

**Kozupeptins, Antimalarial Lipopeptides  
Produced by a Fungus *Paracamarosporium* Species:  
Isolation, Structural Elucidation, Total Synthesis, Bioactivity,  
Development of a New Synthetic Method,  
and Structure-Activity Relationship**

Yumi Hayashi

Graduate school of infection control sciences, Kitasato University

2021

## Acknowledgement

The author would like to express her sincerest gratitude to Distinguished Emeritus Professor Satoshi Ōmura at Kitasato University for his constant guidance and instructive discussions during the course of the studies in this thesis.

The studies presented in this dissertation have been carried out under the supervision of Professor Toshiaki Sunazuka at Laboratory of Bioorganic Chemistry, Graduate School of Infection Control Sciences, Kitasato University during 2018-2021. The author would like to express her deep appreciation to Professor Toshiaki Sunazuka for his helpful guidance and great supports.

The author would also like to express her sincerest appreciation to Professor Hideaki Fujii (School of Pharmacy, Kitasato University), Emeritus Professor Eisuke Kaji (Kitasato University), Associate Professor Masato Iwatsuki (Tropical Disease Centers, Graduate School of Infection Control Sciences, Kitasato University), and Associate Professor Tatsuya Shirahata (School of Pharmacy, Kitasato University) for their valuable advice and guidance during the writing of this thesis.

The author would like to thank Office Manager Ms. Yoko Suzuki for her heartwarming encouragement.

The author would also express her deep gratitude to Dr. Aki Ishiyama (Tropical Disease Centers, Graduate School of Infection Control Sciences, Kitasato University) and Dr. Rei Hokari (Tropical Disease Centers, Ōmura Satoshi Memorial Institute) for evaluation of antimalarial activity and their advice about bioactivity.

The author would like to thank Associate Professor Kenichi Nonaka (Research Center for Microbial Resources, Graduate School of Infection Control Sciences, Kitasato University) for his fermentation and isolation work of the fungus described in this work.

The author would also like to thank Mr. Wataru Fukasawa (Laboratory of Applied Microbial Chemistry, Graduate School of Infection Control Sciences, Kitasato University) for his isolation and structural elucidation work of the natural products described in this thesis.

The author would also like to express her sincerest appreciation to Associate Professor Tomoyasu Hirose for his practical guidance, constant advice, helpful discussions, and invaluable suggestions throughout this work. The author feels so fortunate to have the opportunity to work with Professor Toshiaki Sunazuka and Associate Professor Tomoyasu Hirose at Laboratory of Bioorganic Chemistry.

The author also appreciates Dr. Yoshihiko Noguchi, Dr. Akari Ikeda, Dr. Aoi Kimishima, and all the other members of Sunazuka group.

Furthermore, the author would like to thank Dr. Kenichiro Nagai and Ms. Noriko Sato (School of Pharmacy, Kitasato University) for various instrumental analyses. The author would also like to thank Mr. Toshiyuki Tokiwa (Research Center for Microbial Resources, Ōmura Satoshi Memorial Institute) for photographing the fungus.

The author's life in Tokyo during the studies in this thesis was supported by Sumitomo Chemical Co., Ltd. The author would like to express her sincerest gratitude to Dr. Noriyasu Sakamoto, Dr. Tetsuya Ikemoto, Mr. Koji Yoshikawa, and Dr. Ichiro Komoto (Health & Crop Sciences Research Laboratory, Sumitomo Chemical

Co., Ltd.) for their continued encouragement.

During the studies in this thesis, the author was supported by a large number of people, including her colleagues, friends of hers, her former teachers and so on. The author would like to express her deep gratitude to all of them.

Finally, the author is deeply grateful to her mother Ms. Mieko Hayashi and her deceased father Mr. Kenichi Hayashi for giving birth and raising her.

February 2021

Yumi Hayashi

# Table of Contents

<b>Table of Contents</b>	1
<b>List of Abbreviation</b>	3
<b>Chapter 1. Background and Introduction</b>	6
1-1. Parasitic diseases	7
1-2. Microbial metabolites from nature as drug candidates	9
1-3. Peptides as drug candidates	10
1-4. Peptide synthesis	11
1-5. Malaria	15
1-5-1. Symptoms and prevalence of malaria	15
1-5-2. Lifecycle of malaria parasite	17
1-5-3. Existing malaria drugs and their problems	19
<b>Chapter 2. Kozupeptins, Antimalarial Agents Produced by <i>Paracamarosporium</i> Species: Isolation, Structural Elucidation, Total Synthesis, and Bioactivity</b>	21
2-1. Introduction	22
2-2. Isolation of kozupeptins A and B	23
2-3. Structural elucidation by spectroscopic techniques	25
2-4. Total synthesis and determination of the absolute configuration of kozupeptin A	33
2-5. Evaluation of antimalarial activity <i>in vitro</i> and <i>in vivo</i> (i.p.)	39
2-6. Conclusion	41
<b>Chapter 3. Synthesis of the Antimalarial Peptide Aldehyde, a Precursor of Kozupeptin A, Utilizing a Newly Designed Hydrophobic Anchor Molecule</b>	42
3-1. Introduction	43
3-2. Design and preparation of a new hydrophobic anchor molecule	46
3-3. Peptide elongation utilizing a newly designed hydrophobic anchor molecule	48
3-4. Reduction to the aldehyde	50
3-5. Application to rapid analog synthesis	52
3-6. Conclusion	55

<b>Chapter 4. Synthesis of Analogs and Evaluation of Antimalarial Activity <i>in vitro</i></b>	56
<b>Chapter 5. Summary</b>	61
<b>Experimental Section</b>	64
<b>References</b>	276

## List of Abbreviation

AA	amino acid
Ac	acetyl
ACT	artemisinin-based combination therapy
Ala	alanine
APAD	3-acetyl pyridine NAD
aq.	aqueous
Asn	asparagine
Asp	aspartic acid
ATPase	adenosine triphosphatase
Boc	<i>t</i> -butoxycarbonyl
Bu	butyl
Bzl	benzyl
<sup>13</sup> C	carbon
CDC	Centers for Disease Control and Prevention
Co.	company
Co., Inc.	incorporated company
COMU	(1-cyano-2-ethoxy-2-oxoethylidenaminoxy)dimethylamino-morpholino-carbenium hexafluorophosphate
COSY	correlation spectroscopy
DALY	disability adjusted life years
DBU	1,8-diazabicyclo[5.4.0]undec-7-ene
DCC	<i>N,N'</i> -dicyclohexylcarbodiimide
DCM	dichloromethane
DEPBT	3-(diethoxyphosphoryloxy)-1,2,3-benzotriazin-4(3 <i>H</i> )-one
DEAD	diethyl azodicarboxylate
DIBAL	Diisobutylaluminum hydride
DIC	<i>N,N'</i> -diisopropylcarbodiimide
DMF	<i>N,N</i> -dimethylformamide
DMSO	dimethyl sulfoxide
dr	diastereomeric ratio
EDC	1-ethyl-3-(3-dimethylaminopropyl)-carbodiimide
EI	electron ionization
eq	equivalent
ESI	electrospray ionization

Et	ethyl
FAB	fast atom bombardment
FDA	Food and Drug Administration
FDLA	<i>N</i> <sup>α</sup> -(5-fluoro-2,4-dinitrophenyl)-alaninamide
Fmoc	9-fluorenylmethyloxycarbonyl
GC	gas chromatography
Gln	glutamine
Glu	glutamic acid
Gly	glycine
GPCRs	G-protein-coupled receptors
h	hour (s)
<sup>1</sup> H	proton
HATU	1-[bis(dimethylamino)methylene]-1 <i>H</i> -1,2,3-triazolo[4,5- <i>b</i> ]pyridinium 3-oxide hexafluorophosphate
HBTU	1-[bis(dimethylamino)methylene]-1 <i>H</i> -benzotriazolium 3-oxide hexafluorophosphate
His	histidine
HMBC	heteronuclear multiple bond correlation
HOBt	1-hydroxybenzotriazole
HPLC	high performance liquid chromatography
HRMS	high-resolution MS
IC <sub>50</sub>	half maximal inhibitory concentration
Ile	isoleucine
IR	infrared
K-Selectride <sup>®</sup>	potassium tri- <i>sec</i> -butylborohydride
LAH	lithium aluminum hydride
LC	liquid chromatography
Leu	leucine
LPPS	liquid-phase peptide synthesis
Lys	lysine
M	mol/liter
MBHA	4-methylbenzhydrylamine
Me	methyl
Met	methionine
mp	melting point
Pro	proline
quant.	quantitative
min	minute (s)

MOA	mode of action
MS	mass spectrometer
N/A	not available
NAD	nicotinamide adenine dinucleotide (oxidized)
NADH	nicotinamide adenine dinucleotide (reduced)
NBA	3-nitrobenzylalcohol
NIH	National Institute of Health
NMR	nuclear magnetic resonance
ODS	octadecylsilyl
Ph	phenyl
Phe	phenylalanine
PLC	preparative thin-layer chromatography
p-LDH	parasite lactate dehydrogenase
PyAOP	(7-azabenzotriazol-1-yloxy)tripyrrolidinophosphonium hexafluorophosphate
PyBroP	Bromotripyrrolidinophosphonium hexafluorophosphate
Red-Al <sup>®</sup>	sodium bis(2-methoxyethoxy)aluminum hydride
ROESY	rotating frame nuclear Overhauser effect spectroscopy
rpm	revolutions per minute
SARs	structure-activity relationships
<i>sec-</i>	secondary
Ser	serine
SPPS	solid-phase peptide synthesis
<i>t-</i>	tertiary
<i>tert-</i>	tertiary
TFA	trifluoroacetic acid
THF	tetrahydrofuran
Thr	threonine
TOCSY	total correlation spectroscopy
US	The United States of America
UV	ultraviolet
Val	valine
Z	benzyloxycarbonyl

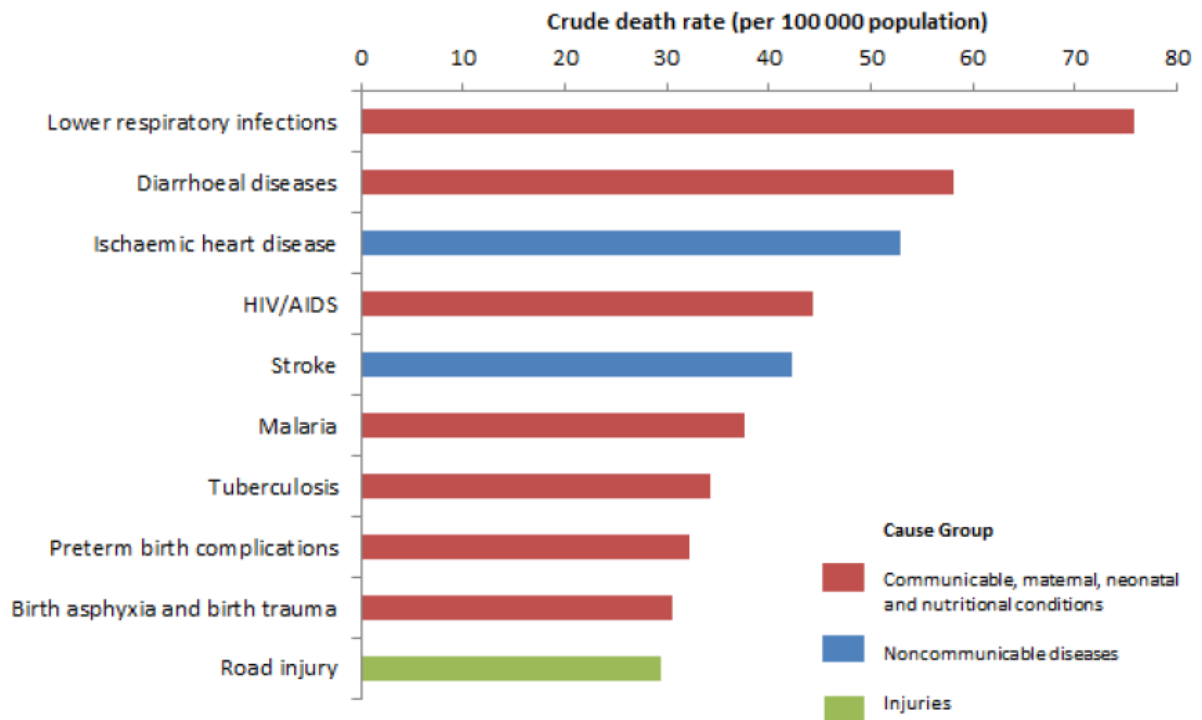
# **Chapter 1**

## **Background and introduction**

## 1-1. Parasitic diseases

Parasitic infections, caused by parasites that have sustained contact with another organism to the detriment of the host organism, remain a serious health problem, especially in low-income countries such as Africa, South-East Asia, and so on.<sup>[1]</sup> Parasites which cause infections are classified into two categories: protozoa that is an unicellular eukaryote and helminth that is a multicellular eukaryote. Protozoan infections usually have a high mortality rate. For example, particularly as for malaria, annual number of patients is estimated 229 million and that of death is reported 409 thousand in 2019.<sup>[2]</sup> On the other hand, helminth infections tend to be chronic and are persistent in certain areas, causing long-term disabilities. The severity of these diseases becomes evident not only from the high mortality rate but also from the high DALY (Disability Adjusted Life Years) values, which are considered to be major obstacles to economic development in low-income countries.<sup>[3]</sup> On the other hand, the number of parasitic diseases is decreasing in high-income countries.<sup>[1]</sup> In particular, in Japan, most parasitic diseases have been suppressed by the spread of mass-screening and development of examination method and useful therapeutic agents, in addition to the improvement of hygienic environments such as water supply and sewerage systems and modernization of agricultural forms using chemical fertilizers. Therefore, in developed countries including Japan, awareness of parasitic infections is not high and pharmaceutical companies have been reluctant to develop new therapeutic drugs for such diseases due to their low profitability.

## Top 10 causes of deaths in low-income countries in 2016



## Top 10 causes of deaths in high-income countries in 2016

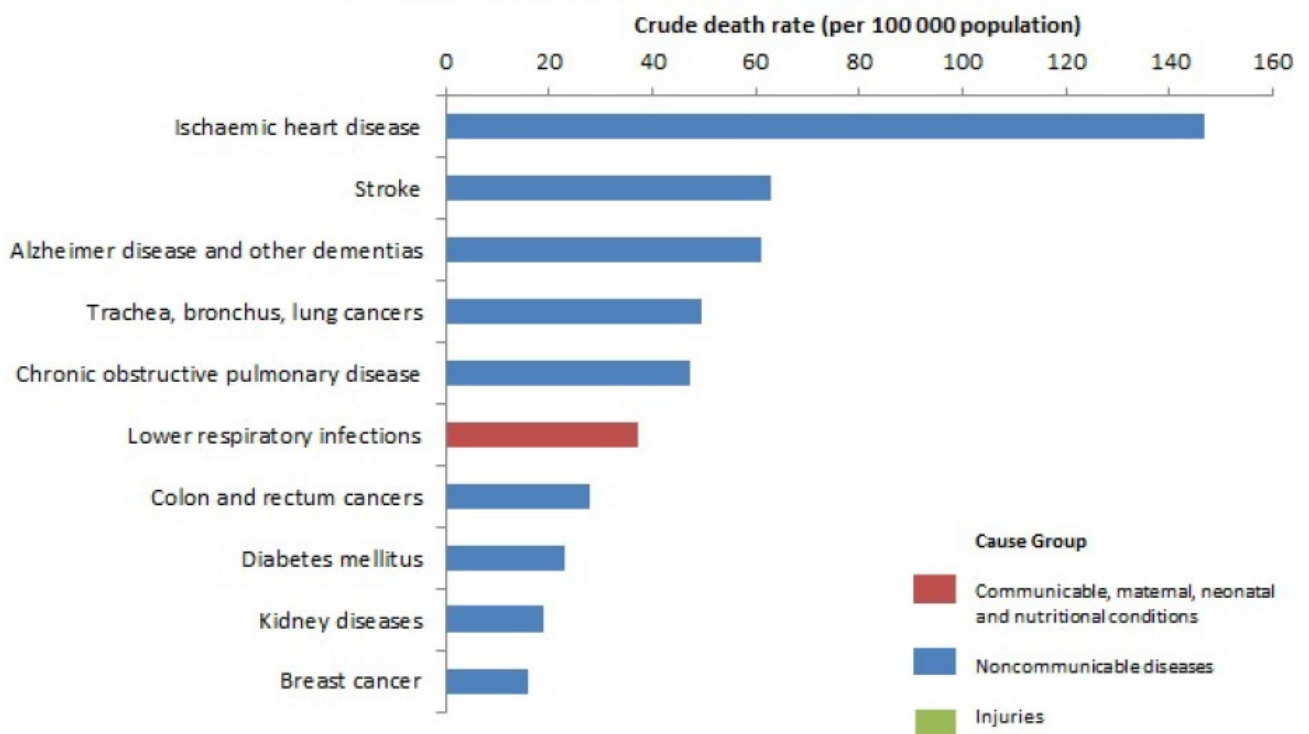


**Figure 1.** Comparison of the top 10 causes of death between low-income countries and high-income countries in 2016<sup>[1a]</sup>

## 1-2. Microbial metabolites from nature as drug candidates

The antibiotic research on natural products derived from microorganisms has been widely developed since the discovery of penicillin by Fleming in 1929.<sup>[4]</sup> As a result of the frenzied research of the past 90 years, a large number of antibiotics were found from nature and have been used as therapeutic agents for infectious diseases and have contributed to human health. Furthermore, in addition to antibacterial agents, a great number of bioactive compounds such as antitumor agents, immunosuppressive agents, and enzyme inhibitors have been discovered from microorganisms.<sup>[5]</sup>

Natural products play a dominant role in the discovery of leads for the development of drugs for the treatment of human diseases. Newman et al. in NIH (National Institute of Health) reported that among the all 1,211 small-molecule drugs approved by U. S. FDA (Food and Drug Administration) during the 34 years from 1981 to 2014, 65% were made based on natural products (**Figure 2**),<sup>[6]</sup> which shows the usefulness of natural products as lead compounds for drug discovery.

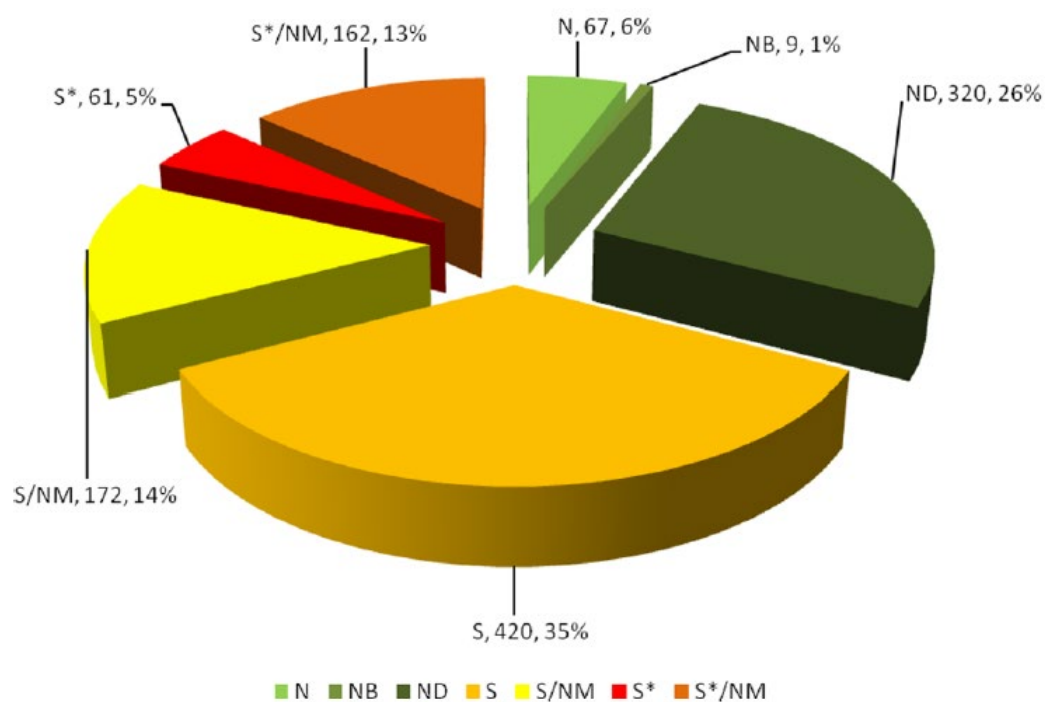


**Figure 2.** All small-molecule approved drugs 1981-2014s; n = 1211.<sup>[6]</sup> N: Unaltered natural product, NB: Botanical drug (defined mixture), ND: Natural product derivative, S: Synthetic drug, S\*: Synthetic drug (NP pharmacophore), /NM: Mimic of natural product.

### 1-3. Peptides as drug candidates

Peptides would be ideal drugs for interfering with protein–protein interactions or serve as ligands for membrane-bound receptors, such as G-protein-coupled receptors (GPCRs) or cell-adhesion receptors (integrins).<sup>[7,8]</sup> As the mainstream modalities of drug discovery shift from small molecules to biological entities, an increasing number of peptide-based drugs and drug candidates have been developed in recent years.<sup>[7,9]</sup> There are already many applications of peptide drugs. Over 60 peptides have been approved in the United States, Europe and Japan, and more than 150 peptides are in active clinical development (**Figure 3**).<sup>[7]</sup> The worldwide market for peptide therapeutics is expected to grow from US\$ 21.3 billion to US\$ 46.6 billion between 2015 and 2024,<sup>[10]</sup> which increases the requirement for improvement in discovery of bioactive peptides and peptide synthesis.

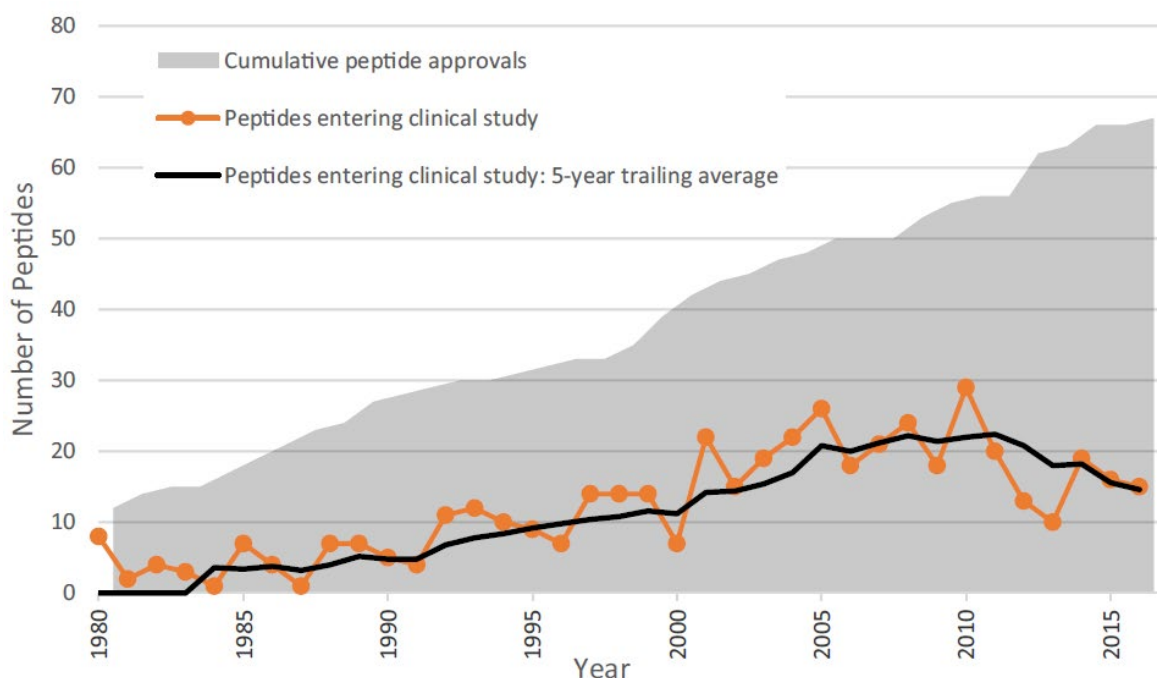


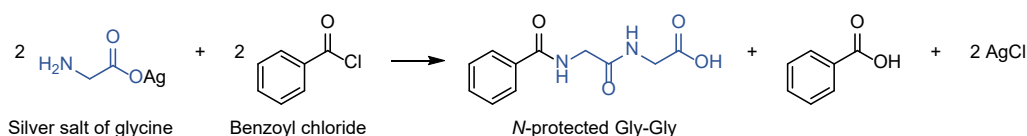
**Figure 3.** Cumulative number of peptides approved in major pharmaceutical markets and the number of peptides entering clinical development<sup>[7]</sup>

## 1-4. Peptide synthesis

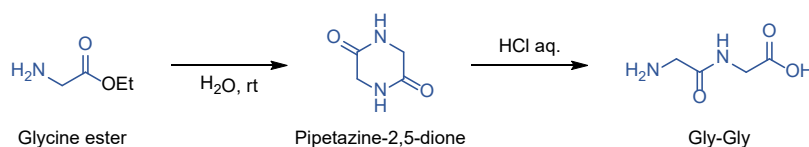
The first peptide synthesis was achieved by Curtius in 1882 in his Ph. D. research with Kolbe.<sup>[11]</sup> Benzoyl glycylglycine, the first *N*-protected dipeptide, was synthesized by reacting the silver salt of glycine with benzoyl chloride (**Scheme 1a**). Nineteen years later, in 1901, Fischer and Fourneau reported the synthesis of glycylglycine, the first free dipeptide, which was achieved by hydrolysis of the diketopiperazine of glycine (**Scheme 1b**).<sup>[12]</sup> In 1902, Fischer first introduced the term “peptides” at the 14<sup>th</sup> meeting of the German scientists and physicians in Karisbad.<sup>[13]</sup> Since then, many researchers, including the above mentioned people, Bergmann, Zervas, Vigneaud, etc., contributed to the development of this research area, and in the 1950s, synthesis of small peptides reached a certain mature stage.<sup>[14]</sup>

**Scheme 1.** Early works for the peptide syntheses

**a)** *N*-protected dipeptide: First ever peptide synthesis by T. Curtius in 1882<sup>[11]</sup>

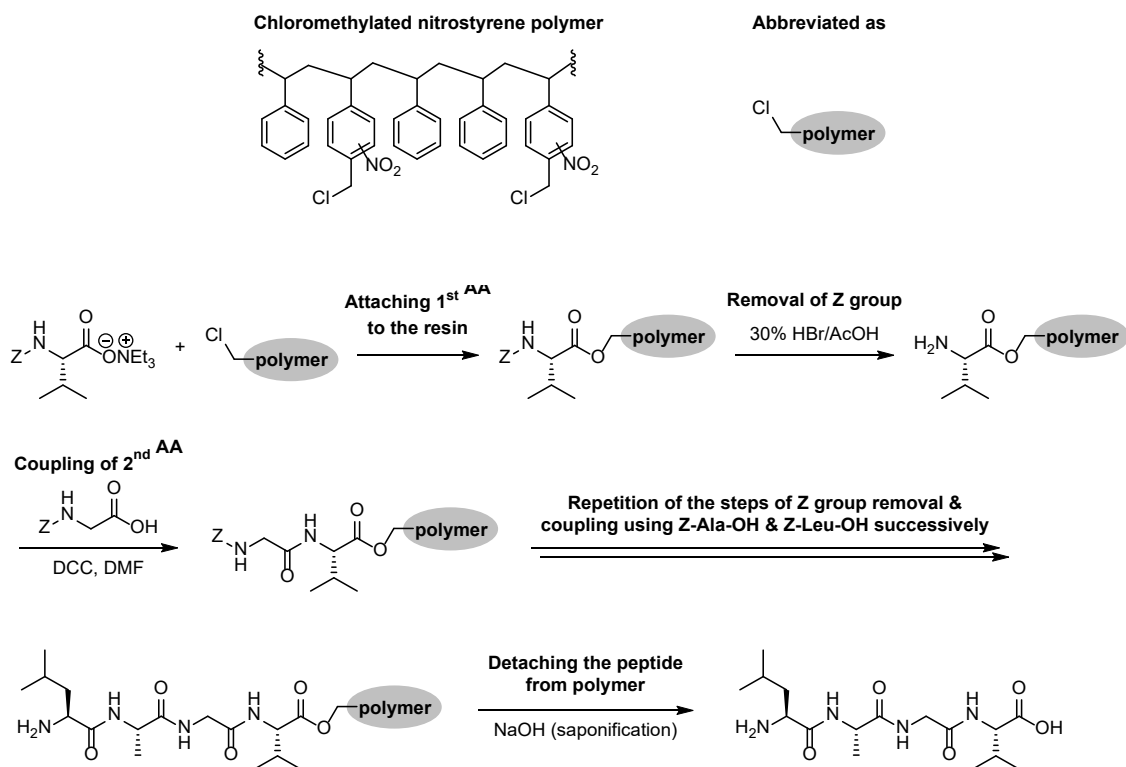


**b)** Free dipeptide: First ever unprotected peptide synthesis by E. Fischer in 1901<sup>[12]</sup>



Synthetic methods of peptides are classified into two categories. The first involves peptide synthesis on an insoluble resin (SPPS, solid-phase peptide synthesis). The second strategy uses a protecting group which is soluble in the reaction medium (LPPS, liquid-phase peptide synthesis). The first ever SPPS was published by Merrifield in 1963.<sup>[15]</sup> In the original procedure, chloromethylnitrostyrene polymer resin was utilized to synthesize a tetrapeptide (**Scheme 2**). Since this fantastic work, SPPS have been improved substantially by many groups over the years, which has greatly contributed to the development of peptide therapeutics. Recent development of various condensation reagents and new solid-phase resins, advances in HPLC purification methods, and development of automated peptide synthesizers have made SPPS the usual method for peptide synthesis.<sup>[16]</sup> Although SPPS offers many advantages with regard to compound isolation and ease of handling, the insoluble nature of resin-supported compounds makes it difficult to monitor the reactions in heterogeneous solutions, to characterize the each synthetic intermediate, and to make reagents access to the reactive site on a solid support. These properties are excellently suitable for initial derivative synthesis for drug discovery but has not shown satisfactory efficiency for scale-up or industrial application. On the other hand, in conventional LPPS, although it is easy to monitor the reaction, reaction and purification conditions largely depend on the amino acid sequence of the peptide, which makes the method suitable to scale-up but unsuitable for divergent peptide synthesis.

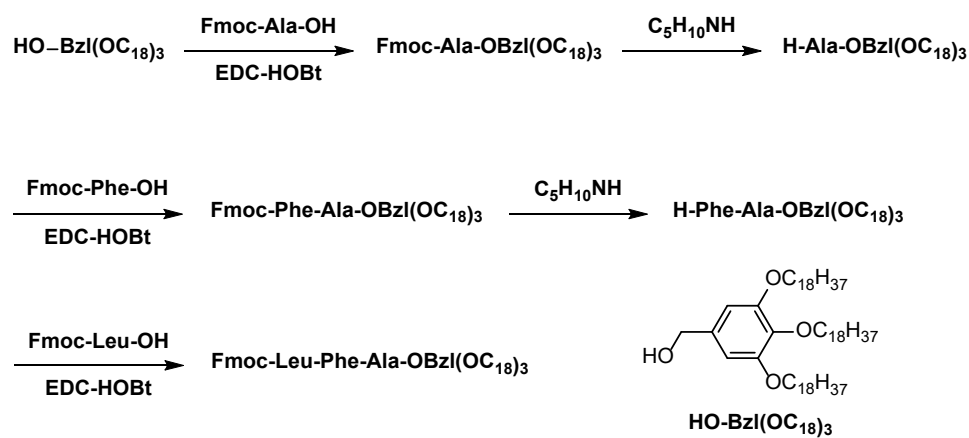
**Scheme 2.** Merrifield's original solid-phase peptide synthesis published in 1963<sup>[15]</sup>



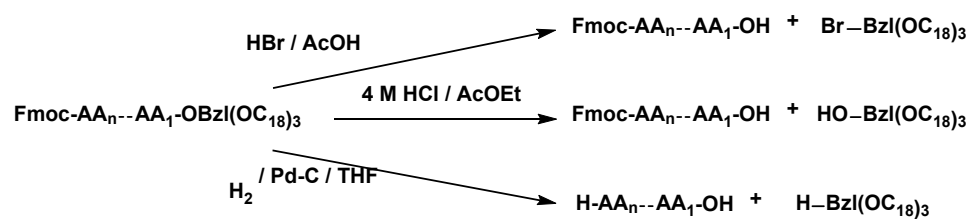
In 2001, Tamiaki *et al.* reported a new type of LPPS utilizing a hydrophobic anchor molecule, which can combine the best characteristics of conventional LPPS with the benefits of SPPS.<sup>[17]</sup> They reported a protocol using a benzyl alcohol derivative having long-alkyl chains as a hydrophobic anchor molecule in which peptide intermediates were purified by simple crystallization combined with flash chromatography if necessary (**Scheme 3**). Afterward, Chiba *et al.* and our group used this protocol to synthesize several peptides including bioactive ones.<sup>[18,19]</sup> Fluorene-derived anchor supported compounds and a synthetic protocol called AJIPHASE<sup>®</sup> were developed by Ajinomoto Co., Inc.<sup>[20]</sup> In spite of the prominent use of this methodology, limited examples illustrated the strategic use of it.

**Scheme 3.** Liquid-phase peptide synthesis utilizing a hydrophobic anchor molecule reported by Tamiaki's group<sup>[17]</sup>

a) Peptide elongation

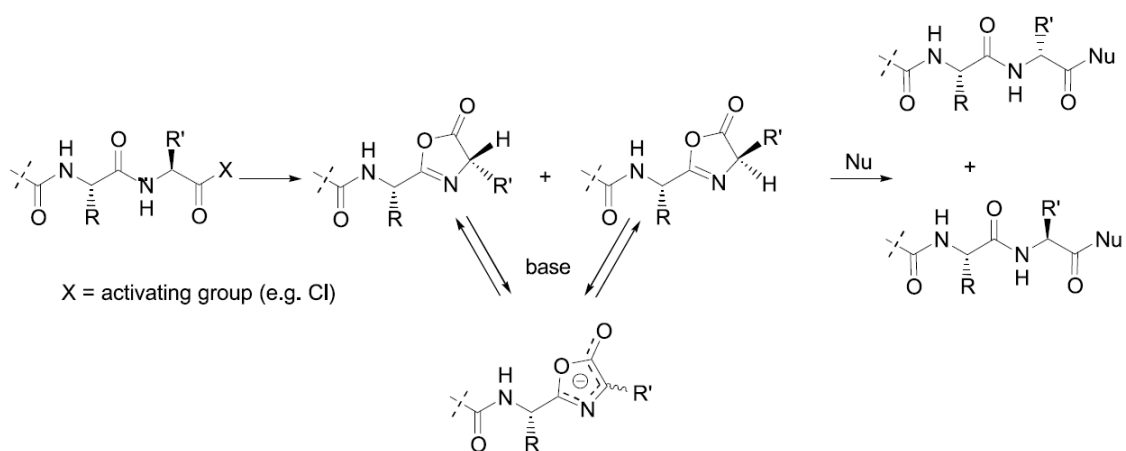


b) Deprotection of the anchor molecule



Amido bond formation in peptide synthesis can often present the problem of racemization. To face this challenge, numerous mild coupling reagents and methods have been developed potentially to help prevent racemization of neighbouring chiral centers.<sup>[16]</sup> Peptide elongation at the *N*-terminus under mild activation conditions using *N*-carbamate protected  $\alpha$ -amino acid such as Boc group or Fmoc group is the most representative example. On the other hand, when the *C*-terminal acid peptide is activated, racemization often occurs because it leads to the formation of the corresponding oxazolone. Even under mild basic conditions, it undergoes racemization due to the formation of conjugated anionic intermediate. The resulting oxazolone mixture reacts then with a nucleophile, which explains the loss of chirality of the coupled material (**Scheme 4**).<sup>[21]</sup>

**Scheme 4.** Oxazolone-mediated racemization occurring during peptide coupling<sup>[21]</sup>



## 1-5. Malaria

### 1-5-1. Symptoms and prevalence of malaria

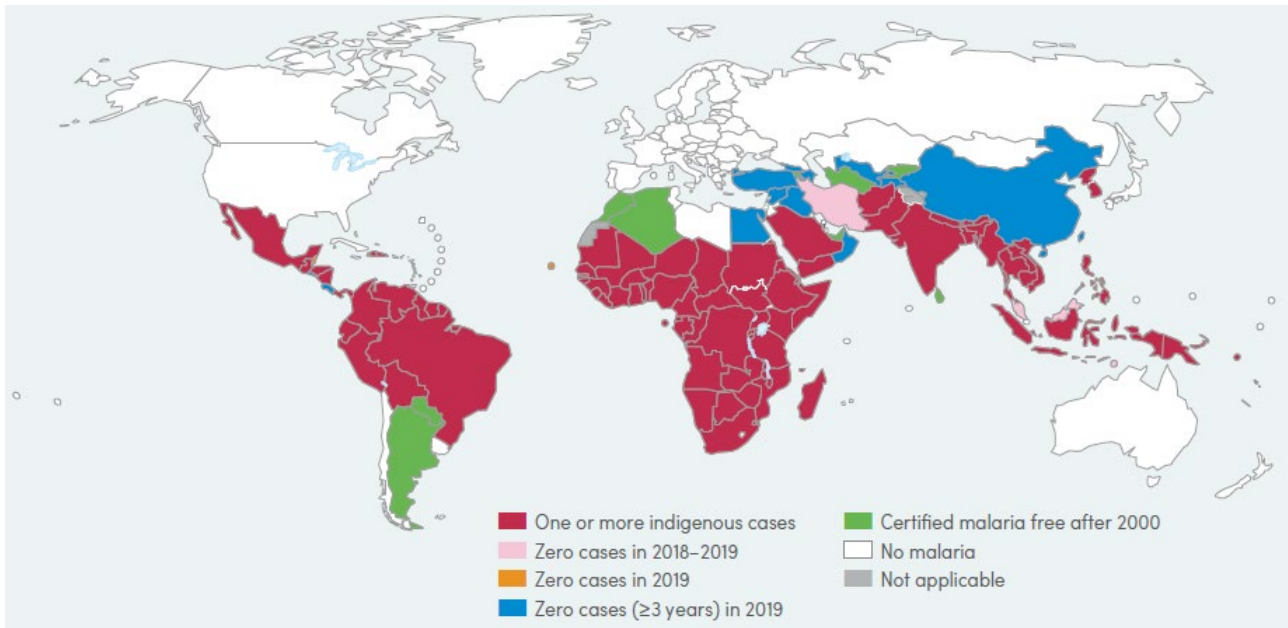


**Figure 4.** Countries with indigenous cases in 2000 and their status by 2019<sup>[2]</sup>

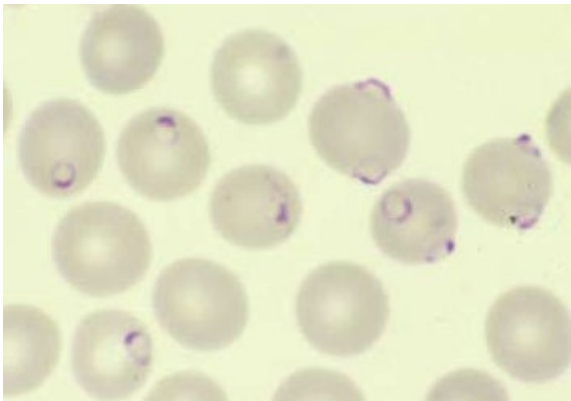


**Figure 5.** *Plasmodium falciparum*

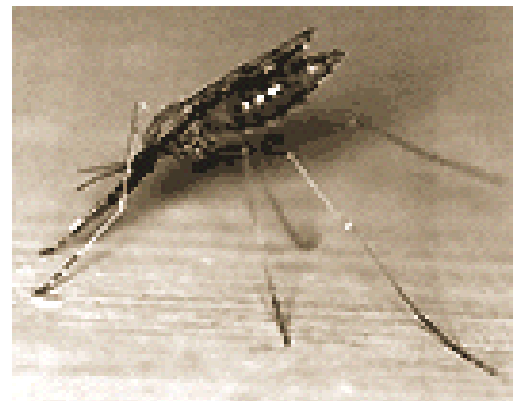


**Figure 6.** *Anopheles* spp.

Malaria, caused by *Plasmodium* species, is a protozoal infection which is widespread throughout the world, especially in the tropical and subtropical regions of sub-Saharan Africa (**Figure 4**).<sup>[2]</sup> The symptoms are characterized by repeated fever around 40°C and antipyretic with splenomegaly, anemia, and so on after a certain incubation period after infection with *Plasmodium* species. There are five kinds of *Plasmodium* species that infects humans: *Plasmodium falciparum* (**Figure 5**), *Plasmodium vivax*, *Plasmodium malariae*, *Plasmodium ovale*, and *Plasmodium knowlesi*. Infection with the most highly pathogenic *P. falciparum*,<sup>[22]</sup> in a severe case, causes death due to acute encephalopathy or renal failure within one to two weeks after onset. According to World Malaria Report 2020 by the World Health Organization (WHO), the estimated annual number of malaria cases is 229 million and that of deaths is 409 thousand in the world in 2019.<sup>[2,23]</sup> In

particular, there are many deaths in children with weak immunity, accounting for high percentage of mortality cause of infants under the age of five due to infectious diseases.<sup>[2,23]</sup> The main cause of malaria epidemic is considered to be underdeveloped medical environment and health services in low-income countries. In addition, with the expansion of the habitat of *Anopheles* (**Figure 6**), which is the vector insect of malaria parasites, due to global warming, there is concern about the expansion of endemic areas.<sup>[24]</sup> On the other hand, cases of imported malaria have been reported all over the world even in no malaria areas, where travelers to endemic areas develop malaria after returning. Since this is an onset in a non-endemic area, some cases leading to death have been reported from delays in diagnosis and treatment.<sup>[25]</sup>

## 1-5-2. Lifecycle of malaria parasite

The lifecycle of *P. falciparum* is shown below (Figure 7)<sup>[26]</sup>

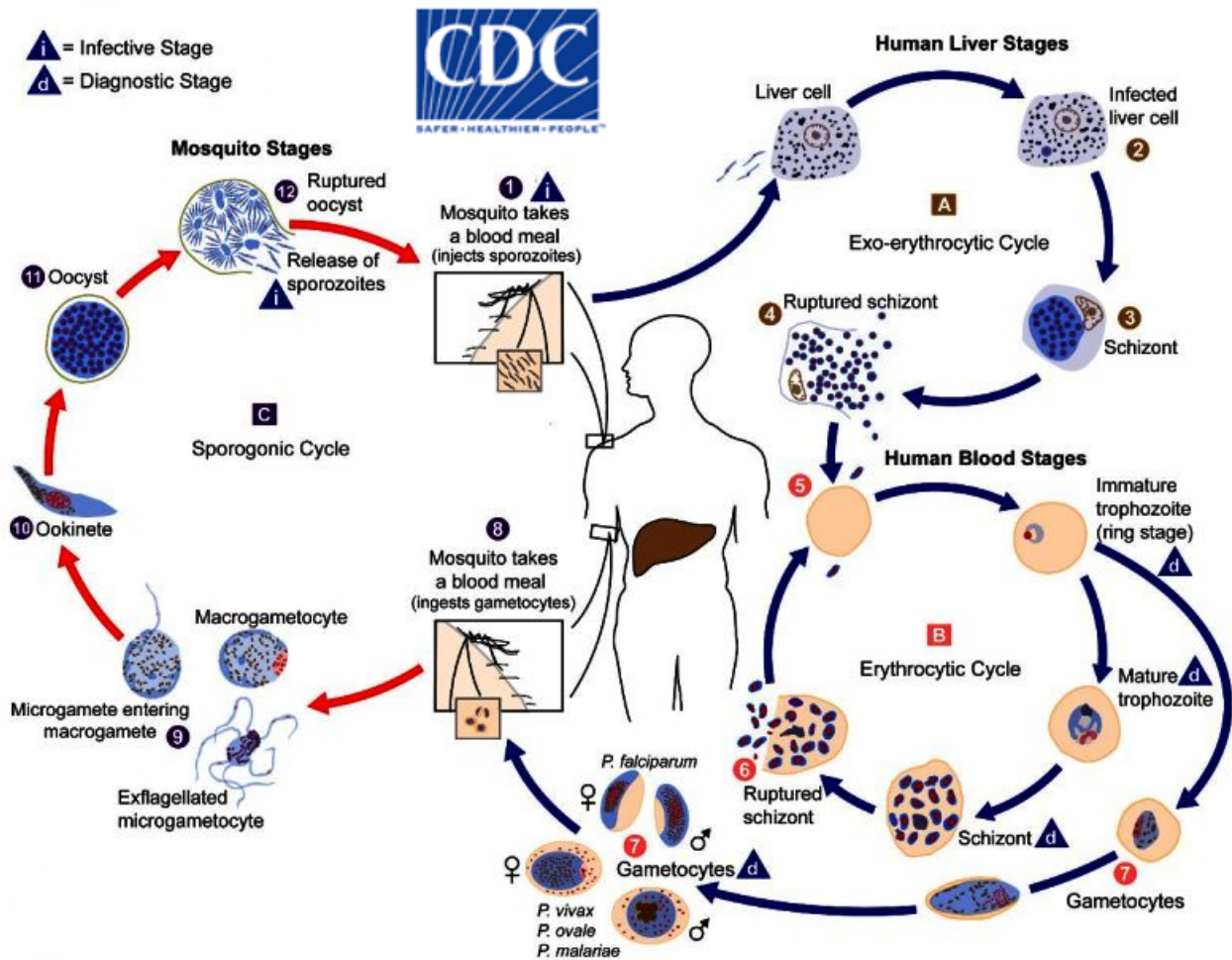


Figure 7. Lifecycle of *P. falciparum*<sup>[26]</sup>

The *Plasmodium* life cycle involves two hosts.

- (1) During a blood diet, a malaria-infected female *Anopheles* mosquito injects sporozoites into the human host.
- (2) Liver cells are infected by the sporozoites.
- (3) The sporozoites mature into schizonts.
- (4) The schizonts rupture and merozoites are released.

After this early replication in the liver (exo-erythrocytic schizogony; A), the parasites undergo asexual reproduction in the erythrocytes (erythrocytic schizogony; B).

- (5) The merozoites infect erythrocytes.
- (6) The ring stage trophozoites mature into schizonts, which rupture and release merozoites.
- (7) Some of parasites differentiate into sexual erythrocytic stages (gametocytes).

Parasites at the blood stage are responsible for the clinical manifestations of the disease.

(8) An *Anopheles* mosquito ingest the gametocytes, male (microgametocytes) and female (macrogametocytes), during a blood meal.

The parasites' multiplication in the mosquito host is known as the sporogonic cycle; C.

(9) In the mosquito's stomach, the microgametes penetrate the macrogametes generating zygotes.

(10) The zygotes become motile and elongated ookinetes.

(11) The ookinetes invade the midgut wall of the mosquito, where they grow into oocysts.

(12) The oocysts develop, rupture, and release sporozoites.

The sporozoites make their way to the mosquito's salivary glands. Inoculation of the sporozoites into a new human host perpetuates the malaria life cycle.

Among the malaria parasites, the growth of *P. falciparum*<sup>[22]</sup> is particularly rapid, which often causes severe symptoms compared to other parasites. The symptoms of malaria are mainly caused by asexual reproduction of *P. falciparum* in erythrocytes. Fever, one of them, is thought to be caused by the release of metabolites of malaria parasites that occurs with the destruction of erythrocytes. Erythrocytes infected with *P. falciparum* are likely to coagulate and occlude the blood vessels of organs such as brain and kidneys, causing necroses of the tissues and making the mortality rate of infected patients high.<sup>[1]</sup>

### 1-5-3. Existing malaria drugs and their problems

Quinine, known as a classic therapeutic agent for malaria, is an alkaloid isolated from *Cinchona* bark, a native plant of the South American Andes in 1820.<sup>[27]</sup> Later, leading the structure of quinine, chloroquine was developed in 1938, and has been used as the most common antimalarial drug for many years.<sup>[28]</sup> Malaria parasites degrade hemoglobin in infected erythrocytes with their proteases and use them as a nutrient source. Although the produced heme is toxic to the protozoa, they have a system that polymerizes heme in the phagosome and detoxifies it as hemozoin. Quinine and chloroquine are thought to exert its antimalarial effect by preventing this polymerization of toxic heme (**Figure 8**).<sup>[29]</sup>

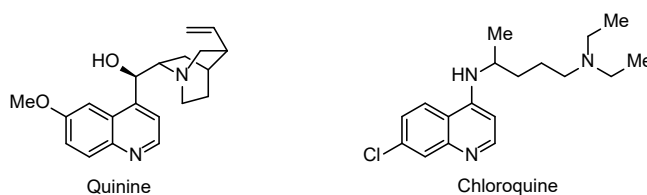


**Figure 8.** Structures of quinine and chloroquine

Chloroquine had been used as an effective treatment even after World War II. However, the chloroquine-resistant *P. falciparum* appeared in Thailand and Colombia in the late 1950s and spread to malaria epidemics around the world, which has significantly reduced the usefulness of it. Chloroquine is selectively toxic to malaria parasites because it attains higher concentrations in parasitized cells than in normal tissue cells. *Plasmodial* resistance to chloroquine is based on an impairment of the mechanism by which such drug levels are accumulated.<sup>[30]</sup> In order to overcome chloroquine-resistant malaria parasites, chloroquine-derivatized mefloquine<sup>[31]</sup> and halofantrine<sup>[32]</sup> have been developed (**Figure 9**). However, their usefulness is decreasing due to the reports of serious side effects and the emergence of resistant protozoa to these drugs.

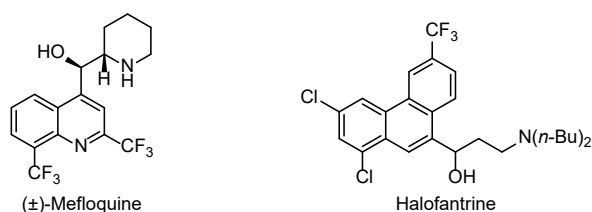


**Figure 9.** Structures of quinine-based existing antimalarial drugs

Artemisinin was first isolated in 1972 from sweet wormwood (*Artemisia annua*), traditionally used for febrile diseases in Chinese medicine.<sup>[33]</sup> Artemisinin, characterized by a cyclic peroxidation structure, shows low toxicity and excellent antimalarial activity. However, since artemisinin is relatively hydrophobic, hydrophilic derivatives such as artesunate have been formulated and used as therapeutics (**Figure 10**).<sup>[34]</sup>

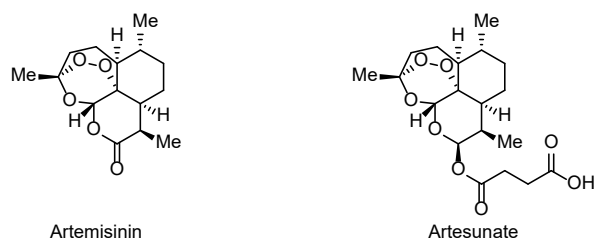


**Figure 10.** Structures of artemisinin-based existing antimalarial drugs

Artemisinins are thought to act on protozoa by being activated by heme in the body, cleaving the cyclic peroxide in the structure and generating reactive oxygen species. It has also been clarified in recent years that antimalarial activity is exhibited by being concentrated and incorporated into protozoa in a high concentration and selectively inhibiting malaria parasite-specific ATPase.<sup>[35]</sup> However, the short half-life and high relapse rate are disadvantages. Relapse is a phenomenon in which a small number of surviving protozoa proliferate and develop the disease again later even after the symptoms of malaria have disappeared and the malaria parasite has not been observed in red blood cells. It is thought that relapse occurs because artemisinins kill the schizont form but only inhibit the growth of ring form trophozoite. Therefore, artemisinin-based combination therapy (ACT) is currently recommended for the treatment of *P. falciparum* malaria by WHO.<sup>[36]</sup> Fast acting artemisinin-based compounds are combined with a drug from a different class. The benefits of ACTs are their high efficacy, fast action and the reduced likelihood of resistance developing. However, since artemisinin drugs cannot easily be chemically synthesized due to their complex structures, they are manufactured by semi-synthesis using the plant extracts, which makes their supply unsustainable and expensive. Moreover, in recent years, malaria parasites resistant to artemisinin or ACT therapy have also been reported.<sup>[37]</sup>

As described above, antimalarial drugs have been developed for a long time and many useful therapeutic agents have been produced. However, the number of resistant parasites is rapidly increasing in any drugs. In addition, vector control has become difficult due to the appearance of *Anopheles* resistant to insecticides, and vaccine development is also difficult because malaria parasites exhibit various antigenic properties. Therefore, the development of novel and safe antimalarial drugs, with new modes of action and structural features, is urgently required.

## Chapter 2

# Kozeptins, Antimalarial Agents Produced by *Paracamarosporium* Species: Isolation, Structural Elucidation, Total Synthesis, and Bioactivity

**ABSTRACT:** Kozeptins A and B, novel antimalarial lipopeptides were isolated from the culture broth of *Paracamarosporium* sp. FKI-7019. They exhibited potent antimalarial activity against chloroquine-sensitive and -resistant *Plasmodium falciparum* strains *in vitro*. The structural elucidation was accomplished by a combination of spectroscopic analyses and chemical approaches including a total synthesis of kozeptin A. Synthetic kozeptin A demonstrated a therapeutic effect *in vivo* and an intermediate exhibited much higher antimalarial activity than kozeptin A.

## 2-1. Introduction

In the course of our screening program to discover antimalarial agents from microbial metabolites which are active against drug-resistant parasites *in vitro* and *in vivo*, we have discovered various metabolites with potent antimalarial properties.<sup>[38]</sup>

Herein, I report the isolation of new potent antimalarial compounds, designated as kozuzeptins A and B (**1a**, **1b**), from the culture broth of *Paracamarosporium* sp. FKI-7019 (**Figure 11**). I also describe an efficient total synthesis and evaluation of the antimalarial activity of these new compounds. This work shows that the kozuzeptins could be a promising leading candidate for development of a new antimalarial drug.

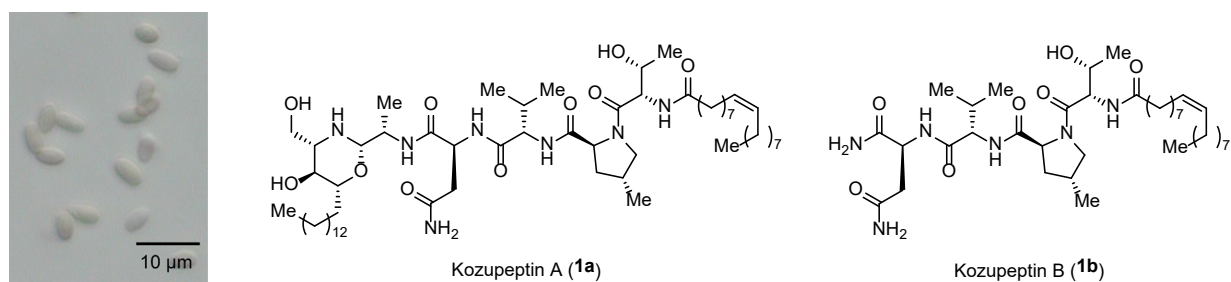
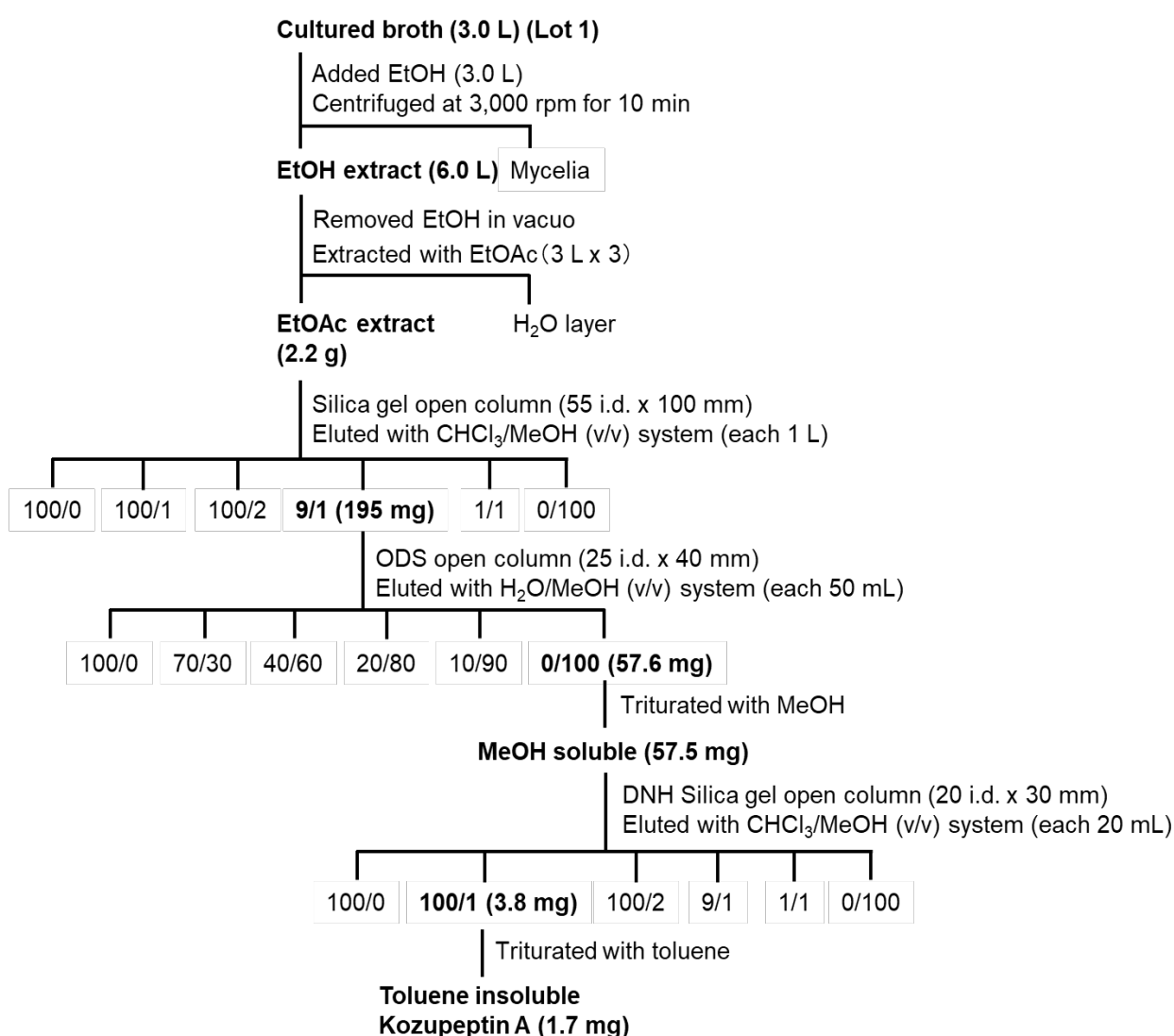


**Figure 11.** *Paracamarosporium* sp. FKI-7019 and structures of kozuzeptins A and B (**1a**, **1b**)

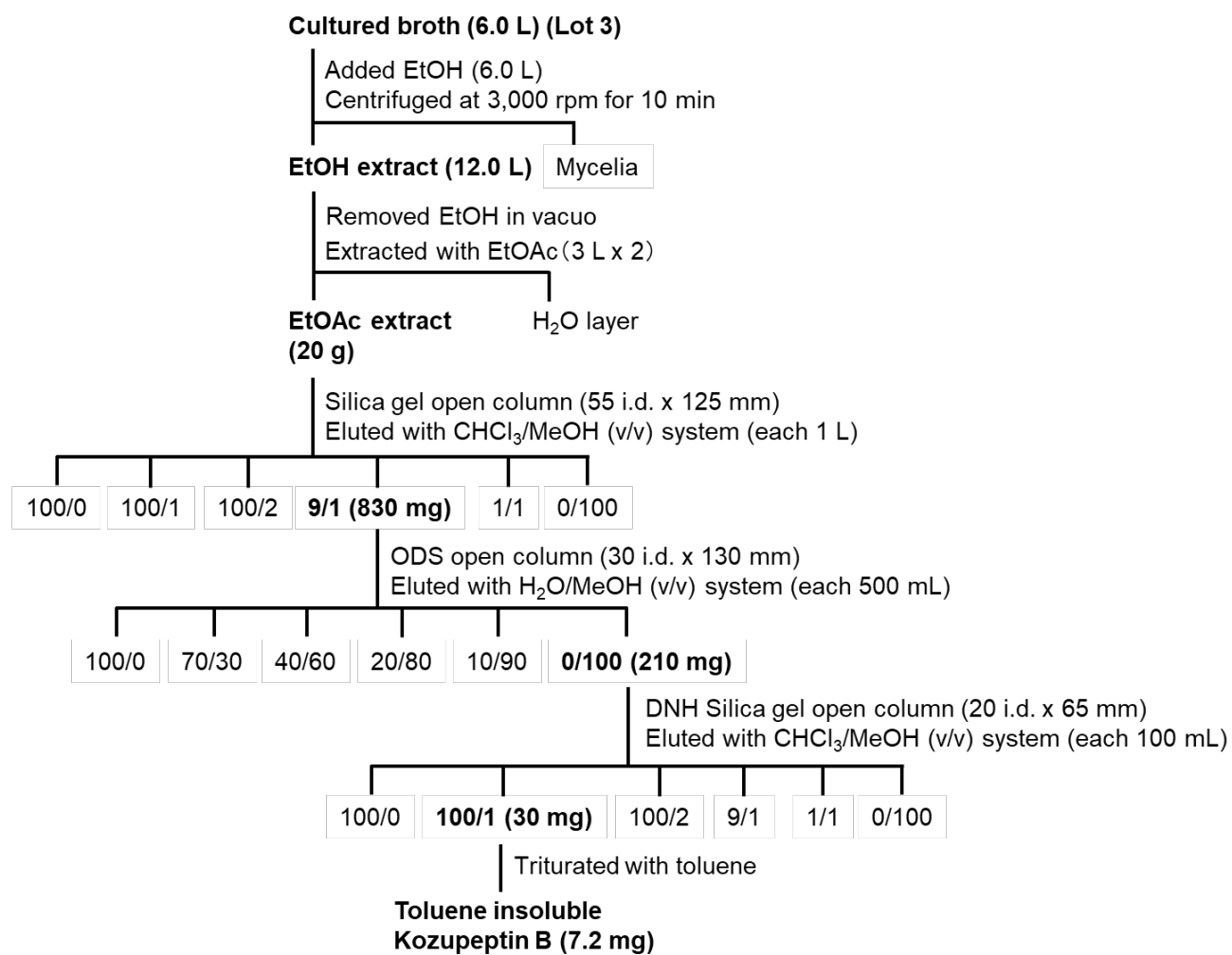
## 2-2. Isolation of kozupeptins A and B

An antimalarial screening program from the fermentation broth of our microorganism library led us to focus on a fungal strain, *Paracamarosporium* sp. FKI-7019 isolated from the soil around a plant in Kozu-Island, Tokyo, Japan. This strain was grown and maintained on an agar slant (see **Experimental Section** for details). The isolation procedure for the kozupeptin A (**1a**) is summarized in **Scheme 5**. The procedure afforded 1.7 mg of kozupeptin A **1a** from an ethanol extracted culture broth of *Paracamarosporium* sp. FKI-7019. From another fermentation lot of ethanol extracted broth (12.0 L), kozupeptin B **1b** (7.2 mg) was obtained (**Scheme 6**).

**Scheme 5.** Isolation procedure of kozupeptin A (**1a**)



**Scheme 6.** Isolation procedure of kozupeptin B (**1b**)



## 2-3. Structural elucidation by spectroscopic techniques

The physico-chemical properties of the isolated compounds kozupeptins A and B (**1a**, **1b**) are summarized in **Table 1**. The molecular formula of kozupeptin A (**1a**) was determined to be  $C_{58}H_{107}N_7O_{10}$  by high-resolution ESI-MS measurement ( $m/z$  1062.8140 calculated for  $C_{58}H_{108}N_7O_{10}$   $[M+H]^+$  1062.8152).

**Table 1.** Physico-chemical properties of kozupeptins A and B (**1a**, **1b**)

	Kozupeptin A ( <b>1a</b> )	Kozupeptin B ( <b>1b</b> )
Appearance	White powder	White powder
Molecular formula	$C_{58}H_{107}N_7O_{10}$	$C_{37}H_{66}N_6O_7$
Molecular weight	1061	706
ESI-MS ( $m/z$ ) ( $[M+H]^+$ )		
calcd.	1062.8152	707.5065
found	1062.8140	707.5060
UV $\lambda_{\text{MeOH}}^{\text{max}}$ nm	End absorption	End absorption
IR $\nu_{\text{KBr}}^{\text{max}}$ $\text{cm}^{-1}$	3436, 3286, 2923, 1647, 1554	3417, 3286, 2923, 1643, 1543
$[\alpha]_D^{26.7}$	-14.7 (c 0.1, DMSO)	-21.1 (c 0.1, DMSO)
Solubility		
soluble	DMSO	DMSO
slightly soluble	MeOH, $\text{CHCl}_3$	MeOH, $\text{CHCl}_3$
insoluble	toluene	toluene
Melting point ( $^{\circ}\text{C}$ )	Not available	207

The structure of **1a** was elucidated by 1D and 2D NMR.  $^1\text{H}$  and  $^{13}\text{C}$  NMR spectral data of the isolated kozupeptins A and B (**1a**, **1b**) are summarized in **Table 2**. The peptide nature of the molecule was immediately inferred from the presence of a number of signals in the amide NH and  $\alpha$ -amino acid proton regions of its  $^1\text{H}$  NMR and of amide carbonyl groups in the  $^{13}\text{C}$  NMR spectra. Furthermore, a monounsaturated fatty acid with one double bond was thought to be present in the molecule due to many methylene signals and an olefin signal. Combined analysis of the  $^1\text{H}$ - $^1\text{H}$  COSY, TOCSY and HMBC spectra identified the structures of four amino acids including one Thr, one 4-methylproline (4-MePro), one Val and one Asn, an alaninal unit, a sphingoid unit, and a fatty acid unit (**Figure 12a**). Thus, kozupeptin A (**1a**) was regarded as a hybrid natural product. The assignment of the sequence was carried out by a combination of HMBC and MS/MS analysis (**Figure 13a**). Consequently, both the fatty acid unit and sphingoid unit were found to have C18, and the planar structure of **1a** was determined to be a novel linear lipopeptide with the sequence fatty acid-Thr-4-MePro-Val-Asn-alaninal-sphingoid.

**Table 2.** NMR data of kozupeptins A and B (**1a**, **1b**) in DMSO-*d*<sub>6</sub>

Kozupeptin A ( <b>1a</b> ) (in DMSO- <i>d</i> <sub>6</sub> )				Kozupeptin B ( <b>1b</b> ) (in DMSO- <i>d</i> <sub>6</sub> )			
	Position	<sup>13</sup> C (100 MHz)	<sup>1</sup> H (J in Hz (400 MHz))		Position	<sup>13</sup> C (100 MHz)	<sup>1</sup> H (J in Hz (400 MHz))
Oleic acid	1	172.1	–	Oleic acid	1	172.2	–
	2	34.8	2.05~2.19 (2H, m)		2	34.8	2.05~2.17 (2H, m)
	3	25.2	1.45 (2H, br t)		3	25.2	1.43 (2H, m)
	4 ~ 7	26.6~31.3	1.20~1.45 (8H, overlapped)		4 ~ 7	26.5~30.1	1.20~1.45 (8H, overlapped)
	8	26.6	2.00(1H, m)		8	25.2	1.95(1H, m)
			1.45(1H, m)				1.43(1H, m)
	9	129.6	5.29~5.34 (1H, m)		9	129.6	5.29~5.34 (1H, m)
	10	129.7	5.30~5.35 (1H, m)		10	129.7	5.30~5.35 (1H, m)
	11	26.6	1.90 (1H, m)		11	26.6	1.90 (1H, m)
			2.00 (1H, m)				2.00 (1H, m)
	12 ~ 17	26.6~31.3	1.20~1.45 (12H, overlapped)		12 ~ 17	21.9~30.1	1.20~1.30 (12H, overlapped)
CH <sub>3</sub>	13.9	0.85 (3H, t, overlapped)	CH <sub>3</sub>	13.9	0.83 (3H, overlapped)		
Thr	1	169.4	–	Thr	1	169.5	–
	2	56.2	4.40 (1H, dd, 7.3, 7.4)		2	56.3	4.38 (1H, dd, 7.8, 7.0)
	3	66.8	3.78 (1H, m)		3	66.8	3.80 (1H, m, overlapped)
	4	19.4	1.09 (3H, d, 6.0)		4	19.3	1.06 (3H, d, 6.8)
	OH	–	4.65 (1H, d, 6.0)		OH	–	4.77 (1H, dr s)
	NH	–	7.86 (1H, d, 7.4)		NH	–	7.91 (1H, d, 7.8)
4-MePro	1	171.7	–	4Me-Pro	1	172.8	–
	2	59.1	4.46 (1H, m)		2	59.2	4.46 (1H, dd, 3.0, 8.6)
	3	36.5	1.65 (1H, ddd, 8.8, 8.8, 12.5)		3	36.4	1.65 (1H, m)
			2.00 (1H, m)				2.00 (1H, m)
	4	32.0	2.35 (1H, m)		4	32.0	2.33 (1H, m)
	5	53.9	3.28 (1H, dd, 9.5, 9.5)		5	53.9	3.24 (1H, d, 8.8, 8.8)
		3.80 (1H, m)			3.78 (1H, m, overlapped)		
CH <sub>3</sub>	17.2	0.97 (3H, d, 6.5)	CH <sub>3</sub>	17.2	0.95 (3H, d, 6.8)		
Val	1	170.6	–	Val	1	170.5	–
	2	57.9	4.05 (1H, dd, 6.5, 8.0)		2	58.4	3.98 (1H, dd, 6.8, 7.9)
	3	29.8	1.92 (1H, m)		3	31.3	1.97 (1H, m)
	CH <sub>3</sub> -1	18.0	0.83 (3H, d, 8.5)		CH <sub>3</sub> -1	18.0	0.81 (3H, overlapped)
	CH <sub>3</sub> -2	19.1	0.84 (3H, d, overlapped)		CH <sub>3</sub> -2	19.1	0.83 (3H, overlapped)
	NH	–	7.82 (1H, d, 8.0)		NH	–	7.94 (1H, d, 7.9)
Asn	1	169.9	–	Asn	1	171.7	–
	2	49.6	4.42 (1H, m)		2	49.5	4.41 (1H, m)
	3	36.8	2.41 (1H, dd, 7.5, 15.5)		3	36.7	2.45 (2H, d, 6.0)
			2.51 (1H overlapped with dms0)		4	172.0	–
	4	171.7	–		NH <sub>2</sub> -1	–	6.95 (1H, s)
	NH <sub>2</sub>	–	7.32 (1H, s)			–	7.02 (1H, s)
		6.87 (1H, s)	NH <sub>2</sub> -4	–	6.85 (1H, s)		
		8.06 (1H, d, 7.5)		–	7.36 (1H, s)		
Alaninal	1	88.3	3.86 (1H, br d, 5.0)	NH	–	8.06 (1H, d, 8.0)	
	2	47.6	3.72 (1H, m)				
	CH <sub>3</sub>	15.4	0.99 (3H, d, 7.0)				
	NH	–	7.32 (1H, d, 8.0)				
Sphingoid	OH-1	–	4.51 (1H, dd, 5.5, 5.5)				
	NH	–	Not observed				
	1	60.4	3.47 (1H, m)				
			3.57 (1H, m)				
	2	61.1	2.36 (1H, m)				
	3	66.9	2.85 (1H, ddd, 9.5, 9.5, 6.8)				
	OH-2	–	4.71 (1H, d, 6.8)				
	4	80.5	3.04 (1H, br ddd)				
	5	31.7	1.77 (1H, br t)				
			1.95 (1H, m)				
	6 ~ 16	26.6~31.3	1.20~1.45 (22H, overlapped)				
17	22.1	1.20~1.45 (2H, overlapped)					
CH <sub>3</sub>	13.9	0.83 (3H, t)					

The absolute configuration of each amino acid residue was determined by advanced Marfey's analysis.<sup>[39]</sup> Acid hydrolysis of **1a** was followed by LC-MS analysis after derivatization of the hydrolysate with D-FDLA. Comparison with the retention times obtained from standards revealed the presence of L-Thr, (2*S*,

4*R*)-4-MePro, L-Val, L-Asn, and L-alaninal (detected as L-Ala by Jones oxidation of the hydrolysate before the reaction with D-FDLA) (**Table 3a**). The monounsaturated fatty acid was deduced to be oleic acid by <sup>1</sup>H NMR and ESI-LCMS using a 2-nitrophenylhydrazide derivative (**Figure 14a**).<sup>[40]</sup> This was also supported by the EI-GCMS fragmentation pattern of pyrrolidine amide derivative (**Figure 15a**).<sup>[41]</sup> Finally, the relative stereochemistry of the six-membered *N,O*-acetal which was deduced to be formed between C18-sphingoid and alaninal was determined by a combination of the correlations of ROESY and the values of the coupling constant in <sup>1</sup>H NMR (**Figure 16**). All substituted groups on the ring proved to be in equatorial positions. However, since the fermentation did not produce **1a** in sufficient quantities and showed poor reproducibility, the absolute configuration of the sphingoid unit was not completely characterized before the total synthesis of **1a** was accomplished in this work (see “Total synthesis and determination of the absolute configuration of kozupeptin A” section below).

The structural elucidation of **1b** was performed in the same way as that of **1a** (**Figure 12b**, **Figure 13b**, **Table 3b**, **Figure 14b**, **Figure 15b**). Consequently, **1b** was found to be an analog of **1a** which lacks both sphingoid and alaninal units (**Figure 11**). The structures predicted by these spectroscopic methods were shown in **Figure 17**.

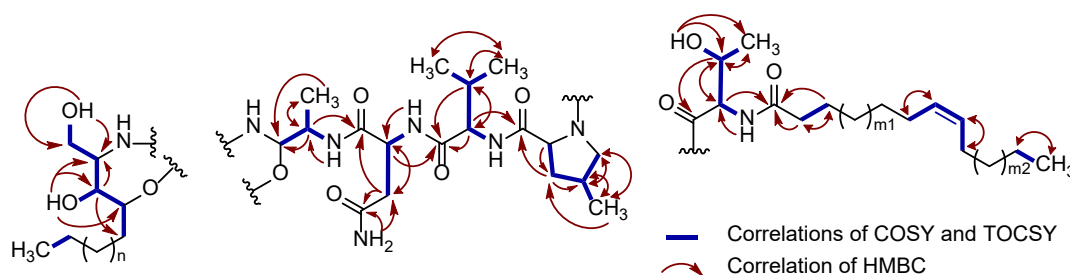


**Figure 12a.** Partial structures of kozupeptin A (**1a**) indicated by the correlations of <sup>1</sup>H–<sup>1</sup>H COSY, TOCSY, and HMBC

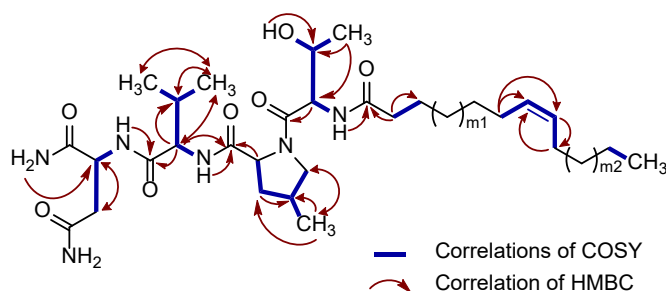


**Figure 12b.** Partial structures of kozupeptin B (**1b**) indicated by the correlations of <sup>1</sup>H–<sup>1</sup>H COSY and HMBC

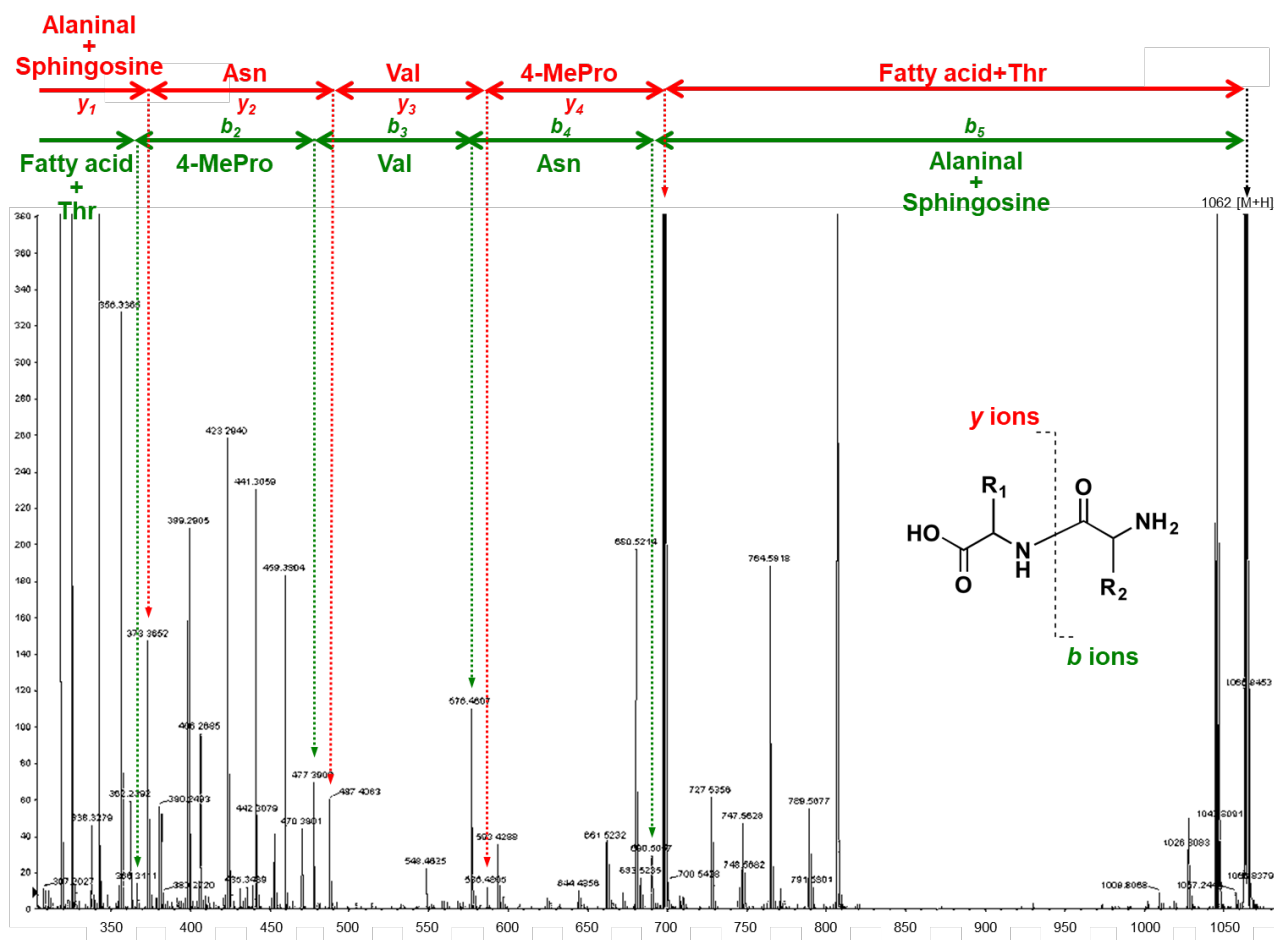


**Figure 13a.** ESI-MS/MS fragment analyses of kozupeptin A (**1a**). The fragmented ions  $b_2$ - $b_5$  as  $b$ -series from the side of N terminus and ions  $y_1$ - $y_4$  as  $y$ -series from the side of C terminus in Biemann nomenclature system, were observed.

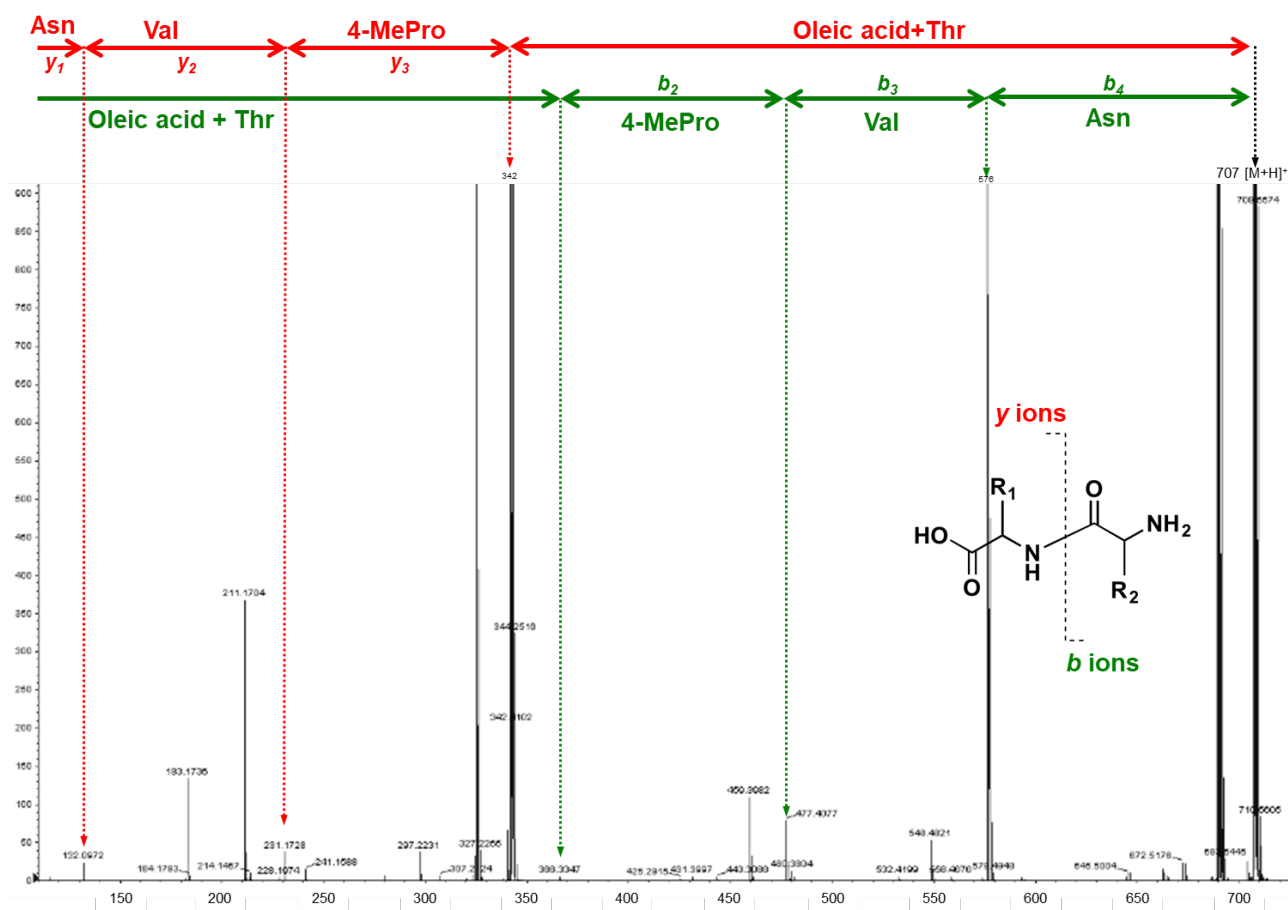


**Figure 13b.** ESI-MS/MS fragment analyses of kozepeptin B (**1b**). The fragmented ions  $b_2$ - $b_4$  as  $b$ -series from the side of N terminus and ions  $y_1$ - $y_3$  as  $y$ -series from the side of C terminus in Biemann nomenclature system, were observed.

**Table 3a.** Advanced Marfey's analysis of kozepeptin A (**1a**)

amino acid-FDLA	$m/z$ [M + H] <sup>+</sup>	retention time (min)			supposed configuration
		authentic L	authentic D	Kozepeptin A ( <b>1a</b> )	Kozepeptin A ( <b>1a</b> )
Thr-D-FDLA	414	4.20	3.58	4.19	L
<i>Allo</i> -Thr-D-FDLA	414	3.93	3.69	not observed	-
Val-D-FDLA	412	5.36	4.49	5.35	L
Asn-D-FDLA	428	3.82	3.70	3.85	L
Ala-D-FDLA	424	4.54	4.03	4.55	L

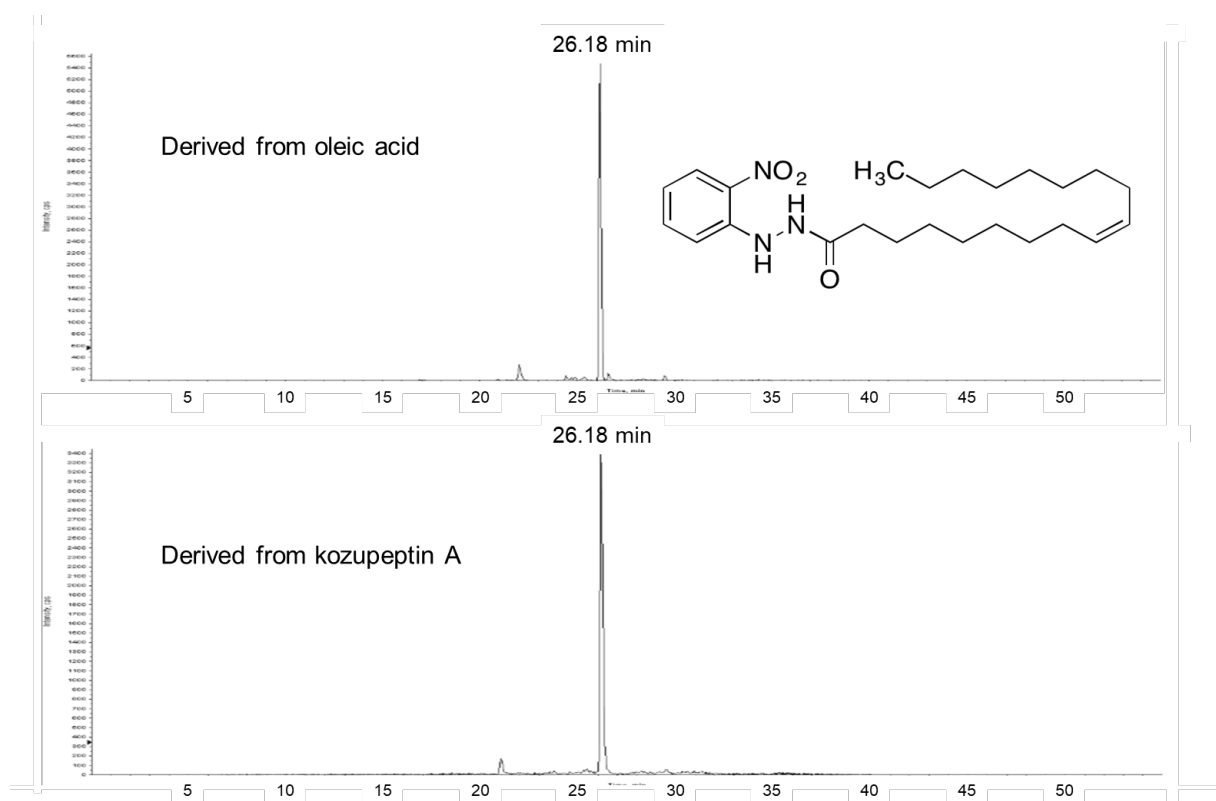
  

amino acid-FDLA	$m/z$ [M + H] <sup>+</sup>	retention time (min)			supposed configuration
		(2S, 4S)	(2S, 4R)	Kozepeptin A ( <b>1a</b> )	Kozepeptin A ( <b>1a</b> )
4-MePro-L-FDLA	424	3.42	3.80	3.79	(2S, 4R)
4-MePro-D-FDLA	424	5.68	5.47	5.40	(2S, 4R)

**Table 3b.** Advanced Marfey's analysis of kozuzeptin B (**1b**)

amino acid-FDLA	$m/z[M + H]^+$	retention time (min)			supposed configuration
		authentic L	authentic D	Kozuzeptin B ( <b>1b</b> )	Kozuzeptin B ( <b>1b</b> )
Thr-D-FDLA	414	4.20	3.58	4.19	L
<i>All</i> o-Thr-D-FDLA	414	3.93	3.69	not observed	-
Val-D-FDLA	412	5.36	4.49	5.36	L
Asn-D-FDLA	428	3.82	3.70	3.82	L

amino acid-FDLA	$m/z[M + H]^+$	retention time (min)			supposed configuration
		(2 <i>S</i> , 4 <i>S</i> )	(2 <i>S</i> , 4 <i>R</i> )	Kozuzeptin B ( <b>1b</b> )	Kozuzeptin B ( <b>1b</b> )
4-MePro-L-FDLA	424	3.42	3.80	3.82	(2 <i>S</i> , 4 <i>R</i> )
4-MePro-D-FDLA	424	5.68	5.47	5.46	(2 <i>S</i> , 4 <i>R</i> )

**Figure 14a.** ESI-LCMS analysis of 2-nitrophenylhydrazide derivatives of oleic acid and the hydrolysate of kozuzeptin A (**1a**)

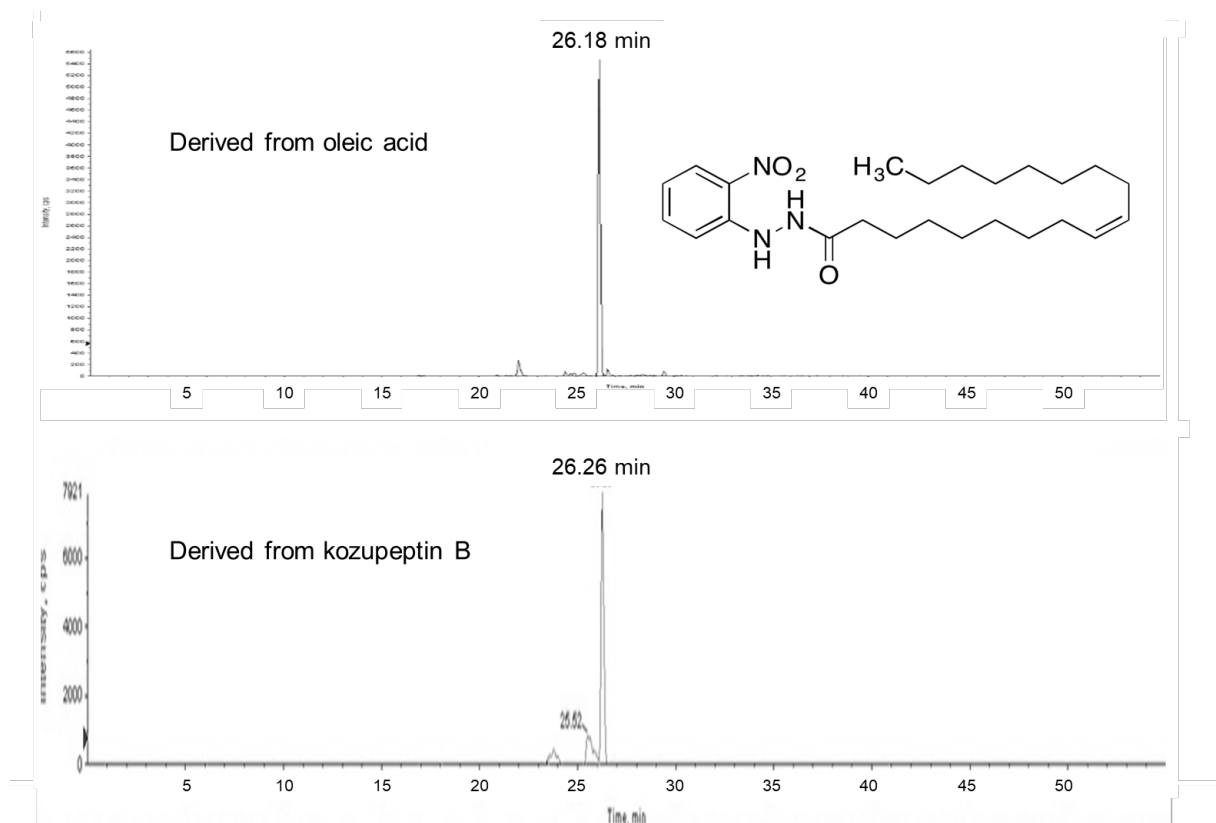


**Figure 14b.** ESI-LCMS analysis of 2-nitrophenylhydrazone derivatives of oleic acid and the hydrolysate of kozuzeptin B (**1b**)

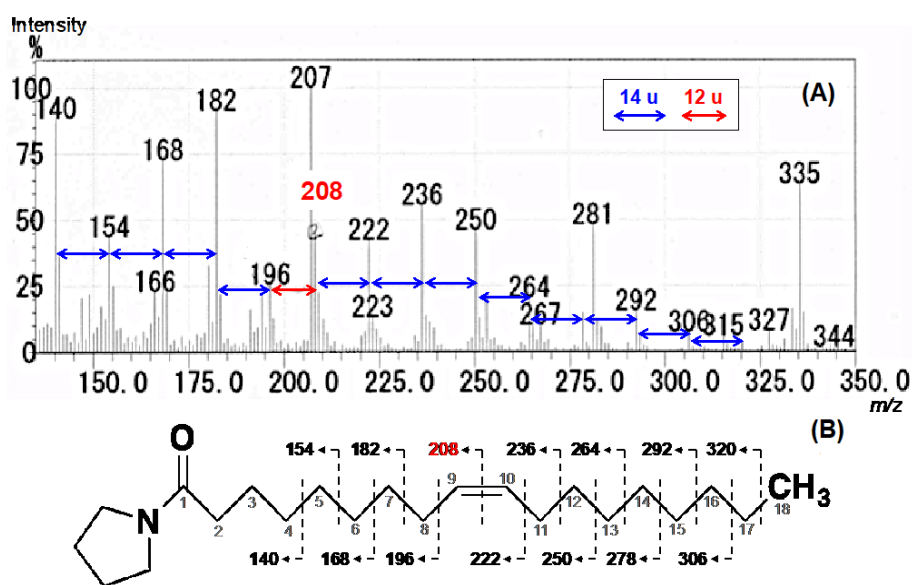


**Figure 15a.** EI-GCMS fragmentation analysis of pyrrolidine derivative of the fatty acid derived from kozuzeptin A (**1a**) (A) and fragment pattern of pyrrolidine derivative of oleic acid (**1b**) (B)

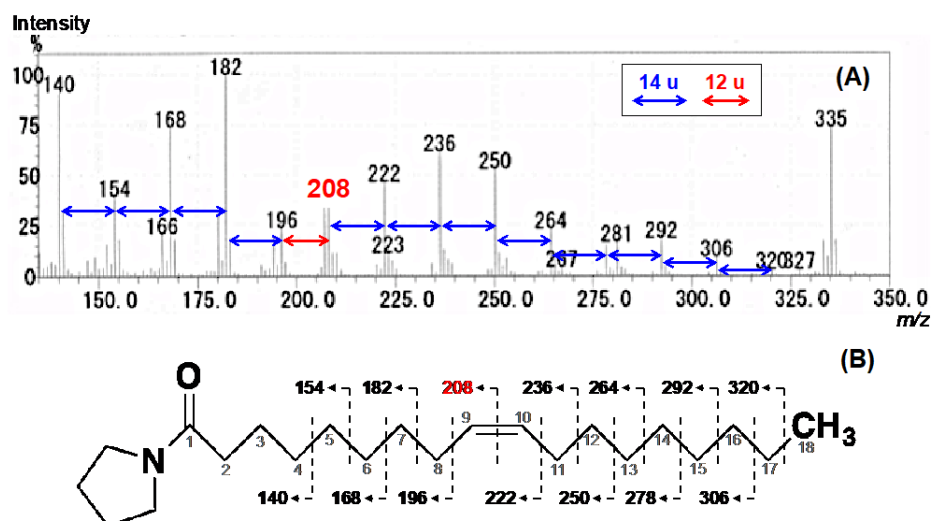


**Figure 15b.** EI-GCMS fragmentation analysis of pyrrolidine derivative of the fatty acid derived from kozupeptin B (**1b**) (A) and fragment pattern of pyrrolidine derivative of oleic acid (B)

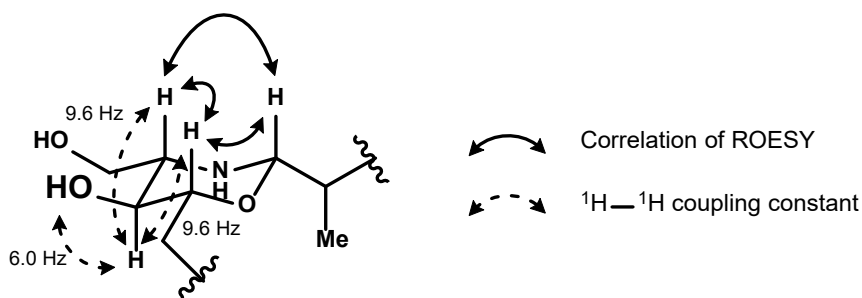


**Figure 16.** ROESY correlation and  $^1\text{H}$  coupling constant of six-membered *N,O*-acetal formed with sphingoid and alaninal

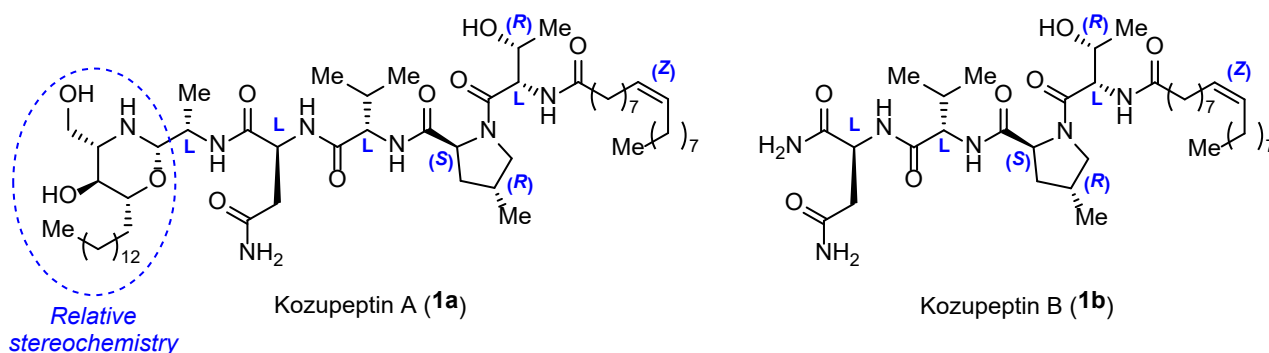


**Figure 17.** The structures predicted by spectroscopic methods

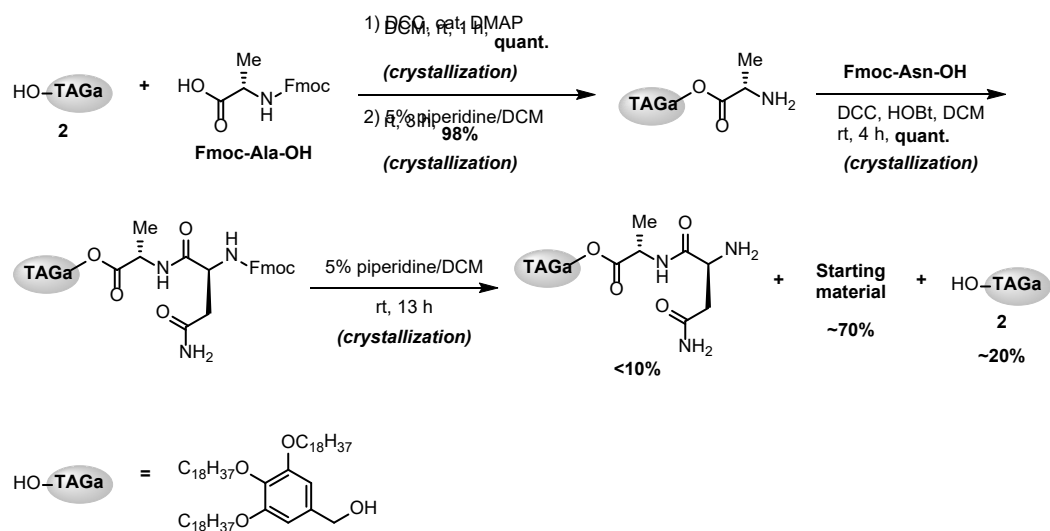
## 2-4. Total synthesis and determination of the absolute configuration of kozupeptin A

To evaluate the predicted structure and determine the absolute stereochemistry, I performed an asymmetric total synthesis of kozupeptin A (**1a**). Aiming for a practical synthesis, I decided to synthesize the peptide unit of **1a** by liquid-phase peptide synthesis (LPPS) utilizing a hydrophobic anchor molecule, which can combine the best characteristics of conventional LPPS with the benefits of solid-phase peptide synthesis (SPPS).<sup>[42,43]</sup> As described in “Peptide synthesis” section of **Chapter 1**, in spite of the highly efficient output of this LPPS-based method, limited examples illustrated the strategic use of it.

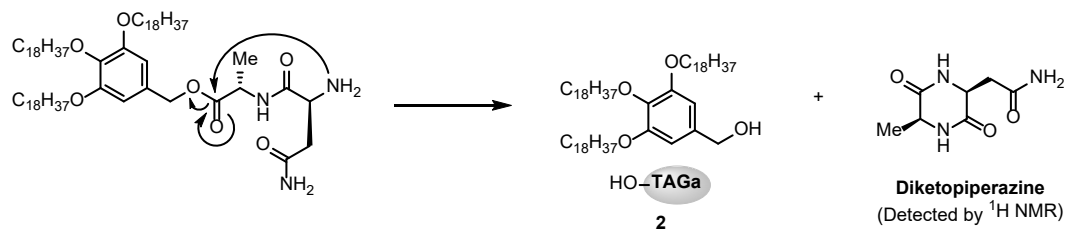
My study began with the use of HO-TAGa (**2**) as an anchor molecule, a known simple one that can be easily synthesized from methyl gallate.<sup>[17]</sup> Condensation with Fmoc-Ala-OH, deprotection of the Fmoc group, and introduction of Fmoc-Asn-OH proceeded without any problems. However, the yield of Fmoc deprotection of Asn was low because of the formation of diketopiperazine and the release of **2** (**Scheme 7a, b**). Although some deprotection conditions were examined, the release of **2** was hardly suppressed.

My next approach was utilizing a fluorene-derived anchor molecule **3**, which was reported that the formation of diketopiperazine was suppressed due to its bulky structure.<sup>[20a]</sup> The synthesis began with the deprotection of the Fmoc group of the known **4**, a fluorene-derived anchor supported Fmoc-Ala (**Scheme 8**).<sup>[20a]</sup> Fortunately, the problematic formation of diketopiperazine during the deprotection of Fmoc group of Asn was greatly suppressed as expected. Thus, the supported amino acid was subsequently subjected to four coupling-deprotection cycles to construct the linear pentapeptide **9** by standard Fmoc peptide synthesis using *N,N'*-diisopropylcarbodiimide (DIC). Each product in peptide elongations could be purified by direct crystallization from the reaction mixture in high yields. Condensation with oleic acid employing the same approach effectively afforded **10**. After synthesis of all the peptide and fatty acid units of **1a** was accomplished, removal of the anchor molecule and deprotection of *t*-Bu group was achieved at the same time under acidic conditions to give carboxylic acid **11** in 75% yield after silica gel flash chromatography separation. Subsequently, to get the C-terminal aldehyde, carboxylic acid **11** was first converted to the Weinreb amide **12** using a condensation reagent. This was the typical method to get a peptide aldehyde, but in our case, epimerization of the  $\alpha$ -position of the C-terminal amino acid became a problem (as described in **Chapter 1-4**). After the screening of condensation reagents, it was eventually suppressed to an acceptable level (dr = 97:3,  $\alpha$ -position of Ala, Weinreb amide **12** did not contain any diastereomers) using 3-(diethoxyphosphoryloxy)-1,2,3-benzotriazin-4(3*H*)-one (DEPBT)<sup>[44]</sup> (**Table 4**). In the literature, DEPBT has been reported to suppress the epimerization,<sup>[44]</sup> which may be due to its neutral and relatively mild character. Reduction of the Weinreb amide utilizing lithium aluminum hydride (LAH) afforded the aldehyde **13**,<sup>[45]</sup> which was treated with natural type phytosphingosine ((2*S*,3*S*,4*R*)-2-amino-1,3,4-octadecanetriol, **14**) to give **1a** in moderate yield over two steps. All the physicochemical data of the synthetic sample were identical to those of the naturally occurring compound and were used to help determine the absolute configuration of **1a** (**Table 5, 6, Figure 17, 18**).

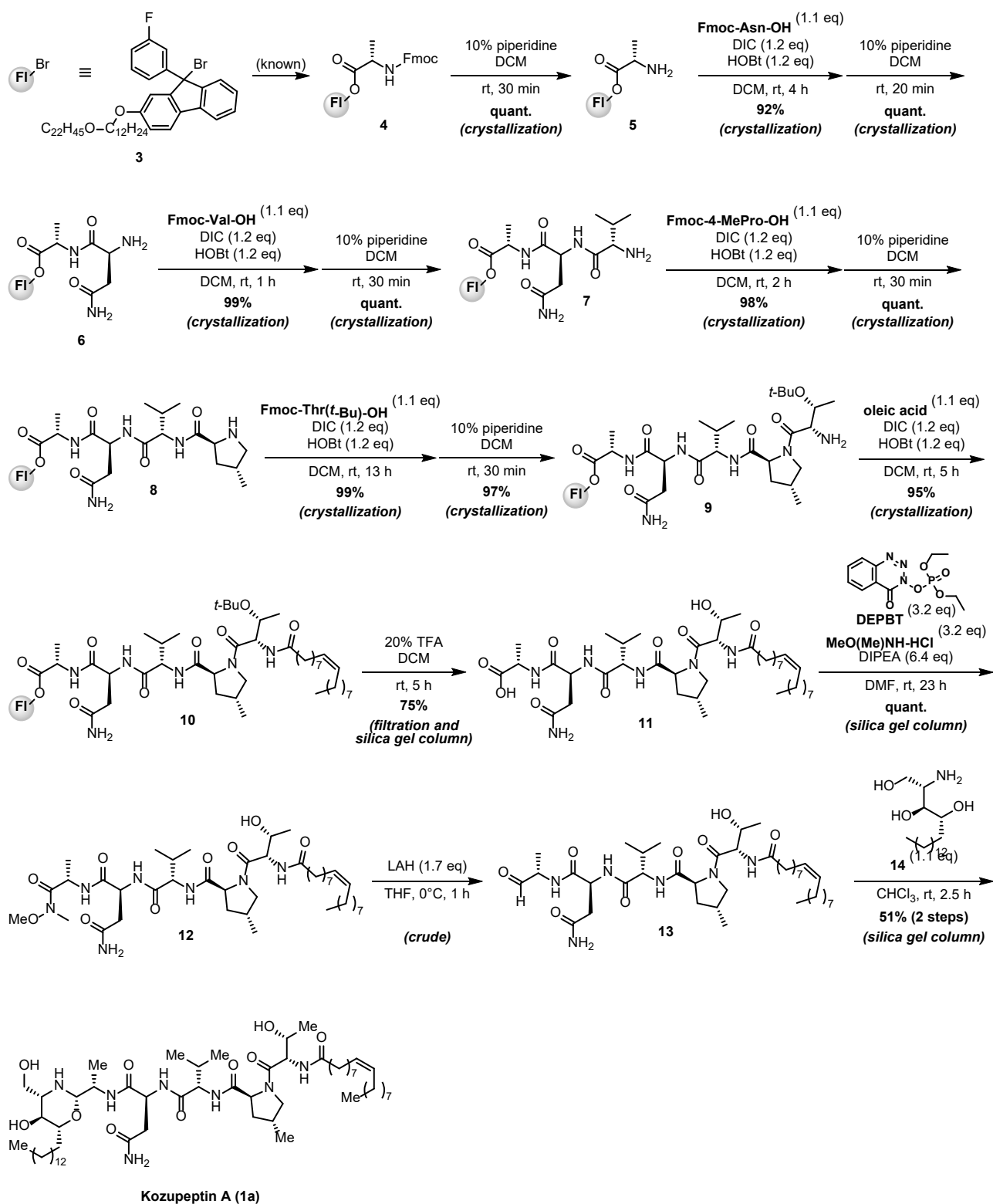
**Scheme 7a.** Synthetic approach using HO-TAGa as a hydrophobic anchor molecule

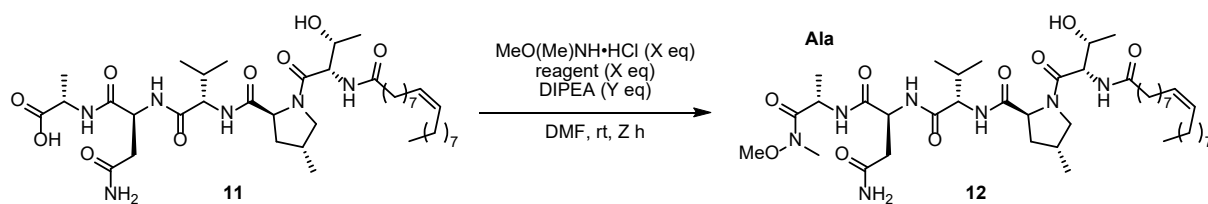


**Scheme 7b.** Formation of diketopiperazine and the release of HO-TAGa



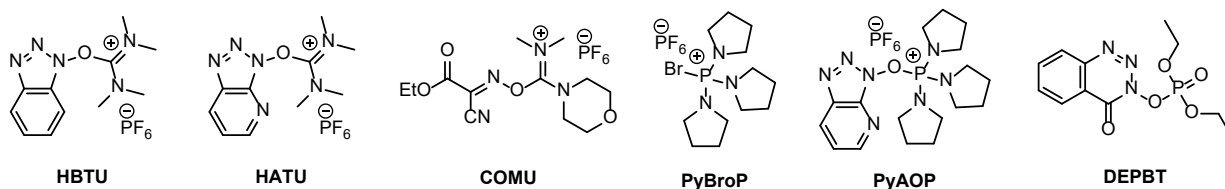
**Scheme 8.** Total synthesis of kozupeptin A (**1a**) utilizing a fluorene-derived hydrophobic anchor molecule



**Table 4.** Screening of condensation reagents in the transformation of carboxylic acid **11** to Weinreb amide **12**

entry	reagent	X eq	Y eq	Z h <sup>[a]</sup>	L/D of Ala <sup>unit</sup> <sup>[b]</sup>	yield (isolated)
1	HBTU	1.2	2.4	3	62/38	–
2	HATU	1.2	2.4	4.5	82/18	–
3	COMU	1.2	2.4	4.5	86/14	–
4	PyBroP	1.8	4.8	5	61/39	–
5	PyAOP	1.2	2.4	6	89/11	–
6	DEPBT	3.2	6.4	16	97/3	quant. <sup>[c]</sup>

<sup>[a]</sup>In all entries, full conv. <sup>[b]</sup>Determined by advanced Marfey's analysis after complete hydrolysis.  
<sup>[c]</sup>120 mg scale of **10** (0.15 mmol). The crude was purified by flash column chromatography on silica gel (CHCl<sub>3</sub>/MeOH).

**Table 5.** Physico-chemical properties of naturally occurring kazupeptin A (**1a**) and synthetic kazupeptin A (**1a**)

	Natural kazupeptin A ( <b>1a</b> )	Synthetic kazupeptin A ( <b>1a</b> )
Appearance	White powder	White powder
Molecular formula	C <sub>58</sub> H <sub>107</sub> N <sub>7</sub> O <sub>10</sub>	C <sub>58</sub> H <sub>107</sub> N <sub>7</sub> O <sub>10</sub>
Molecular weight	1061	1061
ESI-MS ( <i>m/z</i> )		
calcd.	1062.8152 ([M + H] <sup>+</sup> )	1084.7977 ([M + Na] <sup>+</sup> )
found	1062.8140	1084.7968
UV λ <sup>MeOH</sup> <sub>max</sub> nm	End absorption	End absorption
IR ν <sup>KBr</sup> <sub>max</sub> cm <sup>-1</sup>	3436, 3286, 2923, 1647, 1554	3276, 2924, 2853, 1643, 1548, 1456, 1057, 801
[α] <sub>D</sub> <sup>T</sup>	[α] <sub>D</sub> <sup>26.7</sup> = -14.7 (c 0.1, DMSO)	[α] <sub>D</sub> <sup>26.4</sup> = -36.2 (c 0.1, DMSO) <sup>[a]</sup>
Solubility		
soluble	DMSO	DMSO
slightly soluble	MeOH, CHCl <sub>3</sub>	MeOH, CHCl <sub>3</sub>
insoluble	toluene	toluene
Melting point (°C)	Not available	177–179

[a] The difference of absolute values between natural and synthetic ones could be small amount of impurities in naturally isolated one (see <sup>1</sup>H & <sup>13</sup>C NMR spectra in **Figure 17** and **Figure 18**).

**Table 6.**  $^1\text{H}$  and  $^{13}\text{C}$  NMR spectra of naturally occurring kozupeptin A (**1a**) and synthetic kozupeptin A (**1a**) in  $\text{DMSO-}d_6$

	Natural kozupeptin A ( <b>1a</b> ) (in $\text{DMSO-}d_6$ )				Synthetic kozupeptin A ( <b>1a</b> ) (in $\text{DMSO-}d_6$ )		
	Position	$^{13}\text{C}$ (100 MHz)	$^1\text{H}$ (J in Hz (400 MHz))		Position	$^{13}\text{C}$ (125 MHz)	$^1\text{H}$ (J in Hz (500 MHz))
Oleic acid	1	172.1	–	Oleic acid	1	172.2	–
	2	34.8	2.05~2.19 (2H, m)		2	34.9	2.06~2.17 (2H, m)
	3	25.2	1.45 (2H, br t)		3	25.2	1.45 (2H, m, overlapped)
	4 ~ 7	26.6~31.3	1.20~1.45 (8H, overlapped)		4 ~ 7	26.6~31.3	1.13~1.33 (8H, overlapped)
	8	26.6	2.00(1H, m)		8	26.6	2.00(1H, m, overlapped)
			1.45(1H, m)				1.45 (1H, m, overlapped)
	9	129.6	5.29~5.34 (1H, m)		9	129.6	5.29~5.35 (1H, m, overlapped)
	10	129.7	5.30~5.35 (1H, m)		10	129.6	5.29~5.35 (1H, m, overlapped)
	11	26.6	1.90 (1H, m)		11	26.6	1.92 (1H, m, overlapped)
			2.00 (1H, m)				2.00 (1H, m, overlapped)
	12 ~ 17	26.6~31.3	1.20~1.45 (12H, overlapped)		12 ~ 17	26.6~31.3	1.13~1.33 (12H, overlapped)
	$\text{CH}_3$	13.9	0.85 (3H, t, overlapped)		$\text{CH}_3$	14.0	0.85 (3H, t, overlapped)
Thr	1	169.4	–	Thr	1	169.5	–
	2	56.2	4.40 (1H, dd, 7.3, 7.4)		2	56.2	4.40 (1H, m, overlapped)
	3	66.8	3.78 (1H, m)		3	66.8	3.78 (1H, m, overlapped)
	4	19.4	1.09 (3H, d, 6.0)		4	19.4	1.09 (3H, d, 6.0)
	OH	–	4.65 (1H, d, 6.0)		OH	–	4.66 (1H, d, 5.5)
	NH	–	7.86 (1H, d, 7.4)		NH	–	7.86 (1H, d, 7.5)
4-MePro	1	171.7	–	4-MePro	1	171.7	–
	2	59.1	4.46 (1H, m)		2	59.2	4.46 (1H, m, overlapped)
	3	36.5	1.65 (1H, ddd, 8.8, 8.8, 12.5)		3	36.5	1.65 (1H, m)
			2.00 (1H, m)				2.00 (1H, m, overlapped)
	4	32.0	2.35 (1H, m)		4	32.0	2.35 (1H, m)
	5	53.9	3.28 (1H, dd, 9.5, 9.5)		5	54.0	3.29 (1H, dd, 9.0, 9.5)
		3.80 (1H, m)			3.80 (1H, m, overlapped)		
	$\text{CH}_3$	17.2	0.97 (3H, d, 6.5)		$\text{CH}_3$	17.2	0.97 (3H, d, 7.0)
Val	1	170.6	–	Val	1	170.6	–
	2	57.9	4.05 (1H, dd, 6.5, 8.0)		2	57.9	4.05 (1H, dd, 6.5, 8.0)
	3	29.8	1.92 (1H, m)		3	29.8	1.92 (1H, m, overlapped)
	$\text{CH}_3$ -1	18.0	0.83 (3H, d, 8.5)		$\text{CH}_3$ -1	18.0	0.83 (3H, d, overlapped)
	$\text{CH}_3$ -2	19.1	0.84 (3H, d, overlapped)		$\text{CH}_3$ -2	19.1	0.84 (3H, d, overlapped)
	NH	–	7.82 (1H, d, 8.0)		NH	–	7.82 (1H, d, 8.0)
Asn	1	169.9	–	Asn	1	170.0	–
	2	49.6	4.42 (1H, m)		2	49.6	4.42 (1H, m, overlapped)
	3	36.8	2.41 (1H, dd, 7.5, 15.5)		3	36.8	2.41 (1H, dd, 6.5, 15.5)
			2.51 (1H overlapped with dms0)				2.51 (1H overlapped with dms0)
	4	171.7	–		4	171.7	–
	$\text{NH}_2$	–	7.32 (1H, s)		$\text{NH}_2$	–	7.32 (1H, s)
		6.87 (1H, s)			6.88 (1H, s)		
	NH	–	8.06 (1H, d, 7.5)		NH	–	8.08 (1H, d, 8.0)
Alaninal	1	88.3	3.86 (1H, br d, 5.0)	Alaninal	1	88.3	3.86 (1H, app br s)
	2	47.6	3.72 (1H, m)		2	47.6	3.71 (1H, m)
	$\text{CH}_3$	15.4	0.99 (3H, d, 7.0)		$\text{CH}_3$	15.5	0.99 (3H, d, 7.0)
	NH	–	7.32 (1H, d, 8.0)		NH	–	7.32 (1H, d, overlapped)
Sphingoid	OH-1	–	4.51 (1H, dd, 5.5, 5.5)	Sphingoid	OH-1	–	4.51 (1H, m, overlapped)
	NH	–	Not observed		NH	–	Not observed
	1	60.4	3.47 (1H, m)		1	60.4	3.47 (1H, m)
			3.57 (1H, m)				3.57 (1H, m)
	2	61.1	2.36 (1H, m)		2	61.1	2.36 (1H, m)
	3	66.9	2.85 (1H, ddd, 9.5, 9.5, 6.8)		3	66.9	2.86 (1H, m)
	OH-2	–	4.71 (1H, d, 6.8)		OH-2	–	4.71 (1H, d, 6.5)
	4	80.5	3.04 (1H, br ddd)		4	80.6	3.04 (1H, m)
	5	31.7	1.77 (1H, br t)		5	31.7	1.77 (1H, br t)
			1.95 (1H, m)				1.95 (1H, m, overlapped)
	6 ~ 16	26.6~31.3	1.20~1.45 (22H, overlapped)		6 ~ 16	26.6~31.3	1.20~1.45 (22H, overlapped)
	17	22.1	1.20~1.45 (2H, overlapped)		17	22.1	1.20~1.45 (2H, overlapped)
	$\text{CH}_3$	13.9	0.83 (3H, t)		$\text{CH}_3$	14.0	0.83 (3H, t, overlapped)

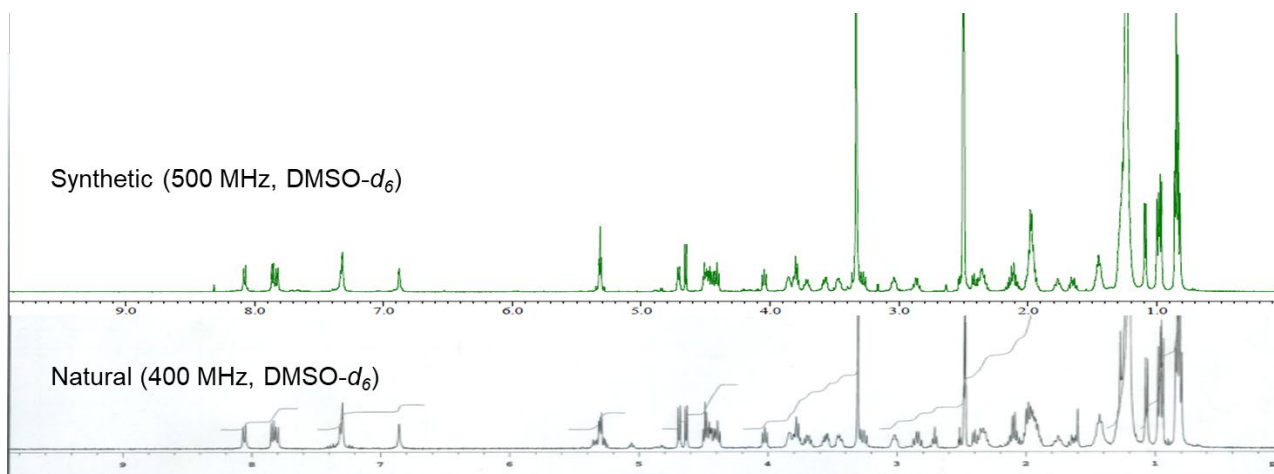


**Figure 17.**  $^1\text{H}$  NMR spectra of naturally occurring kozupeptin A (**1a**) and synthetic kozupeptin A (**1a**) in  $\text{DMSO-}d_6$

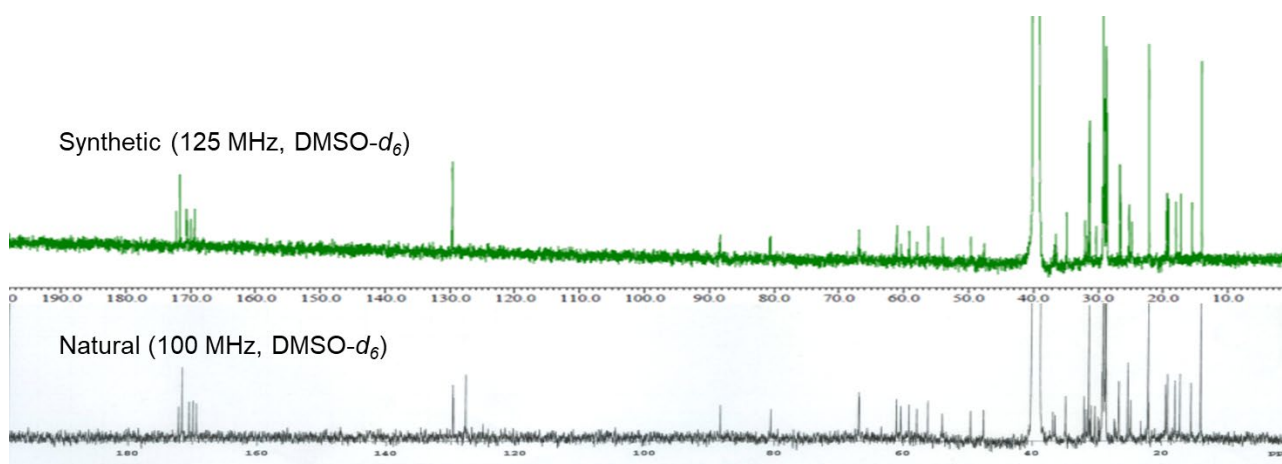


**Figure 18.**  $^{13}\text{C}$  NMR spectra of naturally occurring kozupeptin A (**1a**) and synthetic kozupeptin A (**1a**) in  $\text{DMSO-}d_6$  (Kozupeptin A (**1a**) isolated from the nature includes some impurities and one of them was found to be the one having linoleic acid instead of oleic acid from the results of derivative syntheses in **Chapter 4**. The signal around 128 ppm in “natural” derives from it.)

## 2-5. Evaluation of antimalarial activity *in vitro* and *in vivo* (i.p.)

Naturally occurring kozupeptins, synthesized **1a** and three intermediates in the late stage of our total synthesis were evaluated for *in vitro* antimalarial activity against chloroquine-resistant and -sensitive *P. falciparum* strains (K1 and FCR3 respectively), and cytotoxicity against a human lung fibroblast cell line MRC-5 (Table 7).<sup>[38a]</sup> Synthetic kozupeptin A (**1a**) was found to show a similar IC<sub>50</sub> value (0.3 μM) to that of natural **1a**. Even more surprisingly, aldehyde **13** exhibited potent antimalarial activity (about 20 times stronger than that of **1a**) against both the chloroquine-resistant K1 strain and the chloroquine-sensitive FCR3 strain, which was of the same order as that of artemisinin. In addition, **13** fortunately showed low cytotoxicity against human MRC-5 cells. **1a** would be the prodrug of the most active compound **13**. The antimalarial properties of the Weinreb amide **12** or carboxylic acid **11** were much weaker.

Table 7. *In vitro* antimalarial activity

compound	IC <sub>50</sub> (μM)		
	antimalarial activity		cytotoxicity
	K1 strain <sup>[a]</sup>	FCR3 strain <sup>[b]</sup>	MRC-5
<b>1a</b> (natural)	0.15	0.29	>23
<b>1b</b> (natural)	1.03	1.46	>35
<b>1a</b> (synthetic)	0.30	0.55	>23
<b>13</b> (aldehyde) <sup>[c]</sup>	0.0083	0.013	>32
<b>12</b> (Weinreb amide)	12.5	>15.2	>30
<b>11</b> (carboxylic acid)	>16.0	Not available	>32
chloroquine <sup>[d]</sup>	0.17	0.038	58 <sup>[e]</sup>
artemisinin <sup>[d]</sup>	0.019	0.023	160 <sup>[e]</sup>

[a] Chloroquine-resistant strain. [b] Chloroquine-sensitive strain.

[c] Purified by silica gel column chromatography for the evaluation.

[d] Drugs commonly used to treat malaria. [e] *J. Antibiot.* **2011**, *64*, 183.

Having sufficient **1a** and **13** in hand throughout our total synthesis, *in vivo* antimalarial activity of **1a**, **13**, and one of the standard antimalarial drugs, artesunate, injected i.p. (intraperitoneal), were measured in a mouse model according to Peters' 4-days suppressive test using the rodent malaria *P. berghei* N strain, which is chloroquine-sensitive.<sup>[46,38a,b]</sup> A dose of 30 mg kg<sup>-1</sup> of **1a**, **13**, or artesunate for 4 days each suppressed 52.4%, 99.8%, or 89.9% of malaria parasites (99.8% and 89.9% should not be considered a statistically significant difference in this time period). This initial finding that **1a** and the synthetic intermediate **13** exhibit antimalarial activity not only *in vitro* but also *in vivo*, combined with the rare structure for an antimalarial agent, confirms that the kozupeptins show promise as lead antimalarial compounds with a probable new mode of action (A few compounds which have similar structures to kozupeptins were reported (Figure 19).<sup>[47]</sup>).

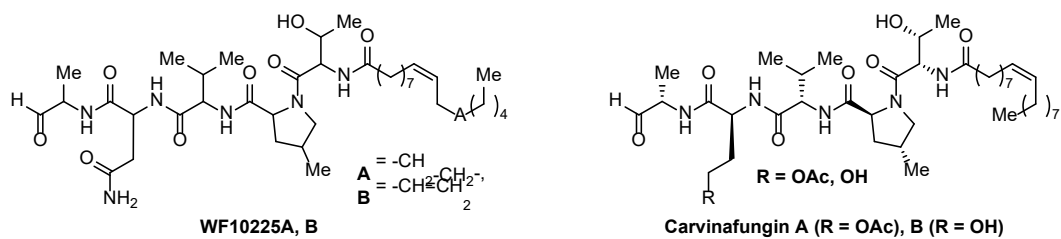


**Figure 19.** Reported compounds that have similar structures to kozupeptins<sup>[47]</sup>

## 2-6. Conclusion

In conclusion, kozupeptins A and B (**1a**, **1b**), new potent antimalarial agents, were isolated from the culture broths of *Paracamarosporium* sp. FKI-7019. An efficient total synthesis of kozupeptin A (**1a**) has been achieved in a practical manner, which confirmed the structure proposed by spectroscopic and chemical techniques and elucidated the absolute configuration of the molecule. It also illustrates the power of an LPPS-based method utilizing a hydrophobic anchor molecule, a concept that can take advantage of the characteristics of both conventional LPPS and SPPS. Kozupeptin A (**1a**) and synthetic intermediates were found to exhibit *in vitro* and *in vivo* antimalarial activity, which showed promise for development of a new antimalarial agent.

## **Chapter 3**

# **Synthesis of the Antimalarial Peptide Aldehyde, a Precursor of Kozupeptin A, Utilizing a Newly Designed Hydrophobic Anchor Molecule**

**ABSTRACT:** In this chapter, I describe an efficient method of synthesizing highly bioactive peptide aldehydes without any concern about epimerization by liquid-phase peptide synthesis (LPPS) through the use of newly designed hydrophobic anchor molecules. Peptide elongation reactions effectively proceeded in less polar solvents, and direct crystallization by the addition of polar solvents enabled easy purification. This method also represents a new concept for efficient synthesis of peptide derivatives. The development of new antimalarial drug candidates will be accelerated using this methodology.

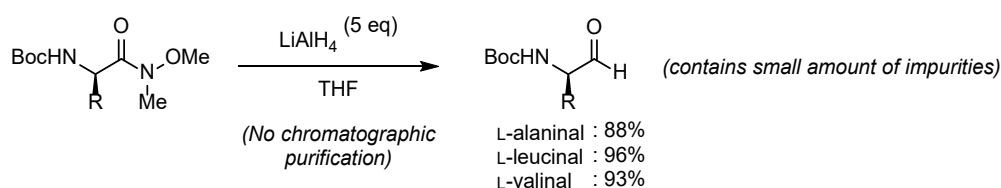
## 2-1. Introduction

As the mainstream modalities of drug discovery shift from small molecules to biological entities, an increasing number of peptide-based drugs and drug candidates have been developed in recent years.<sup>[7-10]</sup> This trend increases the requirement for improvements in peptide synthesis. Among various peptide derivatives, peptide aldehydes stand out because they have been showing inhibitory properties against various proteases,<sup>[48]</sup> probably due to the tetrahedral hydrates of the C-terminal aldehyde function that mimics the transition state of the substrate during hydrolysis by enzymes.<sup>[48b, 49]</sup>

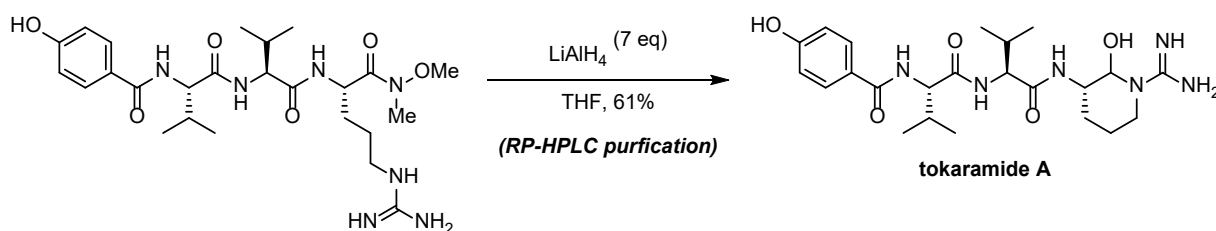
Synthetic methods of peptide aldehydes are classified into two categories.<sup>[50]</sup> The first consists of the prior synthesis of a peptide intermediate, followed by the introduction of aldehyde function by oxidation or reduction. The second strategy uses protected  $\alpha$ -amino aldehydes as starting materials. Among them all, the late-stage reduction of Weinreb amides is the most widely used, but reaction and purification conditions largely depend on the amino acid sequence of the peptide, which sometimes takes a lot of effort (**Scheme 9a, b**).<sup>[45, 51a,b]</sup> This strategy is also applied to solid-phase peptide synthesis (SPPS), which is suitable for the initial derivative synthesis for drug discovery but has not shown satisfactory efficiency for large-scale synthesis because of relatively low yield and intrinsic difficulty in scale-up of solid-phase reaction. (**Scheme 10a, b**)<sup>[51c-e]</sup>

Liquid-phase peptide synthesis (LPPS) utilizing a hydrophobic anchor molecule, which can combine the best characteristics of conventional LPPS with the benefits of SPPS, could become more effective option. As described in “Peptide synthesis” section of **Chapter 1**, despite the prominent use of this methodology, it was met with limited strategic use and there has been no report detailing an efficient synthesis of peptide aldehydes.

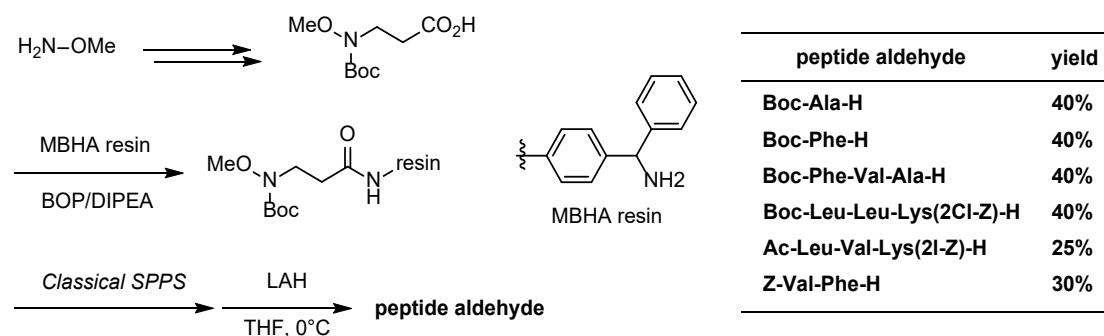
**Scheme 9a.** Synthesis of optically active  $\alpha$ -(Boc-amino)aldehydes from  $\alpha$ -amino acids via Weinreb amides<sup>[51a]</sup>



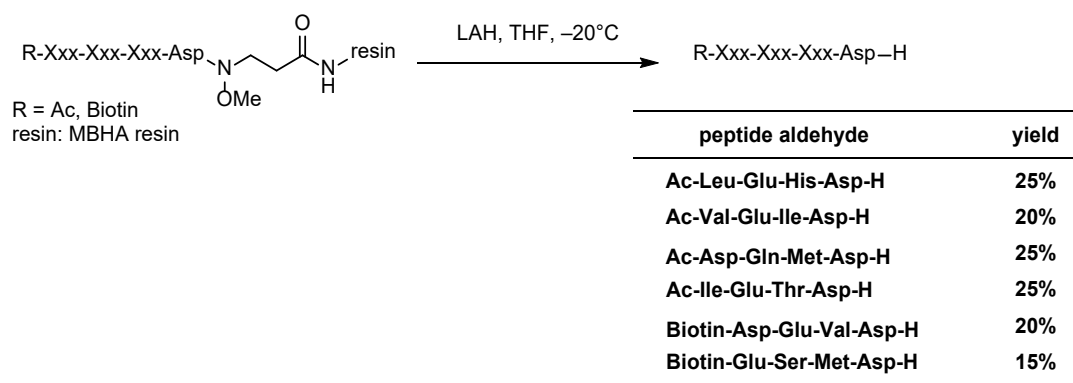
**Scheme 9b.** LPPS of tokaramide A (needs reverse-phase HPLC purification)<sup>[51b]</sup>



**Scheme 10a.** SPPS of C-terminal peptide aldehydes<sup>[51d]</sup>



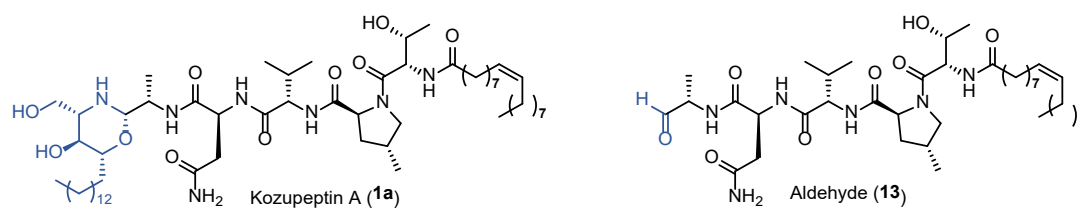
**Scheme 10b.** SPPS of aspartyl peptide aldehydes<sup>[51e]</sup>



In **Chapter 2**, I applied this practical LPPS method for the first total synthesis of kozupeptin A (**1a**), a potent antimalarial lipopeptide isolated through our antimalarial activity-guided screening program of microbial metabolites. The first total synthesis consisted of two parts (**Scheme 8** in **Chapter 2**). One was the synthesis of peptide and fatty acid units by the above described LPPS, utilizing a fluorene-type anchor molecule.<sup>[20a]</sup> The other was the following transformation of the C-terminal by classical organic synthesis in the liquid phase. The anchor deprotected C-terminal carboxylic acid was converted to the Weinreb amide using a condensation reagent and the following reduction gave the C-terminal aldehyde. This was the typical method to get a peptide aldehyde, as described above, but in my case, although it was eventually suppressed to an acceptable level by the screening of condensation reagents, epimerization of the  $\alpha$ -position of the C-terminal amino acid became a problem (**Table 4** in **Chapter 2**). Four steps were needed from the latest anchor-supported intermediate to **1a**. After having accomplished the total synthesis, the intermediates in the late stage were evaluated for *in vitro* antimalarial activity, which revealed that the aldehyde **13**, the precursor of **1a**, exhibited much stronger antimalarial activity than **1a** itself against both a chloroquine-resistant K1 strain and a chloroquine-sensitive FCR3 strain (**Figure 20**).

On the basis of this result and the potential of peptide aldehydes as drug candidates, I started to work on the development of a more efficient method to synthesize a peptide having a C-terminal aldehyde. Herein, I report the design of new hydrophobic anchor molecules that enable practical LPPS to directly afford peptide aldehydes, without any concern for epimerization, and its application for a more effective synthesis of peptide

derivatives.



compound	IC <sub>50</sub> (μM)		
	antimalarial activity		cytotoxicity
	K1 strain <sup>[a]</sup>	FCR3 strain <sup>[b]</sup>	MRC-5
<b>1a</b> (natural)	0.15	0.29	>23
<b>13</b> <sup>[c]</sup>	0.0083	0.013	>32
chloroquine <sup>[d]</sup>	0.17	0.038	58 <sup>[e]</sup>
artemisinin <sup>[d]</sup>	0.019	0.023	160 <sup>[e]</sup>

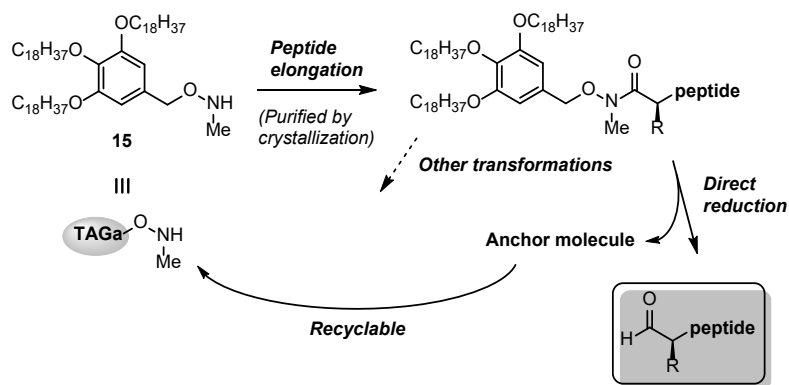
[a] Chloroquine-resistant strain. [b] Chloroquine-sensitive strain.  
 [c] Purified by silica gel column chromatography for the evaluation.  
 [d] Drugs commonly used to treat malaria. [e] *J. Antibiot.* **2011**, *64*, 183.

**Figure 20.** Kozupeptin A (**1a**) and the precursor aldehyde (**13**)

### 3-2. Design and preparation of a new hydrophobic anchor molecule

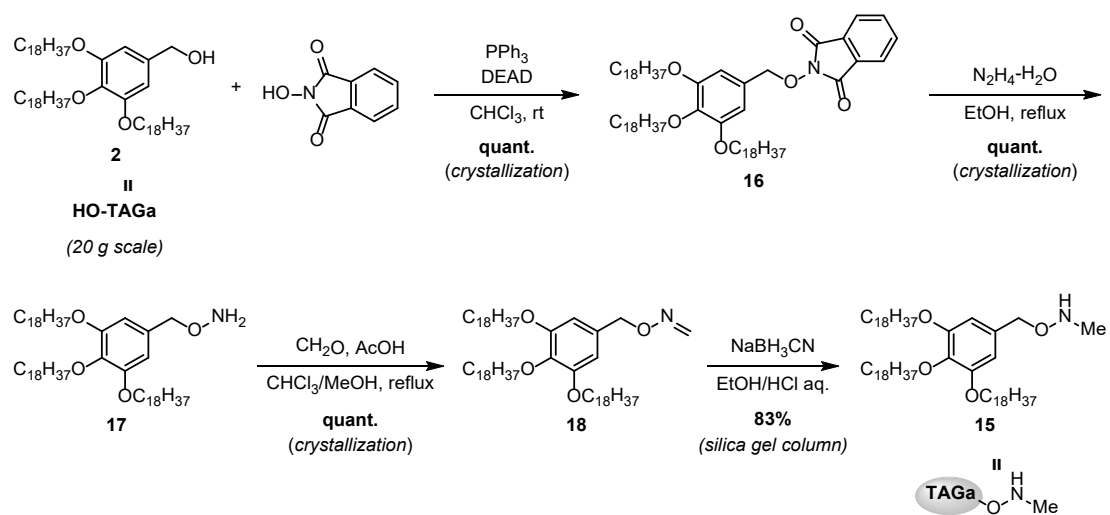
To realize a desired synthetic method, I came up with a new hydrophobic anchor molecule designed to change the anchor-peptide bond which had been an ester structure<sup>[17-20]</sup> to a benzyloxy methyl amide structure (Weinreb amide-type bond) (**Scheme 11**). More specifically, the use of a long-chain alkyl-supported benzyloxy methyl amine **15** as a hydrophobic anchor molecule would enable an efficient LPPS to give the benzyloxy methyl amide structure (Weinreb amide-type structure). The resulting anchor-supported peptide amide would be simultaneously deprotected and reduced to the peptide aldehyde without epimerization using a hydride reductant. The efficiency of reduction in an LPPS method is, in general, higher than in an SPPS method due to the homogeneous system. Other benefits, such as the more stable characteristics of the amide bond under peptide elongation conditions<sup>[52]</sup> and synthetic possibilities for other derivatives such as ketones,<sup>[45]</sup> are expected. Furthermore, the anchor molecule could be directly recycled after the reduction, which would solve the problem of the LPPS method using hydrophobic anchor molecules with poor atom economy.

**Scheme 11.** Design of a new hydrophobic anchor molecule



The designed anchor molecule **15** was readily prepared from HO-TAGa (**2**),<sup>[17]</sup> a known simple anchor molecule that can be easily synthesized from methyl gallate, a commercially available cheap material (**Scheme 12**). Introduction of *N*-hydroxyphthalimide by Mitsunobu reaction, hydrolysis, and reductive amination using formaldehyde gave the target compound **15**.

**Scheme 12.** Synthesis of a new designed hydrophobic anchor molecule



### **3-3. Peptide elongation utilizing a newly designed hydrophobic anchor molecule**

Using the newly designed and prepared anchor molecule, the synthesis of the peptide with oleic acid composing kozupeptin A (**1a**) was effectively accomplished (**Scheme 13**). Every reaction proceeded efficiently with small excess of reagents in less polar solvent such as DCM or CHCl<sub>3</sub>, and the direct addition of polar solvent MeOH to the reaction mixture enabled the easy purification of each intermediate by crystallization (During the deprotection of the Fmoc group of Asn, the release of the anchor molecule described in **Scheme 7, Chapter 2**, was completely suppressed using 1% DBU/1% piperidine conditions). Finally, **24**, having all the required amino acid residues and fatty acid units, was obtained almost quantitatively without any epimerization from the designed anchor molecule **15**.



### 3-4. Reduction to the aldehyde

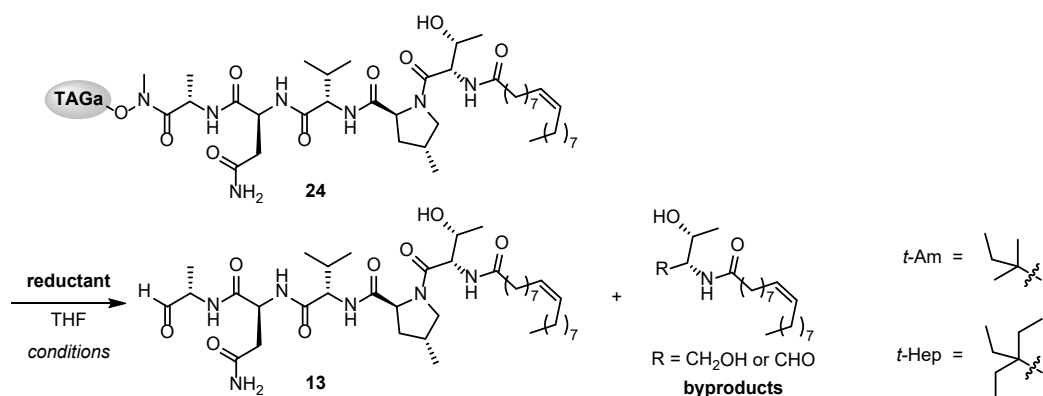
Next, the key reduction of the Weinreb amide-type moiety was examined (**Table 8**). The use of lithium aluminum hydride (LAH), under the same conditions as in the first total synthesis, afforded the desired aldehyde **13** without epimerization, as expected, although the yield was 42% (entry 1). The starting material **24** was fully consumed, and the main side reaction proved to be the reduction of the Thr-4-MePro amide bond (aldehyde and alcohol as the byproducts). It is known that tertiary amides, especially the ones with cyclic amines, can be used as alternatives for the Weinreb amide.<sup>[53]</sup> In addition, the hydroxyl proton of Thr could additionally activate the amide group by hydrogen bonding in this peptide. After the screening of several reductants, lithium tri-*t*-butoxyaluminum hydride (LiAlH(*Ot*-Bu)<sub>3</sub>)<sup>[54]</sup> was found to give the desired peptide aldehyde **13** in 63% yield and an undesired Thr-4-MePro amide bond-cleaved alcohol in 20% yield (entry 3). The use of the reductants having a bulkier alkoxy group such as *Ot*-Am or *Ot*-Hep did not improve the yield (entries 4, 5). Hydride art complexes seemed to be suitable for this reduction. Diisobutylaluminum hydride (DIBAL), which has Lewis acidity due to the aluminum's vacant orbital, did not afford the desired compound **13** at all (entry 6), probably due to high chelation ability of many hetero atoms of the substrate **24**. The use of borane reductants did not give the target aldehyde **13** or improve the yield (entries 7, 8 and 9).

Under the conditions of entry 3, the benzyloxy methyl amine anchor molecule **15** was recovered quantitatively in its hydrogen chloride salt form with high purity, just after aq. HCl quenching and direct crystallization (see **Experimental Section** for details). This reusability of the anchor molecule could eliminate the disadvantage of poor atom economy in the hydrophobic anchor-supported LPPS method.

Incidentally, peptide aldehyde **13** was converted to kozupeptin A (**1a**) in 95% yield by the same procedure described previously (stirring with 1.2 equiv of phytosphingosine in CHCl<sub>3</sub> at room temperature).

I believe that the anchor molecule developed here would offer a highly efficient method suitable for scale-up to synthesize a peptide with a C-terminal aldehyde. Although the yield of peptide aldehyde was moderate, as for kozupeptin A's precursor, when a model anchor-supported substrate **25** without a Thr-Pro amide bond was used, the target aldehyde **26** was obtained in high yield under conditions using LiAlH<sub>4</sub> (**Scheme 14**). Furthermore, it was also converted to methyl ketone **27** using MeLi as a nucleophile, as is the case with usual Weinreb amides (**Scheme 14**).

**Table 8.** Screening of reductants

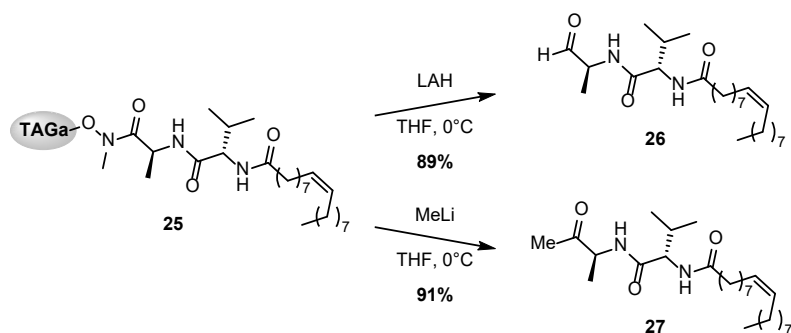


entry	reductant (equivalent)	temperature	isolated (%)	yield	note
1	LAH (1.8 eq)	0°C	42		Full conversion. <b>Byproducts</b> were obtained together in 20-30% yield.
2	Red-Al <sup>®</sup> (9.0 eq)	0°C	37		Full conversion. <b>Byproducts</b> were obtained together in 20-30% yield.
3	LiAlH(O <i>t</i> -Bu) <sub>3</sub> (10 eq)	rt	63		850 mg of substrate <b>24</b> was used. Full conversion. <b>Byproduct</b> alcohol was obtained in 20% yield.
4*	LiAlH(O <i>t</i> -Am) <sub>3</sub> (10 eq)	rt	62		Full conversion. <b>Byproduct</b> alcohol was obtained in around 20% yield.
5*	LiAlH(O <i>t</i> -Hep) <sub>3</sub> (10 eq)	rt	58		Full conversion. <b>Byproduct</b> alcohol was obtained in around 20% yield.
6	DIBAL (10 eq)	-78°C to rt	not obtained		No reaction at -78°C, decomposition at rt.
7	LiBH <sub>4</sub> (4.0 eq)	rt	trace		<b>Byproduct</b> alcohol was observed as a major product in TLC analysis.
8	K-selectride <sup>®</sup> (30 eq)	rt to 40°C	not obtained		No reaction at rt, decomposition at 40°C.
9	LiBHEt <sub>3</sub> (7.0 eq)	0°C	38		Full conversion. <b>Byproducts</b> were obtained together in 20-30% yield.

Unless noted, 40.0 or 50.0 mg of **24** in THF (0.01 M) was used.

\*Prepared by the procedure described in the literature.<sup>[53]</sup>

**Scheme 14.** Use of a model substrate without Thr-Pro amide bond



### 3-5. Application to rapid analog synthesis

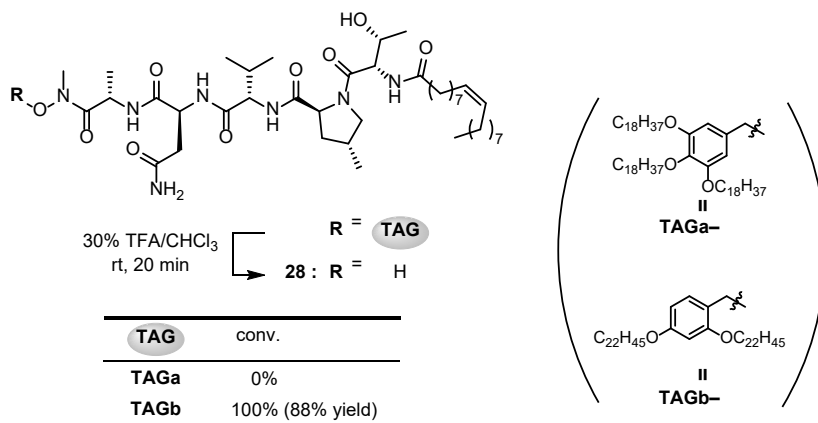
The further application of this new anchor molecule toward more efficient derivative synthesis was successfully demonstrated in the transformation to hydroxamic acid (**Scheme 15**). Although the TAGa benzyl group that had been used tolerated 30% TFA/CHCl<sub>3</sub>/rt conditions, the TAGb benzyl group, known to be a less stable function under acid conditions,<sup>[18a]</sup> was quickly cleaved to afford the desired compound **28** (**Scheme 15a**, the details of the preparation of TAGb-type anchor molecule is shown in **Experimental Section**). This means that deprotection of the anchor molecules can be fully controlled by choosing the suitable TAG.

I herein propose a strategy to accelerate the synthesis of peptide derivatives utilizing these characteristics (**Scheme 15b**). In general, conventional LPPS is unsuitable for divergent synthesis due to the difficulty of separation between peptides having similar properties. Using my LPPS system, the following economical procedure is assumed: (1) peptide intermediates having different TAGs are synthesized in separate flasks, (2) the intermediates are mixed and the peptide elongation is performed in a single flask, which can reduce the number of reactions and flasks, (3) the anchors can be selectively deprotected under acid conditions and the peptides will be separated by crystallization and filtration, and (4) each obtained peptide intermediate can be individually subjected to the next reaction (e.g., reduction to aldehyde). This looks like a combination of split-and-pool method and parallel method in combinatorial chemistry, which could accelerate derivative synthesis for medicinal chemistry.

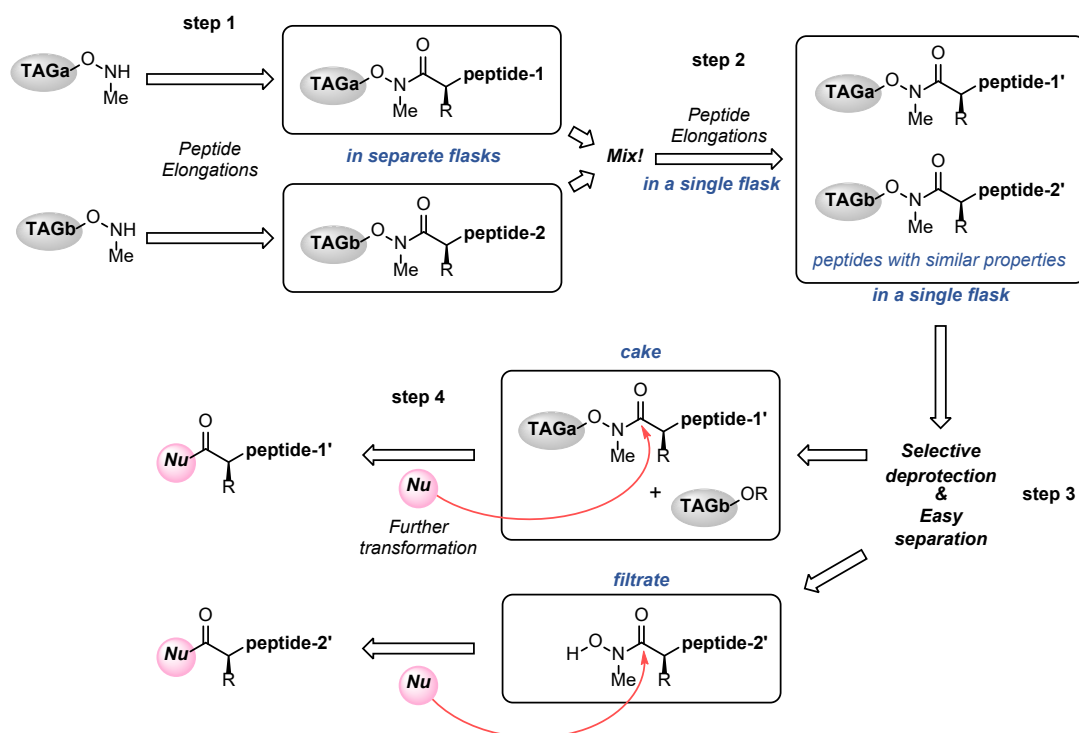
As an initial model experiment, the separation and the following reduction of two peptides having very similar structures from a single flask was demonstrated (**Scheme 15c**). Two peptide aldehydes (**31** and **13**, stearic acid and oleic acid), which could not be separated by the usual crystallization or silica gel chromatography, were, respectively, obtained as pure forms by easy operations from two mixed anchor-supported peptides (**29** and **30**) in a single flask. The deprotection of benzyl TAG was performed with complete selectivity, and the reaction mixture was directly subjected to crystallization. The obtained cake and filtrate were easily purified by silica gel chromatography to afford the corresponding target intermediates (**29** and **28**) in high yields. Afterward, each amide group was reduced to give the target peptide aldehydes **31** and **13**.

**Scheme 15.** Application of orthogonal tags to rapid analog synthesis

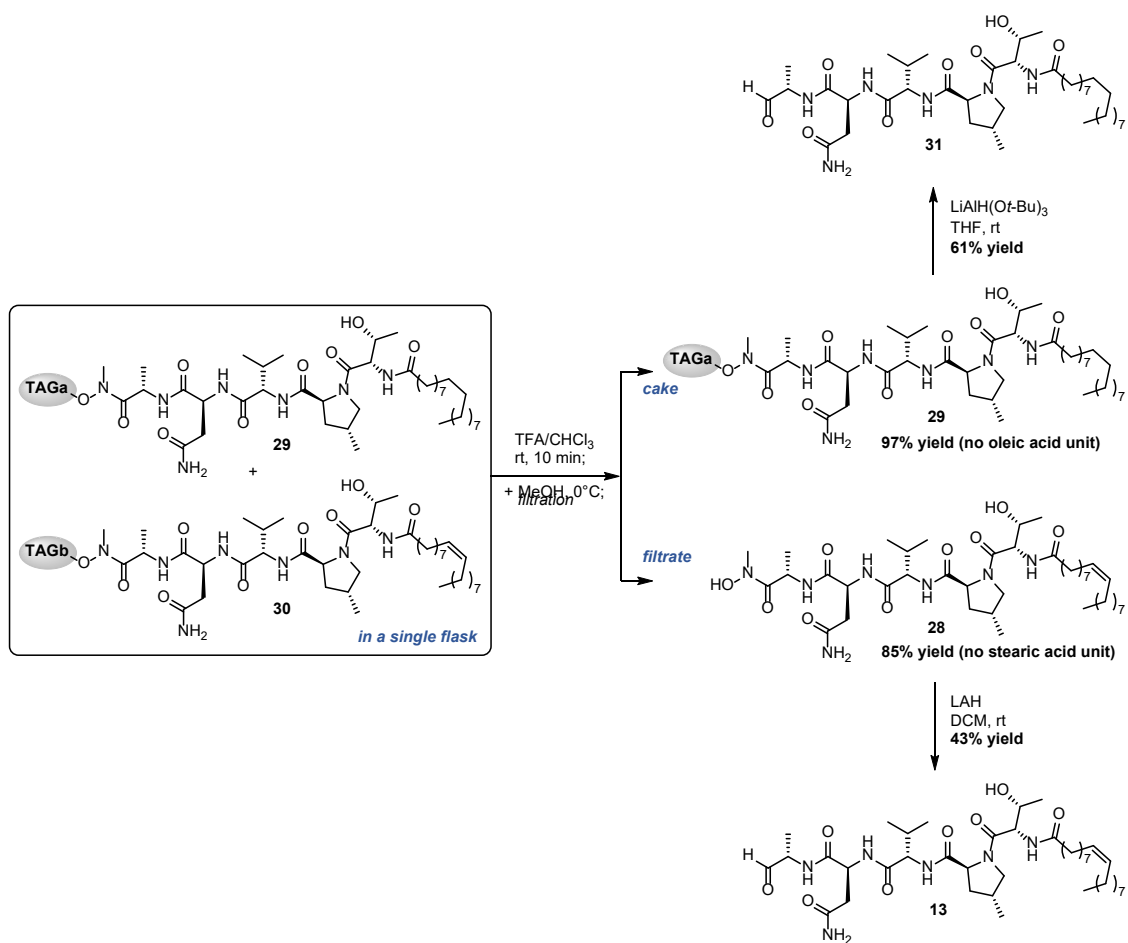
**a) Selective deprotection of TAGs in acid conditions**



**b) Concept of this application**



### c) Initial model experiment



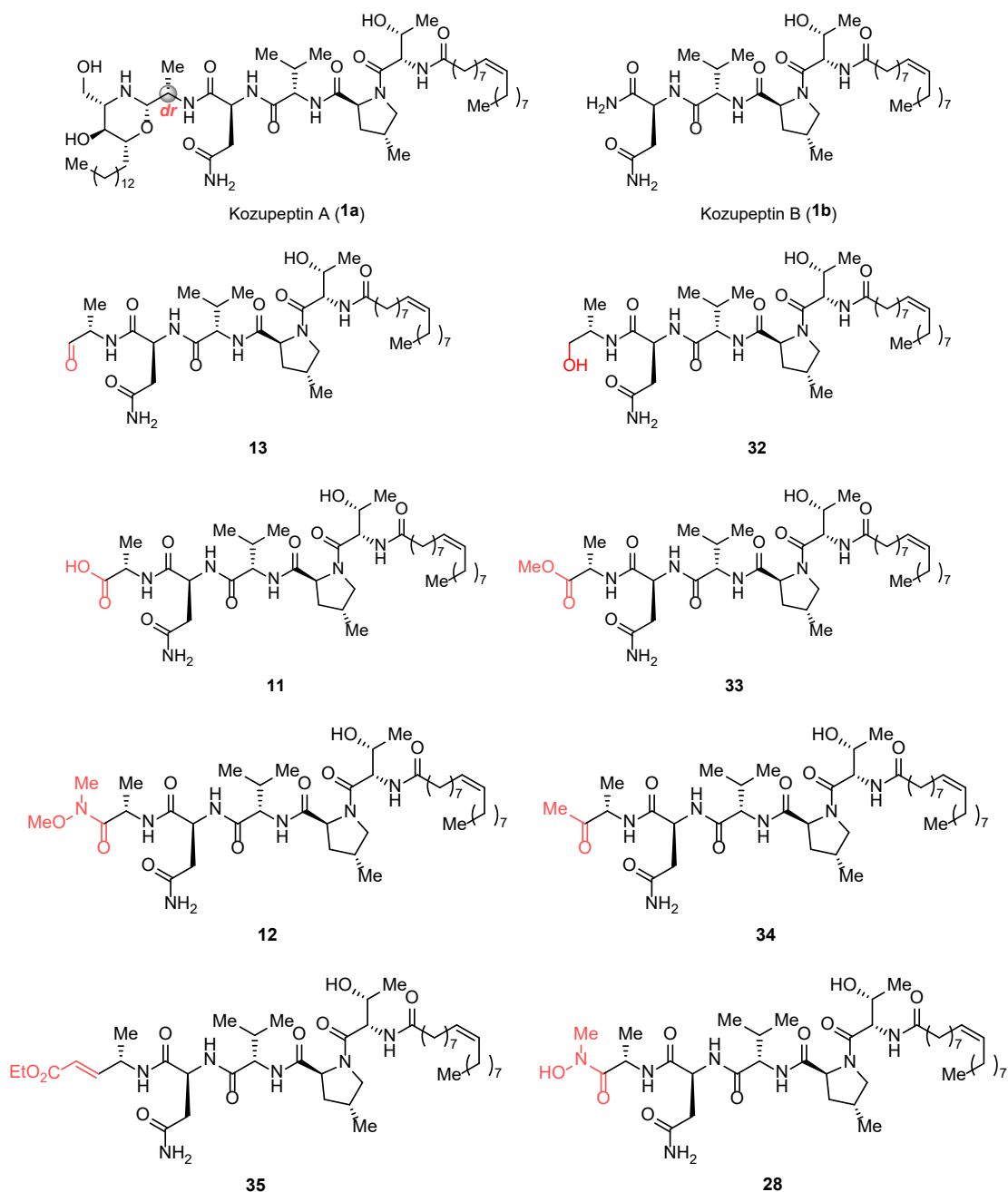
### **3-6. Conclusion**

In summary, I have realized a highly efficient method to synthesize peptide aldehydes and have shown a probable application to derivative synthesis by LPPS utilizing newly designed hydrophobic anchor molecules. This methodology will certainly improve and expand the field of peptide synthesis, whose significance is increasing more and more. It will also accelerate our program for the development of new antimalarial drug candidates.

**Chapter 4**  
**Synthesis of Analogs and Evaluation of**  
**Antimalarial Activity *in vitro***

Based on the synthetic routes established in **Chapters 2** and **3** using hydrophobic anchor molecules, various derivatives of kozupeptins were synthesized and their antimalarial activity against chloroquine-resistant and -sensitive *P. falciparum* strains (K1 and FCR3 respectively) and cytotoxicity against a human lung fibroblast cell line MRC-5 were evaluated (See **Experimental Section** for synthetic details).<sup>[37a]</sup> The results were shown in **Table 9**.

**Table 9.** *In vitro* evaluation of derivatives





entry	compound	IC <sub>50</sub> (μg/ml)			
		antimalarial activity		cytotoxicity	selectivity index
		K1 <sup>[a]</sup>	FCR3 <sup>[b]</sup>	MRC-5	MRC-5/K1
1	<b>1a</b> (natural)	0.16	0.31	>25	>156
2	<b>1b</b> (natural)	0.71	1.01	>25	>35
3	<b>1a</b> (synthetic, single)	0.32	0.58	>25	>78
4	<b>1a</b> (synthetic, dr=62/38)	0.14	0.18	>25	>178
5	<b>13</b>	0.0063	0.010	>25	>3,968
6	<b>32</b>	1.08	2.20	>25	>23
7	<b>11</b>	>12.5	N/A	>25	N/A
8	<b>33</b>	>12.5	N/A	>25	N/A
9	<b>12</b>	5.98	N/A	>25	>4
10	<b>34</b>	4.20	N/A	>25	>5
11	<b>35</b>	1.09	1.43	>25	>22
12	<b>28</b>	10.0	9.76	>25	>2
13	<b>36</b>	1.49	2.46	>25	>17
14	<b>37</b>	1.20	2.32	>25	>21
15	<b>31</b>	0.098	0.13	>12.5	>128
16	<b>38</b>	0.31	0.45	>6.25	>20
17	<b>39</b>	>12.5	N/A	>25	N/A
18	<b>40</b>	10.4	10.8	>12.5	>1.2
19	<b>41</b>	0.33	0.46	>25	>75
20	<b>42</b>	2.50	3.59	>25	>10
21	<b>43</b>	0.020	0.020	4.21	210
22	<b>44</b>	0.072	0.075	>25	>347
23	<b>45</b>	0.53	1.13	>25	>47
24	<b>46</b>	3.08	7.22	>12.5	>4
25	<b>47</b>	>12.5	N/A	>25	N/A
26	chloroquine <sup>[c]</sup>	0.18	0.015	18,570 <sup>[d]</sup>	101
27	artemisinin <sup>[c]</sup>	0.0057	0.0060	45,170 <sup>[d]</sup>	7,925

N/A: Not available.

[a] Chloroquine-resistant strain. [b] Chloroquine-sensitive strain. [c] Drugs commonly used to treat malaria.

[d] *J. Antibiot.* **2011**, *64*, 183. N/A: Not available.

As described in **Chapter 2**, we found that synthetic kozupeptin A (**1a**) showed a similar IC<sub>50</sub> value to that of natural **1a** (entries 1 and 2). The result of entry 4 shows that the stereochemistry of the α-position of the C-terminal alaninal did not significantly affect antimalarial activity. As for the C-terminal, it was found that the aldehyde form showed extremely strong antimalarial activity and other functional groups showed much weaker activity (entries 5~12). The *N,O*-acetal structure of kozupeptin A (**1a**) is an equivalent that produces

the aldehyde when hydrolyzed, which means that kazupeptin A (**1a**) would act as a prodrug. From the results of entries 13 to 18, it was found that the antimalarial activity was the strongest when the *N*-terminal fatty acid was oleic acid, and the activity drastically decreased when the alkyl chain became shorter. These results indicate that, for exhibiting antimalarial activity, a certain or more lipophilic site might be needed to ensure membrane permeability. As for the peptide unit, while the 4-methyl group of Pro and the free hydroxyl group of Thr proved to be important for antiparasitic activity, the stereochemistry of alaninal and the amide group of Asn were found not to significantly affect bioactivity (entries 4, 19~24). Finally, the overall amino acid sequence seems to be important for antimalarial activity because an analog which has only two amino acids showed no bioactivity (entry 25). The current findings are summarized in **Figure 21**.

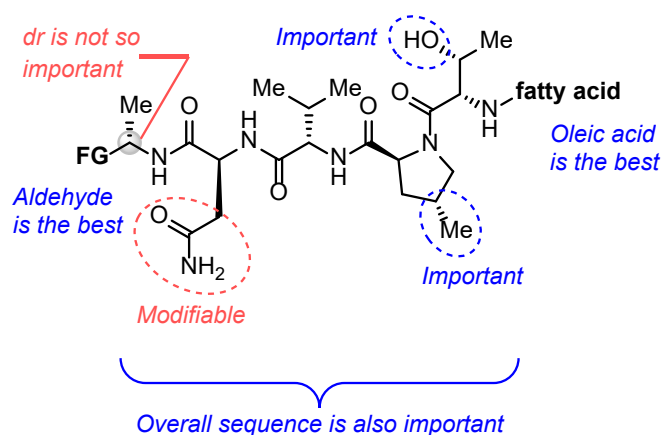
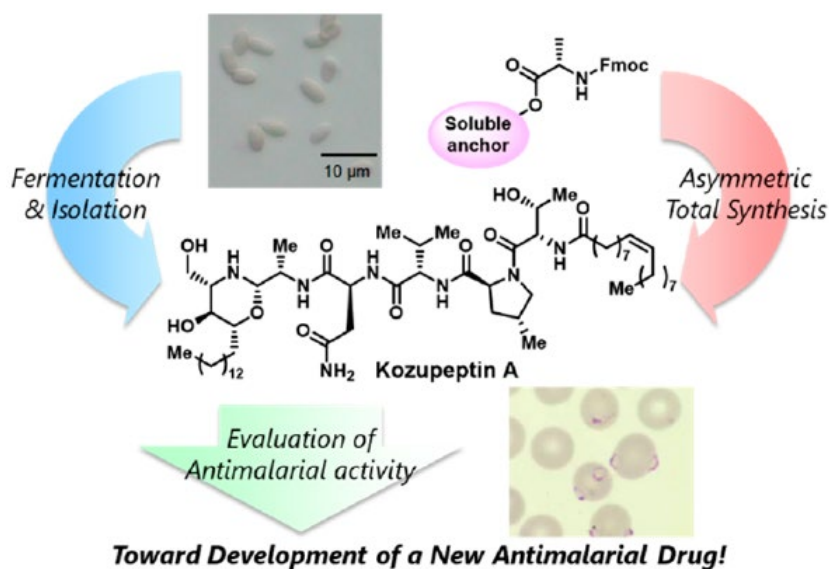


**Figure 21.** Current findings by structure-activity relationships (SARs) study

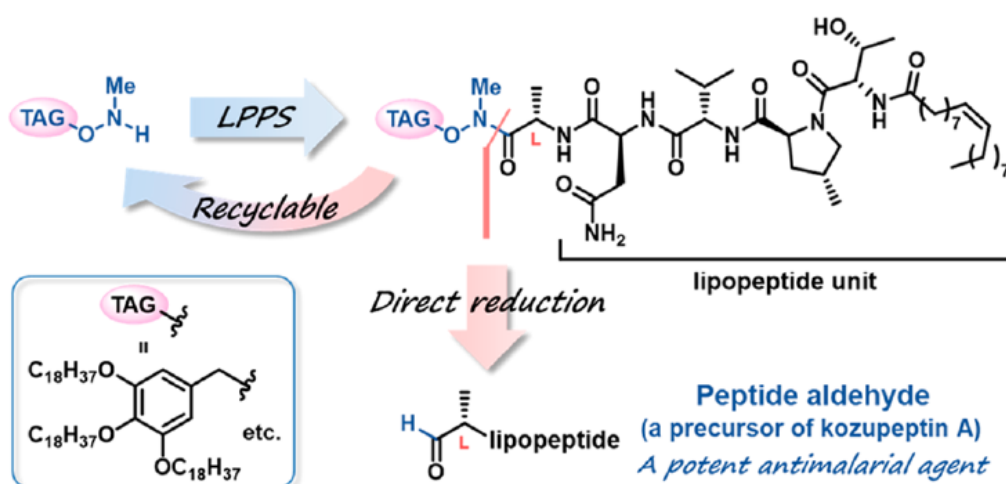
# **Chapter 5**

## **Summary**

In **Chapter 2**, an antimalarial activity-guided screening program from the fermentation broths of our microorganism library led us to focus on a fungal strain, *Paracamarosporium* sp. FKI-7019 isolated from the soil around a plant in Kozu-Island, Tokyo, Japan. Two novel antimalarial lipopeptides, named kozupeptins A and B, were isolated from the culture broths of the above strain. They exhibited potent antimalarial activity against chloroquine-sensitive and -resistant *Plasmodium falciparum* strains *in vitro*. Furthermore, they showed low cytotoxicity against human MRC-5 cells. The structural elucidation, including the absolute configuration of the new molecules, was accomplished by a combination of spectroscopic analyses and chemical approaches including a total synthesis of kozupeptin A. Newly established total synthesis, in which the peptide and fatty acid units were synthesized by liquid-phase peptide synthesis utilizing a hydrophobic anchor molecule that enabled simple purification by crystallization proved to be practical. Synthetic kozupeptin A demonstrated a therapeutic effect *in vivo* and the precursor aldehyde was found to exhibit much stronger antimalarial activity than kozupeptin A itself *in vitro* and *in vivo*, which showed promise for the development of a new antimalarial drug.



In **Chapter 3**, I have developed an efficient method of synthesizing highly bioactive peptide aldehydes without any concern about epimerization by liquid-phase peptide synthesis through the use of newly designed hydrophobic anchor molecules. Peptide elongation reactions effectively proceeded in less polar solvents, and direct crystallization by the addition of polar solvents enabled easy purification. This method also represents a new concept for the efficient synthesis of peptide derivatives. The development of new antimalarial drug candidates will be accelerated using this methodology.



In **Chapter 4**, the structure-activity relationships (SARs) of kozozeptins and synthetic analogs were investigated, which have shown the importance of the C-terminal aldehyde, the kind of fatty acid unit, the 4-methyl group of Pro, the free hydroxyl group of Thr, and the overall amino acid sequence for exhibiting potent antimalarial activity.

Further investigations, including more SARs study and the mode of action (MOA) study, are in progress for development of a new antimalarial drug candidate.

## **Experimental Section**

## Table of Contents for Experimental Section

<b>Table of Contents for Experimental Section</b>	65
<b>General Remarks</b>	66
<b>Supporting Information for Chapter 2</b>	67
1. Taxonomy of the Producing Strain	67
2. Fermentation and Isolation	67
3. Assay of Antimalarial Activity <i>in vitro</i> and <i>in vivo</i>	68
4. Advanced Marfey's Analysis	69
5. Identification of the fatty acid	70
6. Total Synthesis -Experimental Procedures and Compounds Characterization-	71
<b>Supporting Information for Chapter 3</b>	81
1. Preparation of newly designed anchor molecules	81
2. Peptide elongations	85
3. Reduction to afford the aldehyde	92
4. Application of orthogonal TAGs to rapid analog synthesis	97
<b>Supporting Information for Chapter 4</b>	107
1. Syntheses of kozupeptins' analogs	107
<b>IR and NMR Spectra of Compounds</b>	115
1. IR and NMR Spectra of Compounds in <b>Chapter 2</b>	115
2. NMR Spectra of Compounds in <b>Chapter 3</b>	173
3. NMR Spectra of Compounds in <b>Chapter 4</b>	259

## General Remarks

Infrared (IR) spectra were recorded on a Horiba FT-210 spectrometer. UV spectra were measured with a Beckman DU640 spectrophotometer. NMR spectra were measured on an Agilent XL-400 spectrometer with  $^1\text{H}$  NMR at 400 MHz and  $^{13}\text{C}$  NMR at 100 MHz, a JEOL JNM-ECA-500 spectrometer with  $^1\text{H}$  NMR at 500 MHz and  $^{13}\text{C}$  NMR at 125 MHz, or an Agilent Inova 600 spectrometer with  $^1\text{H}$  NMR at 600 MHz and  $^{13}\text{C}$  NMR at 150 MHz. Chemical shifts were reported in ppm from the internal solvent peaks for  $\text{CDCl}_3$  ( $^1\text{H}$ ;  $\delta = 7.26$  ppm,  $^{13}\text{C}$ ;  $\delta = 77.16$  ppm),  $(\text{CD}_3)_2\text{SO}$  ( $^1\text{H}$ ;  $\delta = 2.50$  ppm,  $^{13}\text{C}$ ;  $\delta = 39.52$  ppm), or  $\text{CD}_3\text{OD}$  ( $^1\text{H}$  of  $\text{CH}_3$ ;  $\delta = 3.34$  ppm,  $^{13}\text{C}$ ;  $\delta = 49.86$  ppm).  $^1\text{H}$  NMR data were reported as follows: chemical shift (integration, multiplicity (s = singlet, d = doublet, t = triplet, q = quartet, m = multiplet, br = broad, app = apparent), coupling constants (Hz)). Liquid chromatography-electrospray ionization-tandem mass spectrometry (LC/MS/MS) was performed on an AB Sciex QSTAR Hybrid LC/MS/MS using MeOH solvent system containing 0.1% formic acid. Liquid chromatography-electrospray ionization mass spectrometry (LC/MS) was performed on a Waters AQUITY UPLC H-Class using MeOH solvent system containing 0.05% formic acid. The high-resolution mass spectra (HRMS) were performed on a JEOL JMS-AX505 HA, a JEOL JMS-700 MStation, or a JEOL JMS-T100LP. Optical rotations were measured on a JASCO P-1010 polarimeter. Melting points were measured on a Stanford Research Systems OptiMelt MPA100 apparatus.

For thin layer chromatography (TLC) analysis, Merck precoated TLC plates (silica gel 60 GF254, 0.25 mm) were used. Flash chromatography was carried out with Kanto Chemical silica gel (silica gel 60N, spherical neutral, 0.040–0.050 mm) or Fuji Silysia silica gel (FL60D, avg. 0.060 mm). For purification with preparative thin layer chromatography (PLC), Merck precoated PLC plates (silica gel 60 GF254, 0.5 mm) were used.

Unless otherwise noted, reagents and solvents were commercially available and used without further purification. In experiments requiring dry solvents, dichloromethane (DCM) and tetrahydrofuran (THF) were purchased from Kanto Chemical Co. Inc. as “Dehydrated.” For Fmoc-protected amino acids, Fmoc-Ala-OH, Fmoc-Asn-OH, Fmoc-Val-OH, and Fmoc-Thr-OH $\cdot$ H $_2$ O were purchased from Watanabe Chemical Industries, Ltd. Fmoc-(2*S*, 4*R*)-4-MePro-OH was prepared by the procedure described in the literature.<sup>[55]</sup>

## Supporting Information for Chapter 2

### 1. Taxonomy of the Producing Strain

An antimalarial screening program from the fermentation broths of our microorganism library led us to focus on a fungal strain, *Paracamarosporium* sp. FKI-7019 isolated from the soil around a plant in Kozu-Island, Tokyo, Japan. The photos of the plant and the fungal strain were shown **Figure 22**.



**Figure 22.** The plant (left) and the isolated fungus *Paracamarosporium* sp. FKI-7019 (right)

The producing fungal strain FKI-7019 was identified with the genus *Paracamarosporium* based on its morphology and the internal transcribed spacer of ribosomal RNA gene sequence. We will report taxonomic details elsewhere.

### 2. Fermentation and Isolation

Fermentation and isolation were performed for six times (Lot 1–6). From Lot 1, kozupeptin A (**1a**) was isolated. From Lot 2–6, kozupeptin B (**1b**) was obtained. Described below is the representative procedure.

Strain FKI-7019, isolated from soil around a plant on Kozu-Island, Tokyo, Japan, was grown and maintained on an agar slant consisting of 0.1% glycerol, 0.08%  $\text{KH}_2\text{PO}_4$ , 0.02%  $\text{K}_2\text{HPO}_4$ , 0.02%  $\text{MgSO}_4 \cdot 7\text{H}_2\text{O}$ , 0.02% KCl, 0.2%  $\text{NaNO}_3$ , 0.02% yeast extract and 1.5% agar (adjusted to pH 6.0 before sterilization). A loopful of spores of the strain was inoculated into 100 mL of the seed medium consisting of 2.0% glucose, 0.5% Polypepton (Nihon Pharmaceutical Co., Japan), 0.2% yeast extract, 0.2%  $\text{KH}_2\text{PO}_4$ , 0.05%  $\text{MgSO}_4 \cdot 7\text{H}_2\text{O}$  and 0.1% agar (adjusted to pH 6.0 before sterilization) in each of two 500 mL-Erlenmeyer flasks. The flasks were incubated on a rotary shaker (210 rpm) at 27°C for 3 days. For production of kozupeptins A or B (**1a**, **1b**), 1 mL of seed culture was transferred to 30 (Lot 1) or 60 (Lot 3) 500 mL-Erlenmeyer flasks containing 100 mL of production medium (3.0% soluble starch, 1.0% glycerol, 2.0% soybean meal, 0.3% dry yeast, 0.3% KCl, 0.3%  $\text{CaCO}_3$ , 0.05%  $\text{MgSO}_4 \cdot 7\text{H}_2\text{O}$  and 0.05%  $\text{KH}_2\text{PO}_4$  (adjusted to pH 6.0 before sterilization)) and fermentation was carried out on a rotary shaker (210 rpm) at 27°C for 4 days.

The isolation procedure for kozupeptin A (**1a**) is summarized in **Scheme 5** in **Chapter 2**. The above fermentation broth (Lot 1) was diluted with one equivalent volume of ethanol (3.0 L) and centrifuged. The

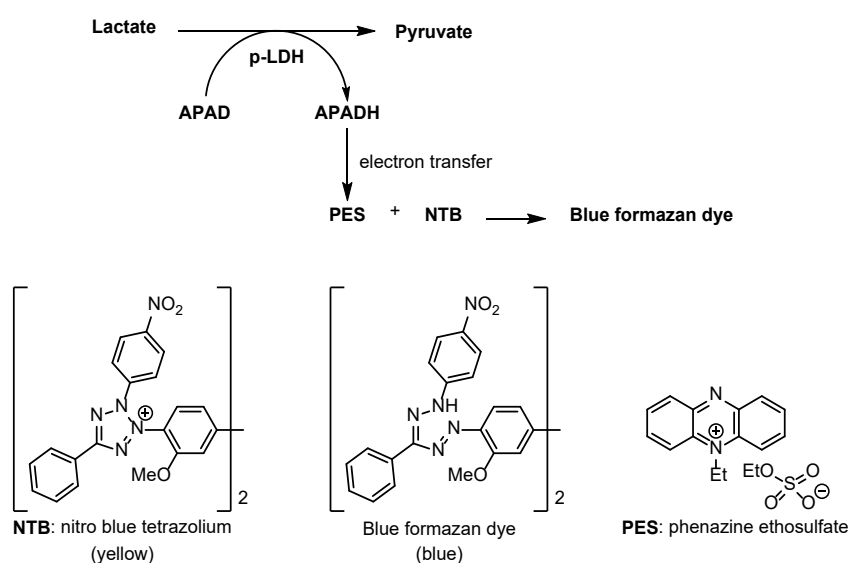
supernatant was concentrated *in vacuo* to remove ethanol. The remaining aqueous solution was extracted with ethyl acetate (3 L×3), and the organic layer was concentrated *in vacuo* to dryness. The ethyl acetate extract was applied to a silica gel column (Merck Co., Germany) using a chloroform/methanol gradient solvent system of increasing polarity, to yield six fractions. The active compound was eluted with chloroform/methanol (9/1 v/v), being concentrated *in vacuo* to dryness before being applied to an ODS chromatography column (YMC Co., Japan) using a H<sub>2</sub>O/methanol gradient solvent system of increasing methanol, to yield six fractions. The active compound was eluted with 100% methanol, being concentrated *in vacuo* to dryness. The residue was applied to a DNH silica gel column (Fuji Silysia Chemical Ltd., Japan) using a chloroform/methanol gradient solvent system of increasing polarity, to yield six fractions. The active compound was eluted with chloroform/methanol (100/1 v/v), being concentrated *in vacuo* to dryness. Finally, the active fraction was triturated with toluene to afford kozozeptin A (**1a**) (1.7 mg). From the fermentation broth Lot 3, kozozeptin B (**1b**) (7.2 mg) was isolated (**Scheme 6 in Chapter 2**).

### 3. Assay of Antimalarial Activity *in vitro* and *in vivo*

#### *In vitro* evaluation

*In vitro* activity against *P. falciparum* strains K1 (chloroquine resistant) and FCR3 (chloroquine sensitive) and cytotoxicity against human diploid embryonic cell line MRC-5 were measured according to the procedure developed in Kitasato Institute using Malstat reagent (**Scheme 16**).<sup>[38a]</sup> This study was approved by “Kitasato Institute Hospital Research Ethics Committee (No12102)” on the donation of human erythrocytes from volunteers.

**Scheme 16.** *In vitro* antimalarial evaluation using Malstat reagent



### ***In vivo* evaluation**

A mouse model using a malaria-derived strain of *P. berghei* N (chloroquine sensitive) was used to assess *in vivo* antimalarial activity according to the procedure developed in Kitasato Institute.<sup>[38a,b]</sup> Male CD-1 (ICR) mice were purchased from Charles River Japan Inc., Japan. Mice at weight of ca. 18–22 g were intravenously infected with  $2 \times 10^6$  parasitized red blood cells of *P. berghei* N strain. Test compounds were prepared by 10% DMSO/0.5% Tween80 aqueous solution and sonicated for 30 min prior to intraperitoneal administration. Treatment was started two hours after the infection (Day 0) and then continued daily for 3 days (Day 1-3). The dosage of all compounds was 30 mg/kg/day. Five mice were used as an each treated and untreated (vehicle) control. On the Day 4, blood smears were made from each mouse to determine parasitaemia. Percentage inhibition was calculated using the following formula.

Percentage inhibition = Treated mice parasitaemia / Untreated (vehicle) mice parasitaemia x 100

The statistical analysis (Dunnett's test and Tukey-Kramer's honestly significant difference test) was using JMP statistical software (JMP® 8 SAS Institute Inc., Cary, NC, USA) and P values < 0.05 were considered statistically significant.

## **4. Advanced Marfey's Analysis**

The absolute configuration of each amino acid residue was determined by advanced Marfey's analysis.<sup>[38]</sup> A sample (100 µg) of kozupeptin A or B (**1a** or **1b**) was dissolved in 6 N HCl (500 µL) and heated for 3 h at 100°C. After cooling to room temperature, the hydrolysate was evaporated to dryness *in vacuo*, and the residue was dissolved in 100 µL of water. 50 µL of the hydrolysate aq. was treated with 25 µL of 1 M NaHCO<sub>3</sub> and 50 µL of 1% 1-fluoro-2,4-dinitrophenyl-5-D or L-leucinamide (D or L-FDLA) in acetone. The mixture was heated for 1 h at 37°C. After cooling to room temperature, the reaction mixture was neutralized with 1M HCl, and concentrated *in vacuo*. The residue was dissolved with 200 µL of acetonitrile, filtered to remove salt and analyzed by UPLC-MS (Waters Co., USA) on reversed-phase column (BEH C18 column; 2.1 x 50 mm, 1.7 µm, 0.5 mL/min) with a linear gradient from 50% to 100% aqueous acetonitrile containing formic acid (mobile phase A; 100% acetonitrile + 0.05% formic acid and mobile phase B; 90% H<sub>2</sub>O / 10% acetonitrile + 0.05% formic acid) for 10 min.

To determine the absolute configuration of the α-position of the alaninal residue of kozupeptin A (**1a**), oxidation was performed. To 50 µL of the hydrolysate aq. of **1a** described above was added 20 µL of Jones reagent (2.5 M CrO<sub>3</sub> in 25% v/v H<sub>2</sub>SO<sub>4</sub> in H<sub>2</sub>O) and stirred at room temperature for 10 min. The reaction mixture was quenched with 40 µL of 2-propanol and concentrated *in vacuo*. The residue was neutralized with 1 M NaHCO<sub>3</sub> and subjected to the derivatization with D-FDLA.

Amino acid standards were adjusted to 1 mM with water and were subjected to advanced Marfey's

analysis as described above. The ESI positive mode for the detection of amino acid-D-FDLA derivatives, and absolute configuration of each amino acid was determined by a comparison of retention time between the derivatives from the hydrolysate of **1a** or **1b** and standards. The retention times of the derivatives of L-Thr, D-Thr, L-*allo*-Thr, D-*allo*-Thr, L-Val, D-Val, L-Asn, D-Asn, L-Ala, and D-Ala were 4.20, 3.58, 3.93, 3.69, 5.36, 4.49, 3.82, 3.70, 4.54, and 4.03 minutes, respectively. Accordingly, the amino acids in **1a** were determined to be L-Thr (4.19 min), L-Val (5.35 min), L-Asn (3.85 min), and L-Ala (4.55 min). The amino acids in **1b** were determined to be L-Thr (4.19 min), L-Val (5.36 min), and L-Asn (3.82 min).

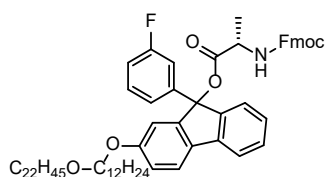
Analysis of the 4-MePro configuration was performed under conditions using a linear gradient from 25% to 100% aqueous acetonitrile containing formic acid (mobile phase A; 100% acetonitrile + 0.05% formic acid and mobile phase B; 90% H<sub>2</sub>O / 10% acetonitrile + 0.05% formic acid) for 10 min. Synthesized diastereoisomers of 4-MePro were used as standards for the analysis. The retention times (min) of the derivatives of (2*S*, 4*S*)-MePro-L-FDLA, (2*S*, 4*R*)-MePro-L-FDLA, (2*S*, 4*S*)-MePro-D-FDLA and (2*S*, 4*R*)-MePro-D-FDLA were 3.42, 3.80, 5.68 and 5.47 min. The retention times (min) of the derivatives of 4-MePro-L-FDLA and 4-MePro-D-FDLA from the hydrolysate of **1a** were 3.79 and 5.40 min and the absolute configuration was determined to be (2*S*, 4*R*)-MePro. Those from the hydrolysate of **1b** were 3.82 and 5.46 min and the absolute stereochemistry also proved to be (2*S*, 4*R*)-MePro as well. The results are summarized in **Table 3 in Chapter 2**.

## 5. Identification of the fatty acid

Identification of the fatty acid unit of kozupeptin A or B (**1a** or **1b**) was conducted by ESI-LCMS using a 2-nitrophenylhydrazide derivative of **1a** or **1b**. The hydrolysate of **1a** or **1b** was derivatized by 2-nitrophenylhydrazine using Fatty acid analysis kit (YMC Co., Kyoto, Japan) and analyzed by ESI-LCMS (QSTAR Hybrid LC/MS/MS using 50-100% MeOH containing 0.1% formic acid) to compare the retention time with that of standards.<sup>[40]</sup> The retention times (min) of the derivatives of hydrolysate of **1a** and **1b** showed both good matches with those of the derivative of oleic acid (**Figure 14 in Chapter 2**). Geometrical isomerism could also be determined as the *Z* isomer by the coupling constant of olefin <sup>1</sup>H NMR and <sup>13</sup>C NMR shift of allyl methylene.

The position of mono-double bond was also confirmed by GC-MS analysis of pyrrolidine amide derivative.<sup>[41]</sup> Standard fatty acid and the hydrolysate of **1a** or **1b** in toluene containing 25% MeOH were converted to methyl esters by reaction with TMS-diazomethane (ca. 10% in hexane, ca. 0.6 mol/L) at room temperature. Obtained crude methyl esters were heated in pyrrolidine/AcOH for 1 h at 100°C to afford pyrrolidine amide derivatives. GC-MS fragmentation analysis of the pyrrolidine amide derivative of **1a** or **1b** indicated a C9-C10 double bond of the fatty acid (**Figure 15 in Chapter 2**).

## 6. Total Synthesis -Experimental Procedures and Compounds Characterization-



### *Fmoc-Ala-O-Fl (4)*

*Fmoc-Ala-O-Fl (4)* was prepared by the procedure described in the literature as an off-white powder.<sup>[20a]</sup>  $[\alpha]_D^{28.3} = -2.0$  (*c* 0.1, chloroform);  $^1\text{H NMR}$  (500 MHz,  $\text{CDCl}_3$ )  $\delta$  7.74 (2H, d,  $J = 8.0$  Hz), 7.63-7.60 (2H, m, overlapped), 7.55-7.52 (2H, m, overlapped), 7.37 (3H, app t,  $J = 7.5$  Hz), 7.28-7.16 (5H, m, overlapped), 7.04-7.01 (2H, m, overlapped), 6.97-6.90 (2H, m, overlapped), 6.83-6.80 (1H, m), 5.30-5.27 (1H, br m), 4.57-4.53 (1H, m), 4.35 (2H, d,  $J = 7.0$  Hz), 4.17 (1H, t,  $J = 7.0$  Hz), 3.92-3.87 (2H, m, overlapped), 3.39 (4H, t,  $J = 7.0$  Hz), 1.77-1.69 (2H, m, overlapped), 1.58-1.20 (61H, br m, overlapped), 0.89 (3H, t,  $J = 7.0$  Hz);  $^{13}\text{C NMR}$  (125 MHz,  $\text{CDCl}_3$ , peaks were complex because of diastereomers derived from the anchor molecule, rotamers, and C-F coupling)  $\delta$  170.4, 163.9, 162.0, 160.0, 155.6, 147.7, 147.6, 145.6, 145.5, 144.0, 143.87, 143.85, 143.8, 141.4, 140.9, 140.6, 133.2, 133.0, 130.3, 130.2, 129.8, 129.7, 127.8, 127.3-127.2 (overlapped), 125.2, 124.3, 123.9, 121.3, 120.8, 120.1, 119.6, 115.45, 115.36, 114.9, 114.8, 112.6, 112.5, 111.1, 110.9, 89.1, 71.1, 68.5, 67.1, 50.0, 47.2, 32.1, 29.9-29.4 (many signals overlapped), 26.3, 26.2, 22.8, 19.0, 14.3; IR (KBr)  $\nu$  ( $\text{cm}^{-1}$ ) 2918, 2849, 1716, 1613, 1590, 1454, 1117, 740; HRMS (FAB, NBA + NaI matrix) Calcd. for  $\text{C}_{71}\text{H}_{96}\text{FNO}_6$ : 1077.7222 ( $\text{M}^+$ ), Found: 1077.7216.

### General procedure for Fmoc deprotection

The Fmoc protected amino acid or peptide was dissolved into 10% piperidine/ $\text{CH}_2\text{Cl}_2$  (0.036 M for substrate) at room temperature, and the solution was stirred until the reaction was completed (generally 20 min to 30 min). The reaction mixture was subsequently cooled to  $0^\circ\text{C}$  and acetonitrile (generally 5-fold excess of  $\text{CH}_2\text{Cl}_2$ ) was added. The resulting heterogeneous solution was stirred for a further 30 min at  $0^\circ\text{C}$ , and the precipitate was filtered and washed with additional acetonitrile to afford the corresponding amine as a white to off-white powder.

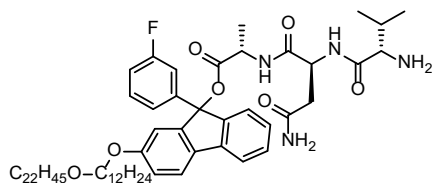
### General procedure for peptide elongation (condensation with Fmoc protected amino acid)

To a solution of Fmoc deprotected amino acid (1.0 eq) in  $\text{CH}_2\text{Cl}_2$  (0.05 M for substrate) were added Fmoc protected amino acid (1.1 eq), HOBt (1.2 eq), and DIC (1.2 eq) at room temperature and stirred until the reaction completed (1 to 13 h). The reaction mixture was subsequently cooled to  $0^\circ\text{C}$  and acetonitrile (generally 5-fold excess of  $\text{CH}_2\text{Cl}_2$ ) was added. The resulting heterogeneous solution was stirred for a further 30 min at  $0^\circ\text{C}$ , and the precipitate was filtered and washed with additional acetonitrile to afford the corresponding Fmoc protected peptide with an anchor molecule as a white to off-white powder.



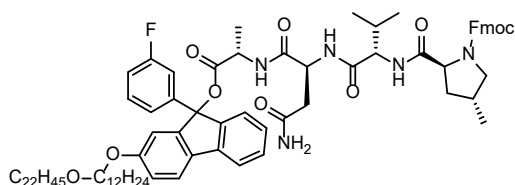


173.6, 173.55, 173.50, 172.0, 171.9, 170.6, 170.54, 170.49, 170.47, 169.9, 169.8, 163.8, 161.8, 159.83, 159.78, 157.0, 147.6, 147.5, 145.6, 145.4, 143.81, 143.76, 141.30, 141.28, 140.6, 140.4, 133.0, 132.9, 130.15, 130.08, 129.5, 129.4, 127.8, 127.15, 127.12, 127.09, 125.13, 125.07, 124.4, 124.0, 121.12, 121.07, 120.8, 120.0, 119.43, 119.40, 115.10, 115.07, 114.7, 114.6, 112.5, 112.3, 111.3, 110.9, 88.8, 71.0, 68.4, 67.1, 60.5, 49.7, 48.7, 48.6, 47.1, 36.7, 36.6, 31.9, 30.9, 29.7-29.3 (many signals overlapped), 26.15, 26.05, 22.7, 19.2, 17.6, 17.3, 17.2, 14.1; IR (KBr)  $\nu$  ( $\text{cm}^{-1}$ ) 3299, 2920, 2851, 1755, 1690, 1670, 1639, 1453, 1438, 1117, 738; HRMS (FAB, NBA + NaI matrix) Calcd. for  $\text{C}_{80}\text{H}_{111}\text{FN}_4\text{O}_9\text{Na}$ : 1313.8233 ( $[\text{M} + \text{Na}]^+$ ), Found: 1313.8241.



### *Val-Asn-Ala-O-Fl (7)*

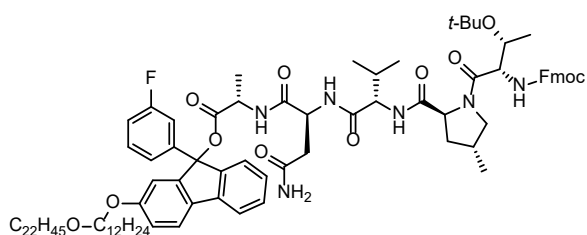
Following the general procedure described for Fmoc deprotection, Fmoc-Val-Asn-Ala-O-Fl (**49**) (2.64 g, 2.04 mmol) was converted to **7** (2.19 g, quant.) as an off-white powder.  $^1\text{H}$  NMR (500 MHz,  $\text{CDCl}_3$ )  $\delta$  8.39 (1H, br d,  $J = 7.5$  Hz), 7.57-7.52 (3H, m, overlapped), 7.35-7.29 (1H, m), 7.25-7.12 (3H, m, overlapped), 7.03-6.99 (2H, m, overlapped), 6.94-6.78 (3H, m, overlapped), 6.07 (1H br s), 5.45-5.35 (1H, br m), 4.68-4.64 (1H, m), 4.62-4.56 (1H, m), 3.93-3.85 (2H, m), 3.38 (4H, t,  $J = 7.0$  Hz), 3.17 (1H, d,  $J = 4.0$  Hz), 2.71-2.64 (1H, m), 2.45-2.39 (1H, m), 2.21-2.14 (1H, m), 1.77-1.70 (2H, m), 1.58-1.53 (4H, m, overlapped), 1.44-1.20 (59H, br m, overlapped), 0.93 (3H, d,  $J = 7.0$  Hz), 0.88 (3H, t,  $J = 7.0$  Hz), 0.77 (3H, d,  $J = 7.0$  Hz);  $^{13}\text{C}$  NMR (125 MHz,  $\text{CDCl}_3$ , peaks were complex because of diastereomers derived from the anchor molecule, rotamers, and C-F coupling)  $\delta$  175.23, 175.21, 173.3, 170.8, 170.7, 170.0, 169.9, 163.9, 161.9, 160.0, 159.9, 147.7, 147.6, 145.64, 145.55, 144.0, 143.94, 143.91, 143.88, 140.7, 140.6, 133.0, 132.9, 130.24, 130.17, 129.65, 129.55, 127.3, 127.2, 124.6, 124.1, 121.3, 121.2, 120.9, 119.62, 119.56, 115.3, 115.2, 114.9, 114.7, 112.6, 112.5, 111.3, 111.0, 88.9, 71.1, 68.5, 60.2, 49.4, 48.79, 48.76, 37.1, 32.1, 31.2, 29.9-29.4 (many signals overlapped), 26.3, 26.2, 22.8, 19.7, 17.9, 17.8, 16.3, 14.3; IR (KBr)  $\nu$  ( $\text{cm}^{-1}$ ) 3299, 2918, 2850, 1753, 1660, 1455, 1118; HRMS (FAB, NBA + NaI matrix) Calcd. for  $\text{C}_{65}\text{H}_{101}\text{FN}_4\text{O}_7\text{Na}$ : 1091.7552 ( $[\text{M} + \text{Na}]^+$ ), Found: 1091.7574.



### *Fmoc-4-MePro-Val-Asn-Ala-O-Fl (50)*

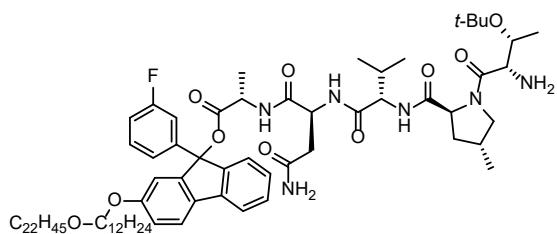
Following the general procedure described for condensation, 4-MePro-Val-Asn-Ala-O-Fl (**7**) (1.28 g, 1.20 mmol) was converted to **50** (1.64 g, 98%) as an off-white powder.  $^1\text{H}$  NMR (500 MHz,  $\text{CDCl}_3$ )  $\delta$  7.78-6.80





***Fmoc-Thr(t-Bu)-4-MePro-Val-Asn-Ala-O-Fl (51)***

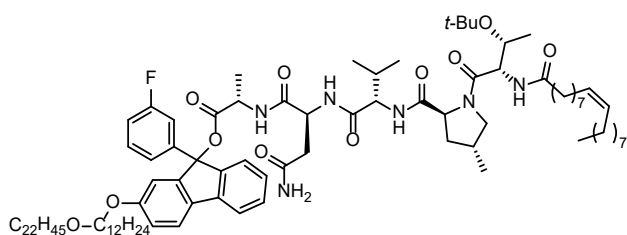
Following the general procedure described for condensation, 4-MePro-Val-Asn-Ala-O-Fl (**8**) (1.37 g, 1.16 mmol) was converted to **51** (1.80 g, 99%) as an off-white powder.  $^1\text{H}$  NMR (500 MHz,  $\text{CDCl}_3$ )  $\delta$  7.76 (2H, d,  $J = 7.5$  Hz), 7.60 (2H, d,  $J = 7.0$  Hz), 7.58-7.52 (2H, m, overlapped), 7.39 (2H, app br t,  $J = 7.0$  Hz), 7.32-6.08 (12H, m, overlapped), 6.19 (1H, br d,  $J = 8.5$  Hz), 5.84 (1H, br dd,  $J = 12.8, 8.5$  Hz), 5.57 (1H, app br d,  $J = 19.5$  Hz), 4.81-4.77 (1H, br m), 4.62-4.53 (3H, m, overlapped), 4.39 (2H, d,  $J = 7.0$  Hz), 4.22-4.17 (3H, m, overlapped), 4.01-3.96 (1H, m), 3.93-3.85 (2H, m, overlapped), 3.38 (4H, t,  $J = 7.0$  Hz), 3.17 (1H, t,  $J = 9.5$  Hz), 2.69-2.57 (2H, m, overlapped), 2.43-2.33 (1H, br m), 2.32-2.25 (1H, br m), 2.24-2.16 (1H, br m), 1.96 (2H, br s), 1.75-1.68 (2H, m, overlapped), 1.58-1.53 (4H, m), 1.43 (3H, app t,  $J = 8.0$  Hz), 1.39-1.20 (62H, br m, overlapped), 1.11 (3H, d,  $J = 6.0$  Hz), 1.06 (3H, d,  $J = 6.5$  Hz), 0.93-0.86 (9H, m, overlapped) (Two protons (NH x 2) were not observed.);  $^{13}\text{C}$  NMR (125 MHz,  $\text{CDCl}_3$ , peaks were complex because of diastereomers derived from the anchor molecule, rotamers, and C–F coupling)  $\delta$  173.1, 173.0, 172.22, 172.20, 171.0, 170.9, 170.53, 170.50, 170.4, 169.7, 169.6, 163.9, 161.9, 160.0, 159.9, 155.9, 147.9, 147.8, 145.9, 145.7, 144.11, 144.08, 144.05, 144.02, 144.0, 143.99, 141.4, 140.64, 140.56, 133.04, 132.99, 130.22, 130.16, 129.5, 129.4, 127.9, 127.2, 125.3, 125.2, 124.5, 124.2, 121.22, 121.18, 121.0, 120.14, 120.12, 119.55, 119.52, 115.3, 114.7, 114.6, 112.7, 112.5, 111.3, 110.9, 88.7, 75.3, 71.1, 68.8, 68.4, 67.1, 61.3, 59.5, 56.5, 55.4, 49.73, 49.67, 48.9, 48.8, 47.3, 37.04, 36.97, 36.4, 33.0, 32.1, 29.9-29.4 (many signals overlapped), 28.2, 26.3, 26.2, 22.8, 19.6, 18.23, 18.16, 17.7, 17.6, 17.0, 14.3; IR (KBr)  $\nu$  ( $\text{cm}^{-1}$ ) 3313, 2923, 2852, 1753, 1652, 1525, 1454, 1190, 1108, 740; HRMS (FAB, NBA + NaI matrix) Calcd. for  $\text{C}_{94}\text{H}_{135}\text{FN}_6\text{O}_{12}\text{Na}$ : 1582.0020 ( $[\text{M} + \text{Na}]^+$ ), Found: 1582.0031.



***Thr(t-Bu)-4-MePro-Val-Asn-Ala-O-Fl (9)***

Following the general procedure described for Fmoc deprotection, Fmoc-Thr(t-Bu)-4-MePro-Val-Asn-Ala-O-Fl (**51**) (0.593 g, 0.38 mmol) was converted to **9** (0.495 g, 97%) as an off-white powder.  $^1\text{H}$  NMR (500 MHz,  $\text{CDCl}_3$ )  $\delta$  8.02-6.78 (13H, m, overlapped), 6.25 (1H, br d,  $J = 11.0$  Hz), 5.63-5.50 (1H, br m), 4.87-4.77 (1H, br m), 4.61-4.52 (2H, m, overlapped), 4.27-4.17 (1H, br m), 4.01

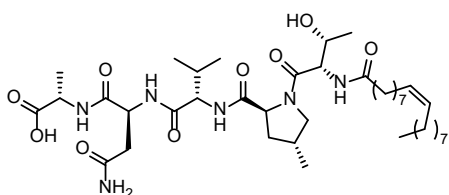
(1H, app t,  $J = 8.5$  Hz), 3.91-3.88 (2H, br m), 3.78-3.71 (1H, m), 3.51 (1H, br d,  $J = 6.5$  Hz), 3.38 (4H, t,  $J = 6.5$  Hz), 3.24-3.07 (1H, m, overlapped), 2.72-2.15 (5H, m, overlapped), 2.14-1.80 (3H, m, overlapped) 1.76-1.69 (2H, m, overlapped), 1.58-1.53 (4H, m), 1.46-1.20 (65H, br m, overlapped), 1.09 (3H, d,  $J = 6.5$  Hz), 1.06 (3H, d,  $J = 6.5$  Hz), 0.93-0.84 (9H, m, overlapped) (Two protons (NH x 2) were not observed.);  $^{13}\text{C}$  NMR (125 MHz,  $\text{CDCl}_3$ , peaks were complex because of diastereomers derived from the anchor molecule, rotamers, and C–F coupling)  $\delta$  174.1, 173.5, 173.2, 172.44, 172.42, 172.39, 171.43, 171.41, 171.04, 171.00, 170.5, 170.4, 170.13, 170.06, 169.8, 169.7, 169.63, 169.58, 163.9, 161.9, 160.0, 159.9, 147.93, 147.86, 147.74, 147.67, 145.9, 145.8, 145.7, 145.6, 144.1 (br), 140.7, 140.62, 140.57, 140.5, 133.0, 132.9, 130.2, 130.1, 129.6, 129.53, 129.49, 129.4, 127.4, 127.25, 127.21, 127.17, 124.6, 124.3, 124.2, 121.23, 121.17, 121.0, 120.9, 119.6, 119.54, 119.49, 115.7, 115.31, 115.29, 114.8, 114.7, 114.6, 114.5, 112.7, 112.5, 111.3, 110.9, 88.8, 88.7, 74.7, 71.7, 71.1, 70.7, 68.5, 61.9, 61.1, 59.6, 59.1, 57.8, 57.7, 55.0, 53.7, 49.7, 49.0, 48.94, 48.88, 39.3, 37.7, 37.6, 36.92, 36.86, 36.0, 33.0, 32.1, 30.8, 30.3, 29.9-29.4 (many signals overlapped), 28.6, 28.4, 26.3, 26.2, 22.8, 19.6, 18.8, 18.7, 18.6, 18.3, 18.0, 17.8, 17.7, 17.6, 17.3, 17.1, 14.3; IR (KBr)  $\nu$  ( $\text{cm}^{-1}$ ) 3299, 2921, 2851, 1755, 1652, 1530, 1455, 1262, 1189, 1115; HRMS (FAB, NBA + NaI matrix) Calcd. for  $\text{C}_{79}\text{H}_{125}\text{FN}_6\text{O}_{10}\text{Na}$ : 1359.9339 ( $[\text{M} + \text{Na}]^+$ ), Found: 1359.9330.



***Oleic acid-Thr(t-Bu)-4-MePro-Val-Asn-Ala-O-Fl (10)***

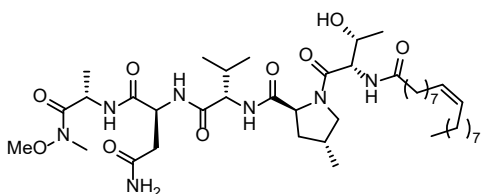
Following the general procedure described for condensation, Thr(*t*-Bu)-4-MePro-Val-Asn-Ala-O-Fl (**9**) (0.900 g, 0.67 mmol) was converted to **10** (1.02 g, 95%) as an off-white powder.  $^1\text{H}$  NMR (500 MHz,  $\text{CDCl}_3$ )  $\delta$  7.59-7.54 (3H, m, overlapped), 7.39-6.80 (11H, m, overlapped), 6.49 (1H, app br t,  $J = 8.0$  Hz), 6.22 (1H, app br d,  $J = 14.0$  Hz), 5.56 (1H, app br d,  $J = 12.5$  Hz), 5.37-5.30 (2H, m, overlapped), 4.81-4.77 (2H, m, overlapped), 4.62-4.53 (2H, m, overlapped), 4.24-4.19 (2H, m, overlapped), 4.04-3.99 (1H, m), 3.93-3.86 (2H, m, overlapped), 3.38 (4H, t,  $J = 6.5$  Hz), 3.25-3.13 (1H, m), 2.69-2.60 (2H, m, overlapped), 2.42-2.32 (1H, m), 2.29-2.17 (4H, m, overlapped), 2.02-1.98 (4H, m, overlapped), 1.76-1.69 (3H, m, overlapped), 1.63-1.53 (7H, m), 1.46-1.20 (85H, br m, overlapped), 1.073 (3H, d,  $J = 6.0$  Hz), 1.065 (3H, d,  $J = 6.0$  Hz), 0.93-0.84 (12H, m, overlapped);  $^{13}\text{C}$  NMR (125 MHz,  $\text{CDCl}_3$ , peaks were complex because of diastereomers derived from the anchor molecule, rotamers, and C–F coupling)  $\delta$  173.1, 173.0, 172.31, 172.29, 171.00, 170.96, 170.7, 170.5, 170.4, 169.7, 169.6, 163.9, 161.9, 160.0, 159.9, 147.9, 147.8, 145.9, 145.8, 144.11, 144.07, 144.02, 140.7, 140.6, 133.05, 132.99, 130.2, 130.1, 129.9, 129.51, 129.46, 127.2, 124.5, 124.2, 121.2, 121.0, 119.5, 115.3, 114.7, 114.6, 112.7, 112.5, 111.3, 110.9, 88.7, 75.3, 71.1, 68.4, 68.3, 61.3, 59.5, 55.4, 54.9, 49.75, 49.70, 48.95, 48.86, 37.2, 37.1, 36.5, 36.4, 33.0, 32.1, 29.9-29.3 (many signals overlapped), 28.4, 28.2, 28.0, 26.3, 26.2, 25.6, 22.8, 19.6, 18.3, 18.2, 17.7, 17.6, 17.0, 14.3; IR (KBr)  $\nu$  ( $\text{cm}^{-1}$ ) 3279, 2919, 2851, 1755, 1646, 1536,

1455, 1191, 1118; HRMS (FAB, NBA + NaI matrix) Calcd. for C<sub>97</sub>H<sub>157</sub>FN<sub>6</sub>O<sub>11</sub>Na: 1624.1792 ([M + Na]<sup>+</sup>), Found: 1624.1804.



*Oleic acid-Thr(t-Bu)-4-MePro-Val-Asn-Ala-OH (11)*

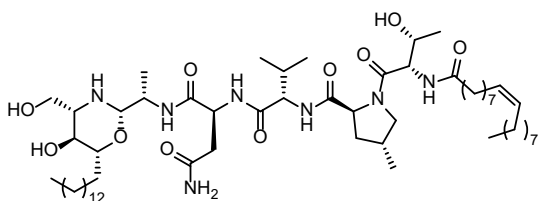
**10** (181 mg, 0.11 mmol) was dissolved into 20% TFA/CH<sub>2</sub>Cl<sub>2</sub> (5.7 mL, 0.02 M for substrate) at room temperature, and the solution was stirred for 5 h. The reaction mixture was subsequently cooled to 0°C and pyridine (1.09 mL, 3.51 mmol, 1.0 eq for TFA) was added dropwise. Methanol (28 mL, 5-fold excess of TFA/CH<sub>2</sub>Cl<sub>2</sub>) was added, and the resulting heterogeneous solution was stirred for a further 30 min at 0°C. The precipitate was filtered and washed with additional methanol, and the filtrate was concentrated *in vacuo*. The residue was dissolved into ethyl acetate (30 mL) and washed with aqueous 1M HCl (3 x 20 mL) and sat. NaCl aq. (20 mL). The organic layer was dried with Na<sub>2</sub>SO<sub>4</sub>, filtered, and concentrated *in vacuo*. The residue was purified by flash column chromatography on silica gel (CHCl<sub>3</sub>/MeOH) to afford carboxylic acid **11** (65.9 mg, 75%) as a white powder. [α]<sub>D</sub><sup>27.2</sup> = -31.3 (*c* 0.1, DMSO); mp 183–186°C; <sup>1</sup>H NMR (500 MHz, DMSO-*d*<sub>6</sub>) δ 8.10 (1H, d, *J* = 7.0 Hz), 7.88 (1H, d, *J* = 8.0 Hz), 7.83 (1H, d, *J* = 8.5 Hz), 7.78 (1H, d, *J* = 7.5 Hz), 7.34 (1H, s), 6.90 (1H, s), 5.35-5.29 (2H, m, overlapped), 4.68 (1H, br s), 4.54-4.48 (2H, m, overlapped), 4.42 (1H, app t, *J* = 7.5 Hz), 4.12-4.07 (2H, m, overlapped), 3.83-3.78 (2H, m, overlapped), 3.27 (1H, app t, *J* = 9.0 Hz), 2.55-2.50 (1H, m, overlapped with DMSO), 2.41 (1H, dd, *J* = 7.5, 15.5 Hz), 2.38-2.30 (1H, m), 2.17-2.06 (2H, m, overlapped), 2.01-1.93 (5H, m, overlapped), 1.67-1.61 (1H, m), 1.48-1.42 (2H, m, overlapped), 1.33-1.13 (24H, app br s, overlapped), 1.08 (3H, d, *J* = 6.0 Hz), 0.97 (3H, d, *J* = 7.0 Hz), 0.86-0.81 (9H, m, overlapped); <sup>13</sup>C NMR (125 MHz, DMSO-*d*<sub>6</sub>) δ 173.8, 172.2, 171.6, 171.5, 170.6, 170.5, 169.4, 129.6, 66.9, 59.2, 57.8, 56.2, 54.0, 49.3, 47.7, 36.7, 36.5, 34.9, 32.0, 31.3, 30.5, 29.1-28.6 (many signals overlapped), 26.62, 26.58, 25.2, 22.1, 19.3, 19.1, 17.9, 17.2, 14.0; IR (KBr) ν (cm<sup>-1</sup>) 3287, 2924, 2854, 1730, 1637, 1541, 1454, 1232, 1199, 1146; HRMS (ESI<sup>+</sup>) Calcd. for C<sub>40</sub>H<sub>70</sub>N<sub>6</sub>O<sub>9</sub>Na: 801.5102 ([M + Na]<sup>+</sup>), Found: 801.5094; HRMS (ESI<sup>-</sup>) Calcd. for C<sub>40</sub>H<sub>69</sub>N<sub>6</sub>O<sub>9</sub>: 777.5126 ([M - H]<sup>-</sup>), Found: 777.5123.



*Oleic acid-Thr-4-MePro-Val-Asn-Ala-N(Me)OMe (12)*

To a solution of **11** (120 mg, 0.15 mmol, 1.0 eq), MeO(Me)NH-HCl (48.1 mg, 0.49 mmol, 3.2 eq), DEPBT (3-(diethoxyphosphoryloxy)-1,2,3-benzotriazin-4(3*H*)-one, 147 mg, 0.49 mmol, 3.2 eq) in DMF (4.3

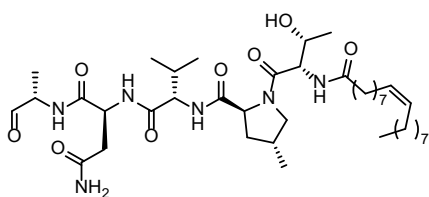
mL, 0.036 M) was added DIPEA (*N,N*-diisopropylethylamine, 127 mg, 0.99 mmol, 6.4 eq) at room temperature. After stirring for 23 h at room temperature, the reaction mixture was then treated with aqueous 1M HCl in an ice bath to quench the excess amine reagent, poured into a separatory funnel containing ethyl acetate (50 mL), and washed with aqueous 1M HCl (2 x 30 mL) and sat. NaCl aq. (30 mL). The organic layer was dried with Na<sub>2</sub>SO<sub>4</sub>, filtered, and concentrated *in vacuo*. The residue was purified by flash column chromatography on silica gel (CHCl<sub>3</sub>/MeOH) to afford Weinreb amide **12** (127 mg, quant, dr = 97:3 ( $\alpha$ -position of Ala, determined by advanced Marfey's analysis described above and <sup>1</sup>H NMR)) as a white powder. [ $\alpha$ ]<sub>D</sub><sup>27.0</sup> = -46.0 (c 0.1, DMSO); mp 176°C; <sup>1</sup>H NMR (500 MHz, DMSO-*d*<sub>6</sub>)  $\delta$  8.10 (1H, d, *J* = 7.0 Hz), 7.86 (1H, d, *J* = 7.5 Hz), 7.83 (1H, d, *J* = 8.0 Hz), 7.77 (1H, d, *J* = 7.0 Hz), 7.32 (1H, s), 6.90 (1H, s), 5.35-5.29 (2H, m, overlapped), 4.65 (1H, d, *J* = 6.0 Hz), 4.68-4.62 (1H, br m), 4.54-4.41 (3H, m, overlapped), 4.09 (1H, dd, *J* = 6.5, 8.0 Hz), 3.83-3.78 (2H, m, overlapped), 3.71 (3H, s), 3.26 (1H, app t, *J* = 9.0 Hz), 3.09 (3H, s), 2.56-2.50 (1H, m, overlapped with DMSO), 2.39 (1H, dd, *J* = 7.5, 15.5 Hz), 2.42-2.29 (1H, m), 2.18-2.06 (2H, m), 2.01-1.92 (5H, m, overlapped), 1.67-1.61 (1H, m), 1.48-1.42 (2H, m, overlapped), 1.33-1.13 (21H, app br s, overlapped), 1.17 (3H, d, *J* = 7.0 Hz), 1.09 (3H, d, *J* = 6.0 Hz), 0.97 (3H, d, *J* = 7.0 Hz), 0.86-0.81 (9H, m, overlapped); <sup>13</sup>C NMR (125 MHz, DMSO-*d*<sub>6</sub>)  $\delta$  171.7, 171.04, 170.98, 170.2, 169.9, 168.9, 129.1, 66.4, 58.7, 57.2, 55.6, 53.5, 48.8, 44.3, 36.2, 36.0, 34.4, 31.5, 30.8, 30.1, 28.6-28.1 (many signals overlapped), 26.12, 26.07, 24.7, 21.6, 18.8, 18.7, 17.4, 16.7, 16.6, 13.5; IR (KBr)  $\nu$  (cm<sup>-1</sup>) 3278, 2924, 2854, 1637, 1542, 1424, 1232; HRMS (ESI<sup>+</sup>) Calcd. for C<sub>42</sub>H<sub>75</sub>N<sub>7</sub>O<sub>9</sub>Na: 844.5524 ([M + Na]<sup>+</sup>), Found: 844.5515.



### Kozupeptin A (**1a**)

To a solution of **12** (16.0 mg, 0.019 mmol, 1.0 eq) in dehydrated THF (3.0 mL, 0.007 M) was added dropwise 0.1 M LAH in dehydrated THF (pre-prepared, 0.331 mL, 1.7 eq) at 0°C. After stirring for 1 h at 0°C, the reaction mixture was then treated with aqueous 1M HCl at 0°C to quench the excess LAH. After stirring for 10 min at room temperature, MeOH (250 mL) was added. The resulting heterogeneous solution was stirred for a further 30 min at room temperature, and the precipitate was filtered and washed with additional MeOH. The filtrate was roughly concentrated *in vacuo*, poured into a separatory funnel containing aqueous 1M HCl (10 mL), and extracted with CHCl<sub>3</sub> (3 × 10 mL). The combined organic extracts were dried with Na<sub>2</sub>SO<sub>4</sub>, filtered, and concentrated *in vacuo* to afford the crude product **13**. To a solution of the crude **13** in CHCl<sub>3</sub> (1.9 mL) was added (*2S,3S,4R*)-phytosphingosine (6.8 mg, 0.021 mmol, 1.1 eq for **12**) at room temperature. After stirring for 2.5 h at room temperature, the reaction mixture was concentrated *in vacuo*. The residue was purified by flash column chromatography on silica gel (CHCl<sub>3</sub>/MeOH) to afford kozupeptin A (**1a**) (10.6 mg,

51% over two steps, dr = 97:3 ( $\alpha$ -position of Ala) as a white powder.  $[\alpha]_D^{26.4} = -36.2$  (*c* 0.1, DMSO); mp 177–179°C;  $^1\text{H NMR}$  (500 MHz, DMSO- $d_6$ )  $\delta$  8.08 (1H, d,  $J = 8.0$  Hz), 7.86 (1H, d,  $J = 7.5$  Hz), 7.82 (1H, d,  $J = 8.0$  Hz), 7.32 (1H, d, overlapped), 7.32 (1H, s), 6.88 (1H, s), 5.35–5.29 (2H, m, overlapped), 4.71 (1H, d,  $J = 6.5$  Hz), 4.66 (1H, d,  $J = 5.5$  Hz), 4.52–4.40 (4H, m, overlapped), 4.05 (1H, dd,  $J = 6.5, 8.0$  Hz), 3.86 (1H, app br s), 3.82–3.78 (2H, m, overlapped), 3.75–3.68 (1H, m), 3.60–3.55 (1H, m), 3.51–3.45 (1H, m), 3.29 (1H, dd,  $J = 9.0, 9.5$  Hz), 3.07–3.01 (1H, m), 2.90–2.84 (1H, m), 2.54–2.50 (1H, m, overlapped with DMSO), 2.41 (1H, dd,  $J = 6.5, 15.5$  Hz), 2.39–2.31 (2H, m), 2.17–2.06 (2H, m, overlapped), 2.02–1.92 (6H, m, overlapped), 1.77 (1H, br t), 1.68–1.62 (1H, m), 1.48–1.42 (3H, m, overlapped), 1.33–1.13 (44H, br m, overlapped), 1.09 (3H, d,  $J = 6.0$  Hz), 0.99 (3H, d,  $J = 7.0$  Hz), 0.97 (3H, d,  $J = 7.0$  Hz), 0.86–0.82 (12H, m, overlapped) (One proton (NH of sphingoid) was not observed);  $^{13}\text{C NMR}$  (125 MHz, DMSO- $d_6$ )  $\delta$  172.2, 171.7, 170.6, 170.0, 169.5, 129.6, 88.3, 80.6, 66.9, 66.8, 61.1, 60.4, 59.2, 57.9, 56.2, 54.0, 49.6, 47.6, 36.8, 36.5, 34.9, 32.0, 31.7, 31.3–26.6 (many signals overlapped), 25.2, 22.1, 19.4, 19.1, 18.0, 17.2, 15.5, 14.0; IR (KBr)  $\nu$  ( $\text{cm}^{-1}$ ) 3276, 2924, 2853, 1643, 1548, 1456, 1057, 801; HRMS (ESI $^+$ ) Calcd. for  $\text{C}_{58}\text{H}_{107}\text{N}_7\text{O}_{10}\text{Na}$ : 1084.7977 ( $[\text{M} + \text{Na}]^+$ ), Found: 1084.7968.

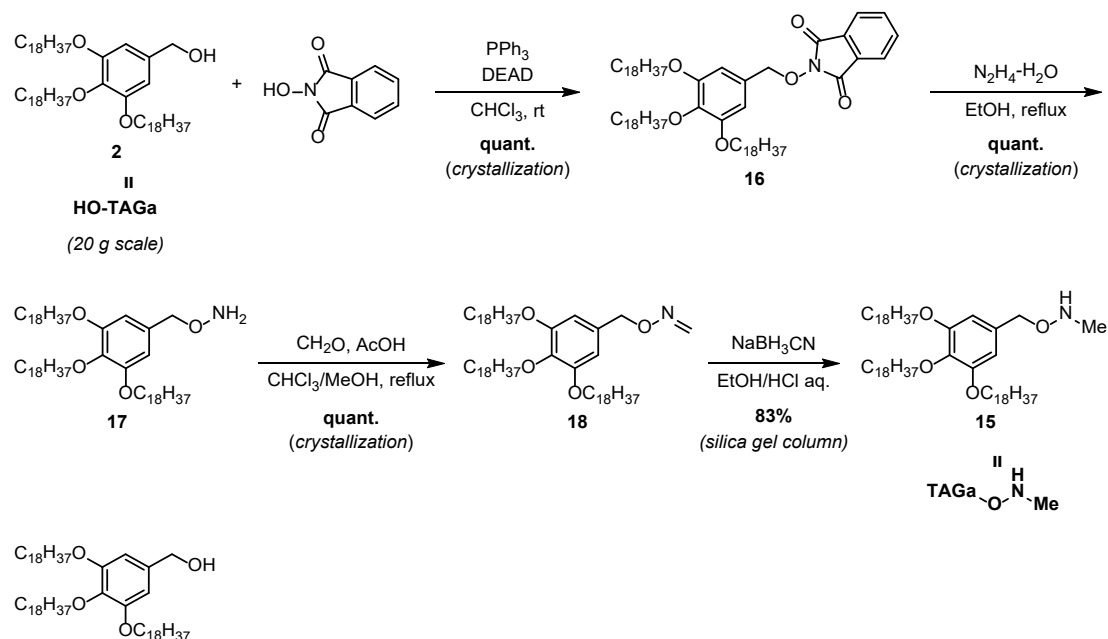


### *Oleic acid-Thr-4-MePro-Val-Asn-Ala-H (13)*

The crude product **13** (48.3 mg), prepared by the same procedure as described above, was purified by flash column chromatography on silica gel ( $\text{CHCl}_3/\text{MeOH}$ ) to afford the aldehyde **13** (31.6 mg, dr = 97:3 ( $\alpha$ -position of Ala) as a white powder.  $[\alpha]_D^{24.8} = -33.5$  (*c* 0.1, DMSO); mp 162–166°C;  $^1\text{H NMR}$  (500 MHz, DMSO- $d_6$ )  $\delta$  9.34 (1H, s), 8.14 (1H, d,  $J = 6.5$  Hz), 8.11 (1H, d,  $J = 7.5$  Hz), 7.87 (2H, app d,  $J = 7.5$  Hz), 7.37 (1H, br s), 6.93 (1H, br s), 5.35–5.29 (2H, m, overlapped), 4.67 (1H, d,  $J = 6.0$  Hz), 4.55–4.47 (2H, m, overlapped), 4.43–4.39 (1H, m), 4.08–3.98 (2H, m, overlapped), 3.83–3.77 (2H, m, overlapped), 3.27 (1H, app t,  $J = 9.0$  Hz), 2.57–2.46 (2H, m, overlapped with DMSO), 2.38–2.30 (1H, m), 2.17–2.06 (2H, m), 2.01–1.94 (5H, m, overlapped), 1.68–1.62 (1H, m), 1.48–1.42 (2H, m, overlapped), 1.33–1.18 (21H, app br s, overlapped), 1.14 (3H, d,  $J = 7.5$  Hz), 1.08 (3H, d,  $J = 6.0$  Hz), 0.97 (3H, d,  $J = 7.0$  Hz), 0.86–0.82 (9H, m, overlapped);  $^{13}\text{C NMR}$  (125 MHz, DMSO- $d_6$ )  $\delta$  201.4, 172.2, 171.9, 171.4, 171.3, 170.6, 169.5, 129.7, 66.9, 59.2, 58.0, 56.2, 54.0, 53.9, 49.5, 36.8, 36.5, 34.9, 32.0, 31.3, 30.4, 29.2–28.6 (many signals overlapped), 26.64, 26.60, 25.3, 22.1, 19.4, 19.1, 18.0, 17.2, 14.0, 13.6; IR (KBr)  $\nu$  ( $\text{cm}^{-1}$ ) 3285, 2924, 2853, 1736, 1639, 1542, 1426, 1235; HRMS (ESI $^+$ ) Calcd. for  $\text{C}_{40}\text{H}_{70}\text{N}_6\text{O}_8\text{Na}$ : 785.5153 ( $[\text{M} + \text{Na}]^+$ ), Found: 785.5151.

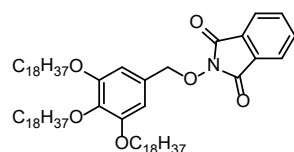
## Supporting Information for Chapter 3

### 1. Preparation of newly designed anchor molecules



#### 3,4,5-Tris(octadecyloxy)benzyl alcohol (**2**) (HO-TAGa)

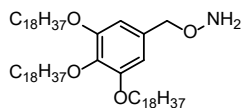
HO-TAGa (**2**) was prepared by the procedure described in the literature as a white powder.<sup>[17]</sup> mp 68–69°C; <sup>1</sup>H NMR (500 MHz, CDCl<sub>3</sub>) δ 6.56 (2H, s), 4.59 (2H, s), 3.98-3.92 (6H, m, overlapped), 1.82-1.71 (6H, m, overlapped), 1.50-1.43 (6H, br m, overlapped), 1.35-1.22 (84H, br m, overlapped), 0.88 (9H, t, *J* = 7.0 Hz); <sup>13</sup>C NMR (125 MHz, CDCl<sub>3</sub>) δ 153.4, 137.7, 136.2, 105.5, 73.6, 69.3, 65.8, 32.1, 30.5, 29.9-29.5 (many signals overlapped), 26.29, 26.26, 22.8, 14.3; IR (KBr) ν (cm<sup>-1</sup>) 3541, 2916, 2848, 1594, 1462, 1439, 1118, 719; HRMS (FAB, NBA matrix) Calcd. for C<sub>61</sub>H<sub>116</sub>O<sub>4</sub>: 912.8874 ([M]<sup>+</sup>), Found: 912.8876.



#### Phthalimide-O-TAGa (**16**)

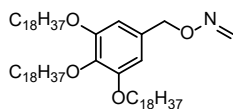
To a solution of **15** (20.0 g, 21.9 mmol, 1.0 eq), triphenylphosphine (11.5 g, 43.8 mmol, 2.0 eq) and *N*-hydroxyphthalimide (7.14 g, 43.8 mmol, 2.0 eq) in CHCl<sub>3</sub> (274 mL, 0.08 M) was added dropwise diethyl azodicarboxylate (DEAD) (40% toluene solution, 19.1 g, 43.8 mmol, 2.0 eq) at 0 °C for 20 min. The mixture was heated to room temperature and stirred for 5 h. Methanol (1370 mL, 5-fold excess of CHCl<sub>3</sub>) was added to the reaction mixture and the resulting heterogeneous solution was stirred for a further 30 min at room temperature. The precipitate was filtered and washed with additional MeOH to afford phthalimide-O-TAGa (**16**) (23.2 g, quant.) as a white powder. mp 81°C; <sup>1</sup>H NMR (500 MHz, CDCl<sub>3</sub>) δ 7.82-7.78 (2H, m), 7.74-7.71 (2H, m), 6.72 (2H, s), 5.13 (2H, s), 3.97-3.92 (6H, m, overlapped), 1.80-1.68 (6H, m, overlapped), 1.48-1.42

(6H, br m, overlapped), 1.35-1.22 (84H, br m, overlapped), 0.88 (9H, t,  $J = 7.0$  Hz);  $^{13}\text{C}$  NMR (125 MHz,  $\text{CDCl}_3$ , peaks were complex because of rotamers)  $\delta$  163.6, 153.3, 139.1, 134.5, 129.0, 128.6, 123.6, 108.4, 80.3, 73.5, 69.3, 32.1, 30.4, 29.9-29.5 (many signals overlapped), 26.2, 22.8, 14.3; IR (KBr)  $\nu$  ( $\text{cm}^{-1}$ ) 2916, 2849, 1739, 1466, 1440, 1112, 700; HRMS (FAB, NBA + Na matrix) Calcd. for  $\text{C}_{69}\text{H}_{119}\text{NO}_6\text{Na}$ : 1080.8935 ( $[\text{M} + \text{Na}]^+$ ), Found: 1080.8942.



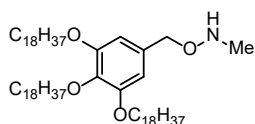
### *NH*<sub>2</sub>-*O*-TAGa (**17**)

To a solution of **16** (23.2 g, 21.9 mmol, 1.0 eq) in EtOH (730 mL, 0.03 M) was added dropwise  $\text{N}_2\text{H}_4 \cdot \text{H}_2\text{O}$  (11.0 g, 219 mmol, 10 eq) at room temperature. The mixture was heated to reflux and stirred for 8 h. After cooling to room temperature, the resulting heterogeneous solution was stirred for a further 30 min at room temperature. The precipitate was filtered and washed with additional EtOH to afford *NH*<sub>2</sub>-*O*-TAGa (**17**) (20.3 g, quant.) as a white powder. mp 69–70°C;  $^1\text{H}$  NMR (500 MHz,  $\text{CDCl}_3$ )  $\delta$  6.55 (2H, s), 5.39 (2H, br s), 4.59 (2H, s), 3.98-3.92 (6H, m, overlapped), 1.82-1.71 (6H, m, overlapped), 1.50-1.43 (6H, br m, overlapped), 1.37-1.22 (84H, br m, overlapped), 0.88 (9H, t,  $J = 7.0$  Hz);  $^{13}\text{C}$  NMR (125 MHz,  $\text{CDCl}_3$ )  $\delta$  153.4, 138.1, 132.4, 106.8, 78.5, 73.5, 69.2, 32.1, 30.5, 29.9-29.5 (many signals overlapped), 26.29, 26.26, 22.8, 14.3; IR (KBr)  $\nu$  ( $\text{cm}^{-1}$ ) 2914, 2848, 1596, 1469, 1243, 1128, 718; HRMS (ESI<sup>+</sup>) Calcd. for  $\text{C}_{61}\text{H}_{118}\text{NO}_4$ : 928.9061 ( $[\text{M} + \text{H}]^+$ ), Found: 928.9056.



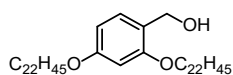
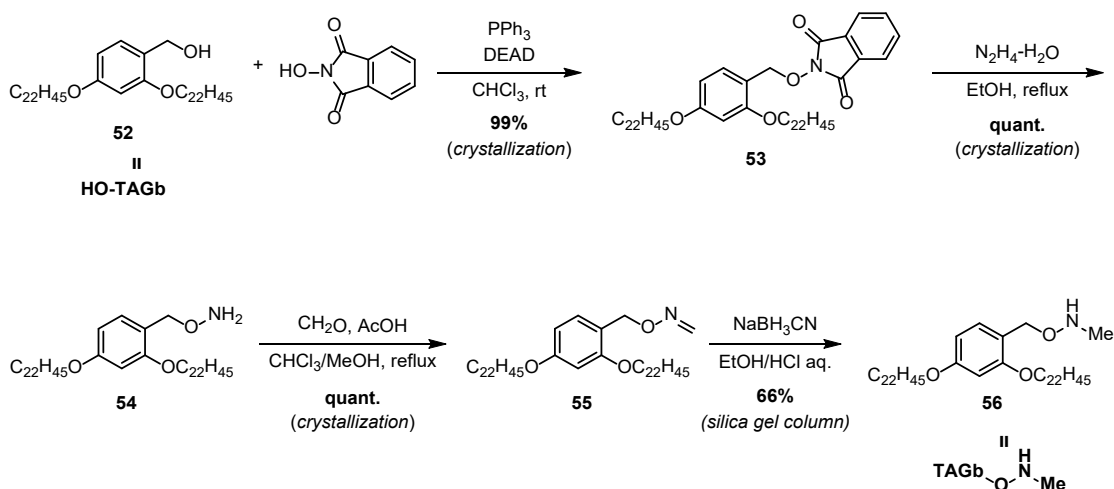
### *CH*<sub>2</sub>=*N*-*O*-TAGa (**18**)

A mixture of **17** (20.3 g, 21.9 mmol, 1.0 eq) and paraformaldehyde (6.56 g, 219 mmol, 10 eq) in  $\text{CHCl}_3/\text{MeOH} = 5/1$  (375 mL, 0.06 M) was heated to reflux and stirred for 3 h. After cooling to room temperature, MeOH (1560 mL, 5-fold excess of  $\text{CHCl}_3$ ) was added to the reaction mixture and was stirred for a further 30 min at room temperature. The precipitate was filtered and washed with additional MeOH to afford *CH*<sub>2</sub>=*N*-*O*-TAGa (**18**) (20.6 g, quant.) as a white powder. mp 71–72°C;  $^1\text{H}$  NMR (500 MHz,  $\text{CDCl}_3$ )  $\delta$  7.09 (1H, d,  $J = 8.5$  Hz), 6.55 (2H, s), 6.48 (1H, d,  $J = 8.5$  Hz), 5.02 (2H, s), 3.98-3.92 (6H, m, overlapped), 1.82-1.70 (6H, m, overlapped), 1.49-1.43 (6H, br m, overlapped), 1.35-1.22 (84H, br m, overlapped), 0.88 (9H, t,  $J = 7.5$  Hz);  $^{13}\text{C}$  NMR (125 MHz,  $\text{CDCl}_3$ )  $\delta$  153.3, 138.1, 137.8, 132.4, 106.9, 76.6, 73.5, 69.2, 32.1, 30.5, 29.9-29.2 (many signals overlapped), 26.29, 26.26, 22.8, 14.3; IR (KBr)  $\nu$  ( $\text{cm}^{-1}$ ) 2914, 2847, 1596, 1469, 1243, 1129, 717; HRMS data is not available because the parent peak was not detected by ESI nor FAB. Only hydrolyzed peaks (928.9 ( $[\text{17} + \text{H}]^+$ ) and 959.9 ( $[\text{17} + \text{Na}]^+$ )) were observed.



### Me-HN-O-TAGa (**15**)

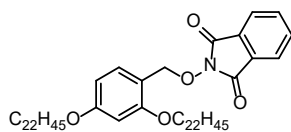
To a solution of **18** (17.6 g, 18.7 mmol, 1.0 eq) and NaBH<sub>3</sub>CN (3.53 g, 56.1 mmol, 3.0 eq) in EtOH/THF = 1/1 (535 mL, 0.035 M) was added dropwise conc. HCl aq. (4.29 g) at room temperature until the pH reached around 3. After stirring for 2 h, MeOH (1338 mL, 5-fold excess of THF) was added to the mixture and the resulting heterogeneous solution was stirred for a further 30 min at room temperature. The precipitate was filtered and washed with additional MeOH to afford Me-HN-O-TAGa (**18**) (17.7 g, app. quant.) as a white powder. Additional purification was performed by column chromatography on silica gel (CHCl<sub>3</sub>/*n*-hexane = 1/1 to 5/1 as eluent) to give highly pure **15** (14.7 g, 83%) as a white powder. mp 53–54°C; <sup>1</sup>H NMR (500 MHz, CDCl<sub>3</sub>) δ 6.55 (2H, s), 5.54 (1H, br s), 4.61 (2H, s), 3.98-3.91 (6H, m, overlapped), 2.75 (3H, s), 1.82-1.70 (6H, m, overlapped), 1.49-1.43 (6H, br m, overlapped), 1.37-1.22 (84H, br m, overlapped), 0.88 (9H, t, *J* = 7.5 Hz); <sup>13</sup>C NMR (125 MHz, CDCl<sub>3</sub>) δ 153.3, 137.9, 133.1, 106.8, 76.1, 73.5, 69.2, 39.4, 32.1, 30.5, 29.9-29.5 (many signals overlapped), 26.29, 26.26, 22.8, 14.3; IR (KBr) ν (cm<sup>-1</sup>) 2916, 2849, 1588, 1468, 1234, 1116, 720; HRMS (ESI<sup>+</sup>) Calcd. for C<sub>62</sub>H<sub>120</sub>NO<sub>4</sub>: 942.9217 ([M + H]<sup>+</sup>), Found: 942.9241.



### 2,4-Bis(docosyloxy)benzyl alcohol (**52**) (HO-TAGb)<sup>[18a]</sup>

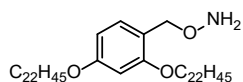
HO-TAGb (**52**) (11.4 g, 15.1 mmol) was prepared by the same procedure as HO-TAGa (**2**) described above as a white powder. mp 69–70°C; <sup>1</sup>H NMR (500 MHz, CDCl<sub>3</sub>) δ 7.13 (1H, d, *J* = 8.5 Hz), 6.45 (1H, d, *J* = 2.5 Hz), 6.42 (1H, dd, *J* = 8.0, 2.0 Hz), 4.61 (2H, d, *J* = 6.5 Hz), 3.98 (2H, t, *J* = 6.5 Hz), 3.93 (2H, t, *J* = 6.5 Hz), 2.27 (1H, t, *J* = 6.5 Hz), 1.83-1.74 (4H, m, overlapped), 1.48-1.41 (4H, br m, overlapped), 1.37-1.22 (72H, br m, overlapped), 0.88 (6H, t, *J* = 7.0 Hz); <sup>13</sup>C NMR (125 MHz, CDCl<sub>3</sub>, peaks were complex because of rotamers) δ 160.3, 158.2, 129.7, 121.8, 104.6, 99.9, 68.3, 68.1, 62.2, 32.1, 29.9-29.4 (many signals overlapped), 26.3, 26.2, 22.8, 14.3; IR (KBr) ν (cm<sup>-1</sup>) 2916, 2848, 1614, 1470, 1180, 1121, 718; HRMS (FAB,

NBA + Na matrix) Calcd. for  $C_{51}H_{96}O_3Na$ : 779.7257 ( $[M + Na]^+$ ), Found: 779.7258.



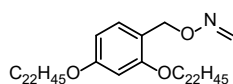
### Phthalimide-O-TAGb (**53**)

Following the same procedure described for phthalimide-O-TAGa (**16**), HO-TAGb (**52**) (6.30 g, 8.3 mmol) was converted to phthalimide-O-TAGa (**53**) (7.40 g, 99%) as a white powder. mp 85–86°C;  $^1H$  NMR (500 MHz,  $CDCl_3$ )  $\delta$  7.80-7.76 (2H, m), 7.72-7.68 (2H, m), 7.32 (1H, d,  $J = 8.5$  Hz), 6.43 (1H, dd,  $J = 8.5, 2.5$  Hz), 6.37 (1H, d,  $J = 2.0$  Hz), 5.20 (2H, s), 3.92 (2H, t,  $J = 6.5$  Hz), 3.82 (2H, t,  $J = 6.5$  Hz), 1.78-1.72 (2H, m), 1.70-1.65 (2H, m), 1.46-1.22 (76H, br m, overlapped), 0.88 (6H, t,  $J = 7.0$  Hz);  $^{13}C$  NMR (125 MHz,  $CDCl_3$ )  $\delta$  163.6, 161.7, 159.4, 134.2, 133.5, 129.2, 123.4, 115.1, 105.0, 99.7, 74.5, 68.5, 68.1, 32.1, 29.9-29.4 (many signals overlapped), 29.1, 26.2, 26.1, 22.8, 14.3; IR (KBr)  $\nu$  ( $cm^{-1}$ ) 2913, 2849, 1745, 1471, 1187, 969, 695; HRMS (FAB, NBA + Na matrix) Calcd. for  $C_{59}H_{99}NO_5Na$ : 924.7421 ( $[M + Na]^+$ ), Found: 924.7426.



### $NH_2$ -O-TAGb (**54**)

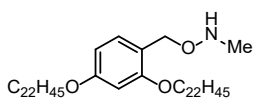
Following the same procedure described for  $NH_2$ -O-TAGa (**17**), phthalimide-O-TAGb (**53**) (7.30 g, 8.1 mmol) was converted to  $NH_2$ -O-TAGb (**54**) (6.25 g, quant.) as a white powder. mp 71–73°C;  $^1H$  NMR (500 MHz,  $CDCl_3$ )  $\delta$  7.23-7.21 (1H, m), 6.46-6.43 (2H, m, overlapped), 5.33 (2H, s), 4.69 (2H, s), 3.96-3.93 (4H, m, overlapped), 1.82-1.74 (4H, m, overlapped), 1.48-1.41 (4H, br m, overlapped), 1.37-1.22 (72H, br m, overlapped), 0.88 (6H, t,  $J = 7.0$  Hz);  $^{13}C$  NMR (125 MHz,  $CDCl_3$ )  $\delta$  160.6, 158.7, 131.4, 117.9, 104.7, 100.0, 73.1, 68.4, 68.2, 32.1, 29.9-29.3 (many signals overlapped), 26.23, 26.21, 22.8, 14.3; IR (KBr)  $\nu$  ( $cm^{-1}$ ) 2915, 2848, 1618, 1471, 1200, 1178, 1041, 717; HRMS (ESI $^+$ ) Calcd. for  $C_{51}H_{98}NO_3$ : 772.7547 ( $[M + H]^+$ ), Found: 772.7550.



### $CH_2=N$ -O-TAGb (**55**)

Following the same procedure described for  $CH_2=N$ -O-TAGa (**18**),  $NH_2$ -O-TAGb (**54**) (3.94 g, 5.1 mmol) was converted to  $CH_2=N$ -O-TAGb (**55**) (4.00 g, quant.) as a white powder. mp 64–65°C;  $^1H$  NMR (500 MHz,  $CDCl_3$ )  $\delta$  7.23-7.21 (1H, m), 7.05 (1H, d,  $J = 8.5$  Hz), 6.45-6.42 (3H, m, overlapped), 5.12 (2H, s), 3.96-3.92 (4H, m, overlapped), 1.81-1.74 (4H, m, overlapped), 1.48-1.41 (4H, br m, overlapped), 1.37-1.22 (72H, br m, overlapped), 0.88 (6H, t,  $J = 7.0$  Hz);  $^{13}C$  NMR (125 MHz,  $CDCl_3$ )  $\delta$  160.6, 158.4, 137.1, 131.1, 118.1, 104.7, 100.0, 71.2, 68.3, 68.2, 32.1, 29.9-29.3 (many signals overlapped), 26.2, 22.8, 14.3; IR (KBr)  $\nu$  ( $cm^{-1}$ ) 2916, 2848, 1613, 1465, 1289, 1183, 1004, 817, 718; HRMS (ESI $^+$ ) Calcd. for  $C_{52}H_{97}NO_3Na$ : 806.7366 ( $[M + Na]^+$ ),

Found: 806.7352.



### *Me-HN-O-TAGb (56)*

Following the same procedure described for Me-HN-O-TAGa (**15**), CH<sub>2</sub>=N-O-TAGb (**55**) (3.95 g, 5.0 mmol) was converted to Me-HN-O-TAGb (**56**) (2.61 g after purification by column chromatography on silica gel (CHCl<sub>3</sub>/*n*-hexane = 1/1 to 5/1 as eluent), 66%) as a white powder. mp 60–61°C; <sup>1</sup>H NMR (500 MHz, CDCl<sub>3</sub>) δ 7.22-7.21 (1H, m), 6.44-6.42 (2H, m, overlapped), 5.49 (1H, br s), 4.70 (2H, s), 3.96-3.91 (4H, m, overlapped), 2.75 (3H, s), 1.81-1.73 (4H, m, overlapped), 1.48-1.41 (4H, br m, overlapped), 1.37-1.22 (72H, br m, overlapped), 0.88 (6H, t, *J* = 7.5 Hz); <sup>13</sup>C NMR (125 MHz, CDCl<sub>3</sub>) δ 160.4, 158.5, 131.2, 118.5, 104.7, 100.0, 70.3, 68.3, 68.2, 39.3, 32.1, 29.9-29.4 (many signals overlapped), 26.3, 26.2, 22.8, 14.3; IR (KBr) ν (cm<sup>-1</sup>) 2915, 2848, 1613, 1466, 1287, 1178, 718; HRMS (ESI<sup>+</sup>) Calcd. for C<sub>52</sub>H<sub>100</sub>NO<sub>3</sub>: 786.7703 ([M + H]<sup>+</sup>), Found: 786.7685.

## 2. Peptide elongations

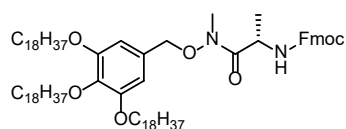
### General procedure for elongation of peptide chain (condensation with Fmoc-protected amino acid)

To a solution of free amine (1.0 eq) in DCM (0.05 M for substrate) were added Fmoc protected amino acid (1.1 eq), 1-hydroxybenzotriazole (HOBt) (1.2 eq), and *N,N'*-diisopropylcarbodiimide (DIC) (1.2 eq (2.3 eq when Fmoc protected amino acid was monohydrate)) in the range of room temperature to 40°C and stirred until the reaction completed (1.5 to 5 h). The reaction mixture was subsequently cooled to 0°C and MeOH (generally 5-fold excess of DCM) was added. The resulting heterogeneous solution was stirred for a further 30 min at 0°C, and the precipitate was filtered and washed with additional MeOH to afford the corresponding Fmoc protected peptide with an anchor molecule as a white to off-white powder.

### General procedure for Fmoc deprotection

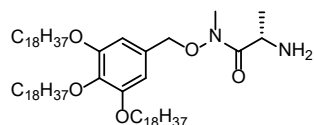
The Fmoc protected amino acid or peptide was dissolved into 10% piperidine/DCM or 1% piperidine/1% 1,8-diazabicyclo[5.4.0]-7-undecene (DBU)/CHCl<sub>3</sub> (0.036 M for substrate) at room temperature, and the solution was stirred until the reaction was completed (generally 0.5 h to 2 h). The reaction mixture was subsequently cooled to 0°C and MeOH (generally 5-fold excess of DCM or CHCl<sub>3</sub>) was added. The resulting heterogeneous solution was stirred for a further 30 min at 0°C, and the precipitate was filtered and washed with additional MeOH to afford the corresponding amine as a white to off-white powder.

## Using TAGa-type anchor molecule



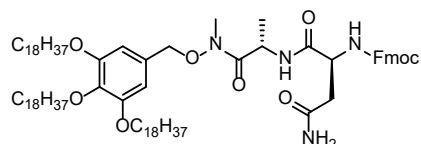
### *Fmoc-Ala-(Me)N-O-TAGa (57)*

Following the general procedure described for condensation, Me-HN-O-TAGa (**15**) (5.00 g, 5.3 mmol) was converted to Fmoc-Ala-(Me)N-O-TAGa (**57**) (6.56 g, quant.) as a white powder.  $[\alpha]_D^{24.3} = +12.1$  (*c* 0.1, CHCl<sub>3</sub>); mp 56–59°C; <sup>1</sup>H NMR (500 MHz, CDCl<sub>3</sub>)  $\delta$  7.77 (2H, d, *J* = 7.5 Hz), 7.62 (2H, t, *J* = 7.5 Hz), 7.40 (2H, t, *J* = 7.5 Hz), 7.32 (2H, t, *J* = 7.5 Hz), 6.63 (2H, s), 5.62 (1H, br d, *J* = 8.5 Hz), 4.92–4.83 (1H, br m), 4.86 (2H, s), 4.40–4.34 (2H, m, overlapped), 4.24 (1H, t, *J* = 7.5 Hz), 4.00–3.94 (6H, m, overlapped), 3.24 (3H, s), 1.83–1.71 (6H, m, overlapped), 1.50–1.44 (6H, br m, overlapped), 1.37–1.22 (87H, br m, overlapped), 0.89 (9H, t, *J* = 7.0 Hz) (Two protons (NH x 2) were not observed.); <sup>13</sup>C NMR (125 MHz, CDCl<sub>3</sub>)  $\delta$  173.9, 155.9, 153.5, 144.1, 143.9, 141.40, 141.38, 138.9, 129.1, 127.8, 127.2, 125.29, 125.25, 120.1, 107.8, 77.7, 73.5, 69.3, 67.1, 47.4, 47.3, 33.9, 32.1, 30.5, 29.9–29.5 (many signals overlapped), 26.2, 22.8, 18.6, 14.2; IR (KBr)  $\nu$  (cm<sup>-1</sup>) 2916, 2849, 1658, 1467, 1243, 1119, 740, 720; HRMS (FAB, NBA + NaI matrix) Calcd. for C<sub>80</sub>H<sub>134</sub>O<sub>7</sub>N<sub>2</sub>Na: 1258.0089 ([M + Na]<sup>+</sup>), Found: 1258.0090.



### *Ala-(Me)N-O-TAGa (19)*

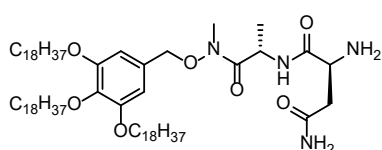
Following the general procedure described for Fmoc deprotection, Fmoc-Ala-(Me)N-O-TAGa (**57**) (3.90 g, 3.2 mmol) was converted to Ala-(Me)N-O-TAGa (**19**) (3.20 g, quant.) as a white powder.  $[\alpha]_D^{24.3} = +5.6$  (*c* 0.1, CHCl<sub>3</sub>); mp 64–65°C; <sup>1</sup>H NMR (500 MHz, CDCl<sub>3</sub>)  $\delta$  6.53 (2H, s), 4.74 (2H, app dd, *J* = 18.5, 10.5 Hz), 3.97–3.93 (6H, m, overlapped), 3.85 (1H, br d, *J* = 6.0 Hz), 3.22 (3H, s), 1.82–1.70 (6H, m, overlapped), 1.49–1.43 (6H, br m, overlapped), 1.37–1.22 (87H, br m, overlapped), 0.87 (9H, t, *J* = 7.0 Hz); <sup>13</sup>C NMR (125 MHz, CDCl<sub>3</sub>)  $\delta$  178.2, 153.5, 139.0, 129.3, 107.7, 77.0, 73.6, 69.4, 47.3, 34.0, 32.1, 30.5, 29.9–29.5 (many signals overlapped), 26.2, 22.8, 20.8, 14.3; IR (KBr)  $\nu$  (cm<sup>-1</sup>) 2915, 2848, 1641, 1469, 1335, 1240, 1123, 719; HRMS (FAB, NBA + NaI matrix) Calcd. for C<sub>65</sub>H<sub>124</sub>O<sub>5</sub>N<sub>2</sub>Na: 1035.9408 ([M + Na]<sup>+</sup>), Found: 1035.9396.



### *Fmoc-Asn-Ala-(Me)N-O-TAGa (58)*

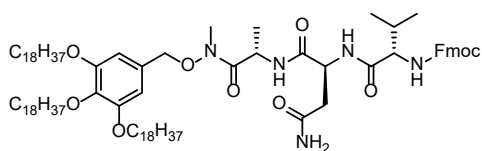
Following the general procedure described for condensation, Ala-(Me)N-O-TAGa (**19**) (5.00 g, 4.9 mmol) was converted to Fmoc-Asn-Ala-(Me)N-O-TAGa (**58**) (6.54 g, 98%) as a white powder.  $[\alpha]_D^{24.4} = +11.9$  (*c* 0.1,

CHCl<sub>3</sub>); mp 134–135°C; <sup>1</sup>H NMR (500 MHz, CDCl<sub>3</sub>) δ 7.75 (2H, d, *J* = 7.5 Hz), 7.60 (2H, br dd, *J* = 7.0, 4.5 Hz), 7.54 (1H, br d, *J* = 7.5 Hz), 7.39 (2H, t, *J* = 7.5 Hz), 7.31 (2H, td, *J* = 7.5, 1.0 Hz), 6.58 (2H, s), 6.36 (1H, br d, *J* = 7.5 Hz), 6.09 (1H, br s), 5.63 (1H, br s), 4.97-4.89 (1H, br m), 4.84 (2H, app dd, *J* = 19.5, 10.0 Hz), 4.60 (1H, br m), 4.41-4.35 (2H, m, overlapped), 4.22 (1H, t, *J* = 7.5 Hz), 3.98-3.93 (6H, m, overlapped), 3.20 (3H, s), 2.93-2.89 (1H, br m), 2.66-2.60 (1H, br m), 1.82-1.71 (6H, m, overlapped), 1.49-1.44 (6H, br m, overlapped), 1.34-1.22 (87H, br m, overlapped), 0.88 (9H, t, *J* = 7.0 Hz); <sup>13</sup>C NMR (125 MHz, CDCl<sub>3</sub>) δ 173.4 (two signals), 170.5, 156.2, 153.5, 144.0, 143.8, 141.4, 138.7, 129.3, 127.8, 127.2, 125.3, 120.1, 107.7, 73.6, 69.3, 67.4, 51.3, 47.2, 46.5, 37.7, 34.0, 32.1, 30.5, 29.9-29.5 (many signals overlapped), 26.3, 22.8, 17.7, 14.3; IR (KBr) ν (cm<sup>-1</sup>) 3403, 3298, 2916, 2848, 1668, 1655, 1468, 1262, 1125, 990, 740, 719; HRMS (FAB, NBA + NaI matrix) Calcd. for C<sub>84</sub>H<sub>140</sub>O<sub>9</sub>N<sub>4</sub>Na: 1372.0518 ([M + Na]<sup>+</sup>), Found: 1372.0538.



#### *Asn-Ala-(Me)N-O-TAGa (20)*

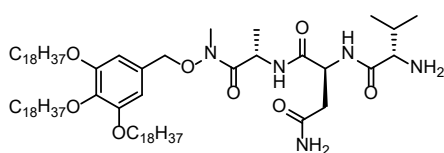
Following the general procedure described for Fmoc deprotection, Fmoc-Asn-Ala-(Me)N-O-TAGa (**58**) (5.00 g, 3.7 mmol) was converted to Asn-Ala-(Me)N-O-TAGa (**20**) (4.18 g, quant.) as a white powder. [ $\alpha$ ]<sub>D</sub><sup>24.5</sup> = -4.2 (*c* 0.1, CHCl<sub>3</sub>); mp 67–69°C; <sup>1</sup>H NMR (500 MHz, CDCl<sub>3</sub>) δ 7.92 (1H, br d, *J* = 7.5 Hz), 6.59 (2H, s), 6.35 (1H, br s), 5.62 (1H, br s), 5.01-4.92 (1H, br m), 4.84 (2H, app dd, *J* = 21.5, 10.5 Hz), 3.98-3.92 (6H, m, overlapped), 3.72-3.68 (1H, m), 3.20 (3H, s), 2.69-2.65 (1H, br m), 2.56-2.51 (1H, br m), 1.82-1.70 (6H, m, overlapped), 1.49-1.43 (6H, br m, overlapped), 1.37-1.21 (87H, br m, overlapped), 0.87 (9H, t, *J* = 7.0 Hz) (Two protons (NH x 2) were not observed.); <sup>13</sup>C NMR (125 MHz, CDCl<sub>3</sub>, Signals were complex due to the rotamers.) δ 173.75, 173.69, 173.55, 173.50, 173.45, 153.4, 138.8, 129.3, 107.8, 77.4, 73.6, 69.3, 52.4, 45.8, 45.6, 40.6, 34.0, 32.1, 30.5, 29.9-29.5 (many signals overlapped), 26.3, 22.8, 18.08, 18.05, 14.3; IR (KBr) ν (cm<sup>-1</sup>) 3366, 2916, 2848, 1659, 1468, 1334, 1122, 719; HRMS (FAB, NBA matrix) Calcd. for C<sub>69</sub>H<sub>131</sub>O<sub>7</sub>N<sub>4</sub>: 1128.0018 ([M + H]<sup>+</sup>), Found: 1128.0023.



#### *Fmoc-Val-Asn-Ala-(Me)N-O-TAGa (59)*

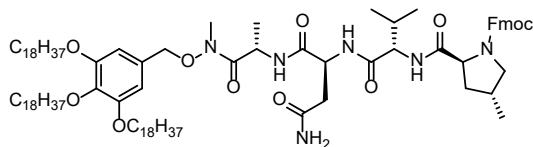
Following the general procedure described for condensation, Asn-Ala-(Me)N-O-TAGa (**20**) (4.10 g, 3.6 mmol) was converted to Fmoc-Val-Asn-Ala-(Me)N-O-TAGa (**59**) (5.27 g, quant.) as a white powder. [ $\alpha$ ]<sub>D</sub><sup>24.5</sup> = -0.1 (*c* 0.1, CHCl<sub>3</sub>); mp 174–179°C; <sup>1</sup>H NMR (500 MHz, CDCl<sub>3</sub>, Signals were complex due to the rotamers.) δ 7.75 (1H, br s), 7.73 (2H, dd, *J* = 7.5, 4.0 Hz), 7.63 (1H, br d, *J* = 7.0 Hz), 7.58 (2H, br d, *J* = 7.5 Hz), 7.36 (2H, app q, *J* = 7.0 Hz), 7.28 (2H, br t, *J* = 7.5 Hz), 6.55 (2H, s), 6.30 (1H, br s), 5.85 (1H, br s), 5.75 (1H, br

d,  $J = 8.0$  Hz), 4.93-4.77 (4H, br m, overlapped), 4.40 (1H, br dd,  $J = 10.5, 8.0$  Hz), 4.31 (1H, br dd,  $J = 10.5, 7.5$  Hz), 4.19 (1H, br t,  $J = 7.0$  Hz), 4.14 (1H, br t,  $J = 7.0$  Hz), 3.97-3.92 (6H, br m, overlapped), 3.17 (3H, s), 2.85-2.81 (1H, m), 2.64-2.60 (1H, m), 2.19-2.12 (1H, m), 1.81-1.71 (6H, m, overlapped), 1.49-1.43 (6H, br m, overlapped), 1.35-1.22 (87H, br m, overlapped), 0.99 (3H, d,  $J = 6.0$  Hz), 0.94 (3H, d,  $J = 7.0$  Hz), 0.88 (9H, t,  $J = 7.0$  Hz);  $^{13}\text{C}$  NMR (125 MHz,  $\text{CDCl}_3$ , Signals were complex due to the rotamers.)  $\delta$  173.6, 173.4, 171.6, 170.2, 156.7, 153.4, 144.0, 143.9, 141.4, 138.8, 129.3, 127.8, 127.22, 127.18, 125.30, 125.25, 120.07, 120.05, 107.7, 73.6, 69.3, 67.3, 60.4, 49.8, 47.3, 46.4, 37.1, 34.0, 32.1, 31.5, 30.5, 29.9-29.5 (many signals overlapped), 26.3, 22.8, 19.4, 17.9, 17.6, 14.3; IR (KBr)  $\nu$  ( $\text{cm}^{-1}$ ) 3272, 2917, 2849, 1639, 1468, 1247, 1120, 719; HRMS (FAB, NBA + NaI matrix) Calcd. for  $\text{C}_{89}\text{H}_{149}\text{O}_{10}\text{N}_5\text{Na}$ : 1471.1202 ( $[\text{M} + \text{Na}]^+$ ), Found: 1471.0200.



#### *Val-Asn-Ala-(Me)N-O-TAGa (21)*

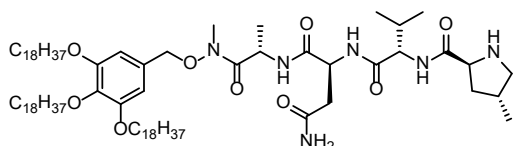
Following the general procedure described for Fmoc deprotection, Fmoc-Val-Asn-Ala-(Me)N-O-TAGa (**59**) (5.21 g, 3.6 mmol) was converted to Val-Asn-Ala-(Me)N-O-TAGa (**21**) (4.41 g, quant.) as a white powder.  $[\alpha]_{\text{D}}^{24.6} = -2.8$  ( $c$  0.1,  $\text{CHCl}_3$ ); mp 81–83°C;  $^1\text{H}$  NMR (500 MHz,  $\text{CDCl}_3$ , Signals were complex due to the rotamers.)  $\delta$  8.40 (1H, d,  $J = 8.0$  Hz), 7.66 (1H, d,  $J = 7.0$  Hz), 6.57 (2H, s), 6.47 (1H, br s), 5.75 (1H, br s), 4.92-4.77 (4H, br m, overlapped), 3.99-3.92 (6H, br m, overlapped), 3.26 (1H, br d,  $J = 3.0$  Hz), 3.18 (3H, s), 2.85-2.81 (1H, m), 2.65-2.60 (1H, m), 2.29-2.20 (1H, m), 1.82-1.70 (6H, m, overlapped), 1.49-1.43 (6H, br m, overlapped), 1.37-1.22 (87H, br m, overlapped), 0.98 (3H, d,  $J = 7.0$  Hz), 0.87 (9H, t,  $J = 7.5$  Hz), 0.83 (3H, d,  $J = 6.5$  Hz) (Two protons ( $\text{NH} \times 2$ ) were not observed.);  $^{13}\text{C}$  NMR (125 MHz,  $\text{CDCl}_3$ , Signals were complex due to the rotamers.)  $\delta$  175.11, 175.05, 173.5, 173.41, 173.36, 170.6, 170.5, 153.4, 138.7, 129.3, 107.7, 73.6, 69.3, 60.3, 49.5, 49.4, 46.45, 46.35, 37.8, 34.0, 32.1, 31.2, 30.5, 29.9-29.5 (many signals overlapped), 26.3, 22.8, 19.8, 17.6, 16.3, 14.2; IR (KBr)  $\nu$  ( $\text{cm}^{-1}$ ) 3277, 2916, 2849, 1637, 1468, 1236, 1121, 720; HRMS (FAB, NBA matrix) Calcd. for  $\text{C}_{74}\text{H}_{140}\text{O}_8\text{N}_5$ : 1227.0702 ( $[\text{M} + \text{H}]^+$ ), Found: 1227.0693.



#### *Fmoc-4-MePro-Val-Asn-Ala-(Me)N-O-TAGa (60)*

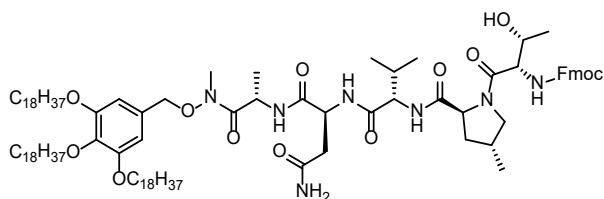
Following the general procedure described for condensation, Val-Asn-Ala-(Me)N-O-TAGa (**21**) (4.40 g, 3.6 mmol) was converted to Fmoc-4-MePro-Val-Asn-Ala-(Me)N-O-TAGa (**60**) (5.60 g, quant.) as a white powder.  $[\alpha]_{\text{D}}^{24.8} = -17.7$  ( $c$  0.1,  $\text{CHCl}_3$ ); mp 169–171°C;  $^1\text{H}$  NMR (500 MHz,  $\text{CDCl}_3$ , Signals were broad and complex due to the rotamers. Those derived from the minor rotamers are not described here.)  $\delta$  7.76-7.69 (3H,

br m, overlapped), 7.61-7.51 (3H, br m, overlapped), 7.39 (2H, br t,  $J = 7.5$  Hz), 7.31 (2H, td,  $J = 7.5, 1.5$  Hz), 6.57 (2H, br s), 6.45 (1H, br s), 5.93 (1H, br s), 5.51 (1H, app br d,  $J = 48$  Hz), 4.92 (1H, br s), 4.86-4.78 (3H, m, overlapped), 4.46-4.33 (3H, br m, overlapped), 4.22 (1H, br t,  $J = 7.0$  Hz), 3.97-3.92 (6H, m, overlapped), 3.65 (1H, br t,  $J = 8.5$  Hz), 3.17 (3H, s), 2.95 (1H, br t,  $J = 10.0$  Hz), 2.79-2.75 (1H, br m), 2.68-2.64 (1H, br m), 2.50-2.06 (4H, br m, overlapped), 1.81-1.70 (6H, m, overlapped), 1.68-1.62 (1H, br m), 1.49-1.43 (6H, br m, overlapped), 1.37-1.22 (87H, br m, overlapped), 1.06 (3H, br d,  $J = 6.5$  Hz), 0.93 (3H, d,  $J = 7.0$  Hz), 0.87 (12H, app t,  $J = 7.0$  Hz);  $^{13}\text{C}$  NMR (125 MHz,  $\text{CDCl}_3$ , Signals were broad and complex due to the rotamers. Those derived from the minor rotamers are not described here.)  $\delta$  173.4 (two signals), 172.4, 171.3, 170.2, 156.3, 153.4, 144.0, 143.8, 141.4, 138.7, 129.4, 127.9, 127.2, 125.1, 120.1, 107.7, 73.6, 69.3, 68.1, 61.3, 58.7, 54.0, 49.9, 47.2, 46.3, 37.2, 36.7, 34.1, 32.7, 32.0, 30.9, 30.5, 29.9-29.5 (many signals overlapped), 26.3, 22.8, 19.5, 17.8, 17.7, 17.3, 14.2; IR (KBr)  $\nu$  ( $\text{cm}^{-1}$ ) 3272, 2916, 2849, 1661, 1638, 1468, 1236, 1122, 739, 720; HRMS (FAB, NBA + NaI matrix) Calcd. for  $\text{C}_{95}\text{H}_{158}\text{O}_{11}\text{N}_6\text{Na}$ : 1582.1886 ( $[\text{M} + \text{Na}]^+$ ), Found: 1582.1896.



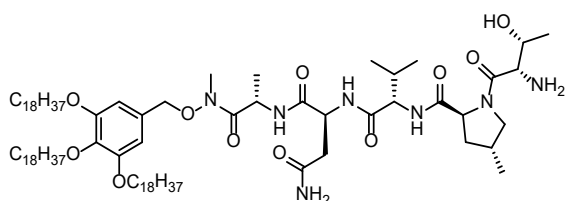
#### 4-MePro-Val-Asn-Ala-(Me)N-O-TAGa (**22**)

Following the general procedure described for Fmoc deprotection, Fmoc-4-MePro-Val-Asn-Ala-(Me)N-O-TAGa (**60**) (5.55 g, 3.6 mmol) was converted to 4-MePro-Val-Asn-Ala-(Me)N-O-TAGa (**22**) (4.76 g, quant.) as a white powder.  $[\alpha]_{\text{D}}^{24.9} = -9.1$  ( $c$  0.1,  $\text{CHCl}_3$ ); mp 100–102°C;  $^1\text{H}$  NMR (500 MHz,  $\text{CDCl}_3$ , Signals were broad and complex due to the rotamers. Those derived from the minor rotamers are not described here.)  $\delta$  8.31 (1H, d,  $J = 8.5$  Hz), 7.81 (1H, br s), 7.61 (1H, d,  $J = 6.5$  Hz), 6.60 (1H, br s), 6.57 (2H, s), 5.88 (1H, br s), 4.91-4.74 (4H, br m, overlapped), 4.28-4.22 (1H, br m), 4.00-3.91 (6H, m, overlapped), 3.81 (1H, br d,  $J = 9.0$  Hz), 3.43-3.35 (1H, br m), 3.17 (3H, s), 3.09-3.02 (1H, br m), 2.81-2.55 (3H, br m, overlapped), 2.30-2.03 (3H, br m, overlapped), 1.81-1.63 (6H, m, overlapped), 1.49-1.43 (6H, br m, overlapped), 1.35-1.22 (87H, br m, overlapped), 0.99 (3H, d,  $J = 6.0$  Hz), 0.95 (3H, d,  $J = 6.5$  Hz), 0.91 (3H, d,  $J = 7.0$  Hz), 0.87 (9H, t,  $J = 7.0$  Hz) (One proton (NH) was not observed.);  $^{13}\text{C}$  NMR (125 MHz,  $\text{CDCl}_3$ , Signals were broad and complex due to the rotamers. Those derived from the minor rotamers are not described here.)  $\delta$  176.4, 173.6, 173.5, 171.6, 170.4, 153.4, 138.7, 129.4, 107.7, 73.6, 69.3, 60.4, 58.1, 54.7, 54.2, 49.9, 48.7, 46.3, 39.0, 36.9, 34.1, 33.3, 32.1, 30.8, 30.5, 29.9-29.5 (many signals overlapped), 26.3, 22.8, 19.6, 17.9, 17.58, 17.56, 14.2; IR (KBr)  $\nu$  ( $\text{cm}^{-1}$ ) 3270, 2916, 2849, 1635, 1468, 1236, 1121, 720; HRMS (FAB, NBA matrix) Calcd. for  $\text{C}_{80}\text{H}_{149}\text{O}_9\text{N}_6$ : 1338.1386 ( $[\text{M} + \text{H}]^+$ ), Found: 1338.1384.



*Fmoc-Thr-4-MePro-Val-Asn-Ala-(Me)N-O-TAGa (61)*

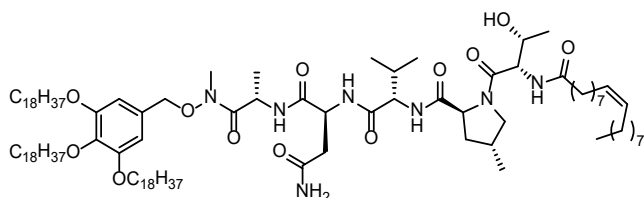
Following the general procedure described for condensation, 4-MePro-Val-Asn-Ala-(Me)N-O-TAGa (**22**) (4.70 g, 3.5 mmol) was converted to Fmoc-Thr-4-MePro-Val-Asn-Ala-(Me)N-O-TAGa (**61**) (5.84 g, quant.) as a white powder.  $[\alpha]_D^{25.0} = -22.8$  ( $c$  0.1,  $\text{CHCl}_3$ ); mp 151–154°C;  $^1\text{H}$  NMR (500 MHz,  $\text{CDCl}_3$ , Signals were broad and complex due to the rotamers. Those derived from the minor rotamers are not described here.)  $\delta$  7.80-7.71 (3H, br m, overlapped), 7.59 (2H, br d,  $J = 7.0$  Hz), 7.37 (2H, br t,  $J = 7.5$  Hz), 7.32-7.28 (3H, br m, overlapped), 7.13 (1H, br d,  $J = 9.5$  Hz), 6.95 (1H, br s), 6.57 (2H, s), 6.31-6.22 (2H, br m, overlapped), 5.01-4.95 (2H, br m, overlapped), 4.84 (1H, d,  $J = 10.5$  Hz), 4.79 (1H, d,  $J = 10.5$  Hz), 4.70 (1H, dd,  $J = 9.5, 3.5$  Hz), 4.63 (1H, dd,  $J = 9.5, 4.0$  Hz), 4.59-4.53 (1H, br m), 4.46 (1H, dd,  $J = 11.0, 7.5$  Hz), 4.35 (1H, dd,  $J = 10.5, 7.0$  Hz), 4.33-4.27 (1H, br m), 4.19 (1H, t,  $J = 6.5$  Hz), 4.03 (1H, br t,  $J = 8.0$  Hz), 3.97-3.92 (6H, m, overlapped), 3.32 (1H, br t,  $J = 9.0$  Hz), 3.17 (3H, s), 2.81-2.69 (2H, br m, overlapped), 2.52-2.41 (1H, br m), 2.24-2.16 (2H, br m, overlapped), 1.96-1.89 (1H, m), 1.80-1.70 (6H, m, overlapped), 1.49-1.42 (6H, br m, overlapped), 1.35-1.22 (90H, br m, overlapped), 1.09 (3H, d,  $J = 6.0$  Hz), 0.94 (3H, d,  $J = 6.5$  Hz), 0.87 (12H, app t,  $J = 7.0$  Hz) (One proton (NH or OH) was not observed.);  $^{13}\text{C}$  NMR (125 MHz,  $\text{CDCl}_3$ , Signals were broad and complex due to the rotamers. Those derived from the minor rotamers are not described here.)  $\delta$  173.9, 173.3, 172.2, 171.7, 171.3, 169.9, 156.4, 153.4, 143.9, 143.8, 141.4, 138.7, 129.5, 127.9, 127.2, 125.21, 125.16, 120.1, 107.7, 73.6, 69.3, 68.0, 67.0, 61.5, 58.1, 57.0, 54.6, 50.5, 47.3, 46.2, 42.3, 37.8, 37.1, 34.2, 33.0, 32.1, 31.0, 30.5, 29.9-29.5 (many signals overlapped), 26.3, 23.6, 22.8, 19.5, 18.8, 18.0, 17.9, 17.4, 14.3; IR (KBr)  $\nu$  ( $\text{cm}^{-1}$ ) 3286, 2917, 2849, 1638, 1467, 1439, 1236, 1119, 720; HRMS (FAB, NBA + NaI matrix) Calcd. for  $\text{C}_{99}\text{H}_{165}\text{O}_{13}\text{N}_7\text{Na}$ : 1683.2363 ( $[\text{M} + \text{Na}]^+$ ), Found: 1683.2360.



*Thr-4-MePro-Val-Asn-Ala-(Me)N-O-TAGa (23)*

Following the general procedure described for Fmoc deprotection, Fmoc-Thr-4-MePro-Val-Asn-Ala-(Me)N-O-TAGa (**61**) (5.78 g, 3.5 mmol) was converted to Thr-4-MePro-Val-Asn-Ala-(Me)N-O-TAGa (**23**) (5.01 g, quant.) as a white powder.  $[\alpha]_D^{25.1} = -35.3$  ( $c$  0.1,  $\text{CHCl}_3$ ); mp ca. 190°C (decomp.);  $^1\text{H}$  NMR (500 MHz,  $\text{CDCl}_3$ , Signals were broad and complex due to the rotamers. Those derived from the minor rotamers are not described here.)  $\delta$  7.34-7.30 (3H, br m, overlapped), 7.17 (1H, br s), 6.81 (1H, br s), 6.58 (2H, s), 5.01-4.92 (1H, br m), 4.93 (1H, dd,  $J = 9.5, 4.5$  Hz), 4.85 (1H, d,

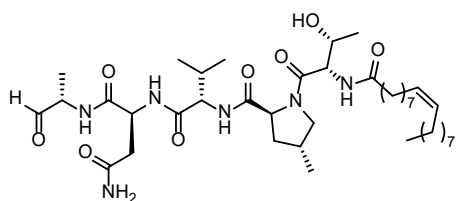
$J = 10.0$  Hz), 4.79 (1H, d,  $J = 10.5$  Hz), 4.66-4.58 (2H, br m), 4.14-4.08 (1H, br m), 3.98-3.92 (6H, m, overlapped), 3.84-3.74 (1H, br m), 3.33-3.28 (1H, br m), 3.26-3.12 (1H, br m, overlapped), 3.17 (3H, s, overlapped), 2.78-2.63 (2H, br m, overlapped), 2.50-2.39 (1H, br m), 2.24-2.19 (1H, br m), 2.16-2.08 (2H, m), 1.89-1.67 (7H, m, overlapped), 1.49-1.43 (6H, br m, overlapped), 1.37-1.22 (90H, br m, overlapped), 1.09 (3H, d,  $J = 6.0$  Hz), 0.94 (3H, d,  $J = 7.0$  Hz), 0.87 (12H, app t,  $J = 7.0$  Hz) (One proton (NH or OH) was not observed.);  $^{13}\text{C}$  NMR (125 MHz,  $\text{CDCl}_3$ , Signals were broad and complex due to the rotamers. Those derived from the minor rotamers are not described here.)  $\delta$  174.2, 173.3 (two signals), 172.4, 171.5, 170.1, 153.4, 138.8, 129.4, 107.7, 73.6, 70.1, 69.3, 61.7, 57.7, 56.4, 54.5, 50.5, 46.0, 37.6, 37.2, 34.1, 32.9, 32.1, 30.5, 29.9-29.5 (many signals overlapped), 26.3, 22.8, 19.5, 18.0, 17.9, 17.5, 17.3, 14.2; IR (KBr)  $\nu$  ( $\text{cm}^{-1}$ ) 3292, 2917, 2849, 1644, 1468, 1237, 1117, 720; HRMS (FAB, NBA matrix) Calcd. for  $\text{C}_{84}\text{H}_{155}\text{O}_{11}\text{N}_7$ : 1439.1863 ( $[\text{M} + \text{H}]^+$ ), Found: 1439.1868.



#### *Oleic acid-Thr-4-MePro-Val-Asn-Ala-(Me)N-O-TAGa (24)*

Following the general procedure described for condensation using oleic acid instead of Fmoc protected amino acid, Thr-4-MePro-Val-Asn-Ala-(Me)N-O-TAGa (**23**) (2.97 g, 2.1 mmol) was converted to oleic acid-Thr-4-MePro-Val-Asn-Ala-(Me)N-O-TAGa (**24**) (3.52 g, quant.) as a white powder. Advanced Marfey's method for all the amino acid residues after complete acid hydrolysis in the same way as described above in **Table 7** in **Chapter 3** confirmed that no epimerization occurred.  $[\alpha]_{\text{D}}^{25.1} = -11.9$  ( $c$  0.1,  $\text{CHCl}_3$ ); mp 151–152°C;  $^1\text{H}$  NMR (500 MHz,  $\text{CDCl}_3$ )  $\delta$  7.78 (1H, br d,  $J = 8.0$  Hz), 7.30 (1H, br d,  $J = 7.5$  Hz), 7.09 (1H, d,  $J = 9.5$  Hz), 7.03 (1H, br s), 6.77 (1H, br d,  $J = 8.5$  Hz), 6.57 (2H, s), 6.37 (1H, br s), 5.37-5.29 (2H, m, overlapped), 4.98 (1H, dd,  $J = 7.5, 4.0$  Hz), 4.95-4.89 (2H, br m, overlapped), 4.85 (1H, d,  $J = 10.5$  Hz), 4.80 (1H, d,  $J = 10.5$  Hz), 4.59 (1H, dd,  $J = 9.0, 4.0$  Hz), 4.55 (1H, dd,  $J = 9.0, 6.5$  Hz), 4.46 (1H, d,  $J = 6.0$  Hz), 4.32-4.26 (1H, m), 4.03 (1H, dd,  $J = 9.5, 7.5$  Hz), 3.98-3.92 (6H, m, overlapped), 3.36 (1H, br t,  $J = 9.5$  Hz), 3.18 (3H, s), 2.81-2.78 (1H, m), 2.72-2.68 (1H, m), 2.52-2.41 (1H, m), 2.34 (2H, t,  $J = 8.0$  Hz), 2.20-2.15 (2H, br m, overlapped), 2.20-1.98 (3H, m, overlapped), 1.93-1.87 (1H, m), 1.82-1.72 (6H, m, overlapped), 1.66-1.58 (2H, br m, overlapped), 1.49-1.43 (6H, br m, overlapped), 1.37-1.22 (110H, br m, overlapped), 1.09 (3H, d,  $J = 7.0$  Hz), 0.94 (3H, d,  $J = 6.5$  Hz), 0.89-0.86 (15H, m, overlapped) (One proton (NH or OH) was not observed.);  $^{13}\text{C}$  NMR (125 MHz,  $\text{CDCl}_3$ )  $\delta$  173.8, 173.4 (two signals), 172.2, 171.7, 171.5, 169.9, 153.5, 138.8, 130.1, 129.9, 129.4, 107.7, 73.6, 69.4, 67.9, 61.5, 58.0, 54.7, 50.6, 46.2, 37.7, 37.1, 36.6, 34.1, 33.0, 32.1, 31.3, 30.5, 29.9-29.3 (many signals overlapped), 27.4, 27.3, 26.3, 25.7, 22.8, 19.5, 18.9, 17.93, 17.86, 17.3, 14.3; IR (KBr)  $\nu$  ( $\text{cm}^{-1}$ ) 3279, 2917, 2849, 1640, 1438, 1238, 1121, 719; HRMS (FAB, NBA + NaI matrix) Calcd. for  $\text{C}_{102}\text{H}_{187}\text{O}_{12}\text{N}_7\text{Na}$ : 1725.4135 ( $[\text{M} + \text{Na}]^+$ ), Found: 1725.4131.

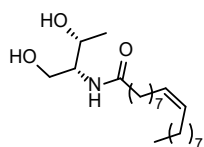
### 3. Reduction to afford the aldehyde



#### *Oleic acid-Thr-4-MePro-Val-Asn-Ala-H (13)*

To a solution of **24** (850 mg, 0.50 mmol, 1.0 eq) in dehydrated THF (50 mL, 0.01 M) was added dropwise 1.0 M LiAlH(*Or*-Bu)<sub>3</sub> in dehydrated THF (4.99 mL, 10 eq, prepared by the procedure described in the literature.<sup>[53]</sup>) at room temperature. After stirring for 1 h at room temperature, the reaction mixture was then treated with aqueous 1M HCl (25 mL) at 0°C to quench the excess LiAlH(*Or*-Bu)<sub>3</sub>. After stirring for 10 min at room temperature, MeOH (250 mL) was added. The resulting heterogeneous solution was stirred for a further 30 min at room temperature, and the precipitate was filtered and washed with additional MeOH. The filtrate was roughly concentrated *in vacuo*, poured into a separatory funnel containing aqueous 1M HCl (20 mL), and extracted with CHCl<sub>3</sub> (3 × 20 mL). The combined organic extracts were dried with Na<sub>2</sub>SO<sub>4</sub>, filtered, and concentrated *in vacuo*. The residue was purified by flash column chromatography on silica gel (CHCl<sub>3</sub>/MeOH = 50/1 to 10/1 as eluent) to afford aldehyde **13** (240.0 mg, 63%) as a white powder and MePro-Thr amide bond-cleaved alcohol **62** (37.5 mg, 20% yield) as a colorless oil (the structure is shown below).

$[\alpha]_D^{24.6} = -33.8$  (*c* 0.1, DMSO),  $[\alpha]_D^{24.6} = -29.6$  (*c* 0.1, CHCl<sub>3</sub>); mp 170–175°C; <sup>1</sup>H NMR (500 MHz, DMSO-*d*<sub>6</sub>, Signals derived from the diastereomer of the α-position of alaninal moiety were not observed at all.) δ 9.34 (1H, s), 8.14 (1H, d, *J* = 6.5 Hz), 8.11 (1H, d, *J* = 7.5 Hz), 7.87 (2H, app dd, *J* = 8.0, 1.5 Hz), 7.37 (1H, br s), 6.93 (1H, br s), 5.35-5.29 (2H, m, overlapped), 4.67 (1H, d, *J* = 6.0 Hz), 4.55-4.47 (2H, m, overlapped), 4.41 (1H, t, *J* = 7.5 Hz), 4.09-3.98 (2H, m, overlapped), 3.83-3.76 (2H, m, overlapped), 3.27 (1H, t, *J* = 9.5 Hz), 2.55-2.46 (2H, m, overlapped with solvent residual signals), 2.38-2.30 (1H, m), 2.17-2.06 (2H, m, overlapped), 2.01-1.94 (6H, m, overlapped), 1.68-1.62 (1H, m), 1.48-1.42 (2H, m, overlapped), 1.32-1.19 (20H, br m, overlapped), 1.14 (3H, d, *J* = 7.5 Hz), 1.08 (3H, d, *J* = 6.0 Hz), 0.97 (3H, d, *J* = 7.0 Hz), 0.86-0.82 (9H, m, overlapped); <sup>13</sup>C NMR (125 MHz, DMSO-*d*<sub>6</sub>) δ 201.4, 172.2, 171.9, 171.4, 171.3, 170.6, 169.5, 129.7, 66.9, 59.2, 58.0, 56.2, 54.0, 53.9, 49.5, 36.8, 36.5, 34.9, 32.0, 31.3, 30.4, 29.2-28.6 (many signals overlapped), 26.64, 26.60, 25.3, 22.1, 19.4, 19.1, 18.0, 17.2, 14.0, 13.6; IR (KBr) ν (cm<sup>-1</sup>) 3285, 2924, 2853, 1736, 1639, 1542, 1426, 1235; HRMS (ESI<sup>+</sup>) Calcd. for C<sub>40</sub>H<sub>70</sub>N<sub>6</sub>O<sub>8</sub>Na: 785.5153 ([M + Na]<sup>+</sup>), Found: 785.5151.

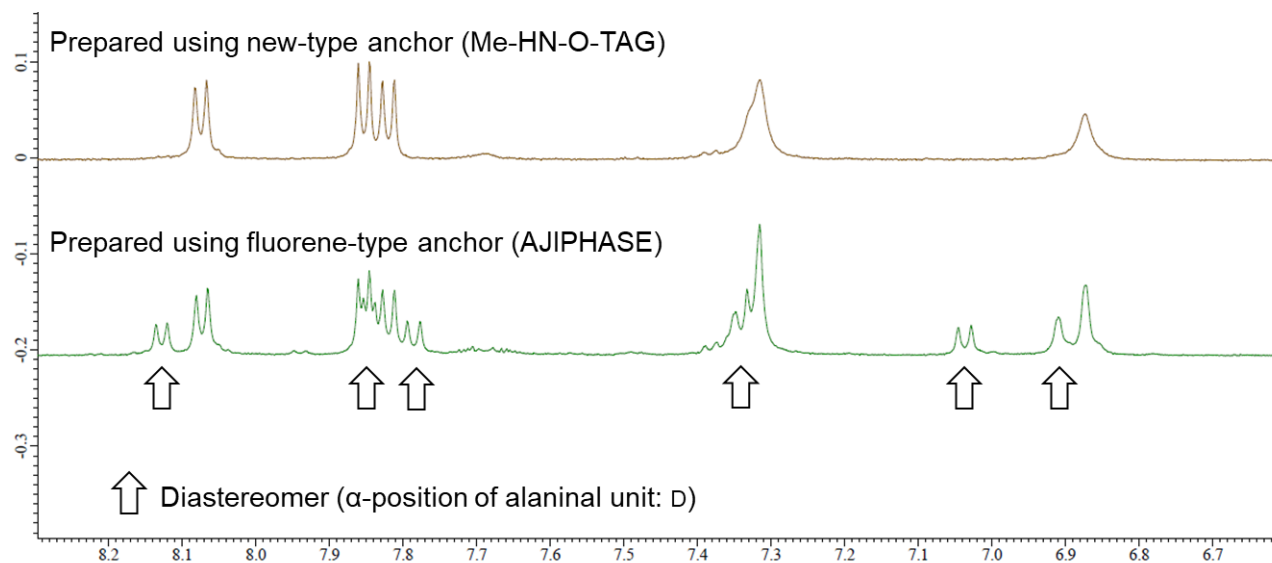


#### *MePro-Thr amide bond-cleaved alcohol 62*

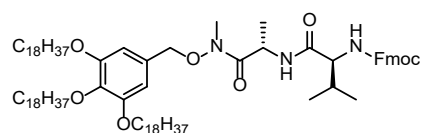
$[\alpha]_D^{25.2} = -25.7$  (*c* 0.1, CHCl<sub>3</sub>); <sup>1</sup>H NMR (500 MHz, DMSO-*d*<sub>6</sub>) δ 7.24 (1H, br d, *J* = 9.0 Hz), 5.35-5.28 (2H, m, overlapped), 4.55-4.51 (2H, br m, overlapped), 3.85 (1H, br m), 3.62 (1H, m), 3.42 (1H, br m), 3.29



$^1\text{H}$  NMR (DMSO- $d_6$ , 500 MHz) of kozupeptin A (**1a**)

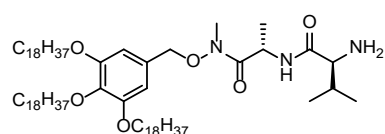


### Use of a model substrate



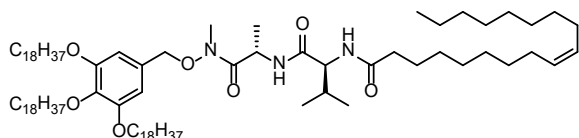
#### *Fmoc-Val-Ala-(Me)N-O-TAGa* (**63**)

Following the general procedure described for condensation, Ala-(Me)N-O-TAGa (**19**) (817 mg, 0.81 mmol) was converted to Fmoc-Val-Ala-(Me)N-O-TAGa (**63**) (1.08 g, quant.) as a white powder.  $[\alpha]_D^{24.3} = -13.8$  ( $c$  0.1,  $\text{CHCl}_3$ ); mp 65–69°C;  $^1\text{H}$  NMR (500 MHz,  $\text{CDCl}_3$ )  $\delta$  7.76 (2H, d,  $J = 7.5$  Hz), 7.61 (2H, br dd,  $J = 7.5, 4.0$  Hz), 7.39 (2H, br td,  $J = 7.5, 2.0$  Hz), 7.33–7.29 (2H, m), 6.63 (1H, br s, overlapped), 6.60 (2H, s), 5.43 (1H, br d,  $J = 9.0$  Hz), 5.08–5.01 (1H, br m), 4.85 (2H, br s), 4.45 (1H, dd,  $J = 10.5, 7.5$  Hz), 4.36 (1H, dd,  $J = 11.0, 6.5$  Hz), 4.23 (1H, t,  $J = 7.0$  Hz), 4.07 (1H, br dd,  $J = 8.5, 6.5$  Hz), 3.99–3.94 (6H, m, overlapped), 3.21 (3H, s), 2.17–2.08 (1H, m), 1.82–1.71 (6H, m, overlapped), 1.50–1.44 (6H, br m, overlapped), 1.36–1.22 (87H, br m, overlapped), 0.97 (3H, d,  $J = 6.5$  Hz), 0.94 (3H, d,  $J = 7.0$  Hz), 0.88 (9H, t,  $J = 7.5$  Hz);  $^{13}\text{C}$  NMR (125 MHz,  $\text{CDCl}_3$ , Signals were complex due to the rotamers.)  $\delta$  173.4, 170.8, 156.4, 153.5, 144.1, 143.9, 141.4, 138.9, 129.1, 127.8, 127.2, 125.3, 125.2, 120.11, 120.09, 107.8, 77.6, 73.6, 69.3, 67.2, 60.3, 47.3, 46.0, 34.1, 32.1, 31.7, 30.5, 29.9–29.5 (many signals overlapped), 26.3, 22.8, 19.3, 18.3, 17.9, 14.3; IR (KBr)  $\nu$  ( $\text{cm}^{-1}$ ) 3290, 2916, 2849, 1644, 1468, 1237, 1119, 739, 721; HRMS (FAB, NBA + NaI matrix) Calcd. for  $\text{C}_{85}\text{H}_{143}\text{N}_3\text{O}_8\text{Na}$ : 1357.0773 ( $[\text{M} + \text{Na}]^+$ ), Found: 1357.0785.



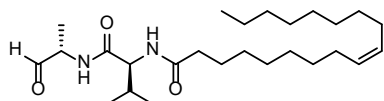
#### *Val-Ala-(Me)N-O-TAGa* (**64**)

Following the general procedure described for Fmoc deprotection, Fmoc-Val-Ala-(Me)N-O-TAGa (**63**) (965 mg, 0.72 mmol) was converted to Val-Ala-(Me)N-O-TAGa (**64**) (804 mg, quant.) as a white powder.  $[\alpha]_D^{24.4} = -10.0$  ( $c$  0.1,  $\text{CHCl}_3$ ); mp 58–59°C;  $^1\text{H NMR}$  (500 MHz,  $\text{CDCl}_3$ )  $\delta$  7.82 (1H, br d,  $J = 8.0$  Hz), 6.62 (2H, s), 5.13-5.06 (1H, br m), 4.89 (1H, d,  $J = 10.0$  Hz), 4.84 (1H, d,  $J = 10.5$  Hz), 4.01-3.91 (6H, m, overlapped), 3.25 (1H, d,  $J = 4.0$  Hz), 3.20 (3H, s), 2.31-2.22 (1H, m), 1.82-1.70 (6H, br m, overlapped), 1.49-1.43 (6H, br m, overlapped), 1.36-1.22 (87H, br m, overlapped), 1.00 (3H, d,  $J = 7.0$  Hz), 0.89-0.85 (12H, m, overlapped) (Two protons ( $\text{NH} \times 2$ ) were not observed.);  $^{13}\text{C NMR}$  (125 MHz,  $\text{CDCl}_3$ , Signals were complex due to the rotamers.)  $\delta$  173.94, 173.87, 153.5, 138.8, 129.3, 107.9, 77.7, 73.6, 69.3, 60.3, 45.3, 34.0, 32.1, 31.2, 30.5, 29.9-29.5 (many signals overlapped), 26.3, 22.8, 19.8, 18.5, 16.4, 14.3; IR (KBr)  $\nu$  ( $\text{cm}^{-1}$ ) 2916, 2849, 1659, 1467, 1236, 1119, 720; HRMS (FAB, NBA matrix) Calcd. for  $\text{C}_{70}\text{H}_{134}\text{O}_6\text{N}_3$ : 1113.0273 ( $[\text{M} + \text{H}]^+$ ), Found: 1113.0282.



#### *Oleic acid-Val-Ala-(Me)N-O-TAGa (25)*

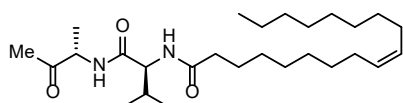
Following the general procedure described for condensation using oleic acid instead of Fmoc protected amino acid, Val-Ala-(Me)N-O-TAGa (**64**) (770 mg, 0.72 mmol) was converted to oleic acid-Val-Ala-(Me)N-O-TAGa (**25**) (933 mg, 98%) as a white powder.  $[\alpha]_D^{24.4} = -11.6$  ( $c$  0.1,  $\text{CHCl}_3$ ); mp 54–55°C;  $^1\text{H NMR}$  (500 MHz,  $\text{CDCl}_3$ )  $\delta$  6.70 (1H, br d,  $J = 7.0$  Hz), 6.59 (2H, s), 6.11 (1H, br d,  $J = 7.5$  Hz), 5.36-5.29 (2H, m, overlapped), 5.05-4.97 (1H, br m), 4.83 (2H, s), 4.36 (1H, dd,  $J = 8.5, 6.5$  Hz), 3.99-3.93 (6H, m, overlapped), 3.20 (3H, s), 2.27-2.17 (2H, m), 2.10-2.03 (1H, m), 2.01-1.98 (3H, br m, overlapped), 1.82-1.70 (6H, m, overlapped), 1.68-1.59 (2H, br m, overlapped), 1.49-1.43 (6H, br m, overlapped), 1.36-1.22 (107H, br m, overlapped), 0.94 (3H, d,  $J = 7.0$  Hz), 0.92 (3H, d,  $J = 6.5$  Hz), 0.87 (12H, t,  $J = 7.0$  Hz) (One proton ( $\text{NH}$ ) was not observed.);  $^{13}\text{C NMR}$  (125 MHz,  $\text{CDCl}_3$ , Signals were complex because of the rotamers.)  $\delta$  173.4, 173.2, 170.8, 153.5, 138.9, 130.1, 129.9, 129.2, 107.8, 77.6, 73.6, 69.3, 58.0, 45.9, 36.9, 34.1, 32.1, 32.0, 31.7, 30.5, 29.9-29.3 (many signals overlapped), 27.34, 27.30, 26.3, 25.9, 22.8, 19.3, 18.19, 18.16, 14.2; IR (KBr)  $\nu$  ( $\text{cm}^{-1}$ ) 3303, 2917, 2849, 1638, 1467, 1235, 1118, 721; HRMS (FAB, NBA + NaI matrix) Calcd. for  $\text{C}_{88}\text{H}_{165}\text{N}_3\text{O}_7\text{Na}$ : 1399.2545 ( $[\text{M} + \text{Na}]^+$ ), Found: 1399.2542.



#### *Oleic acid-Val-Ala-H (26)*

To a solution of **25** (20.0 mg, 0.015 mmol, 1.0 eq) in dehydrated THF (1.8 mL, 0.008 M) was added dropwise 2.0 M  $\text{LiAlH}_4$  in dehydrated THF (8.7  $\mu\text{L}$ , 1.2 eq) at 0°C. After stirring for 15 min at 0°C, the reaction mixture was then treated with aqueous 1M HCl (0.9 mL) at 0°C to quench the excess  $\text{LiAlH}_4$ . After

stirring for 10 min at room temperature, MeOH (9.0 mL) was added. The resulting heterogeneous solution was stirred for a further 30 min at room temperature, and the precipitate was filtered and washed with additional MeOH. The filtrate was roughly concentrated *in vacuo*, poured into a separatory funnel containing aqueous 1M HCl (10 mL), and extracted with CHCl<sub>3</sub> (3 × 10 mL). The combined organic extracts were dried with Na<sub>2</sub>SO<sub>4</sub>, filtered, and concentrated *in vacuo*. The residue was purified by flash column chromatography on silica gel (CHCl<sub>3</sub>/MeOH = 200/1 to 20/1 as eluent) to afford aldehyde **26** (5.6 mg, 89%) as a white powder.  $[\alpha]_D^{24.5} = -12.5$  (*c* 0.1, CHCl<sub>3</sub>); mp 96–99°C; <sup>1</sup>H NMR (500 MHz, DMSO-*d*<sub>6</sub>, Signals were broad and complex due to the rotamers. Those derived from the minor rotamers are not described here.) δ 9.37 (1H, s), 8.45 (1H, d, *J* = 6.0 Hz), 7.83 (1H, d, *J* = 7.5 Hz), 5.35-5.29 (2H, m, overlapped), 4.22-4.17 (1H, m), 4.10-4.04 (1H, m), 2.21-2.07 (2H, m, overlapped), 1.99-1.91 (5H, m, overlapped), 1.53-1.42 (2H, m, overlapped), 1.30-1.22 (20H, br m, overlapped), 1.16 (3H, d, *J* = 7.5 Hz), 0.88-0.84 (9H, m, overlapped); <sup>13</sup>C NMR (125 MHz, DMSO-*d*<sub>6</sub>, Signals were broad and complex due to the rotamers. Those derived from the minor rotamers are not described here.) δ 201.9, 173.2, 172.5, 130.5, 58.2, 54.7, 36.1, 32.2, 31.3, 30.0-29.5 (many signals overlapped), 27.53, 27.49, 26.3, 23.0, 20.1, 19.1, 14.9, 14.4; IR (KBr) ν (cm<sup>-1</sup>) 3284, 2919, 2850, 1733, 1633, 1541, 1466, 1386, 693; HRMS (FAB, NBA matrix) Calcd. for C<sub>26</sub>H<sub>49</sub>O<sub>3</sub>N<sub>2</sub>: 437.3743 ([M + H]<sup>+</sup>), Found: 437.3747.



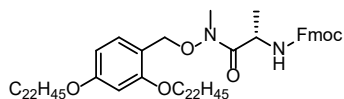
#### Oleic acid-Val-Ala-Me (**27**)

To a solution of **25** (20.0 mg, 0.015 mmol, 1.0 eq) in dehydrated THF (1.8 mL, 0.008 M) was added dropwise 1.11 M MeLi in dehydrated diethyl ether (Et<sub>2</sub>O) (131 μL, 10 eq) at 0°C. After stirring for 20 min at 0°C, the reaction mixture was then treated with aqueous 1M HCl (0.9 mL) at 0°C to quench the excess MeLi. After stirring for 10 min at room temperature, MeOH (9.0 mL) was added. The resulting heterogeneous solution was stirred for a further 30 min at room temperature, and the precipitate was filtered and washed with additional MeOH. The filtrate was roughly concentrated *in vacuo*, poured into a separatory funnel containing aqueous 1M HCl (10 mL), and extracted with CHCl<sub>3</sub> (3 × 10 mL). The combined organic extracts were dried with Na<sub>2</sub>SO<sub>4</sub>, filtered, and concentrated *in vacuo*. The residue was purified by PLC on silica gel (CHCl<sub>3</sub>/MeOH = 10/1) to afford methyl ketone **27** (5.9 mg, 91%) as a white powder.  $[\alpha]_D^{24.5} = -9.0$  (*c* 0.1, CHCl<sub>3</sub>); mp 93–97°C; <sup>1</sup>H NMR (500 MHz, DMSO-*d*<sub>6</sub>, Signals were broad and complex due to the rotamers.) δ 8.34-8.30 (1H, m), 7.84-7.79 (1H, m), 5.35-5.29 (2H, m, overlapped), 4.23-4.11 (2H, m, overlapped), 2.20-2.07 (2H, m, overlapped), 2.06 & 2.04 (3H, two s, presumed to be derived from two rotamers) 1.99-1.90 (5H, m, overlapped), 1.51-1.42 (2H, br m, overlapped), 1.30-1.22 (20H, br m, overlapped), 1.15 (3H, t, *J* = 7.0 Hz), 0.87-0.83 (9H, m, overlapped); <sup>13</sup>C NMR (125 MHz, DMSO-*d*<sub>6</sub>, Signals were complex due to the rotamers.) δ 208.0, 207.4, 172.3, 172.2, 171.3, 171.1, 129.6, 57.7, 57.3, 54.1, 54.0, 35.1, 31.3, 30.4, 30.2, 29.1-28.6 (many signals overlapped), 26.61, 26.57, 26.1, 25.7, 25.41, 25.38, 22.1, 19.24, 19.19, 18.4, 18.1,

15.8, 15.6, 14.0; IR (KBr)  $\nu$  ( $\text{cm}^{-1}$ ) 3284, 2921, 2851, 1720, 1633, 1540, 1467, 1386, 719; HRMS (ESI<sup>+</sup>) Calcd. for  $\text{C}_{27}\text{H}_{50}\text{N}_2\text{O}_3\text{Na}$ : 473.3719 ( $[\text{M} + \text{Na}]^+$ ), Found: 473.3720.

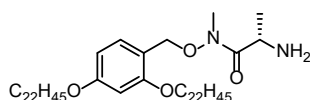
## 4. Application of orthogonal TAGs to rapid analog synthesis

### Peptide elongation using TAGb-type anchor molecule



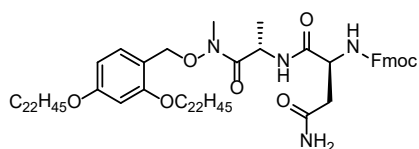
#### *Fmoc-Ala-(Me)N-O-TAGb (65)*

Following the general procedure described for condensation, Me-HN-O-TAGb (**56**) (1.50 g, 1.9 mmol) was converted to Fmoc-Ala-(Me)N-O-TAGb (**65**) (2.03 g, 99%) as a white powder.  $[\alpha]_{\text{D}}^{24.3} = 23.6$  ( $c$  0.1,  $\text{CHCl}_3$ ); mp 53–54°C;  $^1\text{H}$  NMR (500 MHz,  $\text{CDCl}_3$ )  $\delta$  7.76 (2H, d,  $J = 7.5$  Hz), 7.62 (2H, d,  $J = 7.0$  Hz), 7.40 (2H, t,  $J = 7.5$  Hz), 7.32 (2H, t,  $J = 7.5$  Hz), 7.24 (1H, br d,  $J = 8.0$  Hz), 6.45–6.43 (2H, br m, overlapped), 5.59 (1H, br d,  $J = 8.5$  Hz), 4.97 (1H, d,  $J = 9.5$  Hz), 4.88–4.84 (2H, br m, overlapped), 4.39–4.31 (2H, m, overlapped), 4.23 (1H, t,  $J = 7.5$  Hz), 4.04–3.95 (2H, br m, overlapped), 3.91 (2H, t,  $J = 7.0$  Hz), 3.27 (3H, s), 1.84–1.79 (2H, m), 1.76–1.70 (2H, m), 1.48–1.38 (4H, br m, overlapped), 1.34–1.22 (75H, br m, overlapped), 0.88 (6H, t,  $J = 7.0$  Hz);  $^{13}\text{C}$  NMR (125 MHz,  $\text{CDCl}_3$ , Signals were complex due to the rotamers.)  $\delta$  173.7, 161.7, 159.1, 155.7, 144.2, 144.0, 141.43, 141.40, 133.0, 127.8, 127.2, 125.4, 125.3, 120.1, 114.6, 104.9, 99.9, 71.6, 68.33, 68.27, 67.0, 47.4, 47.3, 33.5, 32.1, 29.9–29.3 (many signals overlapped), 26.23, 26.17, 22.8, 18.8, 14.3; IR (KBr)  $\nu$  ( $\text{cm}^{-1}$ ) 3315, 2916, 2849, 1717, 1669, 1468, 1253, 1178, 1131, 1034, 739; HRMS (FAB, NBA + NaI matrix) Calcd. for  $\text{C}_{70}\text{H}_{114}\text{N}_2\text{O}_6\text{Na}$ : 1101.8575 ( $[\text{M} + \text{Na}]^+$ ), Found: 1101.8588.



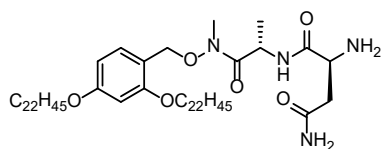
#### *Ala-(Me)N-O-TAGb (66)*

Following the general procedure described for Fmoc deprotection, Fmoc-Ala-(Me)N-O-TAGb (**65**) (1.67 g, 1.6 mmol) was converted to Ala-(Me)N-O-TAGb (**66**) (1.30 g, 98%) as a white powder.  $[\alpha]_{\text{D}}^{24.4} = 15.2$  ( $c$  0.1,  $\text{CHCl}_3$ ); mp 55°C;  $^1\text{H}$  NMR (500 MHz,  $\text{CDCl}_3$ )  $\delta$  7.16 (1H, d,  $J = 8.0$  Hz), 6.45–6.42 (2H, m, overlapped), 4.86 (1H, d,  $J = 10.0$  Hz), 4.77 (1H, d,  $J = 9.5$  Hz), 3.98–3.92 (5H, m, overlapped), 3.25 (3H, s), 1.84–1.73 (4H, m, overlapped), 1.48–1.41 (4H, br m, overlapped), 1.35–1.20 (75H, br m, overlapped), 0.87 (6H, t,  $J = 7.0$  Hz) (Two protons ( $\text{NH} \times 2$ ) were not observed.);  $^{13}\text{C}$  NMR (125 MHz,  $\text{CDCl}_3$ )  $\delta$  177.6, 161.7, 159.1, 132.9, 114.8, 104.9, 99.8, 71.0, 68.34, 68.30, 46.8, 33.4, 32.1, 29.9–29.3 (many signals overlapped), 26.24, 26.17, 22.8, 20.4, 14.3; IR (KBr)  $\nu$  ( $\text{cm}^{-1}$ ) 2915, 2849, 1658, 1614, 1470, 1181, 1131, 718; HRMS (FAB, NBA + NaI matrix) Calcd. for  $\text{C}_{55}\text{H}_{104}\text{N}_2\text{O}_4\text{Na}$ : 879.7894 ( $[\text{M} + \text{Na}]^+$ ), Found: 879.7898.



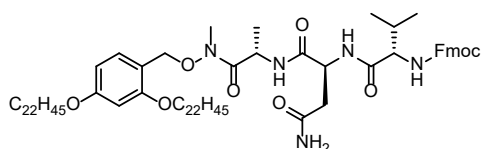
***Fmoc-Asn-Ala-(Me)N-O-TAGb (67)***

Following the general procedure described for condensation, Ala-(Me)N-O-TAGb (**66**) (1.25 g, 1.5 mmol) was converted to Fmoc-Asn-Ala-(Me)N-O-TAGb (**67**) (1.74 g, quant.) as a white powder.  $[\alpha]_D^{24.4} = 20.5$  (*c* 0.1, CHCl<sub>3</sub>); mp 75–79°C; <sup>1</sup>H NMR (500 MHz, CDCl<sub>3</sub>)  $\delta$  7.75 (2H, d, *J* = 7.5 Hz), 7.60 (2H, br dd, *J* = 7.0, 4.5 Hz), 7.53 (1H, br d, *J* = 5.0 Hz), 7.39 (2H, t, *J* = 7.5 Hz), 7.31 (2H, t, *J* = 7.5 Hz), 7.23 (1H, br d, *J* = 8.0 Hz), 6.44-6.42 (2H, br m), 6.38 (1H, br d, *J* = 7.5 Hz), 6.13 (1H, br s), 5.65 (1H, br s), 5.01-4.96 (2H, br m, overlapped), 4.85 (1H, d, *J* = 9.0 Hz), 4.64-4.56 (1H, br m), 4.41-4.34 (2H, br m, overlapped), 4.22 (1H, t, *J* = 7.5 Hz), 4.02-3.92 (4H, m, overlapped), 3.24 (3H, s), 2.95-2.88 (1H, br m), 2.69-2.60 (1H, br m), 1.81-1.74 (4H, br m, overlapped), 1.47-1.41 (4H, br m, overlapped), 1.35-1.22 (75H, br m, overlapped), 0.88 (6H, t, *J* = 7.5 Hz); <sup>13</sup>C NMR (125 MHz, CDCl<sub>3</sub>, Signals were complex due to the rotamers.)  $\delta$  173.4, 173.3, 170.3, 161.7, 159.1, 156.2, 144.0, 143.9, 141.4, 133.0, 127.8, 127.2, 125.3, 120.1, 114.7, 104.9, 99.9, 71.6, 68.3, 67.4, 51.3, 47.2, 46.5, 37.8, 33.5, 32.1, 29.9-29.3 (many signals overlapped), 26.2, 22.8, 17.8, 14.3; IR (KBr)  $\nu$  (cm<sup>-1</sup>) 3421, 2917, 2849, 1661, 1469, 1265, 1178, 1130, 1040, 737; HRMS (FAB, NBA + NaI matrix) Calcd. for C<sub>74</sub>H<sub>120</sub>N<sub>4</sub>O<sub>8</sub>Na: 1215.9004 ([M + Na]<sup>+</sup>), Found: 1215.8998.



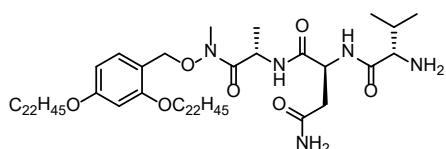
***Asn-Ala-(Me)N-O-TAGb (68)***

Following the general procedure described for Fmoc deprotection, Fmoc-Asn-Ala-(Me)N-O-TAGb (**67**) (1.70 g, 1.4 mmol) was converted to Asn-Ala-(Me)N-O-TAGb (**68**) (1.38 g, quant.) as a white powder.  $[\alpha]_D^{24.5} = 17.5$  (*c* 0.1, CHCl<sub>3</sub>); mp ca. 190°C (decomp.); <sup>1</sup>H NMR (500 MHz, CDCl<sub>3</sub>)  $\delta$  7.82 (1H, br d, *J* = 8.0 Hz), 7.24 (1H, d, *J* = 8.0 Hz), 6.44-6.43 (2H, m, overlapped), 6.18 (1H, br s), 5.35 (1H, br s), 5.03-4.97 (2H, br m, overlapped), 4.83 (1H, d, *J* = 9.5 Hz), 4.04-3.93 (4H, m, overlapped), 3.69 (1H, app br s), 3.24 (3H, s), 2.70-2.66 (1H, m), 2.60-2.55 (1H, m), 1.83-1.74 (4H, m, overlapped), 1.48-1.41 (4H, br m, overlapped), 1.35-1.22 (75H, br m, overlapped), 0.88 (6H, t, *J* = 7.5 Hz) (Two protons (NH x 2) were not observed.); <sup>13</sup>C NMR (125 MHz, CDCl<sub>3</sub>/CD<sub>3</sub>OD = 10/1, Signals were complex due to the rotamers.)  $\delta$  174.1, 173.5 (two signals), 161.6, 160.5, 159.0, 158.5, 132.9, 131.2, 118.0, 114.6, 104.9, 104.7, 99.9, 99.8, 71.6, 70.2, 68.23, 68.18, 52.1, 45.7, 39.89, 39.87, 38.9, 33.4, 32.0, 29.8-29.2 (many signals overlapped), 26.15, 26.10, 22.7, 17.6, 14.2; IR (KBr)  $\nu$  (cm<sup>-1</sup>) 3360, 2916, 2849, 1660, 1468, 1177, 1130, 719; HRMS (FAB, NBA + NaI matrix) Calcd. for C<sub>59</sub>H<sub>110</sub>N<sub>4</sub>O<sub>6</sub>Na: 993.8323 ([M + Na]<sup>+</sup>), Found: 993.8315.



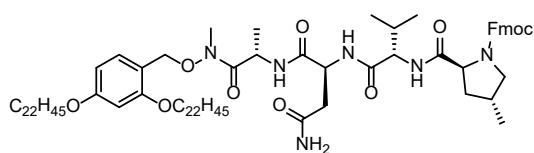
*Fmoc-Val-Asn-Ala-(Me)N-O-TAGb (69)*

Following the general procedure described for condensation, Asn-Ala-(Me)N-O-TAGb (**68**) (1.34 g, 1.4 mmol) was converted to Fmoc-Val-Asn-Ala-(Me)N-O-TAGb (**69**) (1.66 g, 93%) as a white powder.  $[\alpha]_D^{24.5} = 9.6$  (*c* 0.1, CHCl<sub>3</sub>); mp 185–190°C; <sup>1</sup>H NMR (500 MHz, CDCl<sub>3</sub>, Signals were broad and complex due to the rotamers.)  $\delta$  7.76-7.72 (3H, br m, overlapped), 7.60-7.57 (3H, br m, overlapped), 7.38-7.35 (2H, br m), 7.28 (2H, t, *J* = 7.5 Hz), 7.20 (1H, d, *J* = 8.5 Hz), 6.43-6.40 (2H, overlapped), 6.30 (1H, br s), 5.86 (1H, br s), 5.76 (1H, br d, *J* = 8.5 Hz), 5.00-4.92 (2H, br m, overlapped), 4.86-4.77 (2H, br m, overlapped), 4.41-4.29 (2H, br m, overlapped), 4.21-4.14 (2H, br m, overlapped), 4.00-3.91 (4H, br m, overlapped), 3.20 (3H, br s), 2.87-2.79 (1H, br m), 2.67-2.60 (1H, br m), 2.20-2.12 (1H, br m), 1.81-1.73 (4H, br m, overlapped), 1.47-1.40 (4H, br m, overlapped), 1.35-1.22 (75H, br m, overlapped), 0.99 (3H, d, *J* = 6.5 Hz), 0.95 (3H, d, *J* = 7.0 Hz), 0.88 (6H, t, *J* = 7.5 Hz); <sup>13</sup>C NMR (125 MHz, CDCl<sub>3</sub>, Signals were broad and complex due to the rotamers.)  $\delta$  173.5, 173.3, 171.6, 170.1, 161.6, 159.0, 156.7, 144.1, 143.9, 141.4, 132.9, 127.8, 127.22, 127.18, 125.32, 125.29, 120.1, 114.7, 104.8, 99.8, 71.6, 68.3, 67.2, 60.3, 49.8, 47.3, 46.4, 37.2, 33.5, 32.1, 31.5, 29.8-29.2 (many signals overlapped), 26.18, 26.16, 22.8, 19.4, 17.8, 17.7, 14.3; IR (KBr)  $\nu$  (cm<sup>-1</sup>) 3288, 2917, 2849, 1642, 1535, 1468, 1292, 1248, 1180, 1131, 1032, 740, 718; HRMS (FAB, NBA + NaI matrix) Calcd. for C<sub>79</sub>H<sub>129</sub>N<sub>5</sub>O<sub>9</sub>Na: 1314.9688 ([M + Na]<sup>+</sup>), Found: 1314.9697.



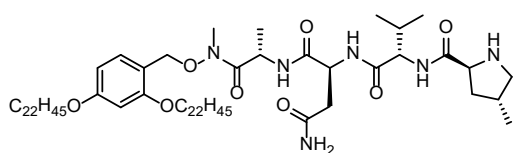
*Val-Asn-Ala-(Me)N-O-TAGb (70)*

Following the general procedure described for Fmoc deprotection, Fmoc-Val-Asn-Ala-(Me)N-O-TAGb (**69**) (1.61 g, 1.2 mmol) was converted to Val-Asn-Ala-(Me)N-O-TAGb (**70**) (1.33 g, quant.) as a white powder.  $[\alpha]_D^{24.5} = 7.7$  (*c* 0.1, CHCl<sub>3</sub>); mp 101–102°C; <sup>1</sup>H NMR (500 MHz, CDCl<sub>3</sub>)  $\delta$  8.39 (1H, br d, *J* = 7.5 Hz), 7.61 (1H, br d, *J* = 7.5 Hz), 7.22 (1H, d, *J* = 9.0 Hz), 6.50 (1H, br s), 6.44-6.42 (2H, m, overlapped), 5.78 (1H, br s), 4.97-4.91 (2H, br m, overlapped), 4.84-4.78 (2H, br m, overlapped), 4.01-3.92 (4H, m, overlapped), 3.28 (1H, d, *J* = 4.0 Hz), 3.22 (3H, s), 2.86-2.82 (1H, m), 2.66-2.61 (1H, m), 2.29-2.20 (1H, m), 1.82-1.73 (4H, m, overlapped), 1.47-1.41 (4H, br m, overlapped), 1.35-1.22 (75H, br m, overlapped), 0.98 (3H, d, *J* = 7.0 Hz), 0.89-0.83 (9H, m, overlapped) (Two protons (NH x 2) were not observed.); <sup>13</sup>C NMR (125 MHz, CDCl<sub>3</sub>)  $\delta$  174.9, 173.4, 173.3, 170.4, 161.6, 159.0, 132.9, 114.7, 104.8, 99.8, 71.6, 68.2, 60.3, 49.6, 46.4, 37.9, 33.5, 32.0, 31.2, 29.8-29.2 (many signals overlapped), 26.1, 22.8, 19.7, 17.7, 16.4, 14.2; IR (KBr)  $\nu$  (cm<sup>-1</sup>) 3286, 2916, 2849, 1654, 1469, 1179, 1131, 719; HRMS (FAB, NBA matrix) Calcd. for C<sub>64</sub>H<sub>120</sub>N<sub>5</sub>O<sub>7</sub>: 1070.9188 ([M + H]<sup>+</sup>), Found: 1070.9191.



#### *Fmoc-4-MePro-Val-Asn-Ala-(Me)N-O-TAGb (71)*

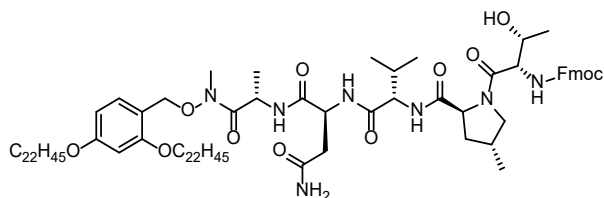
Following the general procedure described for condensation, Val-Asn-Ala-(Me)N-O-TAGb (**70**) (1.28 g, 1.2 mmol) was converted to Fmoc-4-MePro-Val-Asn-Ala-(Me)N-O-TAGb (**71**) (1.68 g, quant.) as a white powder.  $[\alpha]_D^{24.6} = -9.7$  ( $c$  0.1,  $\text{CHCl}_3$ ); mp 160–161°C;  $^1\text{H NMR}$  (500 MHz,  $\text{CDCl}_3$ , Signals were broad and complex due to the rotamers. Those derived from the minor rotamers are not described here.)  $\delta$  7.76 (2H, br d,  $J = 6.5$  Hz), 7.63 (1H, br d,  $J = 7.0$  Hz), 7.59 (2H, br d,  $J = 7.5$  Hz), 7.49 (1H, br d,  $J = 7.0$  Hz), 7.40 (2H, br t,  $J = 7.5$  Hz), 7.32 (2H, td,  $J = 7.5, 1.0$  Hz), 7.23 (1H, br d,  $J = 8.0$  Hz), 6.43-6.42 (2H, br m, overlapped), 6.34 (1H, br s), 5.85 (1H, br s), 5.39 (1H, br s), 4.98-4.92 (2H, br m, overlapped), 4.83-4.77 (2H, br m, overlapped), 4.48-4.34 (4H, br m, overlapped), 4.25 (1H, br t,  $J = 6.5$  Hz), 4.01-3.92 (4H, br m, overlapped), 3.66 (1H, br t,  $J = 7.0$  Hz), 3.21 (3H, br s), 2.96 (1H, br t,  $J = 10.0$  Hz), 2.80-2.77 (1H, br m), 2.67-2.63 (1H, br m), 2.28-2.07 (3H, br m, overlapped), 1.80-1.73 (4H, br m), 1.68-1.62 (1H, br m), 1.47-1.41 (4H, br m, overlapped), 1.35-1.22 (75H, br m, overlapped), 1.06 (3H, br d,  $J = 6.0$  Hz), 0.93 (3H, d,  $J = 6.5$  Hz), 0.90-0.86 (9H, m, overlapped);  $^{13}\text{C NMR}$  (125 MHz,  $\text{CDCl}_3$ , Signals were broad and complex due to the rotamers.)  $\delta$  173.4, 173.2, 172.3, 171.2, 170.0, 161.6, 159.0, 156.3, 144.1, 143.8, 141.4, 133.0, 127.9, 127.5, 127.3, 125.2, 120.1, 114.8, 104.8, 99.8, 71.6, 68.3, 68.0, 61.3, 58.7, 54.0, 49.9, 47.3, 46.3, 37.3, 36.7, 33.5, 32.7, 32.1, 30.9, 29.8-29.3 (many signals overlapped), 26.2, 22.8, 19.5, 17.9, 17.8, 17.3, 14.3; IR (KBr)  $\nu$  ( $\text{cm}^{-1}$ ) 3286, 2917, 2849, 1642, 1468, 1418, 1178, 1129, 739, 719; HRMS (FAB, NBA + NaI matrix) Calcd. for  $\text{C}_{85}\text{H}_{138}\text{N}_6\text{O}_{10}\text{Na}$ : 1426.0372 ( $[\text{M} + \text{Na}]^+$ ), Found: 1426.0363.



#### *4-MePro-Val-Asn-Ala-(Me)N-O-TAGb (72)*

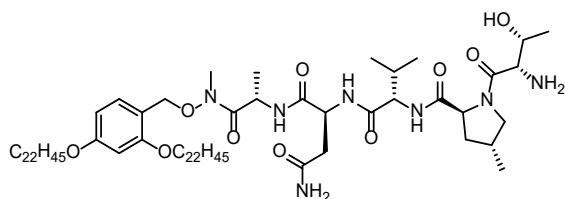
Following the general procedure described for Fmoc deprotection, Fmoc-4-MePro-Val-Asn-Ala-(Me)N-O-TAGb (**71**) (1.64 g, 1.2 mmol) was converted to 4-MePro-Val-Asn-Ala-(Me)N-O-TAGb (**72**) (1.38 g, quant.) as a white powder.  $[\alpha]_D^{24.6} = -2.3$  ( $c$  0.1,  $\text{CHCl}_3$ ); mp 93–95°C;  $^1\text{H NMR}$  (500 MHz,  $\text{CDCl}_3$ )  $\delta$  8.31 (1H, br d,  $J = 8.5$  Hz), 7.78 (1H, br d,  $J = 7.5$  Hz), 7.58 (1H, br d,  $J = 7.0$  Hz), 7.24-7.22 (1H, br m), 6.54 (1H, br s), 6.43-6.42 (2H, br m, overlapped), 5.94 (1H, br s), 4.97-4.92 (2H, br m, overlapped), 4.83-4.75 (2H, m, overlapped), 4.28 (1H, dd,  $J = 9.5, 6.5$  Hz), 4.01-3.92 (4H, m, overlapped), 3.83-3.81 (1H, m), 3.21 (3H, s), 3.08 (1H, dd,  $J = 10.0, 6.5$  Hz), 2.82-2.78 (1H, m), 2.65-2.56 (2H, m, overlapped), 2.26-2.16 (1H, m), 2.13-2.04 (2H, m, overlapped), 1.82-1.68 (5H, m, overlapped), 1.46-1.41 (4H, br m, overlapped), 1.35-1.22 (75H, br m, overlapped), 0.99 (3H, d,  $J = 6.5$  Hz),

0.96 (3H, d,  $J = 6.5$  Hz), 0.91 (3H, d,  $J = 7.0$  Hz), 0.87 (6H, t,  $J = 7.0$  Hz);  $^{13}\text{C}$  NMR (125 MHz,  $\text{CDCl}_3$ )  $\delta$  176.2, 173.6, 173.3, 171.7, 170.2, 161.6, 159.0, 133.0, 114.8, 104.9, 99.8, 71.6, 68.3, 60.4, 58.1, 54.7, 50.0, 46.3, 39.0, 37.2, 33.5, 33.3, 32.1, 30.9, 29.8-29.3 (many signals overlapped), 26.19, 26.17, 22.8, 19.7, 17.9, 17.7, 17.6, 14.3; IR (KBr)  $\nu$  ( $\text{cm}^{-1}$ ) 3271, 2916, 2849, 1643, 1508, 1468, 1179, 1131, 719; HRMS (FAB, NBA matrix) Calcd. for  $\text{C}_{70}\text{H}_{128}\text{N}_6\text{O}_8$ : 1181.9872 ( $[\text{M} + \text{H}]^+$ ), Found: 1181.9851.



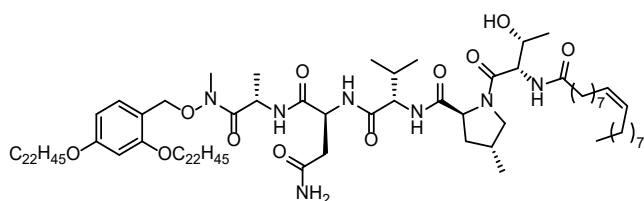
### *Fmoc-Thr-4-MePro-Val-Asn-Ala-(Me)N-O-TAGb (73)*

Following the general procedure described for condensation, 4-MePro-Val-Asn-Ala-(Me)N-O-TAGb (**72**) (657 mg, 0.56 mmol) was converted to Fmoc-Thr-4-MePro-Val-Asn-Ala-(Me)N-O-TAGb (**73**) (818 mg, 98%) as a white powder.  $[\alpha]_{\text{D}}^{24.6} = -11.9$  ( $c$  0.1,  $\text{CHCl}_3$ ); mp 115–125°C;  $^1\text{H}$  NMR (500 MHz,  $\text{CDCl}_3$ , Signals were broad and complex due to the rotamers. Those derived from the minor rotamers are not described here.)  $\delta$  7.78 (1H, br d,  $J = 8.0$  Hz), 7.74 (2H, br d,  $J = 7.5$  Hz), 7.59 (2H, br d,  $J = 7.5$  Hz), 7.38 (2H, br t,  $J = 7.5$  Hz), 7.30 (2H, br td,  $J = 7.5, 2.0$  Hz), 7.30 (1H, br d,  $J = 8.5$  Hz), 7.15 (1H, br d,  $J = 9.0$  Hz), 6.95 (1H, br s), 6.44-6.40 (2H, br m, overlapped), 6.36 (1H, br s), 6.23 (1H, br d,  $J = 8.0$  Hz), 5.05-4.96 (3H, br m, overlapped), 4.80 (1H, br d,  $J = 10.0$  Hz), 4.71 (1H, br dd,  $J = 9.5, 4.0$  Hz), 4.66-4.49 (3H, br m, overlapped), 4.45 (1H, dd,  $J = 11.0, 7.5$  Hz), 4.35 (1H, dd,  $J = 10.5, 7.0$  Hz), 4.32-4.27 (1H, br m), 4.20 (1H, t,  $J = 7.0$  Hz), 4.05 (1H, br t,  $J = 8.0$  Hz), 4.01-3.90 (4H, br m, overlapped), 3.31 (1H, br t,  $J = 9.5$  Hz), 3.21 (3H, s), 2.81-2.77 (1H, br m), 2.72-2.69 (1H, br m), 2.51-2.43 (1H, br m), 2.25-2.17 (2H, br m, overlapped), 1.93 (1H, br m), 1.82-1.73 (4H, br m, overlapped), 1.47-1.41 (4H, br m, overlapped), 1.35-1.22 (78H, br m, overlapped), 1.09 (3H, d,  $J = 6.5$  Hz), 0.95 (3H, d,  $J = 7.0$  Hz), 0.88 (9H, t,  $J = 7.0$  Hz) (One proton (NH or OH) was not observed.);  $^{13}\text{C}$  NMR (125 MHz,  $\text{CDCl}_3$ , Signals were broad and complex due to the rotamers.)  $\delta$  173.8, 173.1, 172.2, 171.6, 171.2, 169.8, 161.6, 159.0, 156.4, 143.9, 143.8, 141.4, 133.0, 127.9, 127.2, 125.23, 125.19, 120.10, 120.08, 114.8, 104.8, 99.8, 71.6, 68.3, 68.1, 67.1, 61.6, 58.0, 56.8, 54.6, 50.5, 47.3, 46.1, 37.8, 37.2, 33.5, 32.9, 32.1, 31.2, 29.8-29.3 (many signals overlapped), 26.2, 22.8, 19.6, 18.6, 18.1, 18.0, 17.4, 14.3; IR (KBr)  $\nu$  ( $\text{cm}^{-1}$ ) 3302, 2917, 2849, 1644, 1508, 1467, 1264, 1179, 740, 721; HRMS (FAB, NBA + NaI matrix) Calcd. for  $\text{C}_{89}\text{H}_{145}\text{N}_7\text{O}_{12}\text{Na}$ : 1527.0849 ( $[\text{M} + \text{Na}]^+$ ), Found: 1527.0854.



### *Thr-4-MePro-Val-Asn-Ala-(Me)N-O-TAGb (74)*

Following the general procedure described for Fmoc deprotection, Fmoc-Thr-4-MePro-Val-Asn-Ala-(Me)N-O-TAGb (**73**) (768 mg, 0.51 mmol) was converted to Thr-4-MePro-Val-Asn-Ala-(Me)N-O-TAGb (**74**) (664 mg, quant.) as a white powder.  $[\alpha]_D^{24.6} = -9.7$  (*c* 0.1, CHCl<sub>3</sub>); mp 70–78°C; <sup>1</sup>H NMR (500 MHz, CDCl<sub>3</sub>, Signals were broad and complex due to the rotamers. Those derived from the minor rotamers are not described here.)  $\delta$  7.97 (1H, br d, *J* = 8.0 Hz), 7.35 (1H, br d, *J* = 9.5 Hz), 7.26-7.23 (1H, br m), 7.16 (1H, br s), 6.96 (1H, br s), 6.43-6.41 (2H, br m, overlapped), 5.04-4.91 (3H, br m, overlapped), 4.82-4.78 (1H, br m), 4.69-4.60 (2H, br m, overlapped), 4.15-4.09 (2H, br m, overlapped), 4.01-3.92 (4H, br m, overlapped), 3.84 (1H, br d, *J* = 5.0 Hz), 3.21 (3H, s), 3.15 (1H, br t, *J* = 9.5 Hz), 2.78-2.72 (1H, br m), 2.67-2.61 (1H, br m), 2.52-2.40 (1H, br m), 2.24-2.08 (3H, br m, overlapped), 1.87-1.73 (5H, br m, overlapped), 1.47-1.40 (4H, br m, overlapped), 1.35-1.22 (78H, br m, overlapped), 1.09 (3H, d, *J* = 6.5 Hz), 0.95 (3H, d, *J* = 6.0 Hz), 0.87 (9H, t, *J* = 7.5 Hz) (Three protons (NH x 2, OH x 1) were not observed.); <sup>13</sup>C NMR (125 MHz, CDCl<sub>3</sub>)  $\delta$  174.0, 173.3, 173.2, 172.4, 171.5, 169.9, 161.6, 159.0, 133.0, 114.8, 104.9, 99.8, 71.6, 70.2, 68.3, 61.7, 57.6, 56.3, 54.5, 50.5, 46.0, 37.6, 37.3, 33.5, 32.8, 32.3, 32.1, 29.8-29.3 (many signals overlapped), 26.2, 22.8, 19.5, 18.2, 17.9, 17.4, 14.3; IR (KBr)  $\nu$  (cm<sup>-1</sup>) 3297, 2917, 2849, 1645, 1508, 1468, 1178, 1131, 719; HRMS (FAB, NBA matrix) Calcd. for C<sub>74</sub>H<sub>136</sub>N<sub>7</sub>O<sub>10</sub>: 1283.0349 ([M + H]<sup>+</sup>), Found: 1283.0349.

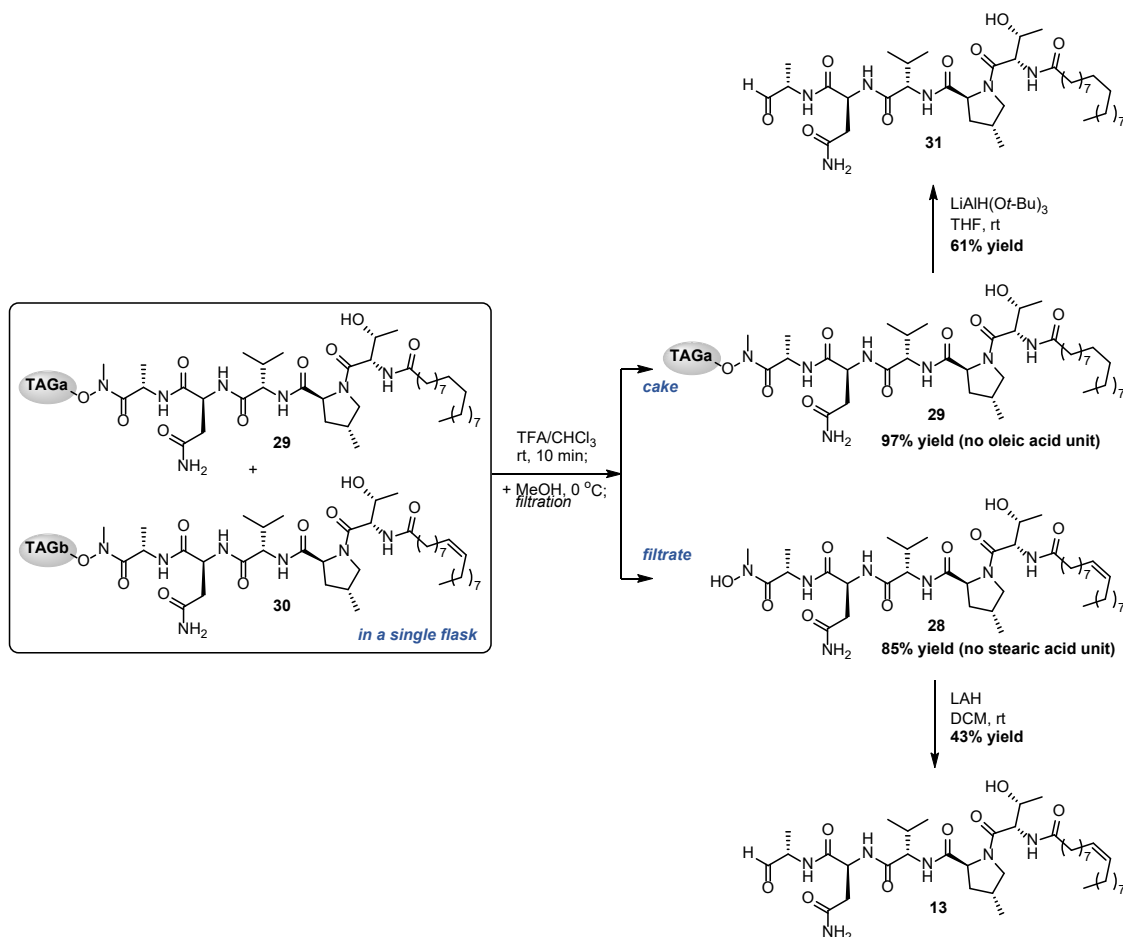


#### *Oleic acid-Thr-4-MePro-Val-Asn-Ala-(Me)N-O-TAGb (30)*

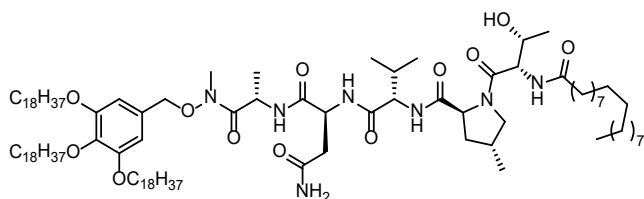
Following the general procedure described for condensation using oleic acid instead of Fmoc protected amino acid, Thr-4-MePro-Val-Asn-Ala-(Me)N-O-TAGb (**74**) (610 mg, 0.48 mmol) was converted to oleic acid-Thr-4-MePro-Val-Asn-Ala-(Me)N-O-TAGb (**30**) (707 mg, 96%) as a white powder.  $[\alpha]_D^{24.6} = -8.5$  (*c* 0.1, CHCl<sub>3</sub>); mp 155–163°C; <sup>1</sup>H NMR (500 MHz, CDCl<sub>3</sub>)  $\delta$  7.84 (1H, br d, *J* = 9.0 Hz), 7.28 (1H, br d, *J* = 7.5 Hz), 7.24 (1H, br d, *J* = 8.5 Hz), 7.16 (1H, br d, *J* = 9.0 Hz), 7.11 (1H, br s), 6.76 (1H, br d, *J* = 8.0 Hz), 6.58 (1H, br s), 6.44-6.42 (2H, br m, overlapped), 5.36-5.29 (2H, m, overlapped), 5.01-4.92 (4H, br m, overlapped), 4.80 (1H, br d, *J* = 9.5 Hz), 4.61-4.58 (2H, br m, overlapped), 4.33-4.26 (1H, br m), 4.09-4.03 (1H, br m), 4.02-3.92 (4H, br m, overlapped), 3.35 (1H, br t, *J* = 9.5 Hz), 3.21 (3H, s), 2.81-2.76 (1H, br m), 2.70-2.66 (1H, br m), 2.52-2.41 (1H, br m), 2.25-2.15 (6H, br m, overlapped), 2.05-1.96 (3H, br m, overlapped), 1.92-1.86 (1H, br m), 1.82-1.73 (4H, br m), 1.66-1.56 (2H, br m), 1.47-1.39 (4H, br m), 1.35-1.22 (98H, br m, overlapped), 1.09 (3H, d, *J* = 6.5 Hz), 0.94 (3H, d, *J* = 6.5 Hz), 0.88-0.86 (12H, m, overlapped); <sup>13</sup>C NMR (125 MHz, CDCl<sub>3</sub>)  $\delta$  173.7, 173.4, 173.2, 172.2, 171.6, 171.3, 169.8, 161.7, 159.0, 133.0, 130.1, 129.9, 114.7, 104.9, 99.8, 71.7, 68.3, 67.9, 61.6, 57.8, 54.6, 54.5, 50.3, 46.1, 37.8, 37.2, 36.6, 33.6, 32.9, 32.1, 31.6, 29.9-29.3 (many signals overlapped), 27.3, 26.2, 25.7, 22.8, 19.5, 18.8, 18.0, 17.9, 17.3, 14.3; IR (KBr)  $\nu$

( $\text{cm}^{-1}$ ) 3284, 2915, 2849, 1645, 1536, 1468, 1180, 1130, 719; HRMS (FAB, NBA + NaI matrix) Calcd. for  $\text{C}_{92}\text{H}_{167}\text{N}_7\text{O}_{11}\text{Na}$ : 1569.2621 ( $[\text{M} + \text{Na}]^+$ ), Found: 1569.2625.

### Selective deprotection of TAG benzyl group under acid conditions and reduction to the aldehydes

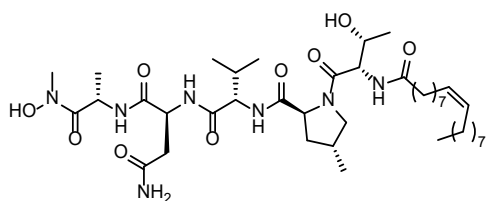


**29** (55.1 mg, 0.032 mmol, 1.0 eq) and **30** (50.0 mg, 0.032 mmol, 1.0 eq) was dissolved into 30% TFA/ $\text{CHCl}_3$  (3.2 mL, 0.01 M for each substrate) at room temperature, and the solution was stirred for 10 min. The reaction mixture was subsequently cooled to 0°C and MeOH (19 mL, 6-fold excess of TFA/ $\text{CHCl}_3$ ) was added. The resulting heterogeneous solution was stirred for a further 30 min at 0°C. The precipitate was filtered and washed with additional MeOH to afford the crude cake **29**. On the other hand, the filtrate was concentrated *in vacuo* to afford the crude **28**. The crude products were respectively purified by PLC on silica gel ( $\text{CHCl}_3/\text{MeOH} = 5/1$  as eluent, respectively) to give **29** (53.5 mg, 97%) as a white powder and hydroxamic acid **28** (22.2 mg, 85%) as a white powder.



### Stearic acid-Thr-4-MePro-Val-Asn-Ala-(Me)N-O-TAGa (**29**)

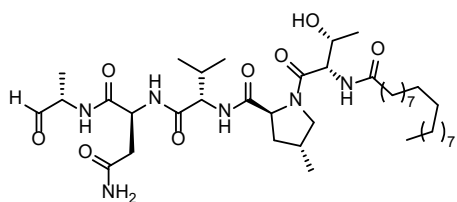
Following the general procedure described for condensation using stearic acid instead of Fmoc protected amino acid, Thr-4-MePro-Val-Asn-Ala-(Me)N-O-TAGa (**23**) (0.300 g, 0.21 mmol) was converted to stearic acid-Thr-4-MePro-Val-Asn-Ala-(Me)N-O-TAGa (**29**) (0.356 g, quant.) as a white powder.  $[\alpha]_D^{24.6} = -15.5$  (*c* 0.1, CHCl<sub>3</sub>); mp 153–154°C; <sup>1</sup>H NMR (500 MHz, CDCl<sub>3</sub>)  $\delta$  7.80 (1H, br d, *J* = 8.5 Hz), 7.33 (1H, br d, *J* = 7.5 Hz), 7.11-7.08 (2H, br m, overlapped), 6.81 (1H, br d, *J* = 8.5 Hz), 6.57 (2H, s), 6.39 (1H, br s), 4.98 (1H, dd, *J* = 8.5, 4.0 Hz), 4.96-4.90 (2H, m, overlapped), 4.85 (1H, br d, *J* = 10.0 Hz), 4.79 (1H, br d, *J* = 10.5 Hz), 4.59 (1H, dd, *J* = 9.0, 4.0 Hz), 4.55 (1H, dd, *J* = 9.0, 6.5 Hz), 4.49 (1H, br s), 4.34-4.24 (1H, br m), 4.03 (1H, br dd, *J* = 9.5, 7.5 Hz), 3.98-3.92 (6H, m, overlapped), 3.36 (1H, t, *J* = 9.5 Hz), 3.18 (3H, s), 2.82-2.78 (1H, m), 2.74-2.65 (1H, m), 2.52-2.41 (1H, m), 2.25-2.15 (4H, m, overlapped), 1.93-1.87 (1H, m), 1.82-1.70 (6H, m, overlapped), 1.65-1.56 (2H, m), 1.49-1.43 (6H, br m, overlapped), 1.36-1.22 (118H, br m, overlapped), 1.09 (3H, t, *J* = 7.0 Hz), 0.94 (3H, t, *J* = 6.5 Hz), 0.89-0.86 (15H, m, overlapped); <sup>13</sup>C NMR (125 MHz, CDCl<sub>3</sub>)  $\delta$  173.8, 173.5, 173.4, 172.2, 171.7, 171.5, 170.0, 153.5, 138.8, 129.4, 107.7, 73.6, 69.3, 67.8, 61.5, 58.0, 54.7, 54.6, 50.6, 46.2, 37.8, 37.1, 36.7, 34.1, 33.0, 32.1, 31.3, 30.5, 29.9-29.5 (many signals overlapped), 26.3, 25.8, 22.8, 19.5, 18.9, 17.9, 17.8, 17.3, 14.3; IR (KBr)  $\nu$  (cm<sup>-1</sup>) 3281, 2916, 2849, 1638, 1543, 1468, 1439, 1239, 1121, 719; HRMS (FAB, NBA + NaI matrix) Calcd. for C<sub>102</sub>H<sub>189</sub>N<sub>7</sub>O<sub>12</sub>Na: 1727.4292 ([M + Na]<sup>+</sup>), Found: 1727.4307.



### Oleic acid-Thr-4-MePro-Val-Asn-Ala-(Me)N-OH (**28**)

**30** (350 mg, 0.23 mmol) was dissolved into 30% trifluoroacetic acid (TFA)/CHCl<sub>3</sub> (11 mL, 0.02 M for substrate) at room temperature, and the solution was stirred for 20 min. The reaction mixture was subsequently cooled to 0°C and MeOH (66 mL, 6-fold excess of TFA/CHCl<sub>3</sub>) was added, and the resulting heterogeneous solution was stirred for a further 30 min at 0°C. The precipitate was filtered and washed with additional MeOH, and the filtrate was concentrated *in vacuo*. The residue was purified by flash column chromatography on silica gel (CHCl<sub>3</sub>/MeOH = 50/1 to 10/1 as eluent) to afford hydroxamic acid **28** (160 mg, 88%) as a white powder.  $[\alpha]_D^{24.6} = -32.1$  (*c* 0.1, DMSO); mp 193–196°C; <sup>1</sup>H NMR (500 MHz, DMSO-*d*<sub>6</sub>)  $\delta$  10.05 (1H, s), 8.15 (1H, d, *J* = 8.0 Hz), 7.86 (1H, d, *J* = 7.5 Hz), 7.82 (1H, d, *J* = 8.5 Hz), 7.59 (1H, br d, *J* = 7.5 Hz), 7.33 (1H, br s), 6.89 (1H, br s), 5.35-5.29 (2H, m, overlapped), 4.80-4.71 (1H, br m), 4.65 (1H, d, *J* =

6.0 Hz), 4.55-4.48 (2H, m, overlapped), 4.42 (1H, t,  $J = 7.5$  Hz), 4.12 (1H, dd,  $J = 8.0, 6.0$  Hz), 3.83-3.76 (2H, m, overlapped), 3.25 (1H, t,  $J = 9.0$  Hz), 3.08 (3H, s), 2.56 (1H, dd,  $J = 11.0, 6.5$  Hz), 2.39-2.30 (2H, m, overlapped), 2.17-2.06 (2H, m, overlapped), 2.01-1.91 (6H, m, overlapped), 1.67-1.61 (1H, m), 1.49-1.40 (2H, br m), 1.30-1.20 (20H, br m, overlapped), 1.16 (3H, d,  $J = 7.0$  Hz), 1.08 (3H, d,  $J = 6.0$  Hz), 0.97 (3H, d,  $J = 6.5$  Hz), 0.86-0.80 (9H, m, overlapped);  $^{13}\text{C}$  NMR (125 MHz, DMSO- $d_6$ )  $\delta$  172.2, 171.7, 171.5, 171.4, 170.8, 170.1, 169.4, 129.7, 67.0, 59.2, 57.5, 56.1, 54.0, 49.3, 45.0, 36.7, 36.6, 35.9, 34.9, 32.0, 31.3, 30.7, 29.2-28.6 (many signals overlapped), 26.64, 26.60, 25.3, 22.1, 19.3, 19.2, 17.9, 17.3, 17.2, 14.0; IR (KBr)  $\nu$  ( $\text{cm}^{-1}$ ) 3283, 2924, 2854, 1636, 1540, 1435, 1199; HRMS (ESI $^+$ ) Calcd. for  $\text{C}_{41}\text{H}_{73}\text{N}_7\text{O}_9\text{Na}$ : 830.5367 ( $[\text{M} + \text{Na}]^+$ ), Found: 830.5358.



#### Stearic acid-Thr-4-MePro-Val-Asn-Ala-H (**31**)

To a solution of **29** (50 mg, 0.029 mmol, 1.0 eq) in dehydrated THF (2.9 mL, 0.01 M) was added dropwise 1.0 M LiAlH(*O*-*t*-Bu) $_3$  in dehydrated THF (293 mL, 10 eq) at room temperature. After stirring for 1 h at room temperature, the reaction mixture was then treated with aqueous 1M HCl (1.5 mL) at 0°C to quench the excess LiAlH(*O*-*t*-Bu) $_3$ . After stirring for 10 min at room temperature, MeOH (15 mL) was added. The resulting heterogeneous solution was stirred for a further 30 min at room temperature, and the precipitate was filtered and washed with additional MeOH. The filtrate was roughly concentrated *in vacuo*, poured into a separatory funnel containing aqueous 1M HCl (10 mL), and extracted with CHCl $_3$  (3  $\times$  10 mL). The combined organic extracts were dried with Na $_2$ SO $_4$ , filtered, and concentrated *in vacuo*. The residue was purified by PLC on silica gel (CHCl $_3$ /MeOH = 5/1 as eluent) to afford aldehyde **31** (13.7 mg, 61%) as a white powder.  $[\alpha]_D^{24.6} = -35.6$  ( $c$  0.1, CHCl $_3$ ); mp 176–177°C;  $^1\text{H}$  NMR (500 MHz, DMSO- $d_6$ )  $\delta$  9.34 (1H, s), 8.13 (1H, d,  $J = 6.5$  Hz), 8.10 (1H, d,  $J = 8.5$  Hz), 7.87 (2H, app d,  $J = 8.5$  Hz, overlapped), 7.37 (1H, br s), 6.92 (1H, br s), 4.69-4.63 (1H, br m), 4.55-4.47 (2H, m, overlapped), 4.45-4.38 (1H, br m), 4.09-3.98 (1H, m), 3.83-3.77 (2H, m, overlapped), 3.30-3.23 (1H, br m), 2.52 (1H, m, overlapped with solvent residual signals), 2.38-2.30 (1H, m), 2.17-2.06 (2H, m), 2.02-1.92 (2H, m, overlapped), 1.68-1.62 (1H, m), 1.50-1.38 (2H, br m), 1.29-1.18 (30H, br m, overlapped), 1.14 (3H, d,  $J = 7.5$  Hz), 1.08 (3H, d,  $J = 6.0$  Hz), 0.97 (3H, d,  $J = 6.5$  Hz), 0.86-0.82 (9H, m, overlapped);  $^{13}\text{C}$  NMR (125 MHz, DMSO- $d_6$ )  $\delta$  201.3, 172.2, 171.8, 171.4, 171.3, 170.6, 169.4, 66.9, 59.2, 56.2, 53.9, 49.5, 36.7, 36.5, 34.8, 32.0, 31.3, 30.3, 29.0-28.7 (many signals overlapped), 25.2, 22.1, 19.3, 19.1, 18.0, 17.2, 14.0, 13.5; IR (KBr)  $\nu$  ( $\text{cm}^{-1}$ ) 3286, 2920, 2851, 1639, 1541, 1419, 1239, 1066; HRMS (ESI $^+$ ) Calcd. for  $\text{C}_{40}\text{H}_{72}\text{N}_6\text{O}_8\text{Na}$ : 787.5309 ( $[\text{M} + \text{Na}]^+$ ), Found: 787.5315.

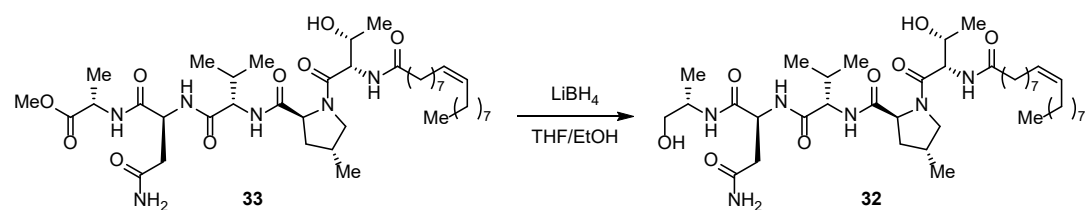


## Supporting Information for Chapter 4

### 1. Syntheses of kozupeptins' analogs

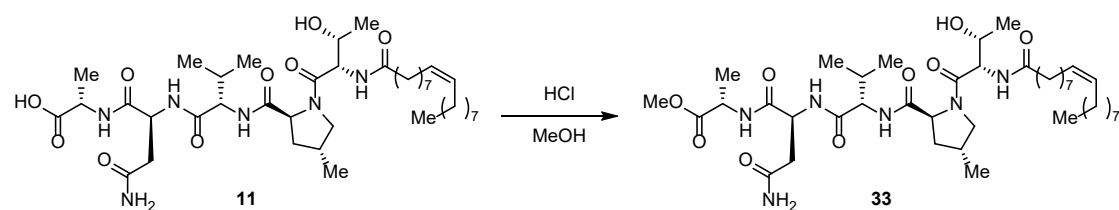
Compounds **13**, **11**, and **12** were synthesized as the intermediates in the first total synthesis of kozupeptin A (**1a**) described in **Chapter 2**. Derivatives **28** and **31** were obtained in the application to rapid analog synthesis described in **Chapter 3**. Lipopeptides **36**, **37**, **39**, **40**, **41**, **42**, **43**, **44**, **45**, **46**, **47**, and **48** were synthesized according to the procedures in **Chapter 2** or **Chapter 3** just by changing the amino acid or fatty acid.

#### Synthesis of C-terminal alcohol **32**



To a solution of **33** (43.0 mg, 0.054 mmol, 1.0 eq) in dehydrated THF (1.8 mL, 0.03 M) was added dropwise 0.3 M LiBH<sub>4</sub> in dehydrated THF (pre-prepared, 0.81 mL, 4.5 eq) and EtOH (1.8 mL) at room temperature. After stirring for 2 h at room temperature, the reaction mixture was then treated with aqueous 1M HCl (10 mL) at 0°C to quench the excess LiBH<sub>4</sub>, poured into a separatory funnel, and extracted with EtOAc (2 × 10 mL). The combined organic extracts were dried with Na<sub>2</sub>SO<sub>4</sub>, filtered, and concentrated *in vacuo*. The residue was purified by PLC on silica gel (CHCl<sub>3</sub>/MeOH = 10/1 as eluent) to afford alcohol **32** (11.9 mg, 29%) as a white powder and MePro-Thr amide bond-cleaved alcohol **63** (13.8 mg, 69% yield) as a colorless oil. <sup>1</sup>H NMR (500 MHz, DMSO-*d*<sub>6</sub>) δ 8.01 (1H, d, *J* = 8.0 Hz), 7.87 (2H, app dd, *J* = 8.0, 2.5 Hz), 7.34 (1H, br s), 7.28 (1H, d, *J* = 8.0 Hz), 6.90 (1H, br s), 5.35-5.29 (2H, m, overlapped), 4.66 (1H, d, *J* = 5.5 Hz), 4.60 (1H, t, *J* = 6.0 Hz), 4.54-4.40 (3H, m, overlapped), 4.03 (1H, dd, *J* = 7.5, 6.5 Hz), 3.83-3.78 (2H, m, overlapped), 3.73-3.68 (1H, m), 3.31-3.26 (2H, m, overlapped), 3.21-3.17 (1H, m), 2.52-2.40 (2H, m, overlapped with solvent residual signals), 2.38-2.31 (1H, m), 2.18-2.06 (2H, m, overlapped), 2.03-1.92 (6H, m, overlapped), 1.69-1.63 (1H, m), 1.48-1.42 (2H, m, overlapped), 1.32-1.19 (20H, br m, overlapped), 1.09 (3H, d, *J* = 6.5 Hz), 0.98 (6H, t, *J* = 6.5 Hz), 0.87-0.83 (9H, m, overlapped); HRMS (ESI<sup>+</sup>) Calcd. for C<sub>40</sub>H<sub>72</sub>N<sub>6</sub>O<sub>8</sub>Na: 787.5309 ([M + Na]<sup>+</sup>), Found: 787.5298.

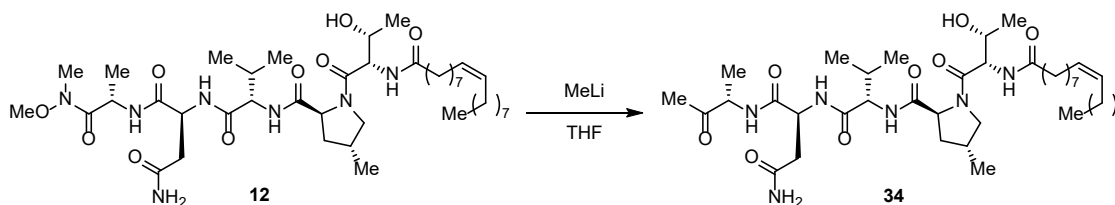
#### Synthesis of C-terminal methyl ester **33**



Compound **11** (20.0 mg, 0.026 mmol) was dissolved into 0.5 M HCl/MeOH (2.6 mL, 0.01 M for

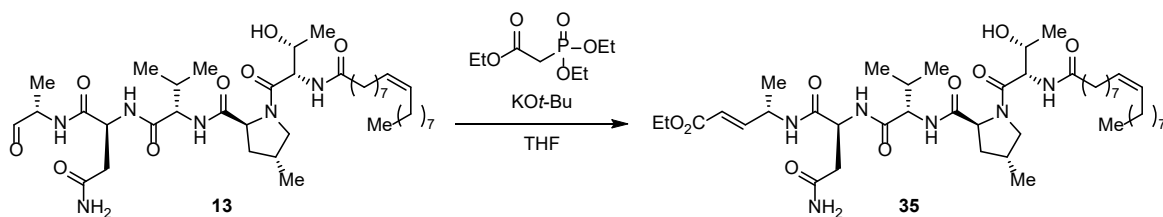
substrate) at room temperature, and the solution was stirred for 1 h. The reaction mixture was roughly concentrated *in vacuo*. The residue was purified by flash column chromatography on silica gel (CHCl<sub>3</sub>/MeOH = 100/1 to 10/1 as eluent) to afford methyl ester **33** (11.5 mg, 56%) as a white powder. <sup>1</sup>H NMR (500 MHz, DMSO-*d*<sub>6</sub>) δ 8.06 (1H, d, *J* = 7.5 Hz), 7.99 (1H, d, *J* = 7.0 Hz), 7.86 (1H, d, *J* = 8.0 Hz), 7.82 (1H, d, *J* = 8.0 Hz), 7.32 (1H, s), 6.92 (1H, s), 5.35-5.29 (2H, m, overlapped), 4.66 (1H, d, *J* = 6.0 Hz), 4.53-4.47 (2H, m, overlapped), 4.41 (1H, app t, *J* = 7.5 Hz), 4.24-4.19 (1H, m), 4.06 (1H, dd, *J* = 8.0, 6.5 Hz), 3.83-3.77 (2H, m, overlapped), 3.60 (3H, s), 3.30-3.25 (1H, m), 2.53-2.48 (1H, m, overlapped with DMSO), 2.46-2.41 (1H, m), 2.38-2.30 (1H, m), 2.17-2.06 (2H, m, overlapped), 2.01-1.92 (5H, m, overlapped), 1.68-1.62 (1H, m), 1.48-1.42 (2H, m, overlapped), 1.32-1.18 (24H, br m, overlapped), 1.08 (3H, d, *J* = 6.5 Hz), 0.97 (3H, d, *J* = 6.5 Hz), 0.86-0.81 (9H, m, overlapped); HRMS (ESI<sup>+</sup>) Calcd. for C<sub>41</sub>H<sub>72</sub>N<sub>6</sub>O<sub>9</sub>Na: 815.5259 ([M + Na]<sup>+</sup>), Found: 815.5262.

#### Synthesis of C-terminal methyl ketone **34**



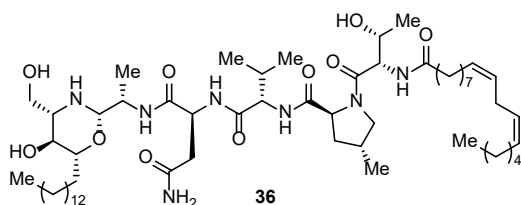
To a solution of **12** (10.0 mg, 0.012 mmol, 1.0 eq) in dehydrated THF (2.4 mL, 0.005 M) was added dropwise 1.11 M MeLi in dehydrated diethyl ether (Et<sub>2</sub>O) (110 μL, 10 eq) at 0°C. After stirring for 1 h at 0°C, the reaction mixture was then treated with aqueous 1M HCl (1.0 mL) at 0°C to quench the excess MeLi, poured into a separatory funnel containing aqueous 1M HCl (10 mL), and extracted with CHCl<sub>3</sub> (3 × 10 mL). The combined organic extracts were dried with Na<sub>2</sub>SO<sub>4</sub>, filtered, and concentrated *in vacuo*. The residue was purified by PLC on silica gel (CHCl<sub>3</sub>/MeOH = 10/1 as eluent) to afford methyl ketone **34** (2.3 mg, 24%) as a white powder. <sup>1</sup>H NMR (500 MHz, DMSO-*d*<sub>6</sub>) δ 8.07 (1H, d, *J* = 7.5 Hz), 8.00 (1H, d, *J* = 7.0 Hz), 7.85 (2H, app d, *J* = 8.0 Hz), 7.35 (1H, br s), 6.91 (1H, br s), 5.35-5.29 (2H, m, overlapped), 4.65 (1H, d, *J* = 6.0 Hz), 4.53-4.47 (2H, m, overlapped), 4.43-4.40 (1H, br m), 4.15-4.09 (1H, m), 4.07-4.04 (1H, dd, *J* = 8.0, 6.0 Hz), 3.83-3.78 (2H, m, overlapped), 3.29-3.25 (1H, m), 2.57-2.49 (1H, m, overlapped with DMSO), 2.48-2.43 (1H, m), 2.38-2.26 (1H, br m), 2.18-2.08 (2H, m, overlapped), 2.04 (3H, s), 2.01-1.94 (5H, m, overlapped), 1.69-1.63 (1H, m), 1.48-1.42 (2H, m, overlapped), 1.31-1.20 (21H, br m, overlapped), 1.14 (3H, d, *J* = 7.5 Hz), 1.08 (3H, d, *J* = 6.0 Hz), 0.97 (3H, d, *J* = 7.0 Hz), 0.87-0.82 (9H, m, overlapped); HRMS (ESI<sup>+</sup>) Calcd. for C<sub>41</sub>H<sub>72</sub>N<sub>6</sub>O<sub>8</sub>Na: 799.5309 ([M + Na]<sup>+</sup>), Found: 799.5310.

#### Synthesis of C-terminal α,β-unsaturated ethyl ester **35**



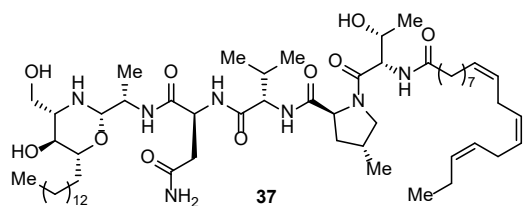
To a solution of ethyl diethylphosphonoacetate (7.4 mg, 0.033 mmol, 2.0 eq) in dehydrated THF (2.3 mL, 0.007 M for **13**) was added dropwise 1.0 M KO $t$ -Bu in dehydrated THF (34  $\mu$ L, 2.1 eq) at 0°C. After stirring for 2 hours at room temperature, **13** was added to this solution at 0°C. After stirring for 30 min at the same temperature, the reaction mixture was then treated with aqueous 1M HCl (10 mL), poured into a separatory funnel, and extracted with CHCl<sub>3</sub> (3  $\times$  10 mL). The combined organic extracts were dried with Na<sub>2</sub>SO<sub>4</sub>, filtered, and concentrated *in vacuo*. The residue was purified by PLC on silica gel (CHCl<sub>3</sub>/MeOH = 10/1) to afford  $\alpha,\beta$ -unsaturated ethyl ester **35** (4.0 mg, 29%) as a white powder. <sup>1</sup>H NMR (500 MHz, DMSO-*d*<sub>6</sub>)  $\delta$  8.02 (1H, d,  $J$  = 7.5 Hz), 7.90 (1H, d,  $J$  = 7.5 Hz), 7.87 (1H, d,  $J$  = 7.5 Hz), 7.74 (1H, d,  $J$  = 8.0 Hz), 7.36 (1H, br s), 6.91 (1H, br s), 6.80 (1H, dd,  $J$  = 16.0, 5.0 Hz), 5.85 (1H, dd,  $J$  = 16.0, 1.5 Hz), 5.35-5.29 (2H, m, overlapped), 4.67 (1H, d,  $J$  = 5.5 Hz), 4.50-4.46 (2H, m, overlapped), 4.40 (1H, t,  $J$  = 7.0 Hz), 4.11 (2H, q,  $J$  = 7.0 Hz), 3.99 (1H, dd,  $J$  = 7.5, 6.6 Hz), 3.81-3.77 (2H, m, overlapped), 3.32-3.24 (1H, m), 2.56-2.52 (1H, m, overlapped with DMSO), 2.50-2.46 (1H, m, overlapped with DMSO), 2.38-2.31 (1H, m), 2.17-2.06 (2H, m, overlapped), 2.01-1.94 (6H, m, overlapped), 1.69-1.63 (1H, m), 1.48-1.42 (2H, m, overlapped), 1.31-1.18 (24H, br m, overlapped), 1.16 (3H, d,  $J$  = 7.0 Hz), 1.08 (3H, d,  $J$  = 6.0 Hz), 0.97 (3H, d,  $J$  = 7.0 Hz), 0.85 (9H, app t,  $J$  = 7.0 Hz); HRMS (ESI<sup>+</sup>) Calcd. for C<sub>44</sub>H<sub>76</sub>N<sub>6</sub>O<sub>9</sub>Na: 855.5572 ([M + Na]<sup>+</sup>), Found: 855.5571.

### Synthesis of *N*-terminal linoleic acid amide **36**



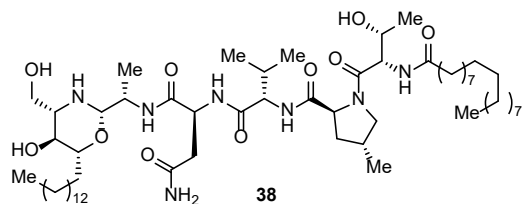
A white powder. <sup>1</sup>H NMR (500 MHz, DMSO-*d*<sub>6</sub>)  $\delta$  8.07 (1H, d,  $J$  = 7.5 Hz), 7.85 (1H, d,  $J$  = 8.0 Hz), 7.82 (1H, d,  $J$  = 8.0 Hz), 7.33 (1H, d, overlapped), 7.31 (1H, s), 6.87 (1H, s), 5.37-5.27 (4H, m, overlapped), 4.70 (1H, d,  $J$  = 6.0 Hz), 4.64 (1H, d,  $J$  = 6.0 Hz), 4.51-4.42 (4H, m, overlapped), 4.05 (1H, app t,  $J$  = 7.0 Hz), 3.86 (1H, app br s), 3.82-3.78 (2H, m, overlapped), 3.75-3.68 (1H, m), 3.60-3.56 (1H, m), 3.50-3.45 (1H, m), 3.30-3.26 (1H, br m), 3.08-3.01 (1H, br m), 2.89-2.84 (1H, m), 2.73 (2H, t,  $J$  = 6.0 Hz), 2.53-2.50 (1H, m, overlapped with DMSO) 2.43-2.32 (2H, m, overlapped), 2.18-2.07 (2H, m, overlapped), 2.03-1.92 (6H, m, overlapped), 1.80-1.73 (1H, br m), 1.68-1.62 (1H, m), 1.49-1.40 (3H, m, overlapped), 1.34-1.15 (40H, m, overlapped), 1.09 (3H, d,  $J$  = 6.0 Hz), 1.00 (3H, d,  $J$  = 7.0 Hz), 0.97 (3H, d,  $J$  = 7.0 Hz), 0.87-0.82 (12H, m, overlapped); HRMS (ESI<sup>+</sup>) Calcd. for C<sub>58</sub>H<sub>106</sub>N<sub>7</sub>O<sub>10</sub>: 1060.8001 ([M + H]<sup>+</sup>), Found: 1060.7991.

### Synthesis of *N*-terminal linolenic acid amide **37**



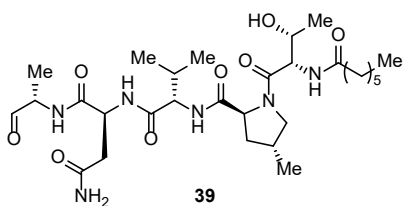
A white powder.  $^1\text{H}$  NMR (500 MHz,  $\text{DMSO-}d_6$ )  $\delta$  8.07 (1H, d,  $J = 8.0$  Hz), 7.85 (1H, d,  $J = 7.5$  Hz), 7.82 (1H, d,  $J = 8.0$  Hz), 7.33 (1H, d, overlapped), 7.31 (1H, s), 6.87 (1H, s), 5.38-5.25 (6H, m, overlapped), 4.70 (1H, br d,  $J = 6.0$  Hz), 4.65 (1H, d,  $J = 6.0$  Hz), 4.51-4.40 (4H, m, overlapped), 4.23-4.13 (1H, br m), 4.05 (1H, app t,  $J = 7.0$  Hz), 3.86 (1H, app br s), 3.82-3.78 (2H, br m, overlapped), 3.75-3.68 (1H, br m), 3.60-3.55 (1H, br m), 3.50-3.45 (1H, br m), 3.30-3.26 (1H, br m), 3.07-3.02 (1H, br m), 2.89-2.84 (1H, m), 2.77 (2H, t,  $J = 6.0$  Hz), 2.54-2.50 (1H, m, overlapped with DMSO), 2.43-2.32 (5H, m, overlapped), 2.18-2.07 (2H, m, overlapped), 2.05-1.92 (6H, m, overlapped), 1.80-1.73 (1H, br m), 1.68-1.62 (1H, m), 1.51-1.41 (3H, m, overlapped), 1.31-1.20 (32H, m, overlapped), 1.09 (3H, d,  $J = 6.0$  Hz), 1.00 (3H, d,  $J = 7.0$  Hz), 0.97 (3H, d,  $J = 7.0$  Hz), 0.87-0.82 (12H, m, overlapped); HRMS ( $\text{ESI}^+$ ) Calcd. for  $\text{C}_{58}\text{H}_{103}\text{N}_7\text{O}_{10}\text{Na}$ : 1080.7664 ( $[\text{M} + \text{Na}]^+$ ), Found: 1080.7669.

### Synthesis of *N*-terminal stearic acid amide **38**



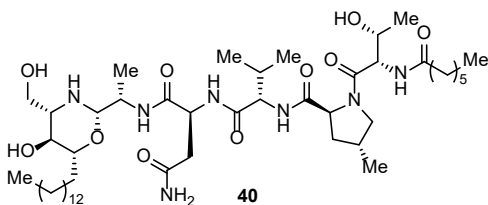
A white powder.  $^1\text{H}$  NMR (500 MHz,  $\text{DMSO-}d_6$ )  $\delta$  8.08 (1H, d,  $J = 8.0$  Hz), 7.87 (1H, d,  $J = 7.5$  Hz), 7.83 (1H, d,  $J = 8.0$  Hz), 7.34 (1H, d, overlapped), 7.32 (1H, s), 6.88 (1H, s), 4.72 (1H, d,  $J = 7.0$  Hz), 4.66 (1H, d,  $J = 5.5$  Hz), 4.53-4.39 (4H, m, overlapped), 4.05 (1H, app t,  $J = 7.0$  Hz), 3.90-3.82 (1H, br m), 3.82-3.76 (2H, m, overlapped), 3.75-3.68 (1H, m), 3.64-3.55 (1H, br m), 3.50-3.45 (1H, br m), 3.33-3.24 (1H, m), 3.09-3.02 (1H, m), 2.91-2.82 (1H, m), 2.54-2.50 (1H, m, overlapped with DMSO), 2.45-2.32 (2H, br m, overlapped), 2.17-2.07 (2H, m, overlapped), 2.02-1.92 (2H, m, overlapped), 1.77 (1H, br t), 1.68-1.62 (1H, m), 1.48-1.42 (4H, m, overlapped), 1.30-1.17 (52H, m, overlapped), 1.09 (3H, d,  $J = 6.0$  Hz), 0.99 (3H, d,  $J = 7.0$  Hz), 0.97 (3H, d,  $J = 7.0$  Hz), 0.86-0.81 (12H, m, overlapped) (One proton (NH or OH) was not observed. It would be NH of sphingoid.); HRMS ( $\text{ESI}^+$ ) Calcd. for  $\text{C}_{58}\text{H}_{109}\text{N}_7\text{O}_{10}\text{Na}$ : 1086.8134 ( $[\text{M} + \text{Na}]^+$ ), Found: 1086.8123.

### Synthesis of *N*-terminal heptanoic acid amide **39**



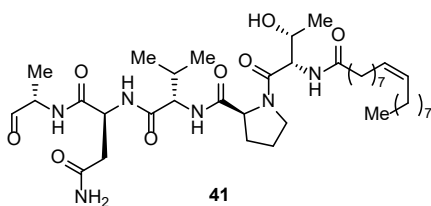
A white powder.  $^1\text{H NMR}$  (500 MHz,  $\text{DMSO-}d_6$ )  $\delta$  9.34 (1H, s), 8.14 (1H, d,  $J = 6.5$  Hz), 8.11 (1H, d,  $J = 7.5$  Hz), 7.89-7.87 (2H, app dd, overlapped), 7.37 (1H, br s), 6.93 (1H, br s), 4.67 (1H, d,  $J = 5.5$  Hz), 4.55-4.47 (2H, m, overlapped), 4.43-4.39 (1H, m), 4.10-3.98 (1H, m), 3.83-3.77 (2H, m, overlapped), 3.30-3.25 (1H, m), 2.56-2.49 (1H, m, overlapped with DMSO), 2.38-2.30 (1H, m), 2.18-2.07 (2H, m, overlapped), 2.01-1.92 (2H, m, overlapped), 1.68-1.62 (1H, m), 1.48-1.42 (2H, br m, overlapped), 1.27-1.20 (8H, br m, overlapped), 1.14 (3H, d,  $J = 7.5$  Hz), 1.09 (3H, d,  $J = 6.0$  Hz), 0.97 (3H, d,  $J = 6.5$  Hz), 0.86-0.82 (9H, m, overlapped); HRMS ( $\text{ESI}^+$ ) Calcd. for  $\text{C}_{29}\text{H}_{50}\text{N}_6\text{O}_8\text{Na}$ : 633.3588 ( $[\text{M} + \text{Na}]^+$ ), Found: 633.3585.

### Synthesis of *N*-terminal heptanoic acid amide **40**



A white powder.  $^1\text{H NMR}$  (500 MHz,  $\text{DMSO-}d_6$ )  $\delta$  8.08 (1H, d,  $J = 7.5$  Hz), 7.88 (1H, d,  $J = 7.5$  Hz), 7.84 (1H, d,  $J = 8.0$  Hz), 7.34 (1H, d, overlapped), 7.33 (1H, s), 6.89 (1H, br s), 4.72 (1H, d,  $J = 6.5$  Hz), 4.67 (1H, d,  $J = 6.0$  Hz), 4.53-4.39 (4H, m, overlapped), 4.05 (1H, dd,  $J = 8.0, 7.0$  Hz), 3.86 (1H, br s), 3.82-3.77 (2H, m, overlapped), 3.75-3.68 (1H, m), 3.59-3.56 (1H, m), 3.51-3.45 (1H, m), 3.30-3.26 (1H, m), 3.09-3.02 (1H, br m), 2.95-2.82 (1H, m), 2.53-2.51 (1H, m, overlapped with DMSO), 2.43-2.32 (3H, m, overlapped), 2.18-2.07 (2H, m, overlapped), 2.02-1.92 (2H, m, overlapped), 1.77 (1H, br t), 1.68-1.62 (1H, m), 1.48-1.42 (3H, m, overlapped), 1.30-1.20 (30H, m, overlapped), 1.09 (3H, d,  $J = 6.0$  Hz), 0.99 (3H, d,  $J = 7.0$  Hz), 0.97 (3H, d,  $J = 7.0$  Hz), 0.86-0.82 (12H, m, overlapped) (One proton (NH or OH) was not observed. It would be NH of sphingoid.); HRMS ( $\text{ESI}^+$ ) Calcd. for  $\text{C}_{47}\text{H}_{87}\text{N}_7\text{O}_{10}\text{Na}$ : 932.6412 ( $[\text{M} + \text{Na}]^+$ ), Found: 932.6400.

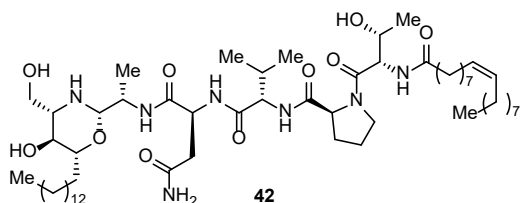
### Substitution of 4-MePro to unsubstituted Pro **41**



A white powder.  $^1\text{H NMR}$  (500 MHz,  $\text{DMSO-}d_6$ )  $\delta$  9.33 (1H, s), 8.14-8.10 (2H, app dd, overlapped), 7.90-7.87 (2H, app dd, overlapped), 7.37 (1H, br s), 6.94 (1H, br s), 5.35-5.29 (2H, m, overlapped), 4.67-4.64

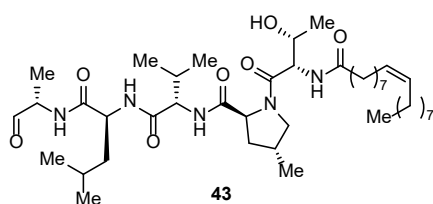
(1H, m), 4.55-4.47 (1H, m), 4.44-4.41 (2H, br m, overlapped), 4.10-3.99 (2H, m, overlapped), 3.81-3.74 (2H, m, overlapped), 3.65-3.59 (1H, br m), 2.57-2.46 (2H, m, overlapped with solvent residual signals), 2.44-2.36 (1H, m), 2.18-2.06 (2H, m, overlapped), 2.03-1.94 (6H, m, overlapped), 1.91-1.81 (2H, m, overlapped), 1.49-1.40 (2H, m, overlapped), 1.32-1.18 (20H, br m, overlapped), 1.09 (3H, dd,  $J = 6.5, 3.0$  Hz), 0.94 (3H, d,  $J = 7.0$  Hz), 0.86-0.82 (9H, m, overlapped); HRMS (ESI<sup>+</sup>) Calcd. for C<sub>39</sub>H<sub>68</sub>N<sub>6</sub>O<sub>8</sub>Na: 771.4996 ([M + Na]<sup>+</sup>), Found: 771.4976.

### Substitution of 4-MePro to unsubstituted Pro 42



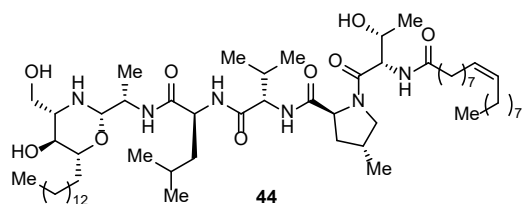
A white powder. <sup>1</sup>H NMR (500 MHz, DMSO-*d*<sub>6</sub>)  $\delta$  8.09 (1H, d,  $J = 8.0$  Hz), 7.88 (1H, d,  $J = 7.5$  Hz), 7.85 (1H, d,  $J = 8.0$  Hz), 7.34 (1H, d, overlapped), 7.33 (1H, s), 6.90 (1H, s), 5.35-5.29 (2H, m, overlapped), 4.73 (1H, d,  $J = 6.5$  Hz), 4.66 (1H, d,  $J = 6.0$  Hz), 4.53 (1H, t,  $J = 5.0$  Hz), 4.47-4.40 (3H, m, overlapped), 4.05 (1H, dd,  $J = 8.0, 7.0$  Hz), 3.85 (1H, app br s), 3.82-3.76 (2H, m, overlapped), 3.75-3.68 (1H, br m), 3.63-3.55 (2H, m, overlapped), 3.50-3.44 (1H, br m), 3.07-3.01 (1H, br m), 2.89-2.84 (1H, m), 2.54-2.50 (1H, m, overlapped with DMSO), 2.43-2.33 (2H, m, overlapped), 2.20-2.06 (2H, m, overlapped), 2.01-1.94 (6H, m, overlapped), 1.91-1.75 (4H, m), 1.48-1.41 (3H, m, overlapped), 1.31-1.20 (44H, m, overlapped), 1.10 (3H, d,  $J = 6.5$  Hz), 0.99 (3H, d,  $J = 7.0$  Hz), 0.86-0.82 (12H, m, overlapped) (One proton (NH or OH) was not observed. It would be NH of sphingoid.); HRMS (ESI<sup>+</sup>) Calcd. for C<sub>57</sub>H<sub>105</sub>N<sub>7</sub>O<sub>10</sub>Na: 1070.7821 ([M + Na]<sup>+</sup>), Found: 1070.7821.

### Substitution of Asn to Leu 43



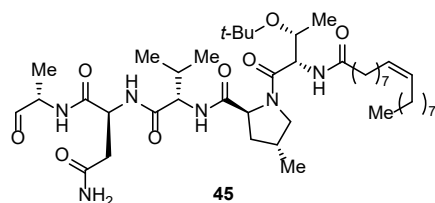
A white powder. <sup>1</sup>H NMR (500 MHz, DMSO-*d*<sub>6</sub>)  $\delta$  9.34 (1H, s), 8.33 (1H, d,  $J = 6.5$  Hz), 7.89 (1H, d, overlapped), 7.88 (1H, d, overlapped), 7.79 (1H, d,  $J = 8.5$  Hz), 5.35-5.29 (2H, m, overlapped), 4.70 (1H, d,  $J = 5.0$  Hz), 4.46-4.40 (2H, m, overlapped), 4.36-4.40 (1H, m), 4.09-4.02 (2H, m, overlapped), 3.85-3.78 (2H, m, overlapped), 3.25 (1H, t,  $J = 9.0$  Hz), 2.36-2.29 (1H, m), 2.18-2.07 (2H, m, overlapped), 1.99-1.89 (5H, m, overlapped), 1.68-1.58 (2H, m, overlapped), 1.50-1.40 (3H, m, overlapped), 1.31-1.19 (22H, br m, overlapped), 1.15 (3H, d,  $J = 7.5$  Hz), 1.09 (3H, d,  $J = 6.0$  Hz), 0.97 (3H, d,  $J = 7.0$  Hz), 0.89 (3H, d,  $J = 6.5$  Hz), 0.86-0.82 (12H, m, overlapped); HRMS (ESI<sup>+</sup>) Calcd. for C<sub>42</sub>H<sub>75</sub>N<sub>5</sub>O<sub>7</sub>Na: 784.5564 ([M + Na]<sup>+</sup>), Found: 784.5561.

### Substitution of Asn to Leu 44



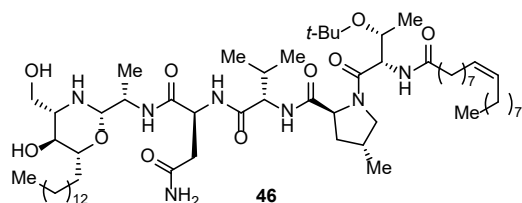
A white powder. <sup>1</sup>H NMR (500 MHz, DMSO-*d*<sub>6</sub>) δ 7.87 (1H, d, *J* = 7.5 Hz), 7.80 (1H, d, *J* = 9.0 Hz), 7.76 (1H, d, *J* = 8.5 Hz), 7.62 (1H, d, *J* = 8.5 Hz), 5.35-5.29 (2H, m, overlapped), 4.69 (2H, app d, *J* = 5.0 Hz), 4.50 (1H, t, *J* = 5.0 Hz), 4.46-4.40 (2H, m, overlapped), 4.30-4.26 (1H, m), 4.06 (1H, dd, *J* = 8.5, 8.0 Hz), 3.90-3.77 (4H, m, overlapped), 3.62-3.58 (1H, br m), 3.47-3.43 (1H, br m), 3.26-3.23 (1H, m), 3.01 (1H, app br t, *J* = 8.0 Hz), 2.91-2.82 (1H, m), 2.36-2.28 (2H, m, overlapped), 2.17-2.07 (2H, m, overlapped), 2.02-1.89 (6H, m, overlapped), 1.80-1.73 (1H, br m), 1.68-1.55 (2H, m, overlapped), 1.51-1.35 (5H, m, overlapped), 1.31-1.18 (44H, br m, overlapped), 1.09 (3H, d, *J* = 6.5 Hz), 1.01 (3H, d, *J* = 7.0 Hz), 0.97 (3H, d, *J* = 7.0 Hz), 0.86-0.81 (18H, m, overlapped) (One proton (NH or OH) was not observed. It would be NH of sphingoid.); HRMS (ESI<sup>+</sup>) Calcd. for C<sub>60</sub>H<sub>112</sub>N<sub>6</sub>O<sub>9</sub>Na: 1083.8389 ([M + Na]<sup>+</sup>), Found: 1083.8388.

### Substitution of unprotected Thr to *t*-Bu protected Thr 45



A white powder. <sup>1</sup>H NMR (500 MHz, DMSO-*d*<sub>6</sub>) δ 9.34 (1H, s), 8.14 (1H, d, *J* = 6.5 Hz), 8.12 (1H, d, *J* = 8.0 Hz), 7.79 (2H, app t, *J* = 8.0 Hz), 7.37 (1H, br s), 6.92 (1H, br s), 5.35-5.29 (2H, m, overlapped), 4.55-4.47 (3H, m, overlapped), 4.15-3.99 (2H, m, overlapped), 3.92 (1H, dd, *J* = 9.5, 7.5 Hz), 3.75-3.70 (1H, m), 3.17 (1H, t, *J* = 9.5 Hz), 2.56-2.45 (2H, m, overlapped with solvent residual signals), 2.41-2.06 (1H, m), 2.18-2.06 (2H, m, overlapped), 2.02-1.94 (6H, m, overlapped), 1.67-1.60 (1H, m), 1.49-1.38 (2H, m, overlapped), 1.30-1.19 (20H, br m, overlapped), 1.12 (9H, s), 1.05 (3H, d, *J* = 6.5 Hz), 0.97-0.94 (6H, m, overlapped), 0.86-0.82 (9H, m, overlapped); HRMS (ESI<sup>+</sup>) Calcd. for C<sub>44</sub>H<sub>78</sub>N<sub>6</sub>O<sub>8</sub>Na: 841.5779 ([M + Na]<sup>+</sup>), Found: 841.5778.

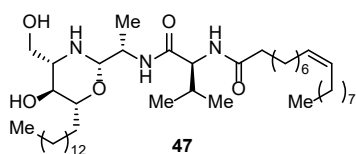
### Substitution of unprotected Thr to *t*-Bu protected Thr 46



A white powder. <sup>1</sup>H NMR (500 MHz, DMSO-*d*<sub>6</sub>) δ 8.11 (1H, d, *J* = 7.5 Hz), 7.79 (1H, d, *J* = 9.0 Hz), 7.73

(1H, d,  $J = 8.0$  Hz), 7.36-7.29 (2H, br m, overlapped), 6.87 (1H, br s), 5.35-5.29 (2H, m, overlapped), 4.71 (1H, d,  $J = 6.5$  Hz), 4.55-4.44 (4H, m, overlapped), 4.11-4.05 (1H, m), 3.94-3.89 (1H, br m), 3.88-3.84 (1H, br m), 3.74-3.70 (2H, m, overlapped), 3.61-3.55 (1H, br m), 3.51-3.45 (1H, m), 3.22-3.15 (1H, m), 3.07-3.02 (1H, br m), 2.92-2.84 (1H, m), 2.53-2.50 (1H, m, overlapped with DMSO), 2.44-2.33 (3H, m, overlapped), 2.18-2.08 (2H, m, overlapped), 2.03-1.94 (6H, m, overlapped), 1.83-1.75 (1H, br m), 1.67-1.61 (1H, m), 1.51-1.39 (3H, m, overlapped), 1.32-1.18 (44H, br m, overlapped), 1.12 (9H, s), 1.06 (3H, d,  $J = 6.0$  Hz), 1.00-0.93 (6H, m, overlapped), 0.86-0.83 (12H, m, overlapped) (One proton (NH or OH) was not observed. It would be NH of sphingoid.); HRMS (ESI<sup>+</sup>) Calcd. for C<sub>62</sub>H<sub>115</sub>N<sub>7</sub>O<sub>10</sub>Na: 1140.8603 ([M + Na]<sup>+</sup>), Found: 1140.8604.

*Synthesis of a C-terminal N,O-acetal model substrate 47*



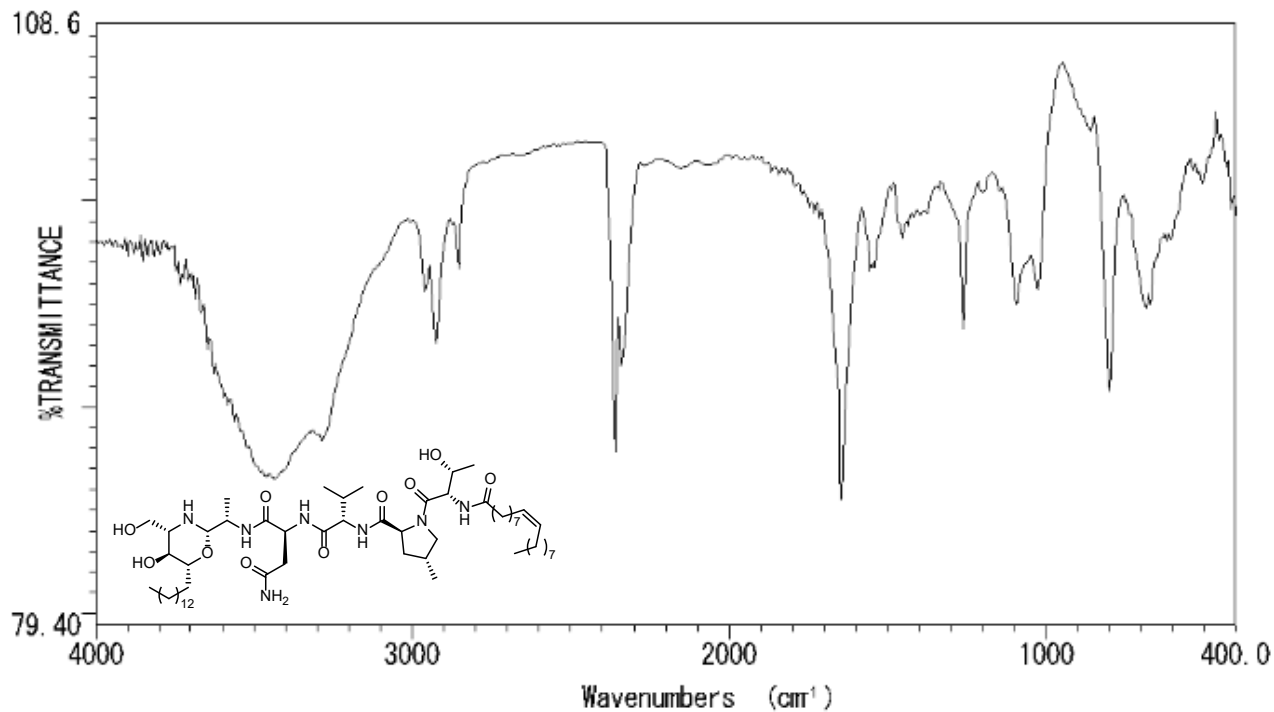
A white powder. <sup>1</sup>H NMR (500 MHz, DMSO-*d*<sub>6</sub>)  $\delta$  7.72 (1H, d,  $J = 9.0$  Hz), 7.69 (1H, d,  $J = 8.0$  Hz), 5.34-5.28 (2H, m, overlapped), 4.67 (1H, d,  $J = 6.5$  Hz), 4.48 (1H, t,  $J = 5.5$  Hz), 4.16 (1H, dd,  $J = 9.0, 7.0$  Hz), 3.90 (1H, br s), 3.87-3.80 (1H, m), 3.63-3.59 (1H, m), 3.46-3.42 (1H, m), 3.02-2.99 (1H, br m), 2.89-2.84 (1H, m), 2.38-2.33 (1H, br m), 2.21-2.15 (1H, m), 2.11-2.05 (1H, m), 1.99-1.89 (6H, m, overlapped), 1.77 (1H, br m), 1.51-1.41 (3H, m, overlapped), 1.30-1.18 (44H, br m, overlapped), 1.01 (3H, d,  $J = 6.0$  Hz), 0.86-0.80 (12H, m, overlapped); HRMS (ESI<sup>+</sup>) Calcd. for C<sub>44</sub>H<sub>86</sub>N<sub>3</sub>O<sub>5</sub>: 736.6568 ([M + H]<sup>+</sup>), Found: 736.6559.

## **IR and NMR Spectra of Compounds in Chapter 2**

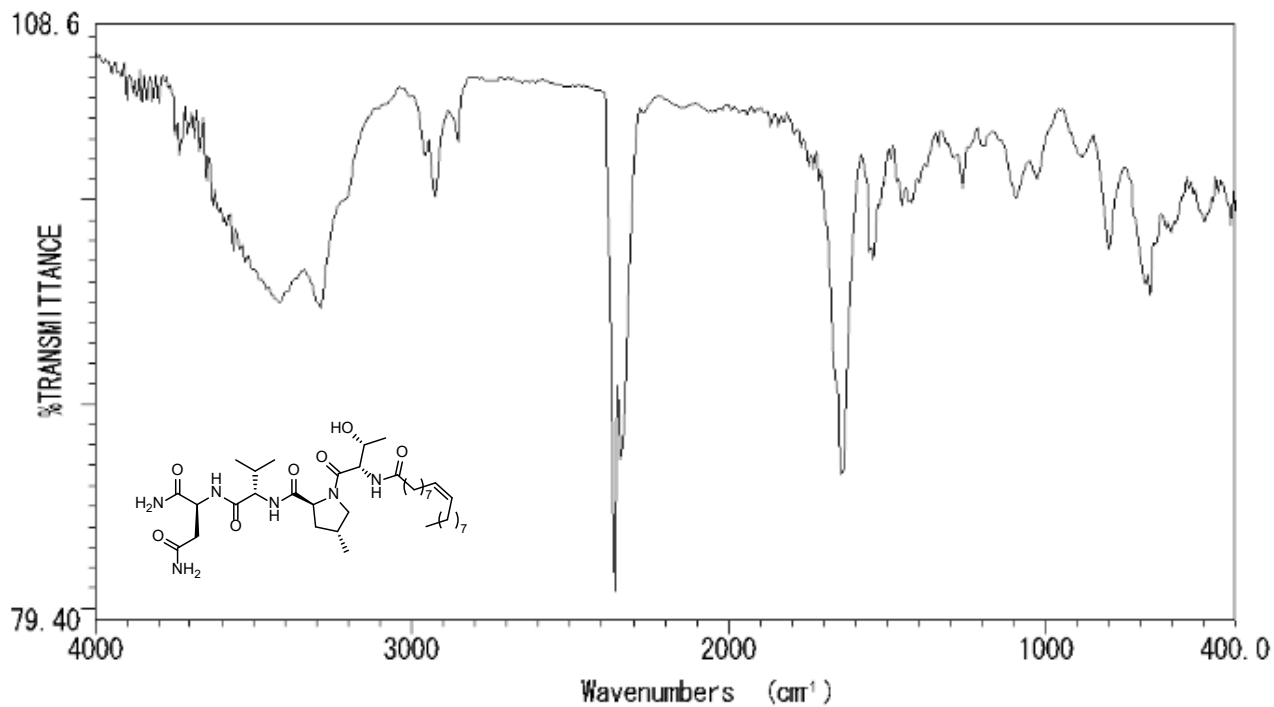
# IR and NMR Spectra of Compounds

## 1. IR spectra of naturally occurring kozupeptins A and B

Natural kozupeptin A (**1a**)

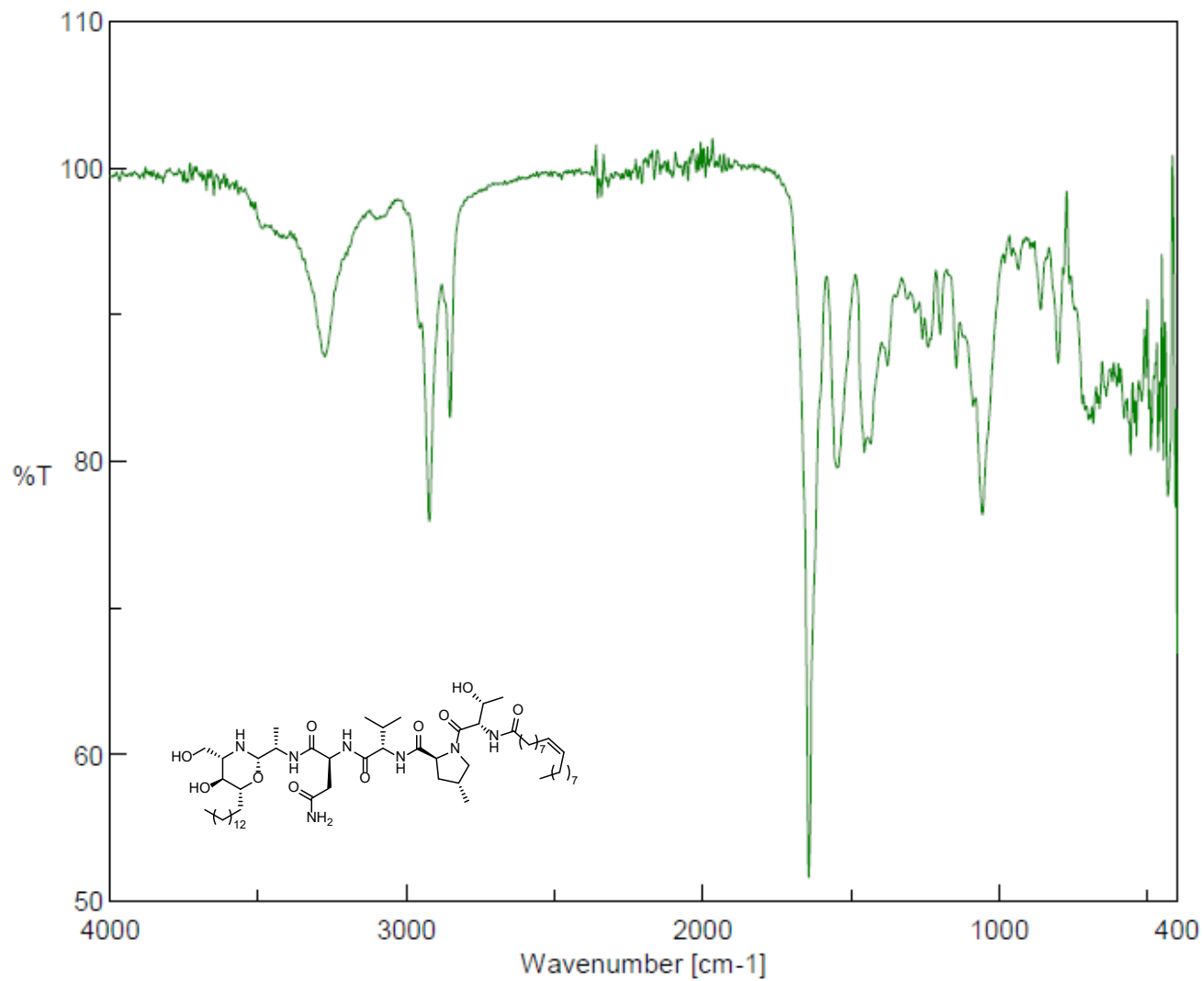


Natural kozupeptin B (**1b**)



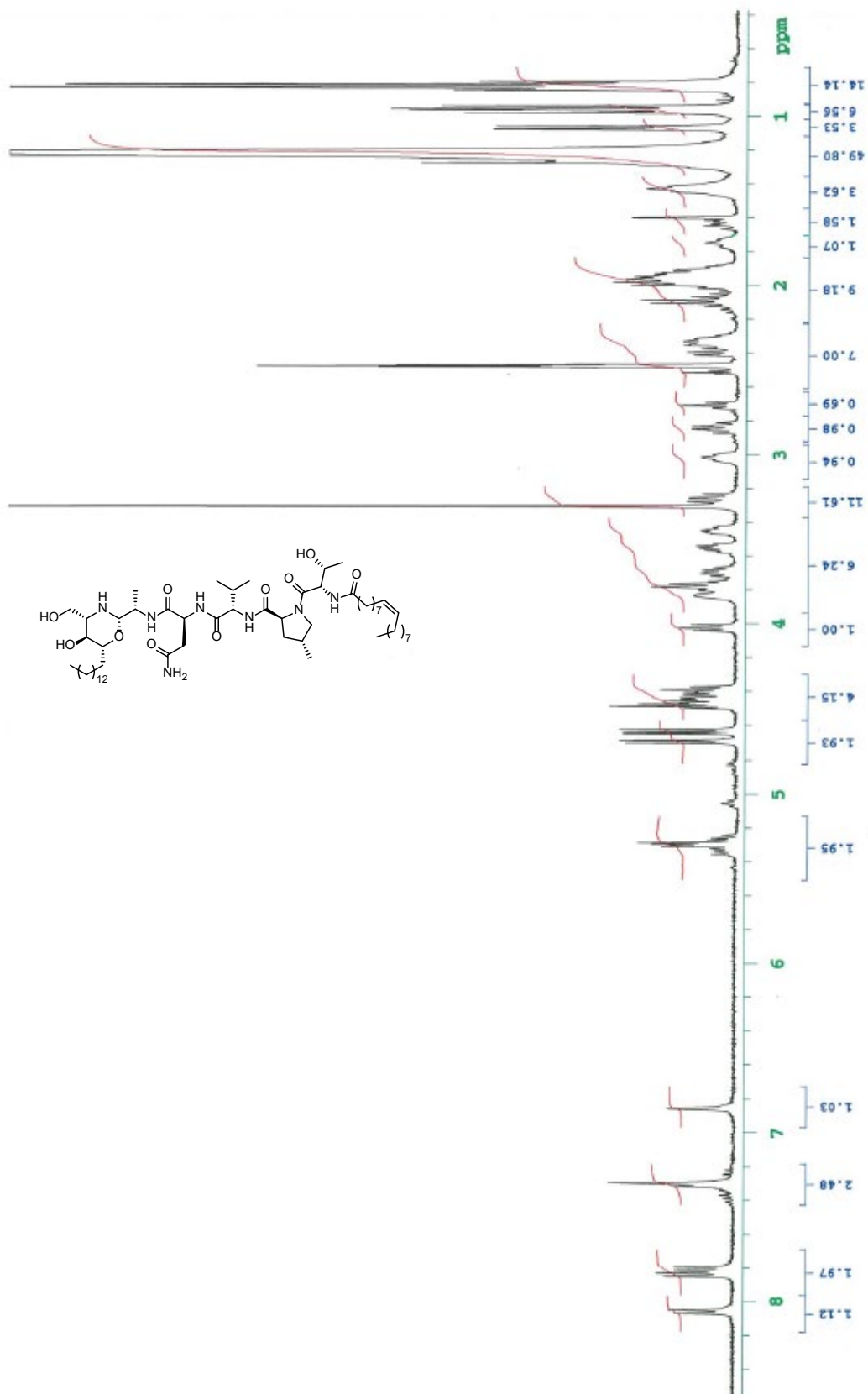
## 2. IR spectra of synthetic kozupeptins A

Synthetic kozupeptin A (**1a**)



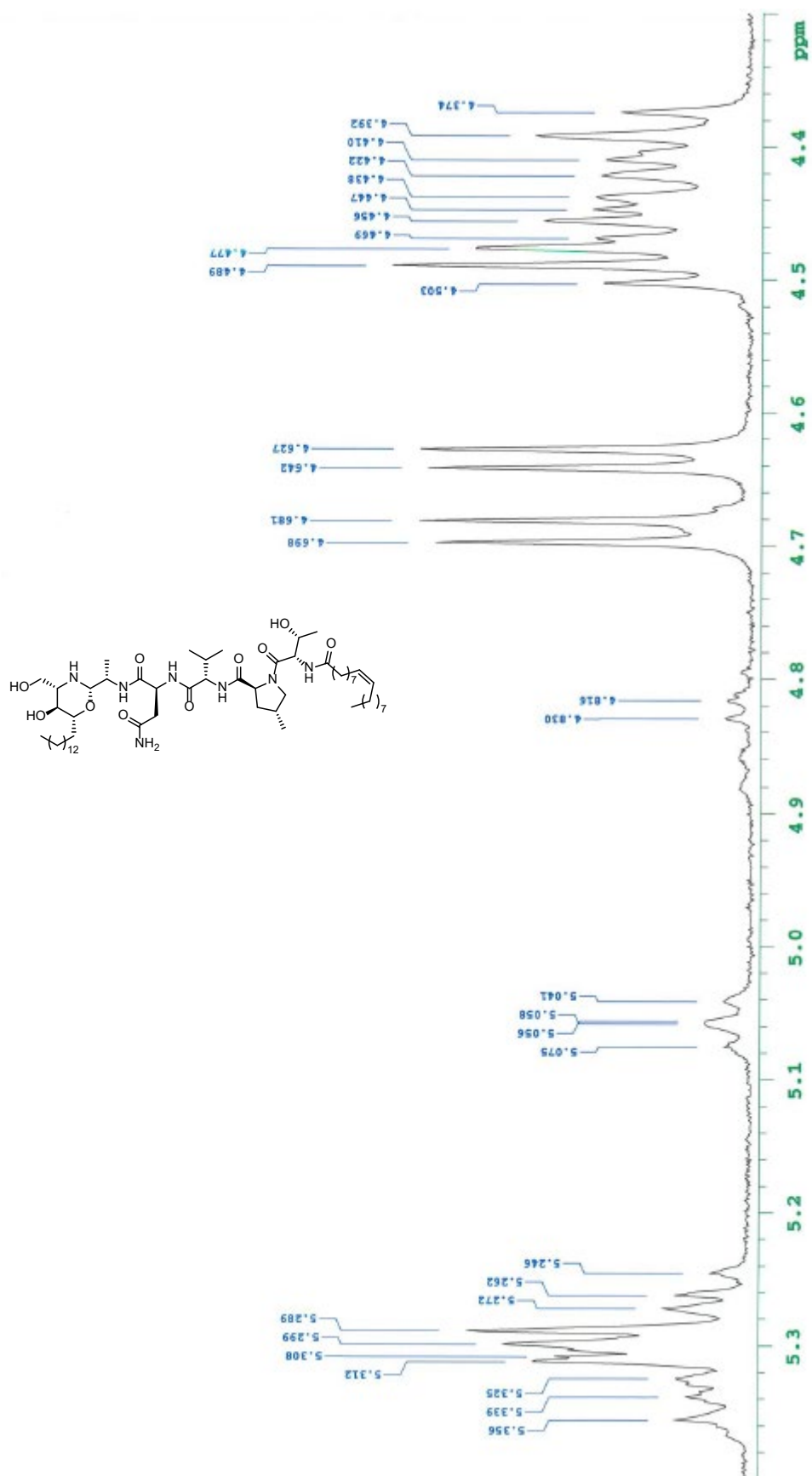
### 3. NMR spectra of naturally occurring kazupeptins A and B

$^1\text{H}$  NMR spectrum of natural kazupeptin A (**1a**) ( $\text{DMSO-}d_6$ )

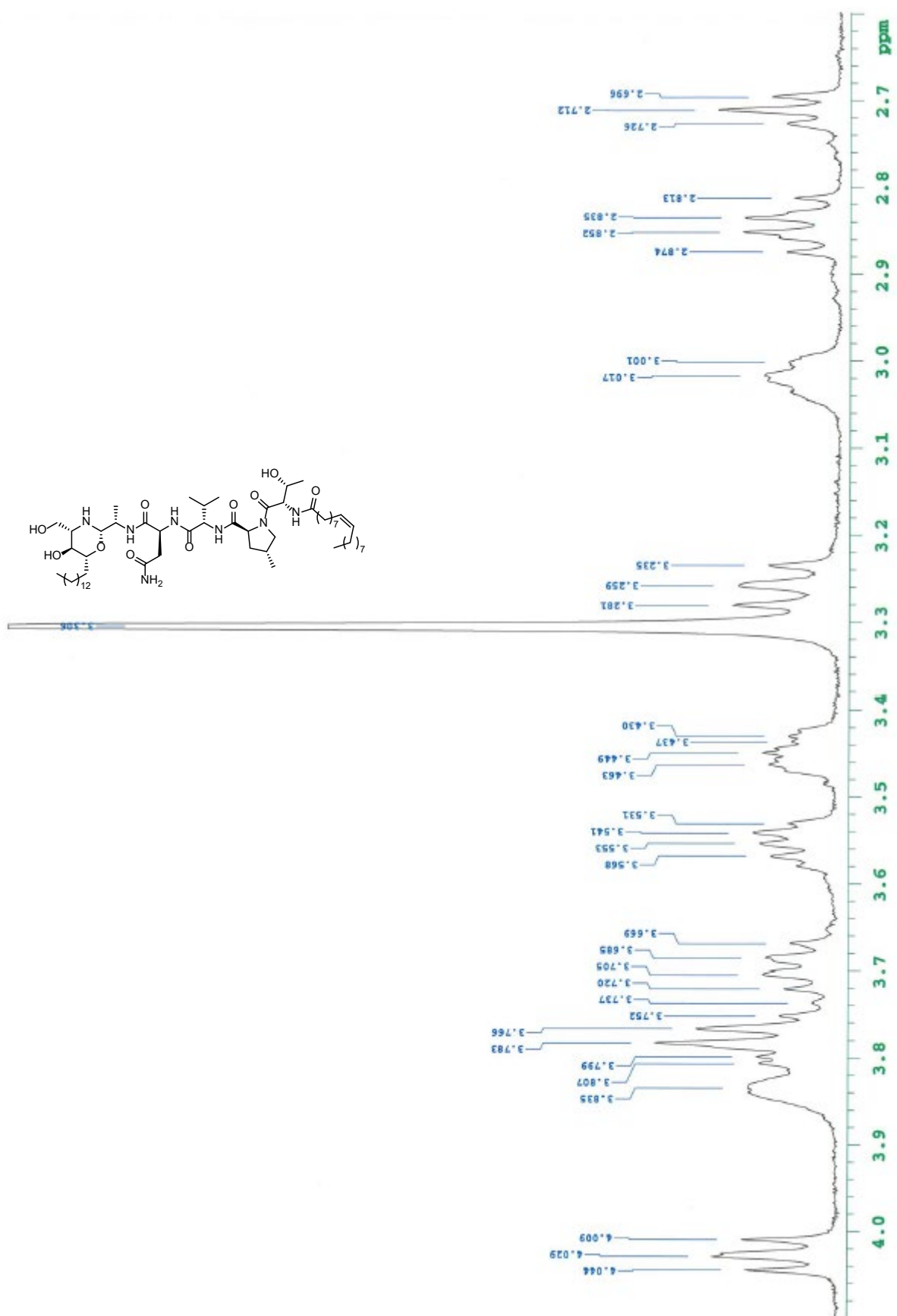




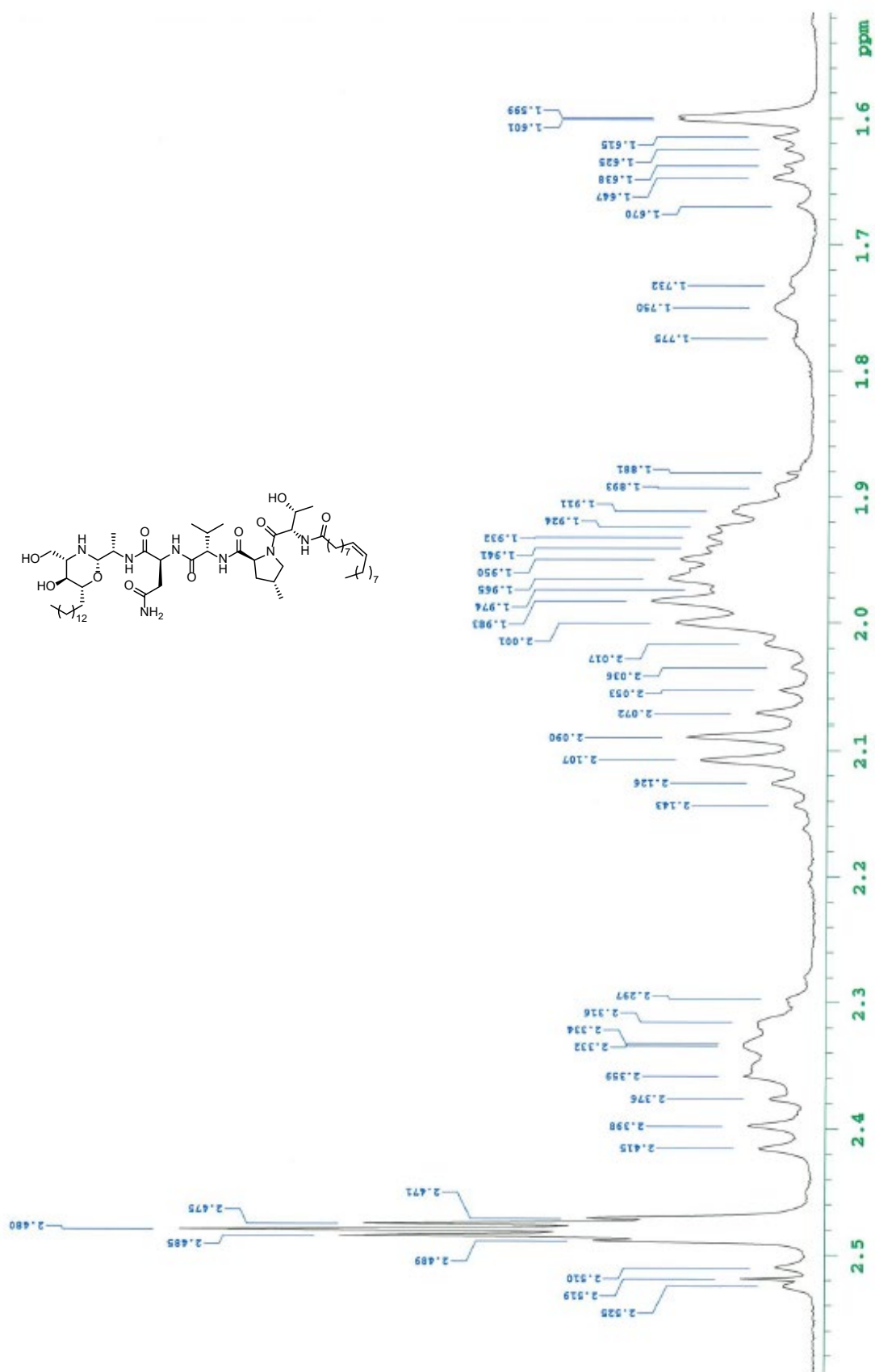
$^1\text{H}$  NMR spectrum of natural kozupeptin A (**1a**) ( $\text{DMSO}-d_6$ )



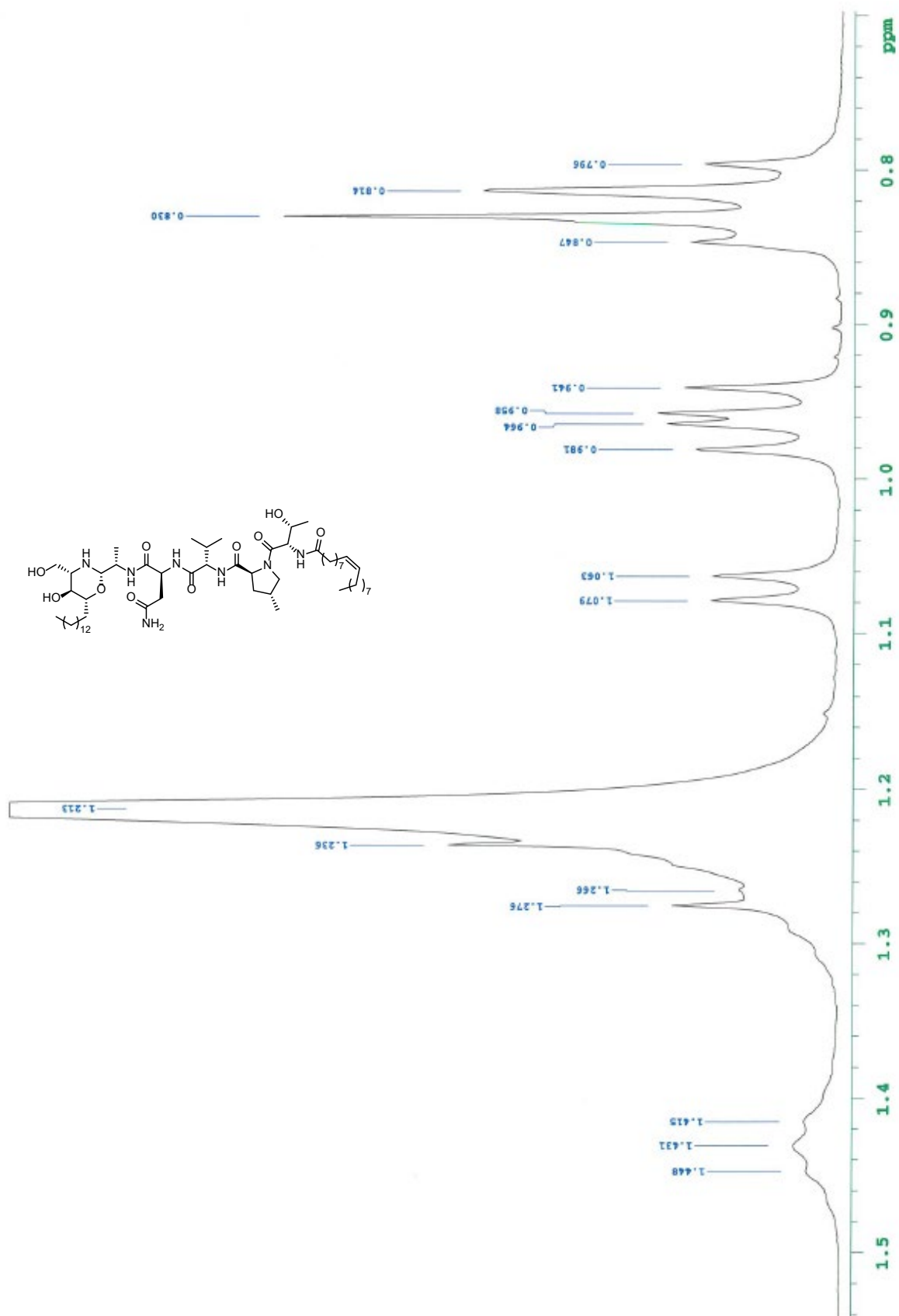
$^1\text{H}$  NMR spectrum of natural kozupeptin A (**1a**) ( $\text{DMSO-}d_6$ )



$^1\text{H}$  NMR spectrum of natural kozupeptin A (**1a**) ( $\text{DMSO-}d_6$ )

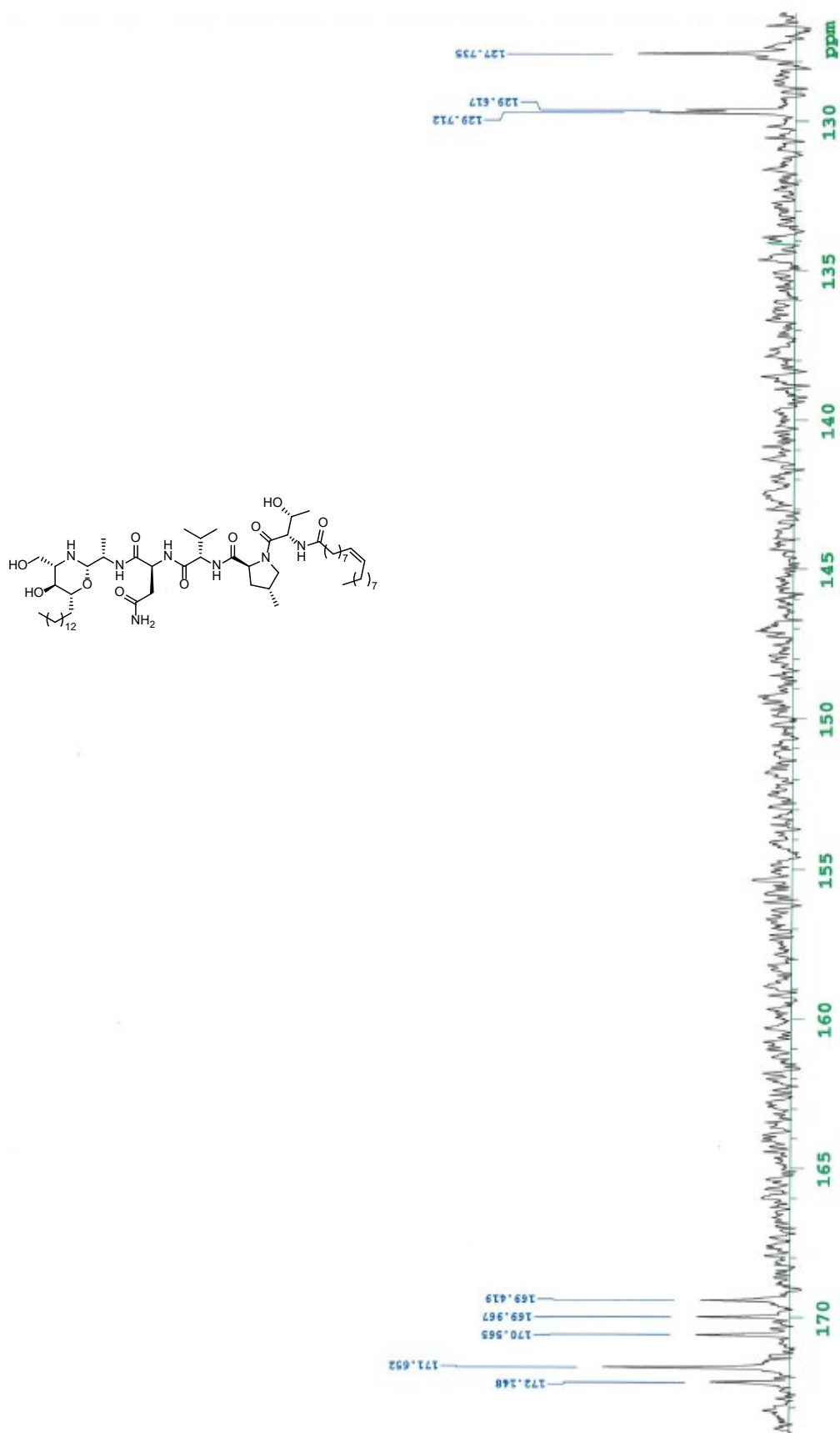


$^1\text{H}$  NMR spectrum of natural kazupeptin A (**1a**) ( $\text{DMSO-}d_6$ )

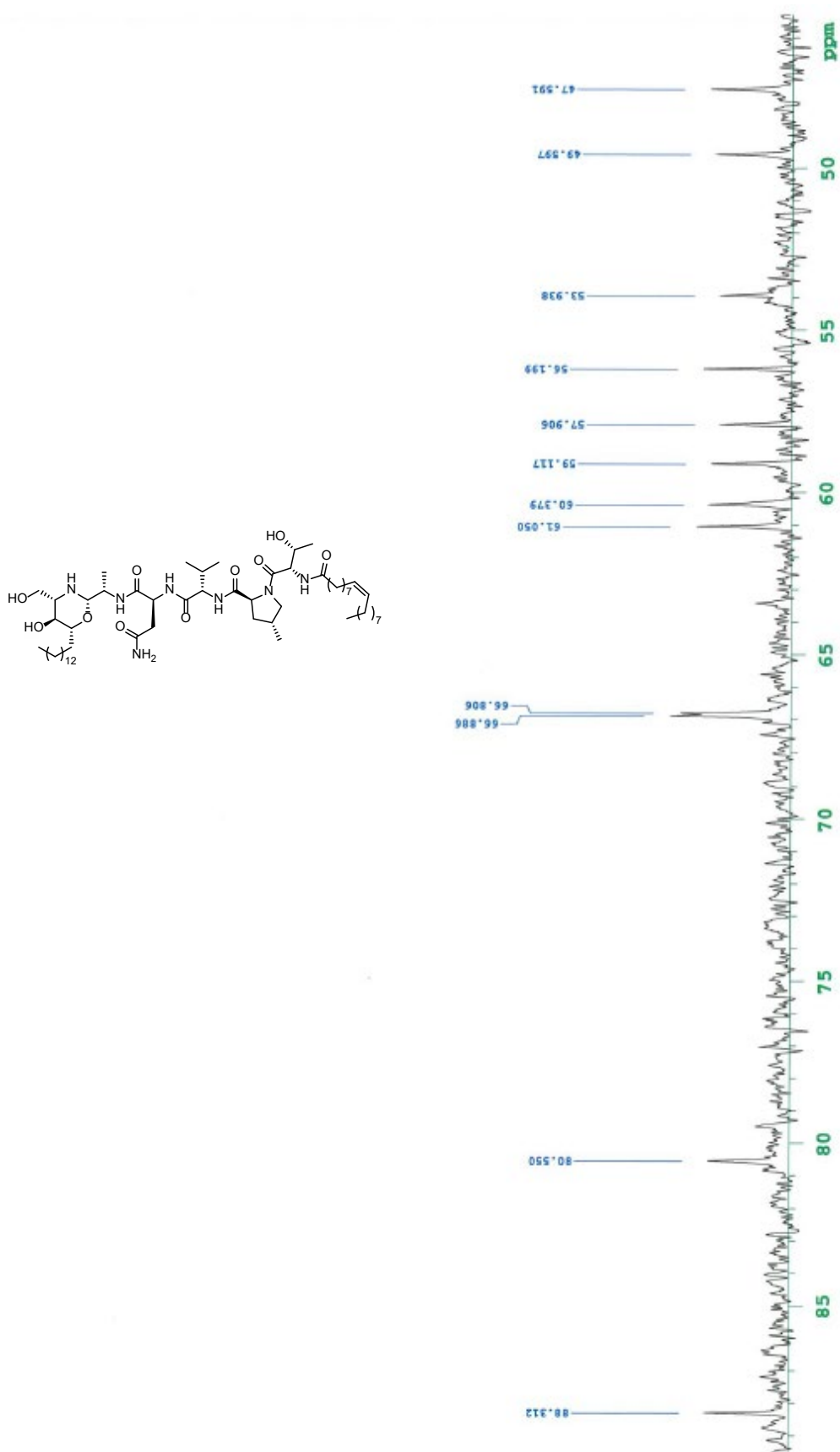




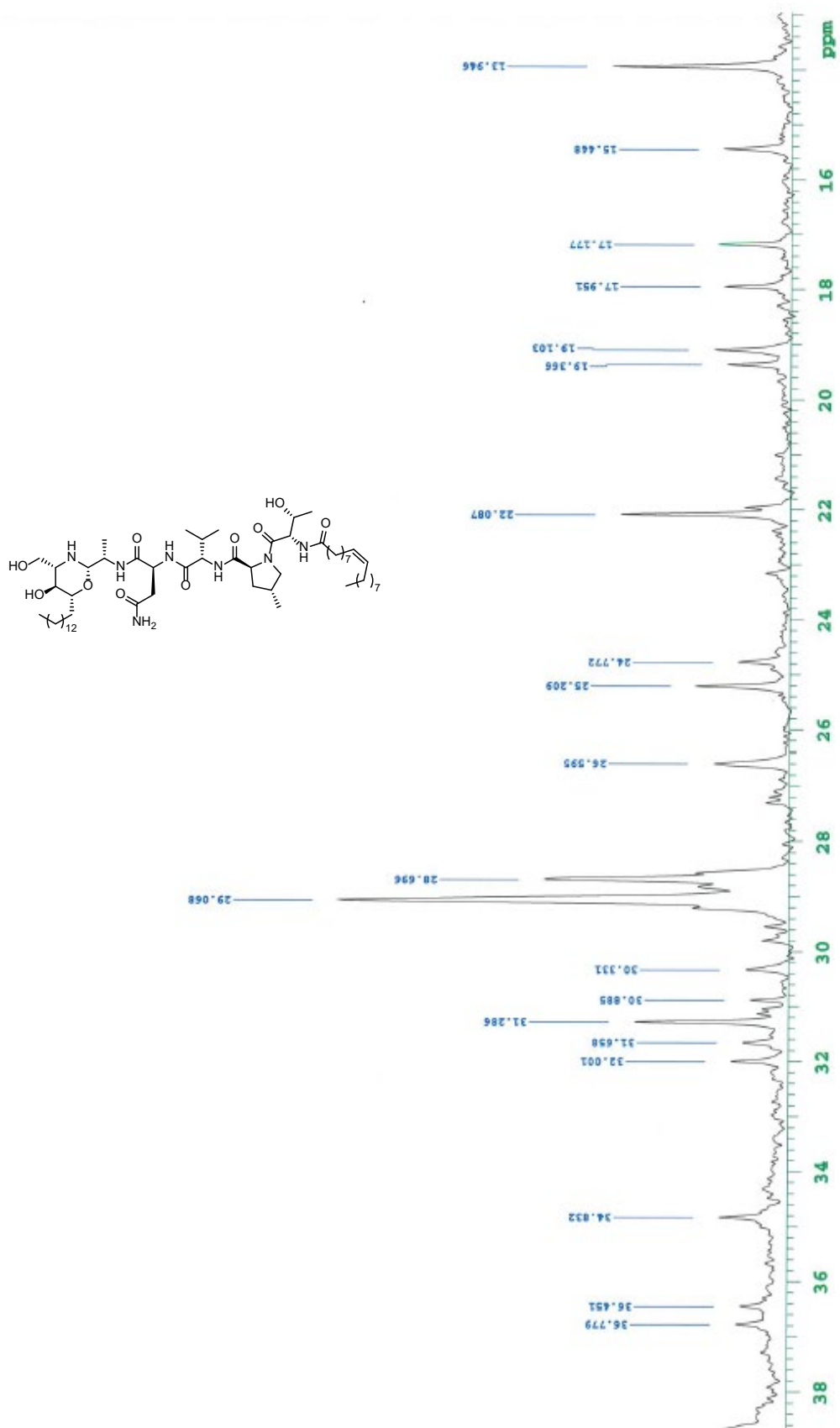
$^{13}\text{C}$  NMR spectrum of natural kozupeptin A (**1a**) ( $\text{DMSO-}d_6$ )



$^{13}\text{C}$  NMR spectrum of natural kozupeptin A (**1a**) ( $\text{DMSO-}d_6$ )



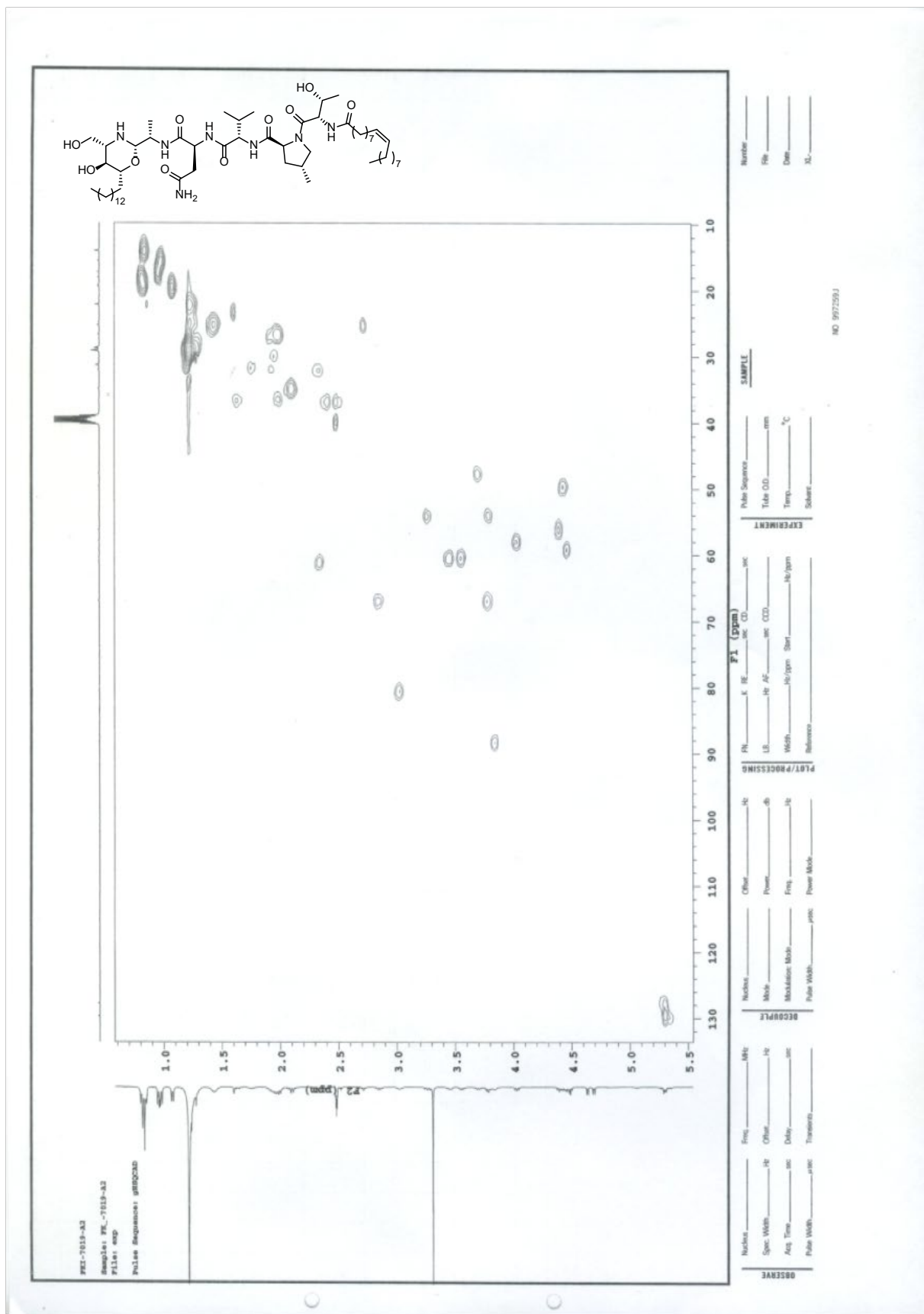
$^{13}\text{C}$  NMR spectrum of natural kozupeptin A (**1a**) ( $\text{DMSO-}d_6$ )



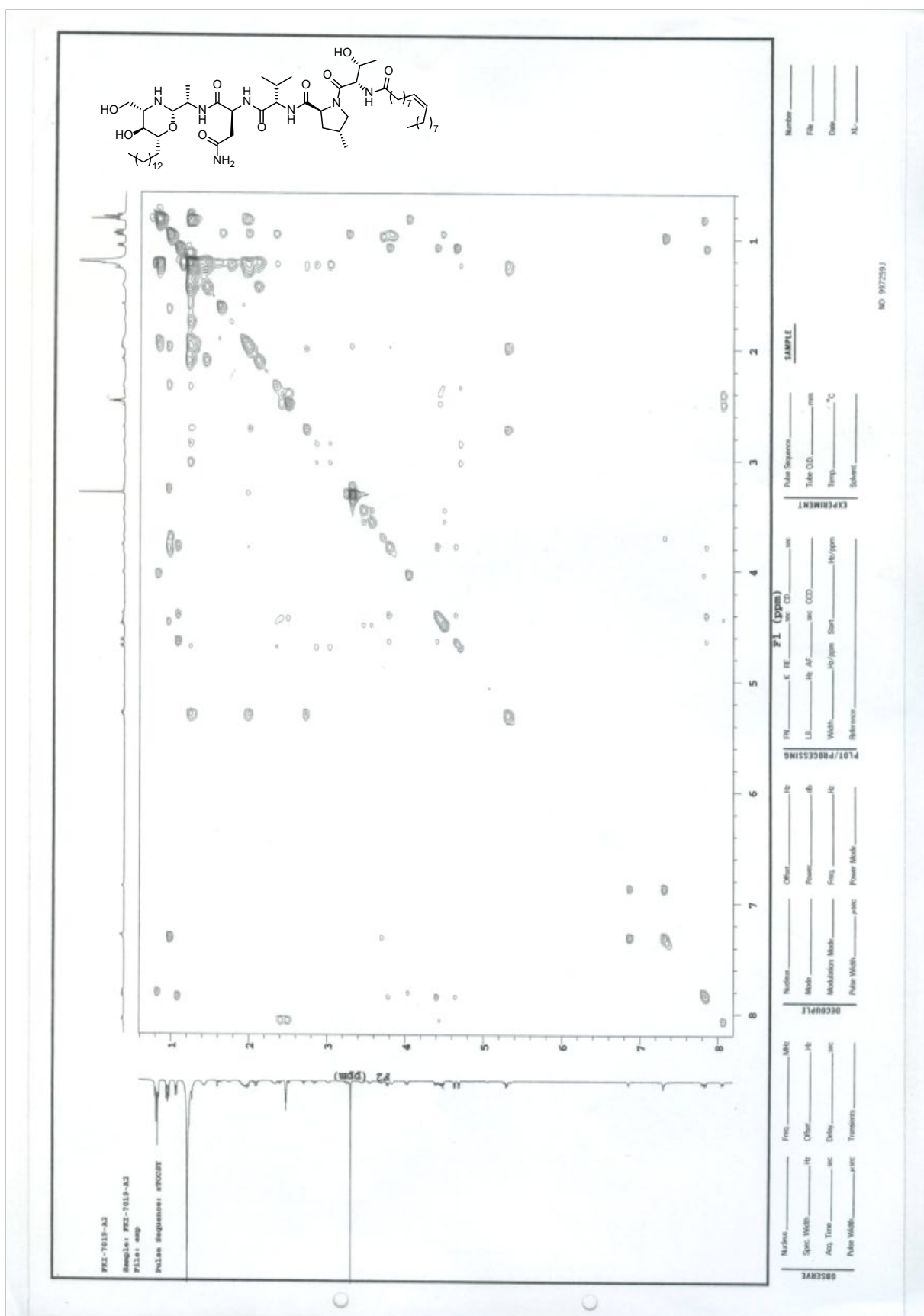




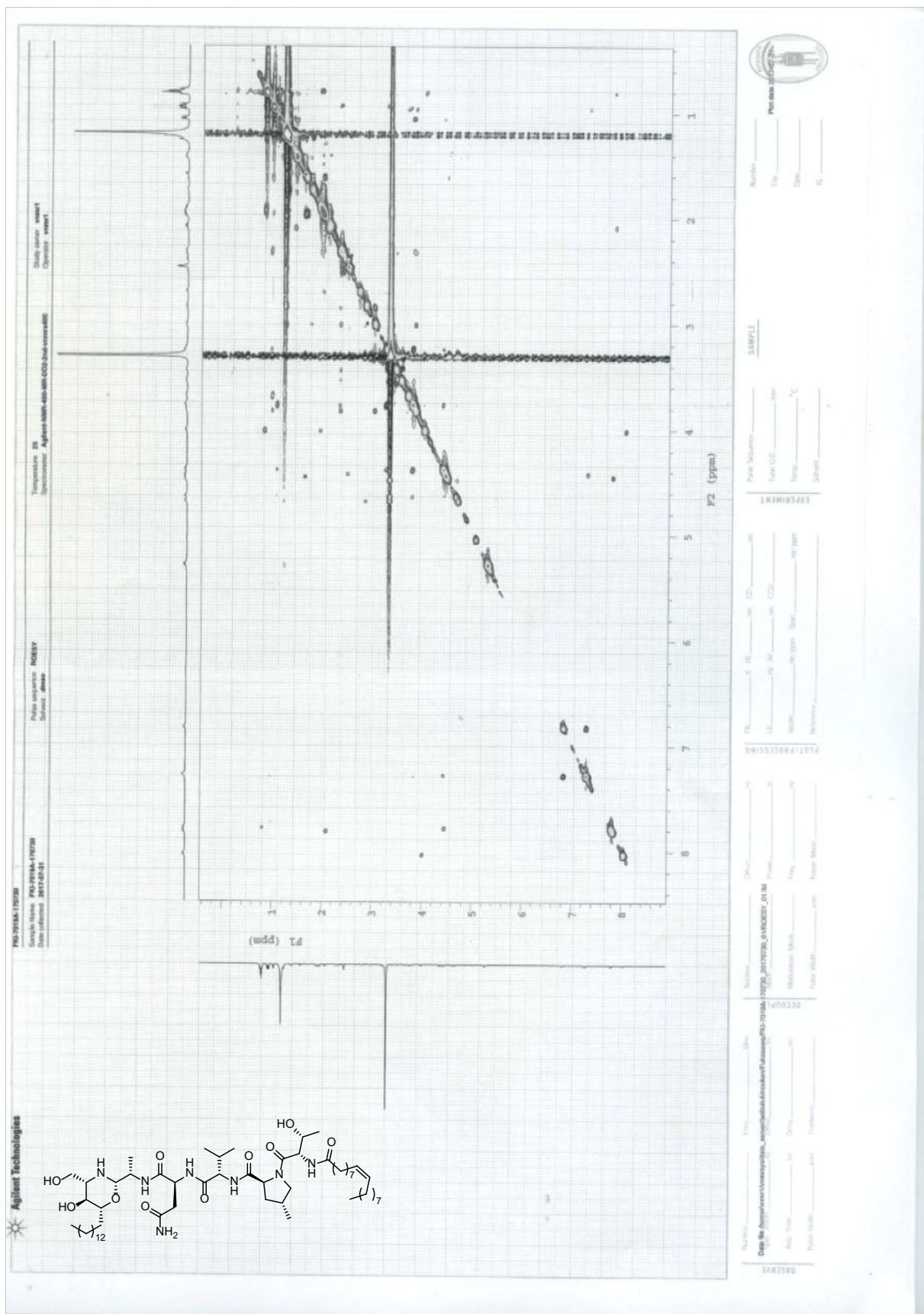
HSQC NMR spectrum of natural kozupeptin A (**1a**) (DMSO-*d*<sub>6</sub>)



TOCSY NMR spectrum of natural kozupeptin A (**1a**) (DMSO-*d*<sub>6</sub>)



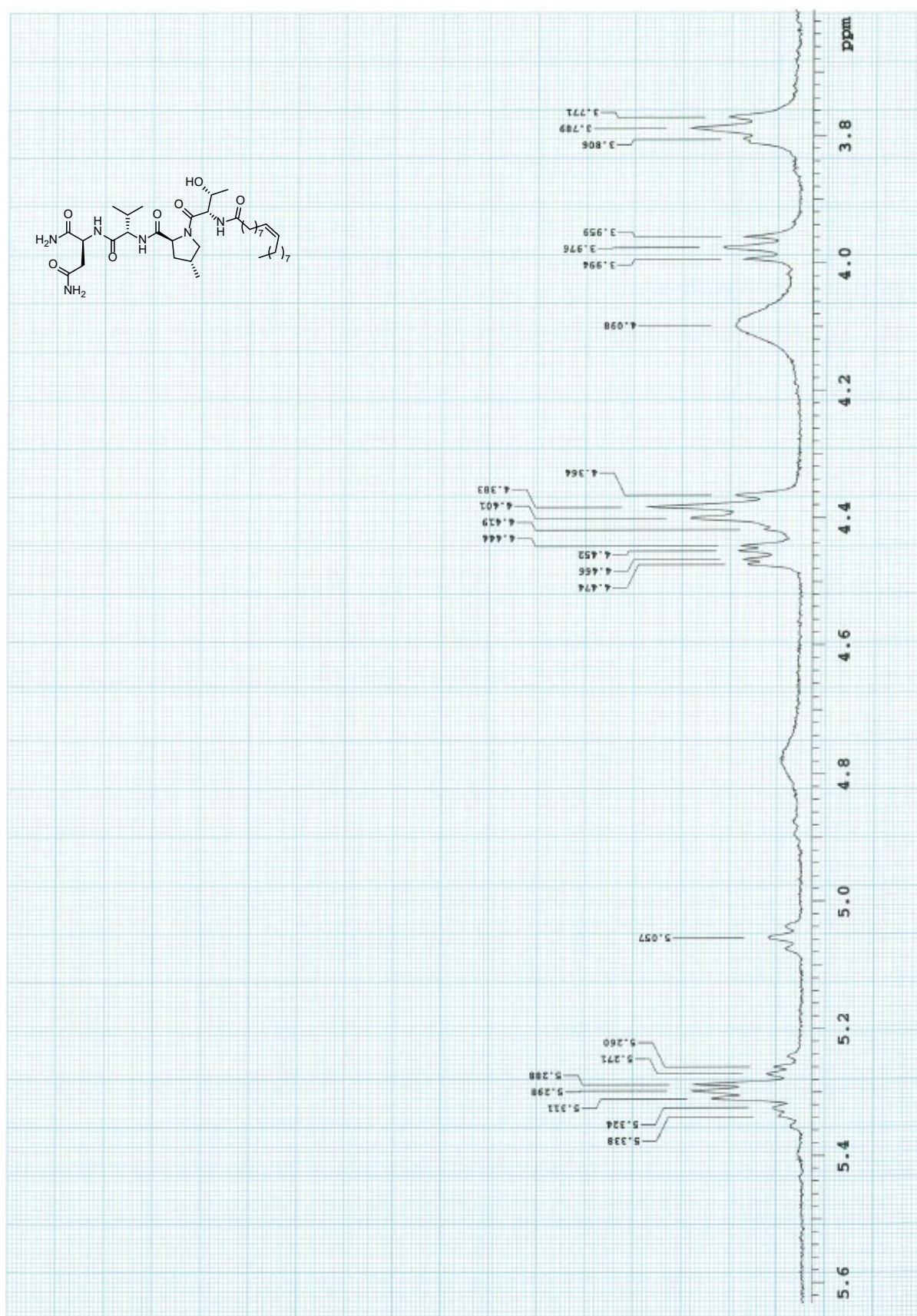
ROESY NMR spectrum of natural kozupeptin A (**1a**) (DMSO-*d*<sub>6</sub>)







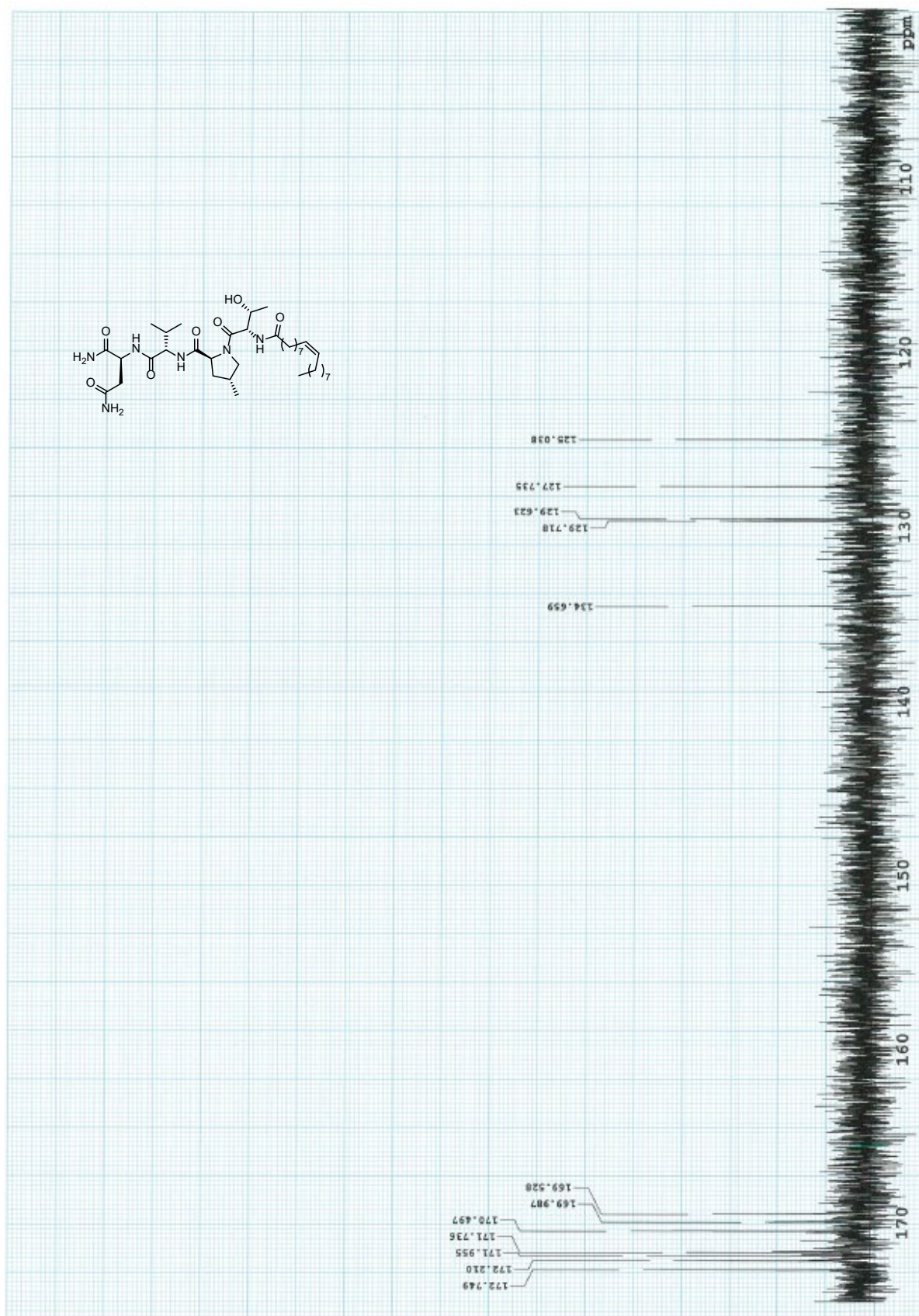
<sup>1</sup>H NMR spectrum of natural kozupeptin B (**1b**) (DMSO-*d*<sub>6</sub>)



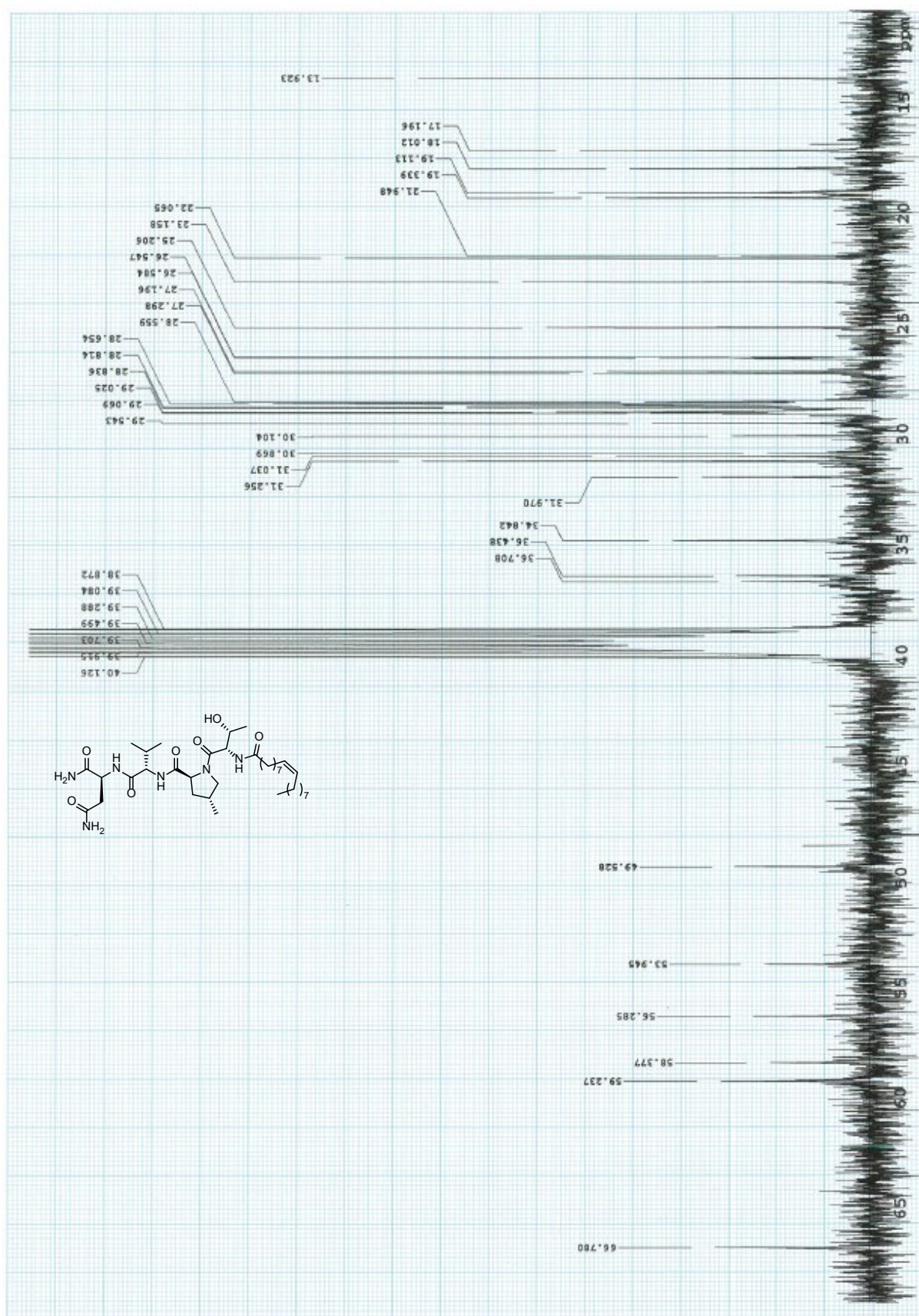




$^{13}\text{C}$  NMR spectrum of natural kozupeptin B (**1b**) (DMSO- $d_6$ )



$^{13}\text{C}$  NMR spectrum of natural kozupeptin B (**1b**) (DMSO- $d_6$ )



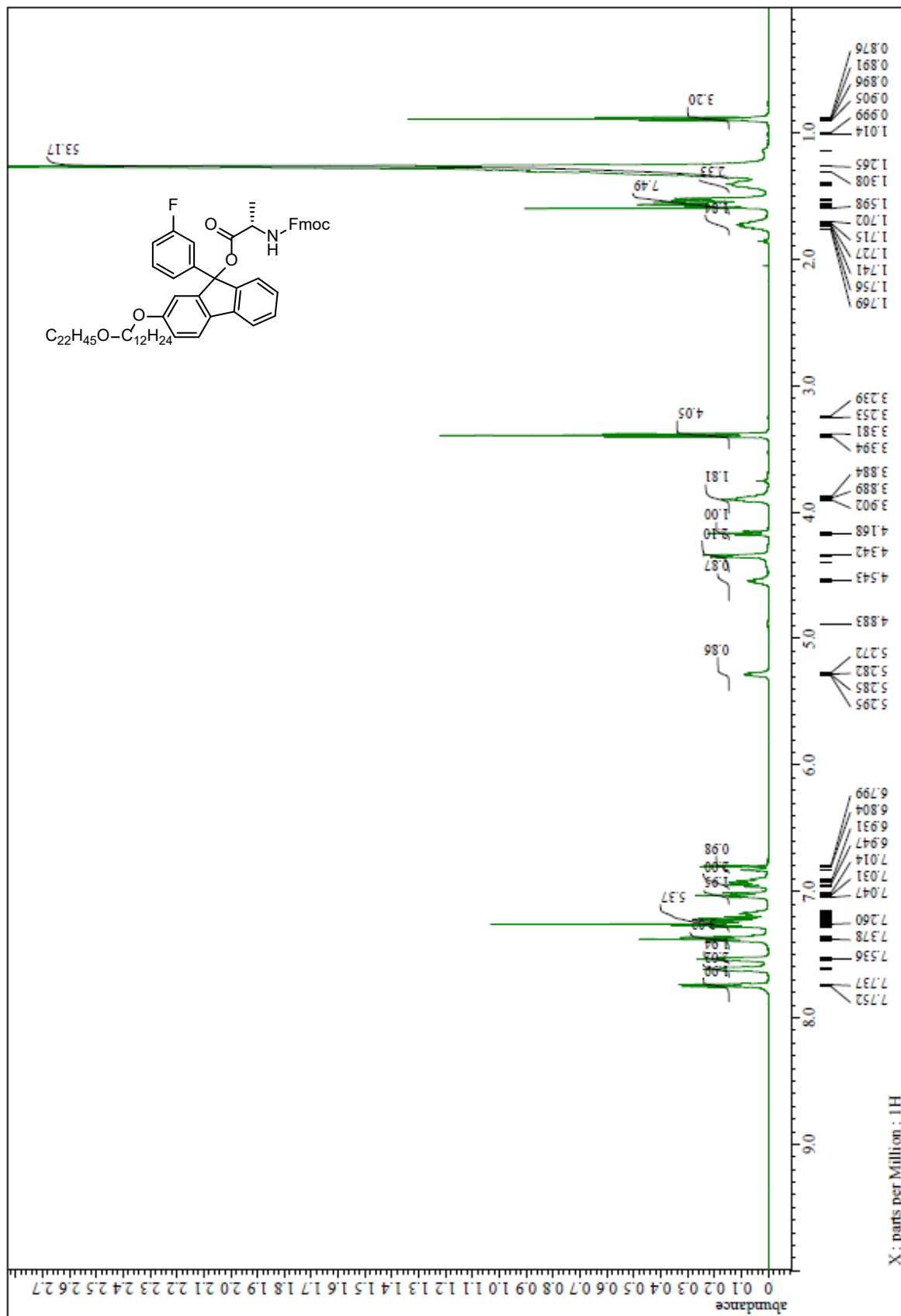




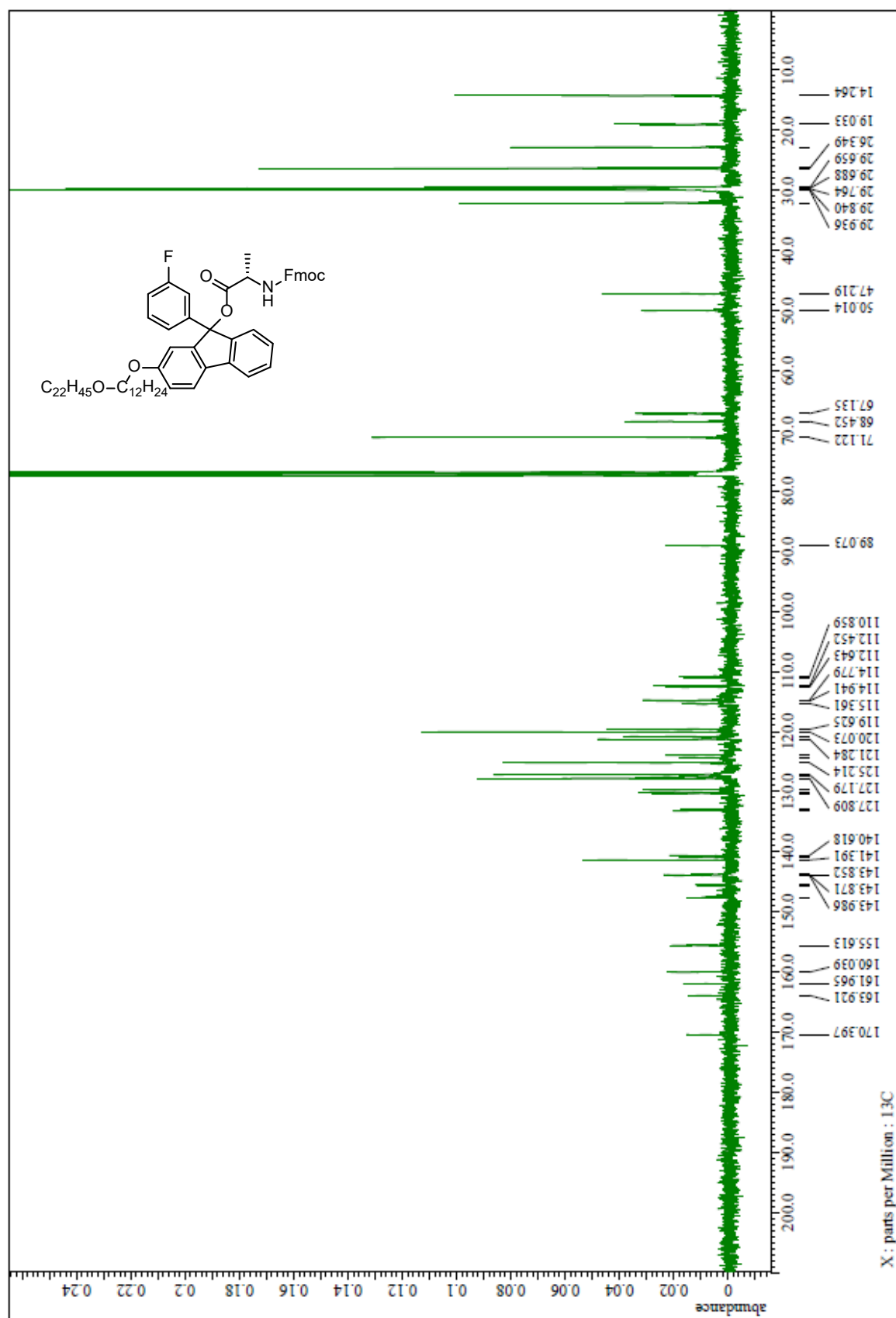


## 4. $^1\text{H}$ and $^{13}\text{C}$ NMR spectra of synthetic compounds

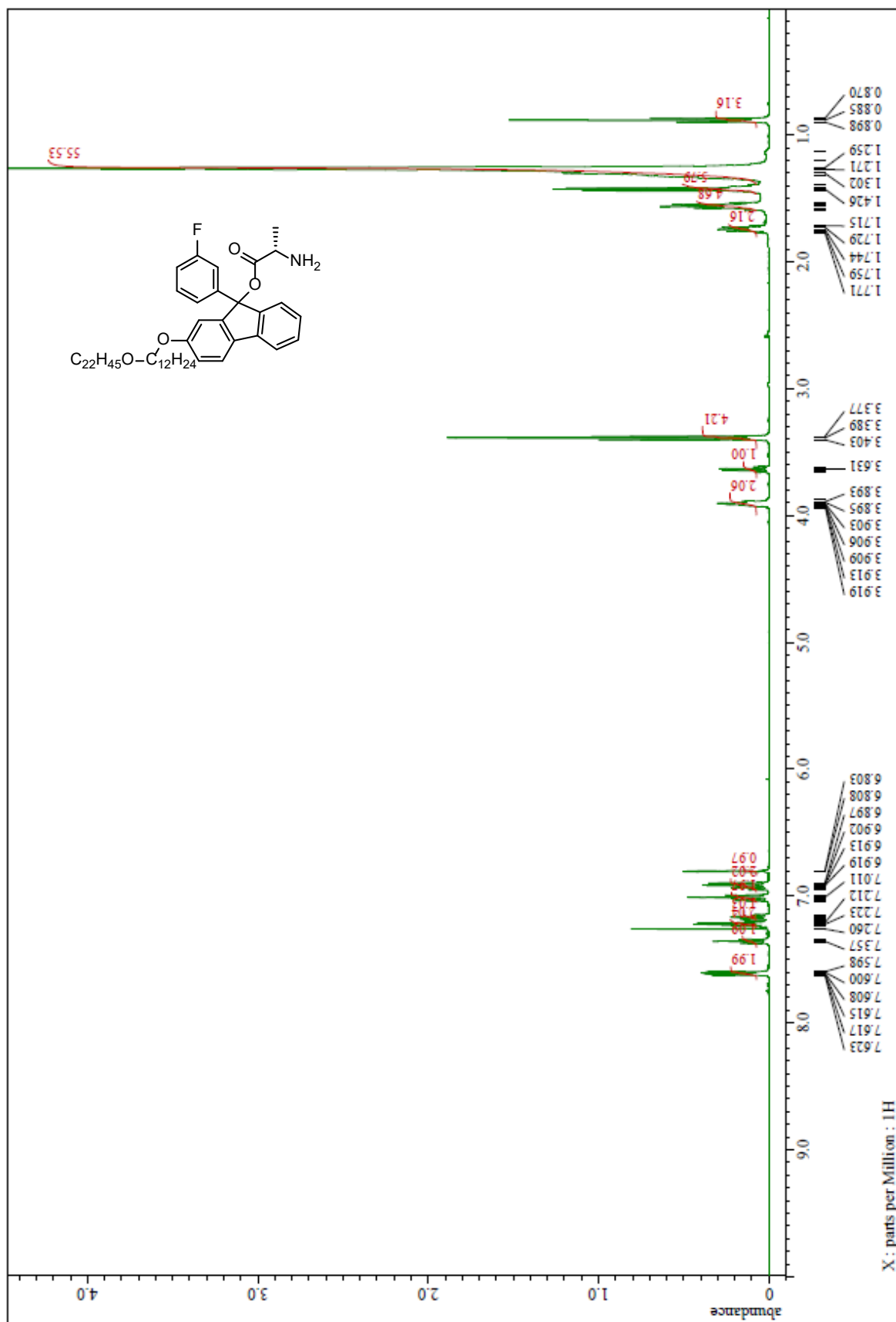
$^1\text{H}$  NMR spectrum of Fmoc-Ala-O-F1 (4) ( $\text{CDCl}_3$ )



$^{13}\text{C}$  NMR spectrum of Fmoc-Ala-O-FI (4) ( $\text{CDCl}_3$ )

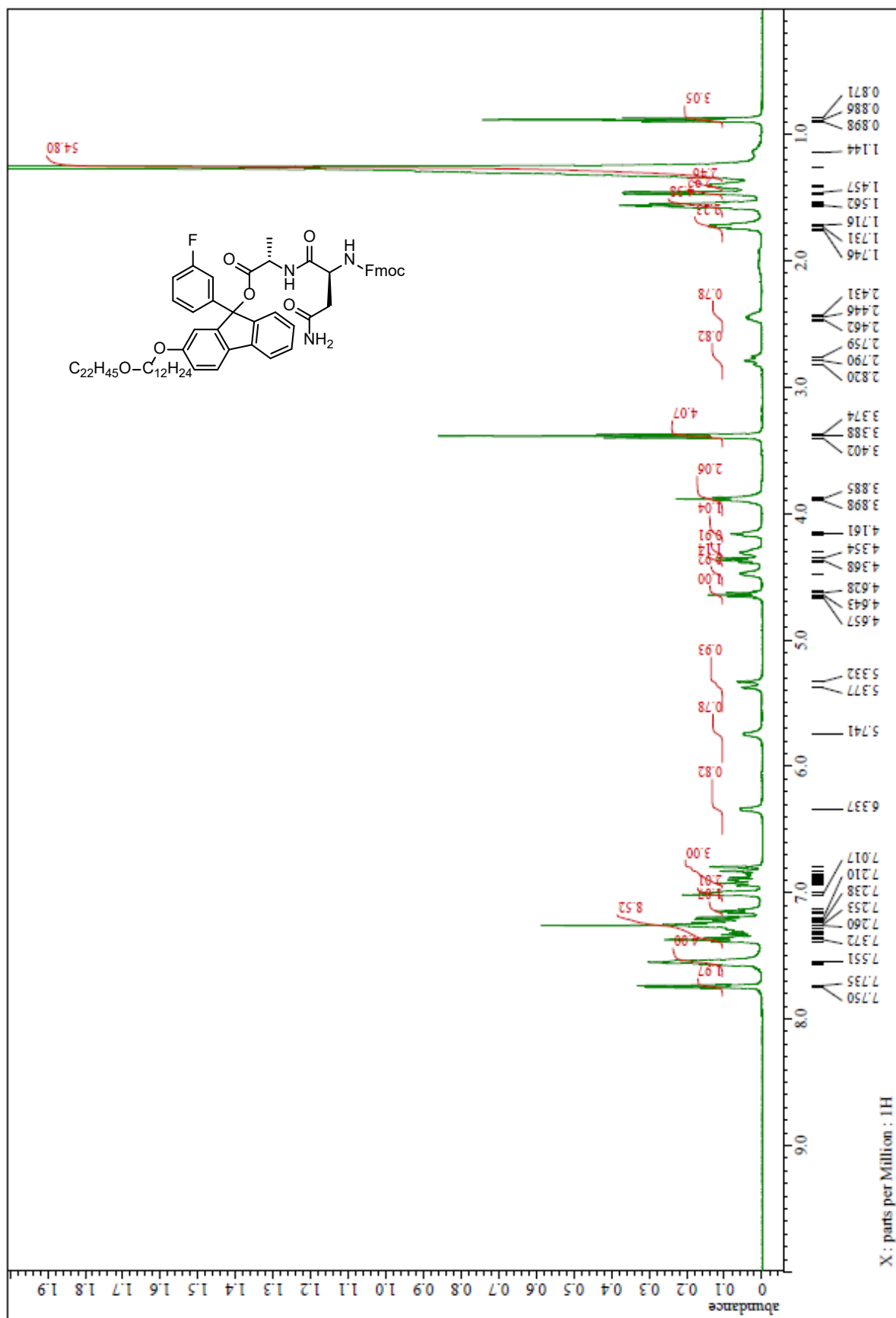


<sup>1</sup>H NMR spectrum of Ala-O-F1 (5) (CDCl<sub>3</sub>)

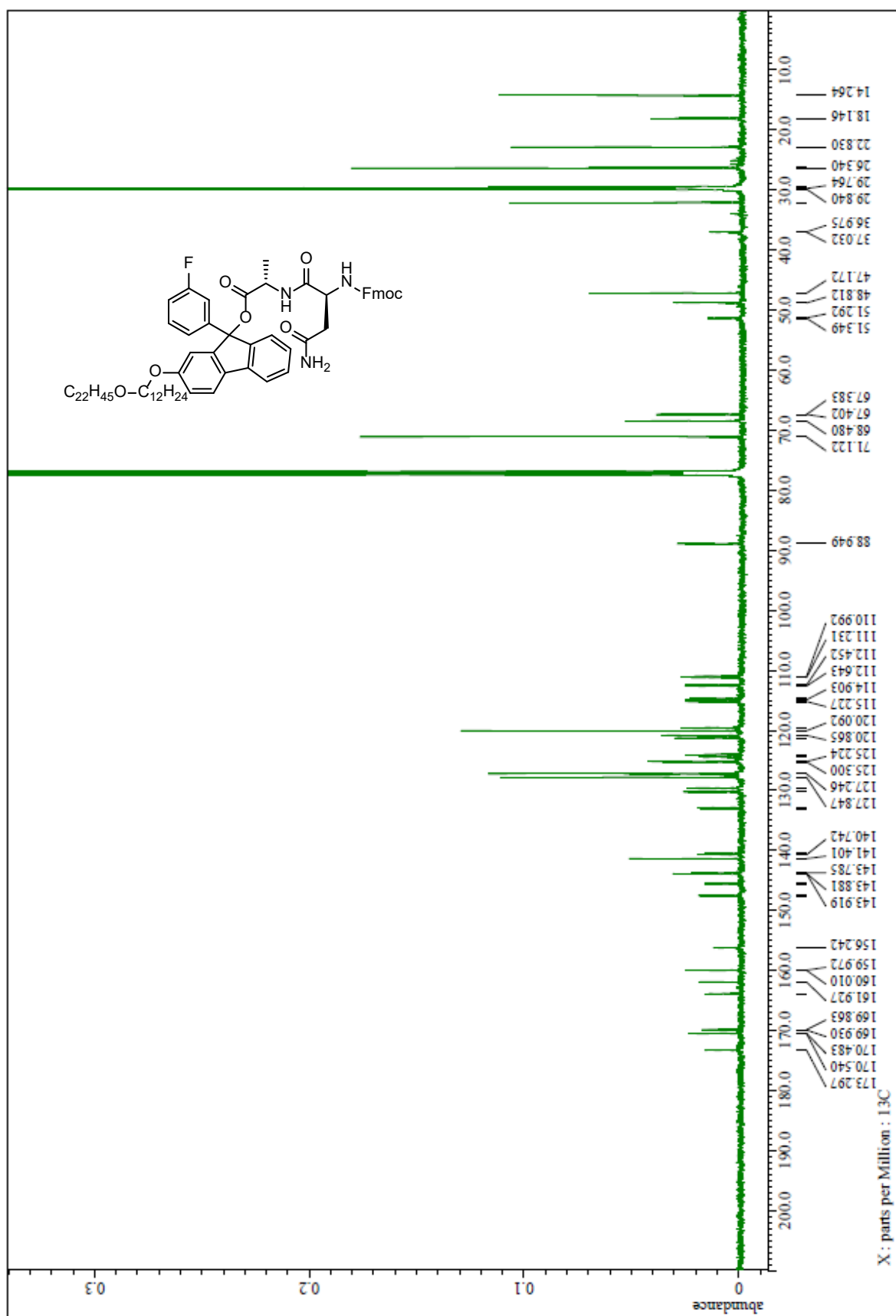




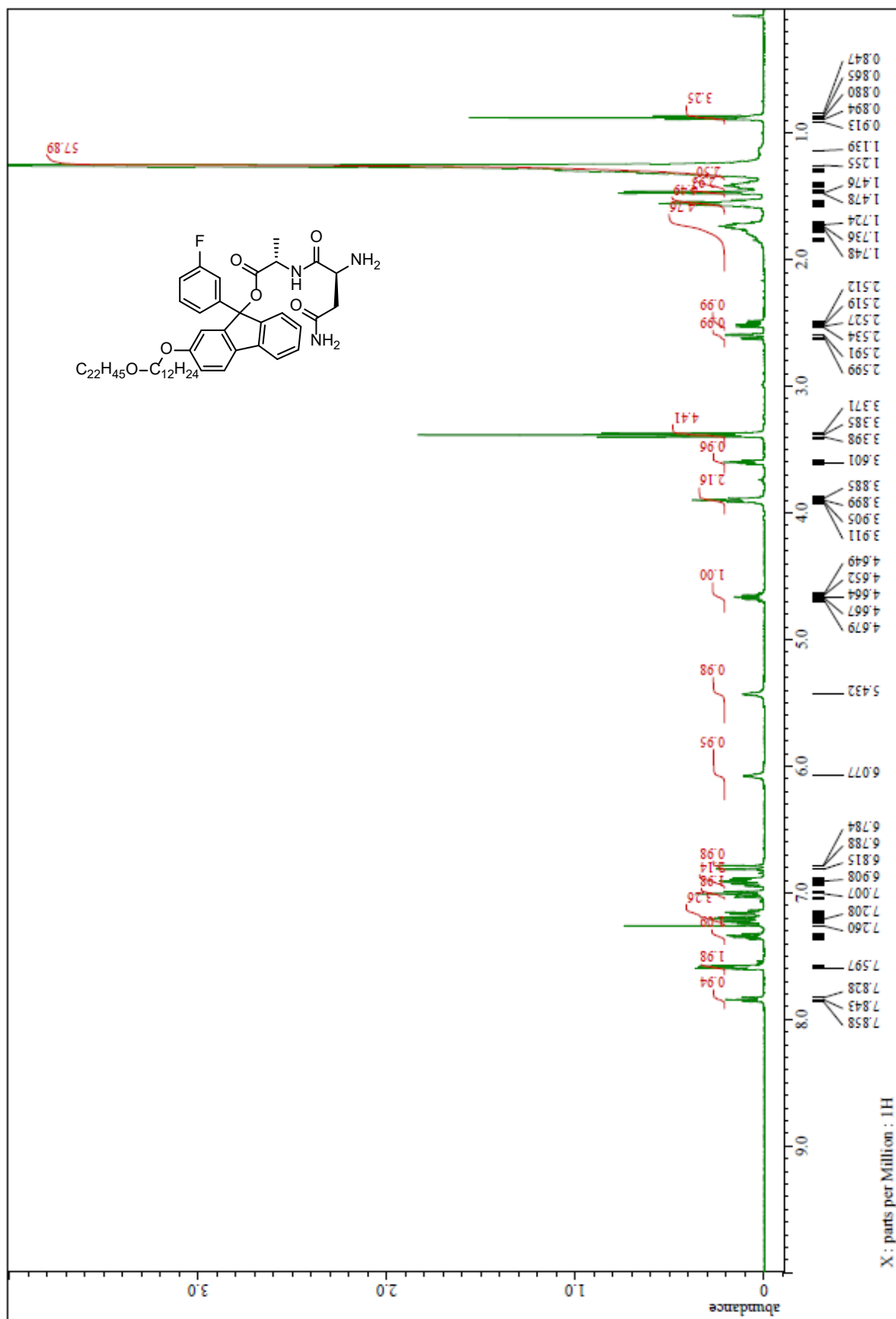
$^1\text{H}$  NMR spectrum of Fmoc-Asn-Ala-O-FI (**48**) ( $\text{CDCl}_3$ )



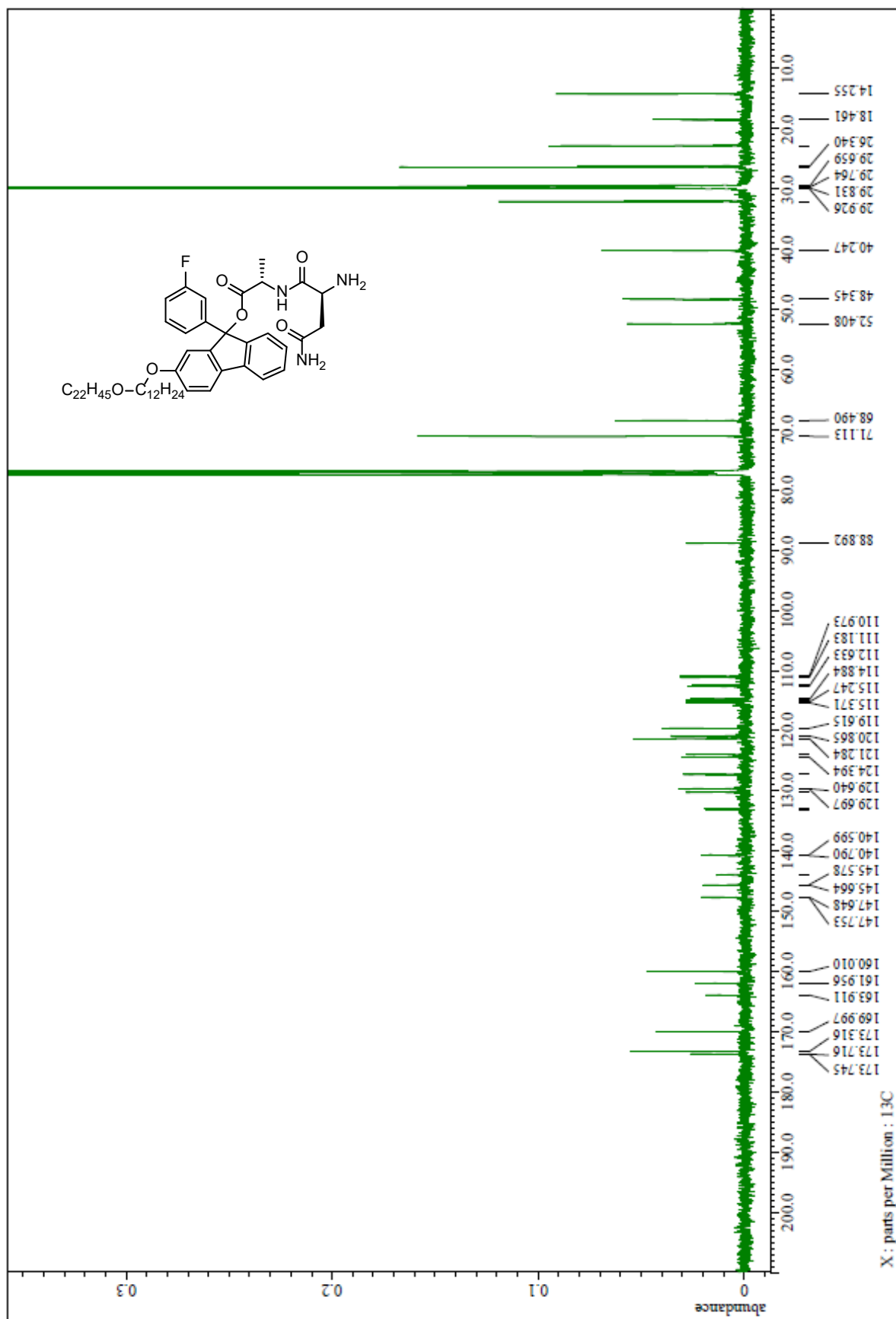
$^{13}\text{C}$  NMR spectrum of Fmoc-Asn-Ala-O-FI (**48**) ( $\text{CDCl}_3$ )



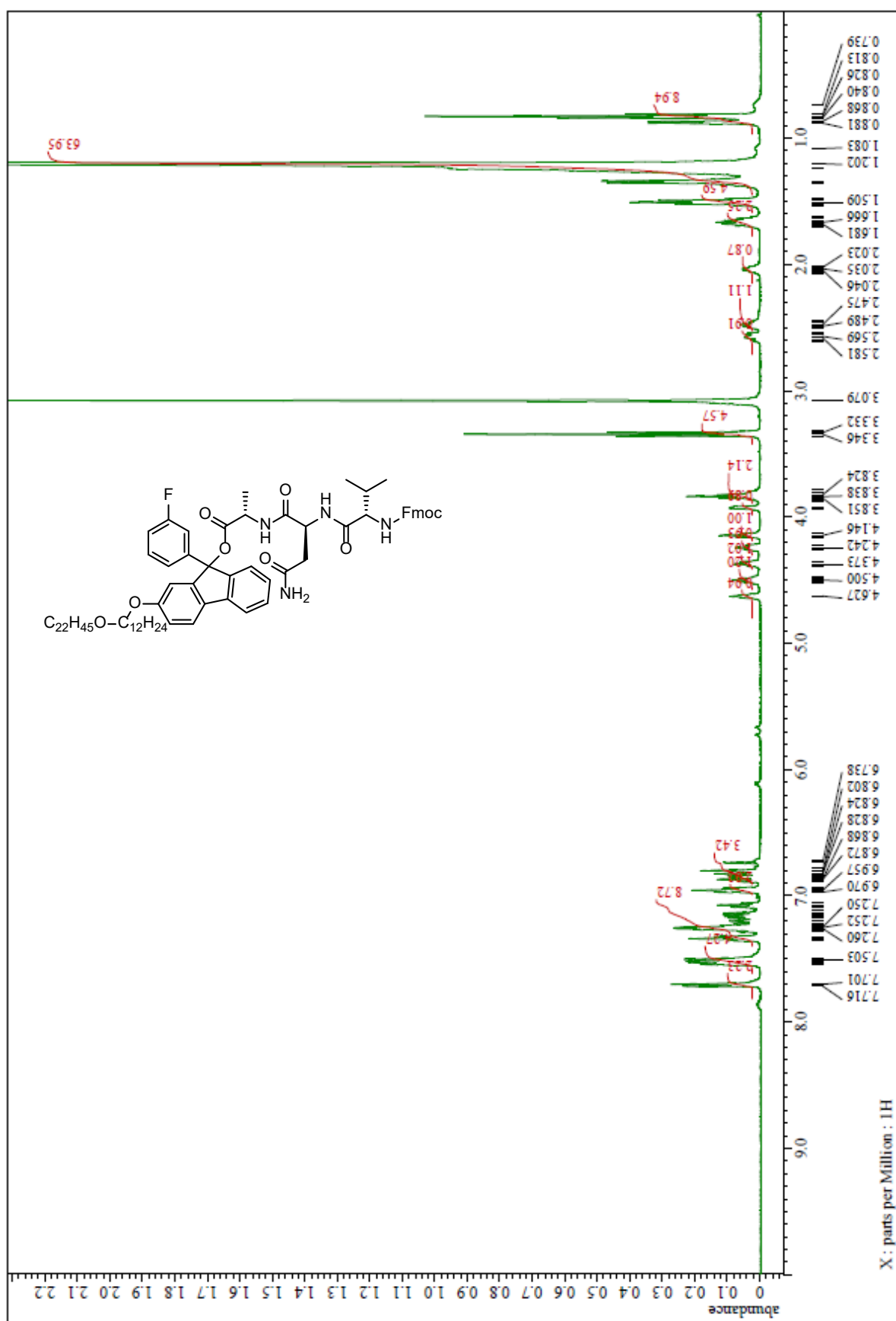
$^1\text{H}$  NMR spectrum of Asn-Ala-O-FI (**6**) ( $\text{CDCl}_3$ )



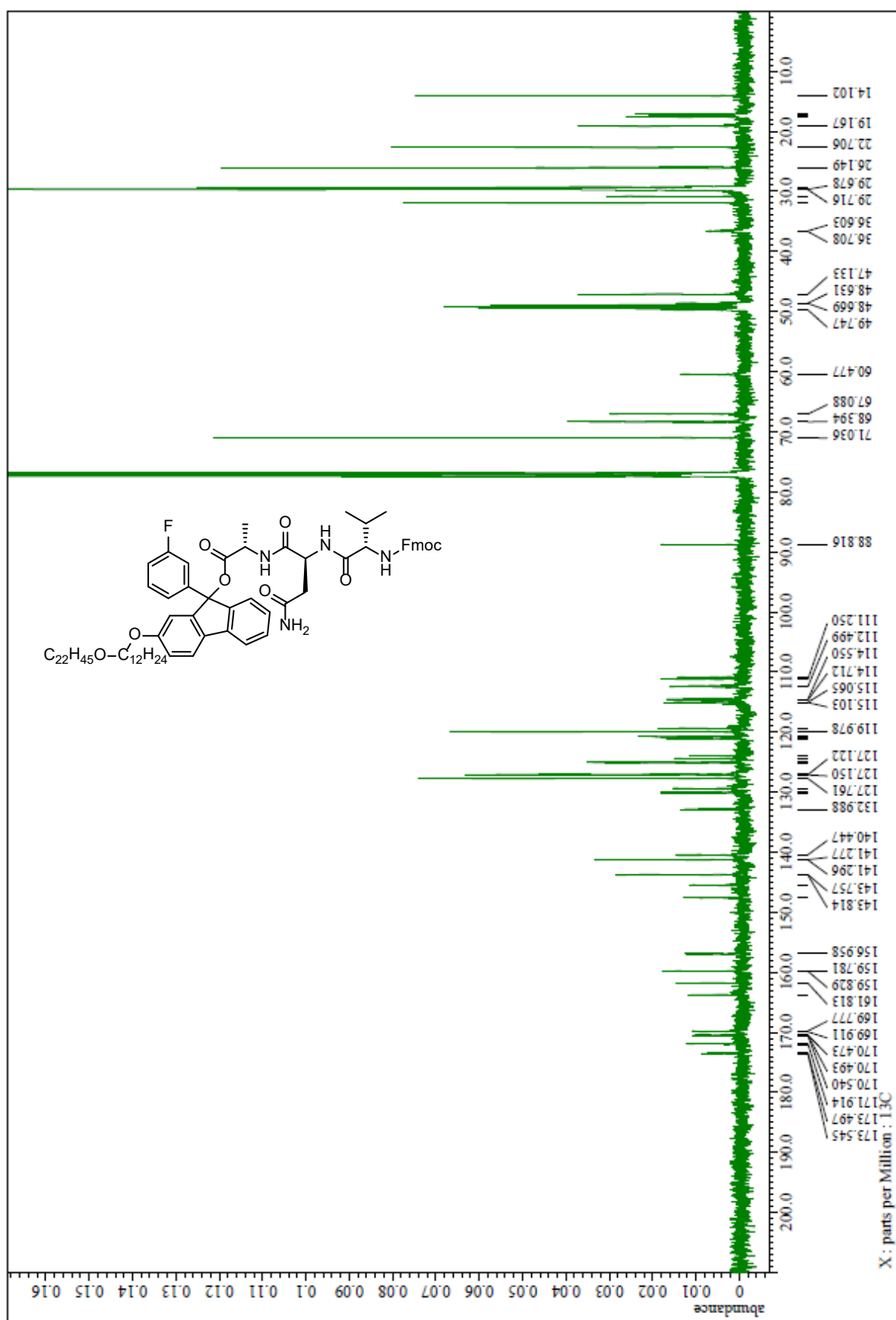
$^{13}\text{C}$  NMR spectrum of Asn-Ala-O-F1 (6) ( $\text{CDCl}_3$ )



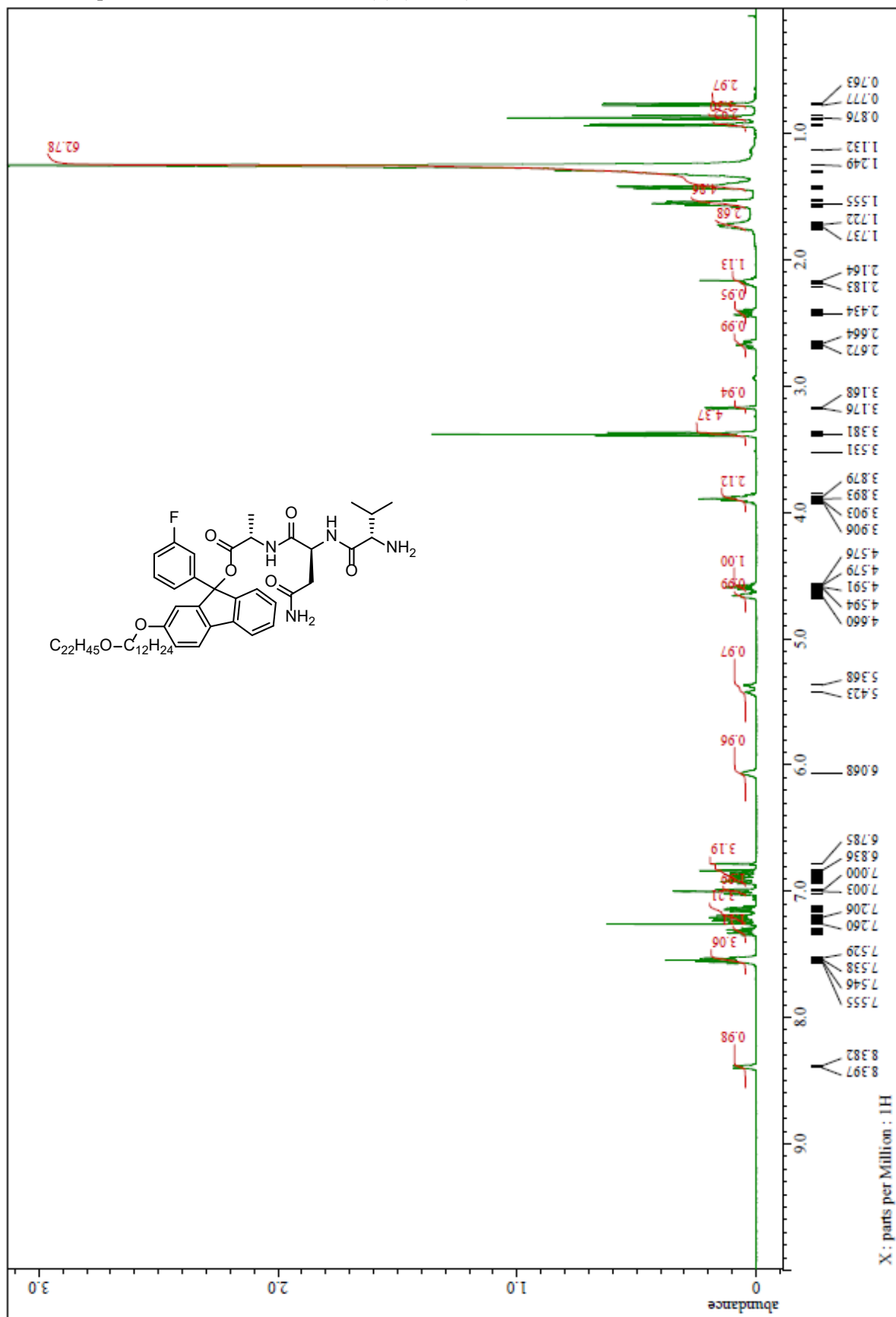
<sup>1</sup>H NMR spectrum of Fmoc-Val-Asn-Ala-O-FI (49) (CDCl<sub>3</sub>/CD<sub>3</sub>OD)



$^{13}\text{C}$  NMR spectrum of Fmoc-Val-Asn-Ala-O-F1 (**49**) ( $\text{CDCl}_3/\text{CD}_3\text{OD}$ )

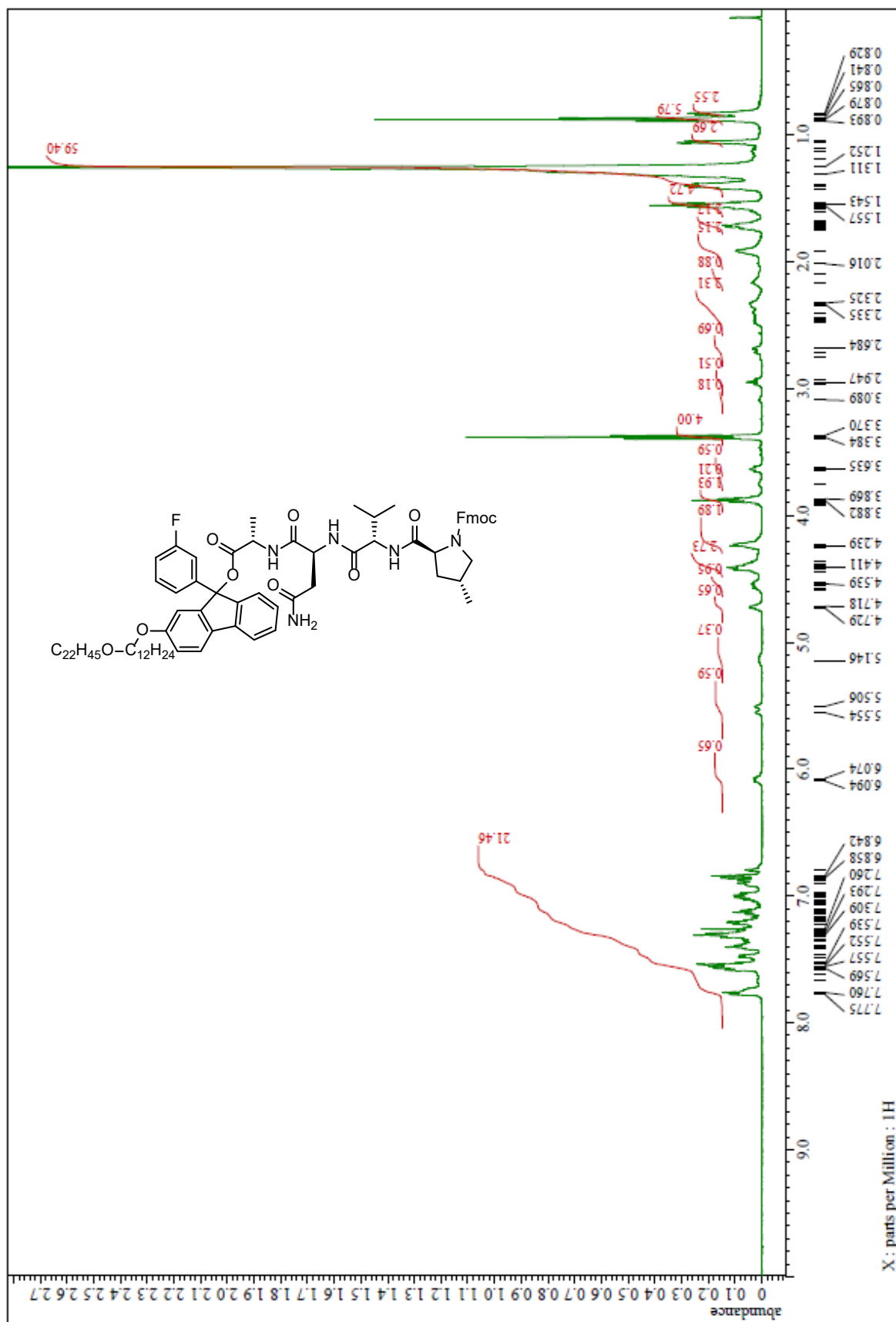


<sup>1</sup>H NMR spectrum of Val-Asn-Ala-O-F1 (7) (CDCl<sub>3</sub>)

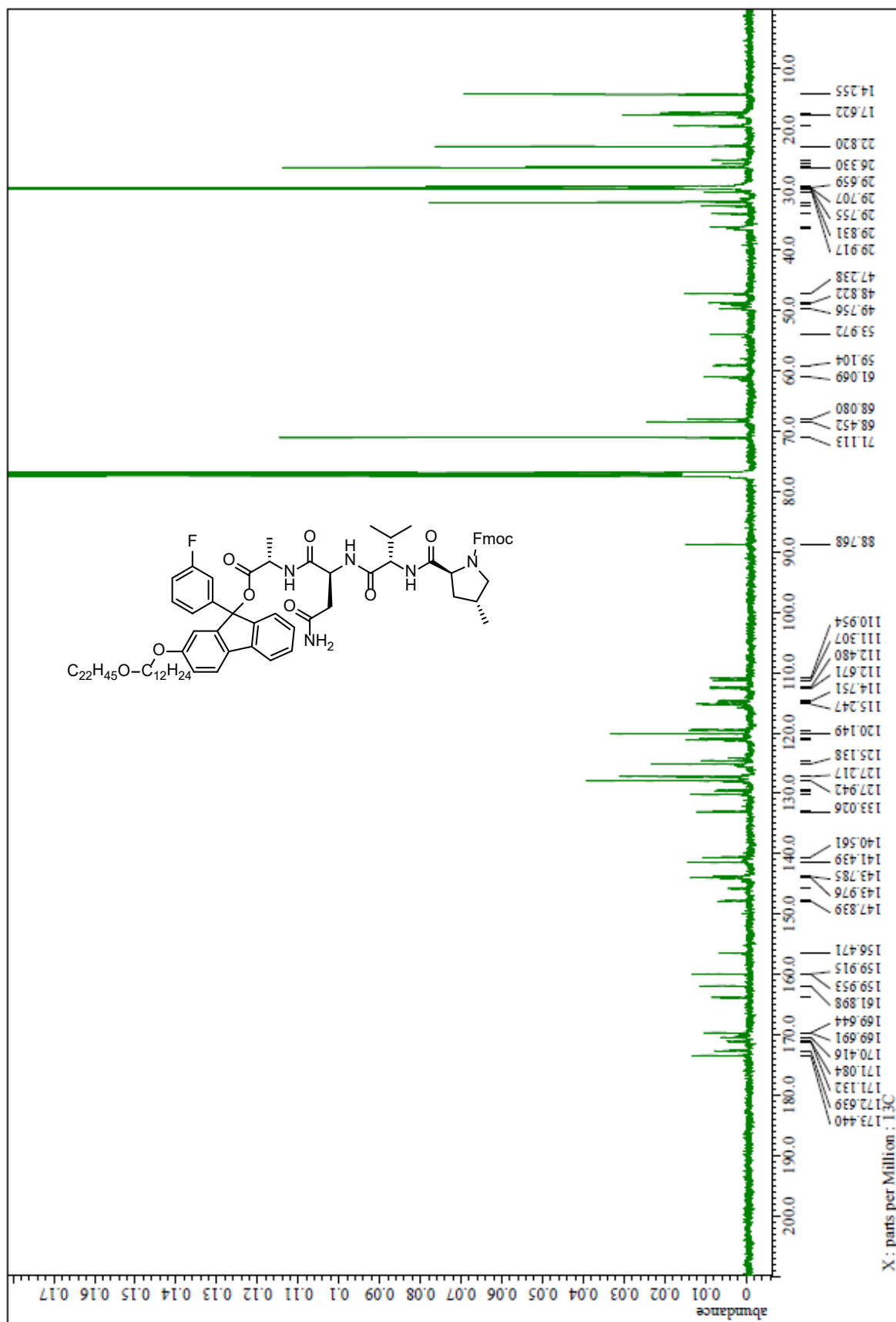




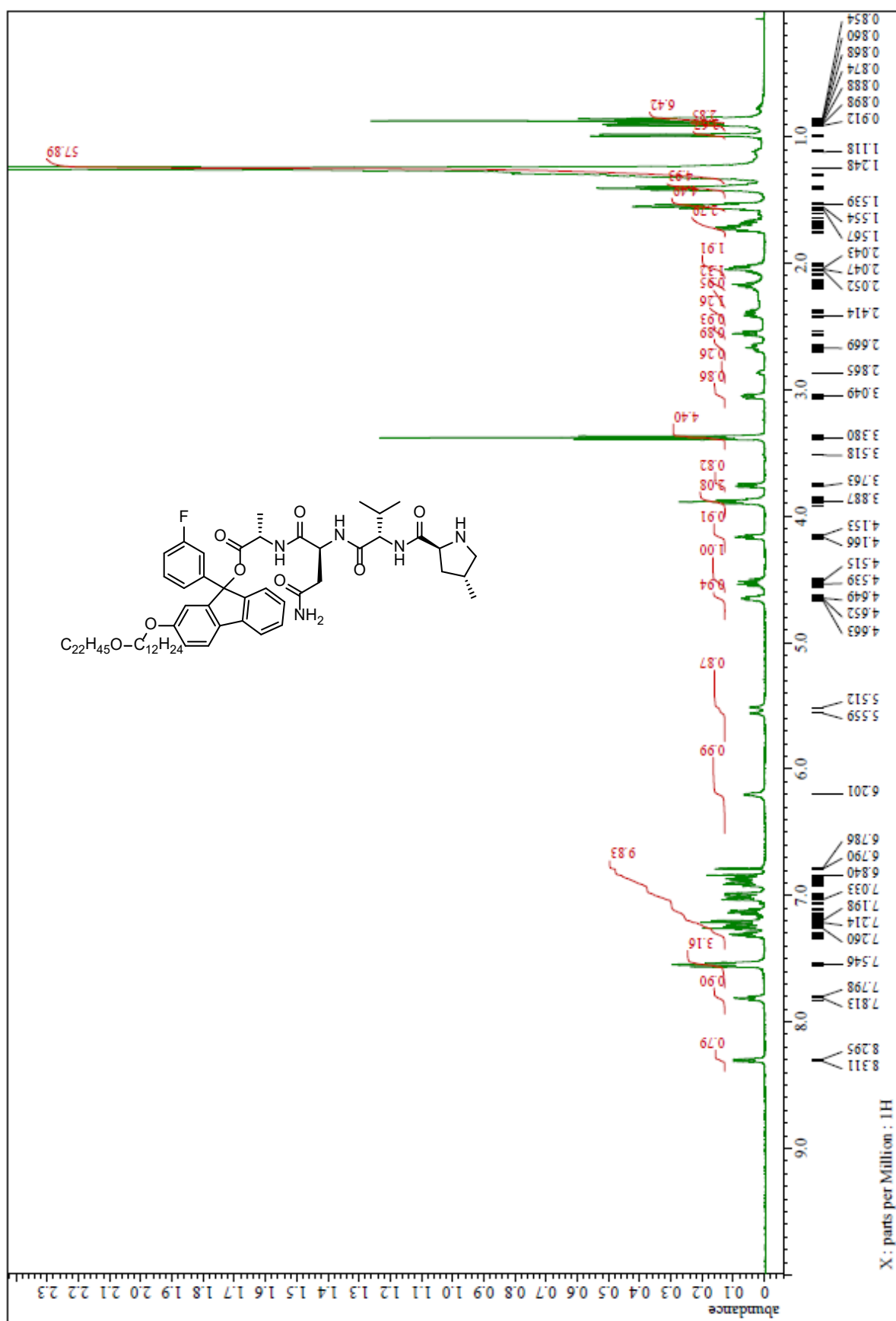
$^1\text{H}$  NMR spectrum of Fmoc-4-MePro-Val-Asn-Ala-O-F1 (**50**) ( $\text{CDCl}_3$ )



$^{13}\text{C}$  NMR spectrum of Fmoc-4-MePro-Val-Asn-Ala-O-F1 (**50**) ( $\text{CDCl}_3$ )



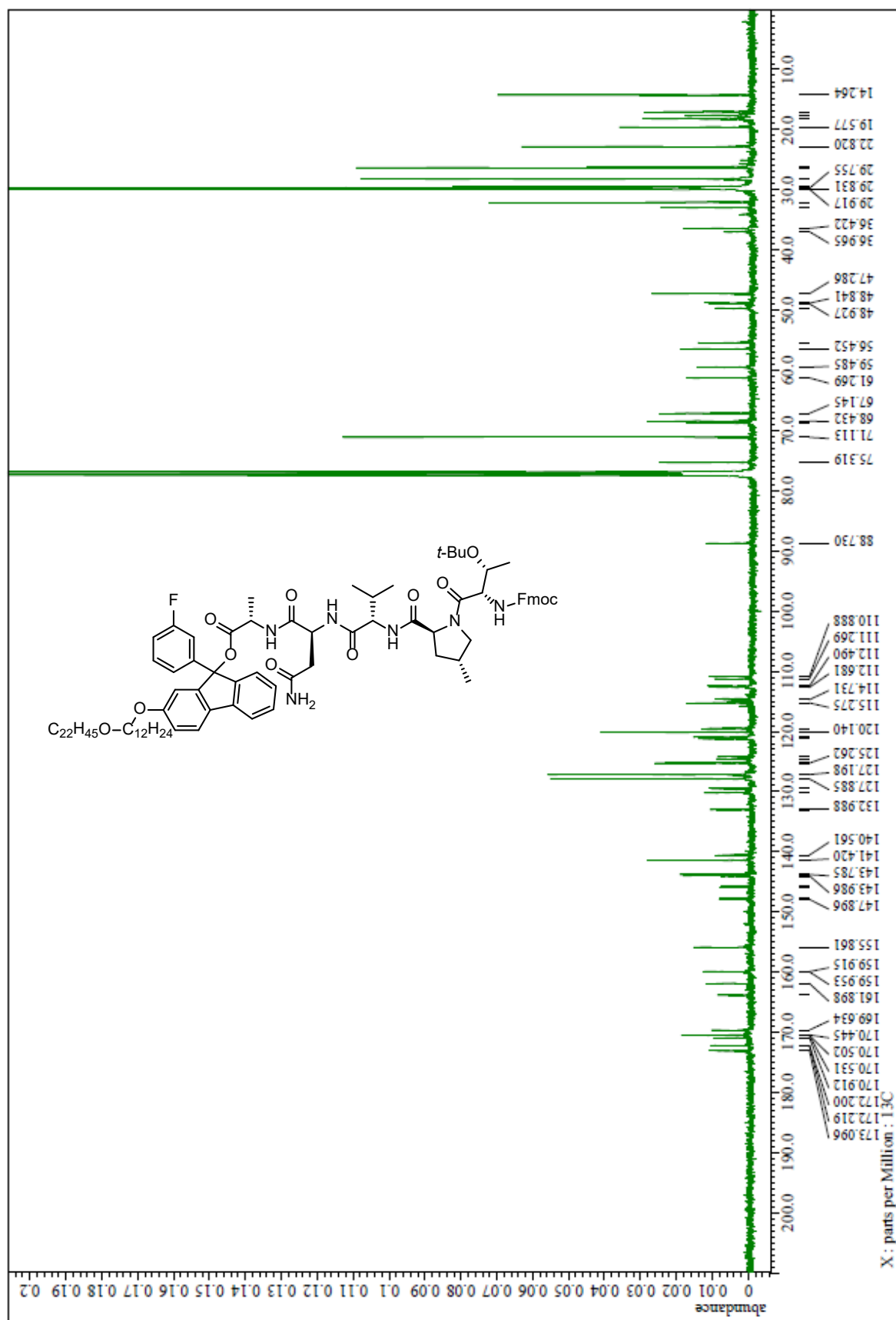
$^1\text{H}$  NMR spectrum of 4-MePro-Val-Asn-Ala-O-F1 (**8**) ( $\text{CDCl}_3$ )



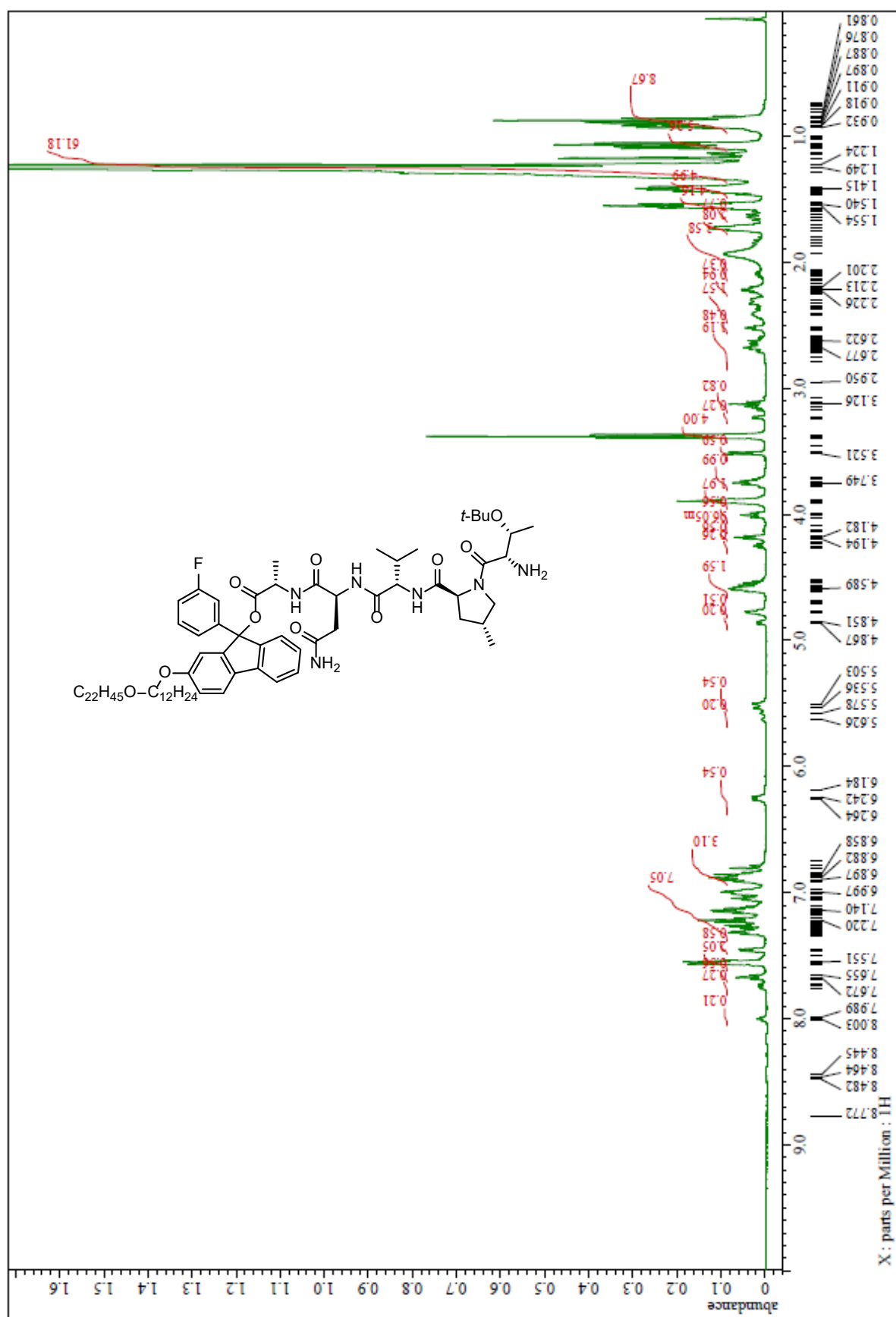




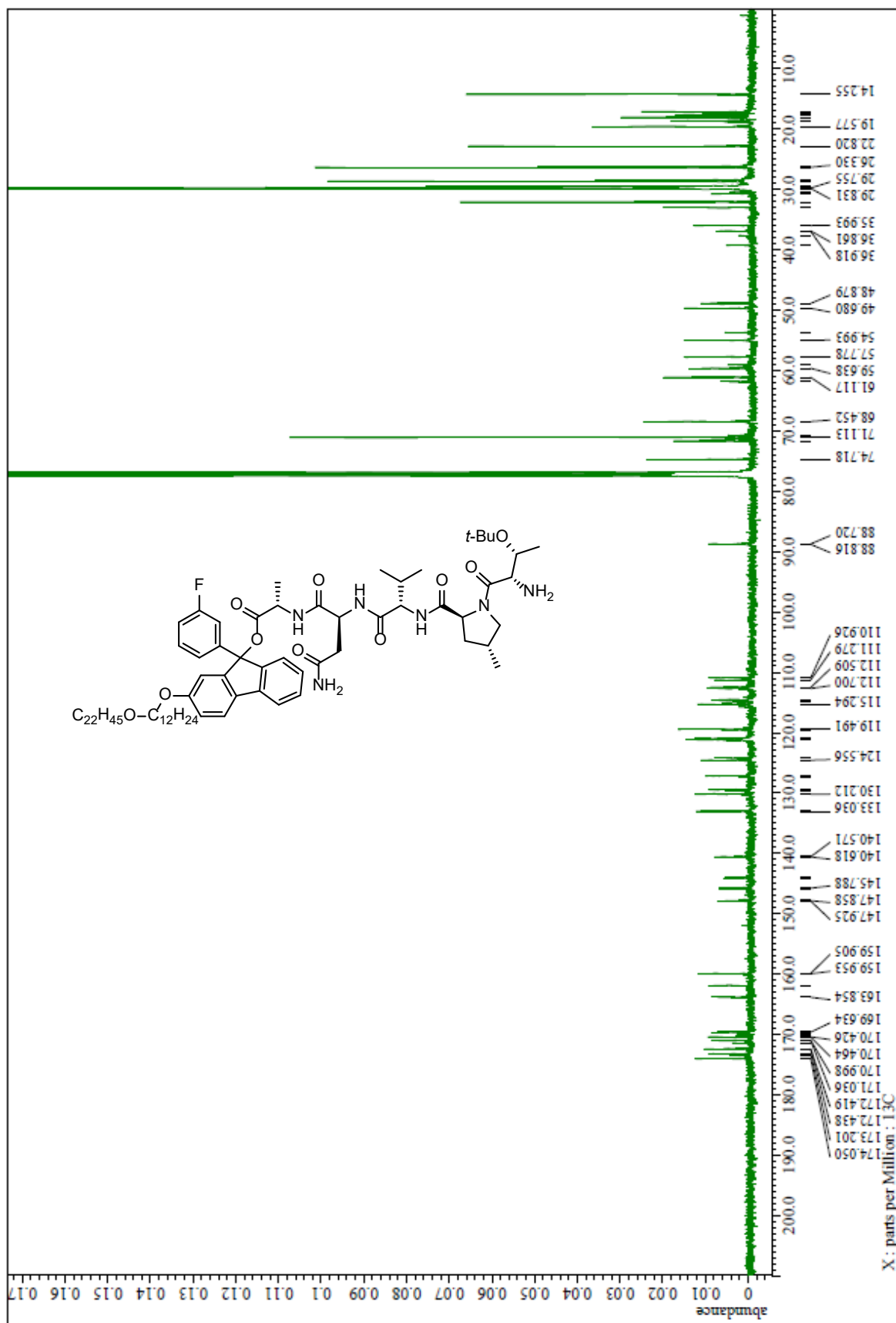
$^{13}\text{C}$  NMR spectrum of Fmoc-Thr(*t*-Bu)-4-MePro-Val-Asn-Ala-O-FI (**51**) ( $\text{CDCl}_3$ )



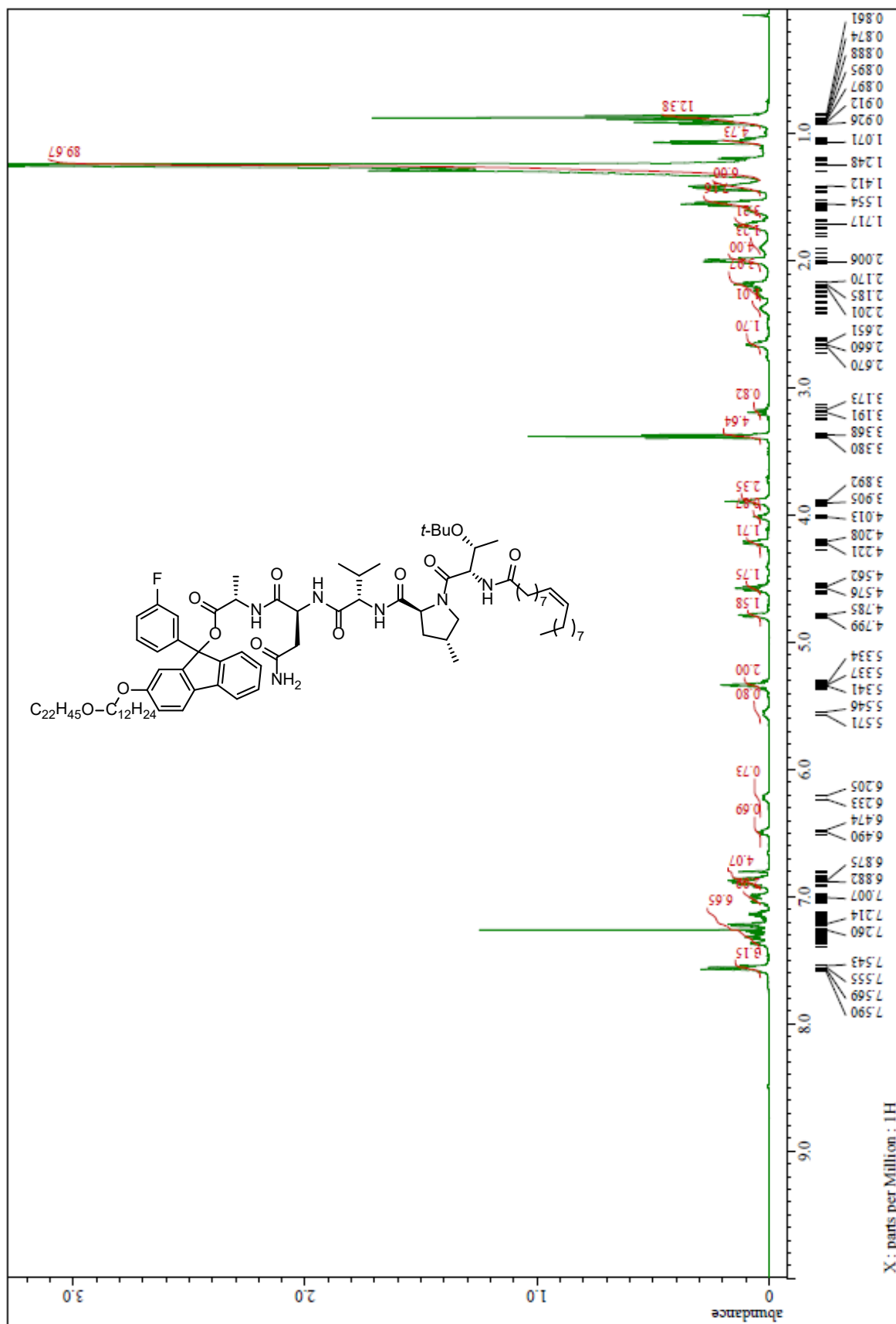
$^1\text{H}$  NMR spectrum of Thr(*t*-Bu)-4-MePro-Val-Asn-Ala-O-F1 (**9**) ( $\text{CDCl}_3$ )



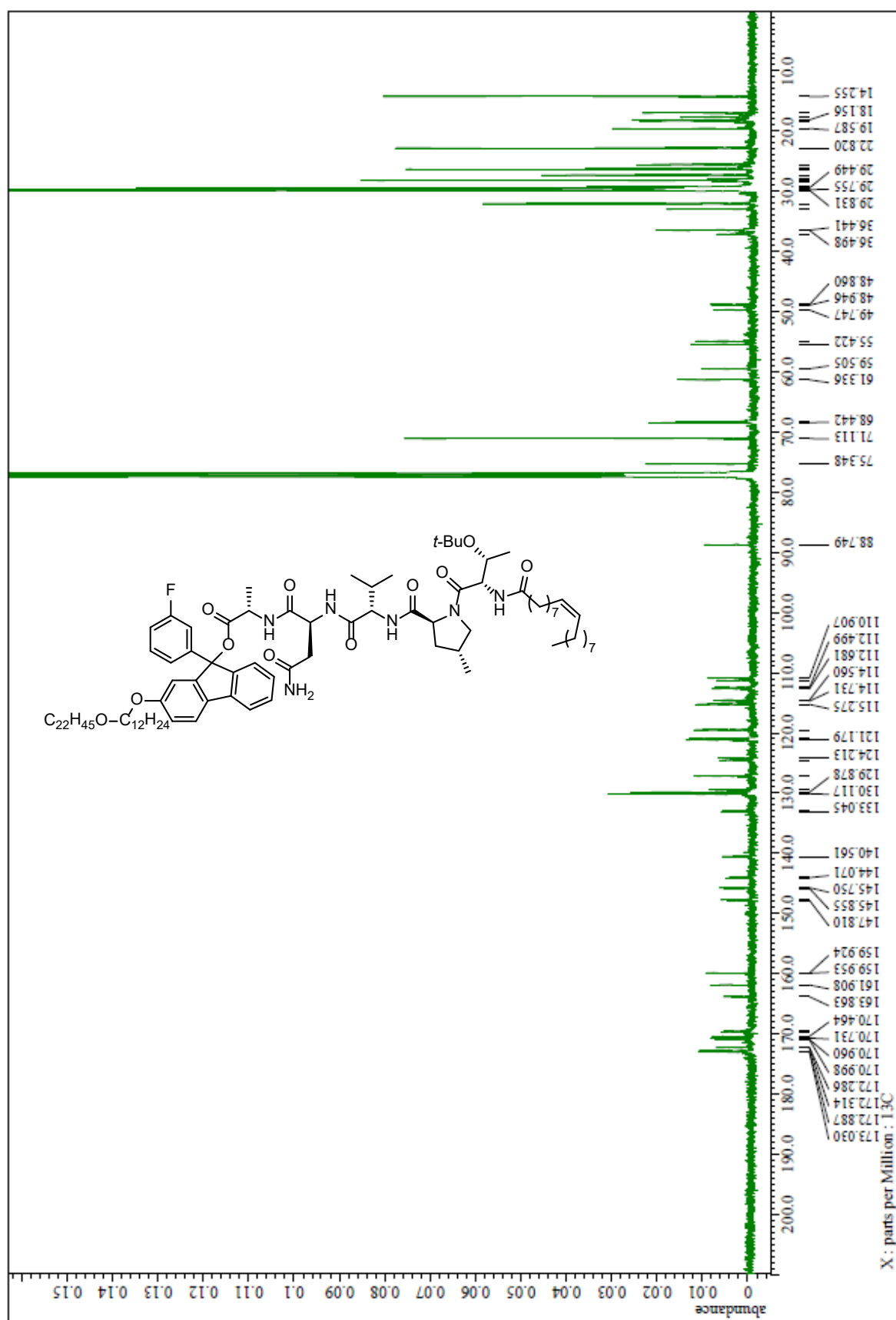
$^{13}\text{C}$  NMR spectrum of Thr(*t*-Bu)-4-MePro-Val-Asn-Ala-O-F1 (**9**) ( $\text{CDCl}_3$ )



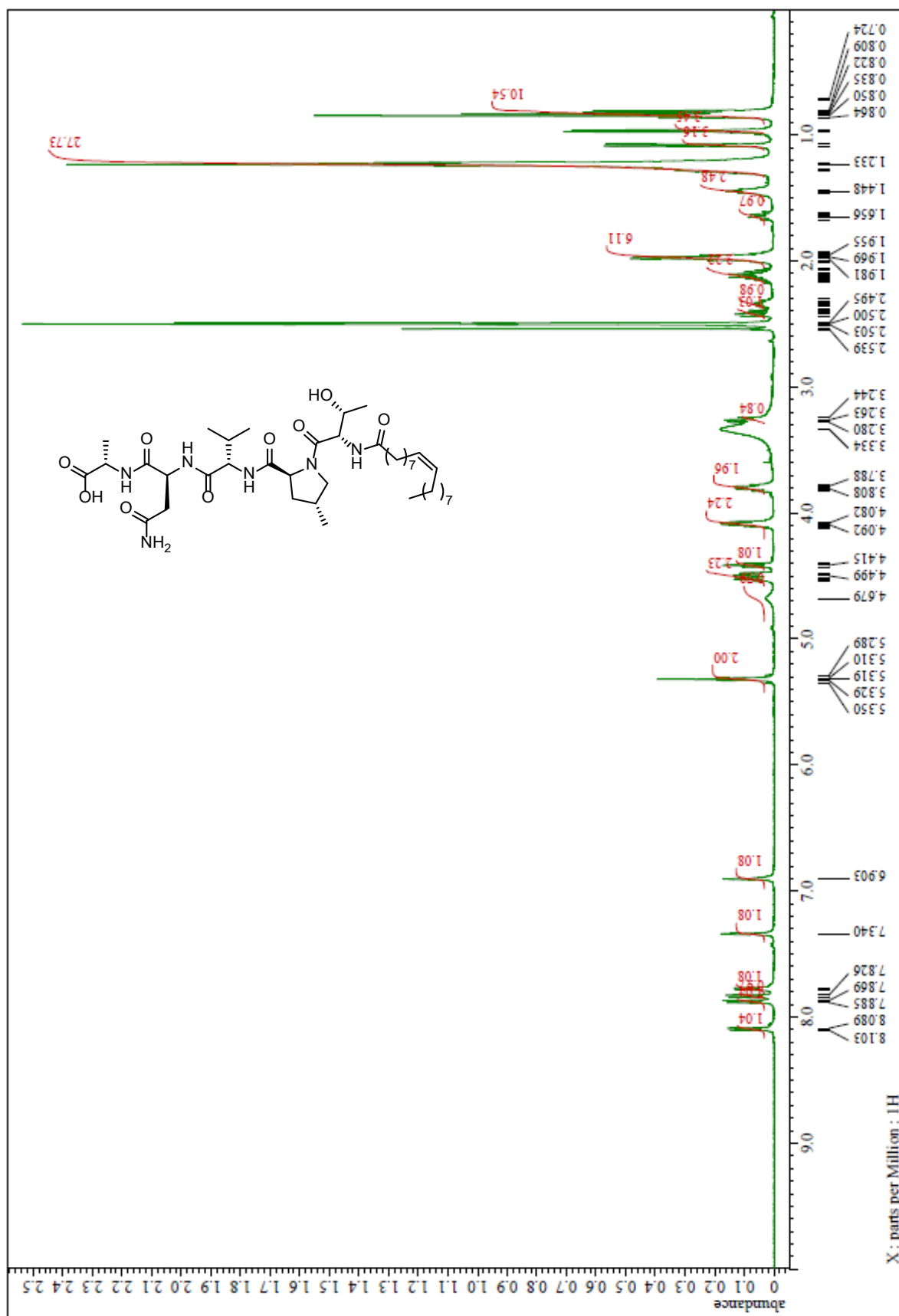
$^1\text{H}$  NMR spectrum of Oleic acid-Thr(*t*-Bu)-4-MePro-Val-Asn-Ala-O-FI (**10**) ( $\text{CDCl}_3$ )



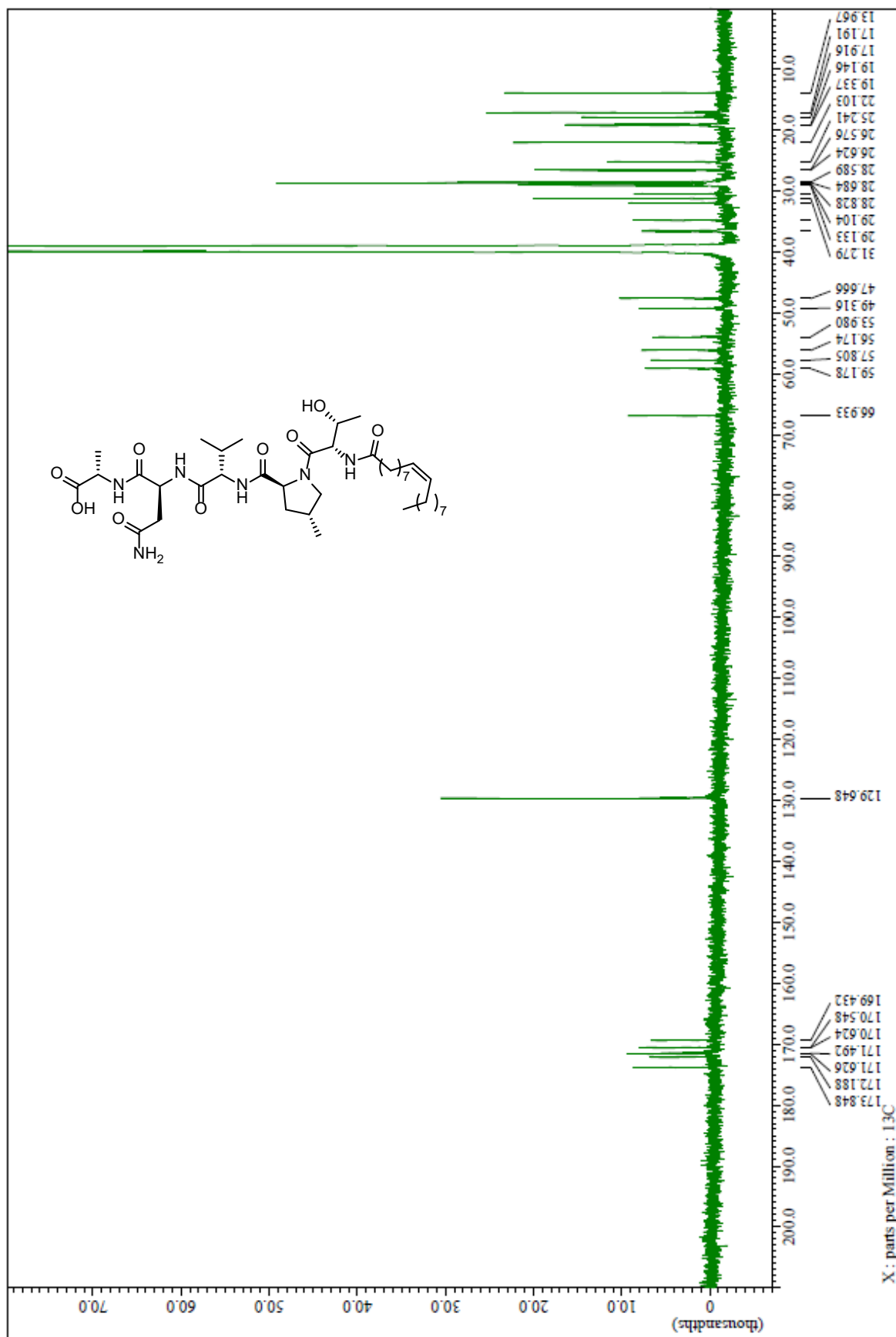
$^{13}\text{C}$  NMR spectrum of Oleic acid-Thr(*t*-Bu)-4-MePro-Val-Asn-Ala-O-FI (**10**) ( $\text{CDCl}_3$ )



<sup>1</sup>H NMR spectrum of Oleic acid-Thr-4-MePro-Val-Asn-Ala-OH (**11**) (DMSO-*d*<sub>6</sub>)

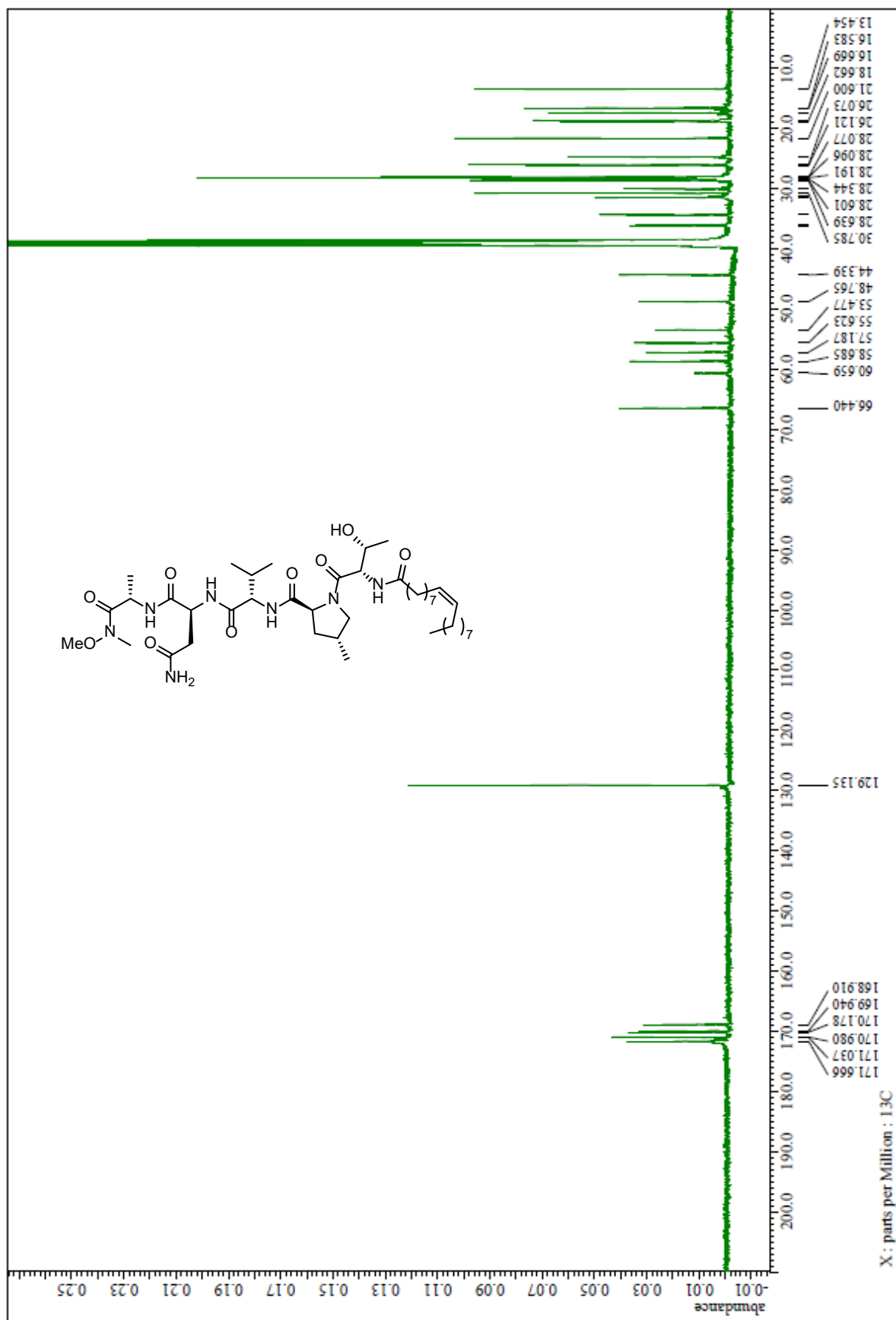


$^{13}\text{C}$  NMR spectrum of Oleic acid-Thr-4-MePro-Val-Asn-Ala-OH (**11**) ( $\text{DMSO-}d_6$ )

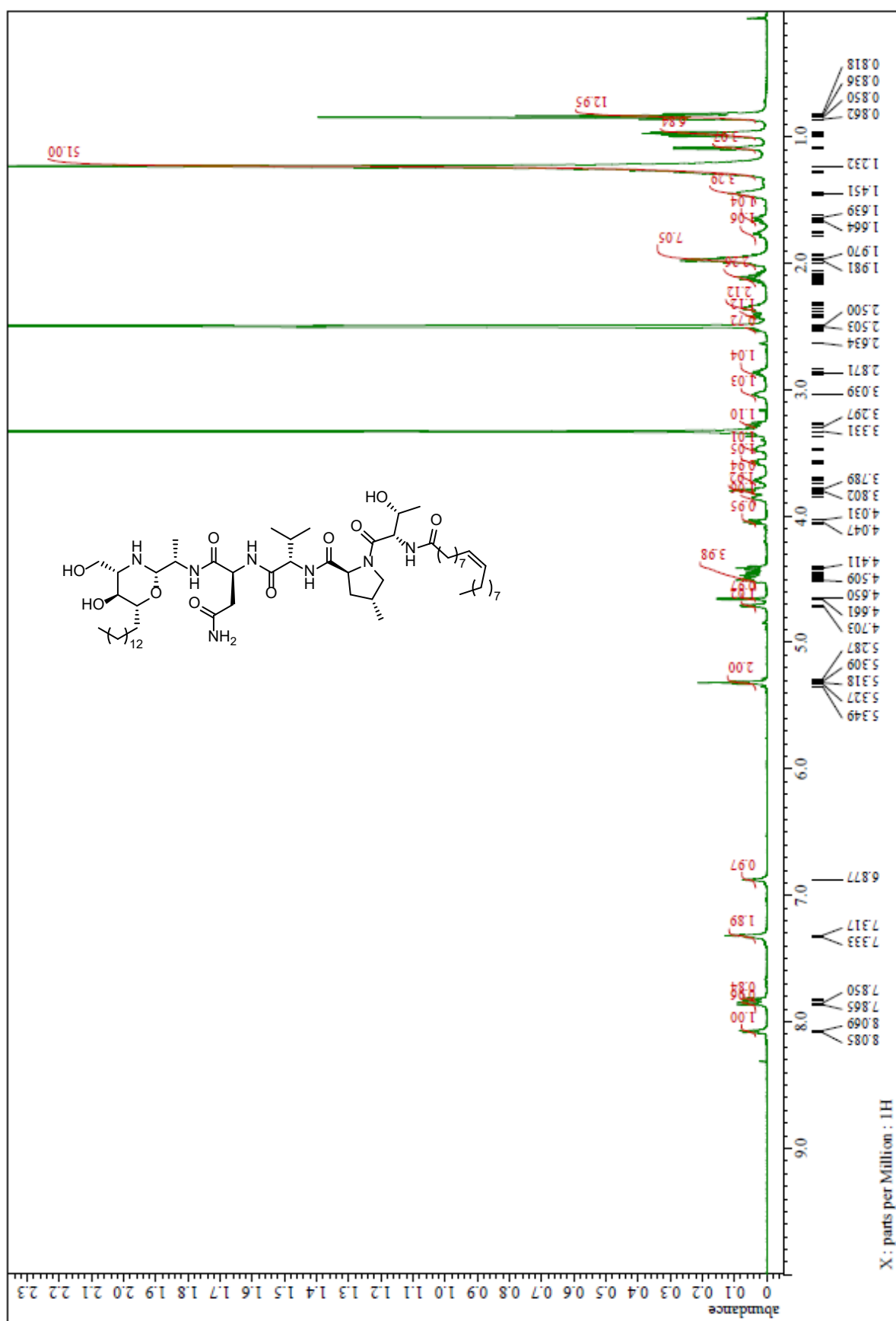




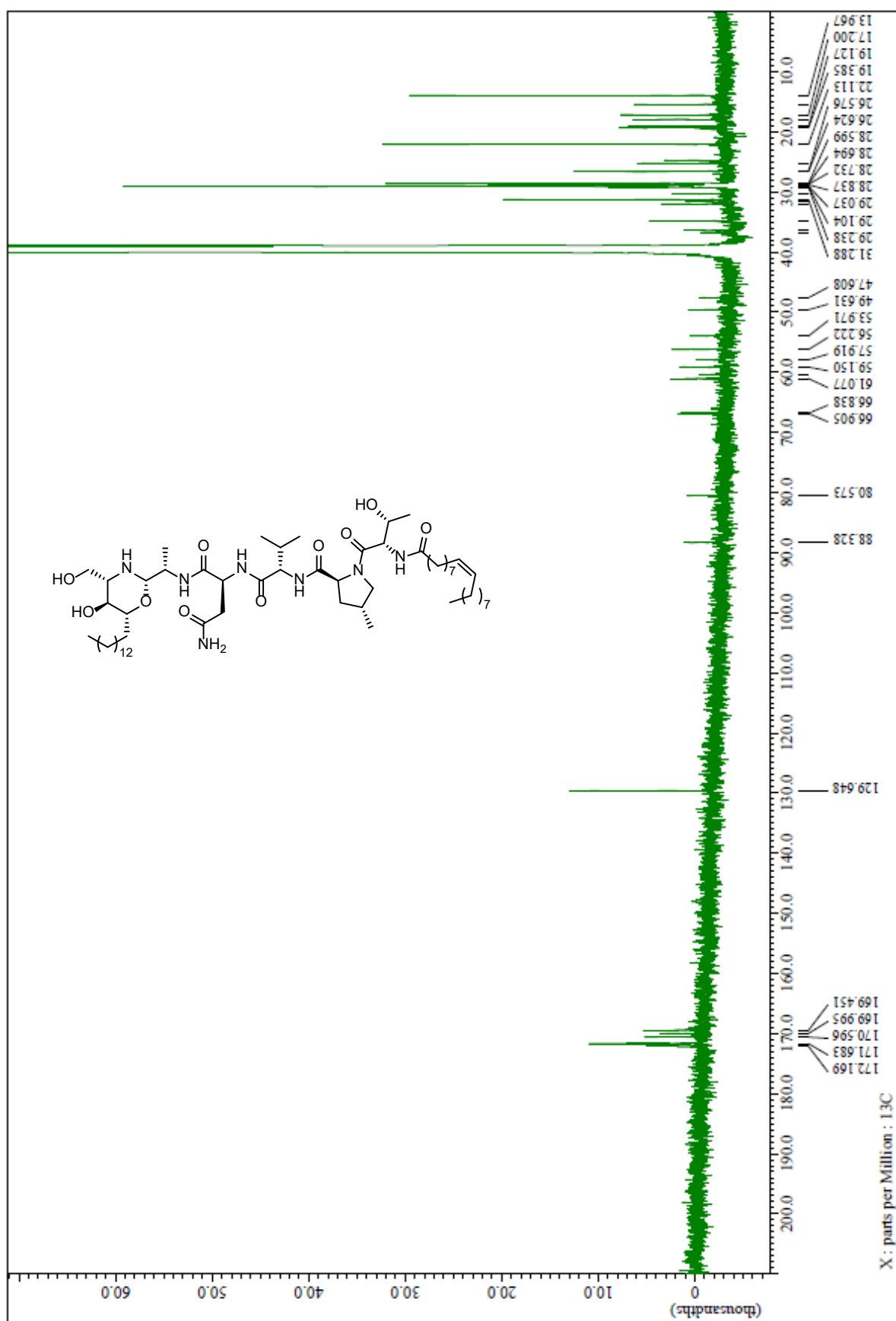
$^{13}\text{C}$  NMR spectrum of Oleic acid-Thr-4-MePro-Val-Asn-Ala-N(Me)OMe (**12**) ( $\text{DMSO-}d_6$ )



<sup>1</sup>H NMR spectrum of kozupeptin A (**1a**) (DMSO-*d*<sub>6</sub>)

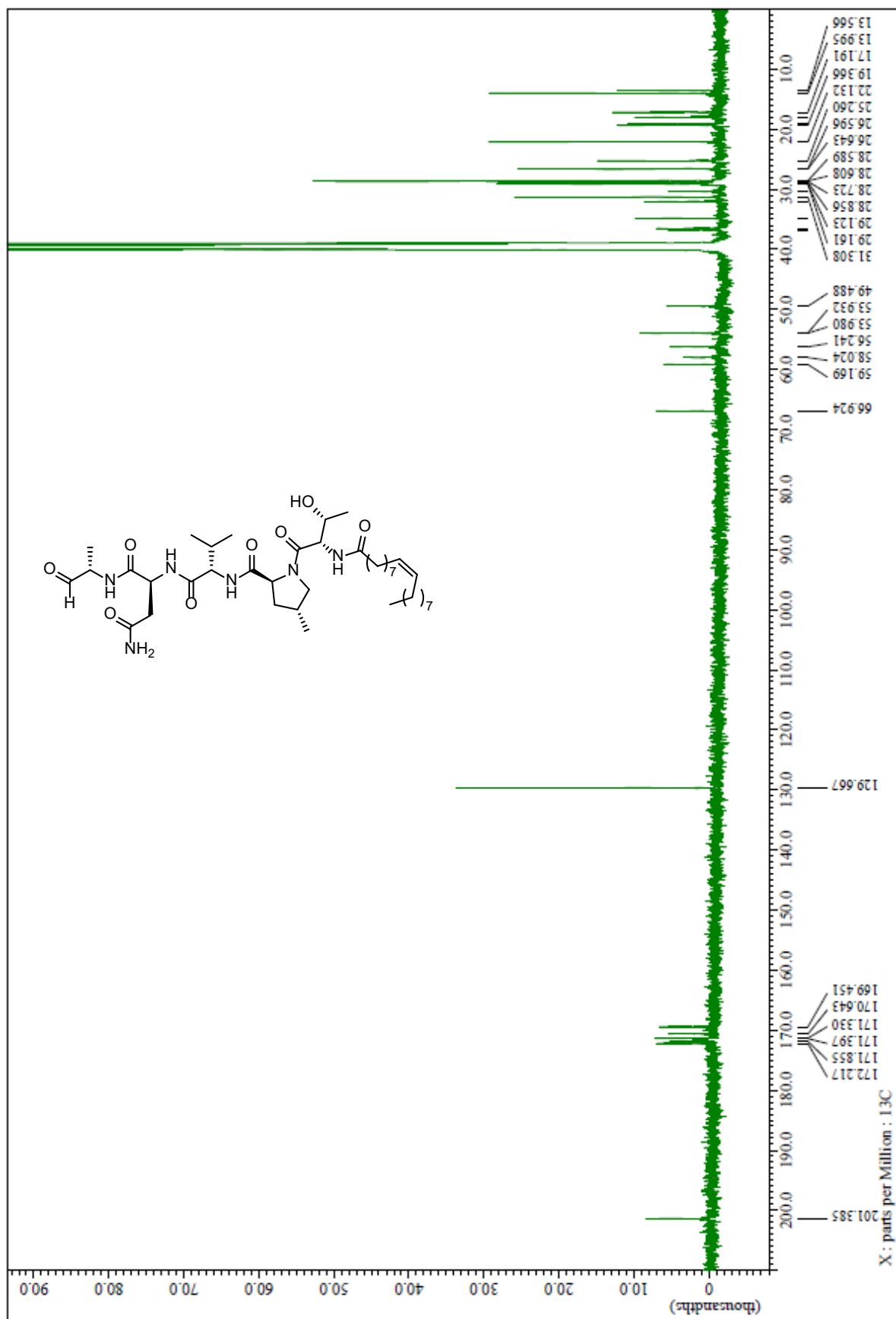


$^{13}\text{C}$  NMR spectrum of kozupeptin A (**1a**) ( $\text{DMSO-}d_6$ )



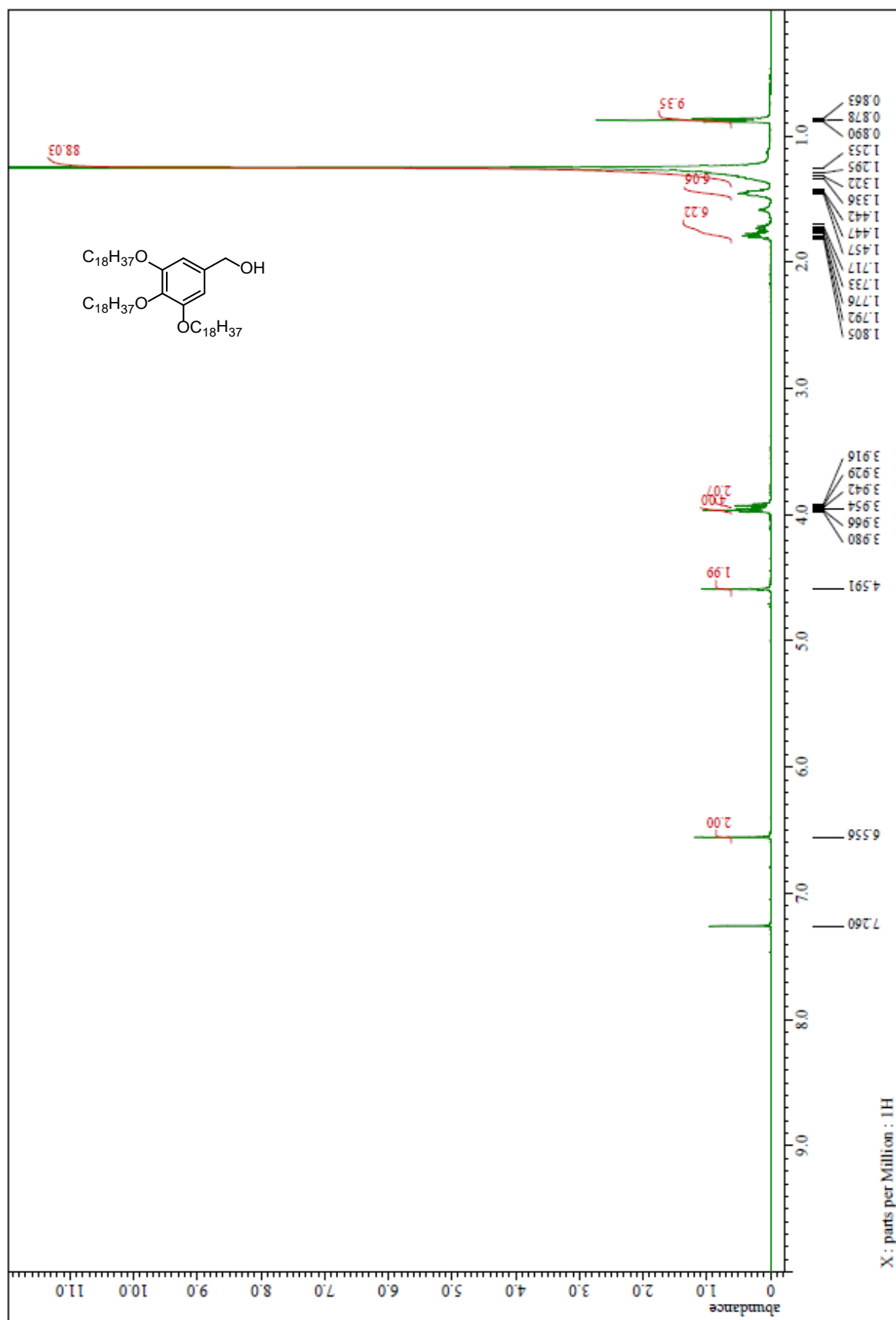


$^{13}\text{C}$  NMR spectrum of Oleic acid-Thr-4-MePro-Val-Asn-Ala-H (**13**) ( $\text{DMSO-}d_6$ )

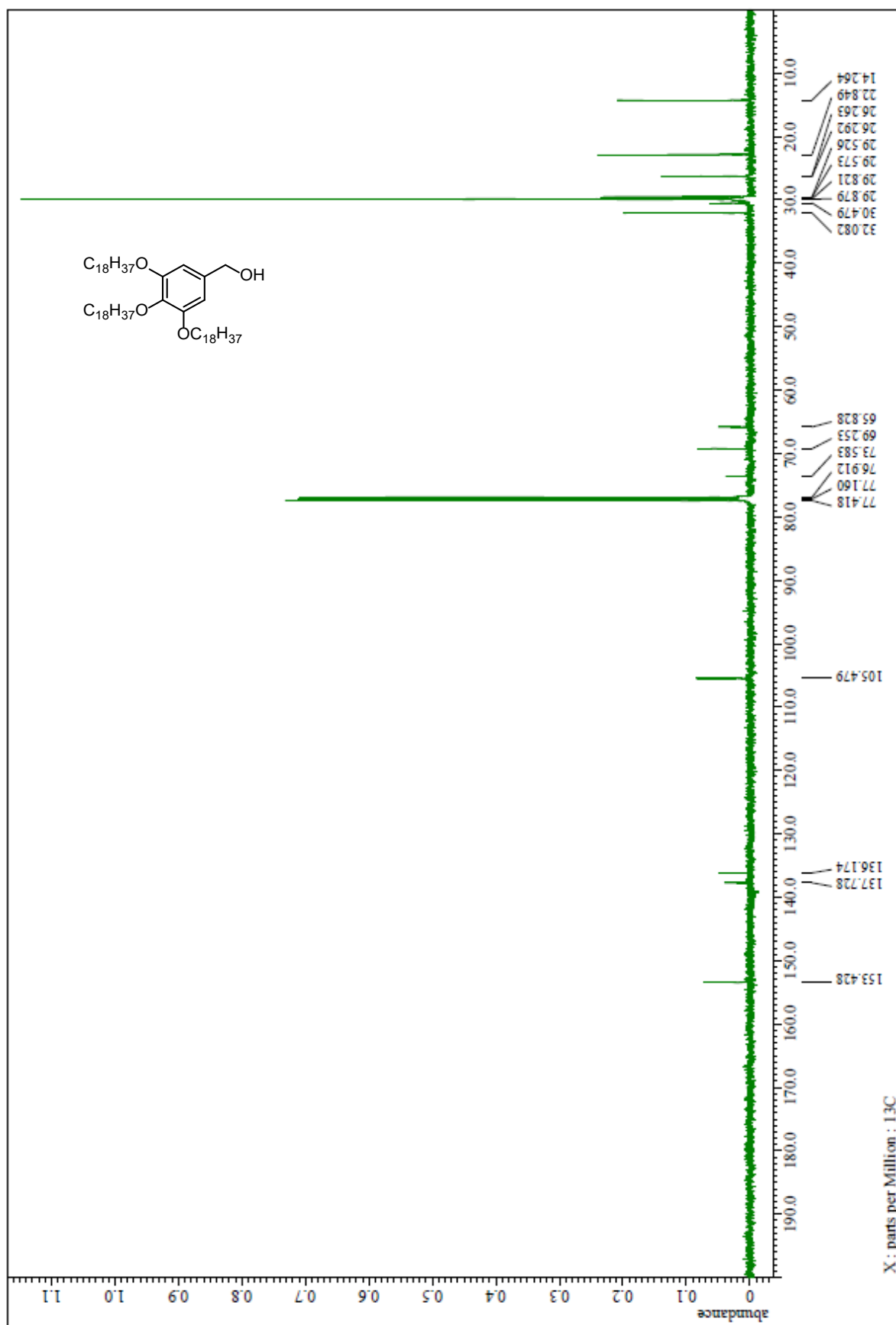


## **NMR Spectra of Compounds in Chapter 3**

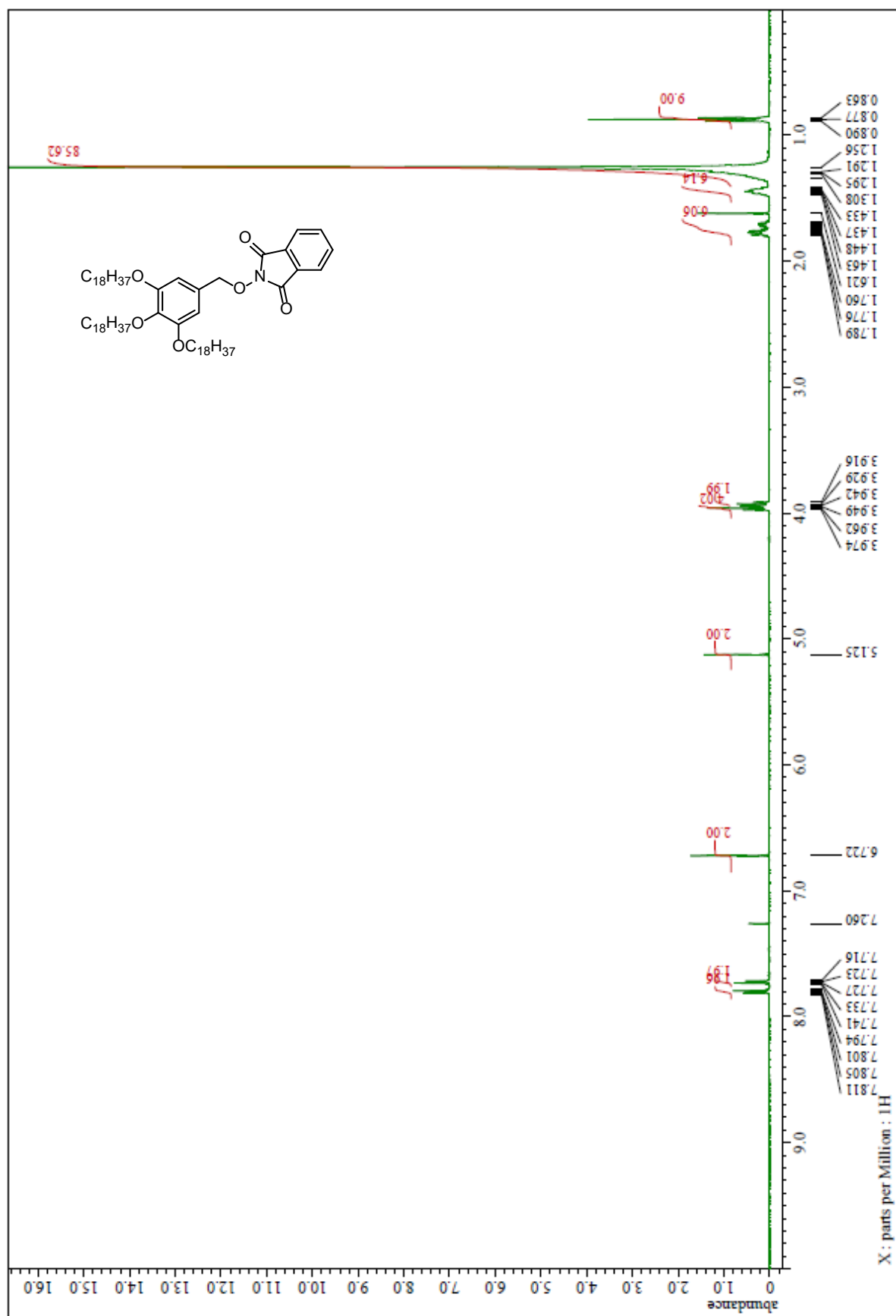
$^1\text{H}$  NMR spectrum of HO-TAGa (**2**) ( $\text{CDCl}_3$ )



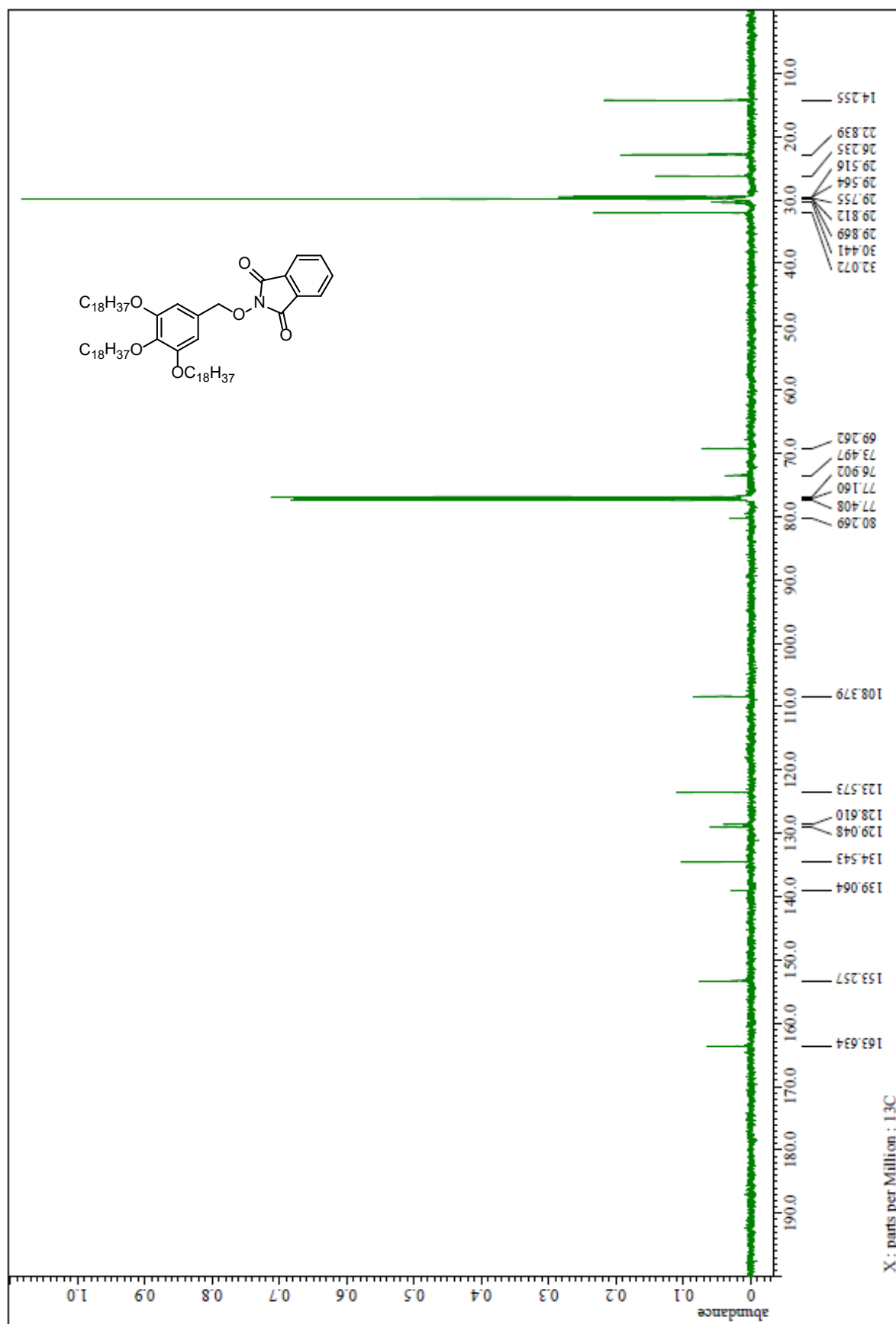
$^{13}\text{C}$  NMR spectrum of Ala-O-FI (**2**) ( $\text{CDCl}_3$ )



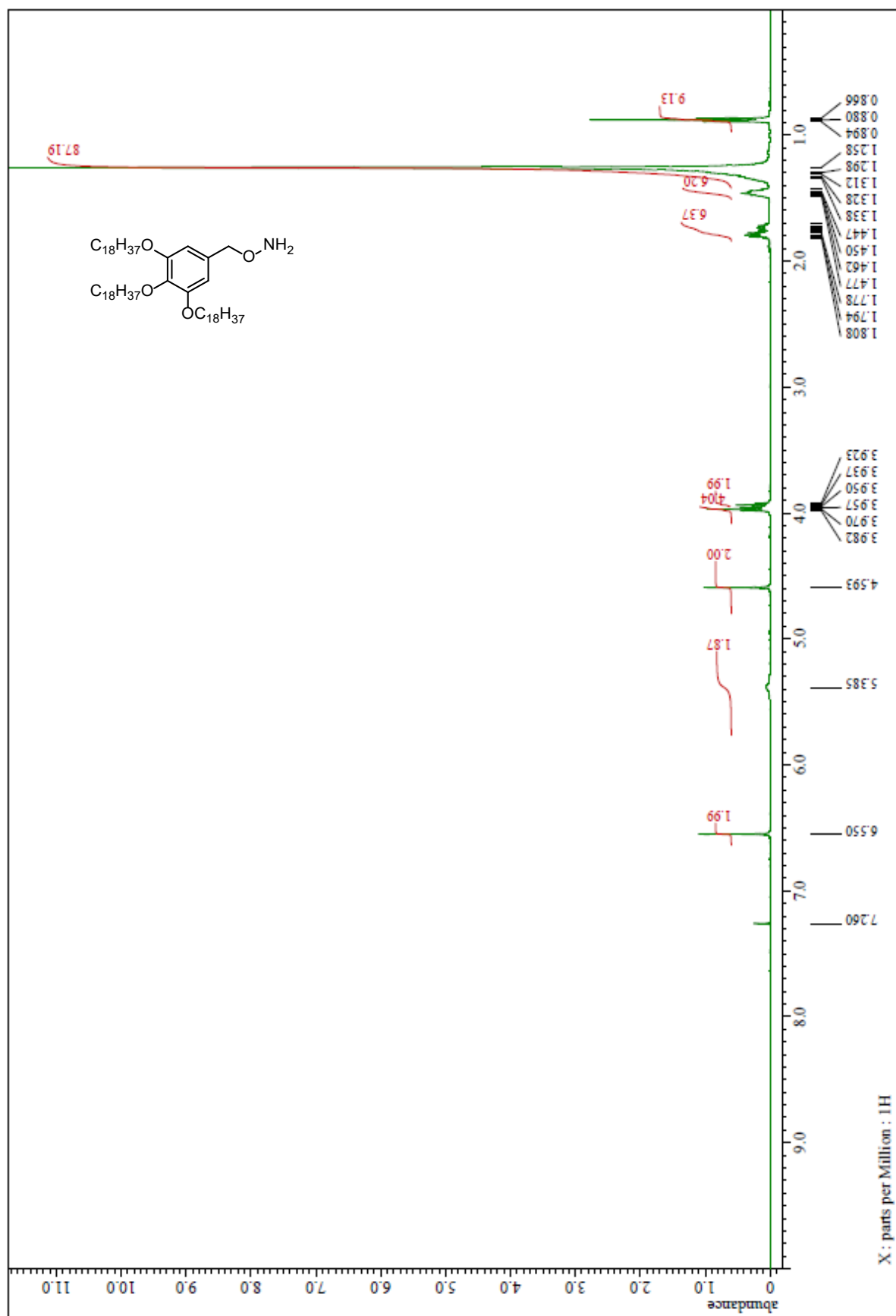
<sup>1</sup>H NMR spectrum of Phthalimide-O-TAGa (**16**) (CDCl<sub>3</sub>)



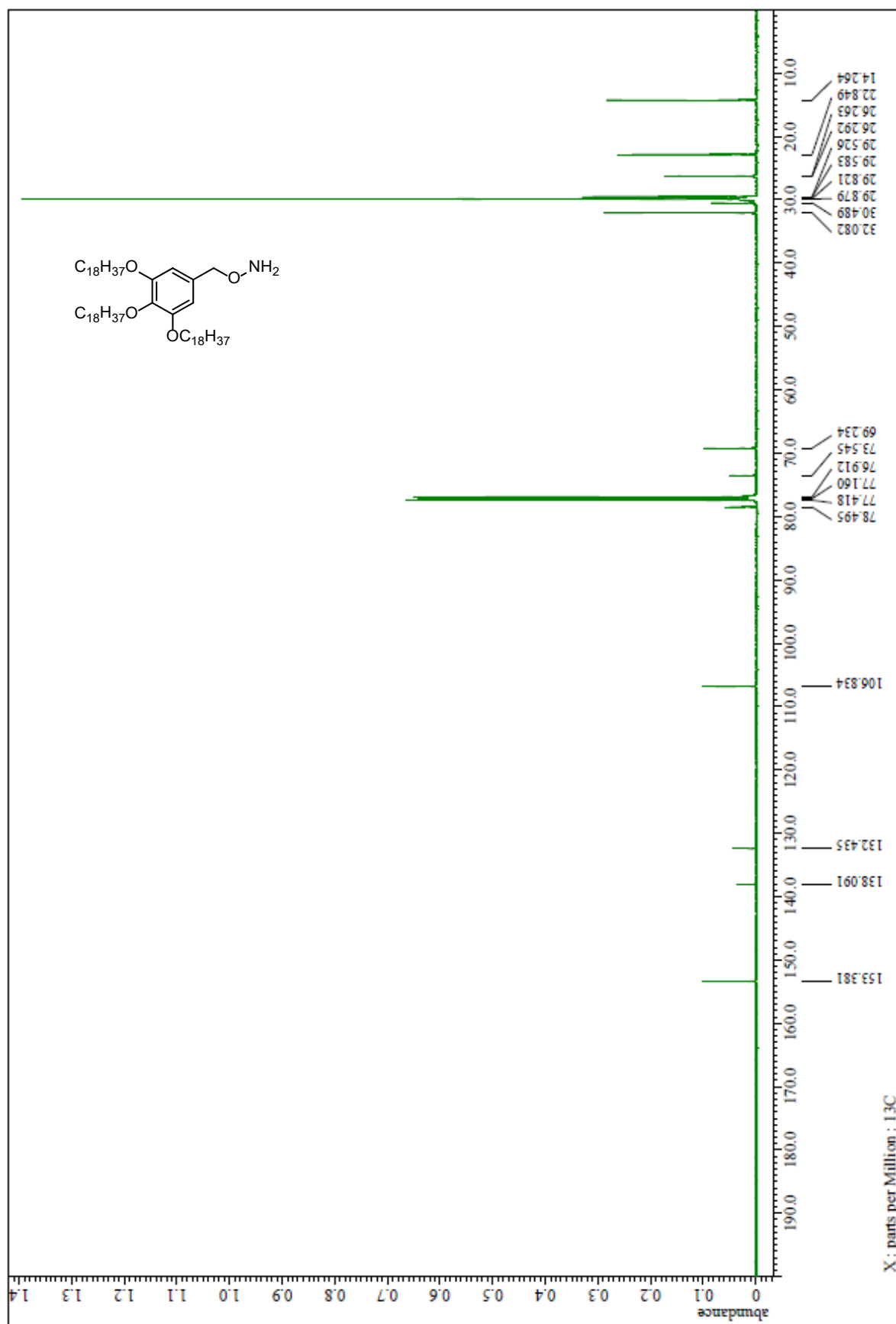
$^{13}\text{C}$  NMR spectrum of Phthalimide-O-TAGa (**16**) ( $\text{CDCl}_3$ )



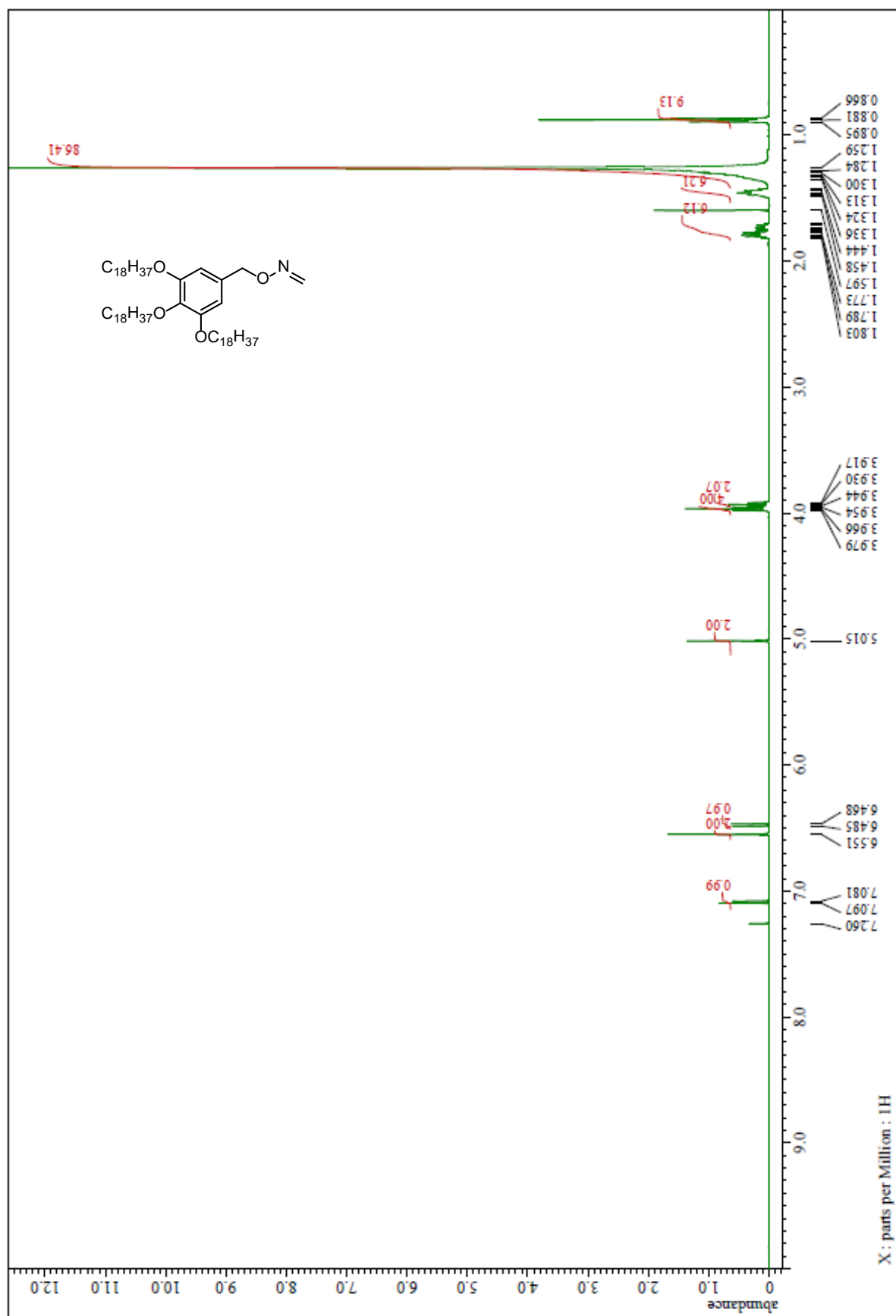
$^1\text{H}$  NMR spectrum of  $\text{NH}_2\text{-O-TAGa}$  (**17**) ( $\text{CDCl}_3$ )



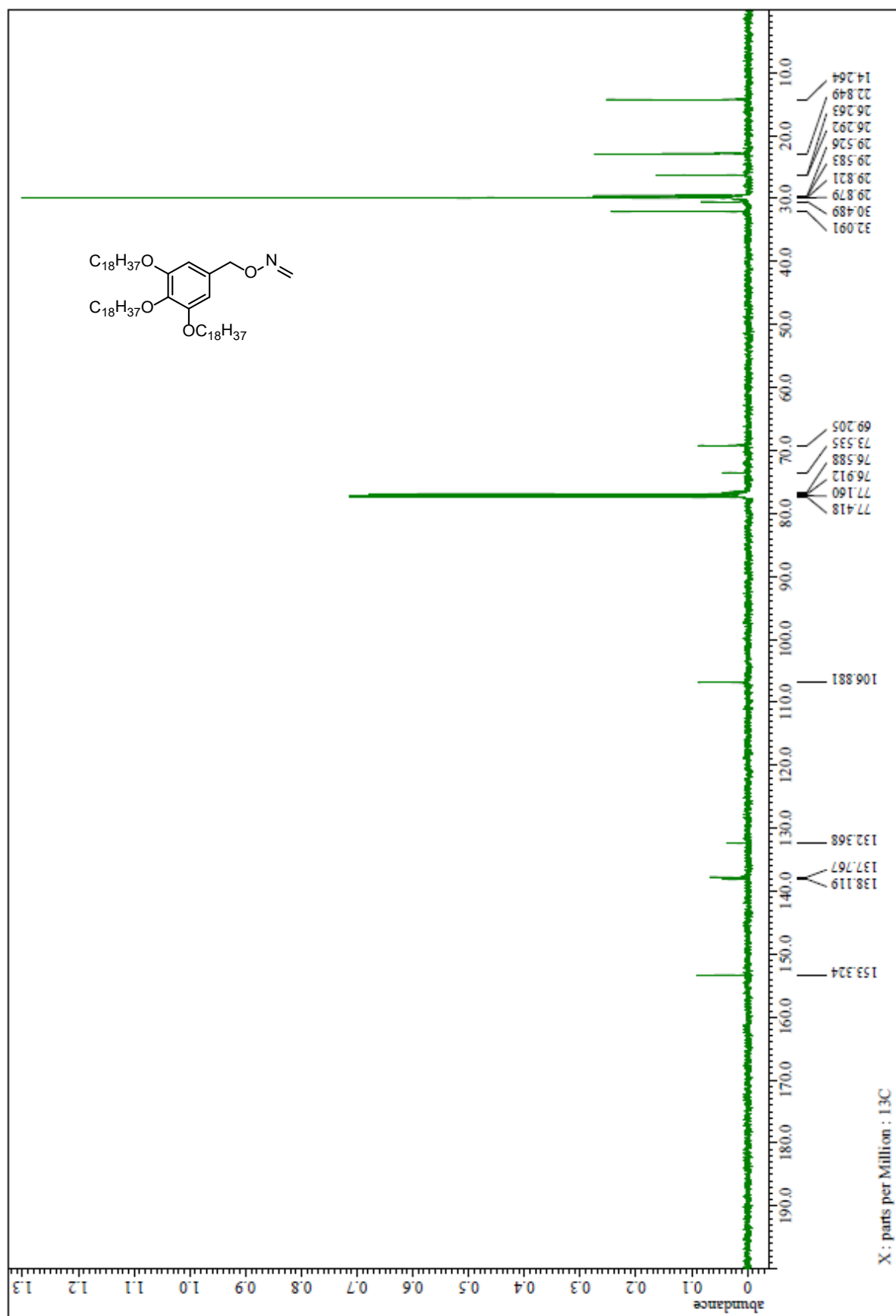
$^{13}\text{C}$  NMR spectrum of  $\text{NH}_2\text{-O-TAGa}$  (**17**) ( $\text{CDCl}_3$ )



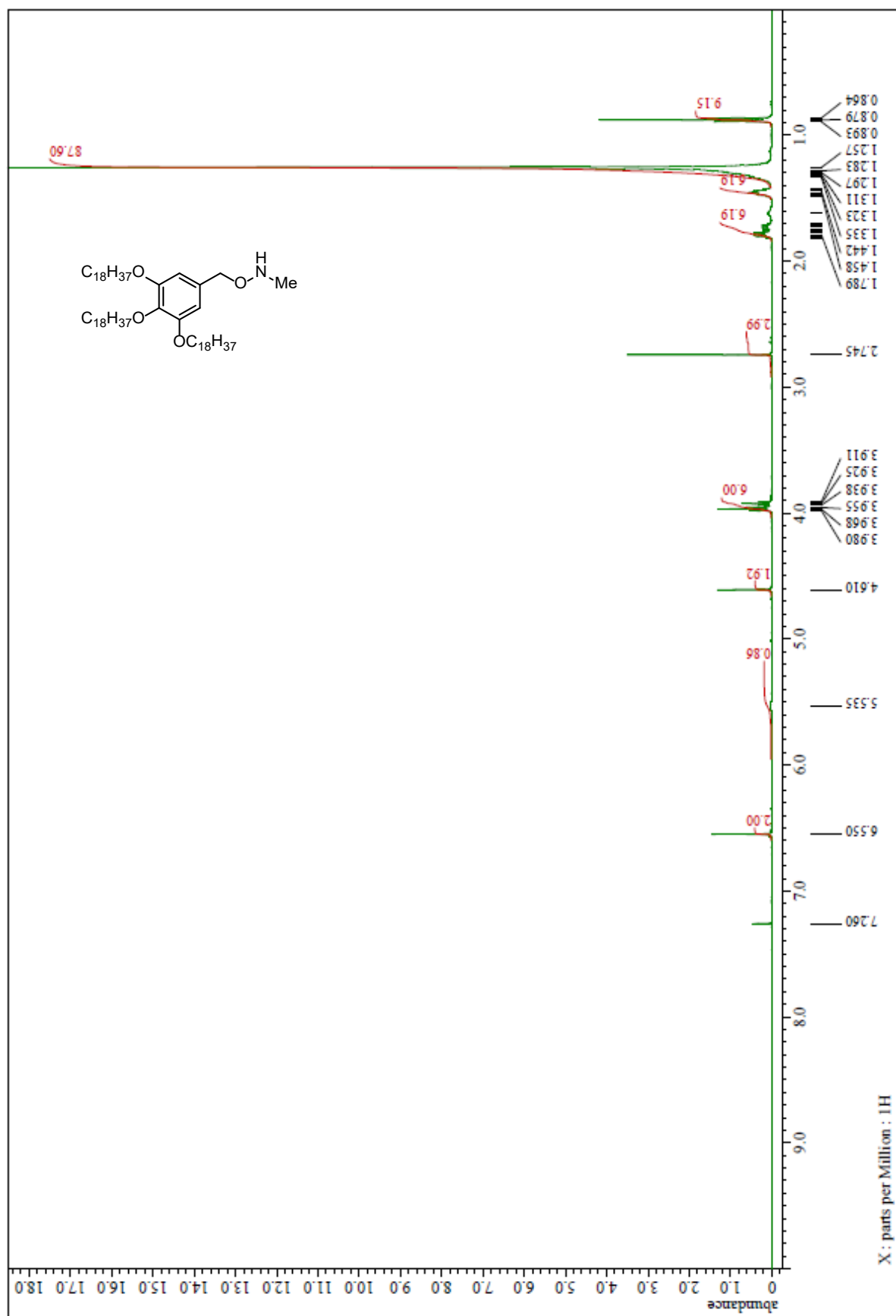
$^1\text{H}$  NMR spectrum of  $\text{CH}_2=\text{N}-\text{O}-\text{TAGa}$  (**18**) ( $\text{CDCl}_3$ )



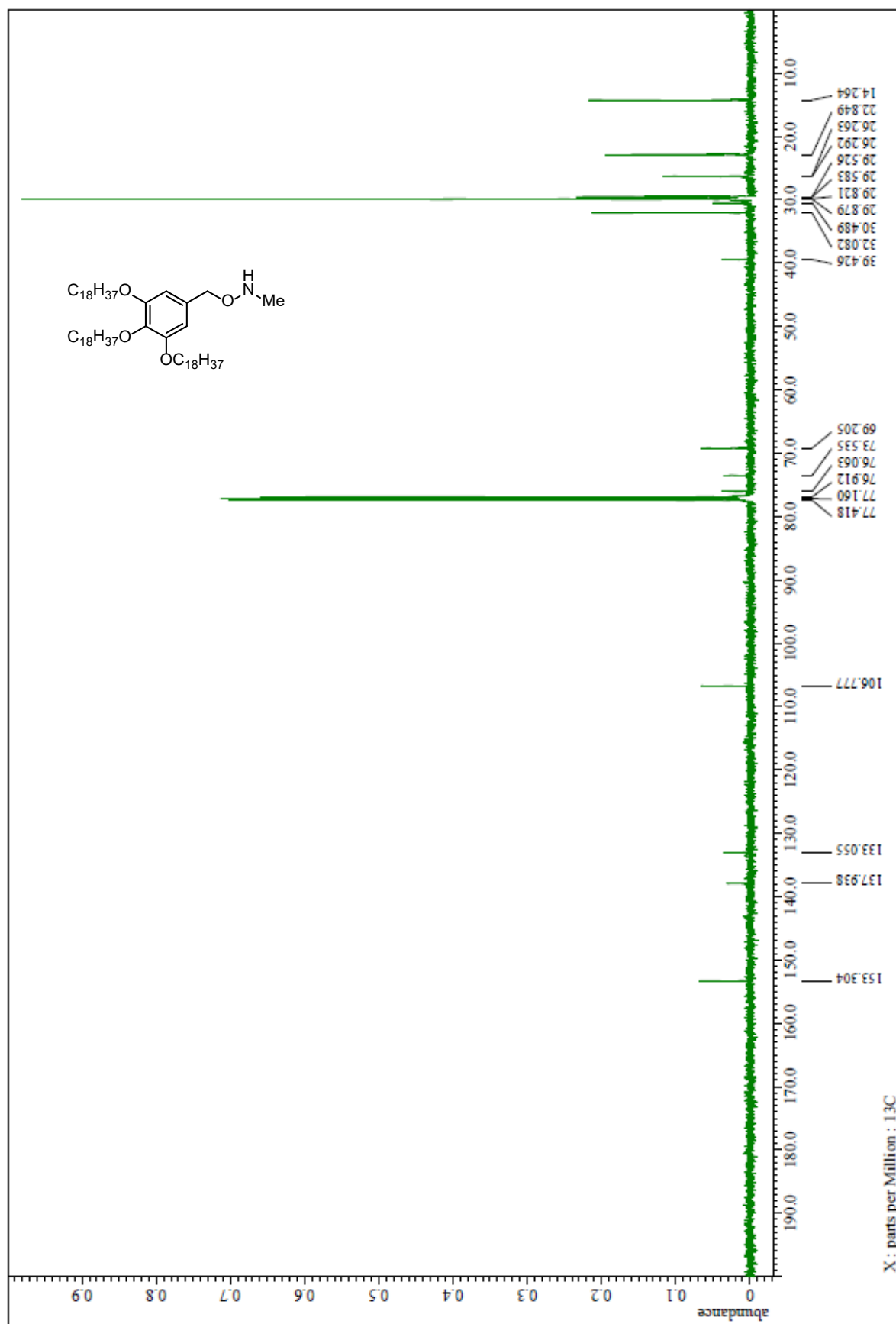
$^{13}\text{C}$  NMR spectrum of  $\text{CH}_2=\text{N}-\text{O}-\text{TAGa}$  (**18**) ( $\text{CDCl}_3$ )



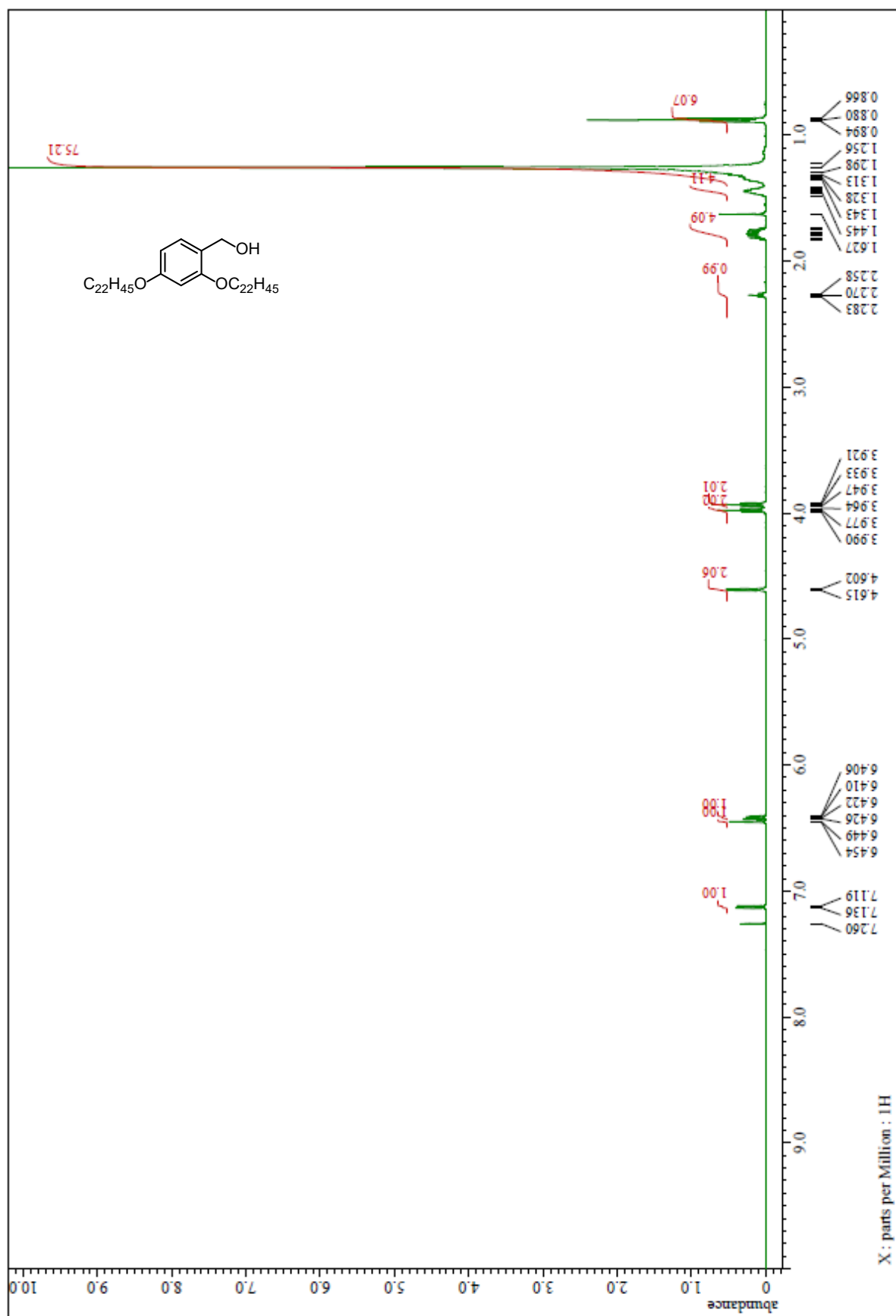
<sup>1</sup>H NMR spectrum of Me-HN-O-TAGa (**15**) (CDCl<sub>3</sub>)



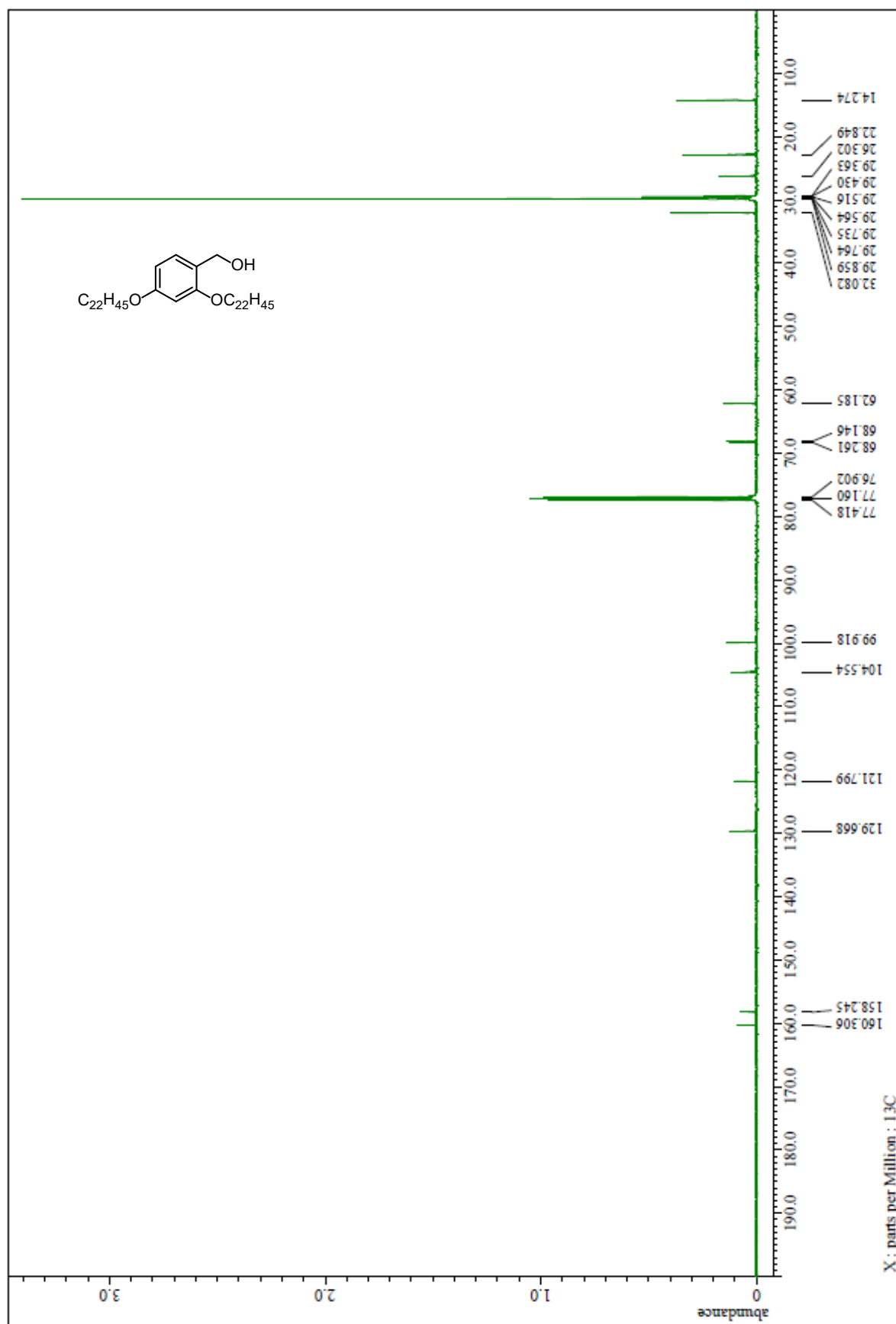
$^{13}\text{C}$  NMR spectrum of Me-HN-O-TAGa (**15**) ( $\text{CDCl}_3$ )



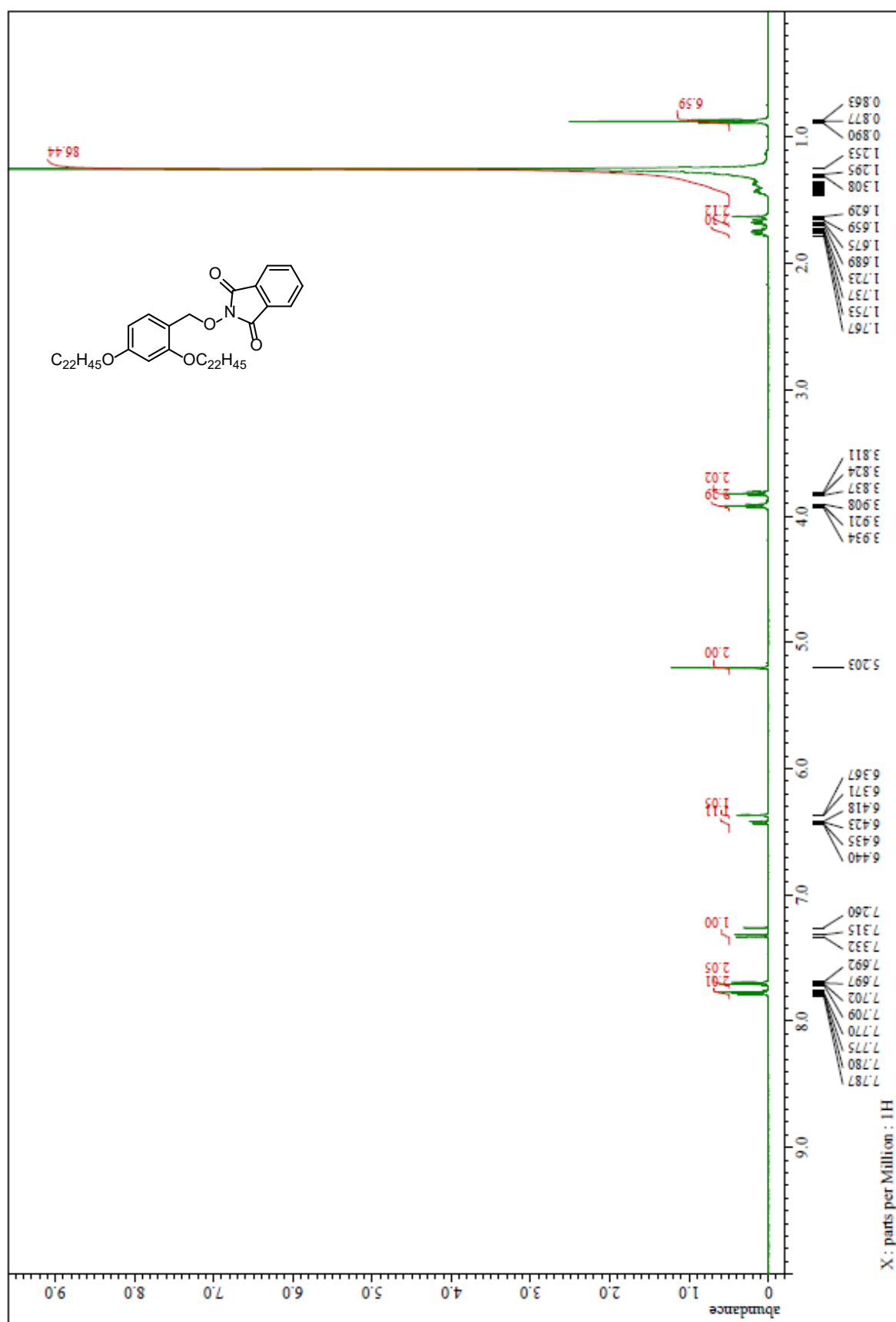
$^1\text{H}$  NMR spectrum of HO-TAGb (**52**) ( $\text{CDCl}_3$ )



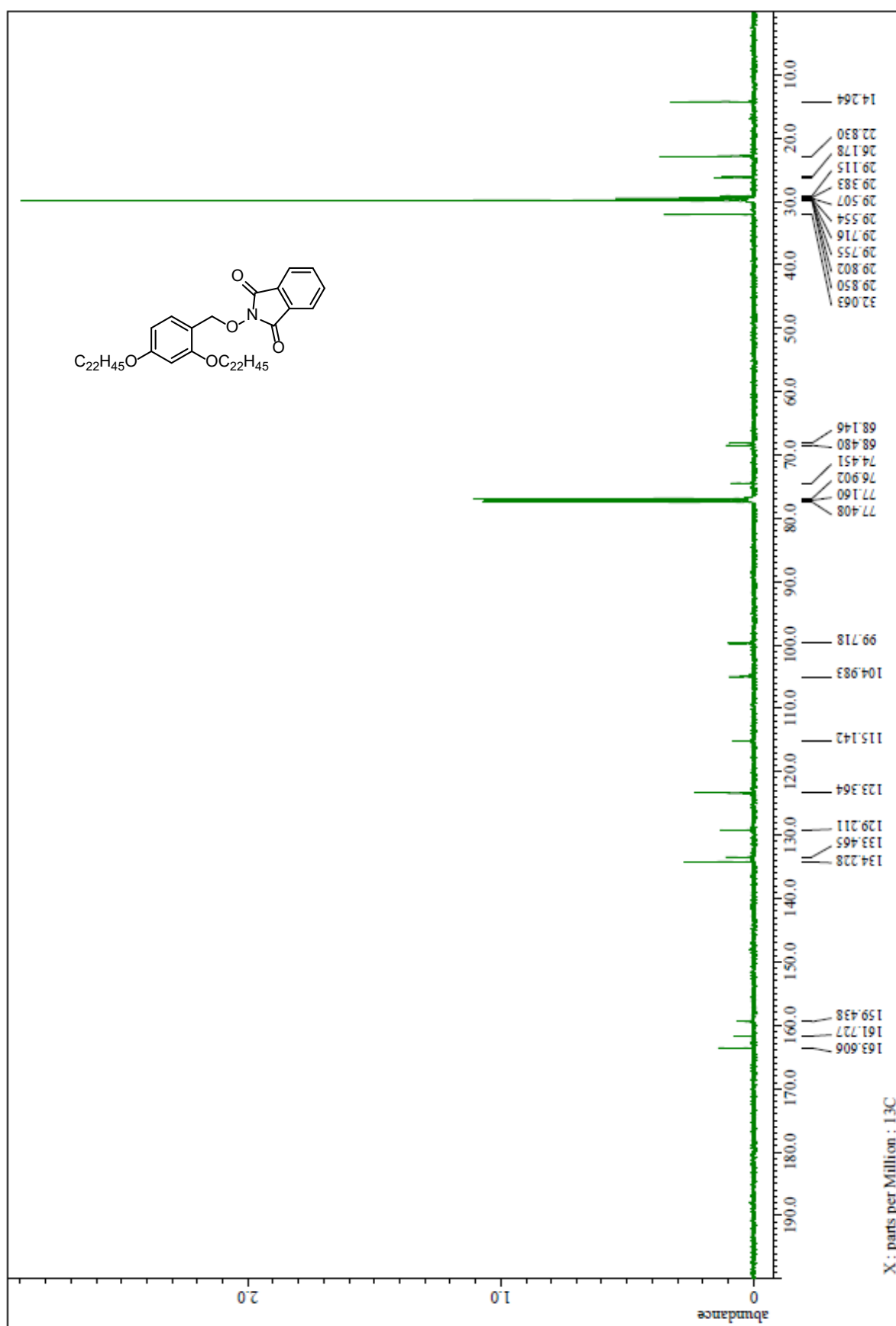
$^{13}\text{C}$  NMR spectrum of HO-TAGb (**52**) ( $\text{CDCl}_3$ )



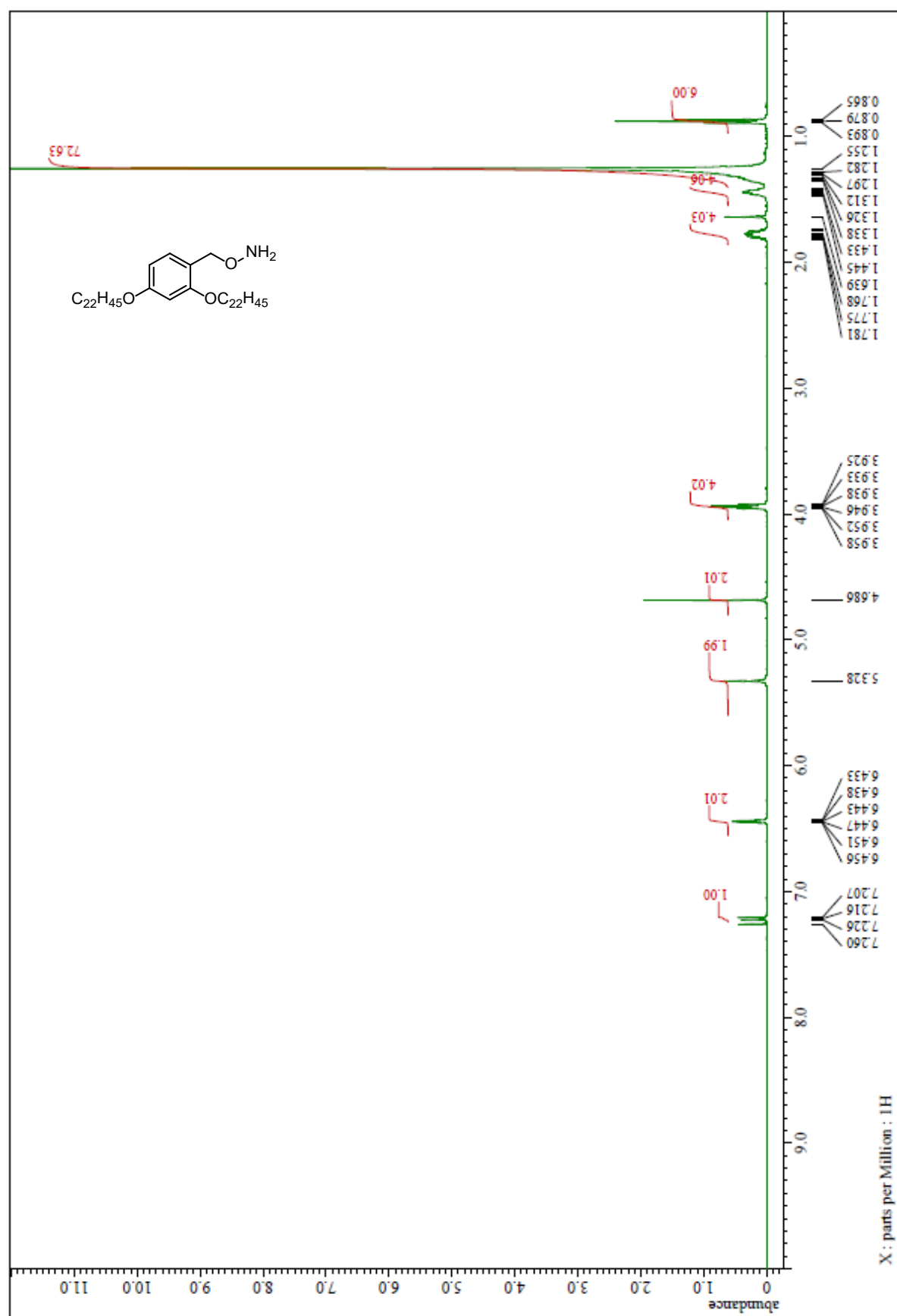
<sup>1</sup>H NMR spectrum of Phthalimide-O-TAGb (**53**) (CDCl<sub>3</sub>)



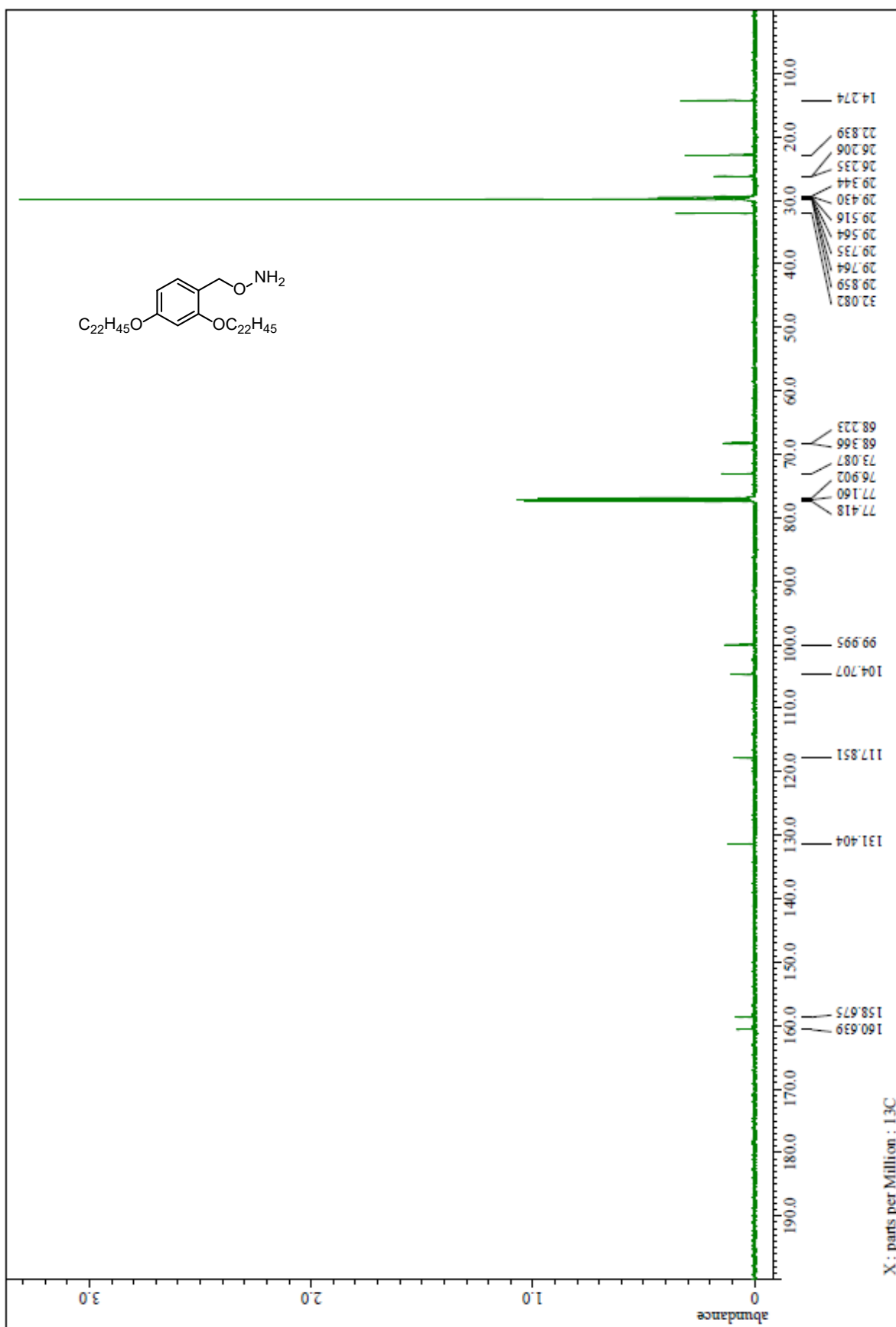
$^{13}\text{C}$  NMR spectrum of Phthalimide-O-TAGb (**53**) ( $\text{CDCl}_3$ )



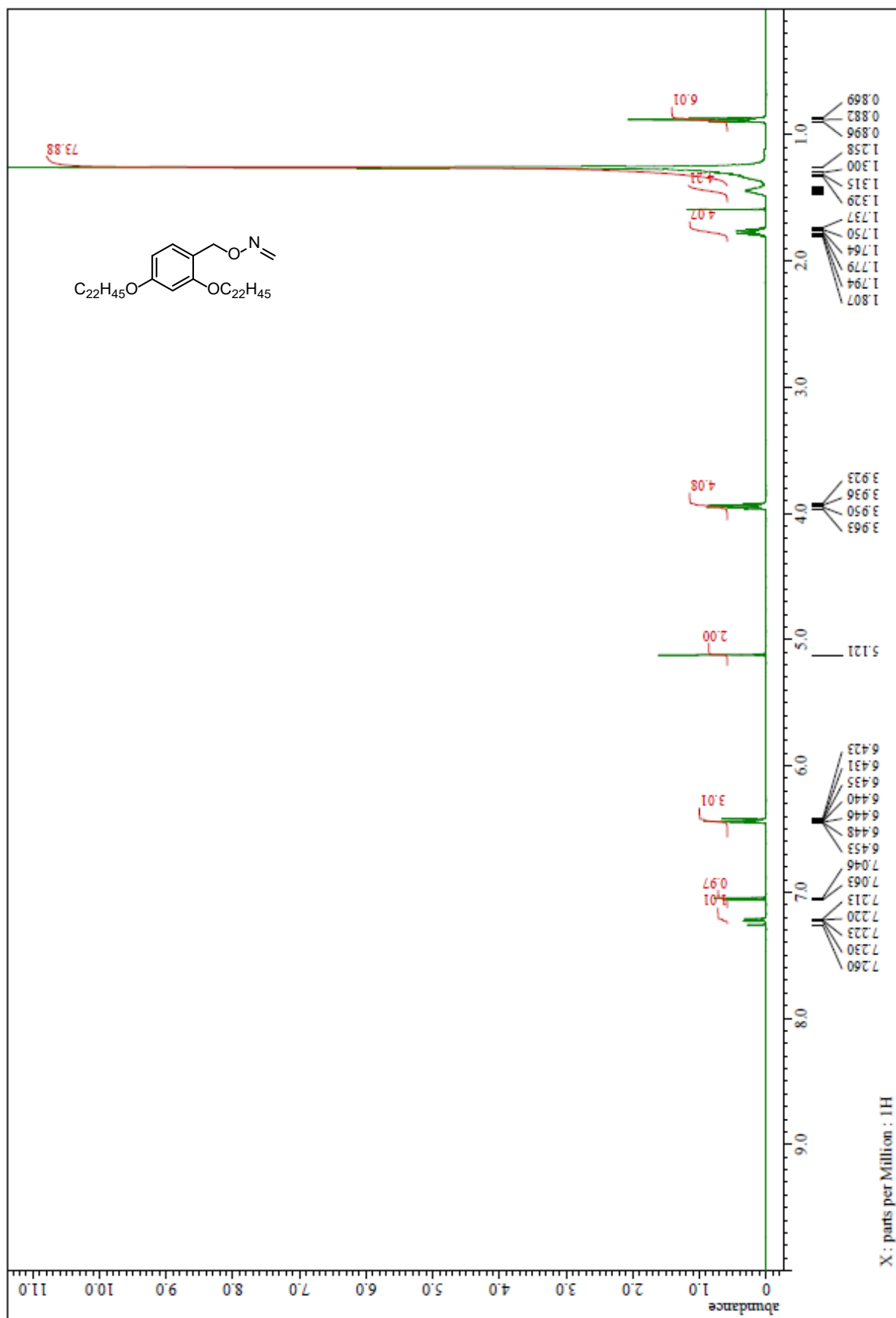
$^1\text{H}$  NMR spectrum of  $\text{NH}_2\text{-O-TAGb}$  (**54**) ( $\text{CDCl}_3$ )



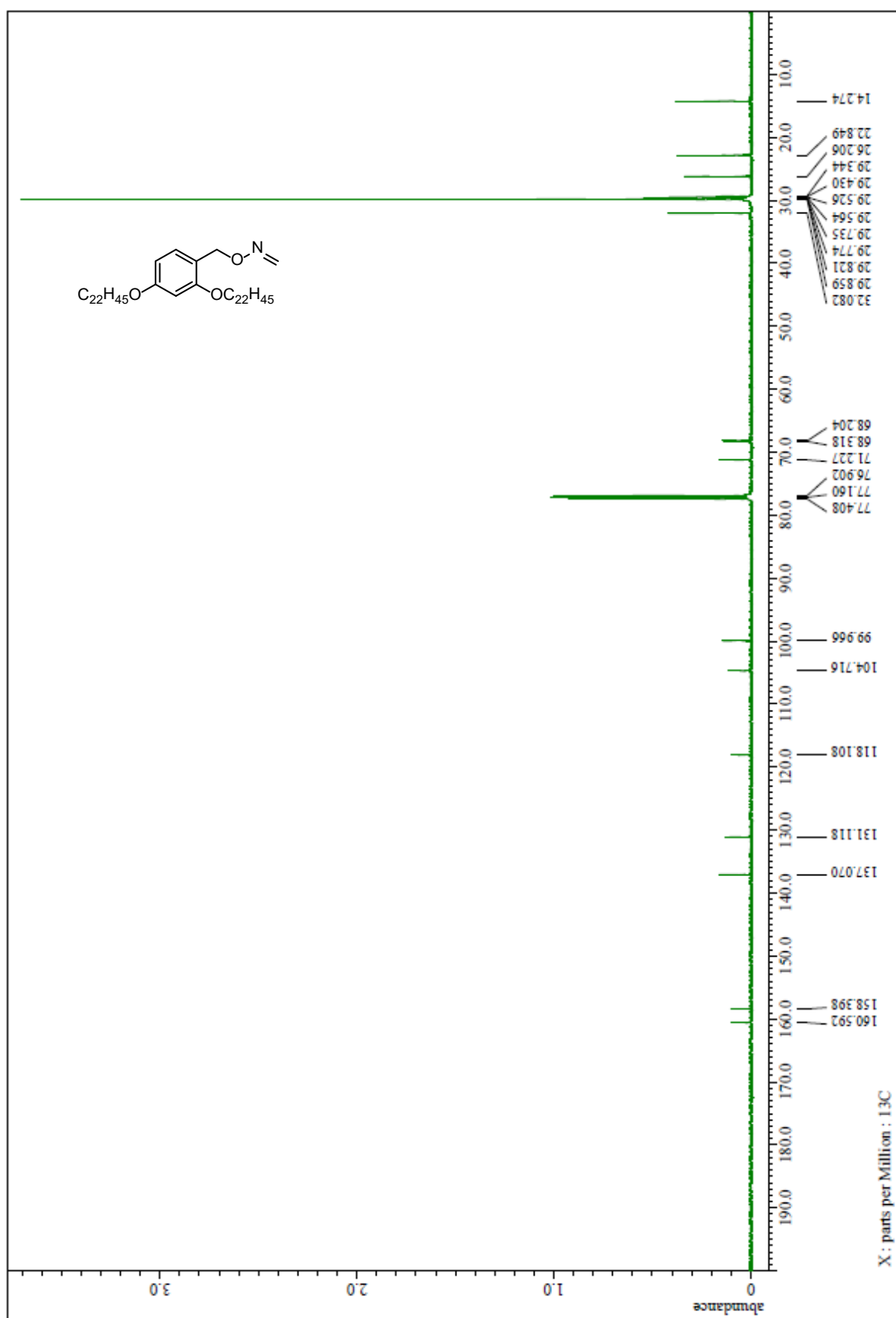
$^{13}\text{C}$  NMR spectrum of  $\text{NH}_2\text{-O-TAGb}$  (**54**) ( $\text{CDCl}_3$ )



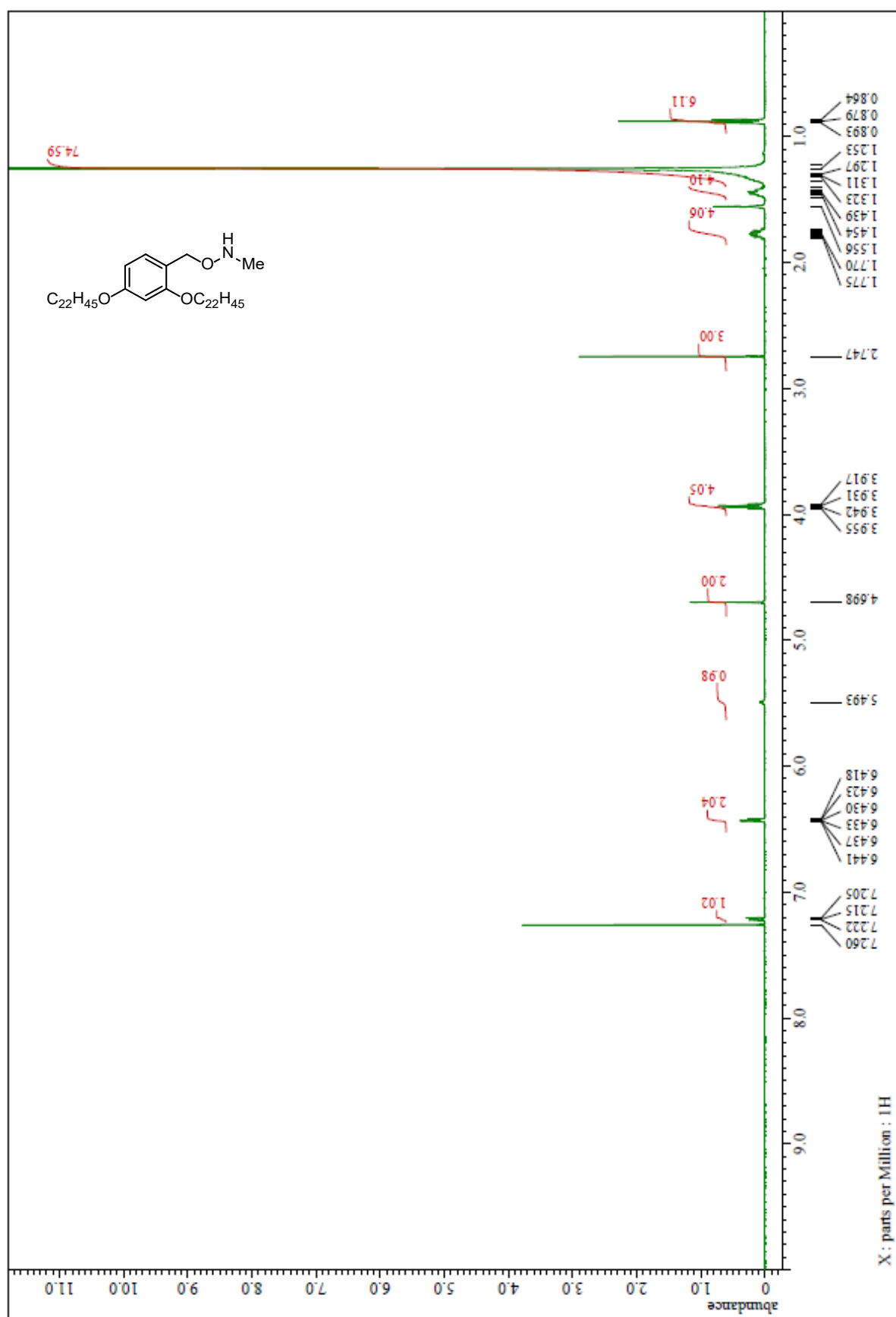
$^1\text{H}$  NMR spectrum of  $\text{CH}_2=\text{N}-\text{O}-\text{TAGb}$  (**55**) ( $\text{CDCl}_3$ )



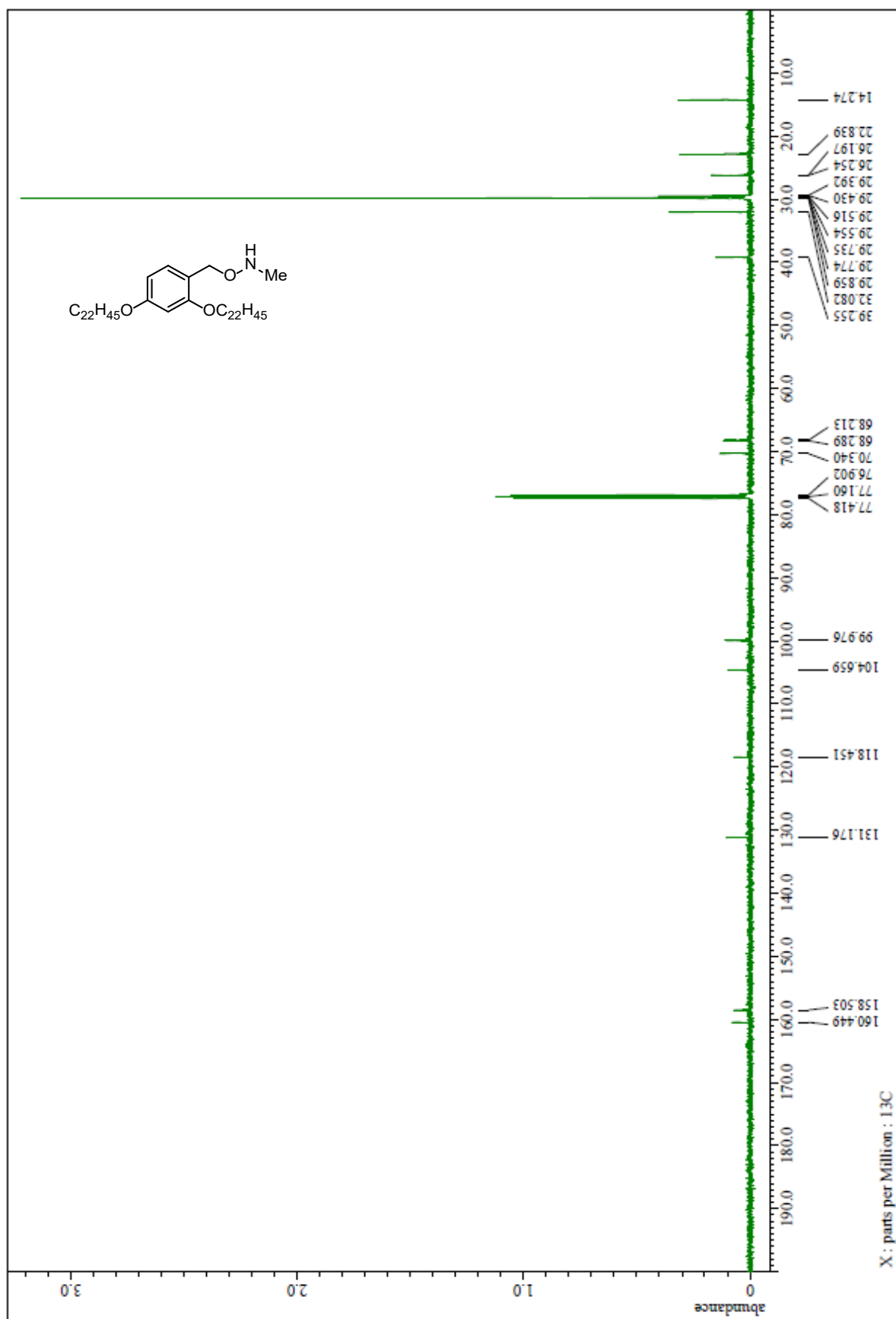
$^{13}\text{C}$  NMR spectrum of  $\text{CH}_2=\text{N}-\text{O}-\text{TAGb}$  (**55**) ( $\text{CDCl}_3$ )



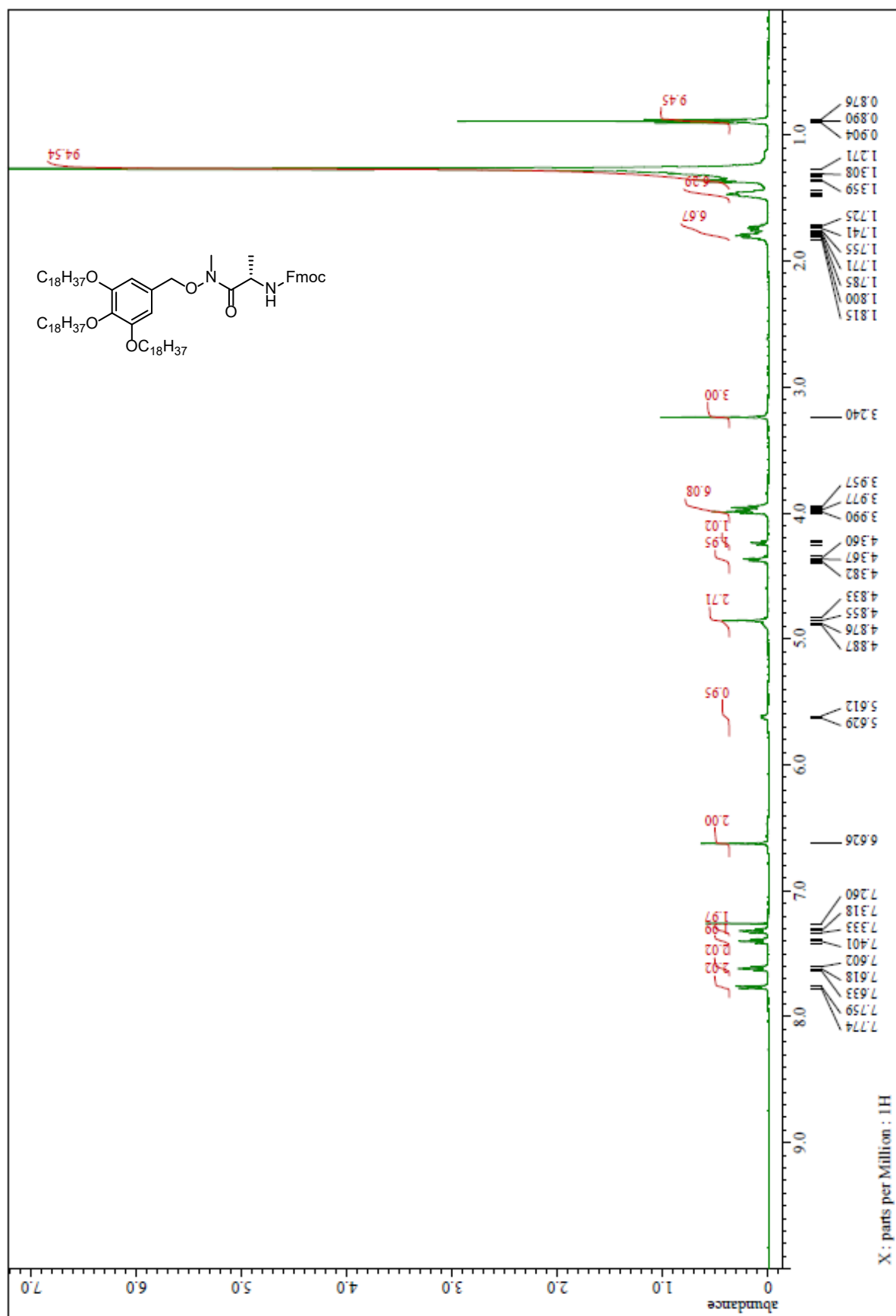
$^1\text{H}$  NMR spectrum of Me-HN-O-TAGb (**56**) ( $\text{CDCl}_3$ )



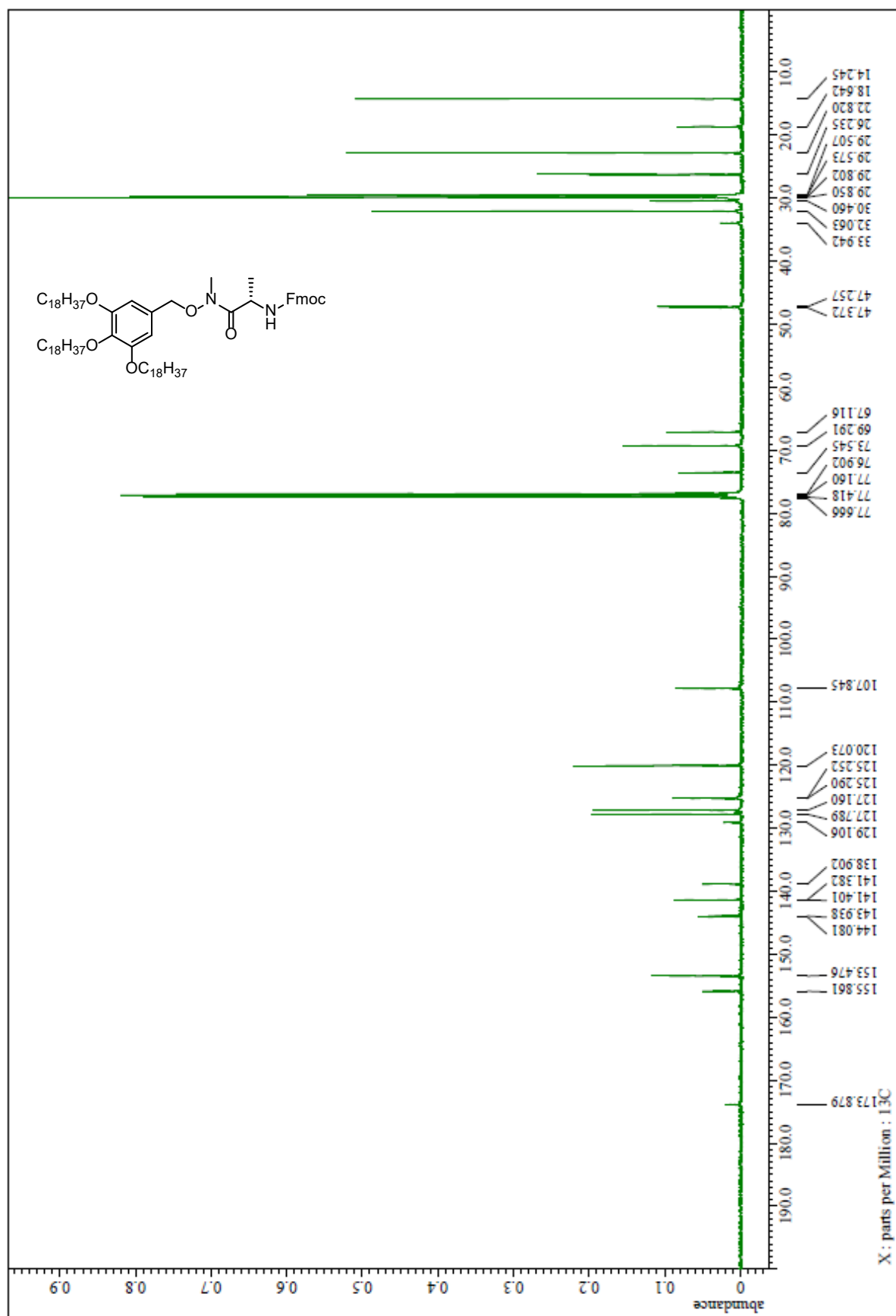
$^{13}\text{C}$  NMR spectrum of Me-HN-O-TAGb (**56**) ( $\text{CDCl}_3$ )



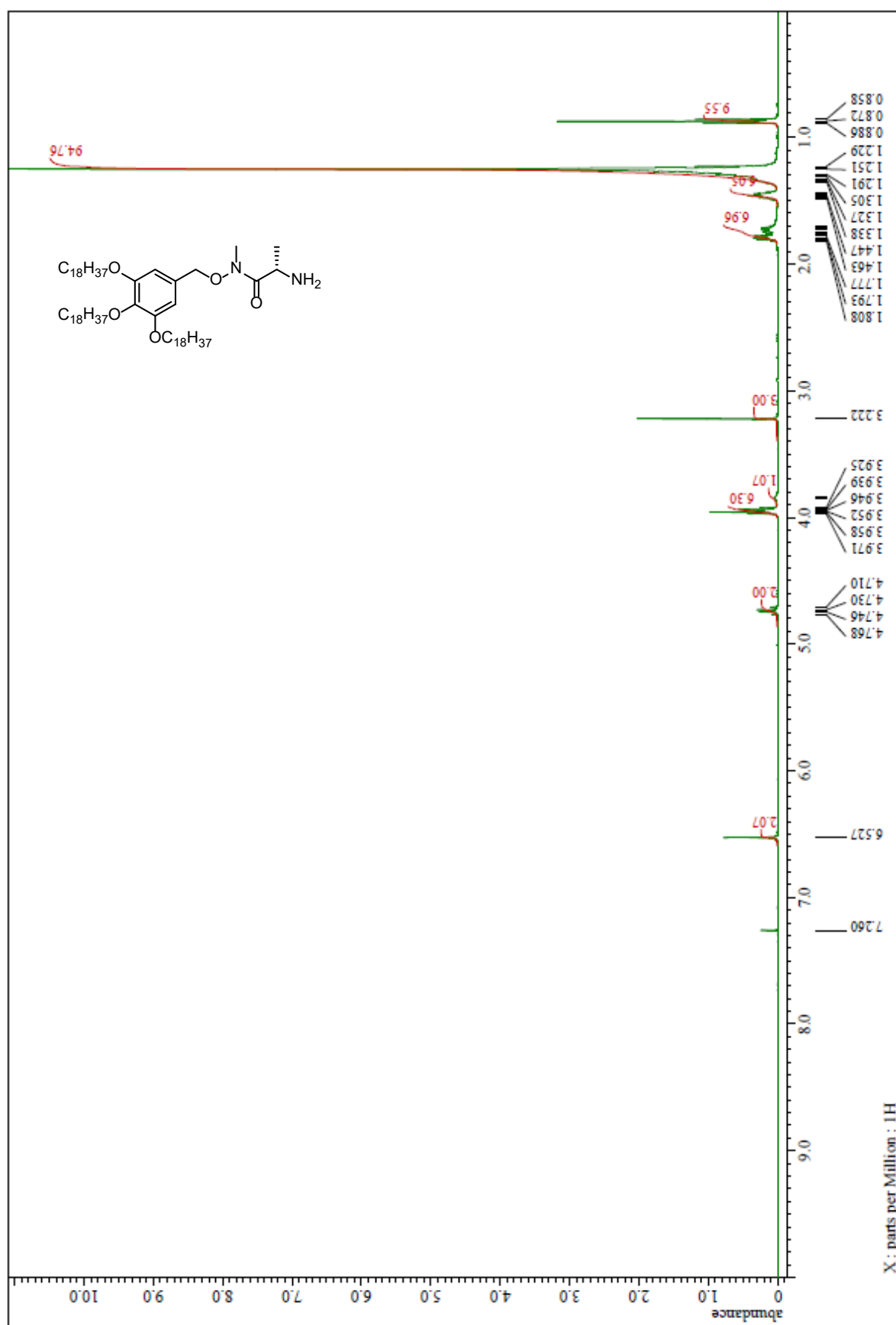
$^1\text{H}$  NMR spectrum of Fmoc-Ala-(Me)N-O-TAGa (**57**) ( $\text{CDCl}_3$ )



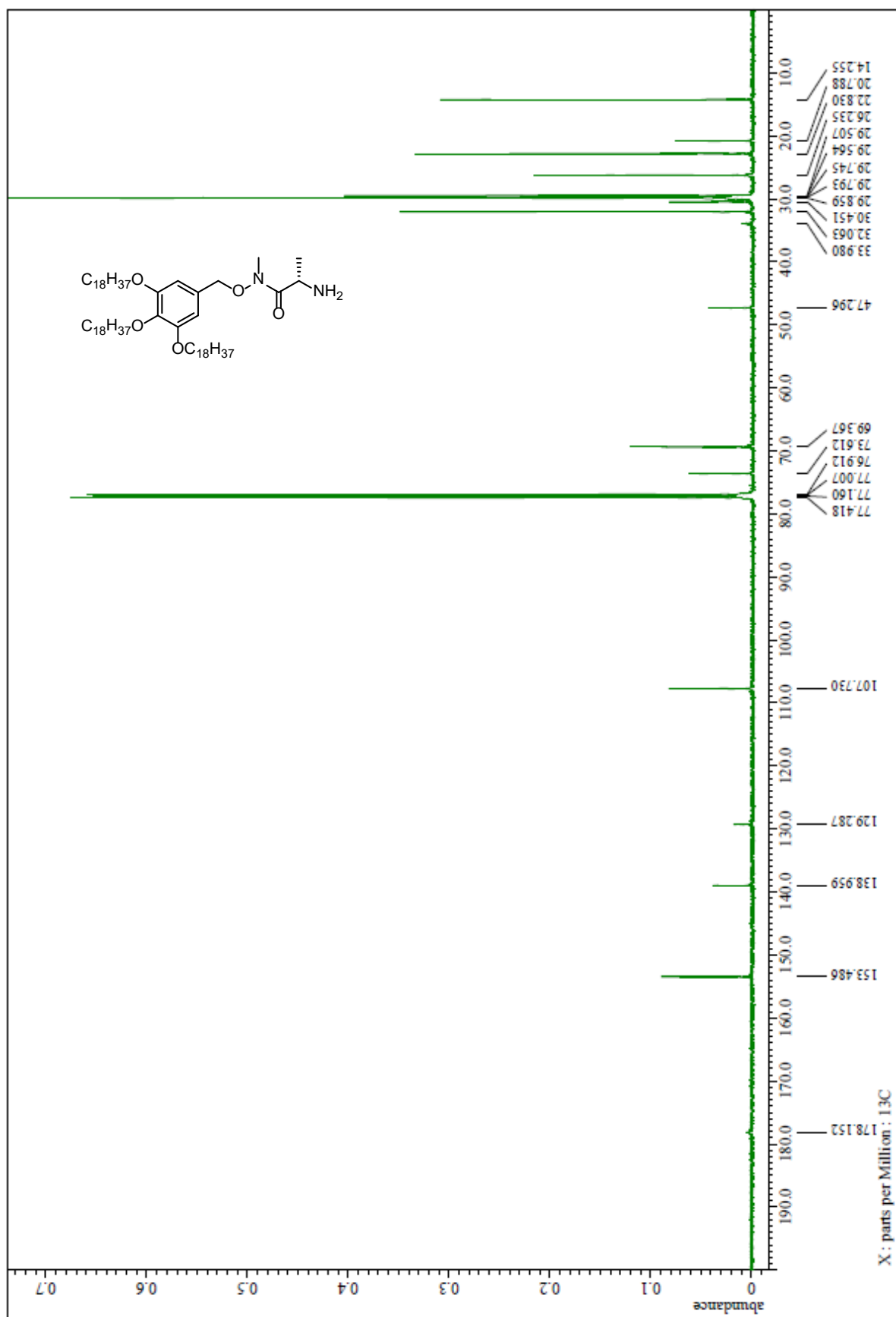
$^{13}\text{C}$  NMR spectrum of Fmoc-Ala-(Me)N-O-TAGa (**57**) ( $\text{CDCl}_3$ )



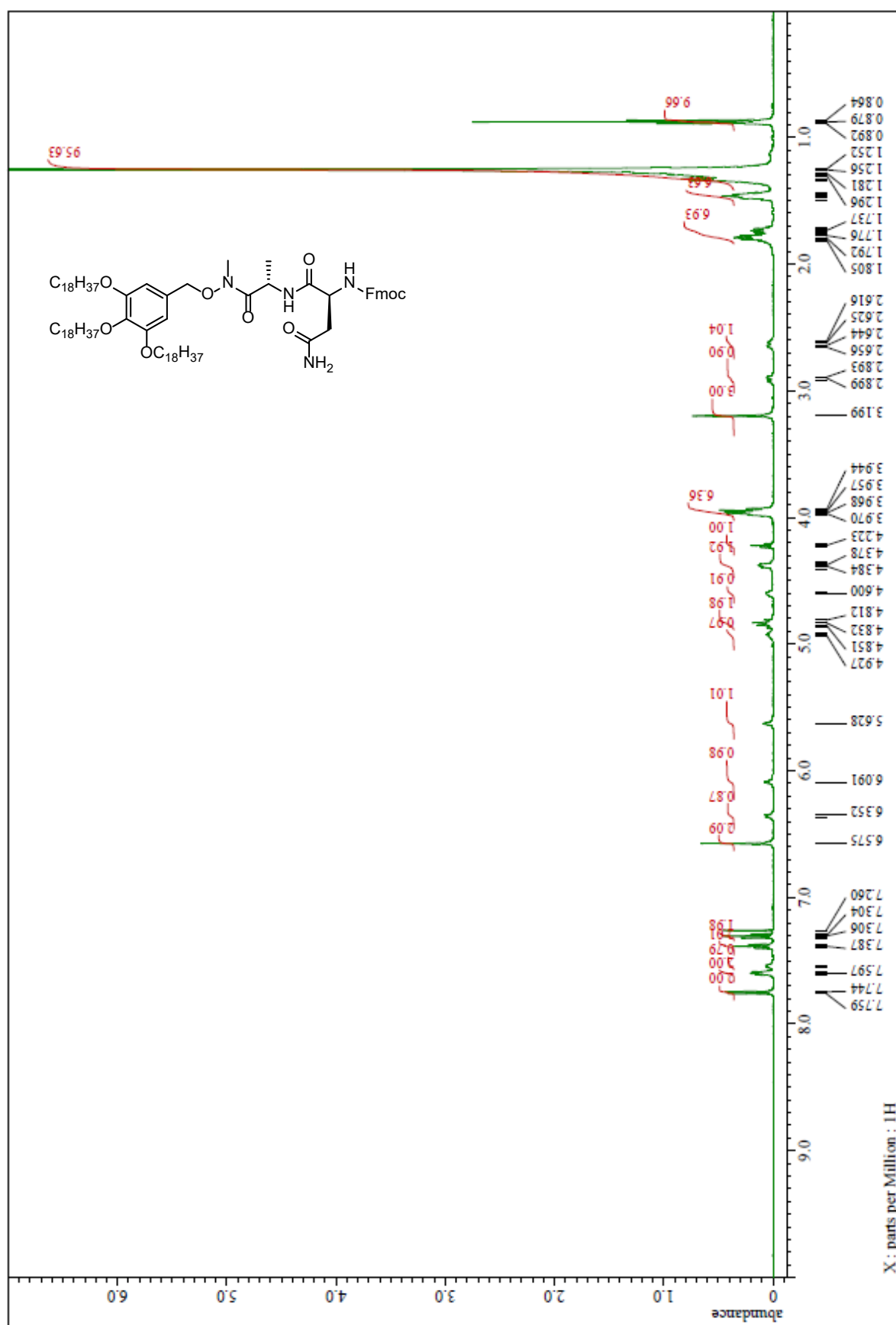
<sup>1</sup>H NMR spectrum of Ala-(Me)N-O-TAGa (**19**) (CDCl<sub>3</sub>)



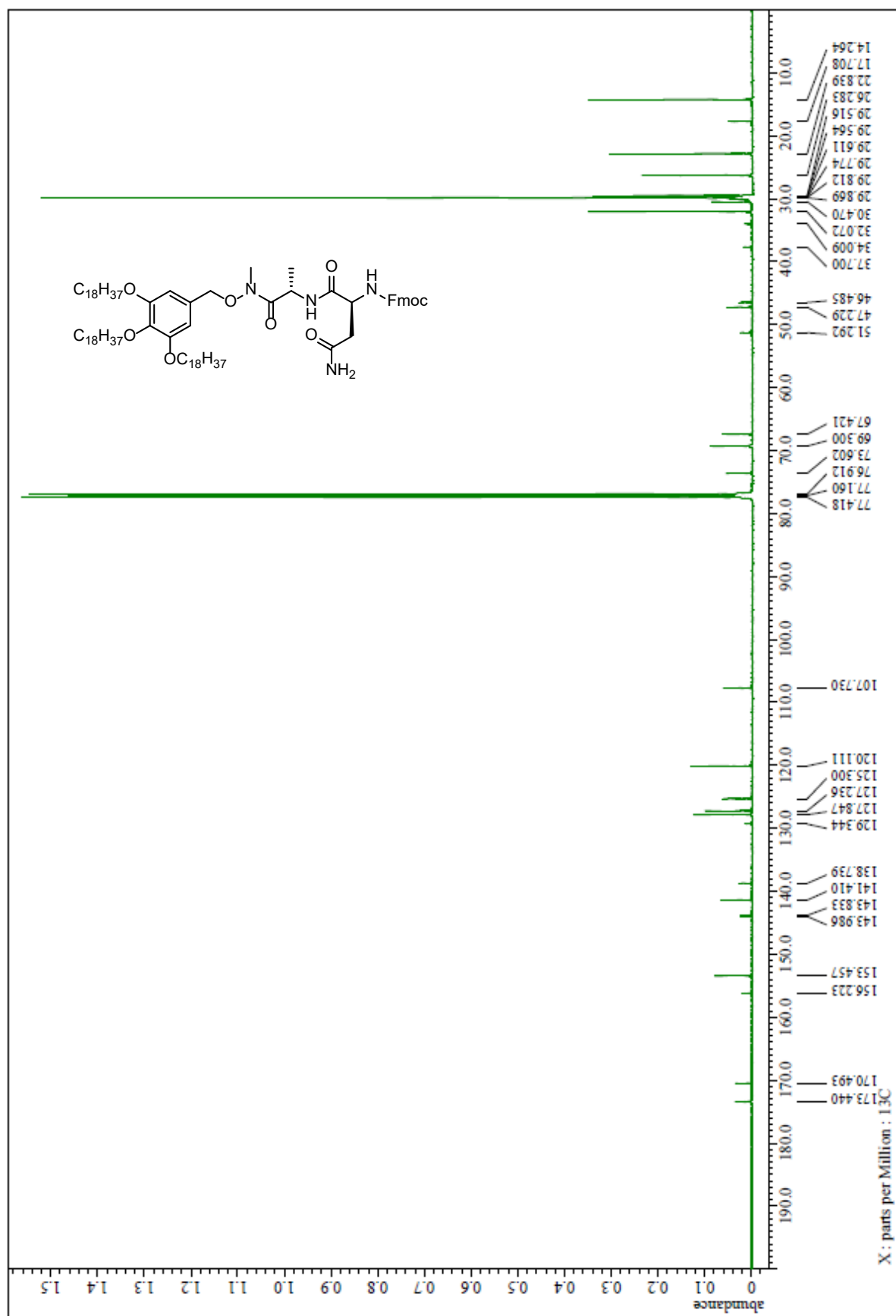
$^{13}\text{C}$  NMR spectrum of Ala-(Me)N-O-TAGa (**19**) ( $\text{CDCl}_3$ )



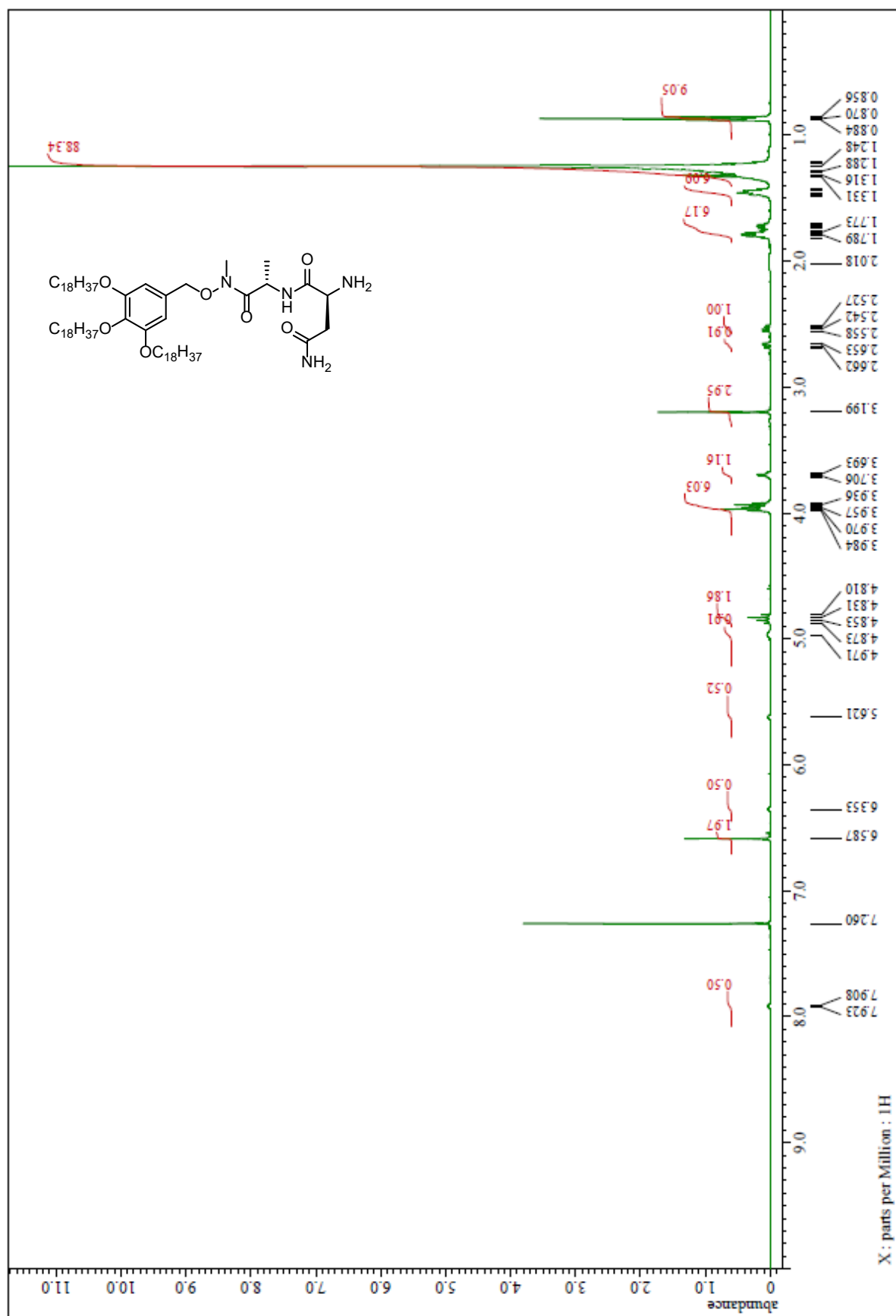
$^1\text{H}$  NMR spectrum of Fmoc-Asn-Ala-(Me)N-O-TAGa (**58**) ( $\text{CDCl}_3$ )



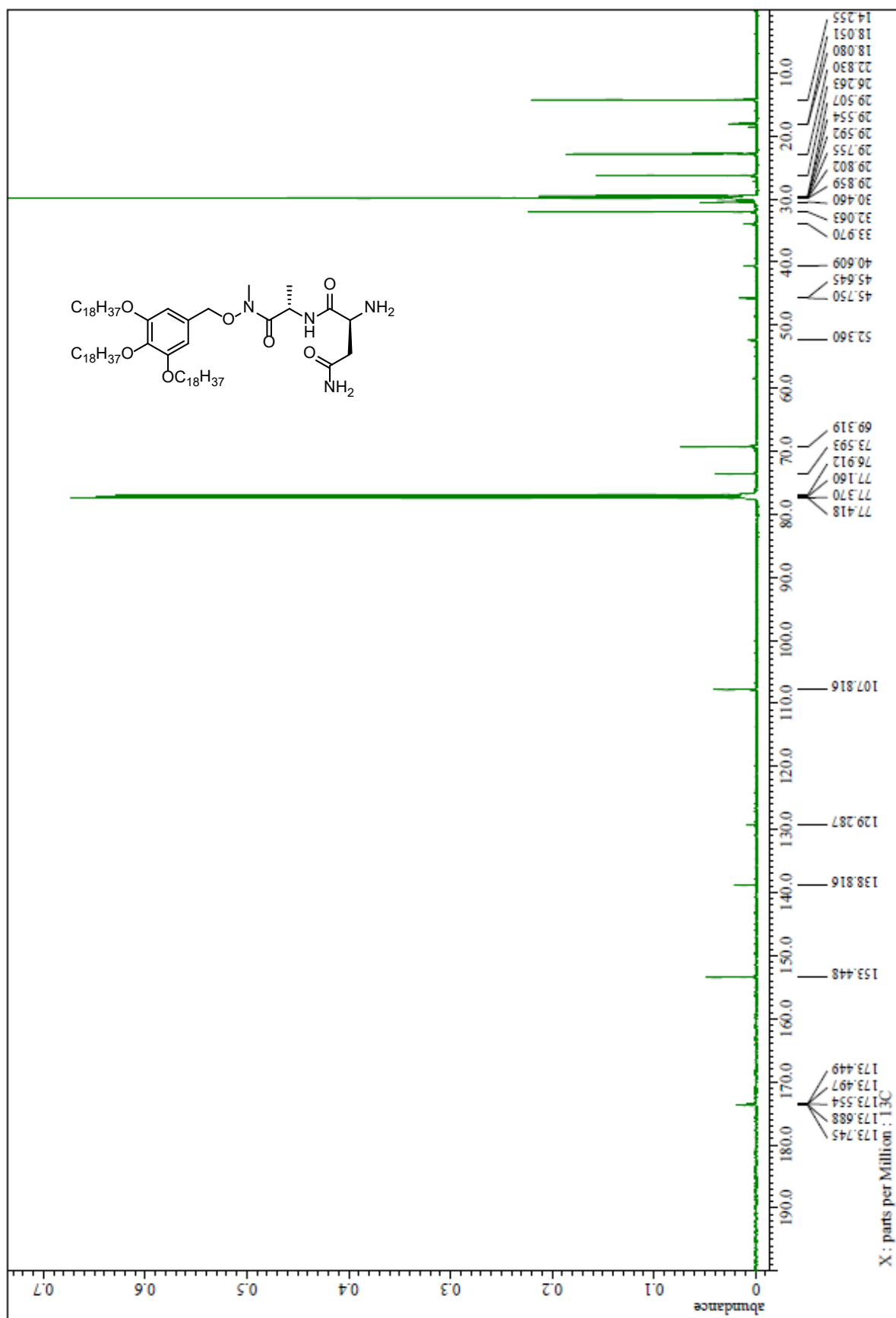
$^{13}\text{C}$  NMR spectrum of Fmoc-Asn-Ala-(Me)N-O-TAGa (**58**) ( $\text{CDCl}_3$ )



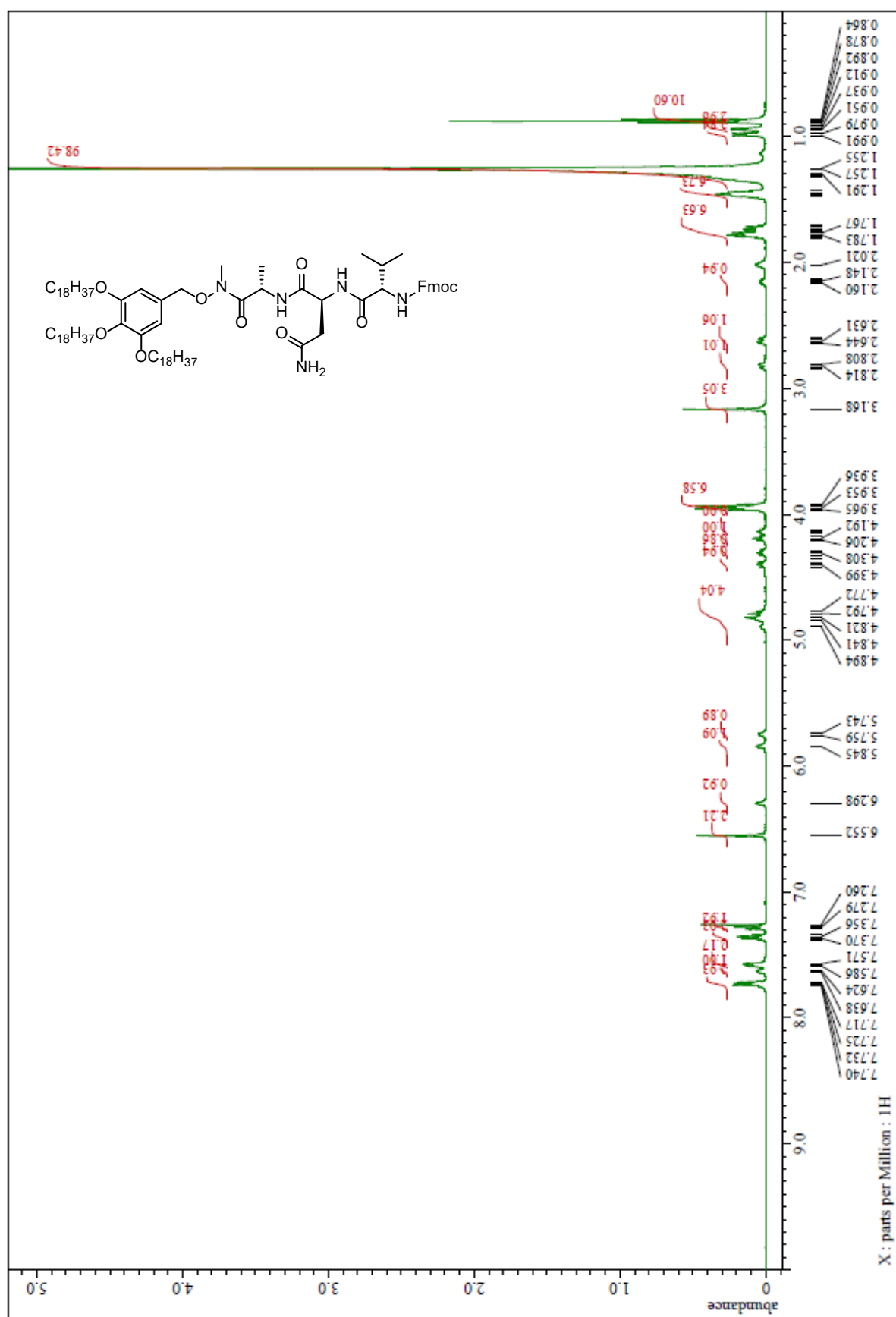
<sup>1</sup>H NMR spectrum of Asn-Ala-(Me)N-O-TAGa (**20**) (CDCl<sub>3</sub>)



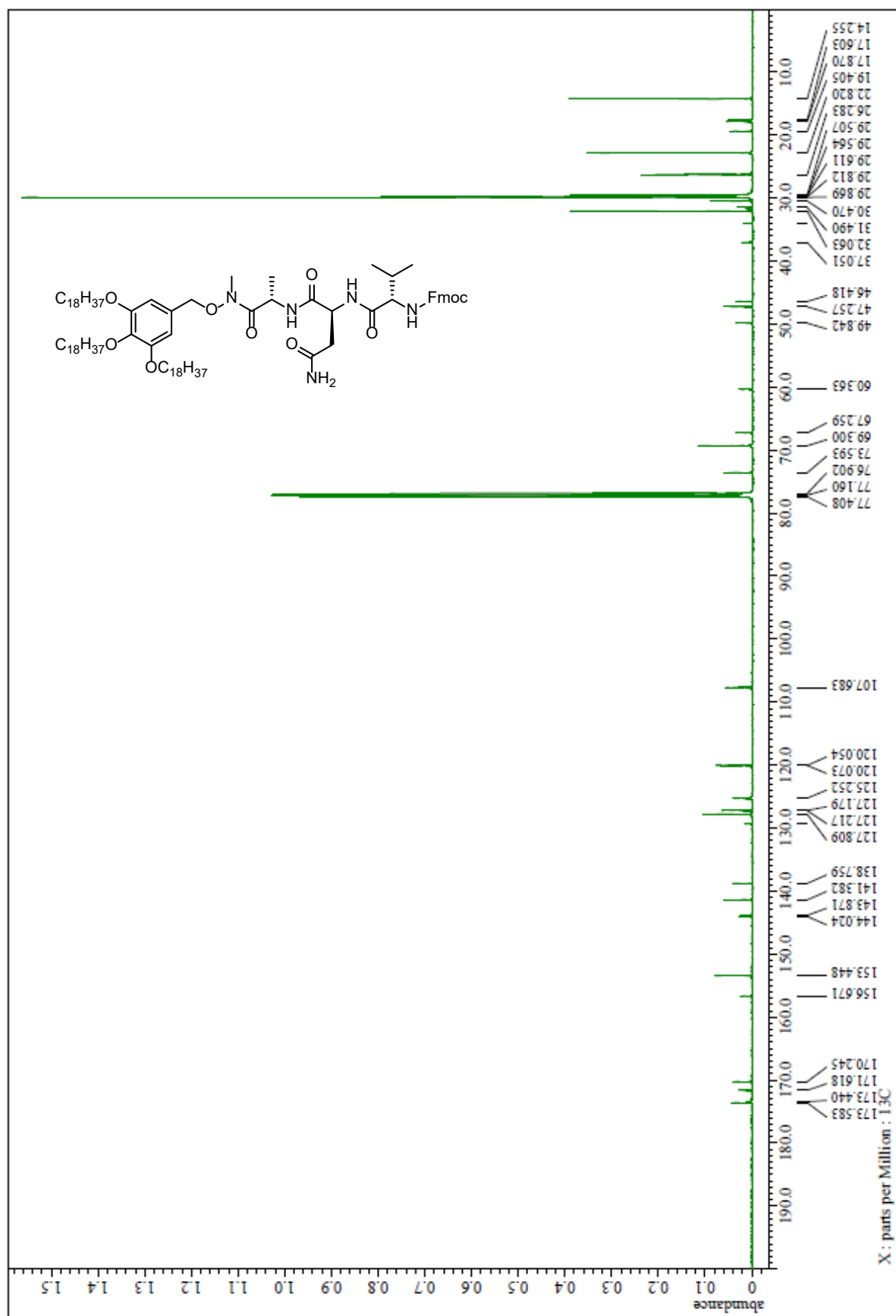
$^{13}\text{C}$  NMR spectrum of Asn-Ala-(Me)N-O-TAGa (**20**) ( $\text{CDCl}_3$ )



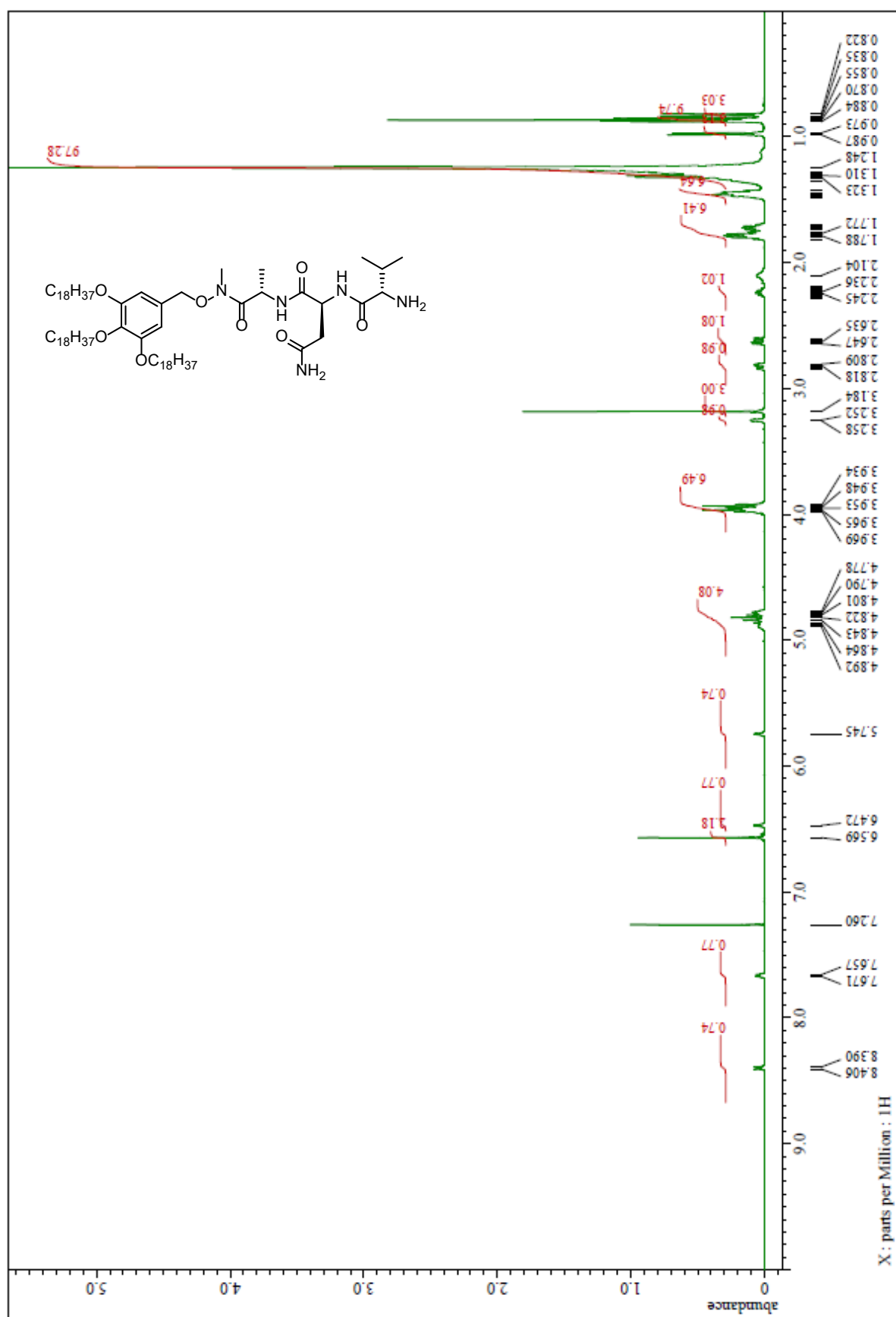
$^1\text{H}$  NMR spectrum of Fmoc-Val-Asn-Ala-(Me)N-O-TAGa (**59**) ( $\text{CDCl}_3$ )



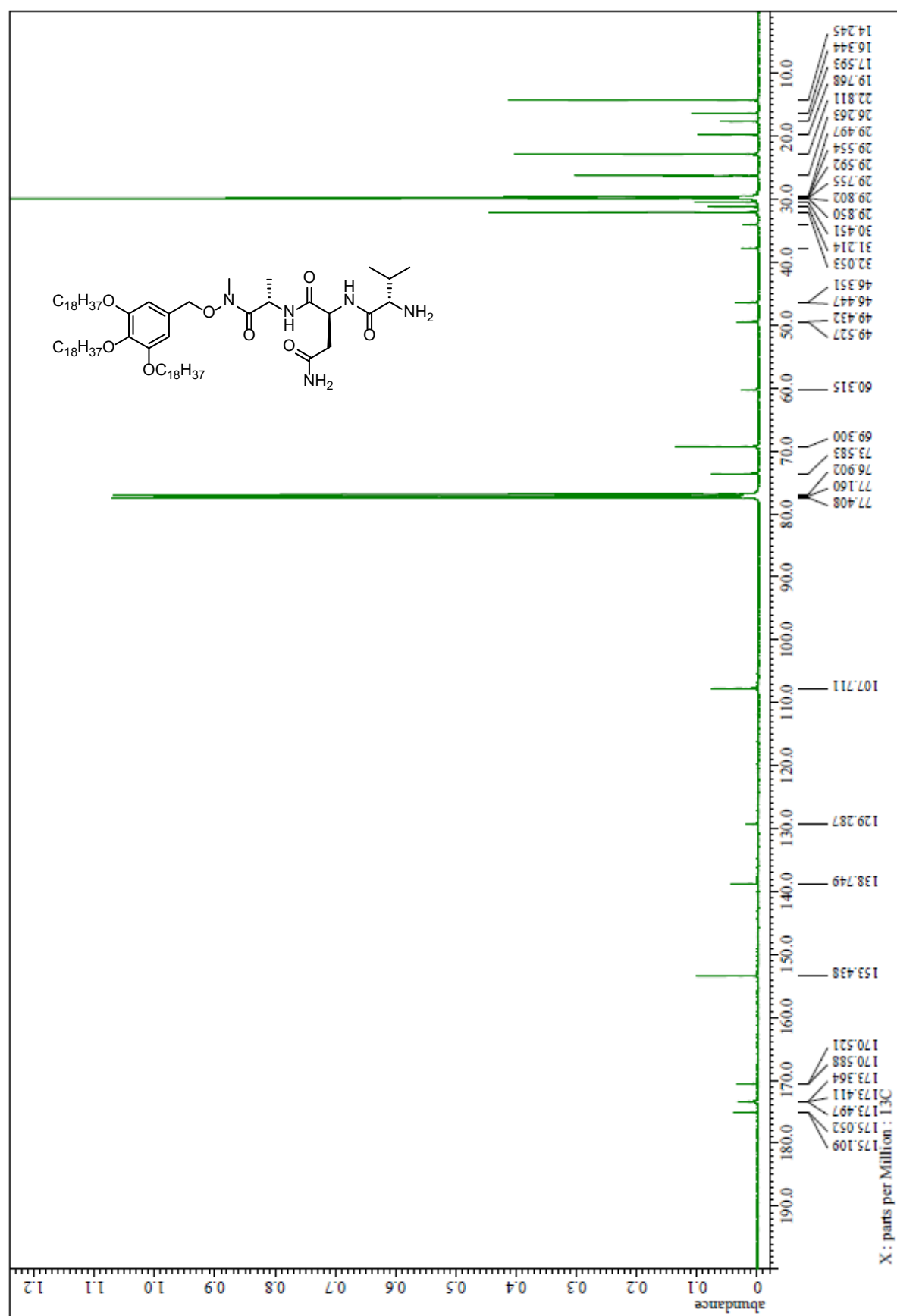
$^{13}\text{C}$  NMR spectrum of Fmoc-Val-Asn-Ala-(Me)N-O-TAGa (**59**) ( $\text{CDCl}_3$ )



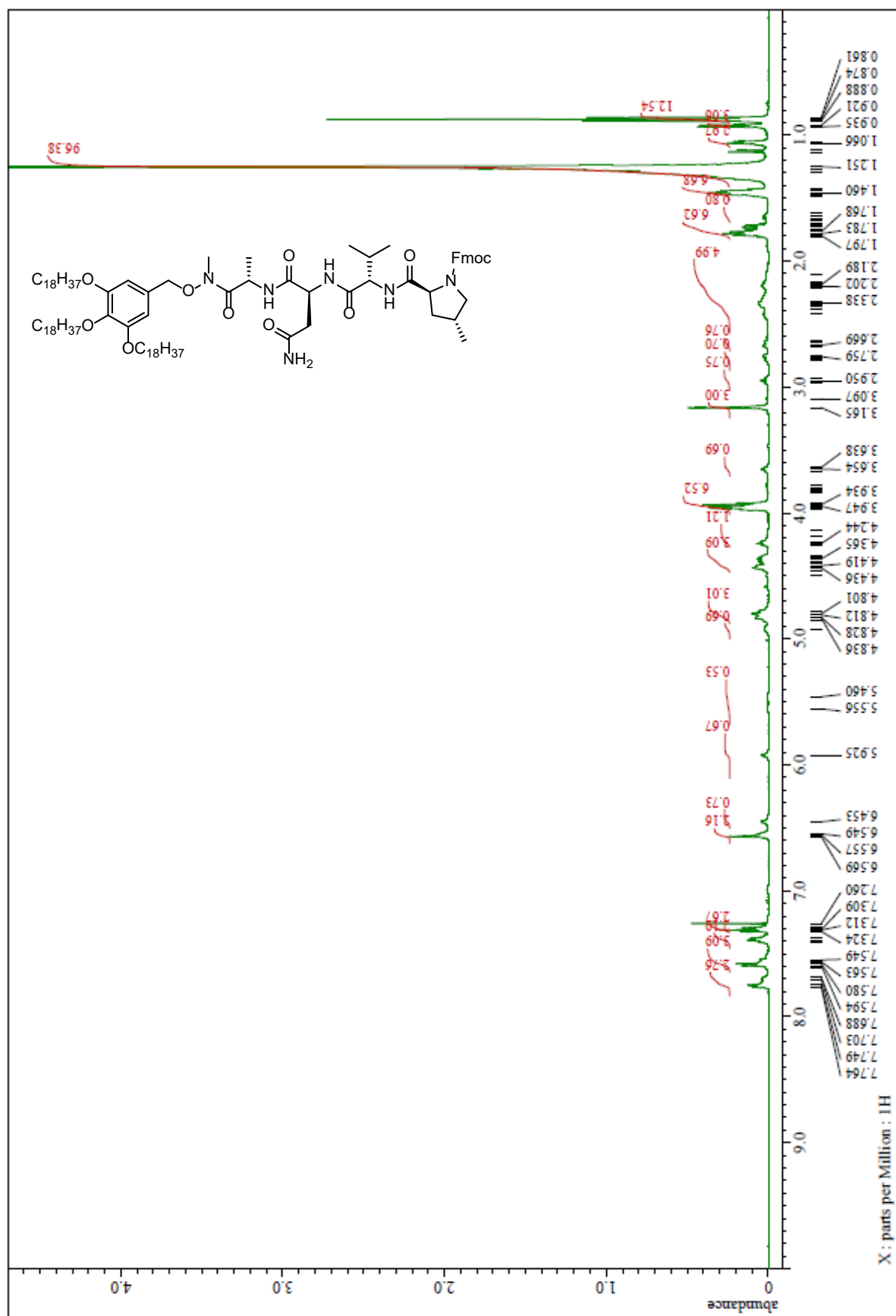
$^1\text{H}$  NMR spectrum of Val-Asn-Ala-(Me)N-O-TAGa (**21**) ( $\text{CDCl}_3$ )



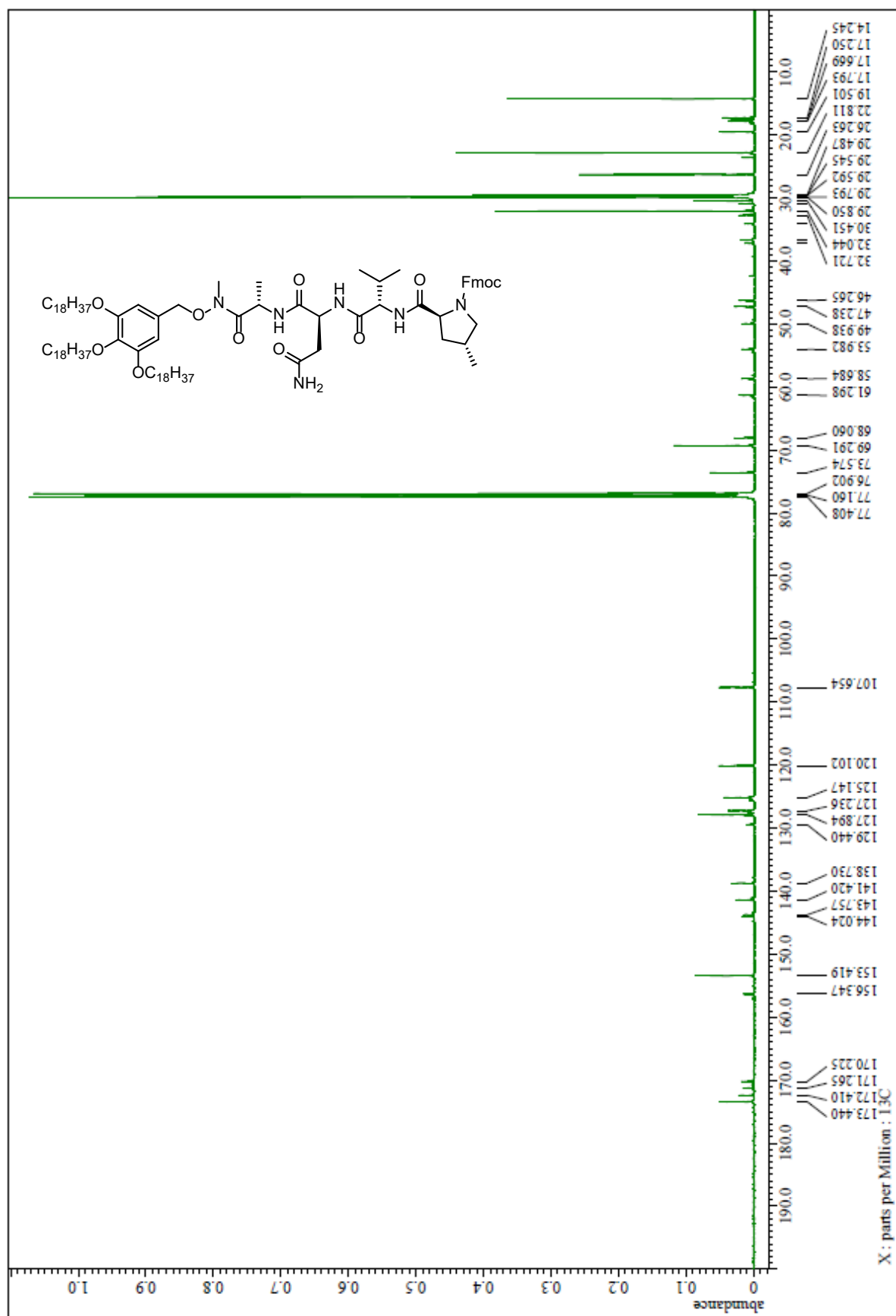
$^{13}\text{C}$  NMR spectrum of Val-Asn-Ala-(Me)N-O-TAGa (**21**) ( $\text{CDCl}_3$ )



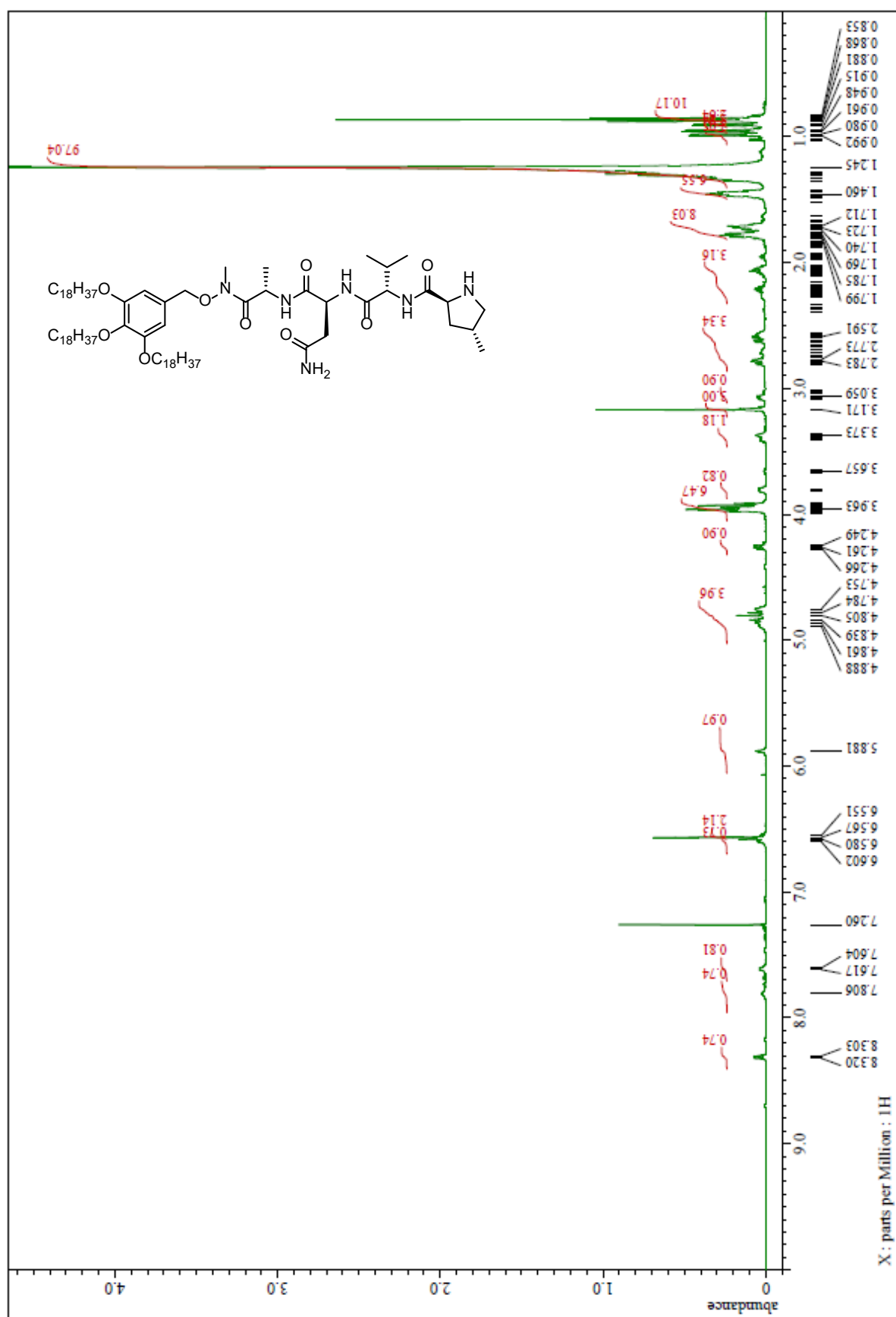
<sup>1</sup>H NMR spectrum of Fmoc-4MePro-Val-Asn-Ala-(Me)N-O-TAGa (**60**) (CDCl<sub>3</sub>)



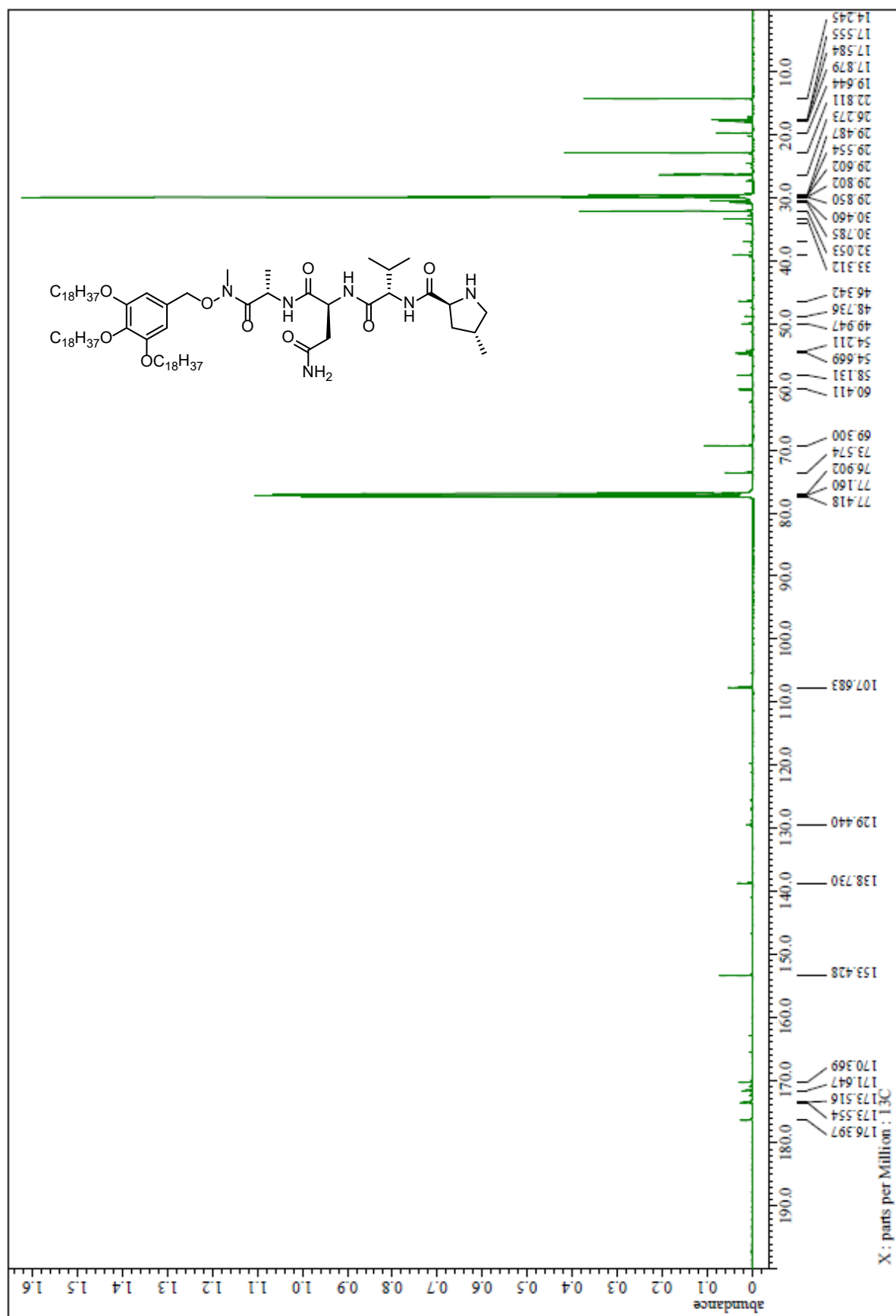
$^{13}\text{C}$  NMR spectrum of Fmoc-4MePro-Val-Asn-Ala-(Me)N-O-TAGa (**60**) ( $\text{CDCl}_3$ )



$^1\text{H}$  NMR spectrum of 4MePro-Val-Asn-Ala-(Me)N-O-TAGa (**22**) ( $\text{CDCl}_3$ )



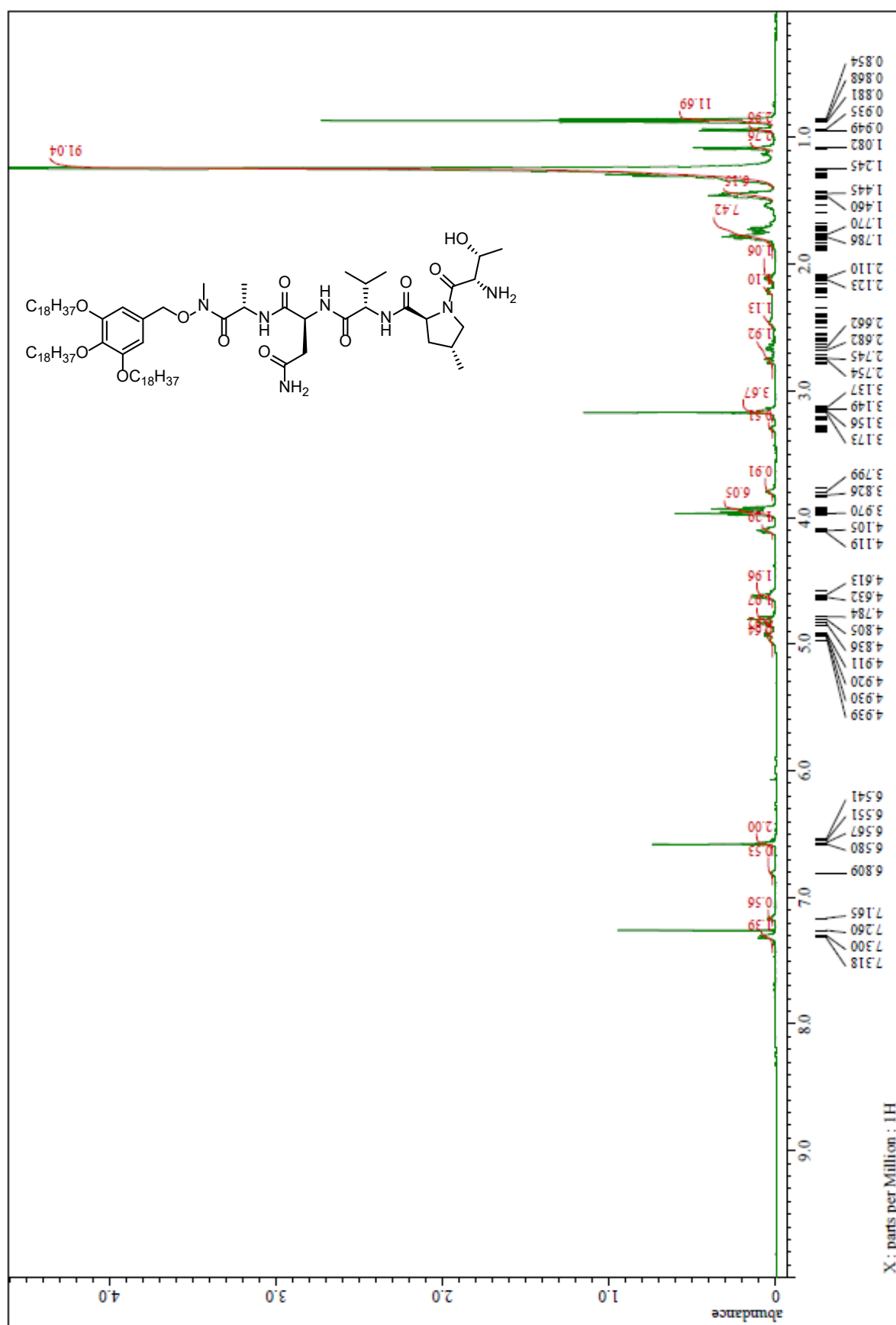
$^{13}\text{C}$  NMR spectrum of 4MePro-Val-Asn-Ala-(Me)N-O-TAGa (**22**) ( $\text{CDCl}_3$ )



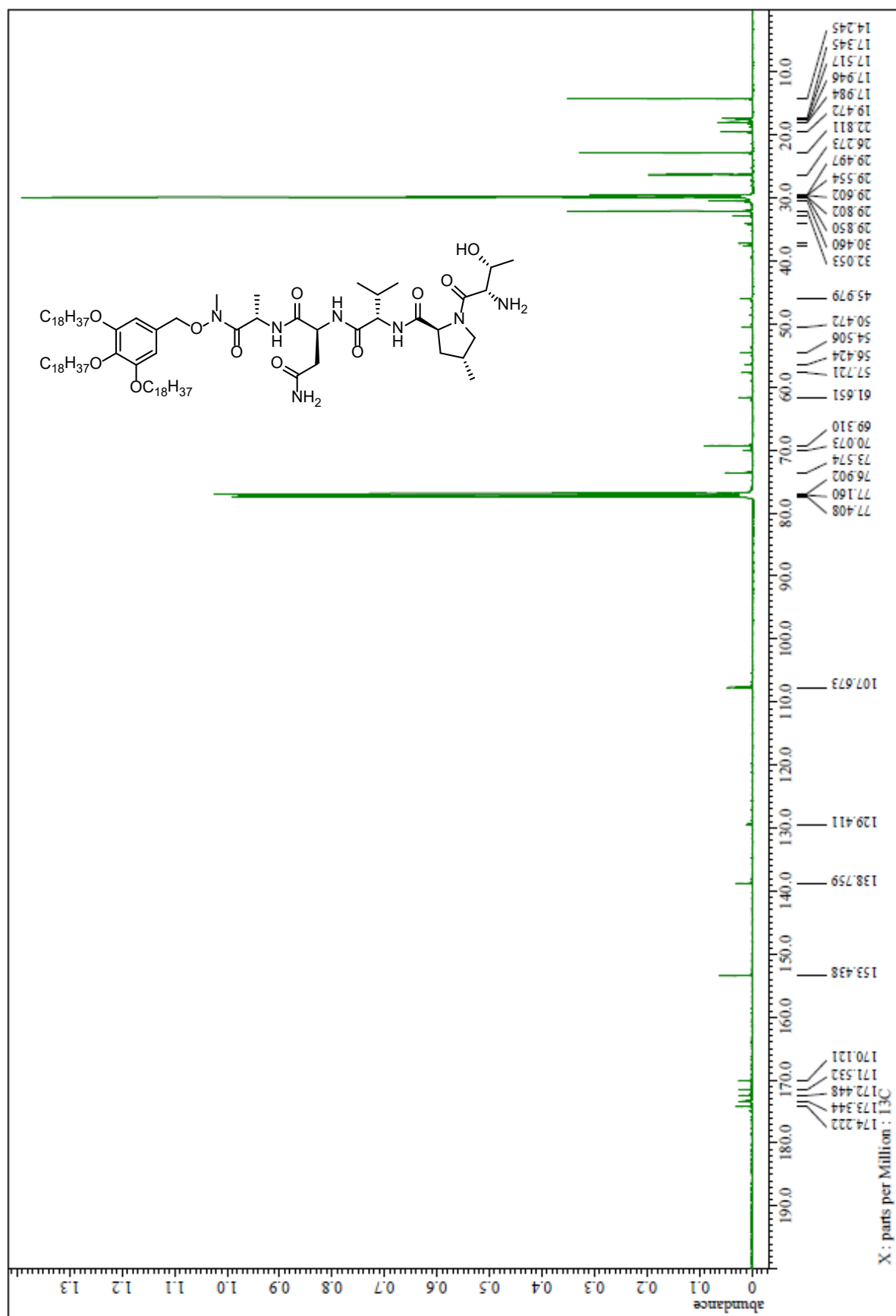




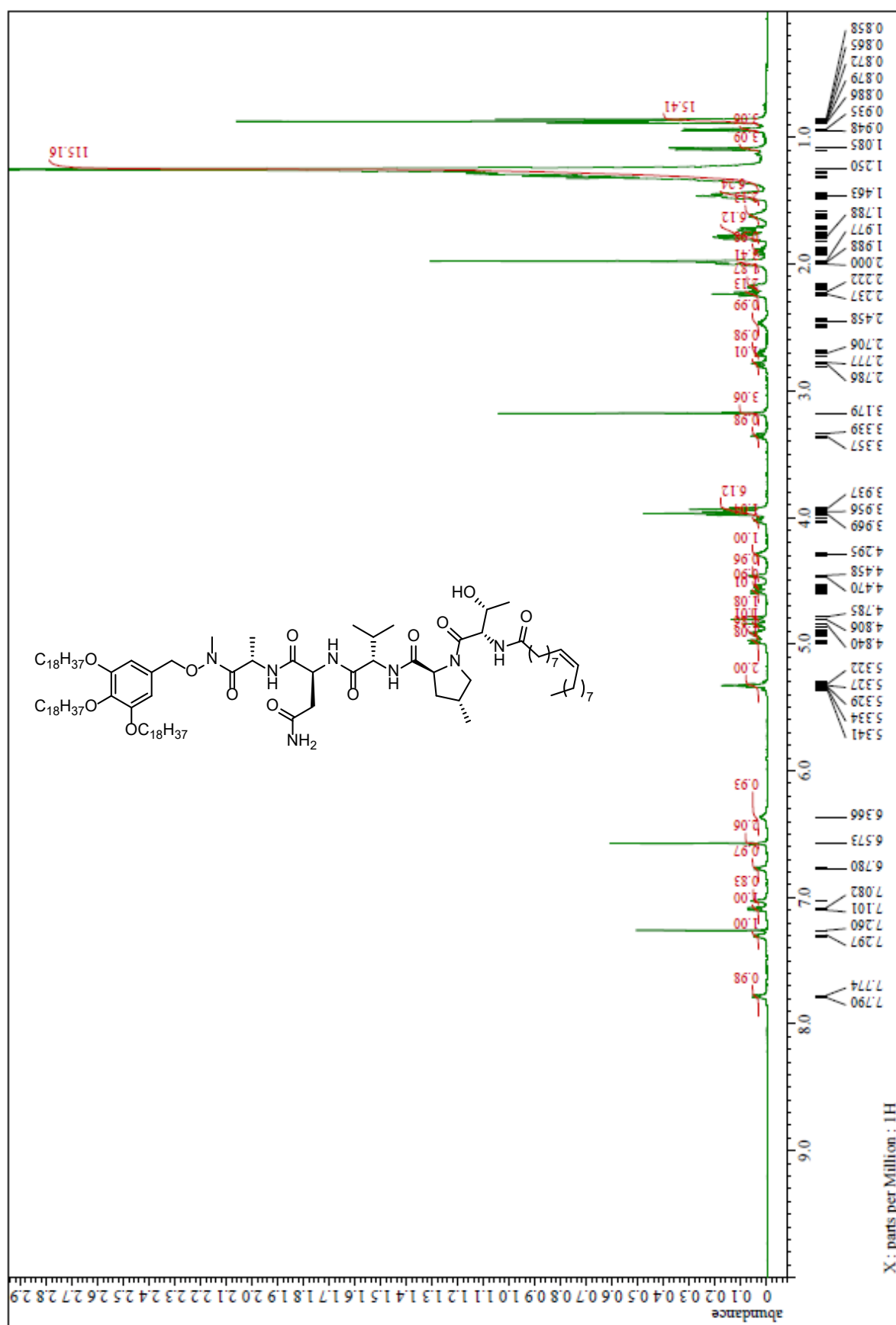
$^1\text{H}$  NMR spectrum of Thr-4MePro-Val-Asn-Ala-(Me)N-O-TAGa (**23**) ( $\text{CDCl}_3$ )



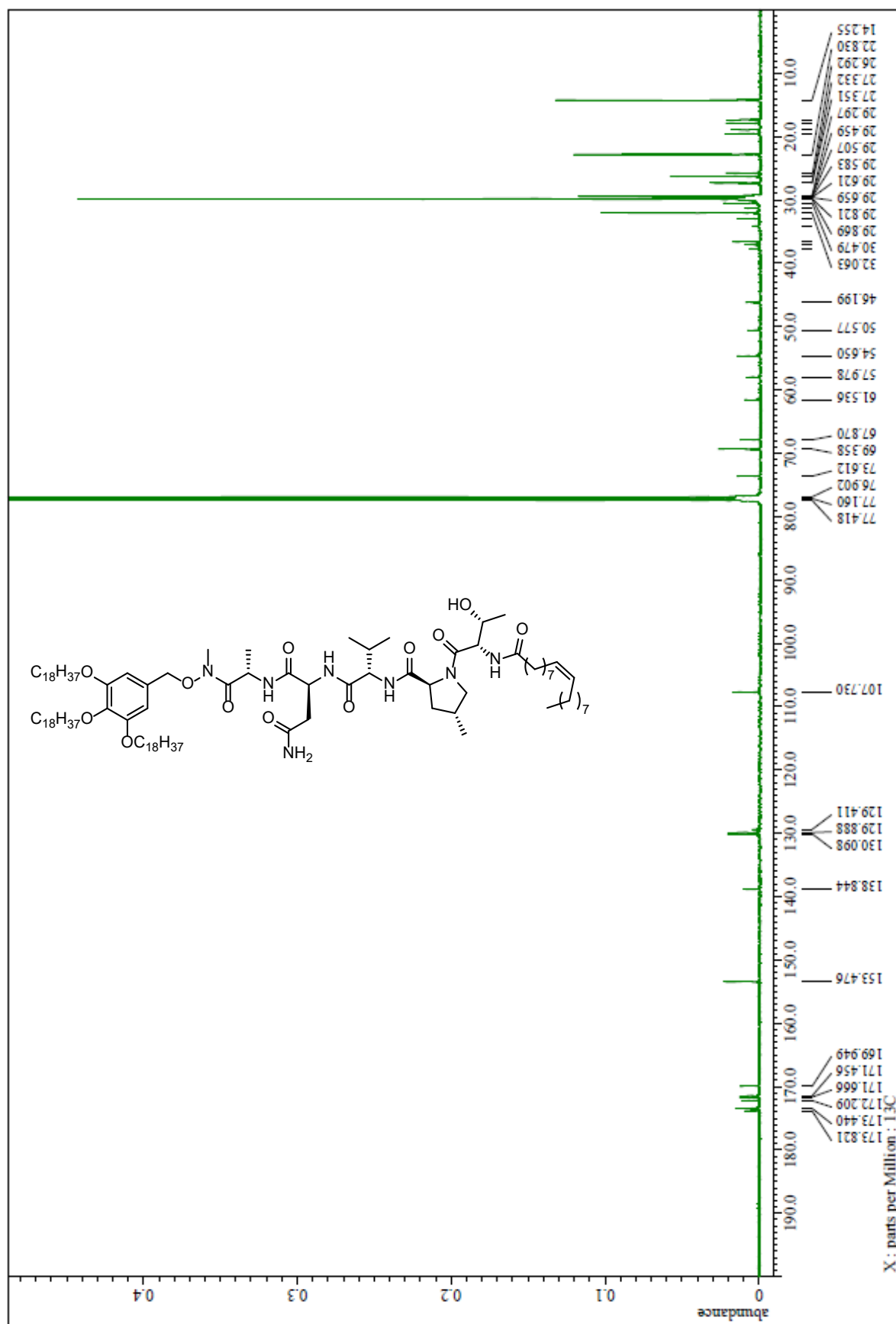
$^{13}\text{C}$  NMR spectrum of Thr-4MePro-Val-Asn-Ala-(Me)N-O-TAGa (**23**) ( $\text{CDCl}_3$ )



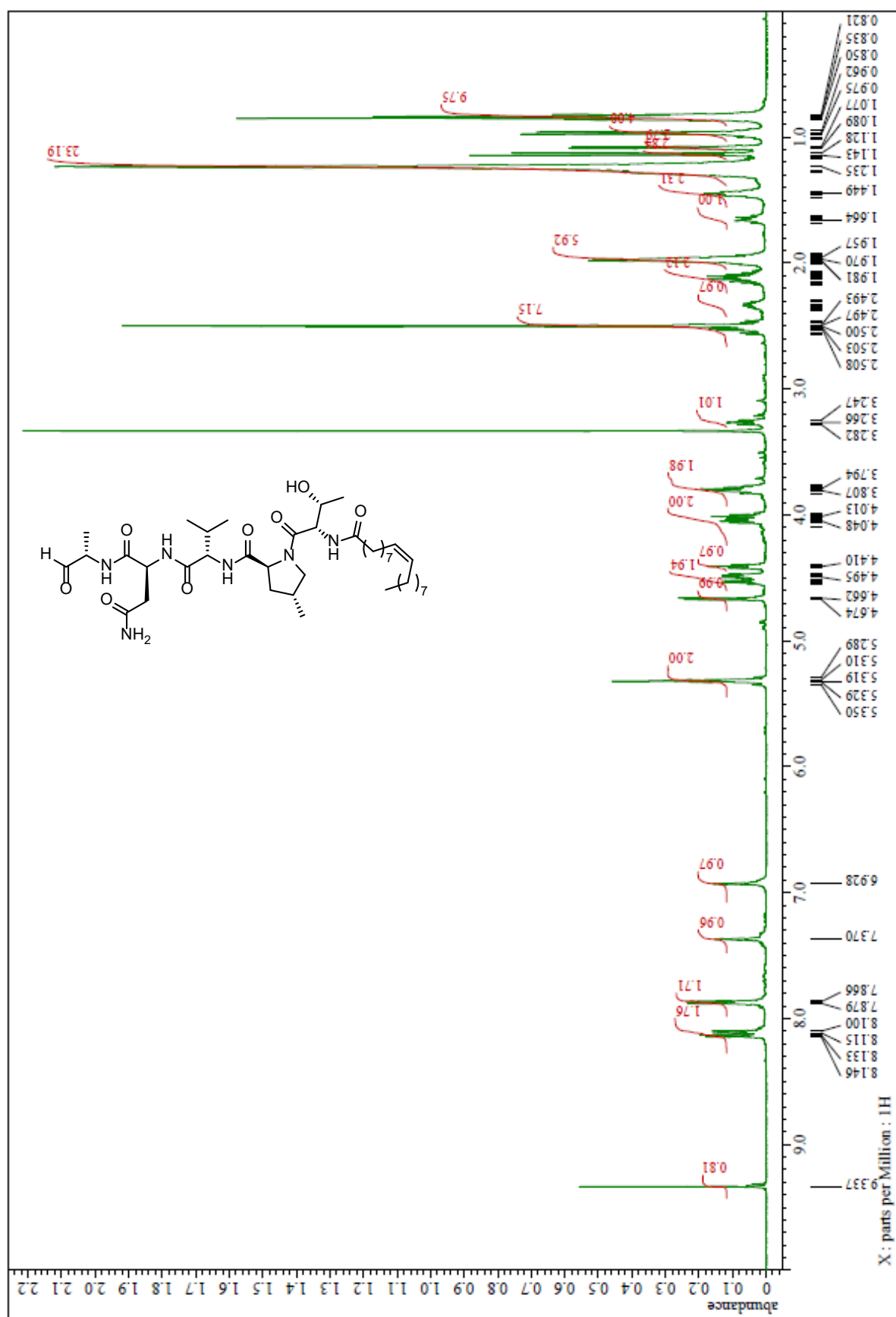
<sup>1</sup>H NMR spectrum of Oleic acid-Thr-4MePro-Val-Asn-Ala-(Me)N-O-TAGa (**24**) (CDCl<sub>3</sub>)



$^{13}\text{C}$  NMR spectrum of Oleic acid-Thr-4MePro-Val-Asn-Ala-(Me)N-O-TAGa (**24**) ( $\text{CDCl}_3$ )

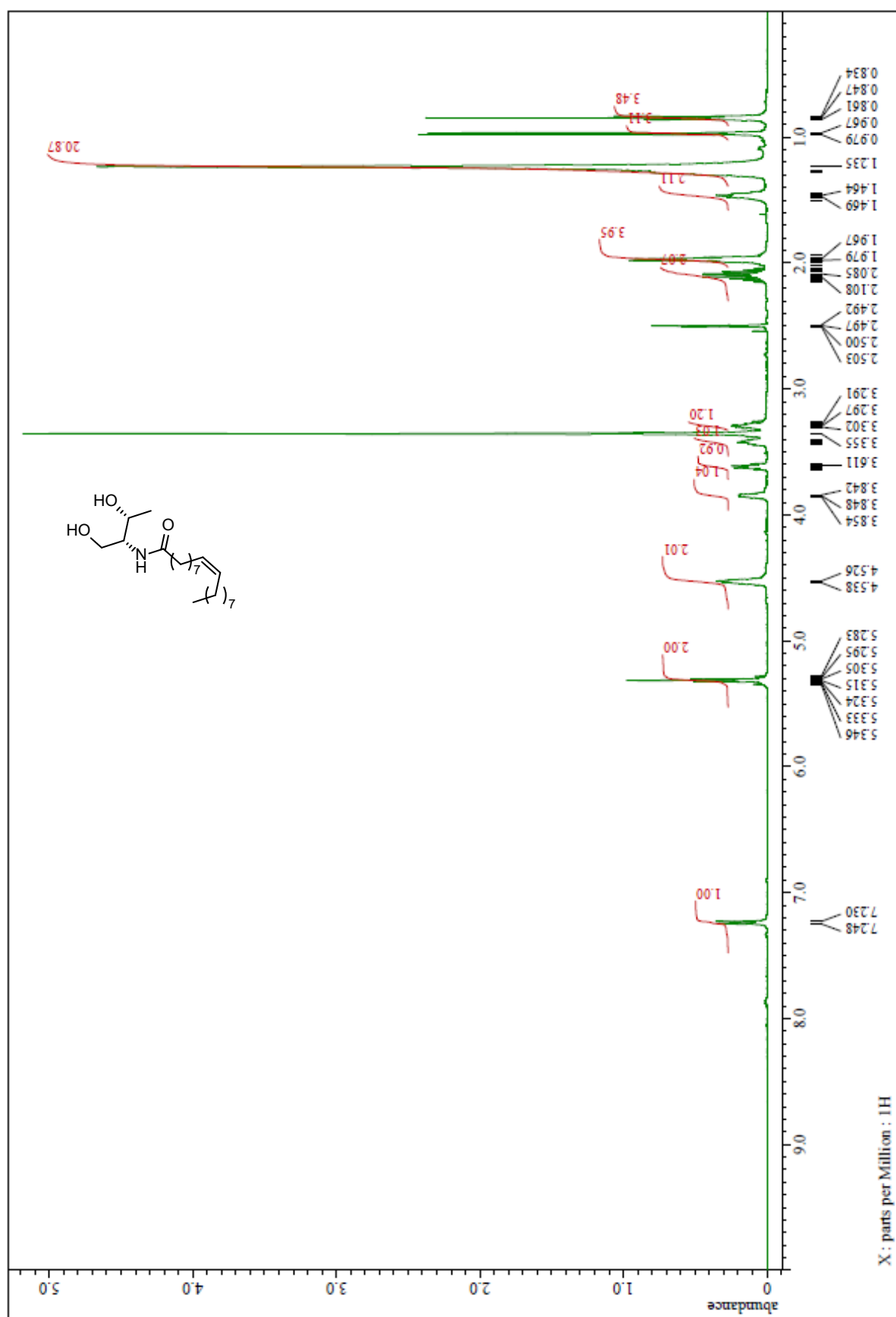


<sup>1</sup>H NMR spectrum of Oleic acid-Thr-4-MePro-Val-Asn-Ala-H (**13**) (DMSO-d<sub>6</sub>)

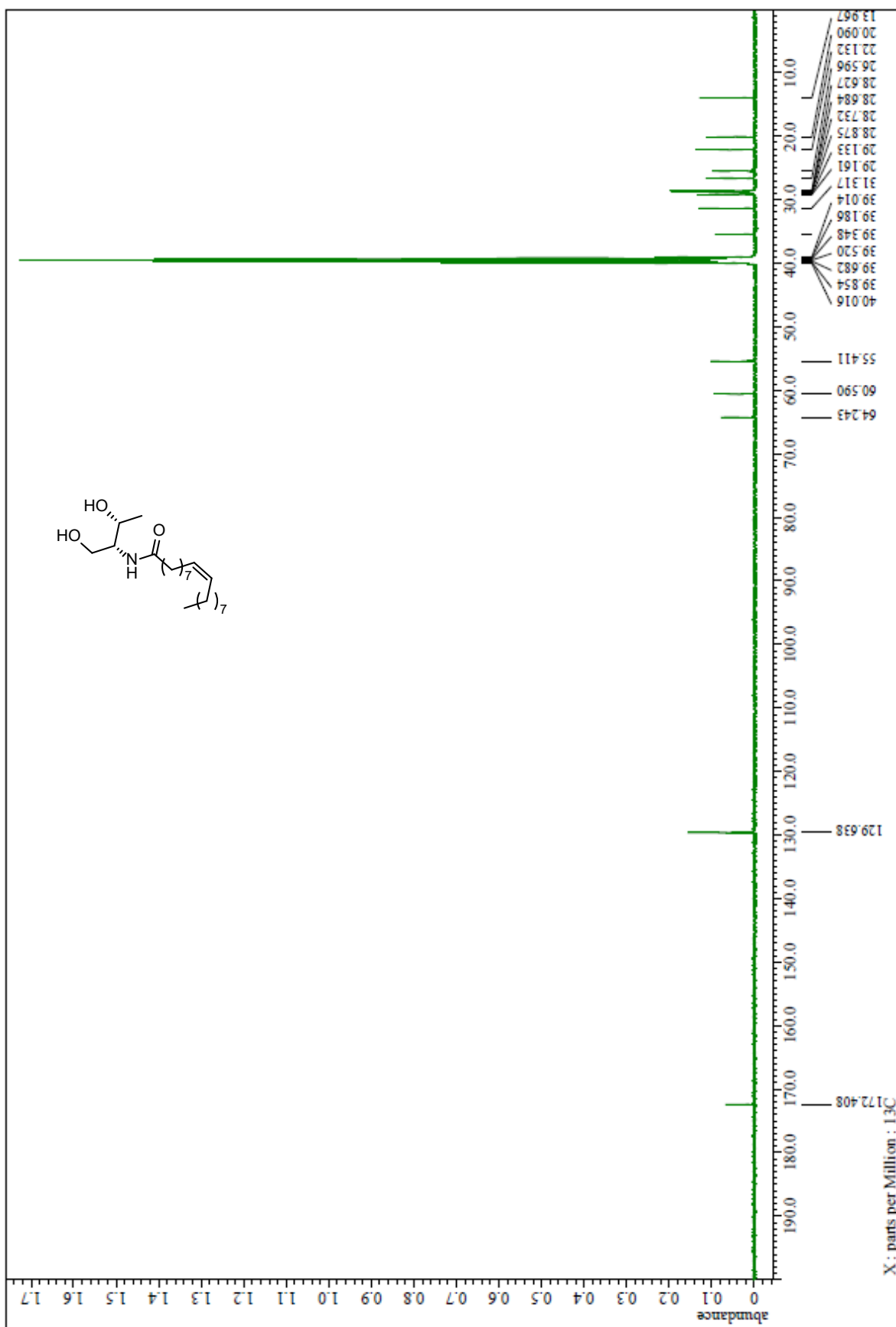




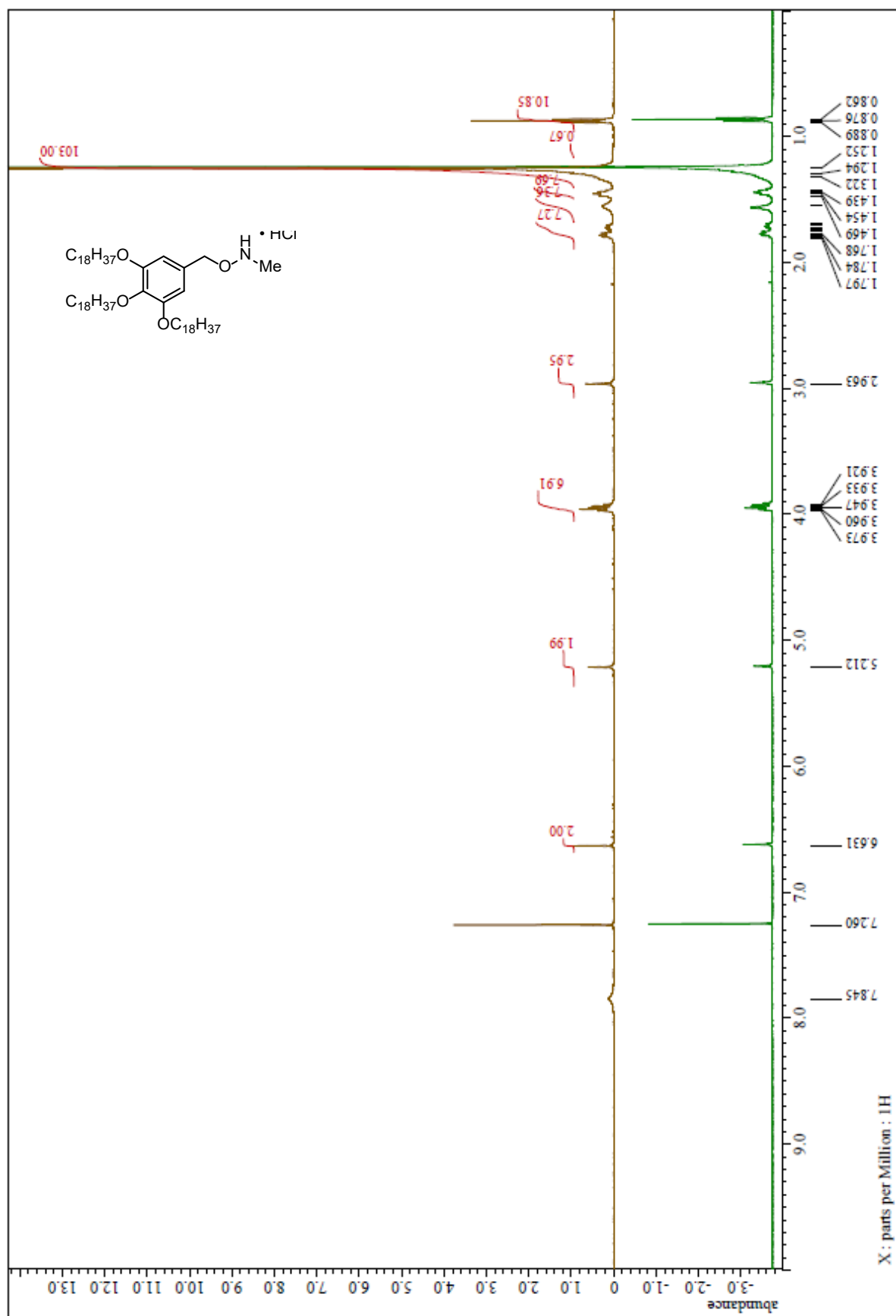
<sup>1</sup>H NMR spectrum of MePro-Thr amide bond-cleaved alcohol (**62**) (DMSO-*d*<sub>6</sub>)



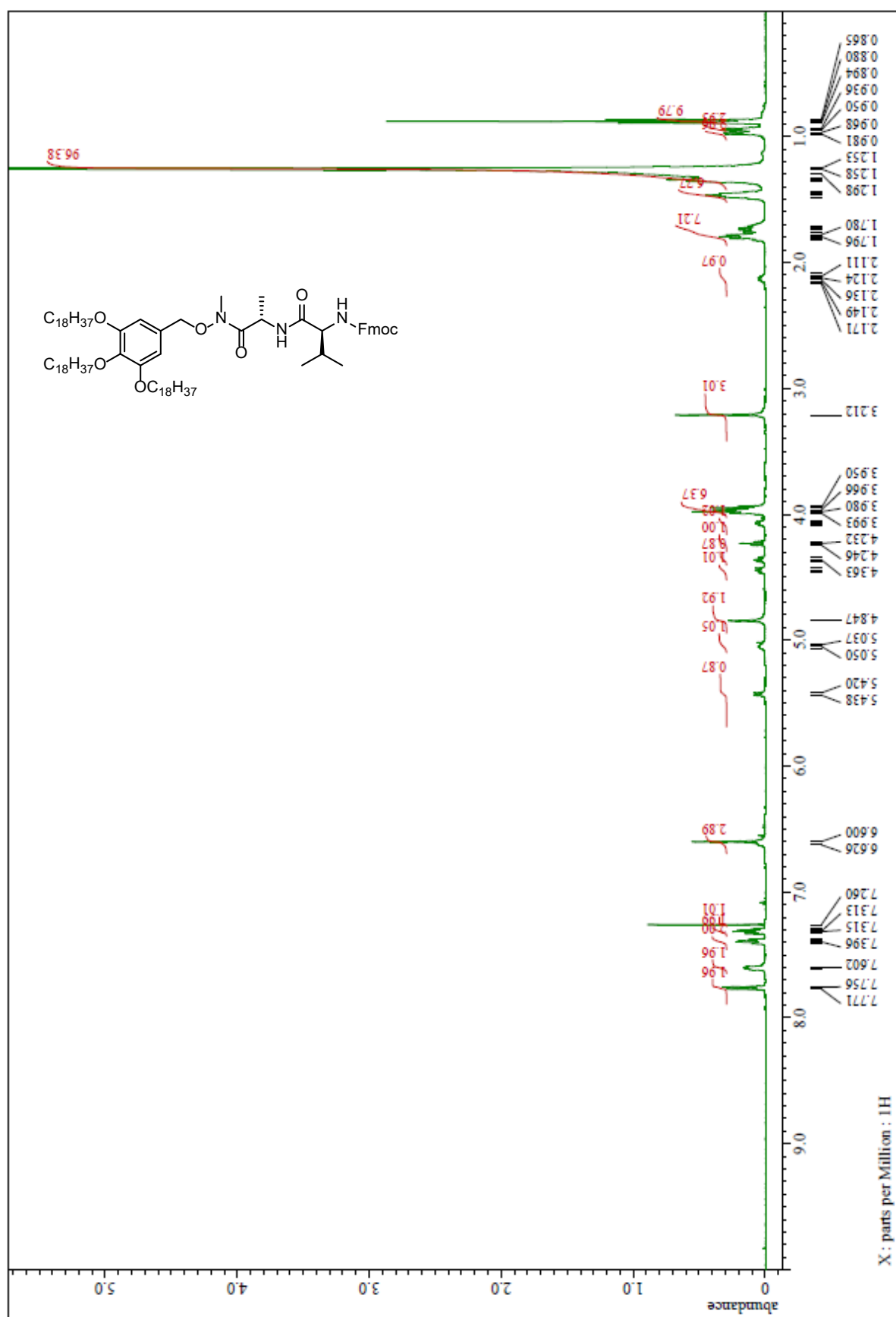
$^{13}\text{C}$  NMR spectrum of MePro-Thr amide bond-cleaved alcohol (**62**) ( $\text{DMSO-}d_6$ )



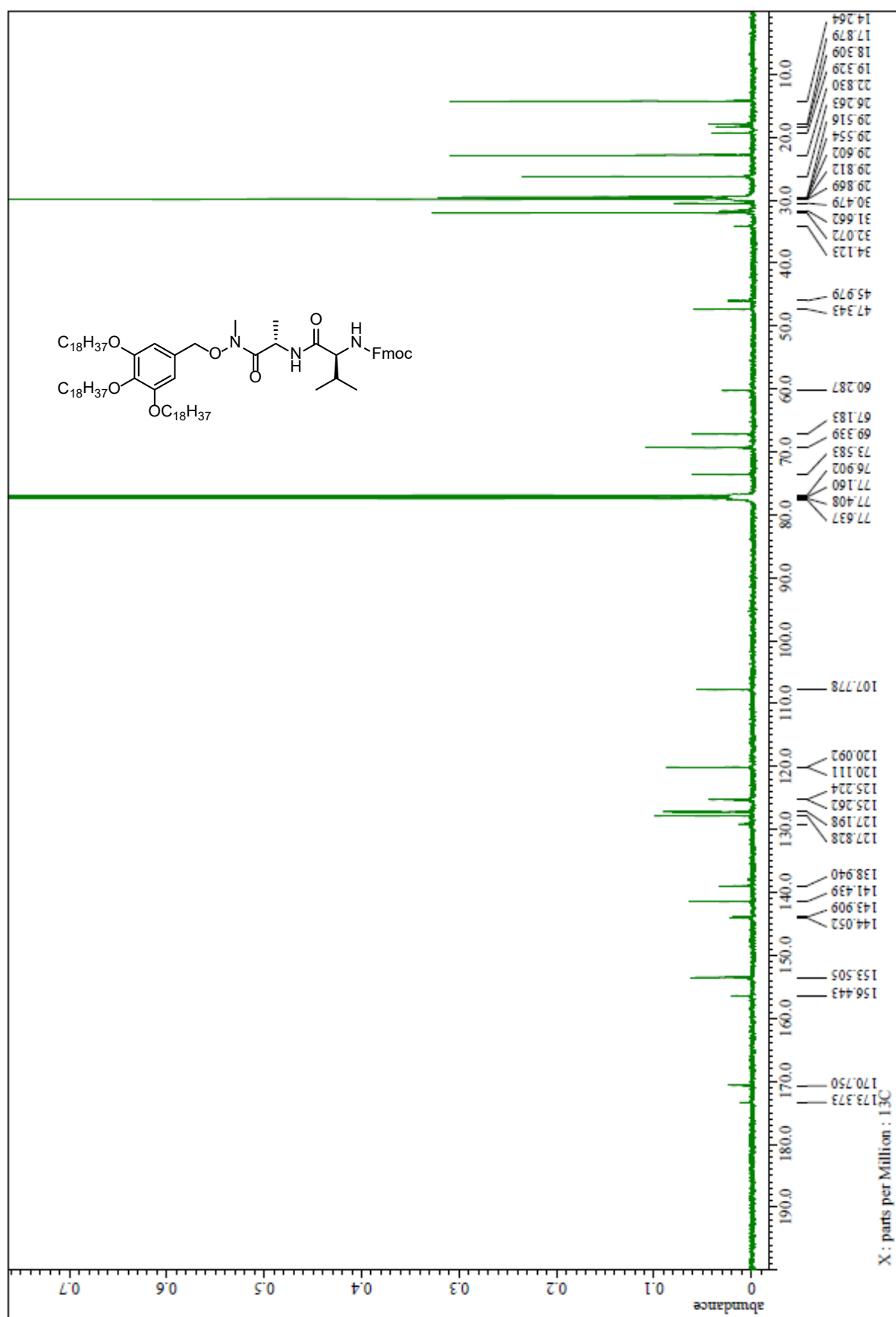
$^1\text{H}$  NMR of recovered Me-HN-O-TAGa (**15**) (up) and newly prepared **15** (down) ( $\text{CDCl}_3$  + conc.  $\text{HCl}$ )



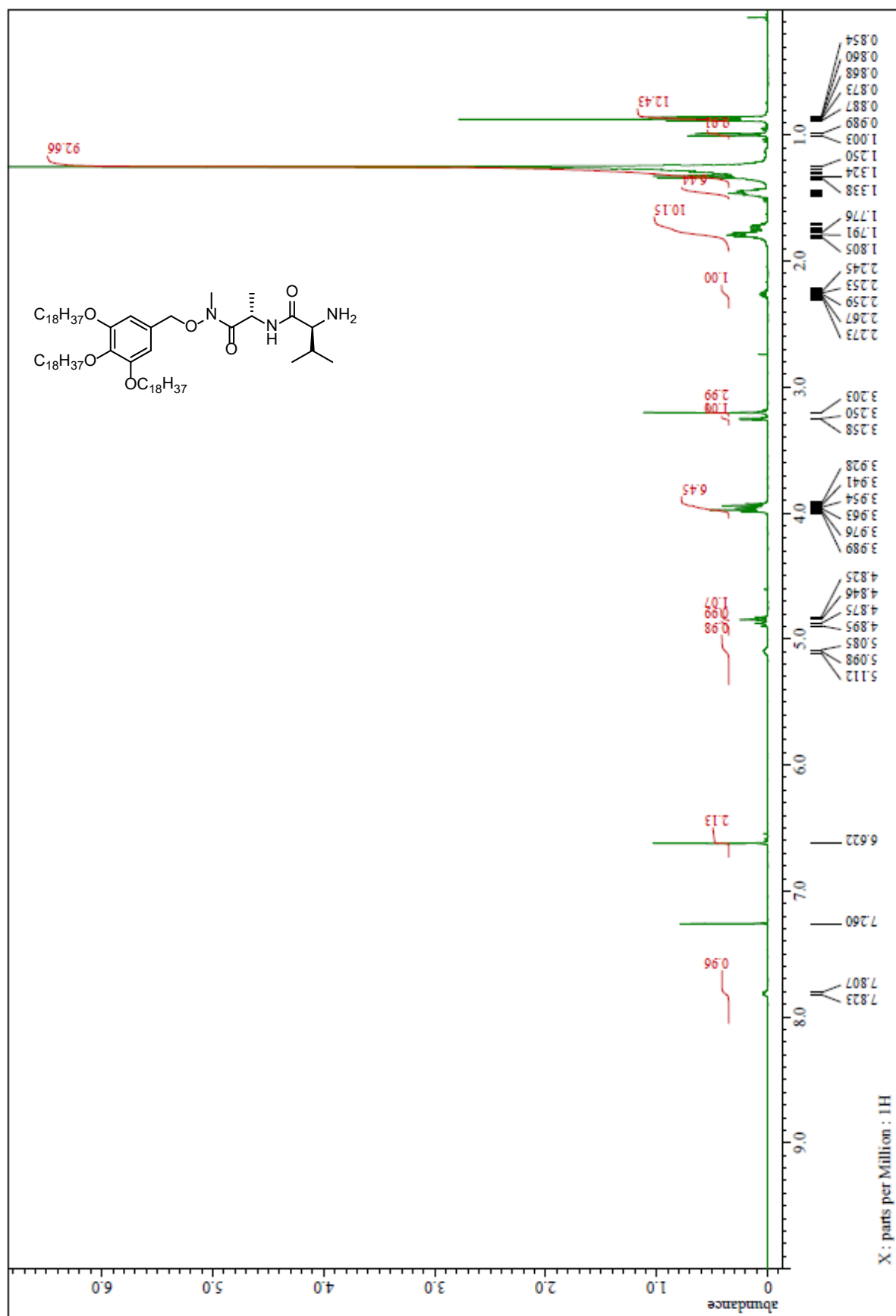
<sup>1</sup>H NMR spectrum of Fmoc-Val-Ala-(Me)N-O-TAGa (**63**) (CDCl<sub>3</sub>)



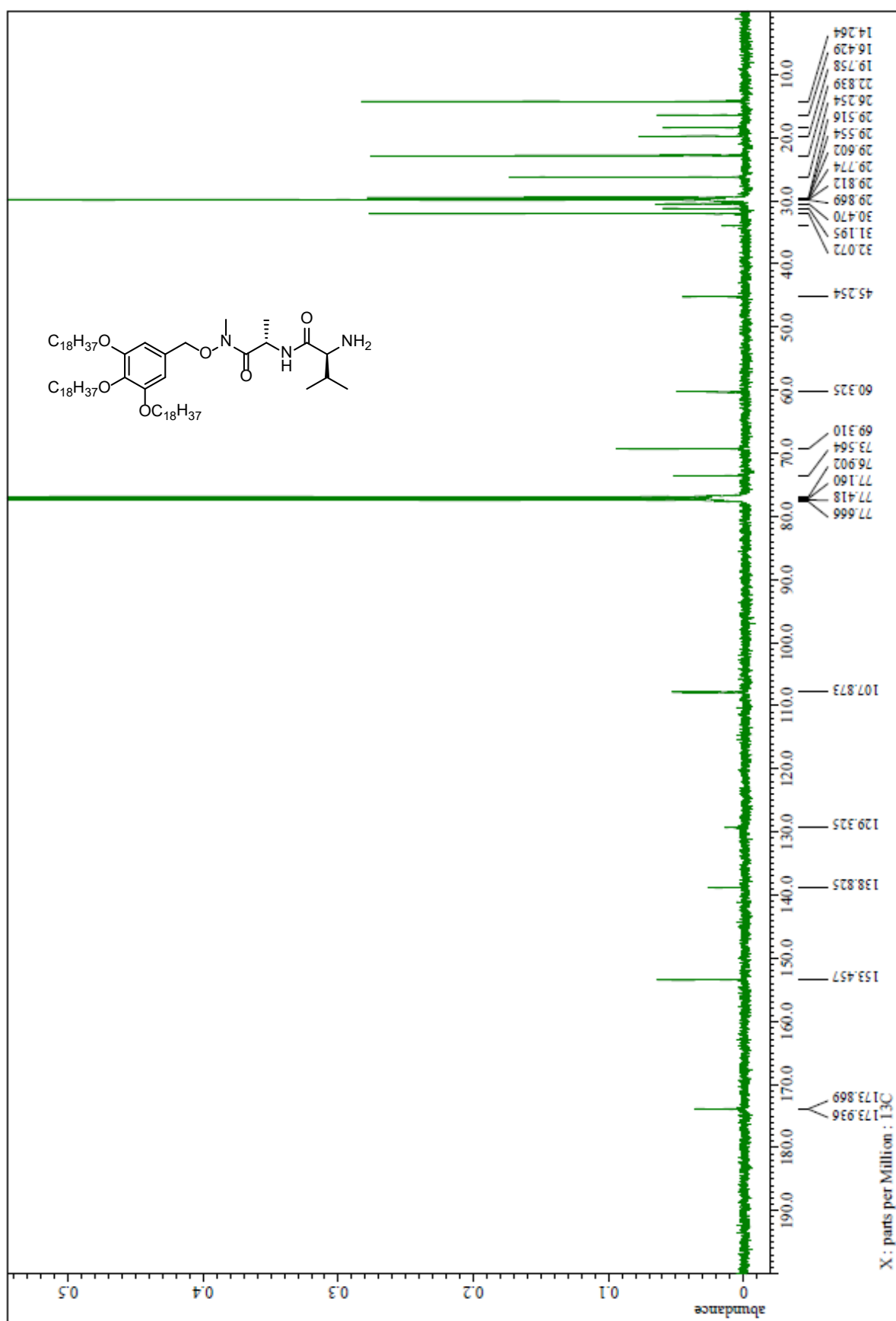
$^{13}\text{C}$  NMR spectrum of Fmoc-Val-Ala-(Me)N-O-TAGa (**63**) ( $\text{CDCl}_3$ )



<sup>1</sup>H NMR spectrum of Val-Ala-(Me)N-O-TAGa (**64**) (CDCl<sub>3</sub>)

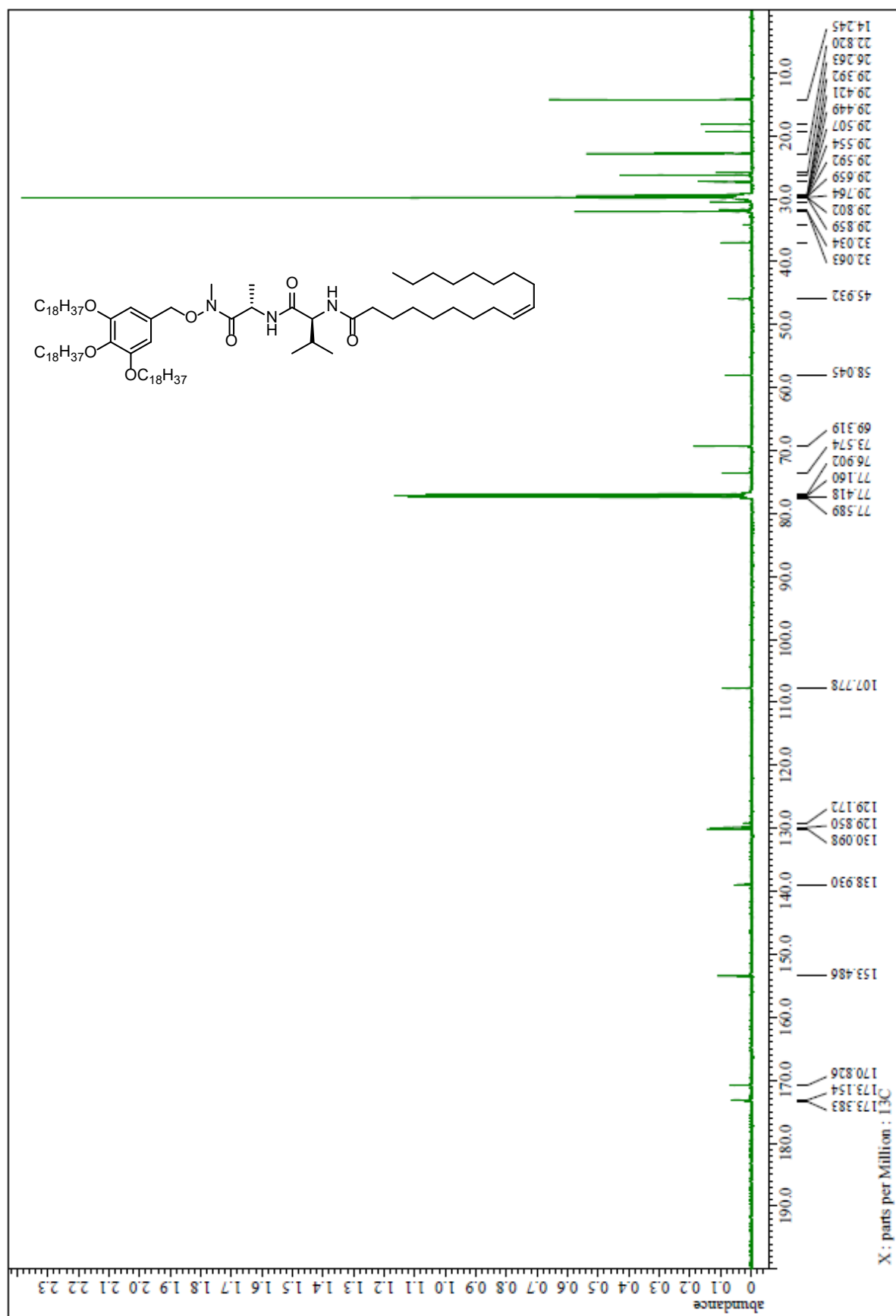


$^{13}\text{C}$  NMR spectrum of Val-Ala-(Me)N-O-TAGa (**64**) ( $\text{CDCl}_3$ )

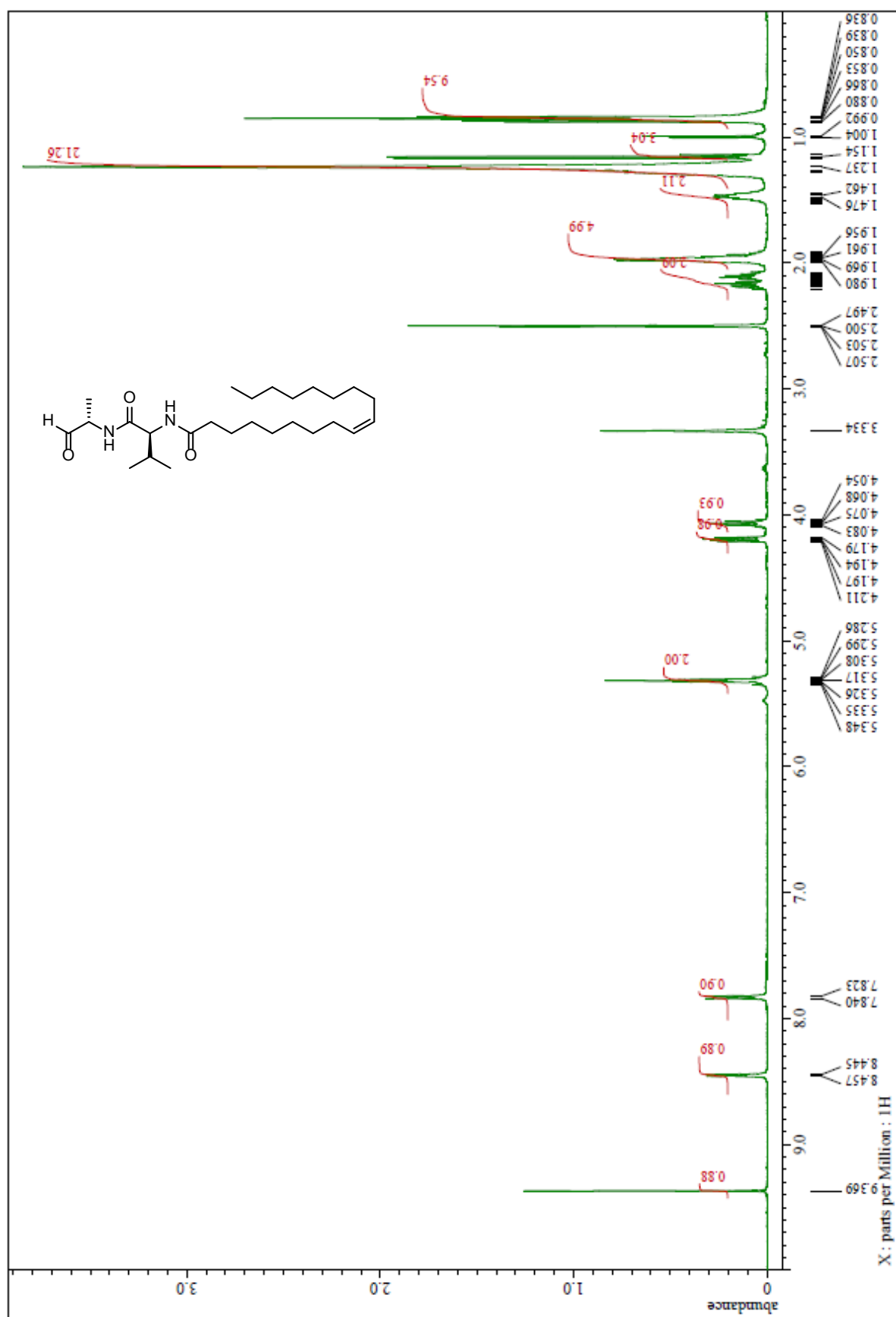




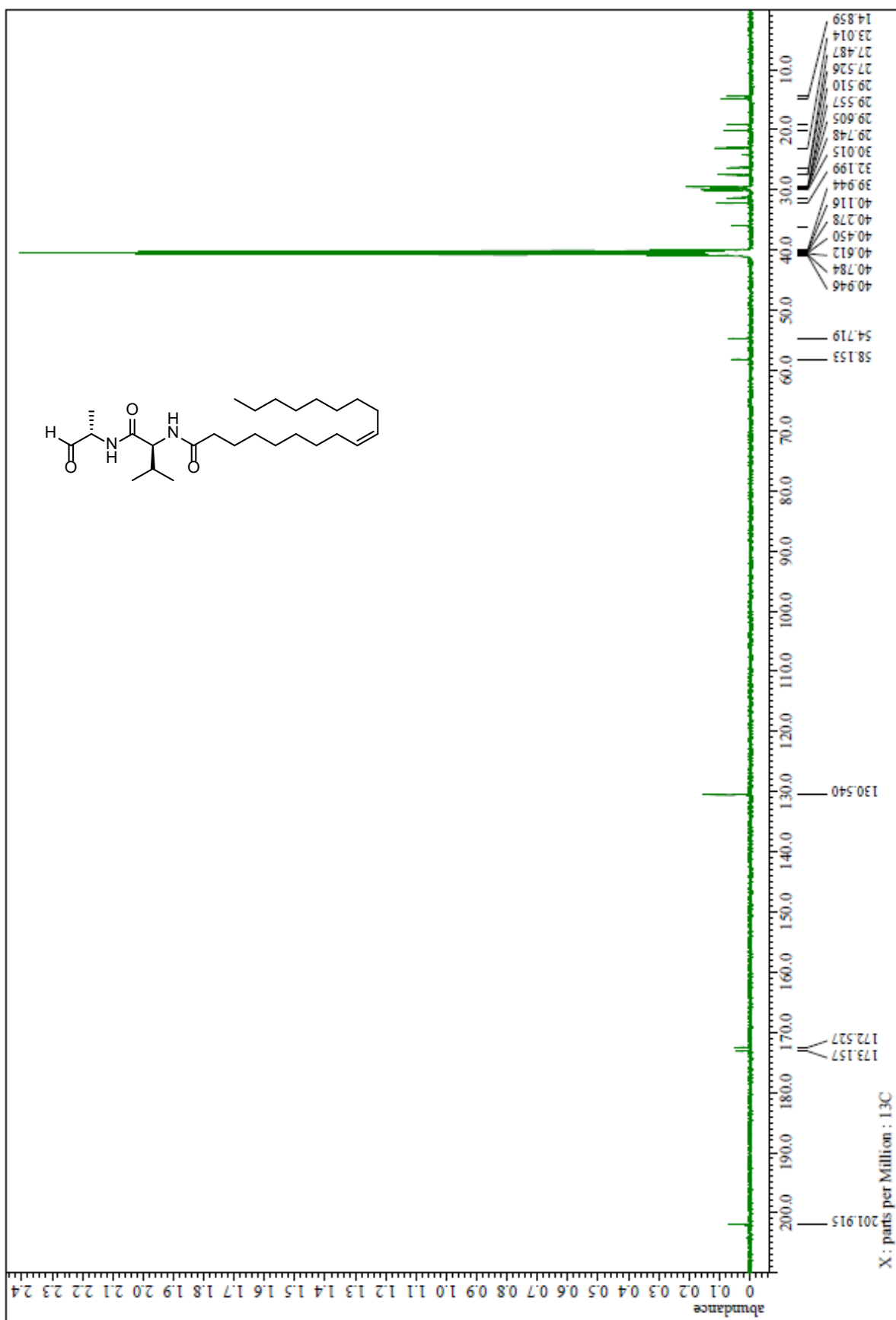
$^{13}\text{C}$  NMR spectrum of Oleic acid-Val-Ala-(Me)N-O-TAGa (**25**) ( $\text{CDCl}_3$ )



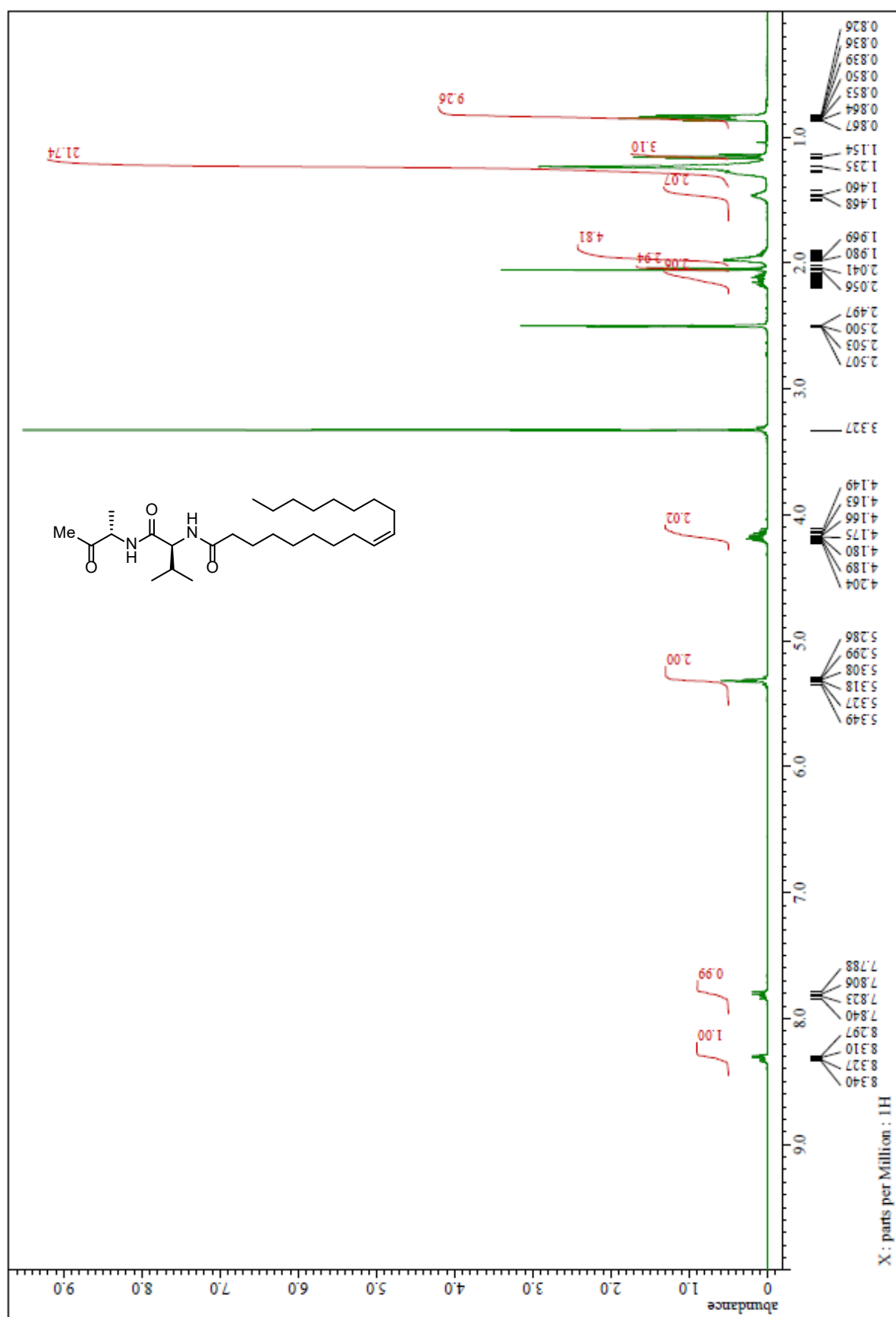
<sup>1</sup>H NMR spectrum of Oleic acid-Val-Ala-H (26) (DMSO-d<sub>6</sub>)



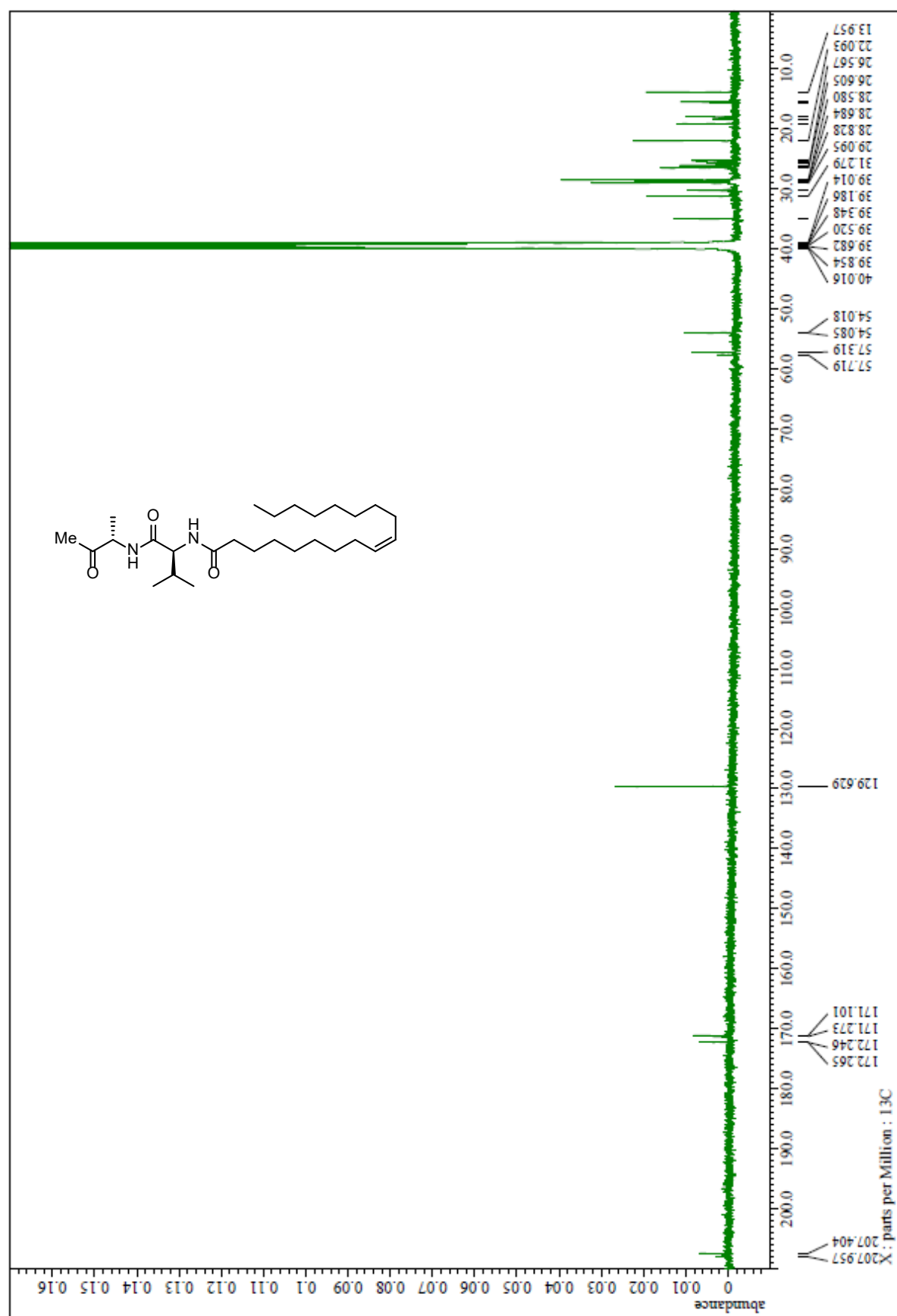
$^{13}\text{C}$  NMR spectrum of Oleic acid-Val-Ala-H (**26**) ( $\text{DMSO-}d_6$ )



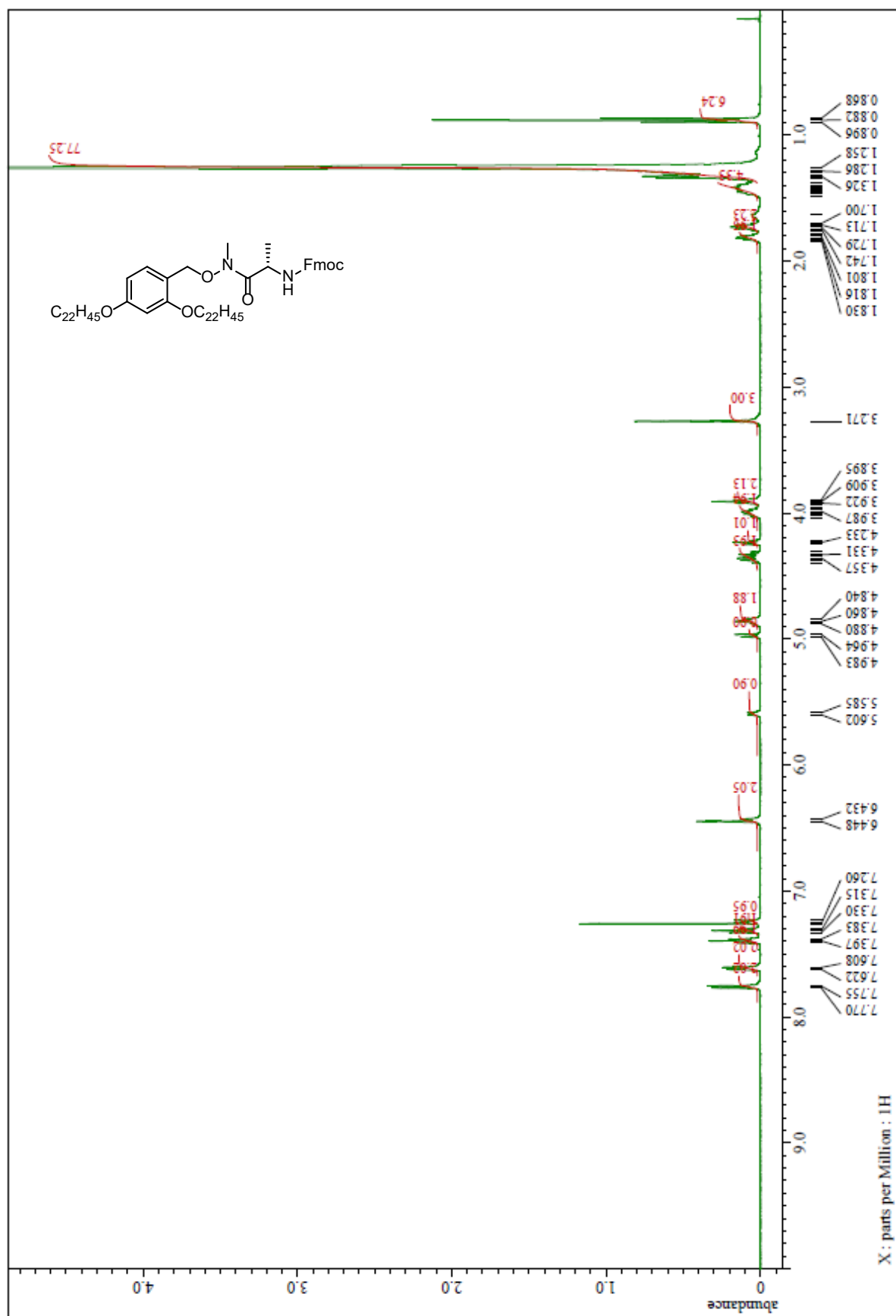
$^1\text{H}$  NMR spectrum of Oleic acid-Val-Ala-Me (27) ( $\text{DMSO-}d_6$ )



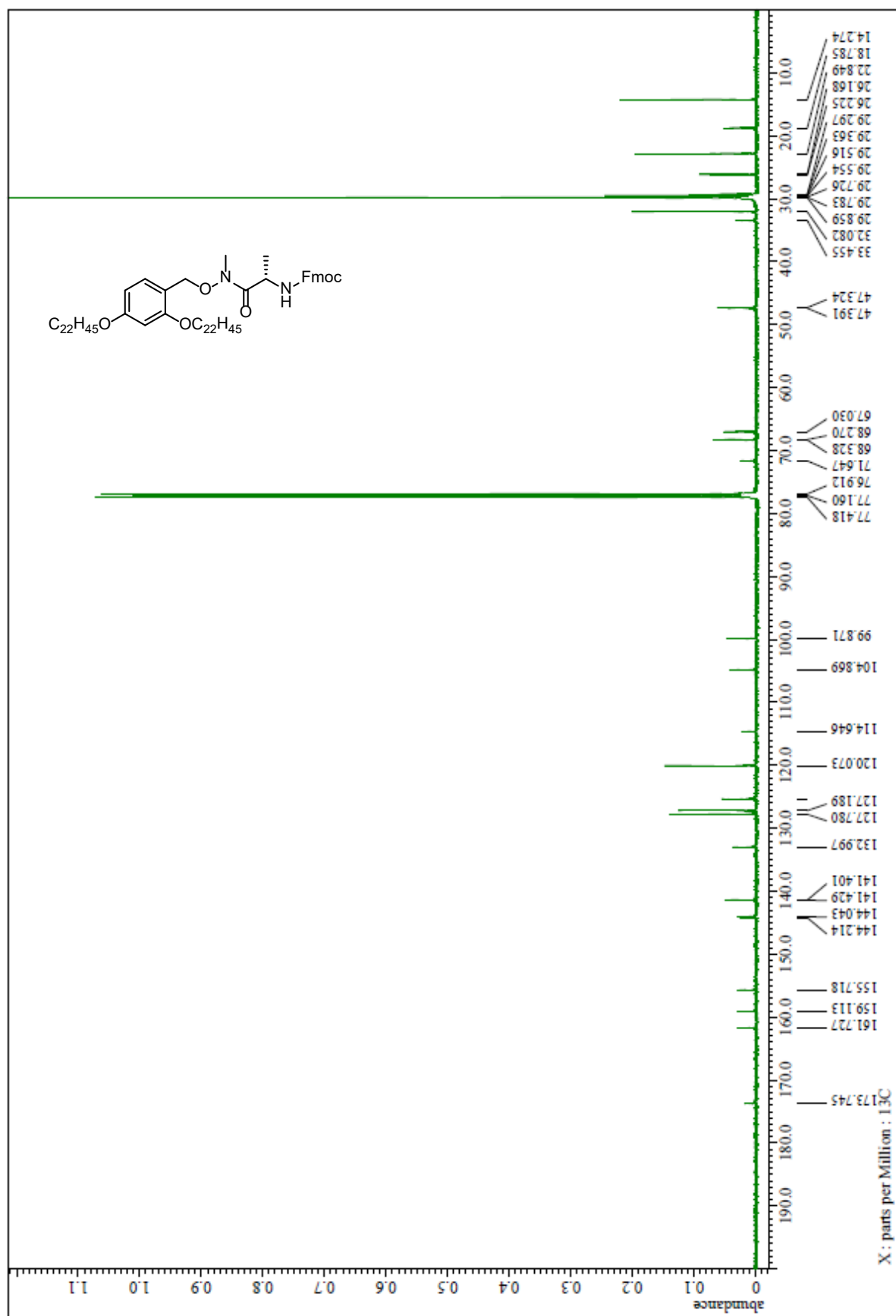
$^{13}\text{C}$  NMR spectrum of Oleic acid-Val-Ala-Me (**27**) ( $\text{DMSO-}d_6$ )



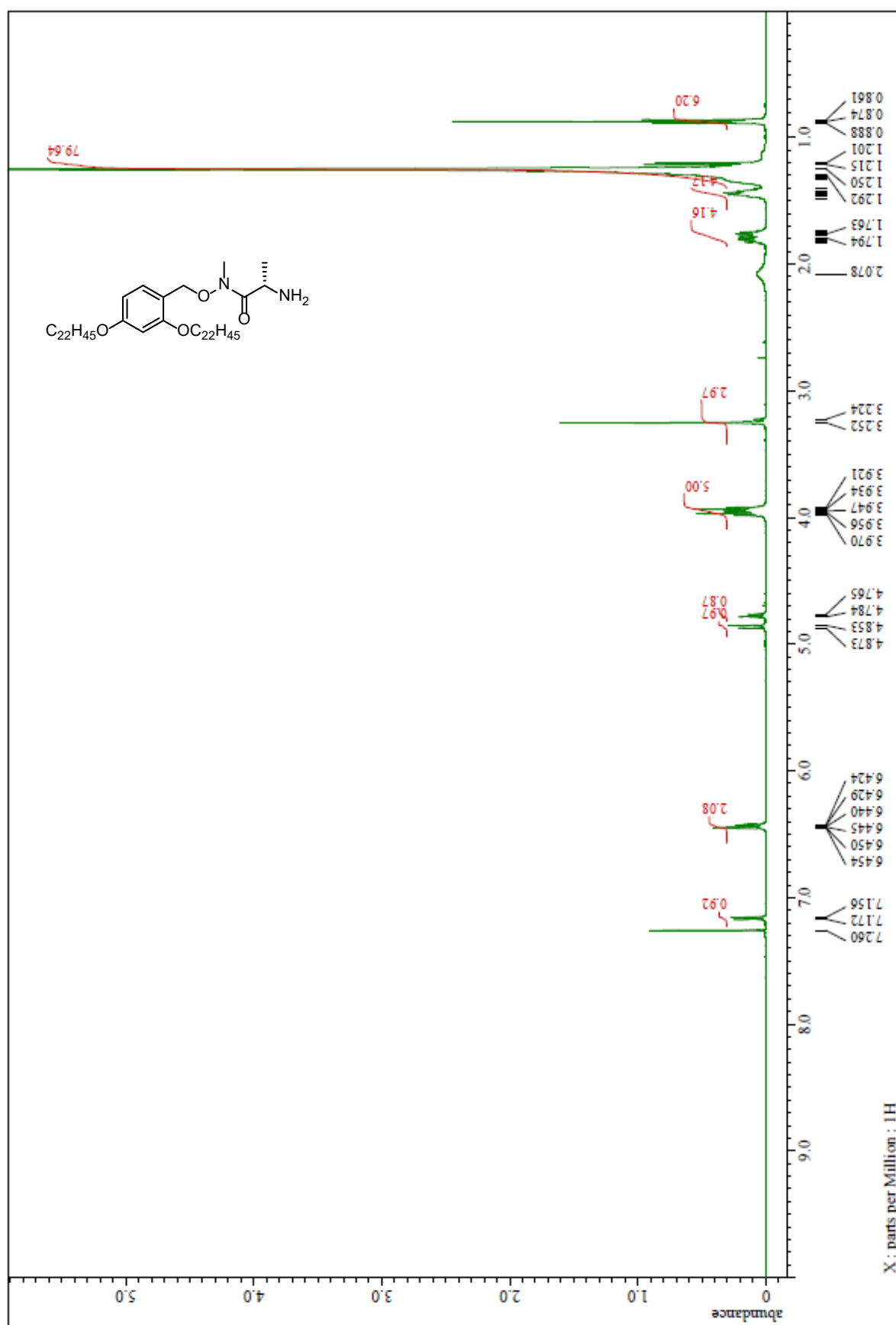
<sup>1</sup>H NMR spectrum of Fmoc-Ala-(Me)N-O-TAGb (65) (CDCl<sub>3</sub>)



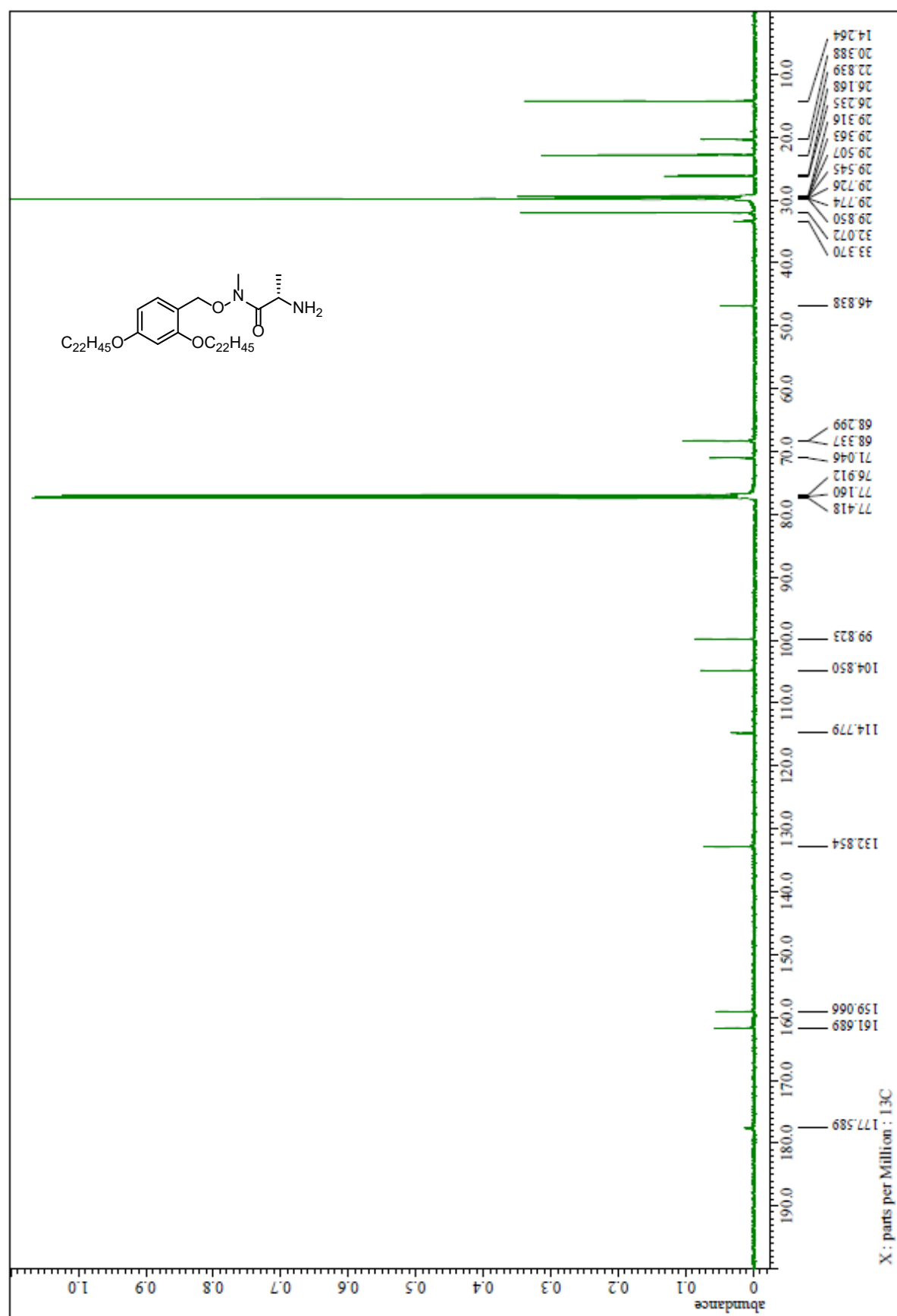
$^{13}\text{C}$  NMR spectrum of Fmoc-Ala-(Me)N-O-TAGb (**65**) ( $\text{CDCl}_3$ )



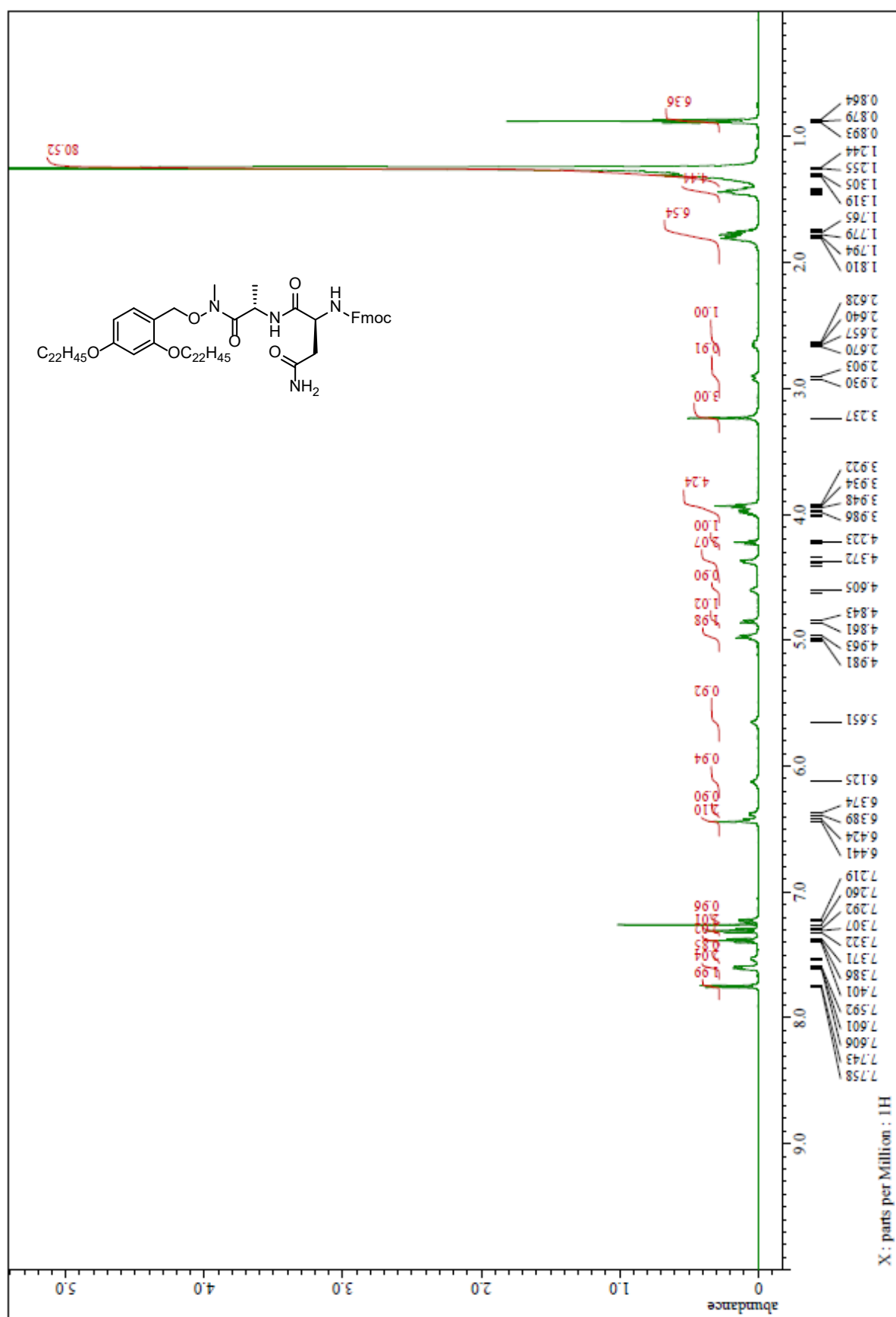
$^1\text{H}$  NMR spectrum of Ala-(Me)N-O-TAGb (**66**) ( $\text{CDCl}_3$ )



$^{13}\text{C}$  NMR spectrum of Ala-(Me)N-O-TAGb (**66**) ( $\text{CDCl}_3$ )

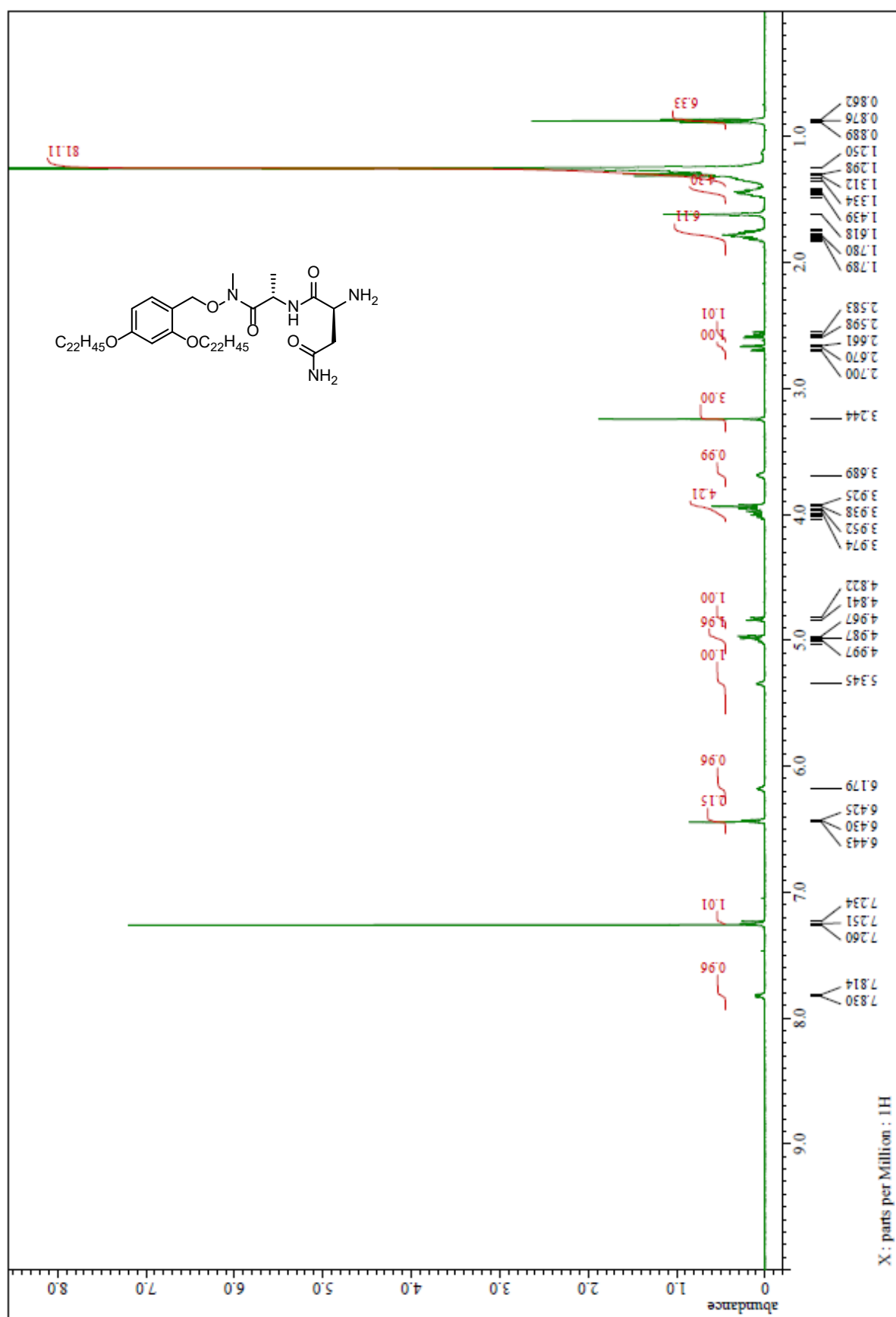


<sup>1</sup>H NMR spectrum of Fmoc-Asn-Ala-(Me)N-O-TAGb (67) (CDCl<sub>3</sub>)

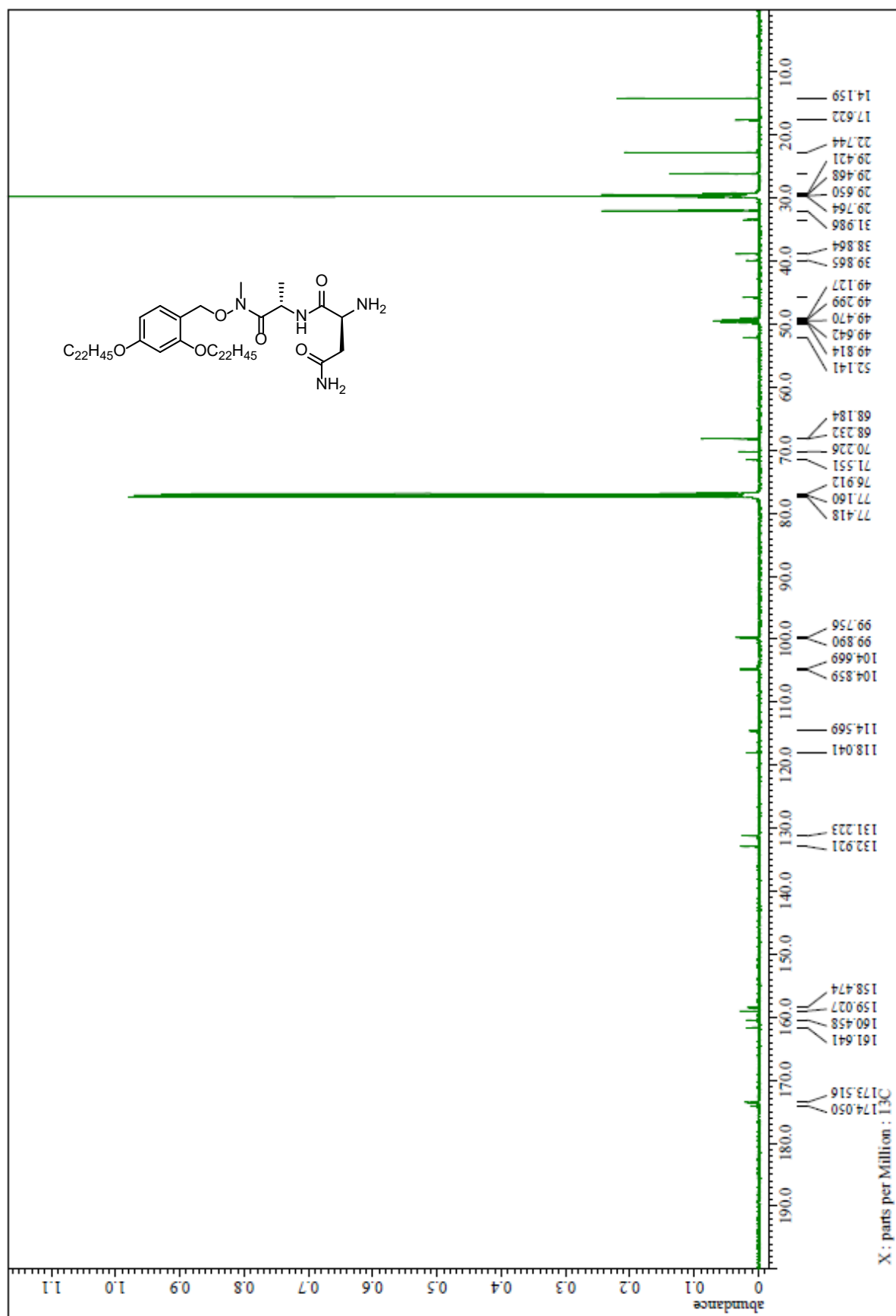




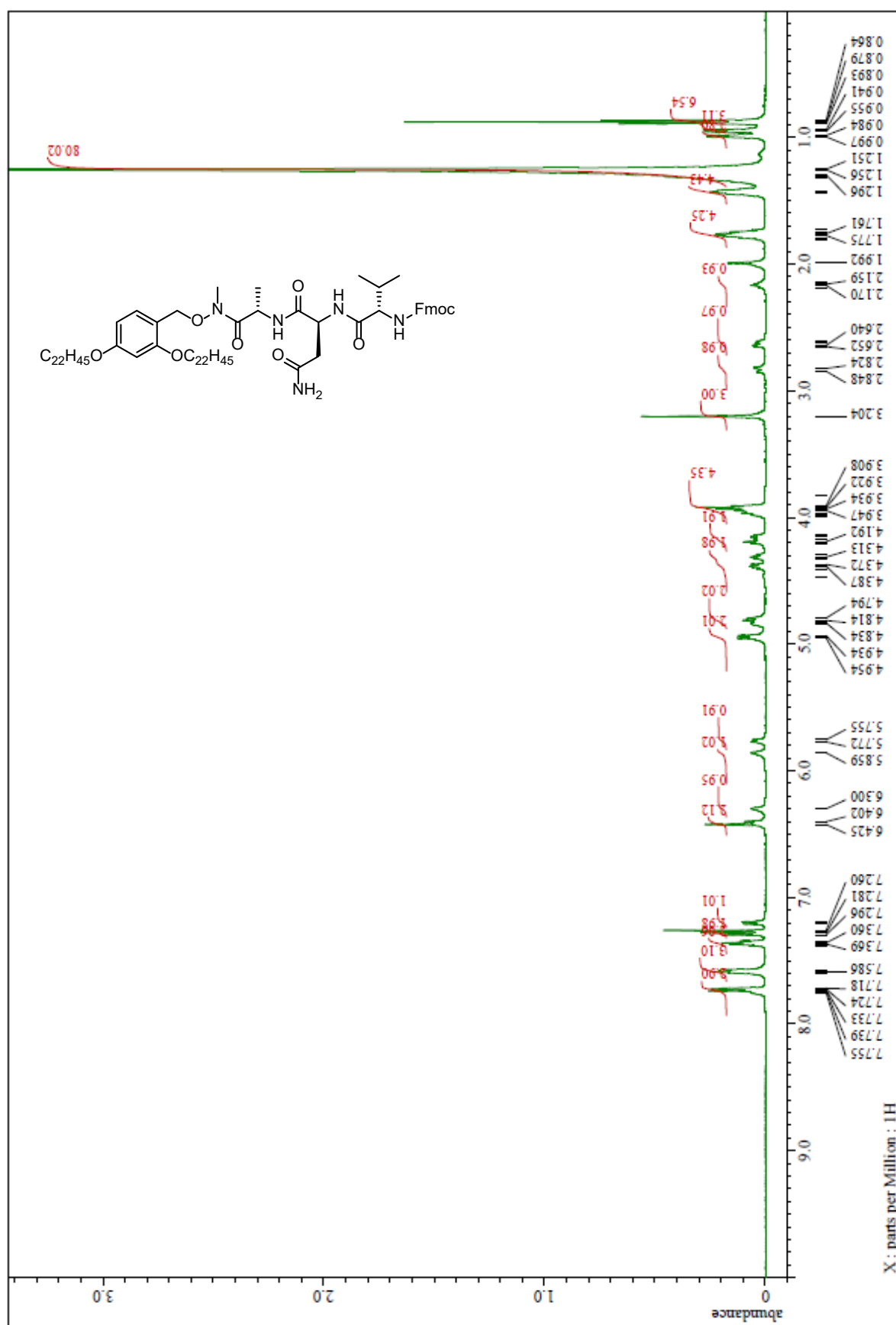
<sup>1</sup>H NMR spectrum of Asn-Ala-(Me)N-O-TAGb (68) (CDCl<sub>3</sub>)



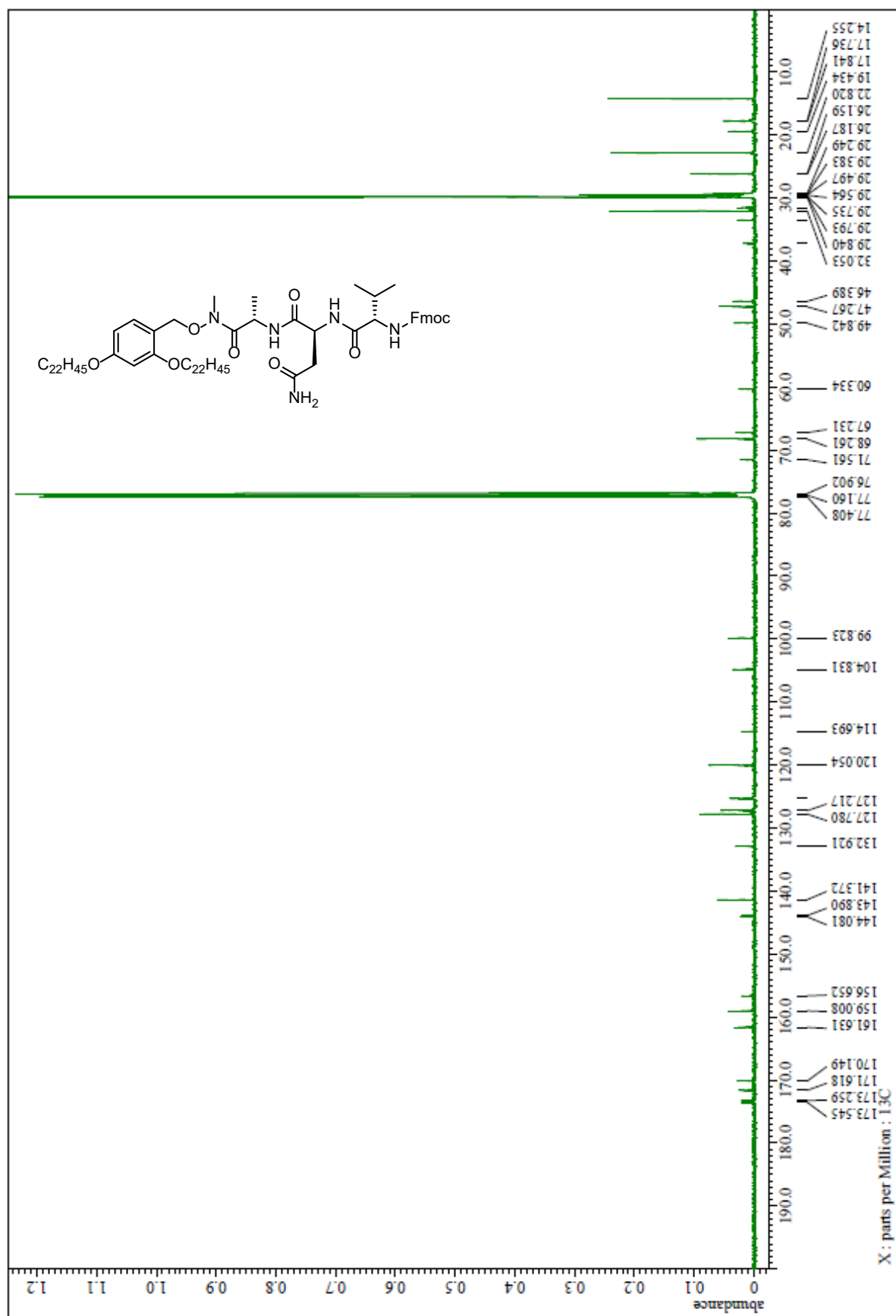
$^{13}\text{C}$  NMR spectrum of Asn-Ala-(Me)N-O-TAGb (**68**) ( $\text{CDCl}_3$ )



<sup>1</sup>H NMR spectrum of Fmoc-Val-Asn-Ala-(Me)N-O-TAGb (69) (CDCl<sub>3</sub>)

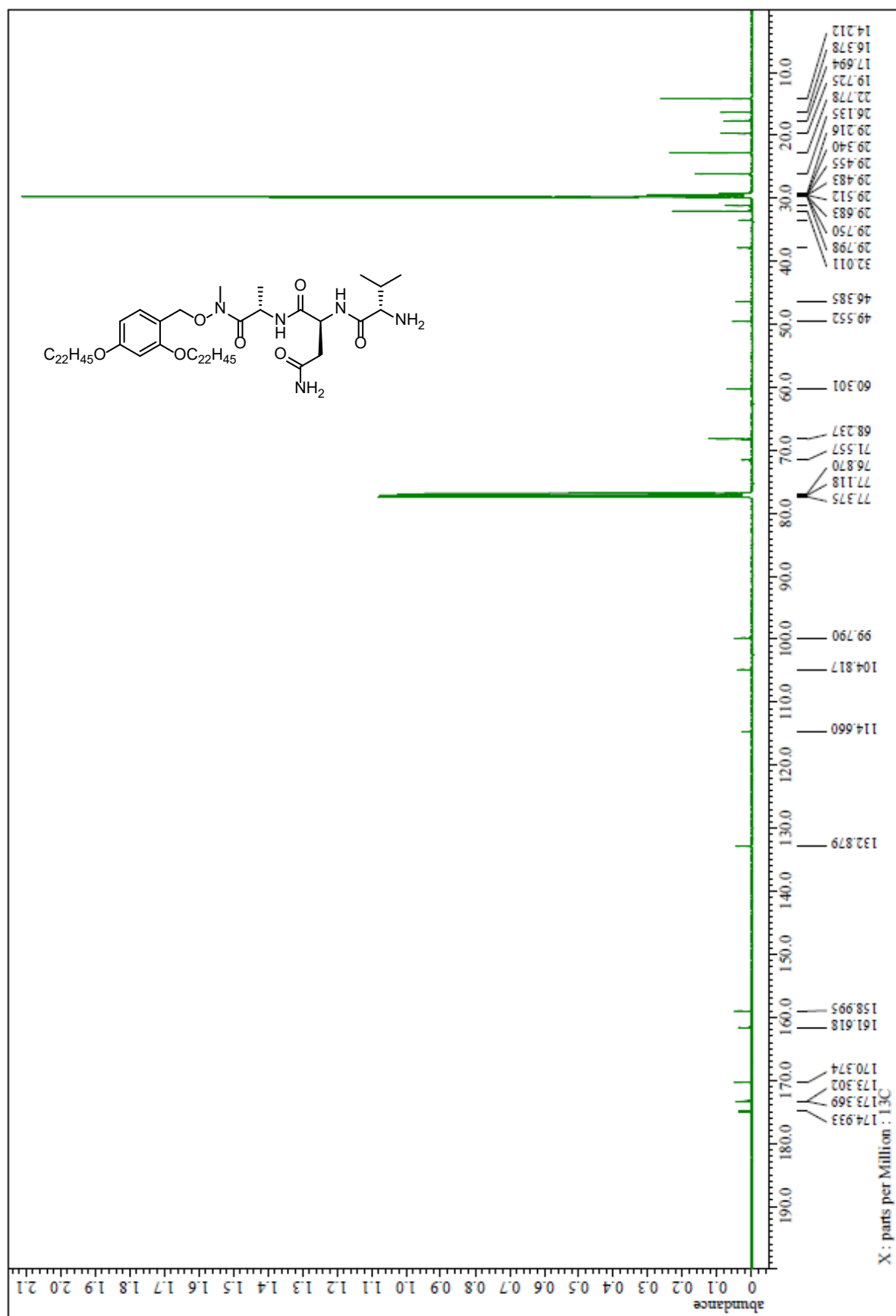


$^{13}\text{C}$  NMR spectrum of Fmoc-Val-Asn-Ala-(Me)N-O-TAGb (**69**) ( $\text{CDCl}_3$ )





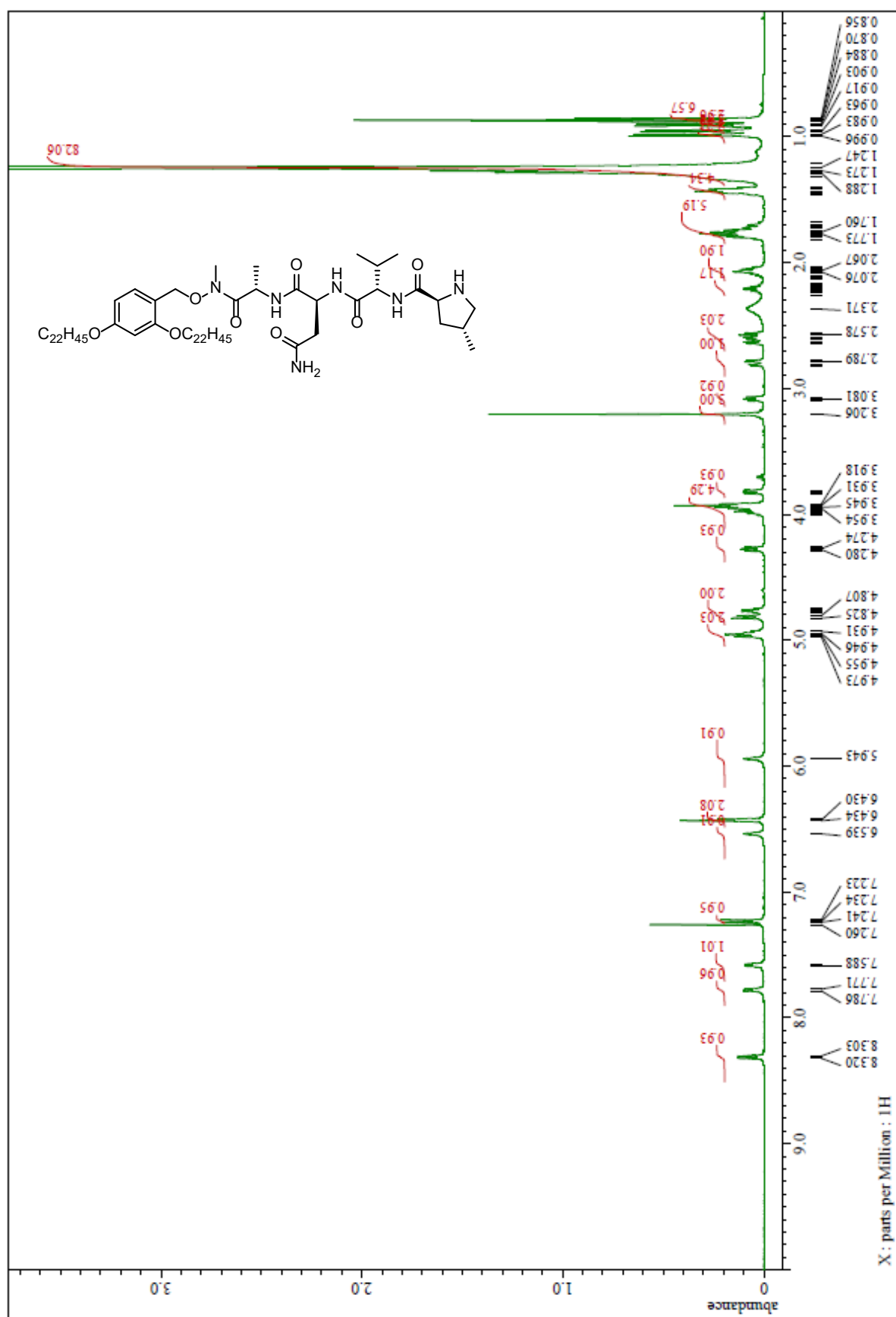
$^{13}\text{C}$  NMR spectrum of Val-Asn-Ala-(Me)N-O-TAGb (**70**) ( $\text{CDCl}_3$ )



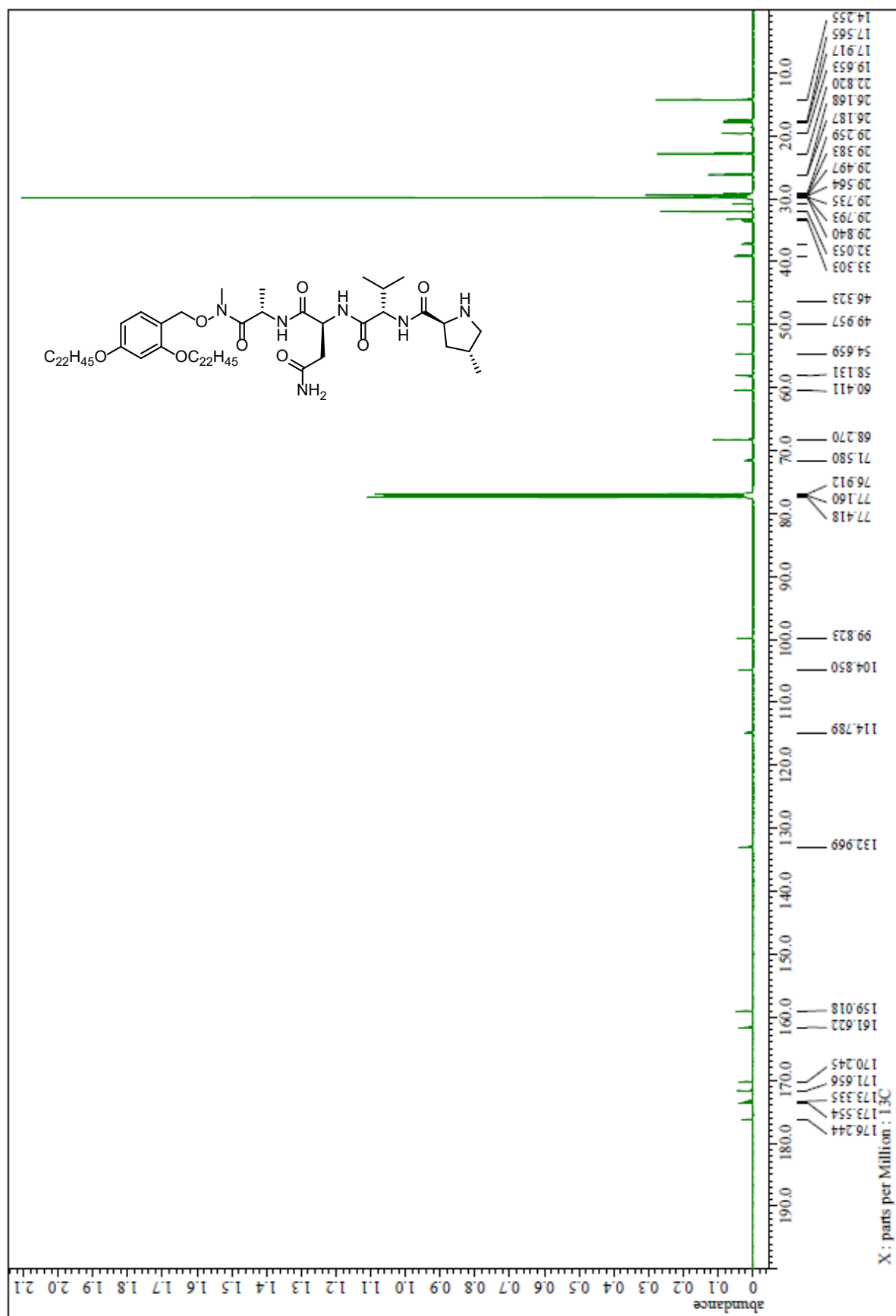




<sup>1</sup>H NMR spectrum of 4MePro-Val-Asn-Ala-(Me)N-O-TAGb (72) (CDCl<sub>3</sub>)



$^{13}\text{C}$  NMR spectrum of 4MePro-Val-Asn-Ala-(Me)N-O-TAGb (**72**) ( $\text{CDCl}_3$ )

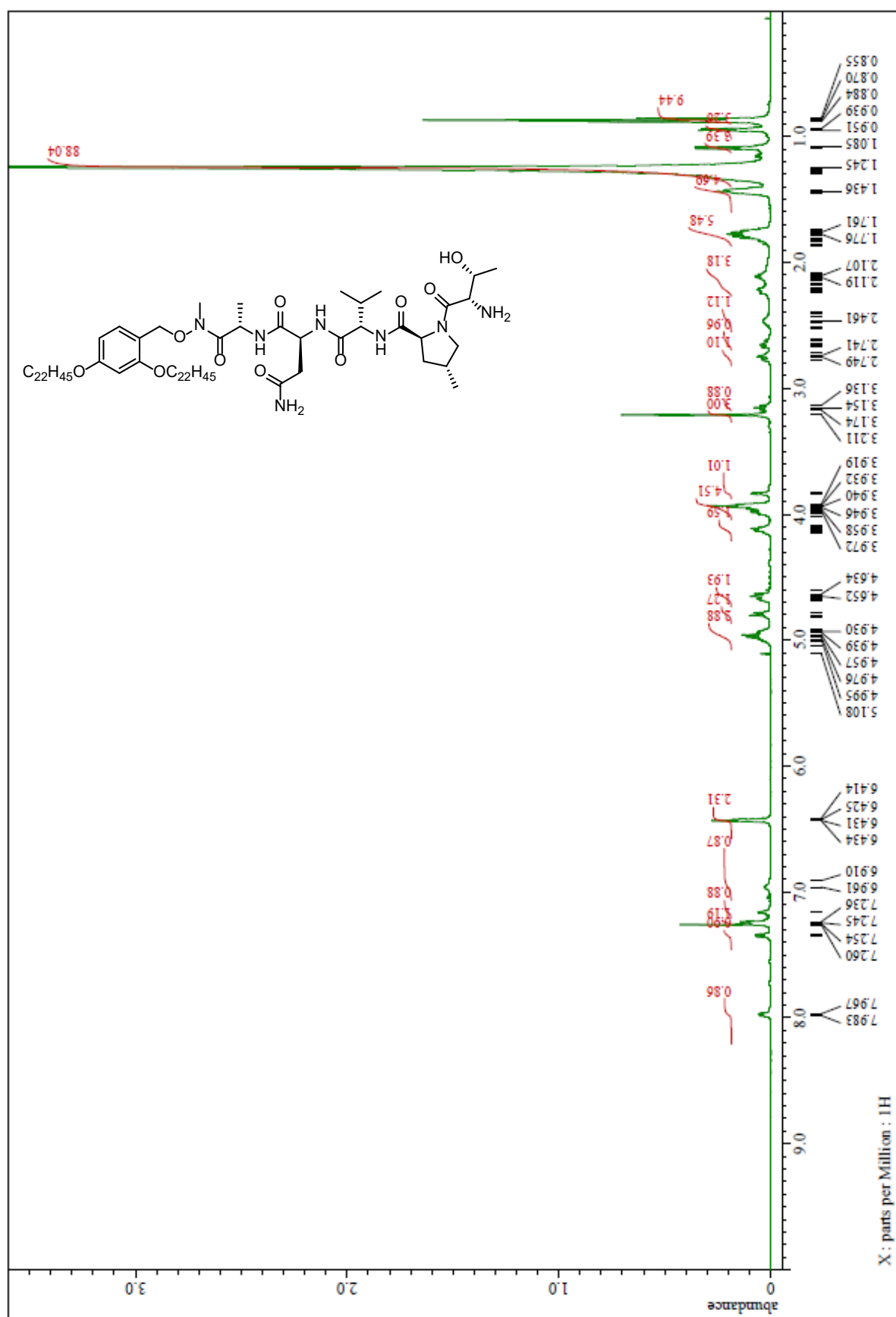


<sup>1</sup>H NMR spectrum of Fmoc-Thr-4MePro-Val-Asn-Ala-(Me)N-O-TAGb (73) (CDCl<sub>3</sub>)

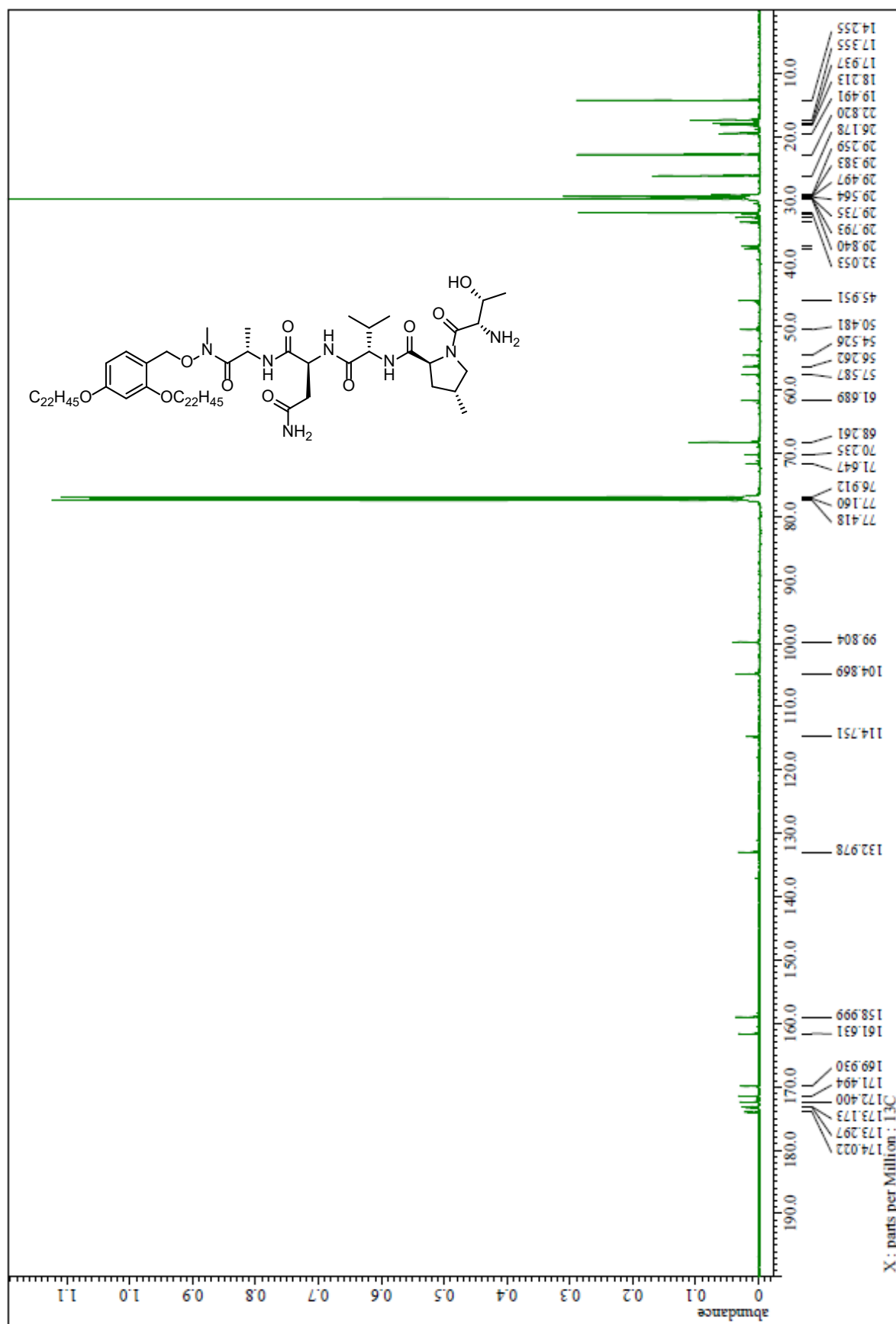




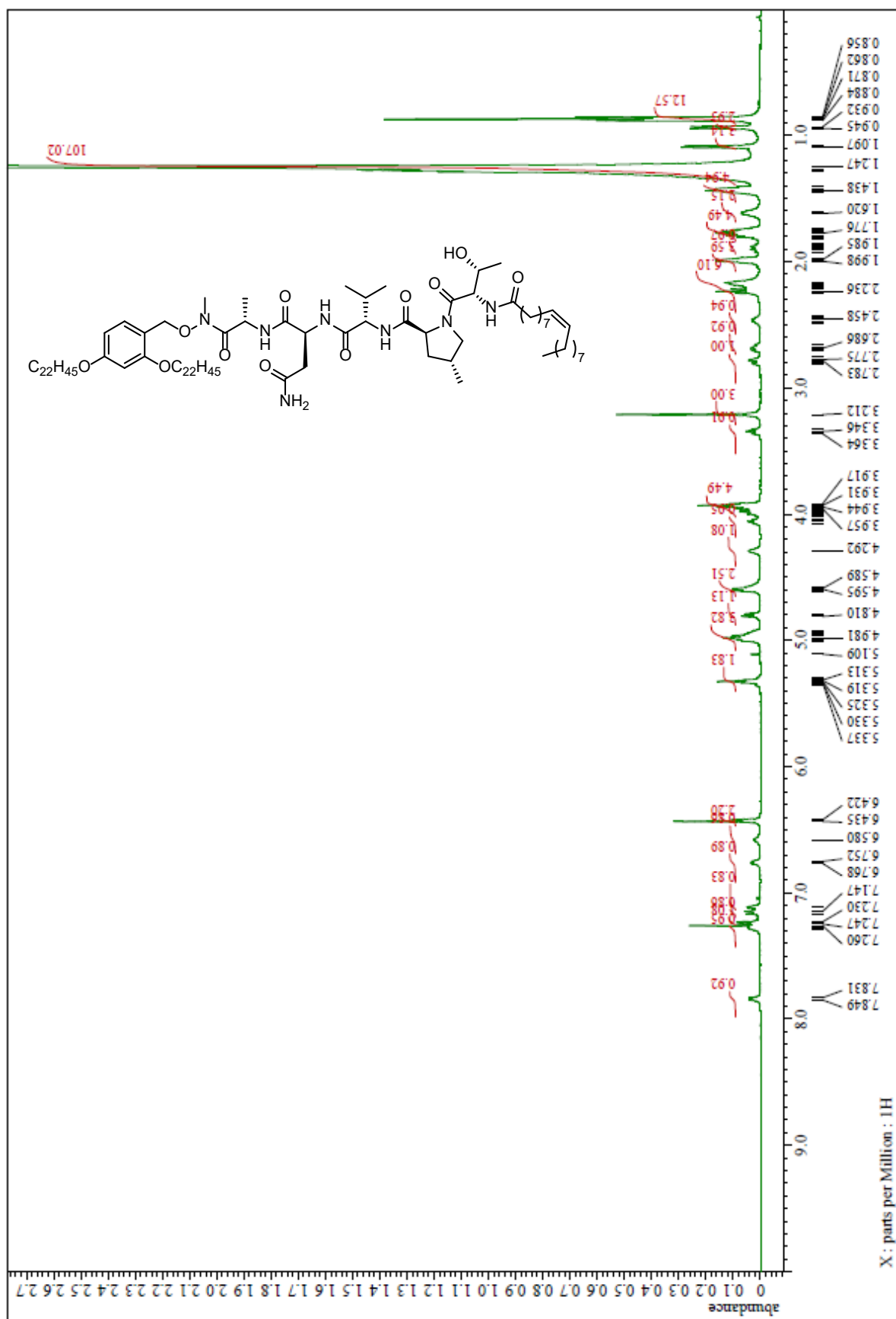
$^1\text{H}$  NMR spectrum of Thr-4MePro-Val-Asn-Ala-(Me)N-O-TAGb (**74**) ( $\text{CDCl}_3$ )



$^{13}\text{C}$  NMR spectrum of Thr-4MePro-Val-Asn-Ala-(Me)N-O-TAGb (74) ( $\text{CDCl}_3$ )



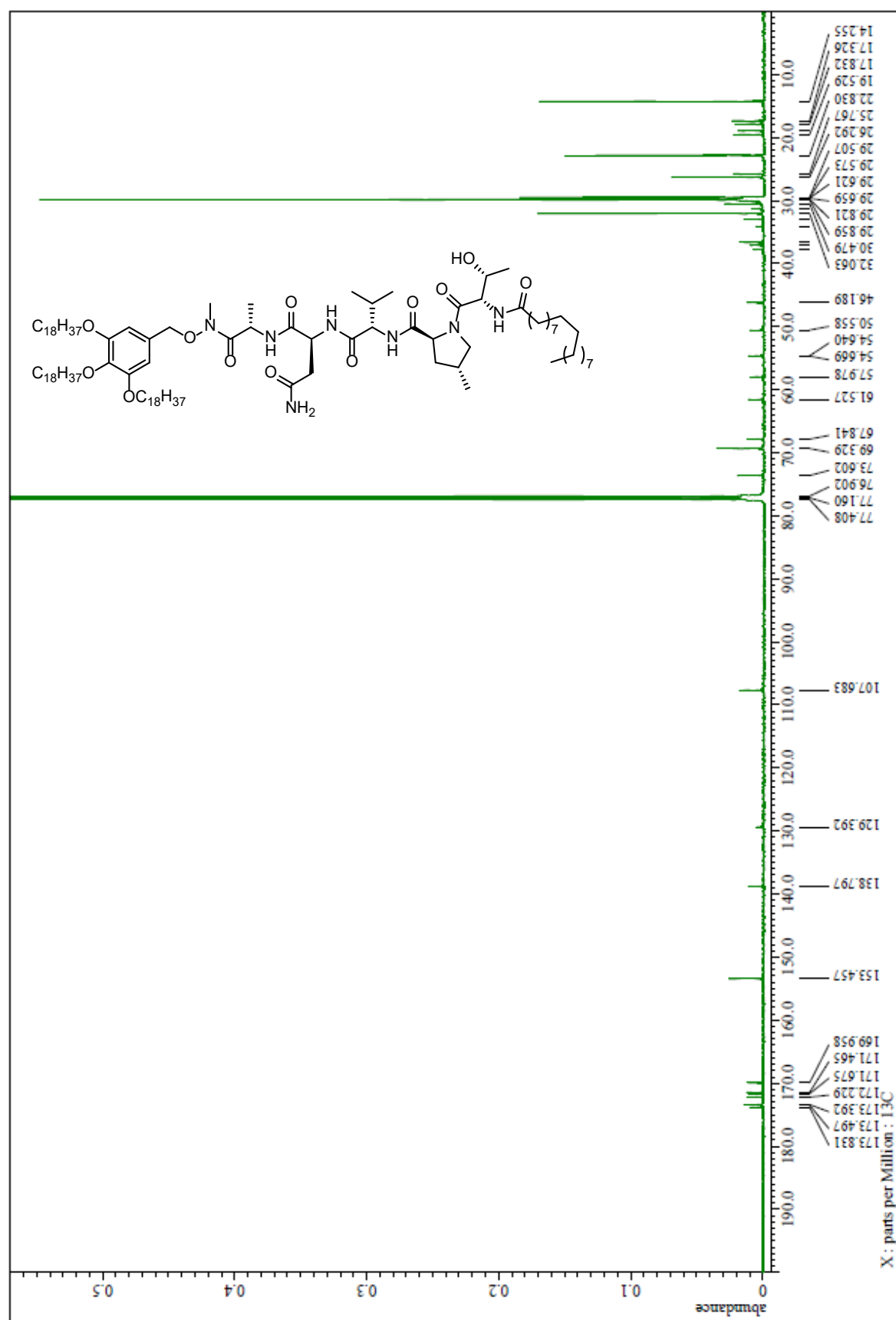
$^1\text{H}$  NMR spectrum of Oleic acid-Thr-4MePro-Val-Asn-Ala-(Me)N-O-TAGb (**30**) ( $\text{CDCl}_3$ )



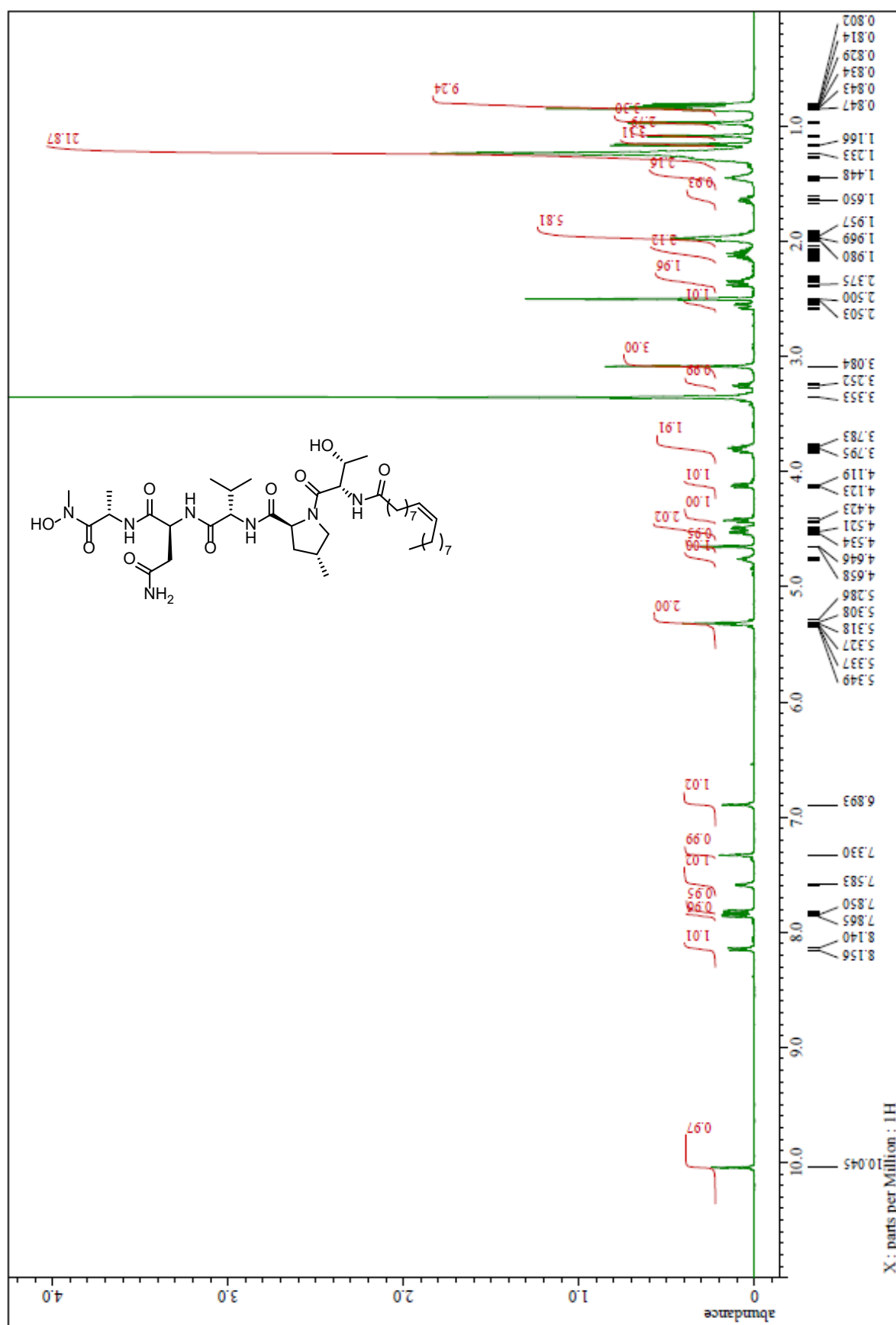




$^{13}\text{C}$  NMR spectrum of Stearic acid-Thr-4MePro-Val-Asn-Ala-(Me) $_7$ N-O-TAGa (**29**) ( $\text{CDCl}_3$ )



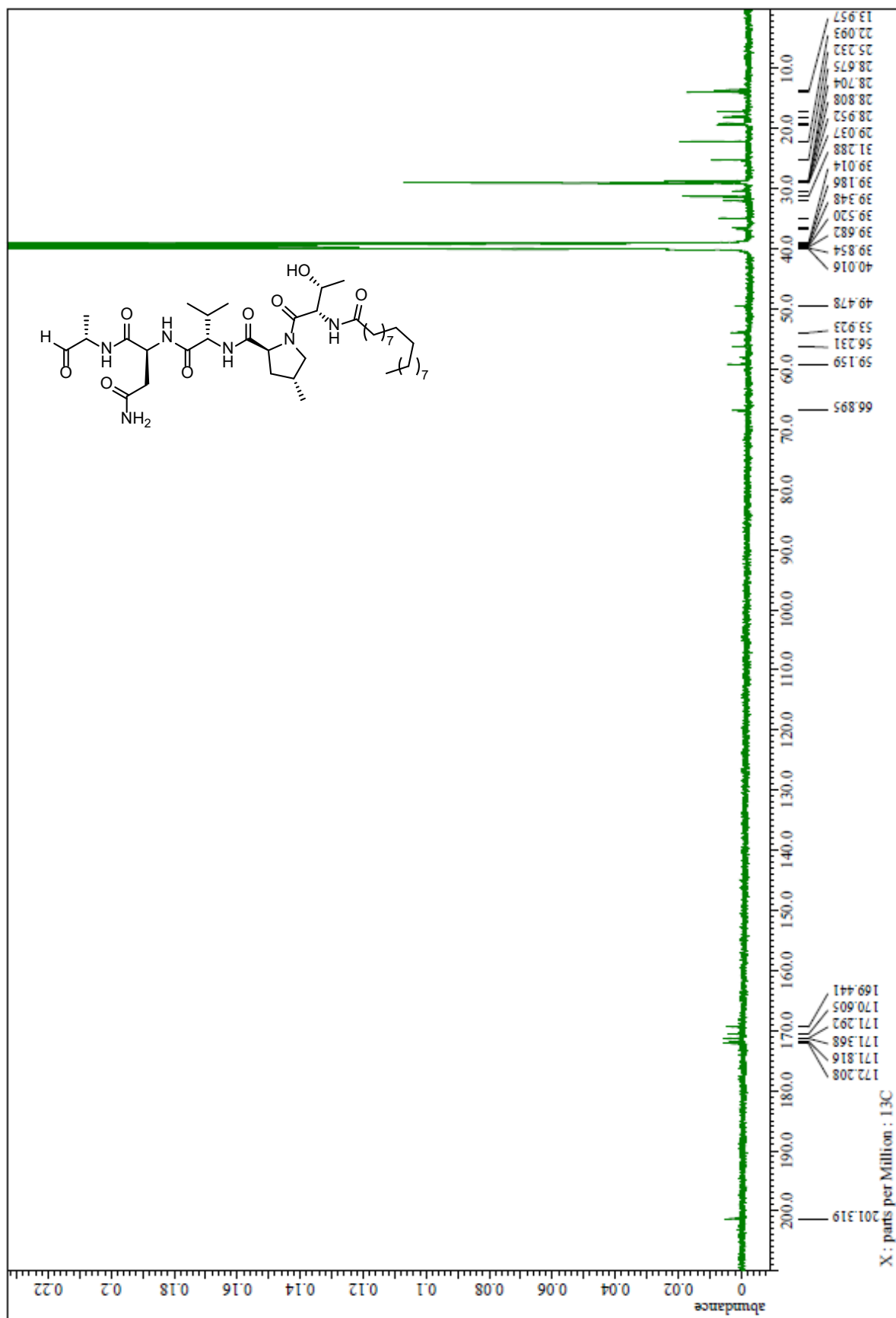
<sup>1</sup>H NMR spectrum of Oleic acid-Thr-4MePro-Val-Asn-Ala-(Me)N-OH (**28**) (DMSO-*d*<sub>6</sub>)





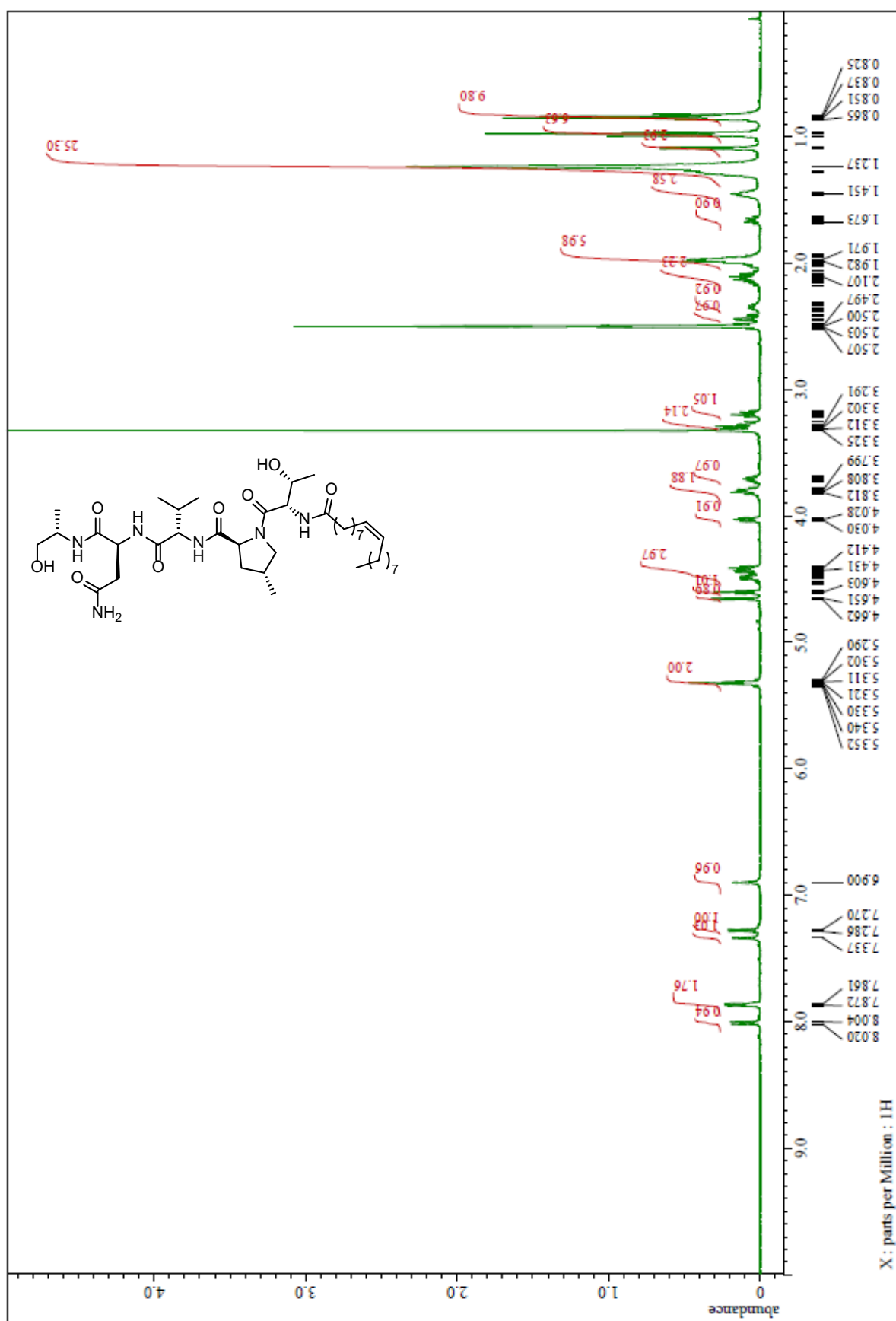


$^{13}\text{C}$  NMR spectrum of Stearic acid-Thr-4MePro-Val-Asn-Ala-H (31) (DMSO- $d_6$ )



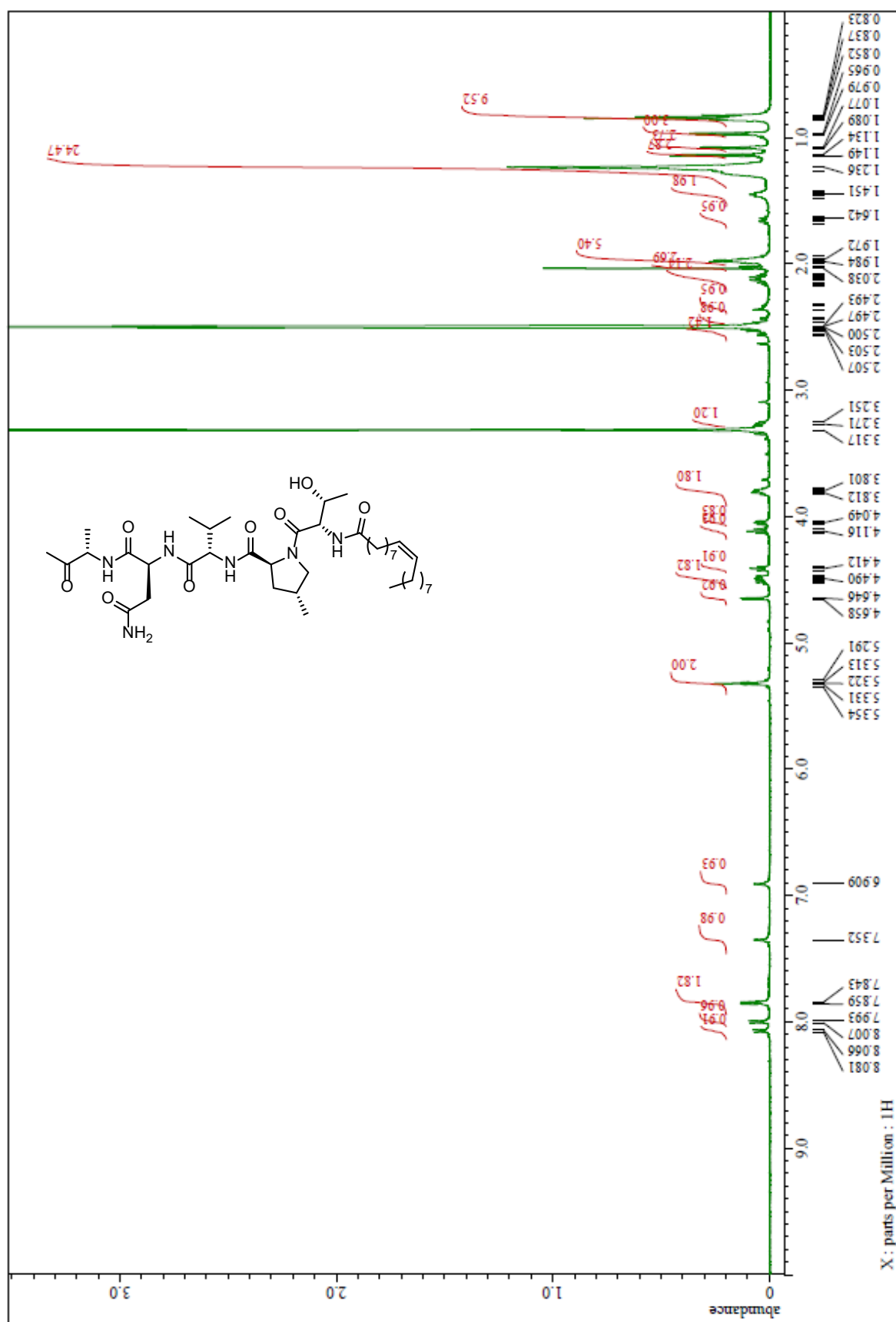
## **NMR Spectra of Compounds in Chapter 4**

<sup>1</sup>H NMR spectrum of Oleic acid-Thr-4MePro-Val-Asn-Alaninol (32) (DMSO-d<sub>6</sub>)

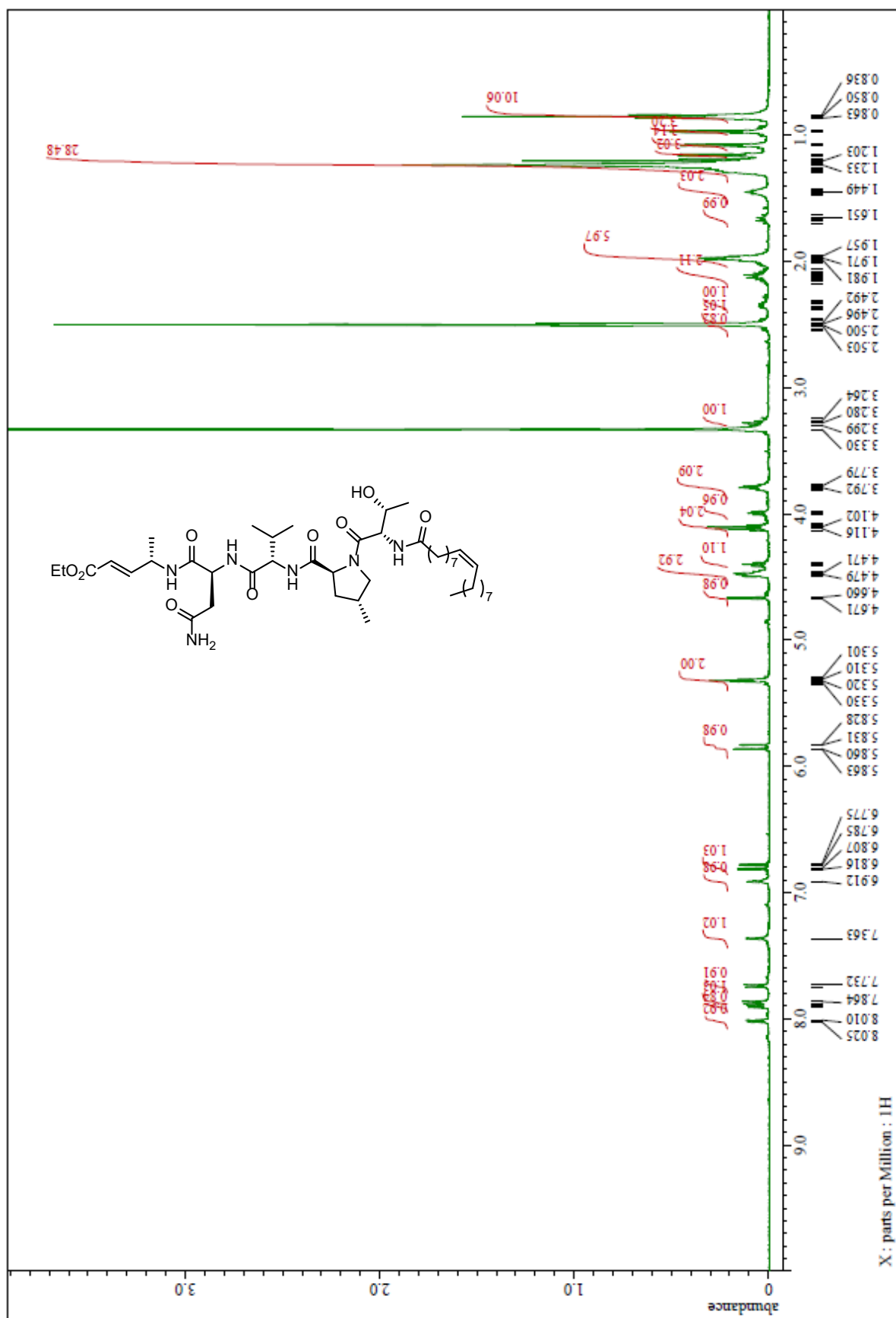




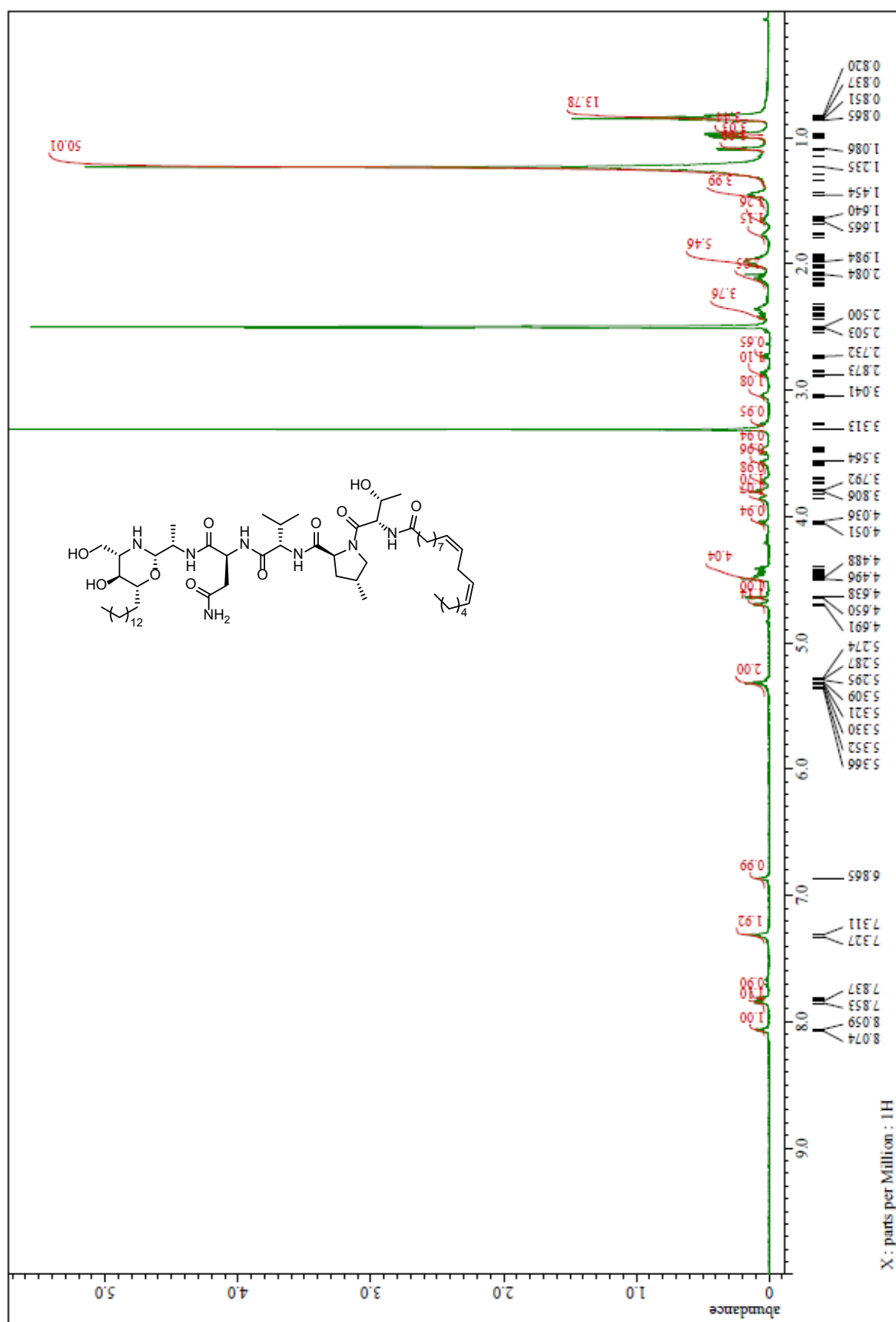
<sup>1</sup>H NMR spectrum of Oleic acid-Thr-4MePro-Val-Asn-Ala-Me (34) (DMSO-d<sub>6</sub>)



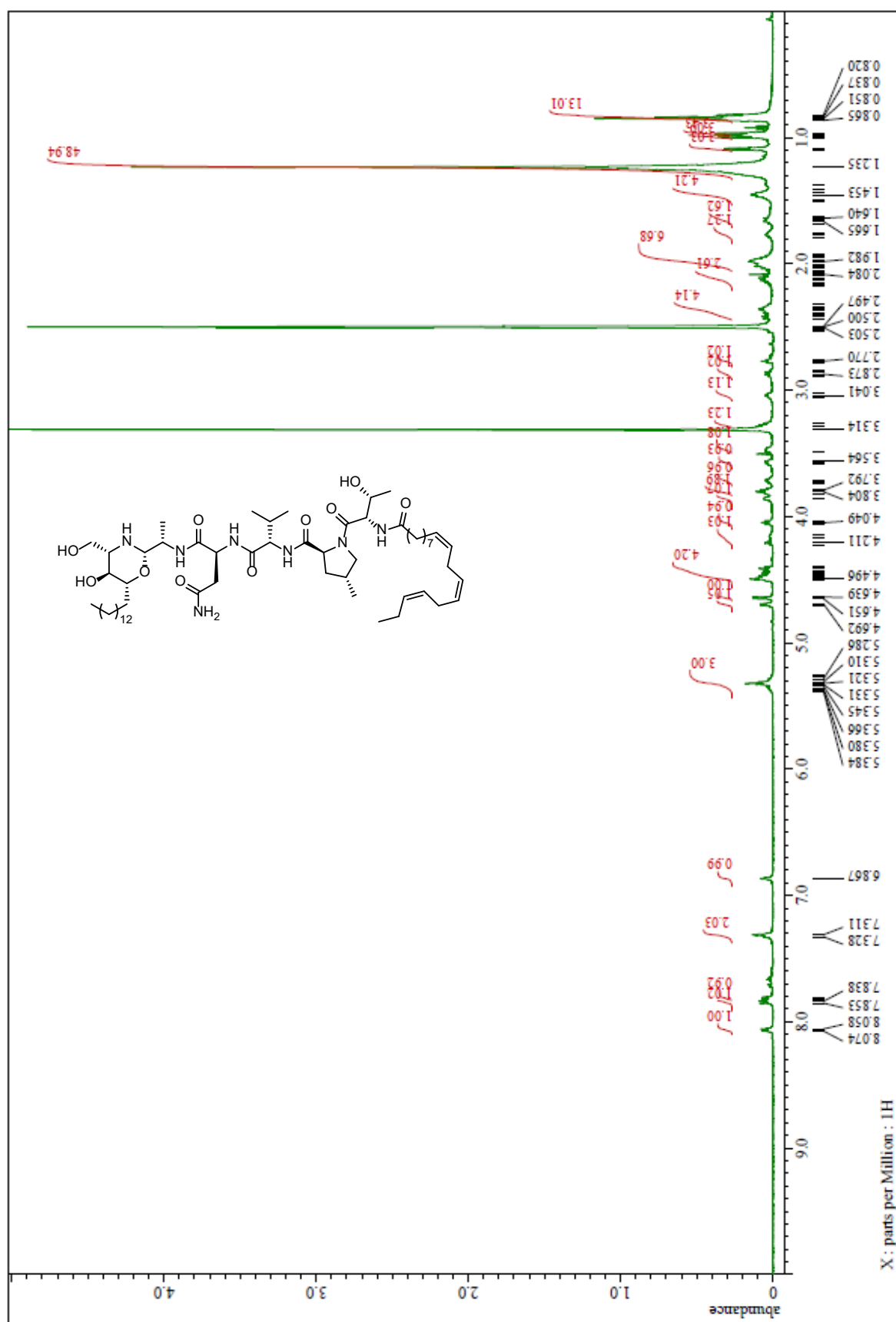
$^1\text{H}$  NMR spectrum of Oleic acid-Thr-4MePro-Val-Asn-Ala-derived unsaturated ester (**35**) ( $\text{DMSO}-d_6$ )



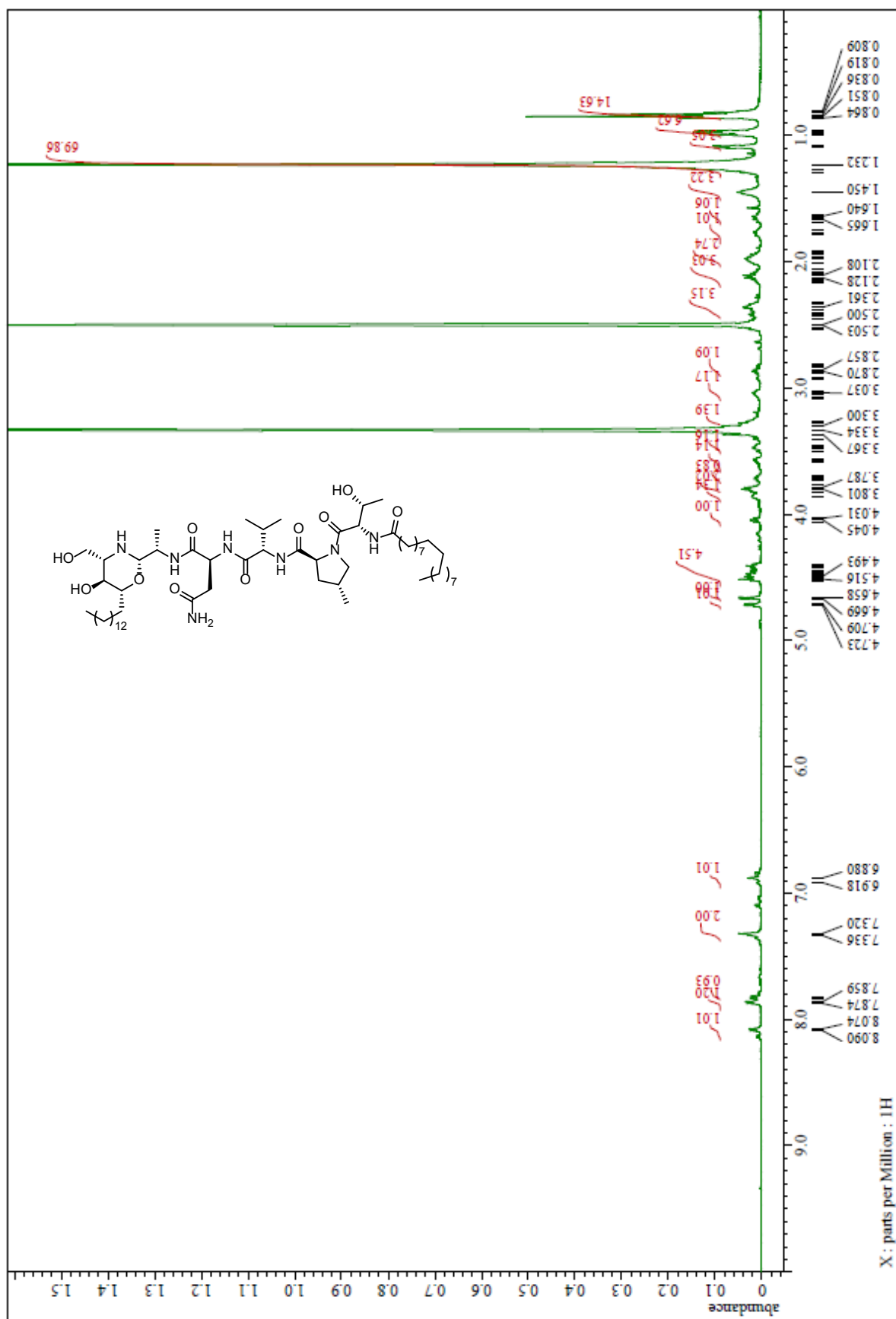
$^1\text{H}$  NMR spectrum of Linoleic acid-Thr-4MePro-Val-Asn-Alaninal-Phytoshingosine (**36**) ( $\text{DMSO-}d_6$ )



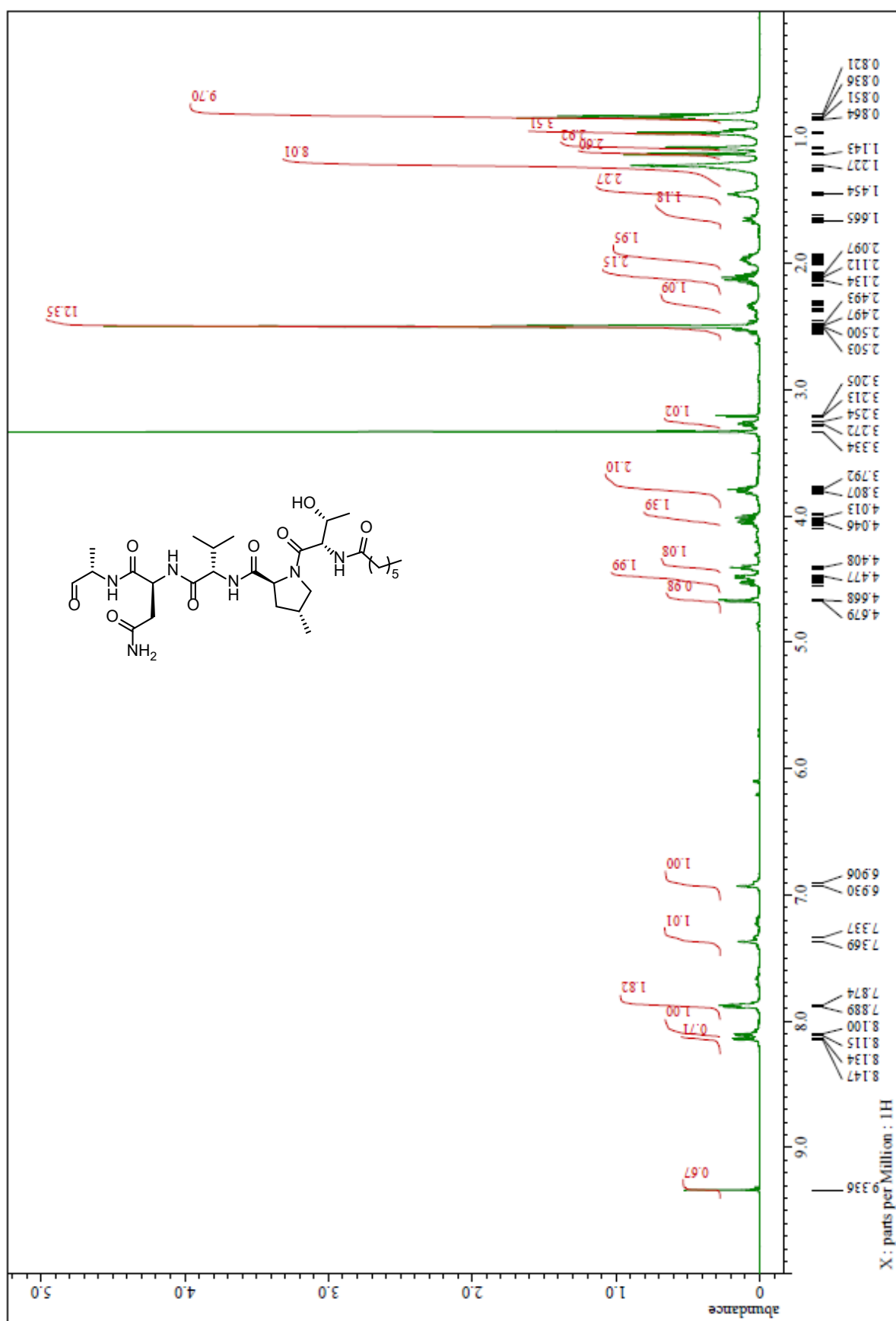
<sup>1</sup>H NMR spectrum of Linolenic acid-Thr-4MePro-Val-Asn-Alaninal-Phytoshingosine (37) (DMSO-d<sub>6</sub>)



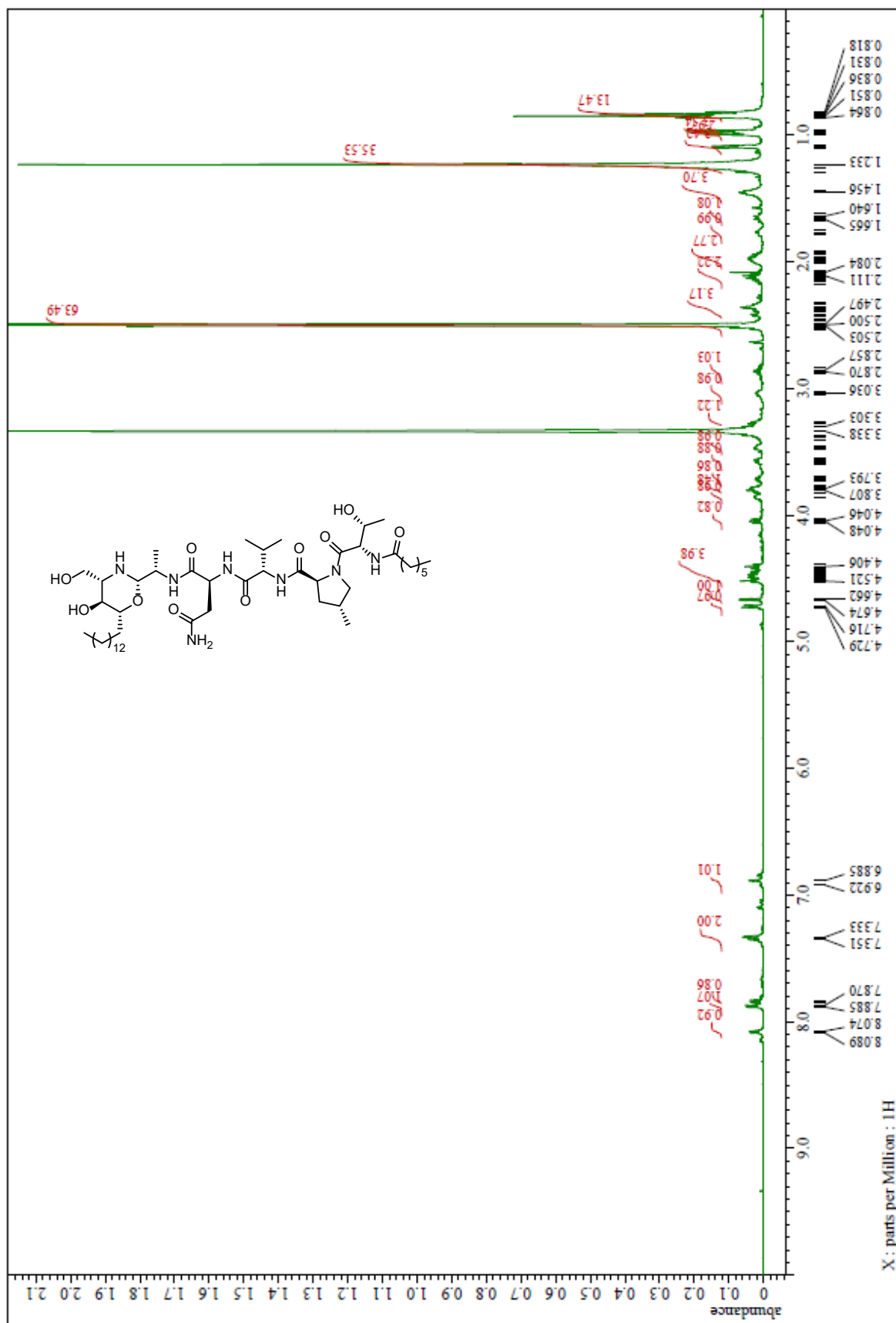
$^1\text{H}$  NMR spectrum of Stearic acid-Thr-4MePro-Val-Asn-Alaninal-Phytoshingosine (**38**) ( $\text{DMSO-}d_6$ )



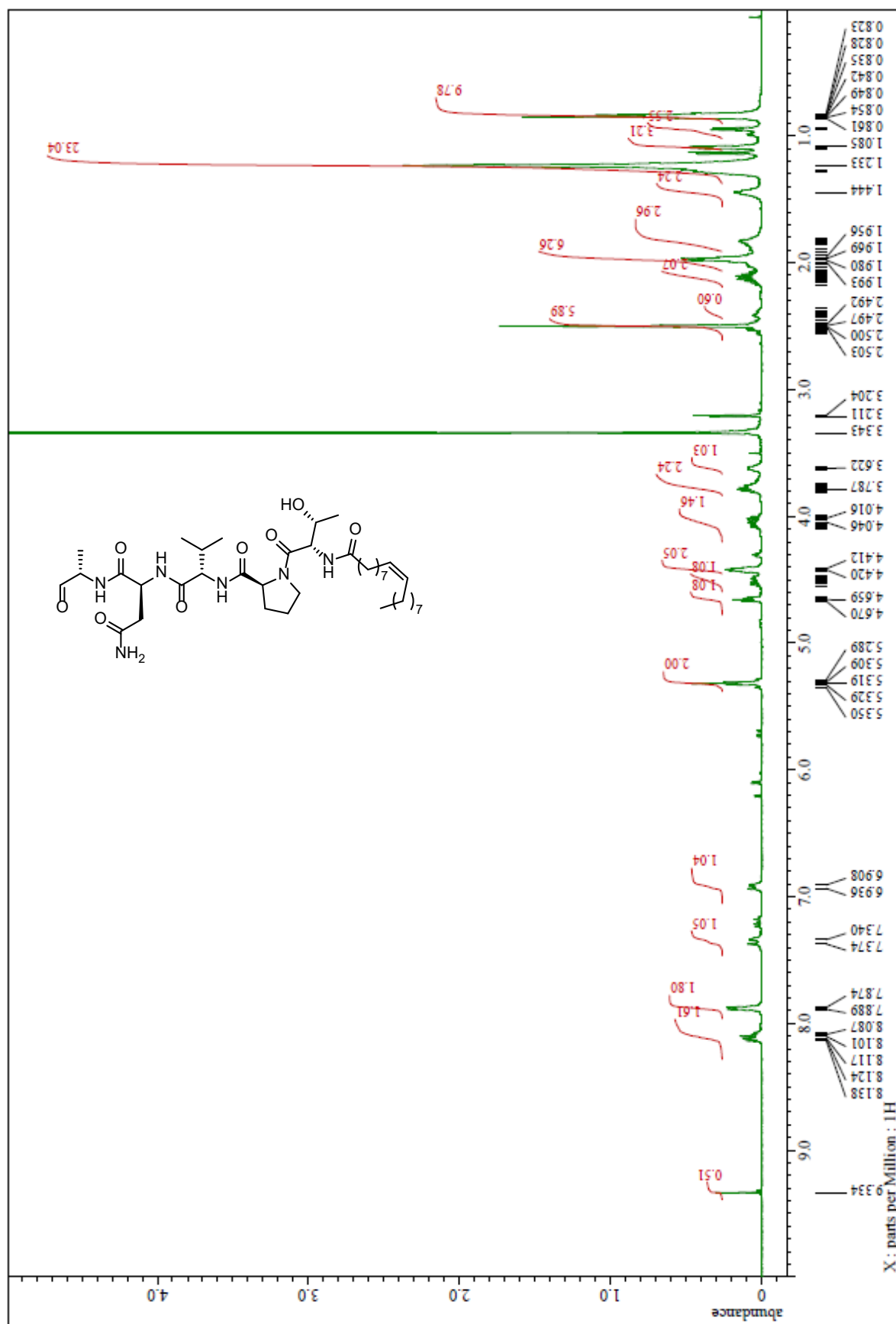
<sup>1</sup>H NMR spectrum of Heptanoic acid-Thr-4MePro-Val-Asn-Ala-H (39) (DMSO-d<sub>6</sub>)



<sup>1</sup>H NMR spectrum of Heptanoic acid-Thr-4MePro-Val-Asn-Alaninal-Phytoshingosine (**40**) (DMSO-*d*<sub>6</sub>)

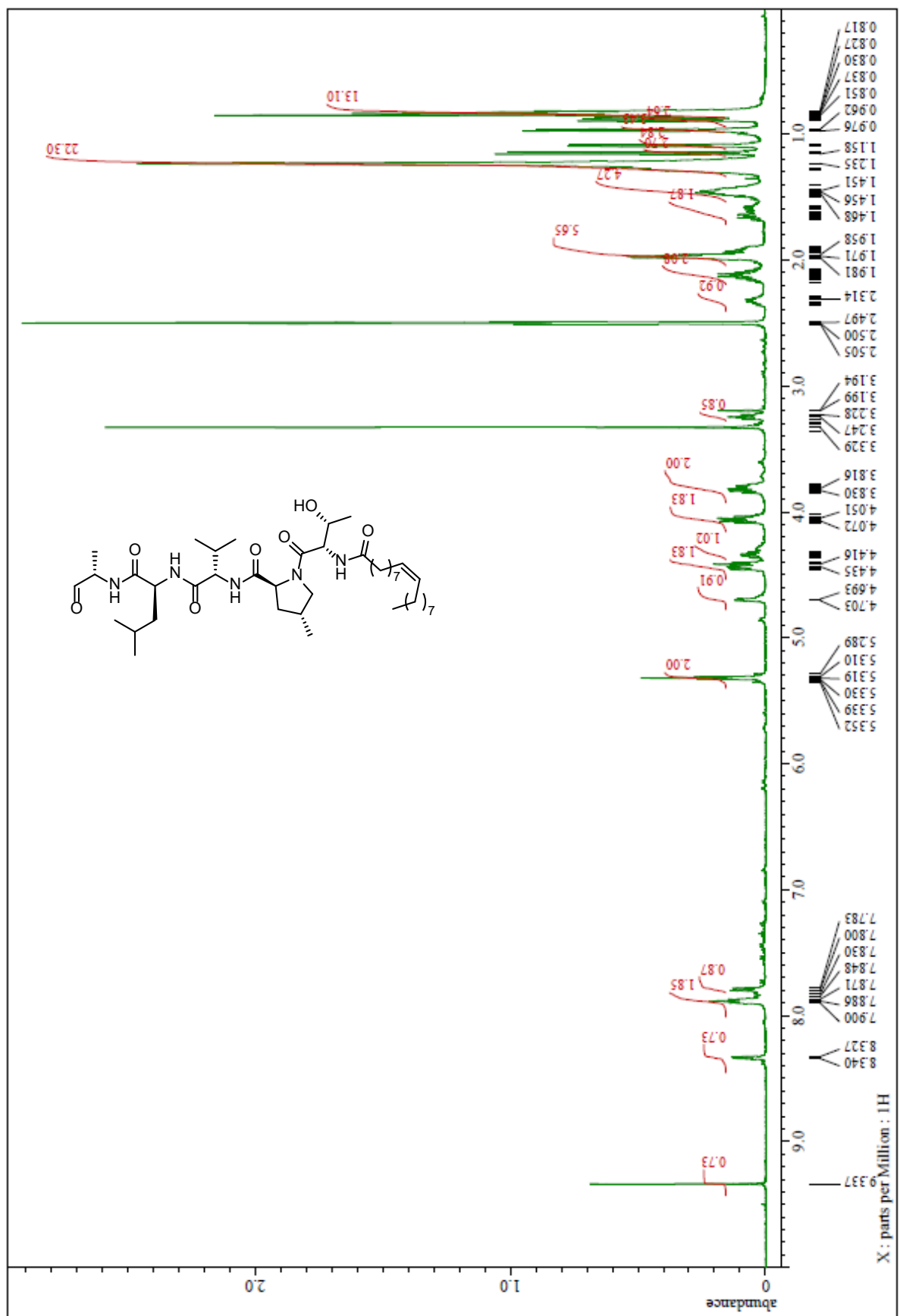


<sup>1</sup>H NMR spectrum of Oleic acid-Thr-Pro-Val-Asn-Ala-H (41) (DMSO-d<sub>6</sub>)

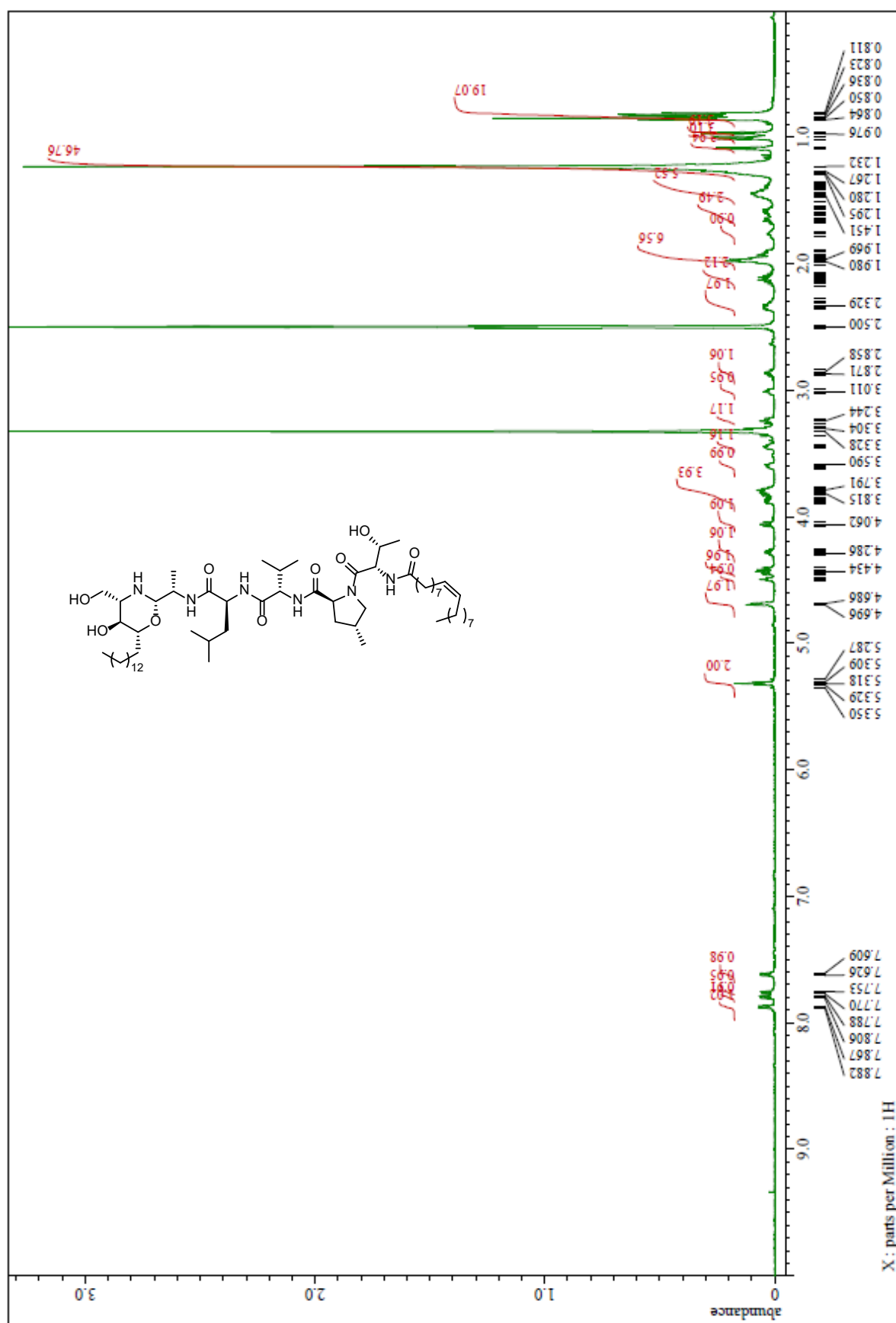




<sup>1</sup>H NMR spectrum of Oleic acid-Thr-4MePro-Val-Leu-Ala-H (43) (DMSO-d<sub>6</sub>)

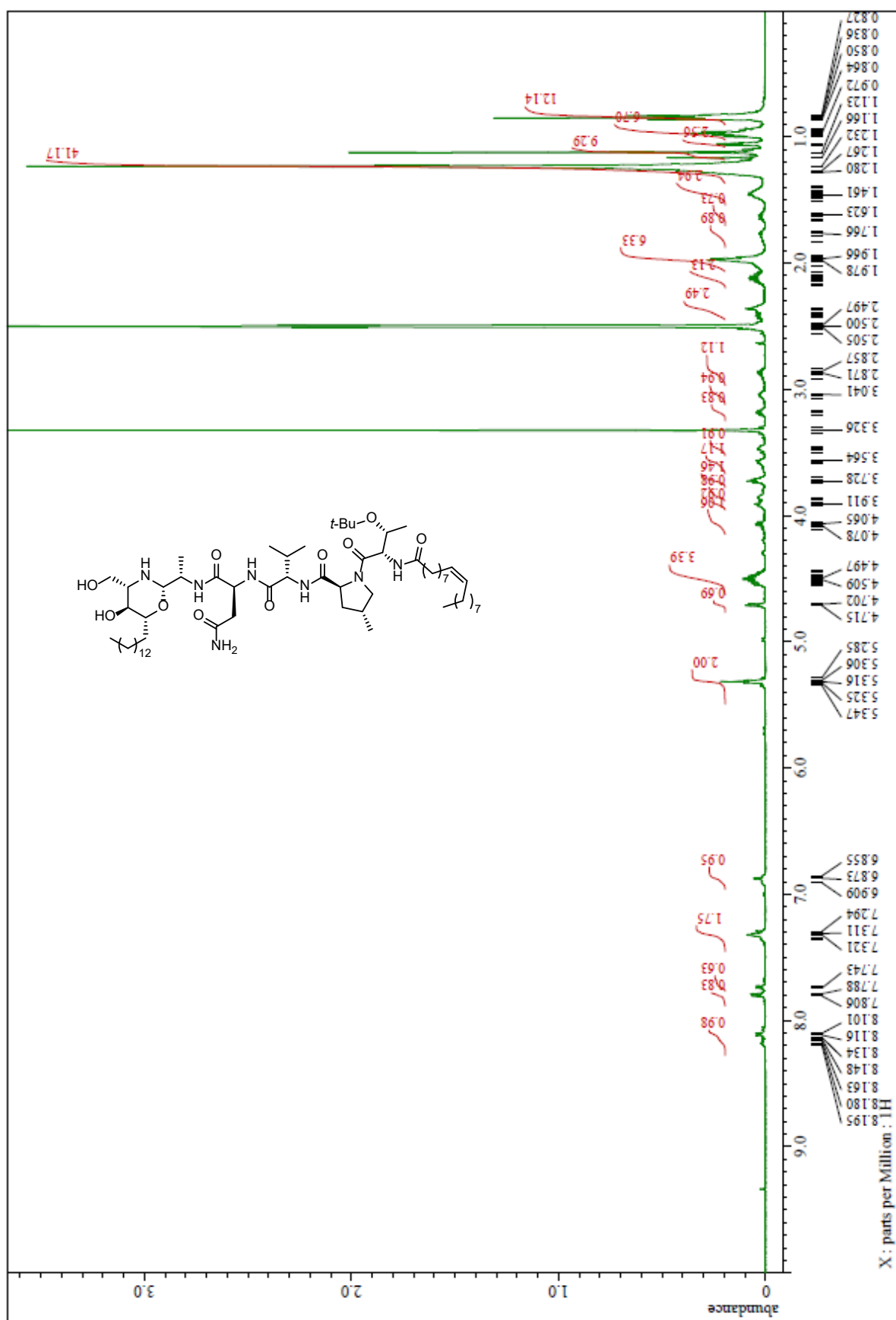


<sup>1</sup>H NMR spectrum of Oleic acid-Thr-4MePro-Val-Leu-Alaninal-Phytoshingosine (**44**) (DMSO-*d*<sub>6</sub>)

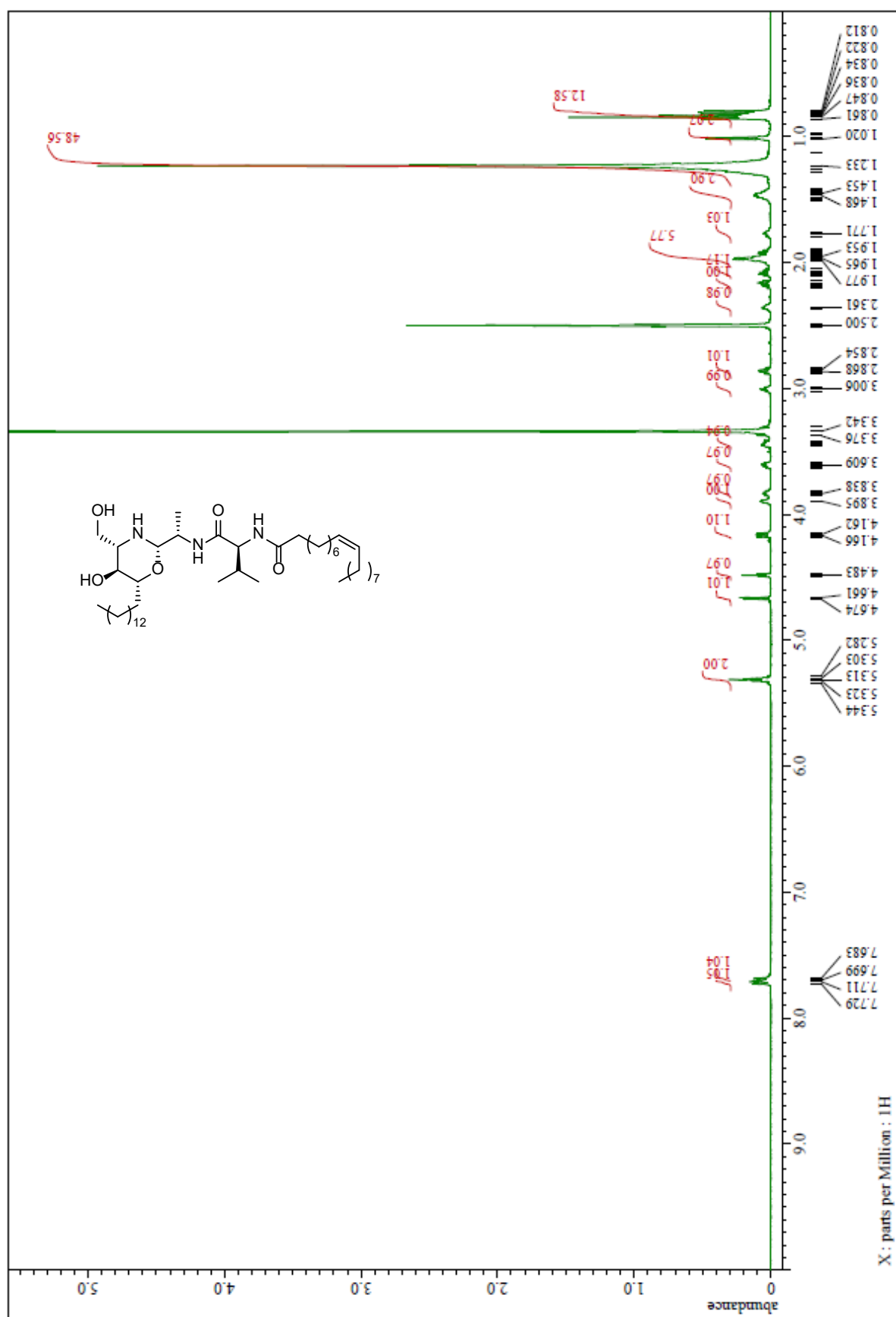




<sup>1</sup>H NMR spectrum of Oleic acid-Thr(*t*-Bu)-4MePro-Val-Asn-Alaninal-Phytoshingosine (**46**) (DMSO-*d*<sub>6</sub>)



<sup>1</sup>H NMR spectrum of Oleic acid- Val- Alaninal-Phytoshingosine (47) (DMSO-d<sub>6</sub>)



# References

## Chapter 1

- (1) (a) World Health Organization, *The top 10 causes of death*. Homepage: <https://www.who.int/news-room/fact-sheets/detail/the-top-10-causes-of-death>. (b) World Health Organization, *Global Health Estimates 2016 Summary Tables: Deaths by Cause, Age and Sex, by World Bank Income Group, 2000-2015*. Homepage: [http://www.who.int/healthinfo/global\\_burden\\_disease/en/](http://www.who.int/healthinfo/global_burden_disease/en/). (c) *The Lancet*, Findings from the Global Burden of Disease Study 2017.
- (2) World Health Organization, *World Malaria Report 2020*.
- (3) (a) Murray, C. J. L. *et al.* Disability-adjusted life years (DALYs) for 291 diseases and injuries in 21 regions, 1990–2010: a systematic analysis for the Global Burden of Disease Study 2010. *Lancet*, **2013**, *380*, 2197. (b) *World Health Organization*, WHO methods and data sources for global burden of disease estimates 2000-2016.
- (4) Fleming, A. On the antibacterial action of cultures of a *Penicillium*, with special reference to their use in the isolation of *B. influenzae*. *J. Exp. Pathol.* **1929**, *10*, 226.
- (5) Bérdy, J. Bioactive Microbial Metabolites. *J. Antibiot.* **2005**, *58*, 1.
- (6) Newman, D. J.; Cragg G. M. Natural Products as Sources of New Drugs from 1981 to 2014. *J. Nat. Prod.* **2015**, *78*, 468. Direct link: <https://pubs.acs.org/doi/10.1021/acs.jnatprod.5b01055>, Notice: further permissions related to **Figure 2** should be directed to the ACS.
- (7) Lau, J. L.; Dunn, M. K. Therapeutic peptides: Historical perspectives, current development trends, and future directions. *Bioorg. Med. Chem.* **2018**, *26*, 2700.
- (8) (a) Vrettos, E. I.; Mező G.; Tzakos, A. G. On the design principles of peptide–drug conjugates for targeted drug delivery to the malignant tumor site. *Beilstein J. Org. Chem.* **2018**, *14*, 930. (b) Lee, A. C.-L.; Harris, J. L.; Khanna, K. K.; Hong, J.-H. *Int. J. Mol. Sci.* **2019**, *20*, 2383.
- (9) Henminot, A.; Collins, J. C.; Nuss, J. M. *J. Med. Chem.* **2018**, *61*, 1382.
- (10) (a) Räder, A. F. B.; Weinmüller, M.; Reichart, F.; Schumacher-Klinger, A.; Merzbach, S.; Gilon, C.; Hoffman, A.; Kessler, H. Orally Active Peptides: Is There a Magic Bullet? *Angew. Chem. Int. Ed.* **2018**, *57*, 2. (b) Transparency Market Research, *Peptide Therapeutics Market–Global Industry Analysis, Size, Share, Growth, Trends and Forecast 2016-2024*. Homepage: <https://www.transparencymarketresearch.com/peptide-therapeutics-market.html>.
- (11) Curtius, T. Ueber einige neue der Hippursäure analog constituirte, synthetisch dargestellte Amidosäuren. *J. Prakt. Chemie.* **1882**, *26*, 145.
- (12) Fischer, E.; Fourneau, E. Ueber einige Derivate des Glykocolls. *Ber. Dtsch. Chem. Ges.* **1901**, *34*, 2868.
- (13) (a) Jaradat, D. M. M. Thirteen decades of peptide synthesis: key developments in solid phase peptide synthesis and amide bond formation utilized in peptide ligation. *Amino Acids* **2018**, *50*, 39. (b) Goodman, M.; Cai, W.; Smith N. D. The Bold Legacy of Emil Fischer. *J. Peptide Sci.* **2003**, *9*, 594. (c) Babu, V. V. S. One hundred years of peptide chemistry. *Resonance* **2001**, *6*, 68.

- (14) For recent representative examples, see: (a) Bergmann, M.; Zervas, L. Über ein allgemeines Verfahren der Peptid-Synthese. *Ber. Dtsch. Chem. Ges.* **1932**, *65*, 1192. (b) Vigneaud, V. d.; Ressler, C.; Swan, C. J. M.; Roberts, C. W.; Katsoyannis, P. G.; Gordon, S. The Synthesis of an Octapeptide Amide with the Hormonal Activity of Oxytocin. *J. Am. Chem. Soc.* **1953**, *75*, 4879. (c) Vigneaud, V. d.; Ressler, C.; Swan, J. M.; Roberts, C. W.; Katsoyannis, P. G. *J. Am. Chem. Soc.* **1954**, *76*, 3115.
- (15) Merrifield, R. B.; Solid Phase Peptide Synthesis. I. The Synthesis of a Tetrapeptide. *J. Am. Chem. Soc.* **1963**, *85*, 2149.
- (16) For representative reviews, see: (a) Edited by B. Dörner and P. White, Novabiochem, *Handbook of Solid-Phase Peptide Synthesis*. Homepage: <https://jp.surveymonkey.com/r/novavio>. (b) Valeur, E.; Bradley, M. Amide bond formation: beyond the myth of coupling reagents. *Chem. Soc. Rev.* **2009**, *38*, 606. (c) Mäde, V.; Els-Heindl, S.; Beck-Sickinger, A. G. Automated solid-phase peptide synthesis to obtain therapeutic peptides. *Beilstein J. Org. Chem.* **2014**, *10*, 1197.
- (17) Tamiaki, H.; Obata, T.; Azefu, Y.; Toma, K. A Novel Protecting Group for Constructing Combinatorial Peptide Libraries. *Bull. Chem. Soc. Jpn.* **2001**, *74*, 733.
- (18) Chiba's group used the protocol to synthesize several peptides, including bioactive ones. For representative reports, see: (a) Tana, G.; Kitada, S.; Fujita, S.; Okada, Y.; Kim, S.; Chiba, K. A practical solution-phase synthesis of an antagonistic peptide of TNF- $\alpha$  based on hydrophobic tag strategy. *Chem. Commun.* **2009**, *46*, 8219. (b) Okada, Y.; Suzuki, H.; Nakae, T.; Fujita, S.; Abe, H.; Nagano, K.; Yamada, T.; Ebata, N.; Kim, S.; Chiba, K. Tag-Assisted Liquid-Phase Peptide Synthesis Using Hydrophobic Benzyl Alcohols as Supports. *J. Org. Chem.* **2013**, *78*, 320. (c) Matsumoto, E.; Fujita, Y.; Okada, Y.; Kauppinen, E. I.; Kamiya, H.; Chiba, K. Hydrophobic benzyl amines as supports for liquid-phase C-terminal amidated peptide synthesis: application to the preparation of ABT-510. *J. Pept. Sci.* **2015**, *21*, 691.
- (19) Our group achieved an efficient total synthesis of argifin, naturally occurring chitinase inhibitors utilizing this LPPS method. See: Hirose, T.; Kasai, T.; Akimoto, T.; Endo, A.; Sugawara, A.; Nagasawa, K.; Shiomi, K.; Ōmura, S.; Sunazuka, T. Solution-phase total synthesis of the hydrophilic natural product argifin using 3,4,5-tris(octadecyloxy)benzyl tag. *Tetrahedron* **2011**, *67*, 6633.
- (20) Fluorene-derived anchor-supported compounds and a synthetic protocol called AJIPHASE were developed by Ajinomoto Co., Inc. See: (a) Takahashi, D.; Yamamoto, T. Development of an efficient liquid-phase peptide synthesis protocol using a novel fluorene-derived anchor support compound with Fmoc chemistry; AJIPHASE<sup>®</sup>. *Tetrahedron Lett.* **2012**, *53*, 1936. (b) Takahashi, D.; Yano, T.; Fukui, T. Novel diphenylmethyl-Derived Amide Protecting Group for Efficient Liquid-Phase Peptide Synthesis: AJIPHASE. *Org. Lett.* **2012**, *14*, 4514. (c) Takahashi, D.; Inomata, T.; Fukui, T. AJIPHASE<sup>®</sup>: A Highly Efficient Synthetic Method for One-Pot Peptide Elongation in the Solution Phase by an Fmoc Strategy. *Angew. Chem., Int. Ed.* **2017**, *56*, 7803.
- (21) Montalbetti, C. A. G. N.; Falque, V. Amide bond formation and peptide coupling. *Tetrahedron* **2005**, *61*, 10827.

- (22) Scientists Against Malaria, *PLASMODIUM FALCIPARUM*.  
Homepage: <https://scientistsagainstmalaria.net/parasite/plasmodium-falciparum>.
- (23) World Health Organization, *Malaria*.  
Homepage: <https://www.who.int/en/news-room/fact-sheets/detail/malaria>.
- (24) Yoshida, Y.; Arizono, N. Nanzando, *Zusetsu Jintai kiseityuu-gaku*, 9<sup>th</sup> edition.
- (25) Research Institute for Microbial Diseases, Osaka University.  
Homepage: <http://www.biken.osaka-u.ac.jp/education/bioscience/>.
- (26) Centers for Disease Control and Prevention, DPDx – Laboratory Identification of Parasites of Public Health Concern, *Malaria*. Homepage: <https://www.cdc.gov/dpdx/malaria/index.html>.
- (27) Achan, J.; Talisuna, A. O.; Erhart, A.; Yeka, A.; Tibenderana, J. K.; Baliraine, F. N.; Rosenthal, P. J.; D'Alessandro, U. Quinine, an old anti-malarial drug in a modern world: role in the treatment of malaria. *Malaria J.* **2011**, *10*, 144.
- (28) (a) Goldsmith, K. A controlled field trial of SN 7618-5 (chloroquine) for the suppression of malaria. *J. Malar. Inst. India* **1946**, *6*, 311. (b) Cooper, R. G.; Magwere, T. Chloroquine: Novel uses & manifestations. *Indian J. Med. Res.* 2008, *127*, 305.
- (29) Sullivan, D. J. Jr.; Gluzman, I. Y.; Russell, D. G.; Goldberg, D. E. On the molecular mechanism of chloroquine's antimalarial action. *Proc. Natl. Acad. Sci. USA* **1996**, *93*, 11865.
- (30) Macomber, P. B.; O'Brien, R. L.; Hahn, F. E. Chloroquine: Physiological Basis of Drug Resistance in *Plasmodium berghei*. *Science* **1966**, *152*, 1374.
- (31) Davidson, M. W.; Griggs, B. G. Jr.; Boykin, D. W.; Wilson, W. D. Mefloquine, a clinically useful quinolinemethanol antimalarial which does not significantly bind to DNA. *Nature* **1975**, *254*, 632.
- (32) Cosgriff, T. M.; Boudreau, E. F.; Pamplin, C. L.; Doberstyn, E. B.; Desjardins, R. E.; Canfield, C. J. valuation of the Antimalarial Activity of the Phenanthrenemethanol Halofantrine (WR 171,669). *Am. J. Trop. Med. Hyg.* **1982**, *31*, 1075.
- (33) (a) Liao, F. Discovery of Artemisinin (Qinghaosu). *Molecules* **2009**, *14*, 5362. (b) Collaboration research group for Qinghaosu. A new sesquiterpene lactone–Qinghaosu (in Chinese). *Kexue Tongbao* **1977**, *3*, 142. (c) Collaboration research group for Qinghaosu. Antimalaria studies on qinghaosu. *Chin. Med. J.* **1979**, *92*, 811.
- (34) White, N. J.; Hien, T. T.; Nosten, F. H. A Brief History of Qinghaosu. *Trends Parasitol.* **2015**, *31*, 607.
- (35) Eckstein-Ludwig, U.; Webb, R. J.; van Goethem, I. D. A.; East, J. M.; Lee, A. G.; Kimura, M.; O'Neill, P. M.; Bray, P. G.; Ward, S. A.; Krishna, S. Artemisinins target the SERCA of *Plasmodium falciparum*. *Nature* **2003**, *424*, 957.
- (36) World Health Organization, *Antimalarial drug combination therapy 2001*.
- (37) Wataya, Y. Search and development of new antimalarial drugs. *Igaku no ayumi* **2009**, *229*, 257.

## Chapter 2

- (38) (a) Otoguro, K.; Kohana, A.; Manabe, C.; Ishiyama, A.; Ui, H.; Shiomi, K.; Yamada, H.; Ōmura, S. Potent Antimalarial Activities of Polyether Antibiotic, X-206. *J. Antibiot.* **2001**, *54*, 658. (b) Otoguro, K.; Ishiyama, A.; Ui, H.; Kobayashi, M.; Manabe, C.; Yan, G.; Takahashi, Y.; Tanaka, H.; Yamada, H.; Ōmura, S. *In Vitro* and *In Vivo* Antimalarial Activities of the Monoglycoside Polyether Antibiotic, K-41 against Drug Resistant Strains of *Plasmodia*. *J. Antibiot.* **2002**, *55*, 832. (c) Otoguro, K.; Ui, H.; Ishiyama, A.; Arai, N.; Kobayashi, M.; Takahashi, Y.; Masuma, R.; Shiomi, K.; Yamada, H.; Ōmura, S. *In Vitro* Antimalarial Activities of the Microbial Metabolites. *J. Antibiot.* **2003**, *56*, 322. (d) Otoguro, K.; Ui, H.; Ishiyama, A.; Kobayashi, M.; Togashi, H.; Takahashi, Y.; Masuma, R.; Tanaka, H.; Tomoda, H.; Yamada, H.; Ōmura, S. *In Vitro* and *in Vivo* Antimalarial Activities of a Non-glycosidic 18-Membered Macrolide Antibiotic, Borrelidin, against Drug-resistant Strains of *Plasmodia*. *J. Antibiot.* **2003**, *56*, 727. (e) Otoguro, K.; Ishiyama, A.; Kobayashi, M.; Sekiguchi, H.; Izuhara, T.; Sunazuka, T.; Tomoda, H.; Yamada, H.; Ōmura, S. *In Vitro* and *In Vivo* Antimalarial Activities of a Carbohydrate Antibiotic, Prumycin, against Drug-resistant Strains of *Plasmodia*. *J. Antibiot.* **2004**, *57*, 400. (f) Ui, H.; Ishiyama, A.; Sekiguchi, H.; Namatame, M.; Nishihara, A.; Takahashi, Y.; Shiomi, K.; Otoguro, K.; Ōmura, S. Selective and Potent *In Vitro* Antimalarial Activities Found in Four Microbial Metabolites. *J. Antibiot.* **2007**, *60*, 220. (g) Iwatsuki, M.; Takada, S.; Mori, M.; Ishiyama, A.; Namatame, M.; Nishihara-Tsukashima, A.; Nonaka, K.; Masuma, R.; Otoguro, K.; Shiomi, K.; Ōmura, S. *In vitro* and *in vivo* antimalarial activity of puberulic acid and its new analogs, viticolins A–C, produced by *Penicillium* sp. FKI-4410. *J. Antibiot.* **2011**, *64*, 183. (h) Hirose, T.; Noguchi, Y.; Furuya, Y.; Ishiyama, A.; Iwatsuki, M.; Otoguro, K.; Ōmura, S.; Sunazuka, T. Structure Determination and Total Synthesis of (+)-16-Hydroxy-16,22-dihydroapparicine. *Chem. - Eur. J.* **2013**, *19*, 10741.
- (39) (a) Marfey, P. Determination of  $\alpha$ -Amino Acids. II. Use of a Bifunctional Reagent, 1,5-Difluoro-2,4-dinitromenzene. *Carlsberg Res. Commun.* **1984**, *49*, 591. (b) Fujii, K.; Ikai, Y.; Mayumi, T.; Oka, H.; Suzuki, M.; Harada, K. A Nonempirical Method Using LC/MS for Determination of the Absolute Configuration of Constituent Amino Acids in a Peptide: Elucidation of Limitations of Marfey's Method and of Its Separation Mechanism. *Anal. Chem.* **1997**, *69*, 3346.
- (40) Miwa, H.; Hiyama, C.; Yamamoto, M. High-Performance Liquid Chromatography of Short-and Long-Chain Fatty Acids as 2-Nitrophenylhydrazides. *J. Chromatogr. A* **1985**, *321*, 165.
- (41) Andersson, B. A.; Holman, R. T. Pyrrolidides for mass spectrometric determination of the position of the double bond in monounsaturated fatty acids. *Lipids* **1974**, *9*, 185.
- (42) For recent representative reviews of SPPS, see: (a) Amblard, M.; Fehrentz, J.-A.; Martinez, J.; Subra, G. Methods and Protocols of Modern Solid Phase Peptide Synthesis. *Mol. Biotechnol.* **2006**, *33*, 239. (b) Behrendt, R.; White, P.; Offer, J. Advances in Fmoc solid-phase peptide Synthesis. *J. Pept. Sci.* **2016**, *22*, 4.
- (43) For LPPS-based methods to address several problems of conventional LPPS, see: (a) Narita, M. Liquid Phase Peptide Synthesis by the Fragment Condensation on Soluble Polymer Support. I. Efficient

- Coupling and Relative Reactivity of a Peptide Fragment with Various Coupling Reagents. *Bull. Chem. Soc. Jpn.* **1978**, *51*, 1477. (b) Pillai, V. N. R.; Mutter, M. New, Easily Removable Poly(ethylene glycol) Supports for the Liquid-Phase Method of Peptide Synthesis. *J. Org. Chem.* **1980**, *45*, 5364. (c) Mizuno, M.; Goto, K.; Miura, T.; Hosaka, D.; Inazu, T. A novel peptide synthesis using fluororous chemistry. *Chem. Commun.* **2003**, 972.
- (44) Li, H.; Jiang, X.; Ye, Y.-h.; Fan, C.; Romoff, T.; Goodman, M. 3-(Diethoxyphosphoryloxy)-1,2,3-benzotriazin-4(3*H*)-one (DEPBT): A New Coupling Reagent with Remarkable Resistance to Racemization. *Org. Lett.* **1999**, *1*, 91.
- (45) Nahm, S.; Weinreb, S. M. *N*-Methoxy-*N*-methylamides as Effective Acylating Agents. *Tetrahedron Lett.* **1981**, *22*, 3815.
- (46) Peters, W.; Portus, J. H.; Robinson, B. L. The chemotherapy of rodent malaria, XXII. The value of drug-resistant strains of *P. berghei* in screening for blood schizontocidal activity. *Ann. Trop. Med. Parasitol.* **1975**, *69*, 155.
- (47) A few compounds which have similar structures to kozupeptins were reported; see: (a) Fujie, K.; Sato, T.; Nishikawa, M.; Hatanaka, H.; Hashimoto, M. JP 09/221497, August 26, 1997. (b) Ortiz-López, F. J.; Monteiro, M. C.; González-Menéndez, V. G.; Tormo, J. R.; Genilloud, O.; Bills, G. F.; Vicente, F.; Zhang, C.; Roemer, T.; Singh, S. B.; Reyes, F. Cyclic Colisporifungin and Linear Cavinafungins, Antifungal Lipopeptides Isolated from *Colispora cavicola*. *J. Nat. Prod.* **2015**, *78*, 468.

### Chapter 3

- (48) For initial representative reports, see: (a) Aoyagi, T.; Takeuchi, T.; Matsuzaki, A.; Kawamura, K.; Kondo, S.; Hamada, M.; Maeda, K.; Umezawa, H. Leupeptins, new protease inhibitors from actinomycetes. *J. Antibiot.* **1969**, *22*, 283. (b) Fehrentz, J.- A.; Heitz, A.; Bertrand, C.; Cazaubon, C.; Nisato, D. Aldehydic peptides inhibiting renin. *FEBS Lett.* **1984**, *167*, 273. (c) Sarubbi, E.; Seneci, P. F.; Angelastro, M. P.; Peet, N. P.; Denaro, M.; Islam, K. Peptide aldehydes as inhibitors of HIV protease. *FEBS Lett.* **1993**, *319*, 253.
- (49) Otto, H.- H.; Schirmeister, T. Cysteine Proteases and Their Inhibitors. *Chem. Rev.* **1997**, *97*, 133.
- (50) Moulin, A.; Martinez, J.; Fehrentz, J.- A. Synthesis of peptide aldehydes. *J. Pept. Sci.* **2007**, *13*, 1.
- (51) (a) Fehrentz, J.- A.; Castro, B. An Efficient Synthesis of Optically Active  $\alpha$ -(*t*-Butoxycarbonylamino)-aldehydes from  $\alpha$ -Amino Acids. *Synthesis* **1983**, *15*, 676. (b) Konno, H.; Nosaka, K.; Akaji, K. Synthesis of tokaramide A, a cysteine protease inhibitor from marine sponge *Theonella aff. Mirabilis*. *Tetrahedron* **2011**, *67*, 9067. (c) Fehrentz, J.- A.; Paris, M.; Heitz, A.; Velek, J.; Liu, C.- F.; Winternitz, F.; Martinez, J. Improved solid phase synthesis of C-terminal peptide aldehydes. *Tetrahedron Lett.* **1995**, *36*, 7871. (d) Fehrentz, J. A.; Paris, M.; Heitz, A.; Velek, J.; Winternitz, F.; Martinez, J. Solid Phase Synthesis of C-Terminal Peptide Aldehydes. *J. Org. Chem.* **1997**, *62*, 6792. (e) Tong, X.- H.; Hong, A. Solid phase synthesis of aspartyl peptide aldehydes. *Tetrahedron Lett.* **2000**, *41*, 8857.

- (52) See **Chapter 2** for details. We tried to use HO-TAGa (**2**) as a hydrophobic anchor molecule. However, in the deprotection of the Fmoc group of Asn under basic conditions, the yield of the desired product was low due to the formation of diketopiperazine. The use of a fluorene-type anchor molecule developed by Ajinomoto Co., Inc. considerably suppressed this undesired reaction.
- (53) (a) Brown, J. D. ASYMMETRIC SYNTHESIS OF NAPROXEN VIA A PINACOL-TYPE REACTION. *Tetrahedron: Asymmetry* **1992**, *3*, 1551. (b) Badioli, M.; Ballini, R.; Bartolacci, M.; Bosica, G.; Torregiani, E.; Marcantoni, E. Addition of Organocerium Reagents to Morpholine Amides: Synthesis of Important Pheromone Components of *Achaea Janata*. *J. Org. Chem.* **2002**, *67*, 8938.
- (54) Brown, H. C.; McFarlin, R. F. The Reaction of Lithium Aluminum Hydride with Alcohols, Lithium Tri-*t*-butoxyaluminumhydride as a New Selective Reducing Agent. *J. Am. Chem. Soc.* **1958**, *80*, 5372.

### Experimental Section

- (55) (a) Valle, J. R. D.; Goodman, M. Asymmetric Hydrogenations for the Synthesis of Boc-Protected 4-Alkylprolinols and Prolines. *J. Org. Chem.* **2003**, *68*, 3923. (b) Shoulders, M. D.; Hodges, J. A.; Raines, R. T. Reciprocity of Steric and Stereoelectronic Effects in the Collagen Triple Helix. *J. Am. Chem. Soc.* **2006**, *128*, 8112.